frontiers | Research Topics

Toxicity mechanisms of environmental pollutants and health risk assessment

Edited by
Mahua Saha, Xiance Sun, Dan Xu and Pu Xia

Published in
Frontiers in Public Health

ISSN 1664-8714
ISBN 978-2-8325-6602-2
DOI 10.3389/978-2-8325-6602-2

Generative AI statement
Any alternative text (Alt text) provided alongside figures in the articles in this ebook has been generated by Frontiers with the support of artificial intelligence and reasonable efforts have been made to ensure accuracy, including review by the authors wherever possible. If you identify any issues, please contact us.

About Frontiers

Frontiers is more than just an open access publisher of scholarly articles: it is a pioneering approach to the world of academia, radically improving the way scholarly research is managed. The grand vision of Frontiers is a world where all people have an equal opportunity to seek, share and generate knowledge. Frontiers provides immediate and permanent online open access to all its publications, but this alone is not enough to realize our grand goals.

Frontiers journal series

The Frontiers journal series is a multi-tier and interdisciplinary set of open-access, online journals, promising a paradigm shift from the current review, selection and dissemination processes in academic publishing. All Frontiers journals are driven by researchers for researchers; therefore, they constitute a service to the scholarly community. At the same time, the *Frontiers journal series* operates on a revolutionary invention, the tiered publishing system, initially addressing specific communities of scholars, and gradually climbing up to broader public understanding, thus serving the interests of the lay society, too.

Dedication to quality

Each Frontiers article is a landmark of the highest quality, thanks to genuinely collaborative interactions between authors and review editors, who include some of the world's best academicians. Research must be certified by peers before entering a stream of knowledge that may eventually reach the public - and shape society; therefore, Frontiers only applies the most rigorous and unbiased reviews. Frontiers revolutionizes research publishing by freely delivering the most outstanding research, evaluated with no bias from both the academic and social point of view. By applying the most advanced information technologies, Frontiers is catapulting scholarly publishing into a new generation.

What are Frontiers Research Topics?

Frontiers Research Topics are very popular trademarks of the *Frontiers journals series*: they are collections of at least ten articles, all centered on a particular subject. With their unique mix of varied contributions from Original Research to Review Articles, Frontiers Research Topics unify the most influential researchers, the latest key findings and historical advances in a hot research area.

Find out more on how to host your own Frontiers Research Topic or contribute to one as an author by contacting the Frontiers editorial office: frontiersin.org/about/contact

Toxicity mechanisms of environmental pollutants and health risk assessment

Topic editors

Mahua Saha — National Institute of Oceanography, Council of Scientific and Industrial Research (CSIR), India

Xiance Sun — Dalian Medical University, China

Dan Xu — Dalian Maritime University, China

Pu Xia — University of Birmingham, United Kingdom

Citation

Saha, M., Sun, X., Xu, D., Xia, P., eds. (2025). *Toxicity mechanisms of environmental pollutants and health risk assessment*. Lausanne: Frontiers Media SA.

doi: 10.3389/978-2-8325-6602-2

Table of contents

frontiers | Frontiers in Public Health

TYPE Original Research
PUBLISHED 12 June 2024
DOI 10.3389/fpubh.2024.1378027

OPEN ACCESS

EDITED BY
Renata Sisto,
National Institute for Insurance against Accidents at Work (INAIL), Italy

REVIEWED BY
Rossanna Rodriguez-Canul,
Center for Research and Advanced Studies – Mérida Unit, Mexico
Sotirios Maipas,
National and Kapodistrian University of Athens, Greece

*CORRESPONDENCE
Aifeng He
✉ 1608427310@qq.com
Wenwen Sun
✉ sww020301@163.com

†These authors have contributed equally to this work and share the corresponding authorship

RECEIVED 29 January 2024
ACCEPTED 28 May 2024
PUBLISHED 12 June 2024

CITATION
Xu L, Yang S, Wang L, Qiu J, Meng H, Zhang L, Sun W and He A (2024) Association between pesticide exposure and thyroid function: analysis of Chinese and NHANES databases. *Front. Public Health* 12:1378027. doi: 10.3389/fpubh.2024.1378027

Association between pesticide exposure and thyroid function: analysis of Chinese and NHANES databases

Leiming Xu[1†], Shengkai Yang[1†], Longqing Wang[1], Jinxin Qiu[1], Hai Meng[1], Lulu Zhang[1], Wenwen Sun[2*] and Aifeng He[1*]

[1]Binhai County People's Hospital Affiliated to Kangda College of Nanjing Medical University, Yancheng, Jiangsu, China, [2]Department of Intensive Care Unit, Changzhou Maternity and Child Health Care Hospital, Changzhou Medical Center, Nanjing Medical University, Changzhou, China

Background: Pesticides are widely used in agricultural activities. Although pesticide use is known to cause damage to the human body, its relationship with thyroid function remains unclear. Therefore, this study aimed to investigate the association between pesticide exposure and thyroid function.

Methods: The Chinese database used included 60 patients with pyrethroid poisoning and 60 participants who underwent health checkups between June 2022 and June 2023. The NHANES database included 1,315 adults enrolled from 2007 to 2012. The assessed pesticide and their metabolites included 2,4-dichlorophenoxyacetic acid (2,4-D), 4-fluoro-3-phenoxybenzoic acid (4F3PB), para-nitrophenol (PN), 3-phenoxybenzoic acid (3P), and trans-dichlorovinyl-dimethylcyclopropane carboxylic acid (TDDC). The evaluated indicators of thyroid function were measured by the blood from the included population. The relationship between pesticide exposure and thyroid function indexes was investigated using linear regression, Bayesian kernel machine regression (BKMR), restricted cubic spline (RCS), and weighted quantile sum (WQS) models.

Results: The Chinese data showed that pesticide exposure was negatively correlated with the thyroid function indicators FT4, TT4, TgAb, and TPOAb (all $p < 0.05$). The BKMR model analysis of the NHANES data showed that the metabolic mixture of multiple pesticides was negatively associated with FT4, TSH, and Tg, similar to the Chinese database findings. Additionally, linear regression analysis demonstrated positive correlations between 2,4-D and FT3 ($p = 0.041$) and 4F3PB and FT4 ($p = 0.003$), whereas negative associations were observed between 4F3PB and Tg ($p = 0.001$), 4F3PB and TgAb ($p = 0.006$), 3P and TgAB ($p = 0.006$), 3P and TPOAb ($p = 0.03$), PN and TSH ($p = 0.003$), PN and TT4 ($p = 0.031$), and TDDC and TPOAb ($p < 0.001$). RCS curves highlighted that most pesticide metabolites were negatively correlated with thyroid function indicators. Finally, WQS model analysis revealed significant differences in the weights of different pesticide metabolites on the thyroid function indexes.

Conclusion: There is a significant negative correlation between pesticide metabolites and thyroid function indicators, and the influence weights of different pesticide metabolites on thyroid function indicators are significantly different. More research is needed to further validate the association between different pesticide metabolites and thyroid disease.

KEYWORDS

pesticides, thyroid function, Bayesian kernel machine regression, restricted cubic spline curve, NHANES database

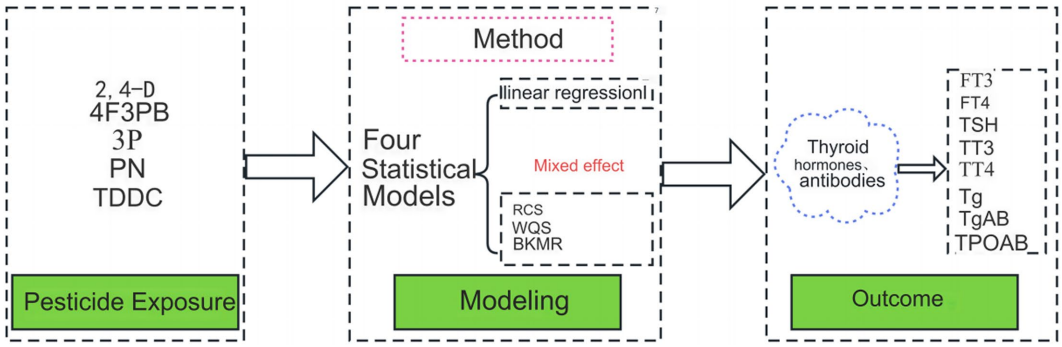

GRAPHICAL ABSTRACT
WQS, weighted quantile sum; BKMR, Bayesian kernel machine regression; RCS, restricted cubic spline; 2,4-D, 2,4-dichlorophenoxyacetic acid; 4F3PB, 4-fluoro-3-phenoxybenzoic acid; 3P, 3-phenoxybenzoic acid; PN, para-nitrophenol; TDDC, trans-dichlorovinyl-dimethylcyclopropane carboxylic acid.

1 Introduction

Pesticides are the most widely used chemical compounds in agriculture, mainly for preventing and eliminating pests and reducing crop damage risk. Current studies suggest that numerous pesticides are more or less harmful to human health. For example, ethyl dithiocarbamate (EBDC) is an extensively applied pesticide worldwide that can cause hypothyroidism in rats, primarily manifesting as decreased FT4 and increased TSH levels (1, 2). Other research has identified the same effect of EBDC on human thyroid function, resulting in decreased thyroid function and serum TSH concentration among people exposed to EBDC compared to those not in contact with EBDC (3). Pyrethroid insecticides and herbicides are not new to the agricultural field, with pyrethroids observed to disrupt thyroid function by binding to hormone receptors due to their structural similarities with the receptors (4). Organophosphorus pesticides (OPs) are another pesticide class popularly employed in agricultural activities. Exposure to these OPs or multiple pesticide classes is associated with genotoxicity and adverse neurobehavioral outcome markers in exposed populations, especially children and farm workers (5). All these research findings highlight that the effects of various pesticides on human health cannot be ignored.

2,4-dichlorophenoxyacetic acid (2,4-D), also known as the "king of grass," is a commonly utilized herbicide and synthetic plant hormone that controls weed growth by mimicking the effects of auxin. Studies have revealed a significant increase in hypothyroidism among people using 2,4-D pesticides (6). Moreover, Goldner et al. (7) identified a significant association between 2,4-D pesticide exposure and hypothyroidism in male pesticide users, whereas no such significant association was detected in the female population. Similar conclusions have been found recently, the United States Environmental Protection Agency's (US EPA) Endocrine Disruptor Screening Program test, which examines potential interactions between 2,4-D and the estrogen, androgen, and thyroid pathways or steroid production, found no convincing evidence on the potential interaction between 2,4-D and estrogen. However, a potential interaction was indicated between 2,4-D and the androgen and thyroid pathways (8, 9). Animal studies have also demonstrated that rats subjected to different doses of 2,4-D exhibited varied effects on thyroid hormone levels as well as on the weight and pathology of the thyroid gland (10).

Para-nitrophenol (PN) and trans-dichlorovinyl-dimethylcyclopropane carboxylic acid (TDDC) are metabolites of the extensively employed OPs and insecticides. OPs are mainly used for controlling pests, such as mosquitoes and fleas, in agriculture, homes, and public places. The primary mechanism of OPs is to produce an insecticidal effect by acetylcholinesterase inhibition in the nervous system of pests. Researchers have determined that compared to the general male population, men exposed to OPs presented with significant changes in the Thyroid Stimulating Hormone (TSH) and other thyroid hormone levels (11). Consistent with the occupational and experimental study findings, OPs can significantly escalate hypothyroidism. The hyperthyroidism changes include increased TSH levels and a reduction, increase, or no significant changes in the T3 and/or T4 levels (12). According to the above findings, OPs and carbamate insecticides may inhibit brain cholinesterase activity by affecting the hypothalamus and pituitary gland via muscarinic and nicotinic receptors, thereby altering thyroid function (12).

Phenoxybenzoic acid (3P) and 4-fluoro-3-phenoxybenzoic acid (4F3PB) are metabolites of pyrethroids, a class of broad-spectrum insecticides popularly used in agriculture and indoor pest control. These compounds cause paralysis and death of the insect pests by interfering with their nervous system excitability (4). These pesticides are ubiquitously used for controlling mosquitoes, moths, fleas, and other pests in fields, greenhouses, homes, and public places. Although this pesticide type has substantial insecticidal activity and is less toxic to humans and mammals, its adverse health effects cannot be ignored. The pyrethroid metabolites have been found to act as thyroid disruptors, affecting the hypothalamic–pituitary-thyroid axis to varying degrees (13). *In vitro* research has shown that pyrethroids can antagonize thyroid receptors and consequently block the thyroid axis, with the possibility of pyrethroids or their metabolites interacting with androgens or estrogen receptors also being indicated (14). Furthermore, *in vivo* experiments have examined the effects of two pyrethroids (permethrin and beta-cypermethrin) and three pyrethroid metabolites (3-phenoxybenzyl alcohol, 3-phenoxybenzaldehyde, and 3-phenoxybenzoic acid) in zebrafish models. The results suggested that pyrethroid insecticides and their metabolites influenced thyroid signaling, motor behavior, and embryonic development in the zebrafish, implying that thyroid disruption may be involved in abnormal larva development (15).

The human body absorbs pesticides not only during agricultural work but also via fruit and vegetable dietary intake as well as direct

pesticide consumption by those attempting suicide. However, pesticide absorption in these population groups is generally linked to two or more pesticides and not a single pesticide. Hence, the effect of multiple pesticides on thyroid function also requires attention. Despite this understanding, most current research focuses on the impact of individual pesticides on the human thyroid function index. Therefore, this study investigated the combined effect of OP, pyrethroid, and herbicide metabolites on thyroid function.

2 Materials and methods

2.1 Analysis of clinical patient and control data

2.1.1 Patients and controls

This retrospective study selected 60 patients hospitalized for pyrethroid pesticide poisoning and 60 healthy control participants who had undergone health examinations at Binhai County People's Hospital between June 2022 and June 2023. This study complied with the criteria outlined in the Declaration of Helsinki (as revised in 2013) and was approved by the Ethics Committee of Binhai County People's Hospital (approval no: 2023-BHKYLL-018). All patients and controls or their relatives provided signed informed consent before study enrollment.

The patient inclusion criteria were as follows: (1) pyrethroid pesticide exposure and (2) age > 20 years. Patients were excluded if they met the following exclusion criteria: (1) previous thyroid disease history or (2) pregnancy or lactation. A total of 60 patients were enrolled based on these criteria.

2.1.2 Data collection

All patient data within 48 h after admission were reviewed and collected from our hospital's electronic medical records as raw data. Acquired data included age, sex, marriage, education, smoking status, alcohol consumption, and laboratory thyroid test results (FT3, FT4, TSH, TT3, TT4, TgAb, and TPOAb levels). Details of the thyroid function indicators are shown in Supplementary Table S1.

2.2 Analysis of participants in the NHANES database

2.2.1 Study design and population

NHANES is a series of cross-sectional, nationally representative surveys conducted annually by the National Center for Health Statistics of the Centers for Disease Control and Prevention to estimate and assess the health and nutritional statuses as well as the potential risk factors of the non-institutionalized civilian population in the United States. All included participants have provided written informed consent before survey inclusion. All NHANES studies receive approval from the National Health Statistics Research Ethics Review Board.[1] All programs comply with the relevant guidelines and regulations.[2]

Three open-access consecutive surveys were retrieved from the NHANES website: 2007–2008, 2009–2010, and 2011–2012. The collected data included demographic, inspection, laboratory, and questionnaire information. The total sample size in the included surveys was 30,442 individuals. Participants <20 years of age and those lacking data on the levels of pesticide metabolites, thyroid hormones, and antibodies were excluded ($n = 28,884$). Additionally, pregnant and lactating women and those with pre-existing thyroid conditions were excluded ($n = 101$). Lastly, individuals with missing covariate data, such as education, marriage, and smoking status, were excluded ($n = 142$). Ultimately, 1,315 individuals were included (Figure 1).

2.2.2 Measurement of pesticide metabolites

The body primarily eliminates absorbed pesticides by excreting their associated metabolites via urine. The metabolites of OPs mainly comprise 2,4-D. Furthermore, 4F3PB, TDDC, and 3P are pyrethroid metabolites, while PN is primarily a herbicide metabolite. Therefore, an urine concentration test for the above metabolites is crucial to detect pesticide poisoning and determine the disease status in patients with pesticide poisoning.

The levels of various pesticide metabolites in the urine were measured and quantified from the participants' urine matrix using an automated solid-phase extraction system. The samples were analyzed via HPLC and a triple quadrupole mass spectrometer with a heated electrospray ionization source (16). The lower limit concentration of 2,4-D detection was 0.15 μg/L; 4F3PB, 0.10 μg/L; 3P, 0.10 μg/L; PN, 0.10 μg/L; and TDDC, 0.60 μg/L. Furthermore, data below the lower limit of their detection (LOD) were specified as LOD divided by the square root of 2 to improve the statistical power and accuracy of effect estimation (17). The official website (NHANES 2007–2012) provides additional laboratory information concerning the applied methods and procedures.

2.2.3 Thyroid hormone

Thyroid blood specimens were processed, stored, and shipped to Collaborative Laboratory Services, Ottumwa, Iowa, United States. A competitive binding immunoenzymatic assay was used to detect TT3, TT4, and FT3 levels. Additionally, a two-step enzyme immunoassay was used to determine FT4 concentration, while a third-generation two-site immunoenzymatic ("sandwich") assay was employed to estimate TSH levels. Lastly, a simultaneous one-step "sandwich" assay was applied to obtain Tg levels, whereas a continuous two-step immunoenzymatic "sandwich" assay was performed to measure TgAb and TPOAb concentrations. The specific details of the methods are available in NHANES 2007–2012.

2.2.4 Covariates

Based on previous studies, relevant variables were selected as the predictors of the preliminary analysis to control for potential confounding effects. The selected covariables included age, sex, race, education level, and obesity. The statistical model was then adjusted using the covariates to reduce the confounding bias on the research results. The adjusted covariates included demographic characteristics such as (a) age (20–39, 40–59, and ≥ 60 years), (b) race (Mexican Americans, non-Hispanic whites, non-Hispanic blacks, other Hispanics, and other races including multiracial groups), (c) gender (male and female), (d) marital status (married, unmarried, and other status including divorced or widowed), and (e) education (below high school, high school, and above high school), as well as characteristics such as (f) smoking status (never smoker, former smoker, and current smoker), (g) alcohol consumption

1 https://www.cdc.gov/nchs/nhanes/irba98

2 https://www.cdc.gov/nchs/data_access/restrictions

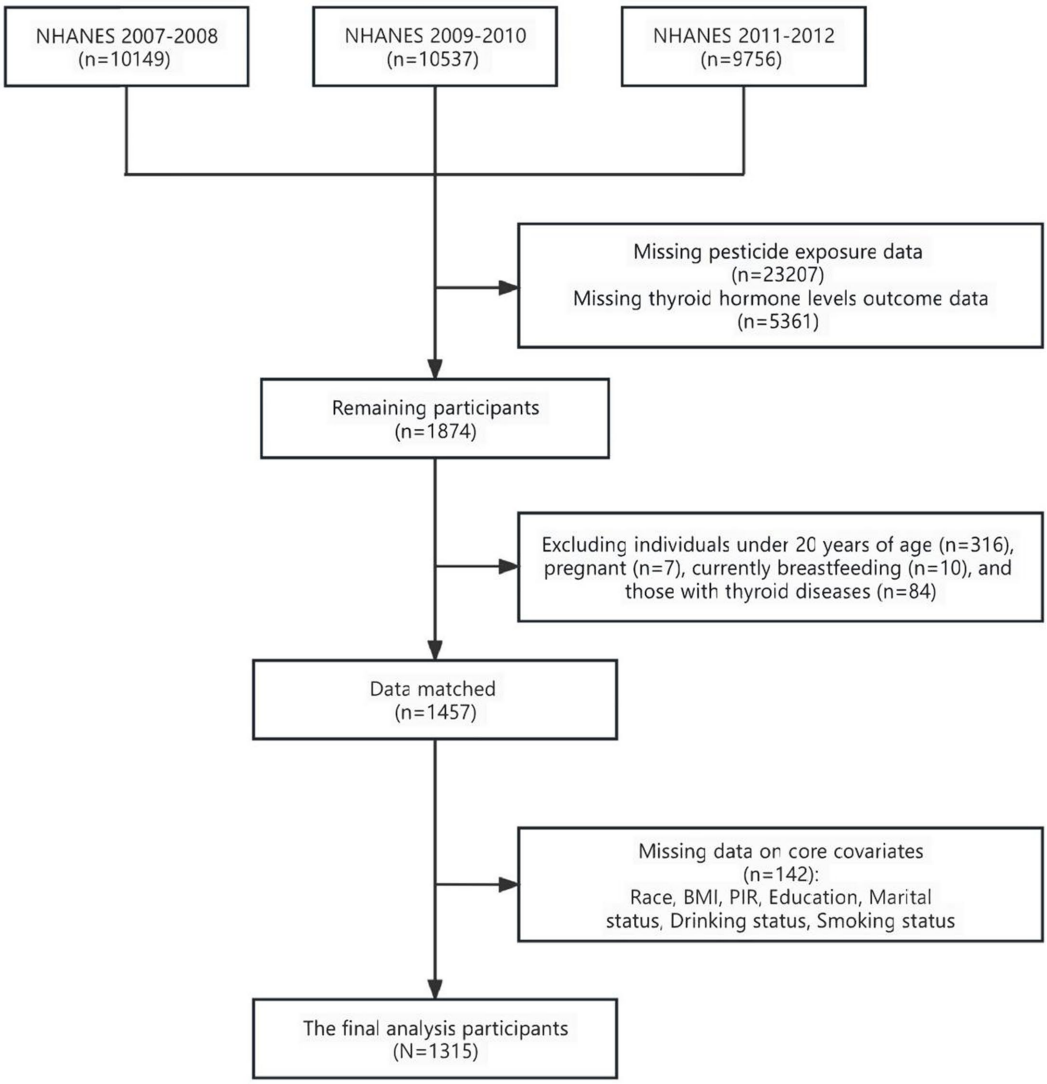

FIGURE 1
Flowchart of study participant selection in the NHANES 2007–2012.

(non-drinkers and moderate drinkers: 1–2 drinks/day for men and 1 drink/day for women; and heavy drinkers: >2 drinks/day for men and > 1 drink/day for women), and (h) body mass index (BMI, normal: 25 kg/m^2, overweight: 25–30 kg/m^2, and obese: ≥30 kg/m^2). The uniform interviews and questionnaires were completed by trained medical professionals.

2.3 Statistical analysis

All statistical analyses were performed using StataMP 17 version, GraphPad Prism 9.5, and R 4.2.3 software, with three statistical packages ("rms," "gWQS," and "bkmr"). A p-value of <0.05 (bilateral) was considered statistically significant.

2.3.1 Descriptive statistical analysis

Normal continuous data were expressed as mean ± standard deviation (mean ± SD), whereas skewed continuous data were presented as median and interquartile distance (IQR). Furthermore, categorical variables were denoted as numbers (percentages). The differences between the age groups were assessed using an independent sample T-test and Mann–Whitney U test for continuous variables and the chi-square test for categorical variables. The pesticide metabolite levels and thyroid function results were naturally log-transformed in an approximately normal distribution. Spearman's rank coefficient was applied to measure the correlation between each pesticide metabolite.

2.3.2 Bayesian kernel machine regression model

The potential complex nonlinear or linear relationships between pesticide metabolites and the various thyroid hormones were evaluated using the BKMR model. BKMR is a nonparametric model combining Bayesian and statistical learning techniques, providing strong adaptability and good model-fitting ability for highly correlated variables common in the environmental epidemiological community (18, 19). Further, we modeled the exposure-response function using a Gaussian approach, followed by the application of the Markov chain Monte Carlo algorithm for 25,000 iterations. Thus, the overall effects

between pesticide metabolites and different thyroid hormones were visualized using BKMR.

2.3.3 Linear regression model

A weighted LRM was employed to determine the correlation between the pesticide metabolites and thyroid function indicators. Model 1 was not adjusted for confounding factors, while model 2 was adjusted for age, sex, race/ethnicity, education level, smoking status, alcohol consumption, and BMI. Additionally, age group analysis was used to understand the effects of pesticide metabolites on thyroid function indexes across different ages. Moreover, we used WTMEC2YR to provide weights for all data to ensure nationally representative results. Finally, we conducted several restricted cubic spline (RCS) analyses to explore the nonlinear dose relationship between pesticide metabolite exposure in the entire population and thyroid hormones.

2.3.4 Weighted quantile sum model

Finally, a WQS regression method was utilized to investigate the effect of the pesticide mixture on thyroid function indicators. The WQS regression technique combines different highly correlated compounds into a composite index, followed by regression analysis on that index. Additionally, WQS regression uses the bootstrap method to assign individual weights to each metabolite, allowing the identification of relatively critical components in the pesticide mixture (20). The weight of each metabolite ranges from 0 to 1, and the sum of the weights is 1. The effect of the metabolite on thyroid function increases with the increase in its weight value. The WQS approach provides better coverage of real-life mixed exposures and is more sensitive than univariate analysis in identifying vital predictors. In this study, 40% of the random samples were used to test and 60% to verify the data.

3 Results

3.1 Characteristics of the clinical study patients and controls

A total of 120 patients and controls from our hospital were included, comprising 60 hospitalized patients with pyrethroid exposure and 60 healthy control participants who underwent physical examination. As depicted in Table 1 and Figure 2, the mean ± SD of the levels of the thyroid function indicators FT4 (22.304 ± 16.188 pmol/L), TT4 (123.73 ± 52.232 nmol/L), TgAb (68.185 ± 119.849 IU/mL), and TPOAb (32.041 ± 60.602 IU/mL) in the healthy group significantly differed from those in the pesticide-exposed group (FT4: 16.488 ± 2.877 pmol/L, $p = 0.008$; TT4: 104.834 ± 21.865 nmol/L, $p = 0.012$; 27.214 ± 10.094 IU/mL, $p = 0.011$; and TPOAb: 14.699 ± 10.316 IU/mL, $p = 0.033$). Sex, age, education, marital status, smoking status, and alcohol consumption were not statistically significant.

3.2 Relationship between pesticide poisoning and thyroid function indicators

Linear regression modeling was used to evaluate the correlation between pesticide poisoning and thyroid function indicators and to understand whether any changes occurred in these parameters after pesticide poisoning (Table 2). The results of model 1, which was not adjusted for covariates, showed that pesticide poisoning in patients was negatively correlated with FT4 ($p = 0.007$), TT4 ($p = 0.011$), TgAb ($p = 0.009$), and TPOAb ($p = 0.031$). Further, considering that numerous potential factors can affect the thyroid function indicators of the patients, covariates such as age and gender were added to re-establish an LRM (model 2) to evaluate the correlation between them (Table 2). The analysis demonstrated that pesticide poisoning in patients was negatively correlated with FT4 ($p = 0.007$), TT4 ($p = 0.01$), TgAb ($p = 0.008$), and TPOAb ($p = 0.04$). Thus, pesticide poisoning was negatively correlated with the thyroid function indicators FT4, TT4, TgAb, and TPOAb, even after adjusting for relevant confounders.

3.3 Association between the metabolic mixture of pesticides and thyroid function indicators (based on the BKMR model)

We developed a BKMR model based on the NHANES data, to understand the effect of the overall metabolic mixture of pesticides on the indicators of thyroid function. Figure 3 illustrates the effects of the mixture of the five pesticide metabolites 2,4-D, 4F3PB, 3P, PN, and TDDC on thyroid function indexes. The mixture exhibited a negative correlation with FT4, TSH, and Tg and with TgAb and TPOAb after the 60th and 70th percentiles, respectively. All these results were consistent with our clinical data, indicating that the metabolic mixture of the pesticides was negatively correlated with thyroid function indexes.

3.4 Basic participant information in the NHANES 2007–2012

Among the 30,442 participants in the NHANES 2007–2012, 1,315 were eventually included according to our study inclusion and exclusion criteria. Table 3 displays the basic characteristic information of the study participants grouped by age. The age groups of 20–39, 40–59, and ≥ 60 years comprised 437, 430, and 448 individuals, respectively. The mean ± SD of the 3P levels was significantly different across the age groups of 20–39 (1.528 ± 4.145 μg/L), 40–59 (1.617 ± 3.802 μg/L), and ≥ 60 (0.954 ± 2.256 μg/L) years. Similarly, the mean ± SD of the levels of FT3 (20–39 years: 3.341 ± 0.383 pg./mL, 40–59 years: 3.183 ± 0.415 pg./mL, and ≥ 60 years: 2.989 ± 0.35 pg./mL), FT4 (20–39 years: 0.78 ± 0.127 ng/dL, 40–59 years: 0.775 ± 0.165 ng/dL, and ≥ 60 years: 0.813 ± 0.176 ng/dL), TSH (20–39 years: 1.758 ± 1.263 mIU/L, 40–59 years: 2.03 ± 3.11 mIU/L, and ≥ 60 years: 2.445 ± 3.328 mIU/L), TT3 (20–39 years: 118.043 ± 20.982 ng/dL, 40–59 years: 114.286 ± 24.429 ng/dL, and ≥ 60 years: 103.089 ± 20.938 ng/dL), and TgAb (20–39 years: 10.722 ± 9.299 IU/mL, 40–59 years: 8.819 ± 81.876 IU/mL, and ≥ 60 years: 19.664 ± 114.705 IU/mL) were significantly different, with all p-values <0.05. Race, marital status, smoking status, alcohol consumption, and BMI were also significantly different between all age groups, with all p-values <0.05.

Next, we conducted a Spearman correlation analysis to understand the relationship between the metabolites of the different pesticides. Supplementary Figure S1 and Supplementary Table S2 present the correlation coefficients (r) between various metabolites, ranging from 0.033 to 0.504. In particular, the r above 0.5 is 3P and TDDC, which are moderately correlated. Furthermore, 3P and PN

TABLE 1 Baseline characteristics of the clinical patients and controls.

Variables	Total (n = 120)	Health examination control group (n = 60)	Pesticide-exposed patient group (n = 60)	p-value
Gender, n (%)				0.449
Male	44 (36.667)	24 (40)	20 (33.333)	
Female	76 (63.333)	36 (60)	40 (66.667)	
Age, n (%)				0.063
20–39 years	29 (24.167)	20 (33.333)	9 (15)	
40–59 years	38 (31.667)	17 (28.333)	21 (35)	
≥60 years	53 (44.167)	23 (38.333)	30 (50)	
Educational level (%)				0.929
Less than high school	74 (61.667)	38 (63.333)	36 (60)	
High school graduate	17 (14.167)	8 (13.333)	9 (15)	
College or above	29 (24.167)	14 (23.333)	15 (25)	
Marital status (%)				0.81
Never married	21 (17.5)	11 (18.333)	10 (16.667)	
Married	99 (82.5)	49 (81.667)	50 (83.333)	
Smoking status, n (%)				0.338
No	92 (76.667)	44 (73.333)	48 (80)	
Yes	28 (23.333)	16 (26.667)	12 (20)	
Drinking status, n (%)				0.071
No	85 (70.833)	38 (63.333)	47 (78.333)	
Yes	35 (29.167)	22 (36.667)	13 (21.667)	
Thyroid function index				
FT3 (pmol/L)	4.748 ± 4.775	5.397 ± 6.643	4.098 ± 1.004	0.139
FT4 (pmol/L)	19.396 ± 11.94	22.304 ± 16.188	16.488 ± 2.877	**0.008**
TSH (uIU/mL)	2.412 ± 2.702	2.122 ± 2.114	2.703 ± 3.175	0.24
TT3 (nmol/L)	1.809 ± 0.76	1.895 ± 1	1.724 ± 0.388	0.22
TT4 (nmol/L)	114.282 ± 40.984	123.73 ± 52.232	104.834 ± 21.865	**0.012**
TgAb (IU/mL)	47.7 ± 87.151	68.185 ± 119.849	27.214 ± 10.094	**0.011**
TPOAb (IU/mL)	23.37 ± 44.152	32.041 ± 60.602	14.699 ± 10.316	**0.033**

Continuous data are displayed as mean ± standard deviation. Categorical variables are presented as n (%), where n is the number of patients or controls and % is the weighted percentage. $p < 0.05$ was considered statistically significant. Not significant (ns), $p > 0.05$; *, $p < 0.05$; **, $p < 0.01$. The bold type means statistically significant.

exhibited a slight correlation (r = 0.5), while the remaining metabolites had a weak correlation (r < 0.3). Lastly, Pearson's correlation coefficients between all metabolites had p-values of <0.05, except for that between 2,4-D and TDDC.

3.5 Association between pesticide metabolites and thyroid function indicators (based on the linear regression model)

Table 4 shows the association between each pesticide metabolite and thyroid function indicators in the LRM. In model 1 (without adjustment for any confounding factors), 2,4-D and FT3 (p = 0.041) as well as 4F3PB and FT4 (p = 0.003) were positively correlated. Additionally, a negative association was detected between 4F3PB and Tg (p = 0.001), 4F3PB and TgAb (p = 0.006), 3P and TgAb (p = 0.006), 3P and TPOAb (p = 0.03), PN and TSH (p = 0.003), PN and TT4 (p = 0.031), and TDDC and TPOAb (p < 0.001). After correcting for the confounding factors such as age, sex, race, education, marital status, smoking status, and alcohol consumption in model 2, the correlations between 2,4-D and FT3 (p = 0.039) as well as 4F3PB and FT4 (p = 0.005) remained. Moreover, the negative correlations persisted between 4F3PB and Tg (p = 0.027), 4F3PB and TgAb (p = 0.024), 3P and TgAb (p = 0.041), 3P and TPOAb (p = 0.047), PN and FT4 (p = 0.034), PN and TSH (p = 0.011), PN and TT4 (p = 0.049), and TDDC and TPOAb (p = 0.003).

Next, we re-established an LRM to assess the relationship between exposure to pesticide metabolites and thyroid function indicators across different age groups (Supplementary Tables S3–S7). Our results showed that 4F3PB was negatively correlated with Tg (p < 0.001) and TgAb (p = 0.046), while PN demonstrated a negative correlation with TSH (p = 0.001) and TPOAb (p = 0.046) in the 20–39 years age group. In the 40–59 years age group, 4F3PB showed a positive correlation with FT4 (p = 0.024) and negative correlations with TSH (p = 0.001) and TPOAb (p = 0.005). Furthermore, 3P was negatively associated with TSH (p = 0.014), TgAb (p = 0.043), and TPOAb (p < 0.001), whereas PN exhibited a negative correlation with TSH (p = 0.017) and TDDC was negatively correlated with TSH (p = 0.001) and TPOAb (p = 0.001). In the ≥60 years age group, a positive correlation was found between 2,4-D and FT3 (p = 0.039),

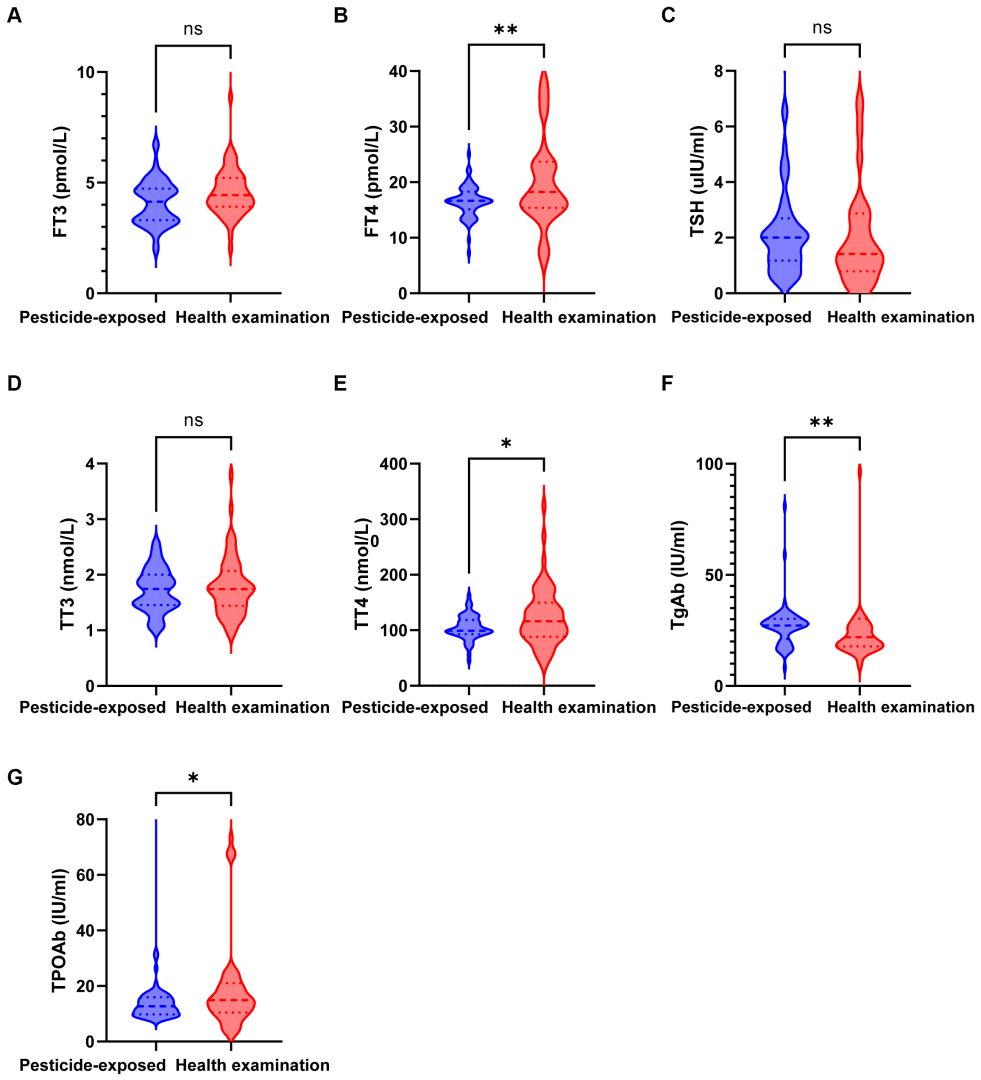

FIGURE 2
Expression levels of thyroid function indicators in the pesticide-exposed and health examination control groups. **(A)** The level of FT3 between the two groups; **(B)** The level of FT4 between the two groups; **(C)** The level of TSH between the two groups; **(D)** The level of TT3 between the two groups; **(E)** The level of TT4 between the two groups; **(F)** The level of TgAb between the two groups; **(G)** The level of TPOAb between the two groups.

while 4F3PB was positively correlated with FT4 ($p < 0.001$) and negatively correlated with FT3 ($p < 0.001$), TT3 ($p < 0.001$), TT4 ($p < 0.001$), Tg ($p < 0.001$), TgAb ($p = 0.004$), and TPOAb ($p < 0.001$). Additionally, whereas negative correlations were demonstrated between PN and TT3 ($p = 0.033$) and TDDC and TPOAb ($p = 0.034$).

3.6 Relationship between pesticide metabolites and thyroid function index (according to the restricted curve spline model)

An RCS model was employed to estimate the dose–response relationship between individual pesticide metabolites and thyroid function indicators (Supplementary Figures S2–S6). In this analysis, 2,4-D was positively correlated with FT3 (Supplementary Figure S2), while 4F3PB exhibited positive correlations with FT4 and TT4 and negative correlations with TT3, Tg, and TPOAb (Supplementary Figure S3). Furthermore, 3P showed positive associations with FT3, FT4, and Tg and negative correlations with TgAb and TPOAb (Supplementary Figure S4), whereas PN demonstrated a negative correlation with TSH and positive correlations with Tg and TgAb (Supplementary Figure S5). Finally, TDDC at <8.731 μg/L was positively correlated with FT4 and Tg and negatively correlated with TSH, whereas TDDC at >8.731 μg/L was positively correlated with TSH (Supplementary Figure S6).

3.7 Relationship between pesticide metabolites and thyroid function index (based on the weighted quantile sum model)

The results of the relationship between the total WQS index and thyroid function indicators as well as the estimated chemical weight of each pesticide metabolite are provided in Figure 4. Based on the fully adjusted model, 2,4-D had the highest weight (0.50) on FT3, followed

TABLE 2 Linear regression analysis of the relationship between pesticide exposure in clinical patients and thyroid function indicators.

Outcome	Model 1		Model 2	
	β (95% CI)	*p*-value	β (95% CI)	*p*-value
FT3	−1.299 (−3.016 to 0.419)	0.137	−1.224 (−3.055 to 0.607)	0.188
FT4	**−5.816 (−10.019 to − 1.613)**	**0.007**	**−6.192 (−10.667 to − 1.718)**	**0.007**
TSH	0.582 (−0.393 to 1.557)	0.24	0.549 (−0.447 to 1.546)	0.277
TT3	−0.171 (−0.4451 to 0.103)	0.219	−0.147 (−0.432 to 0.137)	0.306
TT4	**−18.896 (−33.372 to − 4.420)**	**0.011**	**−20.163 (−35.437 to − 4.889)**	**0.01**
TgAb	**−40.971 (−71.719 to − 10.222)**	**0.009**	**−42.868 (−74.425 to − 11.311)**	**0.008**
TPOAb	**−17.342 (−33.058 to − 1.626)**	**0.031**	**−16.854 (−32.946 to − 0.763)**	**0.04**

Model 1: Non-adjusted model.
Model 2: Adjusted for gender, age, education, marital status, alcohol use, and smoking status.
95% CI, 95% confidence interval. Bold values indicate statistical significance at $p < 0.05$.

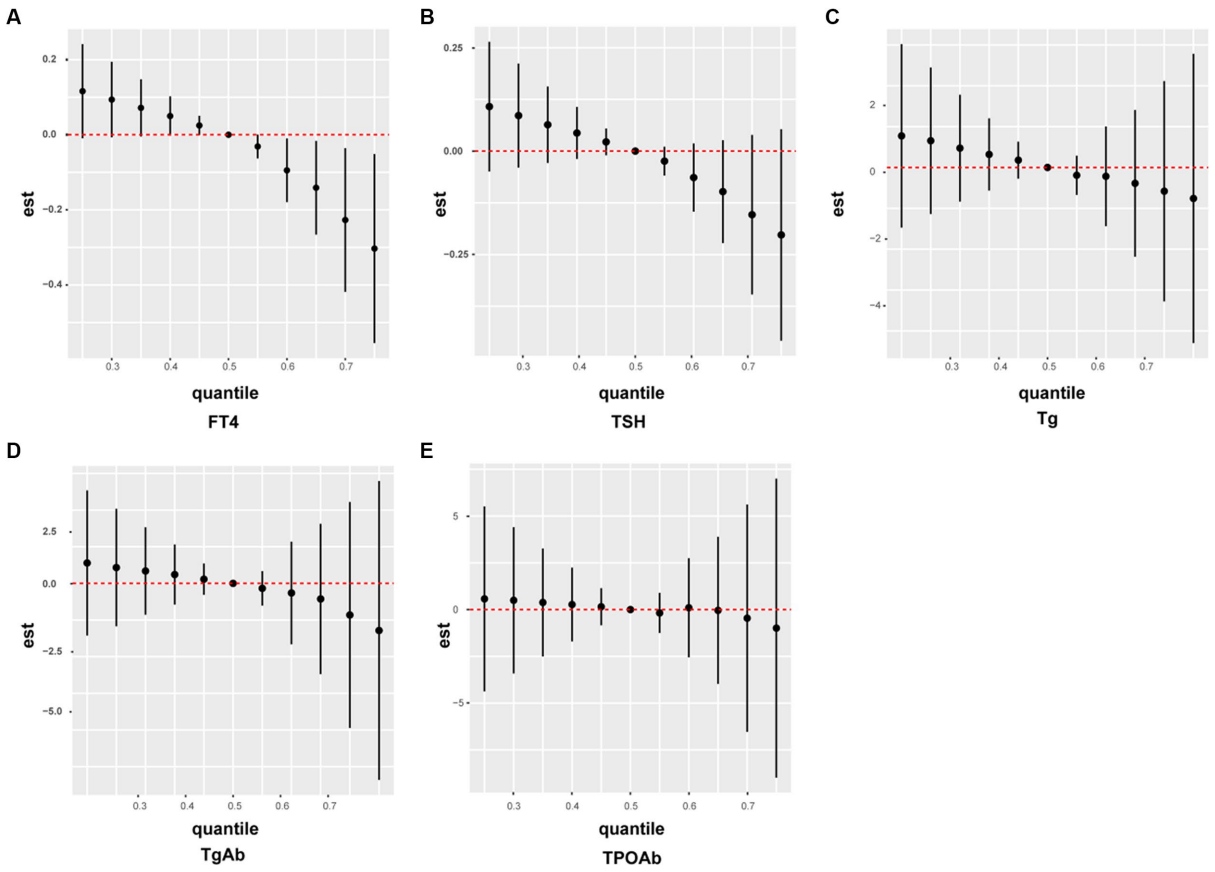

FIGURE 3
A BKMR model to estimate the combined risk effect of the pesticide mixture on thyroid function indicators in the general population. The models were adjusted for gender, age, race, education, marital status, body mass index, smoking status, and alcohol consumption. **(A)** FT4; **(B)** TSH; **(C)** Tg; **(C)** TgAb; **(E)** TPOAb.

by 3P (0.33). Similarly, 4F3PB demonstrated the highest weight on FT4 (0.74); PN on TSH (0.32); 3P on TT3 (0.54); PN on TT4 (0.45); 4F3PB on Tg (0.47); 3P on TgAB (0.45); and 4F3PB on 3P (0.57).

4 Discussion

In this study, we initially revealed that pesticide exposure was negatively correlated with the thyroid function indexes FT4, TT4, TgAb, and TPOAb in patients with pesticide poisoning at our hospital. In a subsequent cross-sectional study of an adult population in the United States (NHANES 2007–2012), BKMR, linear regression, RCS, and WQS models were used to evaluate the individual and combined effects of pesticide metabolites on thyroid function indicators. In terms of the effects of each pesticide metabolite, positive correlations were found between 2,4-D and FT3 and between 4F3PB and FT4. Conversely, we observed a negative correlation of 4F3PB with Tg and TgAb, 3P with TgAb and TPOAb, PN with TSH and TT4, and TDDC with TPOAb.

10.3389/fpubh.2024.1378027

TABLE 3 Weighted characteristics of the NHANES participants from 2007 to 2012 according to age groups.

Variables	Total (*n* = 1,315)	20–39 years (*n* = 437)	40–59 years (*n* = 430)	≥60 years (*n* = 448)	*p*-value
Gender, *n* (%)					0.271
Male	652 (49.582)	217 (49.657)	225 (52.326)	210 (46.875)	
Female	663 (50.418)	220 (50.343)	205 (47.674)	238 (53.125)	
Race, *n* (%)					**0.003**
Mexican American	232 (17.643)	92 (21.053)	81 (18.837)	59 (13.17)	
Other Hispanic	145 (11.027)	45 (10.297)	55 (12.791)	45 (10.045)	
Non-Hispanic White	630 (47.909)	187 (42.792)	192 (44.651)	251 (56.027)	
Non-Hispanic Black	245 (18.631)	87 (19.908)	84 (19.535)	74 (16.518)	
Other races	63 (4.791)	26 (5.95)	18 (4.186)	19 (4.241)	
Educational level (%)					0.337
Below high school	371 (28.213)	121 (27.689)	113 (26.279)	137 (30.58)	
High school	317 (24.106)	99 (22.654)	103 (23.953)	115 (25.67)	
Above high school	627 (47.681)	217 (49.657)	214 (49.767)	196 (43.75)	
Marital status (%)					**<0.001**
Married	236 (17.947)	176 (40.275)	43 (10)	17 (3.795)	
Never married	768 (58.403)	225 (51.487)	282 (65.581)	261 (58.259)	
Widowed/Divorced/ Separated	311 (23.65)	36 (8.238)	105 (24.419)	170 (37.946)	
Smoking status (%)					**<0.001**
Never	685 (52.091)	251 (57.437)	207 (48.14)	227 (50.67)	
Former	317 (24.106)	56 (12.815)	96 (22.326)	165 (36.83)	
Current	313 (23.802)	130 (29.748)	127 (29.535)	56 (12.5)	
Alcohol use (%)					**<0.001**
Non-drinker	221 (16.806)	55 (12.586)	58 (13.488)	108 (24.107)	
Moderate drinker	485 (36.882)	115 (26.316)	153 (35.581)	217 (48.438)	
Heavy drinker	609 (46.312)	267 (61.098)	219 (50.93)	123 (27.455)	
Body mass index (%)					**<0.001**
<25 kg/m^2	381 (28.973)	161 (36.842)	103 (23.953)	117 (26.116)	
25–29.9 kg/m^2	472 (35.894)	147 (33.638)	162 (37.674)	163 (36.384)	
≥30 kg/m^2	462 (35.133)	129 (29.519)	165 (38.372)	168 (37.5)	
Pesticide metabolic compound					
2,4-D (μg/L)	0.595 ± 1.424	0.528 ± 1.04	0.641 ± 2.008	0.616 ± 1.016	0.465
4F3PB (μg/L)	0.088 ± 0.122	0.087 ± 0.097	0.086 ± 0.095	0.092 ± 0.159	0.746
3P (μg/L)	1.361 ± 3.498	1.528 ± 4.145	1.617 ± 3.802	0.954 ± 2.256	**0.009**
PN (μg/L)	1.366 ± 2.736	1.444 ± 2.964	1.268 ± 2.325	1.386 ± 2.868	0.627
TDDC (μg/L)	1.257 ± 3.354	1.154 ± 3.119	1.484 ± 3.728	1.14 ± 3.189	0.233
Thyroid function index					
FT3 (pg/mL)	3.169 ± 0.409	3.341 ± 0.383	3.183 ± 0.415	2.989 ± 0.35	**<0.001**
FT4 (ng/dL)	0.79 ± 0.158	0.78 ± 0.127	0.775 ± 0.165	0.813 ± 0.176	**<0.001**
TSH (mIU/L)	2.081 ± 2.745	1.758 ± 1.263	2.03 ± 3.11	2.445 ± 3.328	**<0.001**
TT3 (ng/dL)	111.72 ± 23.042	118.043 ± 20.982	114.286 ± 24.429	103.089 ± 20.938	**<0.001**
TT4 (μg/dL)	7.862 ± 1.672	7.803 ± 1.656	7.764 ± 1.676	8.014 ± 1.677	0.057
Tg (ng/mL)	16.333 ± 35.266	15.315 ± 31.046	14.103 ± 19.414	19.467 ± 48.357	0.06
TgAb (IU/mL)	10.155 ± 82.148	10.722 ± 9.299	8.819 ± 81.876	19.664 ± 114.705	**0.005**
TPOAb (IU/mL)	19 ± 87.976	14.167 ± 79.862	25.638 ± 108.061	17.345 ± 72.499	0.14

Continuous data are displayed as mean ± standard deviation. Categorical variables are presented as *n* (%), where *n* is the number of participants and % is the weighted percentage. $p < 0.05$ was considered statistically significant. The bold type means statistically significant.

10.3389/fpubh.2024.1378027

TABLE 4 Weighted linear regression analysis of the relationship between pesticide exposure and thyroid function indexes in the NHANES participants from 2007 to 2012.

Exposure outcome		Model 1		Model 2	
		β (95% CI)	*p*-value	β (95% CI)	*p*-value
2,4-D					
	FT3	**0.017 (0.00–10.033)**	**0.041**	**0.019 (0.001–0.038)**	**0.039**
	FT4	0.002 (−0.005 to 0.010)	0.536	0.002 (−0.005 to 0.009)	0.525
	TSH	0.109 (−0.166 to 0.383)	0.438	0.109 (−0.162 to 0.380)	0.43
	TT3	0.431 (−0.408 to 1.270)	0.313	0.457 (−0.354 to 1.267)	0.269
	TT4	−0.029 (−0.118 to 0.061)	0.53	−0.006 (−0.088 to 0.076)	0.892
	Tg	−0.081 (−0.834 to 0.672)	0.833	0.210 (−0.546 to 0.966)	0.586
	TgAb	0.621 (−0.998 to 2.240)	0.452	0.488 (−1.137 to 2.113)	0.556
	TPOAb	1.141 (−2.272 to 4.554)	0.512	2.012 (−1.361 to 5.384)	0.242
4F3PB					
	FT3	−0.142 (−0.361 to 0.078)	0.205	−0.108 (−0.289 to 0.0742)	0.246
	FT4	**0.112 (0.038–0.187)**	**0.003**	**0.107 (0.033–0.182)**	**0.005**
	TSH	−0.077 (−1.054 to 0.900)	0.878	−0.052 (−1.012 to 0.907)	0.914
	TT3	−8.388 (−17.922 to 1.147)	0.085	−6.320 (−14.120 to 1.481)	0.112
	TT4	0.699 (−0.046 to 1.443)	0.066	0.718 (−0.019 to 1.455)	0.056
	Tg	**−9.226 (−14.84 to −3.611)**	**0.001**	**−7.173 (−13.532 to −0.813)**	**0.027**
	TgAb	**−7.835 (−13.383 to −2.287)**	**0.006**	**−8.765 (−16.399 to −1.130)**	**0.024**
	TPOAb	−9.749 (−37.648 to 18.149)	0.493	−10.683 (−36.069 to 14.704)	0.409
3P					
	FT3	0.002 (−0.005 to 0.009)	0.49	−0.001 (−0.007 to 0.005)	0.795
	FT4	0.001 (−0.001 to 0.004)	0.331	0.002 (−0.001 to 0.004)	0.192
	TSH	−0.020 (−0.0407 to 0.001)	0.059	−0.017 (−0.039 to 0.004)	0.111
	TT3	−0.081 (−0.517 to 0.354)	0.714	−0.186 (−0.595 to 0.223)	0.373
	TT4	−0.003 (−0.035 to 0.030)	0.868	0.003 (−0.023 to 0.029)	0.804
	Tg	0.577 (−0.343 to 1.498)	0.219	0.618 (−0.278 to 1.515)	0.176
	TgAb	**−0.368 (−0.632 to − 0.104)**	**0.006**	**−0.282 (−0.553 to − 0.011)**	**0.041**
	TPOAb	**−0.783 (−1.492 to − 0.075)**	**0.03**	**−0.795 (−1.579 to − 0.011)**	**0.047**
PN					
	FT3	−0.005 (−0.018 to 0.009)	0.488	−0.006 (−0.018 to 0.007)	0.38
	FT4	−0.002 (−0.005 to 0.001)	0.099	−0.003 (−0.005 to − 0.001)	0.034
	TSH	**−0.044 (−0.073 to − 0.016)**	**0.003**	**−0.035 (−0.061 to − 0.008)**	**0.011**
	TT3	−0.387 (−0.883 to 0.108)	0.126	−0.270 (−0.739 to 0.199)	0.259
	TT4	**−0.042 (−0.080 to − 0.004)**	**0.031**	**−0.042 (−0.086 to − 0.001)**	**0.049**
	Tg	0.299 (−0.313 to 0.913)	0.337	0.329 (−0.273 to 0.932)	0.284
	TgAb	1.085 (−1.327 to 3.498)	0.378	1.076 (−1.400 to 3.552)	0.394
	TPOAb	−0.715 (−1.748 to 0.317)	0.174	−0.302 (−1.458 to 0.854)	0.609
TDDC					
	FT3	0.001 (−0.006 to 0.007)	0.801	0.001 (−0.004 to 0.006)	0.732
	FT4	0.001 (−0.001 to 0.004)	0.278	0.001 (−0.001 to 0.003)	0.339
	TSH	−0.020 (−0.049 to 0.008)	0.154	−0.022 (−0.052 to 0.008)	0.15
	TT3	−0.127 (−0.519 to 0.265)	0.525	−0.079 (−0.474 to 0.317)	0.696
	TT4	0.001 (−0.026 to 0.027)	0.971	0.001 (−0.022 to 0.023)	0.95

(Continued)

TABLE 4 (Continued)

Exposure outcome		Model 1		Model 2	
		β (95% CI)	*p*-value	β (95% CI)	*p*-value
	Tg	0.770 (−0.603 to 2.143)	0.271	0.748 (−0.607 to 2.104)	0.279
	TgAb	−0.151 (−0.886 to 0.584)	0.686	−0.117 (−0.900 to 0.665)	0.769
	TPOAb	**−1.370 (−2.080 to −0.660)**	**<0.001**	**−1.228 (−2.037 to −0.420)**	**0.003**

Model 1: Non-adjusted model.
Model 2: Gender, age, race, education, marital status, body mass index, alcohol use, and smoking status. 95% CI, 95% confidence interval. Bold values indicate statistical significance at $p < 0.05$.

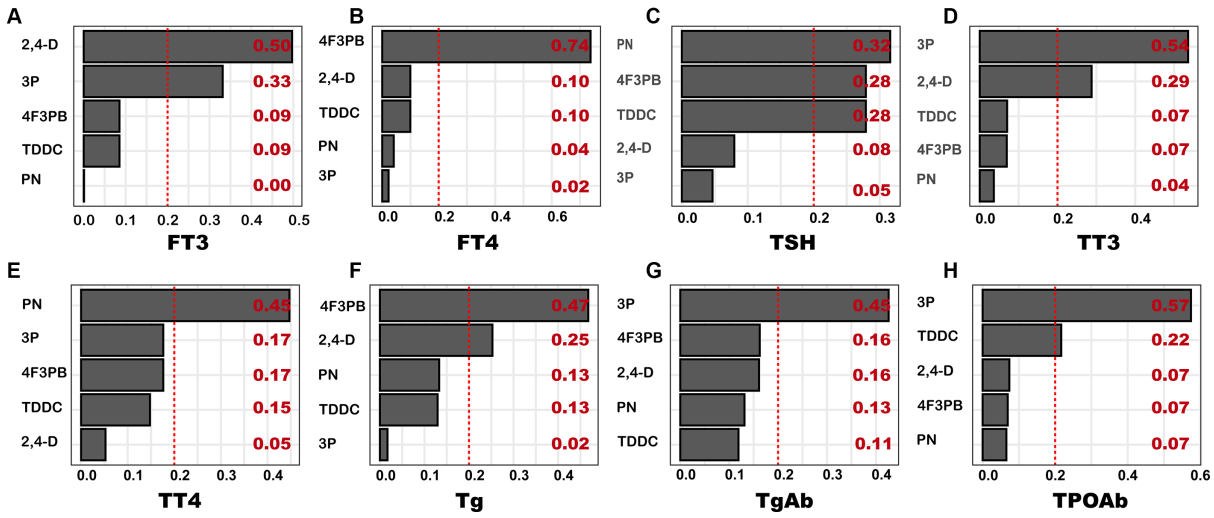

FIGURE 4
WQS-based weights of pesticide metabolites on thyroid function index. The model was adjusted for covariates, including age, sex, race, marital status, education, body mass index, smoking status, and alcohol consumption. **(A)** FT3; **(B)** FT4; **(C)** TSH; **(D)** TT3; **(E)** TT4; **(F)** Tg; **(G)** TgAb; **(H)** TPOAb.

In the case of multi-metabolic compounds, the BKMR model showed that the metabolic mixture of the different pesticides was negatively correlated with FT4, TSH, and Tg as well as with TgAB after the 60th percentile and TPOAb after the 70th percentile, consistent with the clinical data results of the patients in our hospital.

2,4-D is an extensively used herbicide, particularly in the United States and Canada. However, increasing concerns have been raised over its endocrine effects. Moreover, other studies have demonstrated that 2,4-D is an endocrine disruptor that may affect thyroid hormones in male but not in female rodents (8, 9). Similar sex-dependent findings were observed in humans, wherein a significant association was demonstrated between 2,4-D pesticide exposure and hypothyroidism in males, but no such association was detected in females (7). In our study, 2,4-D was positively correlated with FT3 in the general population, which persisted in the age group of ≥60 years. However, no other significant correlation was determined for the remaining thyroid function indicators, consistent with the US EPA findings. Nevertheless, the RCS dose–response curve revealed that thyroid function was affected at a 2,4-D dose exceeding a specific range, highlighting that the effect of the herbicide 2,4-D on the human body must not be overlooked.

In this study, we also analyzed the effects of the OP metabolites PN and TDDC on thyroid function indicators. TDDC is primarily a metabolite of dichlorphos, while PN is a metabolite of many OPs, including parathion and methyl parathion. Research has found that OPs can cause thyroid changes by affecting thyroid hormone regulation at the central nervous system level. In this mechanism, organophosphorus exposure leads to cholinergic overstimulation that further results in somatostatin activation, ultimately inhibiting TSH release (21). A cross-sectional study of adults and children in the United States found that the urinary organophosphorus metabolite 3,5,6-trichloro-2-pyridinol was positively correlated with serum total T4 and negatively associated with TSH in adolescents and adult males (22). Additionally, a rodent model investigation demonstrated that OP exposure could induce changes in thyroid hormone levels; however, the trends in the specific thyroid hormone levels were inconsistent. In particular, rodents that received oral doses of organophosphorus malathion exhibited reduced serum T4 and T3 levels and increased TSH concentrations compared with the mouse pups exposed to OPs *in utero* and postnatally (23). The above results are partially inconsistent with our current study findings, where we observed negative correlations of the OP metabolite PN with TSH and TT4 and that of TDDC with TPOAb. This discrepancy could be because different OP metabolites exert distinct effects on the thyroid gland. Moreover, the different results from the animal model study could be attributed to the variation in the metabolic pathways, species' acceptance thresholds for OPs, or thyroid gland effects occurring during various developmental stages.

Additionally, we investigated the effects of the pyrethroid metabolites 3P and 4F3PB, which are more toxic than the mother compounds. The metabolites 3P and 4F3PB are among the most detectable substances in human urine and blood as well as animal

tissues and thus are commonly used as biomarkers to assess pyrethroid exposure in humans (24–26). Studies on pyrethroid exposure in lizards have found that these pesticides and their metabolites 3P and 4F3PB have unique endocrine-disrupting mechanisms that can impair the thyroid system. Although metabolite exposure did not lead to any significant or slightly significant changes in the thyroid gland or thyroid hormone levels, significant alterations were observed in the expression of the thyroid axis-related genes in the liver and brain of the lizards (27). Several researchers have indicated that 3P has no significant effect on the human thyroid hormone (28), corroborating our current study results. However, apart from thyroid hormone examination, our study also assessed thyroid antibody and antibody protein levels. We demonstrated that although 3P was not significantly correlated with the thyroid hormone, it was negatively correlated with TgAb and TPOAb. Moreover, scarce research exists on the impact of pesticide exposure on these two indicators. Currently, relatively limited information is available on the effects of 4F3PB on thyroid function. The present study showed that 4F3PB was positively correlated with FT4 but negatively correlated with Tg and TgAB. All these thyroid function changes induced by pyrethroids and their metabolites may be ascribed to their structural similarity with the thyroid hormone receptors.

The previously mentioned findings represent individual analyses of the effects of each pesticide and its metabolites on thyroid function indicators. However, pesticide absorption by the human body does not encompass a single pesticide and generally involves two or more types of pesticides. Thus, we further analyzed the effects of pesticide mixtures on thyroid function indicators. A previous comparison study of the toxicity of four organophosphate pesticides (dichlorvos, dimethoate, acephate, and methamidophos) with that of a single pesticide in rats demonstrated that the toxicity of a single pesticide was weak or even non-toxic, but the combination of the four pesticides caused oxidative stress and liver and kidney dysfunction, disrupted lipid and amino acid metabolism, and interfered with thyroid function (29). This study analyzed the effects of OP, herbicide and pyrethroid mixtures on thyroid function in clinical patients in Binhai County People's Hospital. The analyses revealed that the pesticide mixtures were negatively correlated with the thyroid function indicators FT4, TT4, TgAb, and TPOAb. Subsequently, in order to further validate the above findings, the effect of this pesticide mixture on thyroid function indicators was investigated in the NHANES database in the United States. The results showed that based on the BKMR model, the mixture was negatively correlated with FT4, TSH, Tg, and after the 60th percentile with TgAb and after the 70th percentile with TPOAb. These results were generally consistent with the clinical patient data from Binhai County People's Hospital. Next, the weight of the effect of each metabolite in the pesticide mixture on thyroid function indicators was analyzed by the WQS model. Through the above findings, it was speculated that the alteration of thyroid function indicators might be caused by various thyroid damage mechanisms corresponding to each pesticide metabolite. However, the process by which these pesticides interact and cause thyroid damage is not known, and this area was not evaluated in our study. Nevertheless, this aspect is the direction of our future research. Despite these gaps in the literature, various pesticide mixtures have been established to cause damage to the thyroid gland. Thus, the potential harm from pesticide exposure during daily life, consumption of fruits and vegetables, and engagement in agricultural activities should not be disregarded, emphasizing the need to follow protective measures to reduce the health consequences on the human body.

Our study has several advantages that are worth mentioning. We used clinical data to analyze the relationship between patients with pesticide poisoning and thyroid function, along with the NHANES data for further evaluation. Moreover, the current study represents the first attempt to elucidate the link between herbicides, OPs, and pyrethroids (alone and combined) and thyroid function in United States adults. The study results indicated a potential relationship between these pesticides and thyroid function, suggesting the requirement for further mechanistic studies to explore the underlying physiological mechanisms. Another advantage is that we constructed WQS and BKMR models to examine the overall effects of the mixture of herbicides, OPs, and pyrethroids on thyroid function, followed by linear regression and RCS to determine the effects of each pesticide metabolite on thyroid function. These statistical strategies showed the frequency with which people were simultaneously exposed to multiple pesticides in real life. Additionally, combining the advantages and disadvantages of various pesticide approaches might help us better understand their mixed effects, ultimately enabling us to obtain more reliable conclusions and provide valuable scientific information on appropriate pesticide utilization. However, our study has certain limitations that should be acknowledged. The main limitation of this study is that a causal relationship between pesticides and thyroid function could not be confirmed due to the cross-sectional research design. Additionally, herbicides, OPs, and pyrethroids have shorter half-lives that range from a few hours to weeks; thus, the correlation of long-term exposure cannot be determined. Finally, the confounding effects of unmeasured factors cannot be ruled out from the study, even though adjustments were made for some thyroid function-related risk factors.

5 Conclusion

In this study, firstly, pesticides were found to be significantly negatively correlated with thyroid function indicators by analysing the data in the clinical patients in Binhai County People's Hospital, and similarly, pesticide metabolites were found to have a significant difference on the thyroid function indicators in the NHANES database in the United States. Subsequently, through different statistical methods, it was found that there were significant differences in the effects of different metabolite weights on different thyroid function indicators. We initially discussed the effects of various pesticide metabolites on thyroid function indicators. At a later stage, we need to confirm our main findings with a large number of samples, further explore their effects on each thyroid disease, and elucidate the potential mechanisms between various pesticides and thyroid diseases.

Data availability statement

The datasets presented in this study can be found in online repositories. The names of the repository/repositories and accession number(s) can be found at: https://wwwn.cdc.gov/nchs/nhanes/Default.aspx.

Ethics statement

The studies involving humans were approved by Binhai County People's Hospital. The studies were conducted in accordance with the local legislation and institutional requirements. The human samples used in this study were acquired from primarily isolated as part of your previous study for which ethical approval was obtained. Written informed consent for participation was not required from the participants or the participants' legal guardians/next of kin in accordance with the national legislation and institutional requirements.

Author contributions

LX: Conceptualization, Formal analysis, Methodology, Supervision, Writing – review & editing. SY: Data curation, Resources, Software, Writing – review & editing. LW: Project administration, Supervision, Writing – review & editing. JQ: Investigation, Project administration, Supervision, Writing – review & editing. HM: Project administration, Supervision, Writing – review & editing. LZ: Project administration, Supervision, Writing – review & editing. WS: Data curation, Software, Supervision, Validation, Writing – review & editing. AH: Conceptualization, Data curation, Investigation, Methodology, Resources, Software, Supervision, Validation, Visualization, Writing – original draft, Writing – review & editing.

Funding

The author(s) declare financial support was received for the research, authorship, and/or publication of this article. This work was supported by Scientific Research Project of Yancheng Health Commission (YK2023103).

Acknowledgments

The authors thank the National Health and Nutrition Examination Survey created by the United States for providing publicly available data.

Conflict of interest

The authors declare that the research was conducted in the absence of any commercial or financial relationships that could be construed as a potential conflict of interest.

Publisher's note

All claims expressed in this article are solely those of the authors and do not necessarily represent those of their affiliated organizations, or those of the publisher, the editors and the reviewers. Any product that may be evaluated in this article, or claim that may be made by its manufacturer, is not guaranteed or endorsed by the publisher.

Supplementary material

The Supplementary material for this article can be found online at: https://www.frontiersin.org/articles/10.3389/fpubh.2024.1378027/full#supplementary-material

References

1. Axelstad M, Boberg J, Nellemann C, Kiersgaard M, Jacobsen PR, Christiansen S, et al. Exposure to the widely used fungicide mancozeb causes thyroid hormone disruption in rat dams but no behavioral effects in the offspring. *Toxicol Sci*. (2011) 120:439–46. doi: 10.1093/toxsci/kfr006

2. Maranghi F, De Angelis S, Tassinari R, Chiarotti F, Lorenzetti S, Moracci G, et al. Reproductive toxicity and thyroid effects in Sprague Dawley rats exposed to low doses of ethylenethiourea. *Food Chem Toxicol*. (2013) 59:261–71. doi: 10.1016/j.fct.2013.05.048

3. Panganiban L, Cortes-Maramba N, Dioquino C, Suplido ML, Ho H, Francisco-Rivera A, et al. Correlation between blood ethylenethiourea and thyroid gland disorders among banana plantation workers in the Philippines. *Environ Health Perspect*. (2004) 112:42–5. doi: 10.1289/ehp.6499

4. Du G, Shen O, Sun H, Fei J, Lu C, Song L, et al. Assessing hormone receptor activities of pyrethroid insecticides and their metabolites in reporter gene assays. *Toxicol Sci*. (2010) 116:58–66. doi: 10.1093/toxsci/kfq120

5. Zúñiga-Venegas LA, Hyland C, Muñoz-Quezada MT, Quirós-Alcalá L, Butinof M, Buralli R, et al. Erratum: "Health effects of pesticide exposure in Latin American and the Caribbean populations: a scoping review". *Environ Health Perspect*. (2022) 131:89001. doi: 10.1289/EHP13645

6. Shrestha S, Parks CG, Goldner WS, Kamel F, Umbach DM, Ward MH, et al. Pesticide use and incident hypothyroidism in pesticide applicators in the agricultural health study. *Environ Health Perspect*. (2018) 126:97008. doi: 10.1289/EHP3194

7. Goldner WS, Sandler DP, Yu F, Hoppin JA, Kamel F, Levan TD. Pesticide use and thyroid disease among women in the agricultural health study. *Am J Epidemiol*. (2010) 171:455–64. doi: 10.1093/aje/kwp404

8. Marty MS, Neal BH, Zablotny CL, Yano BL, Andrus AK, Woolhiser MR, et al. An F1-extended one-generation reproductive toxicity study in Crl:CD(SD) rats with 2,4-dichlorophenoxyacetic acid. *Toxicol Sci*. (2013) 136:527–47. doi: 10.1093/toxsci/kft213

9. Lacasaña M, López-Flores I, Rodríguez-Barranco M, Aguilar-Garduño C, Blanco-Muñoz J, Pérez-Méndez O, et al. Association between organophosphate pesticides exposure and thyroid hormones in floriculture workers. *Toxicol Appl Pharmacol*. (2010) 243:19–26. doi: 10.1016/j.taap.2009.11.008

10. Campos É, Freire C. Exposure to non-persistent pesticides and thyroid function: a systematic review of epidemiological evidence. *Int J Hyg Environ Health*. (2016) 219:481–97. doi: 10.1016/j.ijheh.2016.05.006

11. Anadón A, Martínez-Larrañaga MR, Martínez MA. Use and abuse of pyrethrins and synthetic pyrethroids in veterinary medicine. *Vet J*. (2009) 182:7–20. doi: 10.1016/j.tvjl.2008.04.008

12. Crofton KM. Thyroid disrupting chemicals: mechanisms and mixtures. *Int J Androl*. (2008) 31:209–23. doi: 10.1111/j.1365-2605.2007.00857.x

13. Xu C, Li X, Jin M, Sun X, Niu L, Lin C, et al. Early life exposure of zebrafish (*Danio rerio*) to synthetic pyrethroids and their metabolites: a comparison of phenotypic and behavioral indicators and gene expression involved in the HPT axis and innate immune system. *Environ Sci Pollut Res Int*. (2018) 25:12992–3003. doi: 10.1007/s11356-018-1542-0

14. Bravo R, Caltabiano LM, Weerasekera G, Whitehead RD, Fernandez C, Needham LL, et al. Measurement of dialkyl phosphate metabolites of organophosphorus pesticides in human urine using lyophilization with gas chromatography-tandem mass spectrometry and isotope dilution quantification. *J Expo Anal Environ Epidemiol*. (2004) 14:249–59. doi: 10.1038/sj.jea.7500322

15. Jayatilaka NK, Restrepo P, Williams L, Ospina M, Valentin-Blasini L, Calafat AM. Quantification of three chlorinated dialkyl phosphates, diphenyl phosphate, 2,3,4,5-tetrabromobenzoic acid, and four other organophosphates in human urine by solid phase extraction-high performance liquid chromatography-tandem mass spectrometry. *Anal Bioanal Chem*. (2017) 409:1323–32. doi: 10.1007/s00216-016-0061-4

16. Bobb JF, Claus Henn B, Valeri L, Coull BA. Statistical software for analyzing the health effects of multiple concurrent exposures via Bayesian kernel machine regression. *Environ Health*. (2018) 17:67. doi: 10.1186/s12940-018-0413-y

17. Bobb JF, Valeri L, Claus Henn B, Christiani DC, Wright RO, Mazumdar M, et al. Bayesian kernel machine regression for estimating the health effects of multi-pollutant mixtures. *Biostatistics*. (2015) 16:493–508. doi: 10.1093/biostatistics/kxu058

18. Keil AP, Buckley JP, O'Brien KM, Ferguson KK, Zhao S, White AJ. A quantile-based g-computation approach to addressing the effects of exposure mixtures. *Environ Health Perspect*. (2020) 128:47004. doi: 10.1289/EHP5838

19. Coady K, Marino T, Thomas J, Sosinski L, Neal B, Hammond L. An evaluation of 2,4-dichlorophenoxyacetic acid in the amphibian metamorphosis assay and the fish short-term reproduction assay. *Ecotoxicol Environ Saf*. (2013) 90:143–50. doi: 10.1016/j.ecoenv.2012.12.025

20. Coady KK, Kan HL, Schisler MR, Gollapudi BB, Neal B, Williams A, et al. Evaluation of potential endocrine activity of 2,4-dichlorophenoxyacetic acid using in vitro assays. *Toxicol In Vitro*. (2014) 28:1018–25. doi: 10.1016/j.tiv.2014.04.006

21. Phillips S, Suarez-Torres J, Checkoway H, Lopez-Paredes D, Gahagan S, Suarez-Lopez JR. Acetylcholinesterase activity and thyroid hormone levels in Ecuadorian adolescents living in agricultural settings where organophosphate pesticides are used. *Int J Hyg Environ Health*. (2021) 233:113691. doi: 10.1016/j.ijheh.2021.113691

22. Fortenberry GZ, Hu H, Turyk M, Barr DB, Meeker JD. Association between urinary 3, 5, 6-trichloro-2-pyridinol, a metabolite of chlorpyrifos and chlorpyrifos-methyl, and serum T4 and TSH in NHANES 1999-2002. *Sci Total Environ*. (2012) 424:351–5. doi: 10.1016/j.scitotenv.2012.02.039

23. Jeong SH, Kim BY, Kang HG, Ku HO, Cho JH. Effect of chlorpyrifos-methyl on steroid and thyroid hormones in rat F0- and F1-generations. *Toxicology*. (2006) 220:189–202. doi: 10.1016/j.tox.2006.01.005

24. Barr DB, Olsson AO, Wong LY, Udunka S, Baker SE, Whitehead RD, et al. Urinary concentrations of metabolites of pyrethroid insecticides in the general U.S. population: National Health and nutrition examination survey 1999–2002. *Environ Health Perspect*. (2010) 118:742–8. doi: 10.1289/ehp.0901275

25. Hwang M, Lee Y, Choi K, Park C. Urinary 3-phenoxybenzoic acid levels and the association with thyroid hormones in adults: Korean National Environmental Health Survey 2012–2014. *Sci Total Environ*. (2019) 696:133920. doi: 10.1016/j.scitotenv.2019.133920

26. Ratelle M, Coté J, Bouchard M. Time profiles and toxicokinetic parameters of key biomarkers of exposure to cypermethrin in orally exposed volunteers compared with previously available kinetic data following permethrin exposure. *J Appl Toxicol*. (2015) 35:1586–93. doi: 10.1002/jat.3124

27. Chang J, Pan Y, Liu W, Xu P, Li W, Wan B. Lambda-cyhalothrin and its common metabolite differentially modulate thyroid disruption effects in Chinese lizards (Eremias argus). *Environ Pollut*. (2021) 287:117322. doi: 10.1016/j.envpol.2021.117322

28. Jain RB. Variability in the levels of 3-phenoxybenzoic acid by age, gender, and race/ethnicity for the period of 2001–2002 versus 2009–2010 and its association with thyroid function among general US population. *Environ Sci Pollut Res Int*. (2016) 23:6934–9. doi: 10.1007/s11356-015-5954-9

29. Du L, Li S, Qi L, Hou Y, Zeng Y, Xu W, et al. Metabonomic analysis of the joint toxic action of long-term low-level exposure to a mixture of four organophosphate pesticides in rat plasma. *Mol BioSyst*. (2014) 10:1153–61. doi: 10.1039/C4MB00044G

frontiers | Frontiers in Public Health

TYPE Perspective
PUBLISHED 28 June 2024
DOI 10.3389/fpubh.2024.1408222

OPEN ACCESS

EDITED BY
Pu Xia,
University of Birmingham, United Kingdom

REVIEWED BY
Christina Maria Socias-Morales,
Centers for Disease Control and Prevention (CDC), United States

*CORRESPONDENCE
Immanuel B. H. Samuel
✉ Immanuel.Samuel@va.gov

RECEIVED 27 March 2024
ACCEPTED 21 May 2024
PUBLISHED 28 June 2024

CITATION
Samuel IBH, Pollin K, Tschida S, Prisco MK, Lu C, Powell A, Mefford J, Lee J, Dupriest T, Forsten R, Ortiz J, Barrett J, Reinhard M and Costanzo M (2024) Linked Exposures Across Databases: an exposure common data elements aggregation framework to facilitate clinical exposure review.
Front. Public Health 12:1408222.
doi: 10.3389/fpubh.2024.1408222

Linked Exposures Across Databases: an exposure common data elements aggregation framework to facilitate clinical exposure review

Immanuel B. H. Samuel[1,2,3]*, Kamila Pollin[2], Sherri Tschida[2,3], Michelle Kennedy Prisco[2], Calvin Lu[1,2,3], Alan Powell[4], Jessica Mefford[4], Jamie Lee[4], Teresa Dupriest[4], Robert Forsten[2,3,5], Jose Ortiz[2,3], John Barrett[2,3,6], Matthew Reinhard[2,3,7] and Michelle Costanzo[2,3,6]

[1]The Henry M. Jackson Foundation for the Advancement of Military Medicine Inc., Bethesda, MD, United States, [2]The War Related Illness and Injury Study Center, Washington, DC, United States, [3]Complex Exposure Threats Center, Department of Veterans Affairs, Washington, DC, United States, [4]Explosive Ordnance Disposal Information Management System (EODIMS), Air Force Civil Engineer Center, Functional Management Office (FMO) (AFCEC/CBS), Joint Base San Antonio, San Antonio, TX, United States, [5]Department of Psychiatry, Uniformed Services University, Bethesda, MD, United States, [6]Department of Medicine, Uniformed Services University, Bethesda, MD, United States, [7]Georgetown University Medical School, Washington, DC, United States

Understanding the health outcomes of military exposures is of critical importance for Veterans, their health care team, and national leaders. Approximately 43% of Veterans report military exposure concerns to their VA providers. Understanding the causal influences of environmental exposures on health is a complex exposure science task and often requires interpreting multiple data sources; particularly when exposure pathways and multi-exposure interactions are ill-defined, as is the case for complex and emerging military service exposures. Thus, there is a need to standardize clinically meaningful exposure metrics from different data sources to guide clinicians and researchers with a consistent model for investigating and communicating exposure risk profiles. The Linked Exposures Across Databases (LEAD) framework provides a unifying model for characterizing exposures from different exposure databases with a focus on providing clinically relevant exposure metrics. Application of LEAD is demonstrated through comparison of different military exposure data sources: Veteran Military Occupational and Environmental Exposure Assessment Tool (VMOAT), Individual Longitudinal Exposure Record (ILER) database, and a military incident report database, the Explosive Ordnance Disposal Information Management System (EODIMS). This cohesive method for evaluating military exposures leverages established information with new sources of data and has the potential to influence how military exposure data is integrated into exposure health care and investigational models.

KEYWORDS

military exposures, data aggregation, exposure model, dose, exposure common data elements

Introduction

The health implications of military exposures are a major concern for clinicians and researchers in the field of Veteran healthcare, with 43% of Veterans expressing toxic exposure concerns to their Veterans Affairs (VA) healthcare providers (1). The recent passing of the PACT Act in 2022 expanded VA care and benefits while increasing presumptive health conditions for various military deployments and exposures. This surge in interest for military toxic exposures necessitates the integration of appropriate data to support investigations between exposures and health outcomes. Capturing the exposome, which measures the multifaceted relationships between environment, behavior, biology, and disease over time, is essential to this understanding (2) as exposures do not cease after military service. Utilizing an exposome model to understand military toxic exposures is crucial because it considers the totality of environmental influences on individuals across their lifetime (3). Similar needs are present in environmental health surveillance programs when integrating existing data. Recently, the United Kingdom completed pilot programs for data integration in communities with high-quality exposure data and paired this data with outcomes in their National Health System (4, 5). Also, current needs demand an expanded Environmental and Public Health Tracking (EPHT) system to emphasize the need of merging, integrating and interpreting exposure data and relating to health outcomes (6, 7). The proposed LEAD framework aims to support efforts to facilitate a unified exposure tracking methodology and help to further understand the exposome.

Linked Exposures Across Databases (LEAD) framework

The LEAD framework unifies diverse exposure sources using common data elements, addressing gaps in sourcing and characterization. Focusing on clinical utility, it develops health applications for siloed sources like military records and incident reports. The LEAD method calculates total exposure dosage as a function of intensity and duration. This method of dosage estimation is used across fields such as radiation exposure capture (8), toxicity research (9) and the military to calculate blast over-pressure as the product of pressure over a set period (10, 11). However, such applications typically focus on specific exposures. LEAD's methodology employs general definitions of Exposure Common Data Elements (ExCDE), enabling comprehensive exposure characterization across various sources while utilizing existing methods and shaping new approaches. This integration facilitates the translation of individual and population-level exposure data for clinical purposes and fosters toxic exposure surveillance and research applications.

While quantitative measures of exposure intensity (e.g., Pascals for blast pressure, micrograms for chemical exposure) and time of exposure (measured in seconds) using sensors are the most objective and quantifiable form of measurement, such information is rarely available at the individual level for Veterans concerned about toxic military exposures. Therefore, the LEAD framework aims to expand the application of intensity and time-based dosage estimation to large sets of qualitative and subjective data. Additionally, potential moderating factors such as protective controls are considered since these factors could moderate exposure-related outcomes.

LEAD characterizes exposure using the following exposure common data elementsExCDEs:

$$Exposure\ Dose \sim f\left(\text{Intensity} \times \text{Time} \mid \text{Moderators}\right)$$

$$Intensity \sim f\left(\text{Route}, \text{Proximity}, \text{Symptoms}\right)$$

$$Time \sim f\left(\text{Duration}, \text{Frequency}, \text{Period}\right)$$

$$Moderators \sim f\left(\text{Environmental Controls}, \text{Personal Protective Controls}\right)$$

The LEAD framework allows for estimating aggregate exposure dosages using proxy measures of intensity and duration, along with factors that may influence these effects (Figure 1). The goal of the LEAD framework is to establish consistent parameters for characterizing exposures. However, like clinical practice where some features hold more weight due to their perceived impact on outcomes, the exposure variables also need to be weighted when evaluating exposure dose. This report provides expert-informed weights for specific variables, demonstrating a practical example of exposure dose estimation. Future analysis with health outcomes data can employ risk-modeling methods (e.g., Cox-Proportion Hazards Model) to assign empirical weights.

To illustrate how the LEAD framework can be used to consolidate exposure data into a unifiable metric, this report will present information from three different exposure data sources relevant to a cohort of Explosive Ordnance Disposal (EOD) Veterans, a complex and very high environmental exposure military occupation. We provide sample data extraction of exposure information from multiple databases and their collation in Table 1. Further, examples of how the data can be used to compare high and low blast exposure using a common scoring methodology is provided in Supplementary Tables S1–S3.

Data sources include:

- Explosive Ordnance Disposal Information Management System (EODIMS): The EODIMS System is an operations specific Classified and Unclassified program for record incident reporting with discoverable data managed by the Air Force supporting joint service EOD units. Focused use of these records for clinically relevant exposure data enables access to the immediate post-exposure reports that are less affected by recall bias and may represent direct evidence of a possible hazardous exposure.
- Veteran Military Occupational and Environmental Exposure Assessment Tool (VMOAT): The VMOAT is a self-reported, structured, and lifespan-based comprehensive assessment of occupational exposures sustained during military service as well as during non-uniformed military and civilian work periods. The VMOAT includes a demographic information section, a lifespan-based occupational and environmental history section, and a comprehensive exposures section based on evidence-based

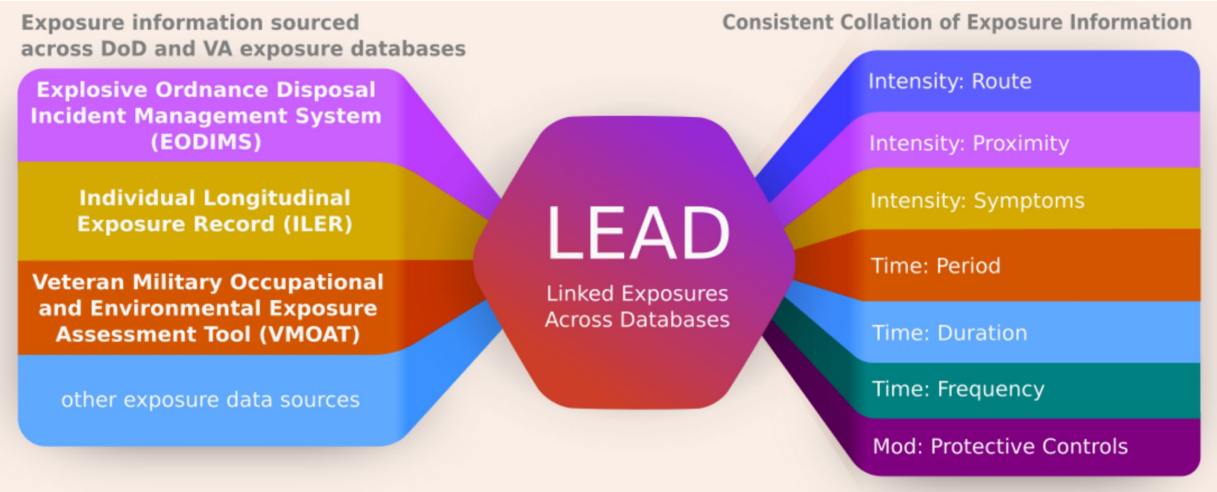

FIGURE 1
The LEAD Framework defines exposure common data elements to enable exposure information collation from a wide range of different databases and obtain a consistent log of exposures. This unform representation of exposures facilitates easy and consistent interpretation to help guide clinical care and research.

TABLE 1 Using the LEAD framework, exposures are characterized according to its route, proximity and symptoms at the time of exposure which reflects exposure intensity as well as the duration, frequency and period of the exposure event which reflects the exposure's temporal characteristics.

1. Exposure collation		Intensity			Time			Moderators
Source	Exposure	Route	Proximity	Symptoms	Period	Duration	Frequency	Protective controls
EODIMS	Blast	Impact	10 feet	Lost consciousness	03/01/1999–03/02/1999	4 h	1 event	Suit
EODIMS	Blast/50lbs NEW	Impact	>150 m	None	07/01/2000–07/02/2000	< 2 min	1 event	Bunker
EODIMS	Blast/<5 lb. NEW	Impact	< 15 m	n/a	11/01/2000–11/02/2000	4 h	1 event	Safe area
VMOAT	Blast	Impact	10 feet	Lost consciousness	03/01/1999–03/02/1999	4 h	Frequent	Suit
ILER-PDHA	Vehicle accident	Impact	n/a	Neck/back injury; LOC <5 min; Disorientation	02/11/2000–02/11/2000	n/a	1 event	Seat belt
ILER-PDHA	Doxycycline (Vibramycin®)	ingestion	n/a	n/a	02/01/2000–11/01/2000	6 months	daily	n/a
ILER-PDHR-A	Sand/Dust	Inhalation	n/a	Coughing, difficulty breathing	04/01/2000–01/01/2001	10 months	n/a	n/a
ILER-EIR	Fuel	Skin, inhalation	10 feet	Rash	03/01/1999–03/02/1999	3 h	Less frequent	Mask, ventilation
ILER-POEMS	Food/water borne disease	Ingestion	n/a	High risk: bacterial diarrhea, hepatitis A, typhoid fever Moderate risk: diarrhea-cholera, diarrhea-protozoal, brucellosis and hepatitis E	04/01/2000–01/01/2001	daily	less frequent	Hepatitis A and typhoid vaccination Food/water consumption only from approved sources

Additionally protective controls used at the time of exposure is also recorded which may moderate the effects of exposure on health outcomes. Transforming exposure information into a consistent format as demonstrated in this table enables faster parsing of exposure information and reduces context switching which is necessary when reviewing exposure data across different databases.

exposure categories such as chemical, physical, injuries, biological, and psychological (12, 13).

- Individual Longitudinal Exposure Record (ILER): The ILER is an individual, electronic record of exposures for each service member and Veteran. ILER contains information from other sources including deployment dates and locations, all-hazard occupation data, environmental hazards, objective monitoring, medical encounter information and medical concerns regarding possible exposures. ILER aims to deliver capabilities and improvements in health care, benefits, collaborations between VA, DoD, Congress, beneficiaries, and other stakeholders (such as Veterans Service Organizations), as well as research and integration of exposure data from VA's environmental health registries (14).

Application of the LEAD to collate exposure variables across exposure databases

Integrating data into exposure variables to be analyzed when determining exposure dose across various hazard categories is a primary function of LEAD. Exposures are categorized according to domains: chemical, biological, physical, ergonomic/injury, and psychological hazards, as defined by the Department of Labor's Occupational Safety and Health Administration (15). A description of each of these variables is detailed, along with examples of exposure information available across EODIMS, VMOAT and ILER.

Intensity

Exposure intensity can be directly estimated by assessing the amount or concentration of hazardous substances that an individual comes into contact. In most cases, intensity exposure characterization occurs retrospectively with limited quantitative exposure data. In such cases, indirect measures of exposure or proxies for intensity such as routes of exposure, proximity to exposure source, and symptoms at the time of the exposure event are the only means of assessing intensity. Such indirect estimates supplement objective information that is often not available.

Route

The route of exposure refers to how a substance enters the body. The EODIMS database does not contain extensive documentation of exposures routes, but routes may be inferred from the incident type and specific exposures reported. For example, an incident report documenting post-blast aerosolized particulate matter may be inferred to have inhalation and skin contact as possible exposure routes. The VMOAT1.0 categorizes exposure routes into the following categories: inhalation, ingestion, skin/eye contact, injection. Psychological exposures routes are categorized as experiencing, seeing, and/or hearing. ILER contains location and group-level exposure records that may be probabilistically associated with chemical (e.g., burn pits) and biological (e.g., infections) exposures.

Proximity

The proximity to the exposure source is directly related to the intensity of exposure, as individuals who are closer to a hazard will generally experience higher exposure intensities and, subsequently, greater doses. Data from EODIMS can provide valuable information regarding proximity, including distances between safe areas and incident sites, as well as frequency of travel between these locations and others involved in the documented response. Although VMOAT1.0 did not estimate proximity, VMOAT2.0 aims to assess proximity to exposure more effectively. Additionally, proximity estimates can be obtained from ILER sources such as VA registries; however, these data are limited in scope and depth of information collected.

Symptoms at the time of exposure

Presence of medical signs and symptoms following exposure may suggest higher exposure intensities. While the purpose of LEAD is not to assess health outcomes, assessing the presence of health changes immediately following exposure can be used as a proxy for estimating exposure intensity especially when objective exposure intensity data is unavailable. We note here that the absence of symptoms or the lack of documentation of symptoms should not be interpreted as a lack of exposure, as devastating health consequences may occur years after exposures (e.g., mesothelioma in asbestos workers) (16–18). While EODIMS documents capture immediate health effects associated with each exposure incident, such capture is neither consistent nor uniformly documented. ILER does contain limited records that ask subjective deployment health questions through DoD's Post Deployment Health Reassessment (PDHRA) such as: "Were you wounded, injured, assaulted or otherwise hurt during your deployment?"

Time

The timing of exposure is important and can be directly estimated with a variety of approaches, ranging from sensors with high sampling rates to subjective reports. Data at the individual level though is sparse and often requires interpreting subjective narratives of exposures that are incomplete and vary from person to person (for example, some individuals recall in detail the timing of an exposure whereas others will report a general time during a deployment). Duration and frequency of an exposure can be used to estimate exposure timing.

Duration and frequency

The duration of exposure refers to how long someone is exposed to a substance or hazard. The longer the duration, such as noise (19), or long-term bio accumulation of Polyfluoroalkyl substances (20, 21), generally the greater the total dose and risk of adverse outcomes. Similarly, frequent repeated exposures even at smaller intensities, such as repeated blast exposures, can lead to chronic health effects (22). The assessment of duration and frequency in databases can be inconsistent due to the lack of standardized measures. Databases like EODIMS provide detailed time and frequency estimates such as start and completion times, while

others like VMOAT measure 'duration' in terms of hours per day and 'frequency' in events within a specific time frame. ILER does not have distinct duration and frequency estimates for most cases, but some exposure Registry assessments consider the number of hours or days an individual may have been exposed in a typical day or month (e.g., airborne hazards including burn pits, fumes, dust, or other similar exposures).

Period or the time of exposure

The exposure period is associated with occupational history or military deployments. The start and end dates for occupational periods are assessed either by asking for the start and end times for exposures in questionnaires, as done in VMOAT, or through administrative records contained in the ILER or EODIMS. Time of exposure and date of birth can be combined to estimate (i) age at exposure, (ii) time since exposure, and (iii) cohort effects across military eras which are key exposure factors that may affect health outcomes.

Moderators

Hazard controls play an important role in moderating health risks associated with occupational exposure (23). While individual factors that affect exposure tolerance (24), are important moderating factors, they are not assessed broadly. Given the growing body of literature on the exposome and potential health outcomes (25, 26) it is important that exposure assessments incorporate these contributing factors as exposure science develops.

Environmental and personal protective controls

The National Institute of Occupational Safety and Health (NIOSH) hierarchy of controls (27) has been developed to control worker exposures, reduce or remove hazards, and reduce risk of illness or injury. When elimination or substitution (i.e., most effective on the hierarchy) of the hazard is not possible, engineering controls such as ventilation systems, administrative controls of rotating work schedules and Personal Protective Equipment (PPE) may reduce cumulative exposures (28). The EODIMS records hazard data, personnel hours, equipment, disposition, and protective controls for many operational and training events. The VMOAT also asks hierarchy of control and PPE questions on its subjective exposure questionnaire. ILER documents Hazard Controls in Defense Occupational and Environmental Health Readiness System (DOEHRS) Industrial Hygiene (IH) reports, but these reports are usually done on a cohort level as opposed to the individual level.

Sample LEAD framework exposure aggregation process

Drawing from the components of the LEAD framework, Table 1 illustrates the process of collating these exposure components across multiple sources into a consistent format. Additionally, Supplementary Table S1 illustrates how blast information can be compared to identify high- and low-level exposure using a simulated data based on typical EOD exposure concerns. Moreover, a translation layer can be used to reduce incompatible scoring between sources and improve consistency and interpretability when estimating exposure dose rates (Supplementary Tables S2, S3).

Discussion

The Existing exposure assessment tools have limited scope, are inconsistently used, and often do not capture metrics that result in meaningful data relevant to clinical and research care. The LEAD framework outlines a consistent method of exposure information aggregation with simplified, exposure common data elements. It aims to improve exposure profiles by offering a standardized template for integrating exposure information across various sources to formulate exposure risk metrics that are easier for clinicians and researchers alike to understand, and integrate this information into Veterans' care. Thus, the LEAD framework promotes consistency in exposure risk communication and interpretation of exposure-related health risks across clinical settings. These efforts aim to advance military exposure science and support exposure-informed clinical care for all Veterans.

Specifically, this framework provides the foundation to summarize exposures that are relevant for clinical care. Ongoing efforts are aimed at condensing detailed exposure records (over 100 exposure incidents) obtained through the LEAD framework into a single-page summary for clinicians, since in many cases, clinicians do not have time to review a Veteran's entire military/exposure history to generate meaningful insights since treatment of acute outcomes like pain take priority. Thus, a systematic method to aggregate a Veteran's prior exposure data and generate clinically relevant summaries will help keep the focus on the patient's immediate clinical need while also considering their past exposures.

The three databases presented in this report are integral exposure resources for the reasons detailed in Table 1. However, there are limitations to each of these resources; for this reason, it is important to integrate and combine information from all three of these sources.

EODIMS records operational incidents with potential exposures, some immediate outcomes, occupational duties, and deployment data. However, due to the classified nature of the data, extensive redaction is necessary before exporting data for healthcare use in VA facilities. The LEAD framework streamlines extraction of non-operational health information for exposure assessment and care at VA clinics. While the examples provided here have a focus on EOD related exposures, the methods detailed in the report can generalize across exposures from other military occupations and civilian settings.

VMOAT is a detailed questionnaire that takes around 45 min to complete. It is not meant to be used as a screener but rather designed for Veterans with more complex exposure histories. While the VMOAT provides valuable data on exposures, it is a subjective questionnaire subject to the limitations of recall biases. Integrating VMOAT information with other VA and DoD records into a cohesive format also requires extensive exposure training. The LEAD offers a potential solution for incorporating VMOAT findings with existing exposure databases.

ILER integrates individual and population-level exposure data from VA and DoD databases. However, its reports are extensive which makes it difficult for non-occupational medicine professionals to understand. Information prioritization is not a key focus area, making clinically relevant information extraction time consuming. Additionally, most of the information in ILER is population-level data which may not reflect individual service members' exposures. Therefore, other sources like EODIMS and VMOAT are needed to identify potential individual level exposures. LEAD enables a holistic framework for how to merge exposure data from multiple sources.

While an expert-informed weighted scoring method can estimate dose, empirical weight assignment using health outcomes is needed for evidence-based risk estimation. It is important to note while interpreting exposures, that exposure-based metrics typically reflects exposure-dose, whereas outcome-based risk estimates reflect exposure toxicity. Additionally, self-report service dates may not reflect official service records (DD214 form). We hope to mitigate this issue by adding both records when available and prioritizing self-reports where available since Veterans many face a variety of barriers to go the appropriate administrative processes to update records. Another inherent limitation is that exposure data can vary across military branches given the unique mandates specific to each branch. To address this aspect, aggregate statistics and sparsity information based on post-hoc analysis specific to each branch of service or units could be reported to help provide context to the exposure profile. Future iterations of LEAD will aim to integrate VA and DoD health records to provide data-driven risk scores to include exposure toxicity in addition to exposure dosage.

Conclusion

To address Veteran exposure concerns, the VA should collaborate with the DoD and other partners to improve models of how military occupational exposures impact health. This can be achieved by using subject matter expertise and reviewing literature in occupational and environmental medicine. The LEAD framework defines exposure common data elements for collecting and extracting exposure information from various databases to create consistent, succinct, insightful, comprehensive, and clinically relevant exposure profiles. Incorporating these elements in future studies ensures consistency, comparability, and robustness in data collection and analysis. Additionally, the LEAD framework aligns with the PACT ACT directives to understand how hazardous exposures affect Veteran health and helps identify new presumptive conditions for care and benefits. The long-term goal of the LEAD framework is to inform clinically relevant exposure summaries utilizing multiple data sources to optimize clinical and research processes associated with exposure data acquisition and use.

Data availability statement

The original contributions presented in the study are included in the article/Supplementary material, further inquiries can be directed to the corresponding author.

Author contributions

IS: Writing – original draft. KP: Writing – review & editing, Data curation. ST: Writing – review & editing, Data curation. MP: Writing – review & editing. CL: Writing – review & editing. AP: Writing – review & editing, Data curation. JM: Writing – review & editing, Data curation. JL: Writing – review & editing, Data curation. TD: Writing – review & editing, Data curation. RF: Writing – review & editing. JO: Writing – review & editing. JB: Writing – review & editing. MR: Writing – review & editing. MC: Writing – review & editing.

Funding

The author(s) declare that no financial support was received for the research, authorship, and/or publication of this article.

Acknowledgments

We would like to acknowledge Lily, Reck R for helping with the manuscript submission process.

Conflict of interest

The authors declare that the research was conducted in the absence of any commercial or financial relationships that could be construed as a potential conflict of interest.

Publisher's note

Author disclaimer

The opinions presented in this article are those of the authors and do not reflect the views of any institution/agency of the U.S. government, Georgetown University, or the Henry M. Jackson Foundation for the Advancement of Military Medicine, Inc.

Supplementary material

The Supplementary material for this article can be found online at: https://www.frontiersin.org/articles/10.3389/fpubh.2024.1408222/full#supplementary-material

References

1. TES, V. A. (2023). VA has screened 5 million veterans for toxic exposures, paving the way for early detection and treatment of health conditions VA Wilmington health care veterans affairs. Available at: https://www.va.gov/wilmington-health-care/news-releases/va-has-screened-5-millionveterans-for-toxic-exposures-paving-the-way-for-early-detection-and-treatment-of/

2. Chung MK, Rappaport SM, Wheelock CE, Nguyen VK, van der Meer TP, Miller GW, et al. Utilizing a biology-driven approach to map the Exposome in health and disease: an 9 essential investment to drive the next generation of environmental discovery. *Environ Health Perspect*. (2021) 129:85001. doi: 10.1289/EHP8327

3. Stingone JA, Buck Louis GM, Nakayama SF, Vermeulen RC, Kwok RK, Cui Y, et al. Toward greater implementation of the Exposome research paradigm within environmental epidemiology. *Annu Rev Public Health*. (2017) 38:315–27. doi: 10.1146/annurev-publhealth-082516-012750

4. Lauriola P, Crabbe H, Behbod B, Yip F, Medina S, Semenza JC, et al. Advancing global health through environmental and public health tracking. *Int J Environ Res Public Health*. (2020) 17:1976. doi: 10.3390/ijerph17061976

5. Thacker SB, Stroup DF, Parrish RG, Anderson HA. Surveillance in environmental public health: issues, systems, and sources. *Am J Public Health*. (1996) 86:633–8. doi: 10.2105/AJPH.86.5.633

6. Hall AL, Batchelor T, Bogaert L, Buckland R, Cowieson AB, Drew M, et al. International perspective on military exposure data sources, applications, and opportunities for collaboration. *Front Public Health*. (2023) 11:1154595. doi: 10.3389/fpubh.2023.1154595

7. Saunders PJ, Middleton JD, Rudge G. Environmental public health tracking: a cost-effective system for characterizing the sources, distribution and public health impacts of environmental hazards. *J Public Health*. (2017) 39:506–13. doi: 10.1093/pubmed/fdw130

8. Lai H, Levitt BB. The roles of intensity, exposure duration, and modulation on the biological e ects of radiofrequency radiation and exposure guidelines. *Electromagn Biol Med*. (2022) 41:230255:230–55. doi: 10.1080/15368378.2022.2065683

9. Di Credico G, Polesel J, Dal Maso L, Pauli F, Torelli N, Luce D, et al. Alcohol drinking and head and neck cancer risk: the joint effect of intensity and duration. *Br J Cancer*. (2020) 123:1456–63. doi: 10.1038/s41416-020-01031-z

10. Ouellet S, Philippens M. The multi-modal responses of a physical head model subjected to various blast exposure conditions. *Shock Waves*. (2017) 28:19–36. doi: 10.1007/s00193-017-0771-3

11. Taylor PA, Ford CC. Simulation of blast-induced early-time intracranial wave physics leading to traumatic brain injury. *J Biomech Eng*. (2009) 131:061007. doi: 10.1115/1.3118765

12. Barrett J., Samuel I., Breneman C., Prisco M., Costanzo M., Krahl P, et al (2022). V MOAT pilot: the comprehensive veteran-military occupational exposure assessment tool. American Occupational Health Conference.

13. Samuel I., Pollin K. U., Breneman C. B., Chun T., Valmas M. M., Brewster R. C., et al. (2022). Effects of military occupational exposures on home-based assessment of veterans self reported health, sleep and cognitive performance measures. International conference on human-computer interaction, 91–102.

14. VA Public Health. (2023). Individual longitudinal exposure record, an individual, electronic record of exposures designed in collaboration between VA and the Department of Defense (DoD) for each service member and future veteran. Available at: https://www.publichealth.va.gov/exposures/publications/ military-exposures/meyh-1/ILER.asp

15. OSHA. (2023). Occupational safety and health administration Hazard Identifcation and assessment-Hazard categories. Available at: https://www.osha.gov/safety-management/hazard-Identification#:~:text=Health%20hazards%20include%20chemical%20hazards,%2C%20repetitive%20motions%2C%20vibrationere

16. Seidman H, Seliko IJ, Hammond EC. Mortality of brain tumors among asbestos insulation workers in the United States and Canada. *Ann N Y Acad Sci*. (1982) 381:160171:160–71. doi: 10.1111/j.1749-6632.1982.tb50380.x

17. Selikoff IJ, Hammond EC, Seidman H. Latency of asbestos disease among insulation workers in the United States and Canada. *Cancer*. (1980) 46:2736–40. doi: 10.1002/1097-0142(19801215)46:12<2736::AID-CNCR2820461233>3.0.CO;2-L

18. CDC. (2022). Incidence of malignant mesothelioma, 19992018 CDC. Available at: https://www.cdc. gov/cancer/uscs/about/data-briefs/no27-incidence-malignant-mesothelioma-1999-2018.htm

19. Kaufman LR, LeMasters GK, Olsen DM, Succop P. E ects of concurrent noise and jet fuel exposure on hearing loss. *J Occup Environ Med*. (2005) 47:212–8. doi: 10.1097/01.jom.0000155710.28289.0e

20. Ankley GT, Cureton P, Hoke RA, Houde M, Kumar A, Kurias J, et al. Assessing the ecological risks of per- and Polyfluoroalkyl substances: current state-of-the science and a proposed path forward. *Environ Toxicol Chem*. (2020) 40:564–605. doi: 10.1002/etc.4869

21. Seals R, Bartell SM, Steenland K. Accumulation and clearance of per uorooctanoic acid (PFOA) in current and former residents of an exposed community. *Environ Health Perspect*. (2011) 119:119–24. doi: 10.1289/ehp.1002346

22. Wang Z, Wilson CM, Mendelev N, Ge Y, Galfalvy H, Elder G, et al. Acute and chronic molecular signatures and associated symptoms of blast exposure in military Breachers. *J Neurotrauma*. (2020) 37:1221–32. doi: 10.1089/neu.2019.6742

23. Hymel PA, Loeppke RR, Baase CM, Burton WN, Hartenbaum NP, Hudson TW, et al. Workplace health protection and promotion: a new pathway for a healthier and safer workforce. *J Occup Environ Med*. (2011) 53:695702:695–702. doi: 10.1097/JOM.0b013e31822005d0

24. Larson GE, Highfill-McRoy RM, Booth-Kewley S. Psychiatric diagnoses in historic and contemporary military cohorts: combat deployment and the healthy warrior effect. *Am J Epidemiol*. (2008) 167:1269–76. doi: 10.1093/aje/kwn084

25. Siroux V, Agier L, Slama R. The exposome concept: a challenge and a potential driver for environmental health research. *Eur Respir Rev*. (2016) 25:124129:124–9. doi: 10.1183/16000617.0034-2016

26. Vermeulen R, Schymanski EL, Barabasi A-L, Miller GW. The exposome and health: where chemistry meets biology. *Science*. (2020) 367:392396:392–6. doi: 10.1126/science.aay3164

27. NIOSH. (2024). Hierarchy of controls, the National Institute for Occupational Safety and Health (NIOSH), Centers for Disease Control and Prevention. Available at: https://www.cdc.gov/niosh/topics/ hierarchy/default.html

28. Reddy SC, Valderrama AL, Kuhar DT. Improving the use of personal protective equipment: applying lessons learned. *Clin Infect Dis*. (2019) 69:S165–70. doi: 10.1093/cid/ciz619

frontiers | Frontiers in Public Health

TYPE Original Research
PUBLISHED 05 July 2024
DOI 10.3389/fpubh.2024.1411123

OPEN ACCESS

EDITED BY
Alesia Coralie Ferguson,
North Carolina Agricultural and Technical State University, United States

REVIEWED BY
Rossanna Rodriguez-Canul,
Center for Research and Advanced Studies - Mérida Unit, Mexico
Jinyi Wu,
Wuhan Fourth Hospital, China
Aziz-Ur-Rahim Bacha,
Harbin Institute of Technology, China

*CORRESPONDENCE
Yurong Wu
✉ wuyurong@xinhuamed.com.cn
Liqing Zhao
✉ zlq3087119019@163.com

†These authors have contributed equally to this work and share first authorship

RECEIVED 02 April 2024
ACCEPTED 27 June 2024
PUBLISHED 05 July 2024

CITATION
Liang Y, Zhang M, Jin W, Zhao L and Wu Y (2024) Association of heavy metals exposure with lower blood pressure in the population aged 8–17 years: a cross-sectional study based on NHANES.
Front. Public Health 12:1411123.
doi: 10.3389/fpubh.2024.1411123

Association of heavy metals exposure with lower blood pressure in the population aged 8–17 years: a cross-sectional study based on NHANES

Yongzhou Liang†, Minjie Zhang†, Wenhao Jin, Liqing Zhao* and Yurong Wu*

Department of Pediatric Cardiology, Xinhua Hospital, School of Medicine, Shanghai Jiao Tong University, Shanghai, China

Background: The existing evidence regarding the joint effect of heavy metals on blood pressure (BP) in children and adolescents is insufficient. Furthermore, the impact of factors such as body weight, fish consumption, and age on their association remains unclear.

Methods: The study utilized original data from the National Health and Nutrition Examination Survey, encompassing 2,224 children and adolescents with complete information on 12 urinary metals (barium, cadmium, cobalt, cesium, molybdenum, lead, antimony, thallium, tungsten, uranium, mercury and arsenic), BP, and core covariates. Various statistical methods, including weighted multiple logistic regression, linear regression, and Weighted Quantile Sum regression (WQS), were employed to evaluate the impact of mixed metal exposure on BP. Sensitivity analysis was conducted to confirm the primary analytical findings.

Results: The findings revealed that children and adolescents with low-level exposure to lead (0.40 μg/L, 95%CI: 0.37, 0.42), mercury (0.38 μg/L, 95%CI: 0.35, 0.42) and molybdenum (73.66 μg/L, 95%CI: 70.65, 76.66) exhibited reduced systolic blood pressure (SBP) and diastolic blood pressure (DBP). Conversely, barium (2.39 μg/L, 95%CI: 2.25, 2.54) showed a positive association with increased SBP. A 25th percentile increase in the WQS index is significantly associated with a decrease in SBP of 0.67 mmHg (95%CI, −1.24, −0.10) and a decrease in DBP of 0.59 mmHg (95% CI, −1.06, −0.12), which remains statistically significant even after adjusting for weight. Furthermore, among individuals who consume fish, heavy metals have a more significant influence on SBP. A 25 percentile increase in the WQS index is significantly associated with a decrease of 3.30 mmHg (95% CI, −4.73, −1.87) in SBP, primarily attributed to mercury (27.61%), cadmium (27.49%), cesium (17.98%), thallium (8.49%). The study also identified a declining trend in SBP among children aged 10–17, whereas children aged 11–18 exhibited lower levels of systolic and diastolic blood pressure, along with a reduced risk of hypertension.

Conclusion: Some heavy metals demonstrate an inverse association with the BP of children and adolescents, particularly notable in groups with fish consumption and older children and adolescents. Future studies are warranted to validate these findings and delve deeper into the interplay of heavy metals.

KEYWORDS
heavy metal, blood pressure, joint effect, children, NHANES

1 Introduction

Hypertension is a well-known risk factor for cardiovascular diseases, with cardiovascular diseases remaining a leading cause of mortality in the United States (1). Over the last two decades, there has been a concerning upward trend in the prevalence of hypertension among children, with a relative growth rate ranging from 75 to 79% between 2000 and 2015 (2). Prolonged elevation of blood pressure (BP) in childhood may result in adult hypertension and increase the risk of cardiovascular diseases in adulthood (3, 4). Successfully reversing childhood hypertension before reaching adulthood could substantially decrease the susceptibility to cardiovascular diseases in the future (5). Hence, the prevention and management of childhood hypertension hold paramount significance in public health strategies.

The onset and progression of hypertension are believed to stem from intricate interactions among environmental factors, pathophysiology, and genetic susceptibility (6). In recent years, there is now a growing interest in the association between metals exposure and hypertension risk (7, 8). Studies have shown that exposure to arsenic (As), cadmium (Cd), lead (Pb), mercury (Hg), and barium (Ba) can increase the risk of hypertension, whereas molybdenum (Mo) is associated with reduced BP (9–12). However, epidemiological data on cobalt (Co), cesium (Cs), thallium (Tl), tungsten (W), and uranium (U) remains sparse, particularly in children and adolescents. Concurrently, research indicates a correlation between Ba exposure and elevated BP among children and adolescents (12). Although several studies have undeniably examined the impact of heavy metal exposure on BP in children, indicating that elevated concentrations of urinary antimony (Sb) might escalate BP, while Ba might exert the opposite effect (13, 14). The findings from epidemiological research regarding the association between environmental heavy metal exposure and the risk of childhood hypertension are inconsistent. Additionally, due to the enactment of diverse public health strategies, the levels of toxic metal exposure in the United States have decreased (15, 16). Given the lack of a clear threshold for the negative consequences of heavy metal exposure on health (17), it remains uncertain whether low-level exposure to multiple heavy metals is detrimental to BP among children and adolescents. Thus, further exploration of the association between heavy metal exposure and BP holds significant clinical and public health implications.

In research, it is necessary to consider the impact of dietary factors on the intake of heavy metals, particularly as certain fish species may accumulate high levels of heavy metals (18). Hence, the consumption of fish could potentially influence the association between heavy metals and BP in children (19). Moreover, as children age and undergo changes in weight, alterations occur in their physiological status and metabolic processes, resulting in variations in heavy metal exposure levels across different age and weight categories (14, 20).

Therefore, this study investigated the potential association of 12 urinary metal concentrations with the levels of BP as well as the risk of hypertension in 8-17-year-old individuals participating in the National Health and Nutritional Examination Surveys (NHANES). Various statistical models were used to study the effects of multiple metals on BP, conducting subgroup analyses to further explore the correlations between different groups.

2 Methods

2.1 Study population

This cross-sectional study focuses on children and adolescents aged 8–17 years. The data was obtained from U.S. NHANES cycles spanning from 2007 to 2016 (five consecutive NHANES cycles). The NHANES conducts a cross-sectional survey using a complex multistage probability design to collect data from the noninstitutionalized U.S. population. This involves conducting household interviews and physical examinations. Prior to participation, all individuals provided written informed consent, and the study protocol received approval from the NCHS Research Ethics Review Board. Out of the total of 9,386 participants, 7,162 had incomplete data, resulting in a final unweighted sample size of 2,224 individuals. The process of data acquisition is depicted in Supplementary Figure S1.

2.2 Blood pressure (BP)

In our study, participants who underwent BP measurements at the Mobile Examination Centers (MECs) were instructed to sit in a seated position with their feet flat on the floor and rest for a duration of 5 min. Trained researchers then performed three consecutive BP measurements using a mercury manometer and an appropriately sized cuff, which were subsequently averaged to obtain the final result (21).

The diagnostic criteria for hypertension were based on the 2017 clinical practice guidelines and previous studies (17, 22). The specific criteria for diagnosis include the following: (1) For children aged 8–12 years, hypertension is diagnosed when their systolic and/or diastolic blood pressure exceeds the 95th percentile compared to children of the same age, gender, and height. Alternatively, a diagnosis of hypertension can also be made if their SBP exceeds 130 mmHg and/or their DBP exceeds 80 mmHg. Conversely, for adolescents aged 13–17 years, hypertension is diagnosed if their SBP exceeds 130 mmHg and/or their DBP exceeds 80 mmHg (22); or (2) Irrespective of the BP level, patients aged ≥16 or the parents/guardians of patients aged <16 report the patient's diagnosis of hypertension or the use of antihypertensive drugs (17, 23).

2.3 Urinary heavy metal collection and exposure assessment

In the NHANES, most metals were detected in urine samples rather than blood samples. The non-invasive, sensitive, and prompt

detection capabilities of urine have increasingly positioned it as an alternative method for metal detection over blood samples. Therefore, all metal detection data in this study was based on urine samples. Upon arriving at the MECs, study participants were instructed by the coordinator to provide urine samples. Subsequently, urine samples undergo processing and analysis using inductively coupled plasma-mass spectrometry (ICP-MS) to determine the concentrations of 12 elements, including Ba, Cd, Co, Cs, Mo, Pb, Sb, TI, W, U, Hg, and As.[1] Comprehensive instructions for laboratory methods utilized to measure the urinary metal concentrations can be found on the NHANES website.[2] In our statistical analysis, the concentrations of urinary metals were used as a variable after being transformed with natural logarithm (Ln). Approximately 70% of the cleared As from the blood is excreted through urine. Thus, we opted to assess As exposure by measuring the total concentration of As in urine, rather than focusing on speciated As. Moreover, these data pertain to the overall healthy population, and restricting the analysis to speciated As may lead to an underestimation of long-term exposure levels. Nonetheless, this study conducted further analysis on speciated As, namely arsenobetaine (AsB), arsenic acid (As(V)), arsenocholine (AsC), arsenous acid (As(III)), monomethylarsinic acid (MMA), and dimethylarsinic acid (DMA). Exclusion of trimethylarsine oxide from the analysis was due to the unavailability of subject data for NHANES 2013–16 cycle (24).

2.4 Covariates

Based on previous literature, several covariates were extracted as potential confounding factors in this study (17, 25, 26). The selected covariates included age, sex, race/ethnicity (Mexican American, other Hispanic, non-Hispanic White, non-Hispanic Black, and other race), family poverty income ratio (PIR, categorical variables: <1.3, 1.3–3.5, >3.5 denote low, middle and high income, respectively), serum creatinine (an indicator of renal function), urinary creatinine (Detection method: Enzymatic Roche Cobas 6,000 Analyzer) and serum cotinine levels (25) (considered to reflect exposure to environmental cigarette smoke). Physical activity was fell into three groups (never, moderate or vigorous, and no record) according to self-reported activity intensity. Consistent with a previous study, the population was divided into three age groups: 8–10 years old, 11–13 years old, and 14–18 years old, representing primary school, junior high school, and senior high school, respectively (27). Additionally, the consumption of fish in the past 30 days (Yes or No) was included as a covariate in the model to account for the impact of dietary factors on urinary heavy metal concentrations. Body mass index (BMI) was calculated using the formula weight (in kilograms) divided by the square of height (in meters). Underweight was an age-and gender-specific BMI below the 5th percentile on the 2000 Centers for Disease Control and Prevention (CDC) age-and gender-specific growth charts, normal weight was a BMI below the 85th percentile but at or above the 5th percentile, overweight was a BMI falling between the 85th and 95th percentiles, and obesity was a BMI at or above the 95th percentile (28).

Additionally, all participants in the NHANES are eligible for two separate 24-h dietary recall interviews. Nonetheless, fewer participants had completed two 24-h dietary recalls. Consequently, the research evaluated the daily intake of total energy, calcium, sodium, and potassium using data from the first recall (23), which were then incorporated as covariates in our analysis.

2.5 Statistical analysis

We utilized the NHANES weighting guidelines to weigh the analysis results. Our study incorporated sample weights, sampling units, and strata provided by NHANES. We combined two groups of 5 years to conform two periods for the calculation of a new multiyear sample, ensuring that the results represent the nationwide non-institutionalized civilian population aged 8–17 years. In descriptive analysis, means ± standard deviation (SD) and counts (percentage) are applied to, respectively, describe quantitative and qualitative data. Spearman's rank correlation analysis was performed to examine the correlations of urinary toxicant concentrations. Subsequently, due to the presence of values below the detection limit for certain individuals, urinary toxicant concentrations were categorized into four quartiles (Q1, Q2, Q3, Q4) as categorical variables, with the quartile containing the lowest metal concentrations serving as the reference group. Survey-weighted logistic regression and survey-weighted multiple linear regression models were employed to calculate odds ratios (ORs), β, and 95% confidence intervals (CIs). The false-discovery rate (FDR) correction was applied to adjusted for errors resulting from multiple testing in regression models.

The WQS approach has been widely utilized to investigate the cumulative effect of environmental mixtures on health outcomes and to assess the contribution of individual metals (29, 30). The urinary metals composing a weighted index were divided into quartiles and then applied in the estimation of empirically deduced weights and a final WQS index by bootstrap sampling (31, 32). This WQS index denotes the cumulative effect of all urinary toxicants on BP. The weights sum to 1 and range from 0 to 1, and they can be applied to identify important urinary metals (the average weight surpasses the threshold of 1 divided by the total number of independent variables) in the mixture (33). The WQS index was constructed from the quartiles of urinary metals, with 40% of participants in this study divided into the test set and 60% into the validation set. Initially, we examined whether the relationship between heavy metal concentration and BP is influenced by body weight by adjusting the BMI category in the WQS model. Subsequently, we divided the samples into two groups depending on fish consumption in the past 30 days to investigate the impact of fish consumption on the association between heavy metals and BP. Lastly, to investigate the impact of heavy metals on BP in children and adolescents across different age groups, we categorized the age of pediatric patients into seven time intervals based on previous research (34). The first group comprised individuals aged 8–14, the second group included those aged 9–15, and so on, in order to analyze the trend of the effect of heavy metal concentration on BP with changing age.

In our sensitivity analysis, we initially considered the potential non-linear and non-additive relationships among urine metals.

1 https://wwwn.cdc.gov/Nchs/Nhanes/2007-2008/UHM_E.htm

2 http://www.cdc.gov/nchs/nhanes/index.htm

Bayesian kernel machine regression (BKMR) was employed to assess the combined effects of all metals and the dose–response relationship between individual metals and BP when fixing other metal concentrations. Secondly, participants were excluded if their urine samples were categorized as either diluted (urine creatinine <30 mg/dL, $n = 139$) or concentrated (urine creatinine concentration > 300 mg/dL, $n = 63$), according to previous study (26, 35). Subsequently, WQS analysis was conducted.

All statistical analyses were performed with R statistical software (V.4.4.0),[3] and a two-sided p value <0.05 was considered statistically significant. The R packages gWQS and nhanesR were applied to construct the WQS model, weighted logistic regression and multiple linear regression, respectively.

3 Results

3.1 Baseline characteristics of the participants

Supplementary Figure S1 illustrates the process of acquiring the study population. Table 1 and Supplementary Table S1 present the weighted general characteristics and urinary metal concentrations of 2,224 children and adolescents aged 8–17 years from NHANES 2007–2008 to 2015–2016. The weighted average age of the participants was 12.81 ± 0.08 years, with male and female proportions of 50.63 and 49.37%, respectively. The overall prevalence of hypertension was 10.48% ($n = 233$). Most of the participants were Mexican American and had attained higher education levels. Among hypertension patients, there was a higher proportion of individuals who were overweight or obese, had increased daily energy and sodium intake, and a lower proportion of those with unavailable serum creatinine values. Additionally, both systolic and diastolic blood pressures were elevated, while no significant differences were observed in other general characteristics. In comparison to children and adolescents without hypertension, hypertensive patients exhibited lower concentrations of Co (0.56 μg/L, 95%CI, 0.49, 0.63), Cs (4.37 μg/L, 95%CI, 3.97, 4.78), TI (0.18 μg/L, 95%CI, 0.16, 0.20), and As (8.74 μg/L, 95%CI,6.62, 10.86) in their urine samples, whereas there were no significant differences in the concentrations of Ba (2.38 μg/L, 95%CI, 1.82, 2.94), Cd (0.08 μg/L, 95%CI, 0.07, 0.10), Mo (75.31 μg/L, 95%CI, 65.28, 85.33), Pb (0.38 μg/L, 95%CI, 0.32, 0.43), Sb (0.08 μg/L, 95%CI, 0.07, 0.09), W (0.19 μg/L, 95%CI, 0.15, 0.22), U (0.02 μg/L, 95%CI, 0.00, 0.03), and Hg (0.38 μg/L, 95%CI, 0.29, 0.46). The proportions of urinary Cd and Hg concentrations exceeding the limits of detection (LOD) were the lowest, at only 65.47 and 76.35%, respectively, whereas the proportions of other urinary metals exceeding the LOD were all above 80% (Supplementary Table S1).

3.2 Correlation of the urinary metals

Supplementary Figure S2 displays weak to moderate correlations ($-0.02 \leq r \leq 0.67$) among all toxic metals, as calculated using Spearman's rank correlation analysis. Cs and TI exhibit the strongest correlation ($r = 0.67$, $p < 0.05$), followed by Mo and W, while the correlation between Cd and W is the weakest. Consequently, it may be necessary to construct a multi-pollution model to detect the impact of toxic metals on BP.

3.3 Association of single metal exposure with blood pressure

Survey-weighted logistic regression and multiple linear regression models were utilized to investigate the association between Ln-transformed urinary metal concentrations and BP. These models were adjusted for selected potential confounding factors. The results presented in Supplementary Table S2 indicate a null significant correlation between urinary metal concentrations and hypertension (all p for trend >0.05). Supplementary Table S3 revealed a negative association between an increase in urinary concentrations of Pb (p for trend =0.036), Hg (p for trend =0.036) and SBP. Moreover, an increase in Ln-transformed Mo concentration was associated with a decreasing trend in DBP (p for trend <0.001). However, for the remaining urinary metal concentrations, no significant trend effects on BP were observed in the single-metal models.

3.4 Association of urinary metal co-exposure with blood pressure

The WQS regression model was employed to examine the impact of mixed metals on BP. After adjusting for all selected confounding factors, null association was observed between low concentrations of urinary metal mixtures and the risk of hypertension (OR_{index}: 0.08, 95%CI: −0.31, 0.47, $p = 0.681$) (Table 2; Figure 1A). Conversely, these mixtures were correlated with lower SBP (β_{index}: −0.67, 95%CI: −1.24, −0.10, $p = 0.002$) and DBP (β_{index}: −0.59, 95%CI: −1.06, −0.12, $p = 0.036$) (Table 2). Metal mixtures primarily affected SBP through Pb (23.62%), As (19.22%), Hg (18.62%), and Co (18.52%) (Figure 1B), while the effects on DBP were primarily attributed to Cs (24.48%), Mo (15.22%), U (14.74%), and Co (11.24%) (Table 2; Figure 1C). Furthermore, excluding the degree of obesity from the model yielded similar results to the obesity-corrected model (Figures 1D–F). Subgroup analyses were conducted to determine how fish consumption influenced the impact of heavy metals on BP. The analyses were based on participants' fish consumption in the past 30 days. The results indicated that heavy metal exposure did not significantly affect BP values in the subgroup without fish consumption (Figures 1G–I). However, in the subgroup with fish consumption, heavy metals were associated with lower SBP (β_{index}: −3.30, 95%CI: −4.73, −1.87, $p \leq 0.001$) (Table 2; Figures 1J–L). The main contributors were Hg (27.61%), Cd (27.49%), Cs (17.98%), and TI (8.49%) (Table 2; Figure 1K).

Following the consideration of potential confounding factors, the impact of urinary heavy metals on the BP of children and adolescents across various age groups was investigated using the WQS regression model. The findings are outlined as follows: within the 10–17 age group, a 25th percentile increase in the WQS index corresponded to a 1.48 mmHg (95% CI, −2.66, −0.30) reduction in SBP. Meanwhile, in the 11–18 age group, each 25th percentile rise in the WQS index led to reductions of 1.42 mmHg (95% CI, −2.44, −0.40) in SBP and

3 https://www.R-project.org

2.62 mmHg (95% CI, −4.00, −1.22) in DBP, contributing to a 0.42 times (95% CI, −0.81, −0.03) decrease in hypertension risk. Notably, no significant association between heavy metal exposure and BP was observed among the 8–15 and 9–16 age groups (Table 3).

To examine the association between speciated As and BP, we adopted the WQS to model these categories, comprising AsB, As(V), AsC, As(III), MMA, and DMA (Supplementary Table S4; Figures 2A–C). A 25th percentile increase in the WQS index was associated with a decrease in SBP by 0.88 mmHg (95% CI, −1.62, −0.13), predominantly influenced by As (III) (40.00%) and AsC (34.04%) (Supplementary Table S5).

3.5 Sensitivity analysis

The results of the BKMR model reveal that when utilizing the median concentration (50th percentile) of all metals as the reference exposure level, a concentration of the mixture at or above the 55th percentile is associated with a downward trend in both systolic and diastolic blood pressure (Figures 2D–F). Furthermore, regardless of the percentile level (25th, 50th, or 75th) of other metals, Ba exhibits a significant association with elevated SBP (Supplementary Figure S3). The analysis yielded consistent results with the preliminary analysis, not just in the subgroups analyzed based on fish consumption, but also among participants with a urine creatinine concentration ranging between 30 mg/dL and 300 mg/dL (Supplementary Table S6; Supplementary Figures S4, S5).

4 Discussion

Several studies provide undeniable epidemiological evidence supporting the link between heavy metal exposure and BP in children and adolescents (12–14). This study is innovative in its investigation of the potential influence of weight and fish consumption on the relationship between heavy metal exposure and BP, and in exploring whether the effects of heavy metal exposure on BP differ across different age groups. The study employed both single metal and mixed metal chemical analysis models to assess the impact of urinary heavy metal concentrations on BP in children and adolescents. The findings are as follows: (1) Single-metal analysis indicated that Pb and Hg were associated with lower SBP. Likewise, Mo demonstrated a reduction in DBP. Moreover, the findings from the analysis of mixed metals further substantiated the impact of Pb, Hg, and Mo on BP reduction. Nevertheless, the BKMR model revealed that Ba was associated with an elevation in SBP; (2) Mixed metal exposure led to reduced systolic and diastolic pressures regardless of participants' body weight; (3) Consumers of fish exhibit lower SBP, mainly attributed to exposure to Hg (27.61%), Cd (27.49%), Cs (17.98%), and TI (8.49%); (4)The effects of heavy metal exposure on BP varied across different age groups. A downward trend in SBP was noted in children aged 10–17, while children aged 11–18 exhibited lower SBP and DBP, along with a reduced risk of hypertension.

It is well known that lifestyle-risk factors can affect BP, but an increasing number of studies have implicated heavy metals as a latent risk factor for hypertension (7, 36). Heavy metals are naturally existing substances widely distributed in the environment and are widely used in industry, households, agriculture, medicine and other fields (37). Children and adolescents are inevitably exposed to these metals simultaneously in their daily activities, of which the most prominent are Pb, Cd, and Hg (22). Our study revealed an association between Pb (0.40 μg/L, 95%CI, 0.37, 0.42), Hg (0.38 μg/L, 95%CI, 0.29, 0.46), Mo (75.31 μg/L, 95%CI, 65.28, 85.33) and lower BP in both the single metal chemical model and the mixed metal chemical model, providing further evidence of children and adolescents' susceptibility to Pb and Hg exposure in their daily activities. Additionally, the BKMR model exhibits an association between Ba (2.39 μg/L, 95%CI, 2.25, 2.54) and higher SBP.

Currently, there is inconsistent research evidence regarding the relationship between Pb，Hg and BP. A study in in Brazilian adults revealed that blood Pb levels (1.97 μg/dL, 95% CI, 1.90–2.04 μg/dL) were correlated with elevated DBP and an augmented hypertension risk (38). Conversely, a study focusing on children and adolescents showed no significant relationship between urinary Pb levels (0.31 μg/L, IQR, 0.18–0.57) and systolic or diastolic blood pressure (17). Another study with children and adolescents found no association between blood Hg (From 0.52 to 0.74 μg/L) and SBP. Nonetheless, a correlation was observed between total Hg and methylmercury, resulting in a DBP reduction (17). Conversely, data from adult epidemiological studies suggests that urinary Hg (0.433 μg/g, 95% CI, 0.400–0.469) was related to hypertension (9, 10). Our study diverges from these findings. Initially, we selected urine samples as the biomarker for assessment. Additionally, our study focuses on children and adolescents as the target population, who may exhibit lower exposure levels. Furthermore, this trend may stem from the limited focus in most studies solely on single metal analyses. In fact, the accumulation of Pb and Hg in the human body promotes arterial atherosclerosis through various mechanisms such as lipid peroxidation, vascular inflammation, endothelial dysfunction, and inhibition of nitric oxide (39, 40). Pb appears to activate the adrenergic system, potentially altering arterial tension, and it may also activate endothelin, resulting in vasoconstriction (40). Consequently, these pathophysiological consequences result in elevated SBP (39).

A study conducted on children and adolescents has demonstrated that a two-fold increase in urinary Ba concentration was associated with a rise of 0.41 mmHg in SBP and 1.04 mmHg in pulse pressure (12). Ba, by means of oxidative stress and inflammation, induces a reduction in the activity of nitric oxide synthase and the bioavailability of nitric oxide (NO), leading to endothelial dysfunction, heightened systemic vascular resistance, and SBP (41, 42). As an essential trace element, Mo is a cofactor of a variety of metabolic enzymes, including xanthine oxidase, sulfite oxidase and nitrate reductase (43). Studies have demonstrated that molybdate and metabolic enzymes containing Mo can improve vascular smooth muscle contraction, leading to a decrease in BP by reducing oxidative stress, enhancing nitric oxide (NO) synthesis, and promoting the release of vascular prostanoid (a vasodilator) (44–46). These findings align with our research results, supporting the conclusion that Ba is capable of inducing an elevation in BP, whereas low concentrations of Mo exhibit a hypotensive effect.

Recent studies have shown a positive association between urinary heavy metal exposure and obesity in children and adolescents (34). A study investigating the impact of heavy metal exposure on hypertension revealed that participants with a BMI ≥ 30 exhibited a positive association between heavy metal exposure and hypertension, whereas no association was found among those with a BMI < 30 (20). Furthermore, within the normal weight range for children and

TABLE 1 Distribution of general characteristics of in children and adolescents in NHANES 2007–2016.

Characteristic	Overall (*n* = 2,224)	No-hypertension (*n* = 1991)	Hypertension (*n* = 233)	*p*-value
Mean ± SD[a]				
Age, years	12.81 ± 0.08	12.85 ± 0.09	12.41 ± 0.24	0.100
Cotinine, ng/ml	5.89 ± 1.07	5.58 ± 1.08	8.78 ± 3.96	0.430
SBP, mmHg	105.69 ± 0.33	104.27 ± 0.31	118.80 ± 0.81	**< 0.001**
DBP, mmHg	57.69 ± 0.43	56.96 ± 0.40	64.45 ± 1.31	**< 0.001**
Urinary creatinine, μg/L	121.60 ± 2.06	122.48 ± 2.13	113.52 ± 6.68	0.200
Total energy, kcal/day	2092.83 ± 25.54	1962.84 ± 47.84	2106.90 ± 28.23	**0.020**
Calcium intake, mg	1063.62 ± 20.13	1010.67 ± 43.19	1069.35 ± 22.61	0.260
Sodium intake, mg	3361.77 ± 52.46	3145.20 ± 98.43	3385.21 ± 55.96	**0.030**
Potassium intake, mg	2234.94 ± 27.50	2169.04 ± 65.84	2242.07 ± 29.09	0.300
N (%)[b]				
Sex				0.970
Female	1,098(49.37)	989(49.91)	109(49.70)	
Male	1,126(50.63)	1,002(50.09)	124(50.30)	
Race/ethnicity				0.060
Mexican American	638(55.78)	579(56.40)	59(50.07)	
Other Hispanic	536(14.82)	469(14.38)	67(18.81)	
Non-Hispanic White	521(13.63)	455(13.12)	66(18.28)	
Non-Hispanic Black	281(8.94)	259(9.17)	22(6.86)	
Other race	248(6.83)	229(6.92)	19(5.99)	
Obesity				**0.002**
Underweight	60(2.7)	57(2.52)	3(0.74)	
Normal weight	1,271(57.15)	1,161(57.73)	110(47.04)	
Overweight	380(17.09)	338(18.22)	42(16.52)	
Obesity	513(23.07)	435(21.53)	78(35.70)	
PIR				0.920
Low income	950(42.72)	841(30.02)	109(35.30)	
Middle income	807(36.29)	715(37.91)	92(40.72)	
High income	467(21)	435(32.08)	32(23.98)	

(Continued)

10.3389/fpubh.2024.1411123

TABLE 1 (Continued)

Characteristic	Overall (*n* = 2,224)	No-hypertension (*n* = 1991)	Hypertension (*n* = 233)	*p*-value
Education				0.080
Primary school	686(30.85)	602(24.82)	84(33.34)	
Junior high school	644(28.96)	581(27.75)	63(27.34)	
Senior high school	894(40.2)	808(47.42)	86(39.32)	
Fish consumption				0.760
No	1,271(57.15)	1,129(59.76)	142(61.06)	
Yes	953(42.85)	862(40.24)	91(38.94)	
Activity				0.580
Never	109(4.74)	97(4.70)	12(5.14)	
Moderate or vigorous	217(11.97)	197(12.23)	20(9.53)	
No record	1898(83.30)	1,697(83.08)	201(85.33)	
Serum creatinine				**0.020**
No	952(42.81)	838(34.38)	114(44.76)	
Yes	1,272(57.19)	1,153(65.62)	119(55.24)	

Complex sampling weights were used for the results.

SBP, systolic blood pressure; DBP, diastolic blood pressure; PIR, family poverty income ratio; SD, standard deviation.

[a]Weighted mean ± weighted SD.

[b]Sample size (weighted percentage).

Bold values indicate statistical significance $p < 0.05$.

10.3389/fpubh.2024.1411123

TABLE 2 Association of WQS indices with blood pressure.

	WQS mixture result[a]	*p*-value	Component (weights)[b]
Hypertension			
Un-adjusted by obesity	−0.05(−0.34, 0.44)	0.791	NA
Adjusted by obesity	0.08(−0.31, 0.47)	0.681	NA
Not fish consumption	−0.59(−1.32, 0.14)	0.114	NA
Fish consumption	0.20(−0.37, 0.77)	0.477	NA
SBP			
Un-adjusted by obesity	−0.74(−1.35, −0.13)	**0.012**	Pb (23.26%), As (20.05%), Hg (18.82%), Co (17.64%)
Adjusted by obesity	−0.67(−1.24, −0.10)	**0.002**	Pb (23.62%), As (19.22%), Hg (18.62%), Co (18.52%)
Not fish consumption	−0.21(−1.48, 1.06)	0.749	NA
Fish consumption	−3.30(−4.73, −1.87)	**<0.001**	Hg (27.61%), Cd (27.49%), Cs (17.98%), TI (8.49%)
DBP			
Un-adjusted by obesity	−0.60(−1.19, −0.01)	**0.034**	Cs (24.45%), Mo (15.39%), U (15.09%), Co (11.13%)
Adjusted by obesity	−0.59(−1.06, −0.12)	**0.036**	Cs (24.48%), Mo (15.22%), U (14.74%), Co (11.24%)
Not fish consumption	−1.51(−3.31, 0.29)	0.101	NA
Fish consumption	−1.19(−2.72, 0.34)	0.125	NA

[a]The estimated parameters (OR_{index} or β_{index}) for the metal mixture in each model, along with the corresponding 95% confidence interval (CI) and *p*-value, were reported. OR_{index} indicates the change in risk of hypertension corresponding to a 25th percentile increase in the WQS index, whereas β_{index} represents the change in blood pressure associated with a 25th percentile increase in the WQS index.

[b]The component (weights) represent the metals in the model that exhibit significant effects and indicate their corresponding percentages.

Bold values indicate statistical significance $p < 0.05$.

SBP, systolic blood pressure; DBP, diastolic blood pressure; NA, not applicable.

adolescents, the study found that a BMI ranging from the 25th to the 84th percentile was positively associated with higher BP and an increased risk of hypertension (47). These findings suggest that body weight acts as a significant confounding factor in the relationship between heavy metal exposure and BP. However, our study revealed that, even after adjusting for obesity, heavy metal exposure exhibited a significant association with lower BP, indicating its independence from body weight in children and adolescents. Further investigation is required to determine the specific mechanisms underlying this relationship.

Fish helps establish a cardioprotective dietary pattern, as advocated by the Mediterranean and Dietary Approaches to Stop Hypertension (DASH) diet (48, 49). Fish provides essential nutrients such as iodine, selenium, vitamin D, and ω-3 long-chain polyunsaturated fatty acids, but it also poses risks of Hg and organic As exposure (50). Reports have suggested that As can induce hypertension through oxidative stress, inflammation, and endothelial dysfunction (51). Our study revealed that the reduction in BP observed in individuals who consume fish is primarily attributed to Hg, suggesting that some fish types can increase Hg exposure. Although there is a correlation between As exposure and decreased SBP, this connection was not evident in fish consumers. To investigate the antihypertensive effects of As, we examined the correlation between speciated As and BP, in addition to total urinary As. Analysis of speciated As including AsB, As(V), AsC, As(III), MMA, and DMA revealed the significant roles of As(III) (40.00%) and AsC (34.04%) in WQS model. However, the detection rate of AsC was only 6.43%, which might not fully account for its impact on BP. Previous research has confirmed the association between As(III) and the risk of hypertension (52). Notably, the single-metal model indicated a relationship between Pb and Hg exposure and decreased SBP. The BKMR model demonstrated associations of Hg, and As with reduced SBP, and Ba with increased SBP. Furthermore, Pb, Hg and As contributed to lowered SBP in the WQS model, but these findings were inconsistent. Previous studies have highlighted that Ba, Pb, and Hg primarily cause hypertension through oxidative stress, inflammation, and endothelial dysfunction (9, 10). Surprisingly, our study revealed a connection between Pb, Hg, As, and decreased BP, contrary to previous studies. In mice, exposure to low levels of methylmercury notably raised plasma renin levels, leading to elevated BP, whereas co-exposure to Pb and Hg reversed this effect (10, 53). These results suggest antagonistic interactions between mixed metal components, aiding in the understanding of our findings. Overall, consuming specific types of fish can lead to heightened exposure to some heavy metals, which warrants further research.

This study confirms that low-level exposure to heavy metals is associated with lower SBP and DBP in older children and is also linked to a lower risk of hypertension. However, the study did not attempt to investigate the long-term effects of chronic heavy metal exposure on BP. More precisely, it only emphasizes whether there are differences in the effects of heavy metal exposure on BP among children and adolescents of different age groups. This limitation arises because most metals detected in urine reflect recent exposure. For instance, inorganic As is excreted within 4 days, Ba is mostly eliminated within 3–42 days after exposure, and the half-life of Hg is generally no longer than 3 months (50). Currently, research on the impact of heavy metal exposure on BP in different age groups of children and adolescents is relatively limited. A previous study focused on preschool children, showing no significant association

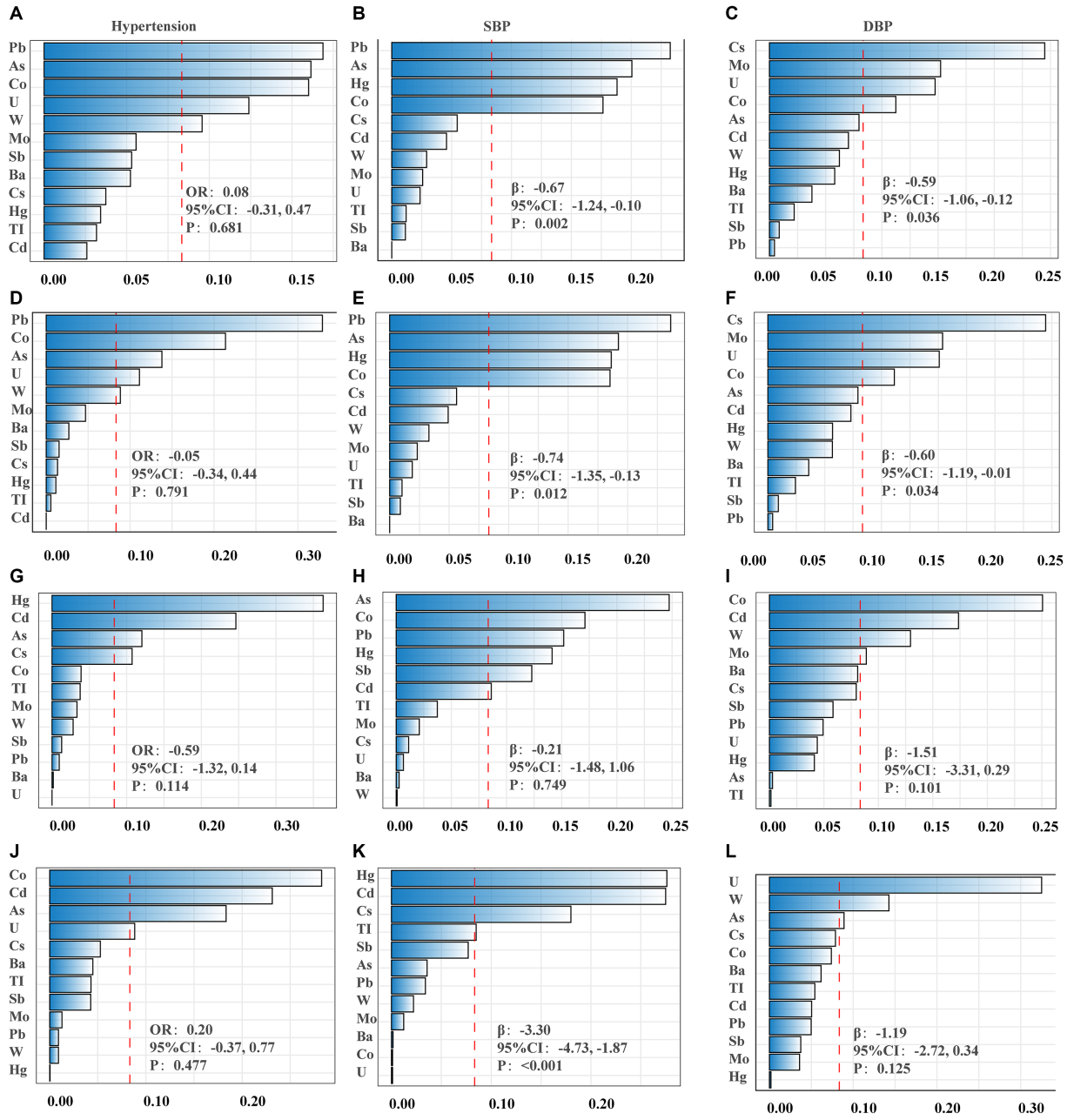

FIGURE 1
The weights of each metal in WQS model regression index for blood pressure. **(A–C)** Models were adjusted for sex, age, race/ethnicity, family poverty income ratio (PIR), obesity, education, serum cotinine, serum creatinine, urinary creatinine, fish consumption, total energy, calcium intake, sodium intake, potassium intake and activity. **(D–F)** Obesity was excluded from the models. **(G–I)** Non-fish consumers. **(J–L)** Fish consumers. **(A,D,G,J)** Presented hypertension; **(B,E,H,K)** presented systolic blood pressure (SBP); **(C,F,I,L)** presented diastolic blood pressure (DBP).

between urinary Ba concentration and DBP among different age groups (ages 2–3, 4, 5, and 6 years) (14). Additionally, an animal experimental study has indicated that Pb exposure during infancy disrupts bone metabolism, with more noticeable effects on bone microstructure compared to childhood and adolescence (54). Similarly, these findings suggest the presence of an important critical period for the effects of heavy metal exposure on BP in children and adolescents, but the specific mechanisms need further elucidation.

This study examined the potential association between urinary metal concentrations and BP as well as hypertension risk in children and adolescents using diverse statistical models. Inevitably, this study has several limitations. Initially, following the methodology of prior studies where missing covariates were coded as categorical variables (55), we categorized the serum creatinine into two groups: available and unavailable. While this study incorporated urinary creatinine, it may not offer an optimal solution, necessitating further investigation in future research. Moreover, covariates associated with BP, such as

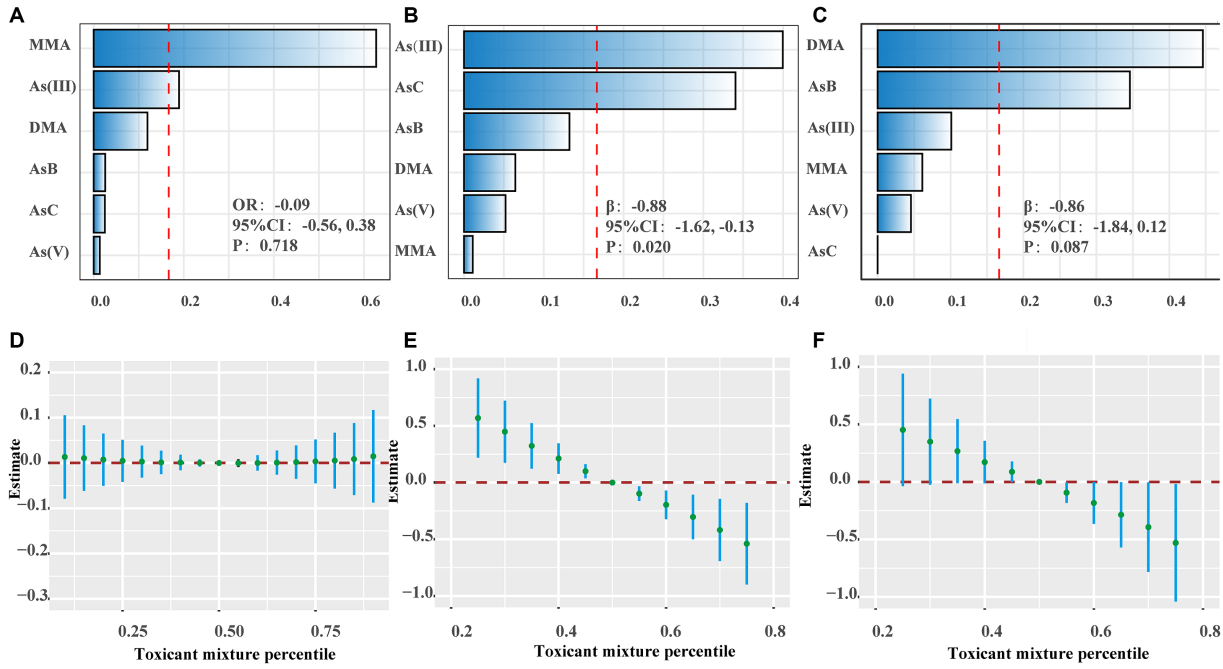

FIGURE 2
The effects of speciated As and metal mixtures on blood pressure. **(A–C)** The weights of speciated As in WQS model regression index for hypertension, systolic blood pressure (SBP) and diastolic blood pressure (DBP). **(D–F)** Joint effects of metal mixtures on hypertension, SBP and DBP using Bayesian kernel machine regression (BKMR). The results were adjusted for sex, age, race/ethnicity, family poverty income ratio (PIR), obesity, education, serum cotinine, serum creatinine, urinary creatinine, fish consumption, total energy, calcium intake, sodium intake, potassium intake and activity.

TABLE 3 Trend analysis of the combined effect (WQS indices) of metal mixtures.

Ranges of age	WQS mixture result	*p*-value
	Hypertension, OR (95%CI)	
8 ~ 15	0.02 (−0.43, 0.47)	0.940
9 ~ 16	−0.02 (−0.51, 0.47)	0.591
10 ~ 17	−0.39 (−0.84, 0.06)	0.173
11 ~ 18	−0.42 (−0.81, −0.03)	**0.021**
	SBP, β (95%CI)	
8 ~ 15	−1.01 (−2.09, 0.07)	0.065
9 ~ 16	−1.18 (−2.40, 0.04)	0.061
10 ~ 17	−1.48 (−2.66, −0.30)	**0.013**
11 ~ 18	−1.42 (−2.44, −0.40)	**0.007**
	DBP, β (95%CI)	
8 ~ 15	−1.29 (−2.70, 0.12)	0.071
9 ~ 16	−1.35 (−2.90, 0.20)	0.089
10 ~ 17	−1.01 (−2.08, 0.07)	0.065
11 ~ 18	−2.62 (−4.00, −1.22)	**<0.001**

Association of WQS index with blood pressure in different age groups was reported, presented as OR_{index} or β_{index} (95% confidence interval, 95%CI).
Bold values indicate statistical significance $p < 0.05$.
SBP, systolic blood pressure; DBP, diastolic blood pressure.

dietary factors (excluding fish), were not completely controlled in this study. Additionally, as a cross-sectional study, it prevents drawing causal inferences that metal exposure causes BP changes. Further studies with a prospective design are necessary to validate these discoveries. Furthermore, given the complex composition of metal mixtures in the environment, it is essential to elucidate the synergistic and antagonistic mechanisms among heavy metals to regulate each metal at its optimal exposure level.

5 Conclusion

Our study revealed a negative correlation between low-level heavy metal exposure and BP in children and adolescents, particularly notable in groups with fish consumption and older children and adolescents. In future research, validating our findings through a prospective cohort study, elucidating the potential interactive mechanisms of heavy metals, and specifying the possible windows of susceptibility affecting childhood BP are crucial.

Data availability statement

The original contributions presented in the study are included in the article/Supplementary material, further inquiries can be directed to the corresponding authors.

Ethics statement

Ethical approval was not required for the study involving humans in accordance with the local legislation and institutional requirements.

Written informed consent to participate in this study was not required from the participants or the participants' legal guardians/next of kin in accordance with the national legislation and the institutional requirements.

Author contributions

YL: Conceptualization, Data curation, Methodology, Writing – original draft, Writing – review & editing. MZ: Validation, Visualization, Writing – review & editing. WJ: Validation, Visualization, Writing – review & editing. LZ: Formal analysis, Funding acquisition, Methodology, Validation, Writing – review & editing. YW: Conceptualization, Funding acquisition, Methodology, Supervision, Writing – review & editing.

Funding

The author(s) declare that financial support was received for the research, authorship, and/or publication of this article. This work was supported in part by grants from the National Natural Science Foundation of China (NSFC Project Numbers: 82171948), and the Shanghai Municipal Health Commission Scientific Research Project (Project Number 20214Y0126). The sponsors of this study had no role in study design, data collection, data analysis, data interpretation, or writing of the report.

Acknowledgments

The authors gratefully acknowledge the National Center for Health Statistics of the Centers for Disease Control and Prevention for sharing the data.

Conflict of interest

The authors declare that the research was conducted in the absence of any commercial or financial relationships that could be construed as a potential conflict of interest.

Publisher's note

Supplementary material

The Supplementary material for this article can be found online at: https://www.frontiersin.org/articles/10.3389/fpubh.2024.1411123/full#supplementary-material

References

1. Benjamin EJ, Muntner P, Alonso A, Bittencourt MS, Callaway CW, Carson AP, et al. Heart disease and stroke Statistics-2019 update: a report from the American Heart Association. *Circulation*. (2019) 139:e56–e528. doi: 10.1161/CIR.0000000000000659

2. Song P, Zhang Y, Yu J, Zha M, Zhu Y, Rahimi K, et al. Global prevalence of hypertension in children: a systematic review and Meta-analysis. *JAMA Pediatr*. (2019) 173:1154–63. doi: 10.1001/jamapediatrics.2019.3310

3. Yang L, Magnussen CG, Yang L, Bovet P, Xi B. Elevated blood pressure in childhood or adolescence and cardiovascular outcomes in adulthood: a systematic review. *Hypertension*. (2020) 75:948–55. doi: 10.1161/HYPERTENSIONAHA.119.14168

4. Schuermans A, Lewandowski AJ. Childhood risk factors and adult cardiovascular events. *N Engl J Med*. (2022) 387:472–4. doi: 10.1056/NEJMc2208135

5. Juhola J, Magnussen CG, Berenson GS, Venn A, Burns TL, Sabin MA, et al. Combined effects of child and adult elevated blood pressure on subclinical atherosclerosis: the international childhood cardiovascular cohort consortium. *Circulation*. (2013) 128:217–24. doi: 10.1161/CIRCULATIONAHA.113.001614

6. Oparil S, Acelajado MC, Bakris GL, Berlowitz DR, Cifkova R, Dominiczak AF, et al. Hypertension[J]. *Nat Rev Dis Primers*. (2018) 4:18014. doi: 10.1038/nrdp.2018.14

7. Cosselman KE, Navas-Acien A, Kaufman JD. Environmental factors in cardiovascular disease[J]. *Nat Rev Cardiol*. (2015) 12:627–42. doi: 10.1038/nrcardio.2015.152

8. Tan Q, Ma J, Zhou M, Wang D, Wang B, Nie X, et al. Heavy metals exposure, lipid peroxidation and heart rate variability alteration: association and mediation analyses in urban adults. *Ecotoxicol Environ Saf*. (2020) 205:111149. doi: 10.1016/j.ecoenv.2020.111149

9. Qu Y, Lv Y, Ji S, Ding L, Zhao F, Zhu Y, et al. Effect of exposures to mixtures of lead and various metals on hypertension, pre-hypertension, and blood pressure: a cross-sectional study from the China National Human Biomonitoring[J]. *Environ Pollut*. (2022) 299:118864. doi: 10.1016/j.envpol.2022.118864

10. Wildemann TM, Siciliano SD, Weber LP. The mechanisms associated with the development of hypertension after exposure to lead, mercury species or their mixtures differs with the metal and the mixture ratio[J]. *Toxicology*. (2016) 339:1–8. doi: 10.1016/j.tox.2015.11.004

11. Zhong Q, Wu HB, Niu QS, Jia PP, Qin QR, Wang XD, et al. Exposure to multiple metals and the risk of hypertension in adults: a prospective cohort study in a local area on the Yangtze River, China. *Environ Int*. (2021) 153:106538. doi: 10.1016/j.envint.2021.106538

12. Zeng H, Wang Q, Wang H, Guo L, Fang B, Zhang L, et al. Exposure to barium and blood pressure in children and adolescents: results from the 2003-2018 National Health and nutrition examination survey. *Environ Sci Pollut Res Int*. (2022) 29:68476–87. doi: 10.1007/s11356-022-20507-4

13. Liu M, Li M, Guo W, Zhao L, Yang H, Yu J, et al. Co-exposure to priority-controlled metals mixture and blood pressure in Chinese children from two panel studies. *Environ Pollut*. (2022) 306:119388. doi: 10.1016/j.envpol.2022.119388

14. Liu Y, Yu L, Zhu M, Lin W, Liu Y, Li M, et al. Associations of exposure to multiple metals with blood pressure and hypertension: a cross-sectional study in Chinese preschool children. *Chemosphere*. (2022) 307:135985. doi: 10.1016/j.chemosphere.2022.135985

15. Muntner P, Menke A, DeSalvo KB, Rabito FA, Batuman V. Continued decline in blood lead levels among adults in the United States: the National Health and nutrition examination surveys[J]. *Arch Intern Med*. (2005) 165:2155–61. doi: 10.1001/archinte.165.18.2155

16. Tellez-Plaza M, Navas-Acien A, Caldwell KL, Menke A, Muntner P, Guallar E. Reduction in cadmium exposure in the United States population, 1988-2008: the contribution of declining smoking rates. *Environ Health Perspect*. (2012) 120:204–9. doi: 10.1289/ehp.1104020

17. Yao B, Lu X, Xu L, Wang Y, Qu H, Zhou H. Relationship between low-level lead, cadmium and mercury exposures and blood pressure in children and adolescents aged 8-17 years: an exposure-response analysis of NHANES 2007-2016. *Sci Total Environ*. (2020) 726:138446. doi: 10.1016/j.scitotenv.2020.138446

18. Benefice E, Luna-Monrroy S, Lopez-Rodriguez R. Fishing activity, health characteristics and mercury exposure of Amerindian women living alongside the Beni River (Amazonian Bolivia). *Int J Hyg Environ Health*. (2010) 213:458–64. doi: 10.1016/j.ijheh.2010.08.010

19. Fillion M, Mergler D, Sousa Passos CJ, Larribe F, Lemire M, Guimaraes JR. A preliminary study of mercury exposure and blood pressure in the Brazilian Amazon. *Environ Health*. (2006) 5:29. doi: 10.1186/1476-069X-5-29

20. Xu J, Engel LS, Rhoden J, Jackson WB 2nd, Kwok RK, Sandler DP. The association between blood metals and hypertension in the GuLF study. *Environ Res*. (2021) 202:111734. doi: 10.1016/j.envres.2021.111734

21. Sharma AK, Metzger DL, Rodd CJ. Prevalence and severity of high blood pressure among children based on the 2017 American Academy of Pediatrics guidelines. *JAMA Pediatr*. (2018) 172:557–65. doi: 10.1001/jamapediatrics.2018.0223

22. Flynn JT, Kaelber DC, Baker-Smith CM, Blowey D, Carroll AE, Daniels SR, et al. Clinical practice guideline for Screening and Management of High Blood Pressure in children and adolescents. *Pediatrics*. (2017) 140:e20171904. doi: 10.1542/peds.2017-1904

23. Yao B, Wang Y, Xu L, Lu X, Qu H, Zhou H. Associations between copper and zinc and high blood pressure in children and adolescents aged 8-17 years: an exposure-response analysis of NHANES 2007-2016. *Biol Trace Elem Res*. (2020) 198:423–9. doi: 10.1007/s12011-020-02095-x

24. Sanders AP, Mazzella MJ, Malin AJ, Hair GM, Busgang SA, Saland JM, et al. Combined exposure to lead, cadmium, mercury, and arsenic and kidney health in adolescents age 12-19 in NHANES 2009-2014. *Environ Int*. (2019) 131:104993. doi: 10.1016/j.envint.2019.104993

25. Zang X, Huang H, Zhuang Z, Chen R, Xie Z, Xu C, et al. The association between serum copper concentrations and cardiovascular disease risk factors in children and adolescents in NHANES. *Environ Sci Pollut Res Int*. (2018) 25:16951–8. doi: 10.1007/s11356-018-1816-6

26. Desai G, Niu Z, Luo W, Frndak S, Shaver AL, Kordas K. Low-level exposure to lead, mercury, arsenic, and cadmium, and blood pressure among 8-17-year-old participants of the 2009-2016 National Health and nutrition examination survey. *Environ Res*. (2021) 197:111086. doi: 10.1016/j.envres.2021.111086

27. Cohen JFW, Lehnerd ME, Houser RF, Rimm EB. Dietary approaches to stop hypertension diet, weight status, and blood pressure among children and adolescents: National Health and nutrition examination surveys 2003-2012. *J Acad Nutr Diet*. (2017) 117:1437–1444.e2. doi: 10.1016/j.jand.2017.03.026

28. Ervin RB, Fryar CD, Wang CY, Miller IM, Ogden CL. Strength and body weight in US children and adolescents. *Pediatrics*. (2014) 134:e782–9. doi: 10.1542/peds.2014-0794

29. Chen L, Zhao Y, Liu F, Chen H, Tan T, Yao P, et al. Biological aging mediates the associations between urinary metals and osteoarthritis among U.S. adults. *BMC Med*. (2022) 20:207. doi: 10.1186/s12916-022-02403-3

30. Guo X, Li N, Wang H, Su W, Song Q, Liang Q, et al. Combined exposure to multiple metals on cardiovascular disease in NHANES under five statistical models. *Environ Res*. (2022) 215:114435. doi: 10.1016/j.envres.2022.114435

31. Czarnota J, Gennings C, Colt JS, De Roos AJ, Cerhan JR, Severson RK, et al. Analysis of environmental chemical mixtures and non-Hodgkin lymphoma risk in the NCI-SEER NHL study. *Environ Health Perspect*. (2015) 123:965–70. doi: 10.1289/ehp.1408630

32. Duan W, Xu C, Liu Q, Xu J, Weng Z, Zhang X, et al. Levels of a mixture of heavy metals in blood and urine and all-cause, cardiovascular disease and cancer mortality: a population-based cohort study. *Environ Pollut*. (2020) 263:114630. doi: 10.1016/j.envpol.2020.114630

33. Carrico C, Gennings C, Wheeler DC, Factor-Litvak P. Characterization of weighted quantile sum regression for highly correlated data in a risk analysis setting. *J Agric Biol Environ Stat*. (2015) 20:100–20. doi: 10.1007/s13253-014-0180-3

34. Shan Q. Trend analysis of the association of urinary metals and obesity in children and adolescents. *Chemosphere*. (2022) 307:135617. doi: 10.1016/j.chemosphere.2022.135617

35. Xue Q, Pan A, Wen Y, Huang Y, Chen D, Yang CX, et al. Association between pyrethroid exposure and cardiovascular disease: a national population-based cross-sectional study in the US. *Environ Int*. (2021) 153:106545. doi: 10.1016/j.envint.2021.106545

36. Wu X, Cobbina SJ, Mao G, Xu H, Zhang Z, Yang L. A review of toxicity and mechanisms of individual and mixtures of heavy metals in the environment. *Environ Sci Pollut Res Int*. (2016) 23:8244–59. doi: 10.1007/s11356-016-6333-x

37. Al Osman M, Yang F, Massey IY. Exposure routes and health effects of heavy metals on children. *Biometals*. (2019) 32:563–73. doi: 10.1007/s10534-019-00193-5

38. Almeida Lopes ACB, Silbergeld EK, Navas-Acien A, Zamoiski R, Martins ADC Jr, Camargo AEI, et al. Association between blood lead and blood pressure: a population-based study in Brazilian adults. *Environ Health*. (2017) 16:27. doi: 10.1186/s12940-017-0233-5

39. Hu XF, Singh K, Chan HM. Mercury exposure, blood pressure, and hypertension: a systematic review and dose-response Meta-analysis. *Environ Health Perspect*. (2018) 126:076002. doi: 10.1289/EHP2863

40. Zachariah JP, Wang Y, Penny DJ, Baranowski T. Relation between Lead exposure and trends in blood pressure in children. *Am J Cardiol*. (2018) 122:1890–5. doi: 10.1016/j.amjcard.2018.08.033

41. Dinh QN, Drummond GR, Sobey CG, Chrissobolis S. Roles of inflammation, oxidative stress, and vascular dysfunction in hypertension. *Biomed Res Int*. (2014) 2014:406960. doi: 10.1155/2014/406960

42. Touyz RM, Alves-Lopes R, Rios FJ, Camargo LL, Anagnostopoulou A, Arner A, et al. Vascular smooth muscle contraction in hypertension. *Cardiovasc Res*. (2018) 114:529–39. doi: 10.1093/cvr/cvy023

43. Li B, Huang Y, Luo C, Peng X, Jiao Y, Zhou L, et al. Inverse Association of Plasma Molybdenum with metabolic syndrome in a Chinese adult population: a case-control study. *Nutrients*. (2021) 13:4544. doi: 10.3390/nu13124544

44. Panneerselvam SR, Govindasamy S. Effect of sodium molybdate on the status of lipids, lipid peroxidation and antioxidant systems in alloxan-induced diabetic rats. *Clin Chim Acta*. (2004) 345:93–8. doi: 10.1016/j.cccn.2004.03.005

45. Webb AJ, Patel N, Loukogeorgakis S, Okorie M, Aboud Z, Misra S, et al. Acute blood pressure lowering, vasoprotective, and antiplatelet properties of dietary nitrate via bioconversion to nitrite. *Hypertension*. (2008) 51:784–90. doi: 10.1161/HYPERTENSIONAHA.107.103523

46. Peredo HA, Andrade V, Donoso AS, Lee HJ, Puyo AM. Sodium molybdate prevents hypertension and vascular prostanoid imbalance in fructose-overloaded rats. *Auton Autacoid Pharmacol*. (2013) 33:43–8. doi: 10.1111/aap.12010

47. Wang M, Kelishadi R, Khadilkar A, Mi Hong Y, Nawarycz T, Krzywinska-Wiewiorowska M, et al. Body mass index percentiles and elevated blood pressure among children and adolescents. *J Hum Hypertens*. (2020) 34:319–25. doi: 10.1038/s41371-019-0215-x

48. Rees K, Takeda A, Martin N, Ellis L, Wijesekara D, Vepa A, et al. Mediterranean-style diet for the primary and secondary prevention of cardiovascular disease. *Cochrane Database Syst Rev*. (2019) 3:CD009825. doi: 10.1002/14651858.CD009825.pub3

49. Sayer RD, Wright AJ, Chen N, Campbell WW. Dietary approaches to stop hypertension diet retains effectiveness to reduce blood pressure when lean pork is substituted for chicken and fish as the predominant source of protein. *Am J Clin Nutr*. (2015) 102:302–8. doi: 10.3945/ajcn.115.111757

50. Martinez-Morata I, Sobel M, Tellez-Plaza M, Navas-Acien A, Howe CG, Sanchez TR. A state-of-the-science review on metal biomarkers. *Curr Environ Health Rep*. (2023) 10:215–49. doi: 10.1007/s40572-023-00402-x

51. Zhao J, Li A, Mei Y, Zhou Q, Li Y, Li K, et al. The association of arsenic exposure with hypertension and blood pressure: a systematic review and dose-response meta-analysis. *Environ Pollut*. (2021) 289:117914. doi: 10.1016/j.envpol.2021.117914

52. Rahman HH, Niemann D, Munson-McGee SH. Environmental exposure to metals and the risk of high blood pressure: a cross-sectional study from NHANES 2015-2016. *Environ Sci Pollut Res Int*. (2022) 29:531–42. doi: 10.1007/s11356-021-15726-0

53. Wildemann TM, Weber LP, Siciliano SD. Combined exposure to lead, inorganic mercury and methylmercury shows deviation from additivity for cardiovascular toxicity in rats. *J Appl Toxicol*. (2015) 35:918–26. doi: 10.1002/jat.3092

54. Zhang Y, Zhou L, Li S, Liu J, Sun S, Ji X, et al. Impacts of lead exposure and chelation therapy on bone metabolism during different developmental stages of rats. *Ecotoxicol Environ Saf*. (2019) 183:109441. doi: 10.1016/j.ecoenv.2019.109441

55. Ma H, Wang X, Xue Q, Li X, Liang Z, Heianza Y, et al. Cardiovascular health and life expectancy among adults in the United States. *Circulation*. (2023) 147:1137–46. doi: 10.1161/circulationaha.122.062457

frontiers | Frontiers in Public Health

TYPE Original Research
PUBLISHED 12 July 2024
DOI 10.3389/fpubh.2024.1408842

OPEN ACCESS

EDITED BY
Mariana Farcas,
Altria, United States

REVIEWED BY
Ann-Charlotte Almstrand,
University of Gothenburg, Sweden
Mariana Farcas,
Altria, United States

*CORRESPONDENCE
C. Wright
✉ Christa.Wright@ul.org

RECEIVED 28 March 2024
ACCEPTED 03 June 2024
PUBLISHED 12 July 2024

CITATION
Barnett LMA, Zhang Q, Sharma S, Alqahtani S, Shannahan J, Black M and Wright C (2024) 3D printer emissions elicit filament-specific and dose-dependent metabolic and genotoxic effects in human airway epithelial cells. *Front. Public Health* 12:1408842. doi: 10.3389/fpubh.2024.1408842

3D printer emissions elicit filament-specific and dose-dependent metabolic and genotoxic effects in human airway epithelial cells

LMA Barnett[1], Q. Zhang[1], S. Sharma[1], S. Alqahtani[2,3], J. Shannahan[2], M. Black[1] and C. Wright[1]*

[1]Chemical Insights Research Institute, UL Research Institutes, Marietta, GA, United States, [2]School of Health Sciences, Purdue University, West Lafayette, IN, United States, [3]Advanced Diagnostic and Therapeutics Technologies Institute, Health Sector, King Abdulaziz City for Science and Technology (KACST), Riyadh, Saudi Arabia

Three-dimensional (3D) printers have become popular educational tools in secondary and post-secondary STEM curriculum; however, concerns have emerged regarding inhalation exposures and associated health risks. Current evidence suggests that filament materials and site conditions may cause differences in the chemical profiles and toxicological properties of 3D printer emissions; however, few studies have evaluated exposures directly in the classroom. In this study, we monitored and sampled particulate matter (PM) emitted from acrylonitrile-butadiene-styrene (ABS) and polylactic acid (PLA) filaments during a 3-hour 3D printing session in a high school classroom using aerosol monitoring instrumentation and collection media. To evaluate potential inhalation risks, Multiple Path Particle Dosimetry (MPPD) modeling was used to estimate inhaled doses and calculate *in vitro* concentrations based on the observed aerosol data and specific lung and breathing characteristics. Dynamic light scattering was used to evaluate the hydrodynamic diameter, zeta potential, and polydispersity index (PDI) of extracted PM emissions dispersed in cell culture media. Small airway epithelial cells (SAEC) were employed to determine cellular viability, genotoxic, inflammatory, and metabolic responses to each emission exposure using MTS, ELISA, and high-performance liquid chromatography-mass spectrometry (HPLC-MS), respectively. Aerosol monitoring data revealed that emissions from ABS and PLA filaments generated similar PM concentrations within the ultrafine and fine ranges. However, DLS analysis showed differences in the physicochemical properties of ABS and PLA PM, where the hydrodynamic diameter of PLA PM was greater than ABS PM, which may have influenced particle deposition rates and cellular outcomes. While exposure to both ABS and PLA PM reduced cell viability and induced MDM2, an indicator of genomic instability, PLA PM alone increased gamma-H2AX, a marker of double-stranded DNA breaks. ABS and PLA emissions also increased the release of pro-inflammatory cytokines, although this did not reach significance. Furthermore, metabolic profiling via high performance liquid chromatography-mass spectrometry (HPLC-MS) and subsequent pathway analysis revealed filament and dose dependent cellular metabolic alterations. Notably, our metabolomic analysis also revealed key metabolites and pathways implicated in PM-induced oxidative stress, DNA damage, and respiratory disease that were perturbed across both tested doses for a given filament. Taken together, these findings suggest that use of ABS and PLA filaments in 3D printers within school settings may potentially contribute to adverse respiratory responses especially in vulnerable populations.

KEYWORDS

3D printer, emissions, exposure dosimetry, particulate matter, respiratory toxicity, metabolomics

Introduction

Fused filament fabrication (FFF) is a form of three-dimensional (3D) printing that employs heating and extrusion of thermoplastics in layers onto a print bed surface to form multi-dimensional objects. FFF has become the most common form of 3D printing and is a popular hands-on educational tool in secondary and higher education settings. However, these benefits are coupled with potential health hazards due to the release of potentially harmful emissions during 3D printing.

3D printers pose potential respiratory hazards to users because they emit ultrafine particles at rates of 2×10^{8} to 2×10^{12} min^{-1} in tandem with gas phase emissions (1–4). This is concerning because ultrafine particles can cause both local and systemic toxicity by penetrating deep into the respiratory tract, passing through the alveolar–capillary barrier, and distributing throughout the body (5). Additionally, 3D printers emit metals such as Cr, As, Pb, Cd, and Co (6–8) and volatile organic compounds (VOCs) such as styrene, formaldehyde, acetaldehyde, ethylbenzene, methylene chloride, methyl-methacrylate, toluene, lactide, and caprolactam that are International Agency for Research on Cancer (IARC) class 1 or 2 carcinogens and/or respiratory hazards (1–3, 9–12). Moreover, total VOC and individual VOCs released by 3D printers have been shown to exceed national and international indoor air quality (IAQ) standards (10, 11). This is especially concerning for indoor environments that are poorly filtered and ventilated, such as older homes, schools, and small offices.

Importantly, the chemical composition of 3D printing emissions depends on printer settings and filament formulations. For example, acrylonitrile butadiene styrene (ABS) filaments have been shown to emit 3 to 4-fold higher emissions than polylactic acid (PLA) filaments (1, 2, 6, 13). This could be because ABS filaments require higher extrusion temperatures relative to PLA filaments and contain unknown additives that elevate emissions (4, 14). Accordingly, regardless of the filament type (ABS vs. PLA), higher extrusion temperatures have been shown to increase particle and VOC emissions from 3D printers (15, 16).

Conversely, relatively few studies have compared different printer settings and filament formulations in terms of their toxicological effects. A recent *in vitro* study from Zhang and coworkers revealed that ABS and PLA 3D printer emission exposures caused a reduction in cell viability and oxidative stress in both macrophages and airway epithelial cells (4). Farcas and coworkers revealed dose-dependent increases in pro-inflammatory cytokine and chemokines, oxidative stress, and cytotoxicity due to ABS emission exposures in small airway epithelial cells (17). Animal studies investigating 3D printing emissions have also found concerning results where 3 h exposures to 1 mg/m^3 of ABS aerosols induced substantial impairments to cardiovascular function in rats (18). Moreover, a recent health survey revealed approximately 60% of participants using 3D printers in commercial prototyping facilities, educational settings, and public libraries experienced weekly respiratory issues along with strong associations between hours worked per week and asthma or allergic rhinitis development (19). Given the rising popularity of 3D printers in educational and residential settings, research on how 3D printer emissions may alter indoor air quality and enhance exposure to hazardous chemicals is critical to protecting human health.

In this study, we characterized the particulate emissions and potential respiratory toxicity resulting from a 3 h 3D printing session at a high school and compared two different filament types, ABS and PLA. Scanning mobility particle sizer (SMPS) and optical particle sizer (OPS) technology were used to compare particle sizes and concentrations and dynamic light scattering (DLS) was used to determine physicochemical properties of ABS and PLA particles including hydrodynamic diameter and zeta potential. Dosimetric analyses using multiple-path particle dosimetry (MPPD) computational software were performed to estimate rate of deposition of 3D printer emissions within the human lung using parameters obtained during aerosol monitoring. Potentially inhaled doses and extrapolated *in vitro* concentrations were calculated using aerosol data consisting of count median diameter, geometric standard deviation, and aerosol concentration along with breathing parameters. Additionally, primary small airway epithelial cells (SAEC) were exposed to ABS and PLA-emitted particles collected and extracted from filters for 24 h, followed by assessments of cell viability, DNA damage, inflammation, and metabolomic responses. Our results suggest that ABS and PLA 3D printing emissions reduce cellular viability, induce genotoxic effects, and elicit metabolic changes in SAEC. Furthermore, metabolic pathways related to oxidative stress, DNA damage, inflammation, and respiratory disease were altered by ABS and PLA across both tested doses. Ultimately, these results advance our understanding of the potential toxicity of 3D printer emissions and their impact on respiratory health.

Methods

Sampling sites and generation of 3D printer emissions

Airborne particulate matter (PM) was collected from a high school located in Atlanta, GA. There were two locations studied for each filament material; one science, technology, engineering, and mathematics (STEM) lab classroom with a 3D printer (hereinafter referred to as the printer room) and an adjacent classroom without a 3D printer (the control room). In the printer room, PM was sampled within one meter of the printer.

One fused filament fabrication (FFF) 3D printer was operated in the printer room for 3 h to generate a cube. Black ABS (extrusion temperature = 245°C, printer chamber temperature = 85°C) or black PLA (extrusion temperature = 200°C, printer chamber temperature = 40°C) filaments were used on two separate days. On each day, PM was monitored during printing in both the printer room

and control room. Support filaments (SR30 for ABS at 240°C and PVA (polyvinyl alcohol) for PLA at 200°C) were loaded to enable printer function following manufacturer's instruction and accounted for a minimal fraction of the printed part.

PM monitoring, sampling, and extraction

Aerosol size distributions were assessed using a scanning mobility particle sizer (NanoScan SMPS, TSI 3910) and an optical particle sizer (OPS, TSI 3330) to detect a particle size range of 10 nm to 10 microns. Fine PM ($PM_{2.5}$, less than 2.5 µm) were collected during printing using PTFE (polytetrafluoroethylene) filters (37 mm, 0.45 µm pore size), personal modular impactors, and portable pumps at a flow rate of 4 L/min. The weight of PM collected on the filter was analyzed using a microbalance (Mettler Toledo XS3DU) by subtracting pre-sampling filter weights from post-sampling filter weights. Filter collected particles were extracted using a solvent-based (75% methanol) method coupled with sonication. Extractions were then concentrated using a vacufuge to remove the solvent extraction fluid and refrigerated until toxicological analysis.

Estimation of inhaled and *in vitro* doses

Estimated inhaled doses were determined by inputting measured aerosol data into the Multiple-Path Particle Dosimetry 2 (MPPD2) computational model. The parameters used by MPPD2 to calculate deposition comprise four areas: the type of airway morphometry was age-specific (14 years old) symmetric; the particle properties included count median diameter (CMD), geometric standard deviation (GSD), and averaged aerosol mass concentration; the exposure was a constant exposure at the measured PM concentration. The exposure time was assumed to be 6 h per day, 5 days per week for a school year of 36 weeks. The total deposited mass across the airways (Generations 1–21) was divided by the surface area of those regions, which provided the total deposited dose within the small airways. To convert the total deposited dose to an *in vitro* dose or concentration, the total deposited dose (µg/cm^2) was multiplied by the surface area of one well within a 96 well plate (0.33 cm^2) then divided by the total exposure volume (100 µL).

Dynamic light scattering

Extracted particles were submerged in cell culture media and analyzed on a Zetasizer Ultra (Malvern Panalytical, Malvern, United Kingdom). Samples were loaded into folded capillary cells/cuvettes (Malvern Panalytical, DTS1070) and polystyrene cells/cuvettes (Malvern Panalytical, DTS0012) for analysis of zeta potential and particle size, respectively.

Cell culture and 3D printer PM exposure parameters

Normal small airway epithelial cells (SAEC) were cultured in small airway basal media (SABM) (Lonza, Walkersville, MD) supplemented with bovine pituitary extract (BPE), hydrocortisone, human epidermal growth factor (hEGF), epinephrine, transferrin, insulin, retinoic acid, triiodothyronine, gentamicin, and amphotericin-B (GA-1000). SAEC were maintained in a humidified atmosphere of 37°C and 5% CO_2 with media renewal every 2–3 days. For 3D printer exposure assessments, SAEC were seeded in 96 well plates at a density of 10,000 cells/well and grown to 70–80% confluency for 5–7 days. Cells were exposed to 5 µg/mL or 10 µg/mL of PM extracts from the printer room and control room for 24 h to cover the range of estimated *in vitro* doses from the MPPD2 model (Table 1). PM extracts were diluted in cell culture media and administered in a volume of 100 µL in triplicate for each dose. In addition, untreated cells in culture media were used as a negative control (NC).

MTS assay

Cell viability was measured after 24 h of exposure to PM using the CellTiter 96 Aqueous One Solution Cell Proliferation Assay (Promega Corp., Madison, WI). This test is based on the reduction of the tetrazolium salt MTS (3-[4,5-dimethylthiazol-2-yl]-5-(3-carboxymethoxyphenyl)-2-(4-sulfophenyl)-2H-tetrazolium) into a soluble purple formazan product by dehydrogenase enzymes in metabolically active cells. After removing the exposure media containing ABS or PLA PM, cells were washed twice with 1X phosphate buffered saline (PBS). A 1:10 dilution of MTS reagent: cell culture media was added to each well for 45 min and absorbance was read at 490 nm using a microplate reader (Cytation 1, Biotek). Triplicate readings were blank-corrected and averaged for each control and sample. In addition, cells that were treated with a hypotonic solution (0.1% Triton-X) served as a positive control (PC). Cells were also treated with blank filter extracts to account for residual solvent during the extraction process.

TABLE 1 Aerosol characterization, estimated inhaled doses, and calculated *in vitro* doses of particles emitted during 3 h of 3D printing.

Sample location	Count median diameter (nm)	Geometric standard deviation	Aerosol concentration (µg/m^3)	Inhaled dose (µg/cm^2)	*In vitro* dose (µg/mL)
Control room	125 ± 4.0	1.77 ± 0.12	4.22 ± 0.48	2.08	6.87
Printer room during ABS printing	87.4 ± 4.9	1.94 ± 0.24	4.33 ± 0.81	1.46	4.81
Printer room during PLA printing	130 ± 3.0	1.77 ± 0.32	4.44 ± 0.79	2.16	7.14

Endotoxin assay

The Pierce Chromogenic Endotoxin Quant Kit (Pierce Biotechnology, Rockford, IL) was used to assess the potential for bacterial endotoxin contamination when cells were exposed to particulate matter samples. Due to limited sample, cell lysates were assessed rather than cell culture supernatants. All steps were performed according to the manufacturer's protocol. Briefly, 50 µL lysates, standards, and blanks were added in triplicate to a 96-well plate. After adding 50 µL Amebocyte Lysate Reagent to each well, the plate was incubated at 37°C for the time indicated on the lysate vial. Next, 100 µL/well of Chromogenic Substrate Solution was added, followed by 6 min incubation at 37°C. To stop the reaction, 50 µL Stop Solution was added to each well. Absorbance was read at optical density (OD) 405 nm using a Cytation C10 plate reader (Agilent, Santa Clara, CA). The blank-corrected absorbance for standards and samples was calculated by subtracting the average absorbance of blank wells. The corresponding endotoxin concentration of each sample was calculated by plotting a standard curve of the average blank-corrected absorbance of each standard vs. the known endotoxin concentration in EU/mL.

DNA damage evaluation

The MILLIPLEX 7-Plex DNA Damage/Genotoxicity Magnetic Bead Kit (Millipore Sigma) was used to measure changes in a panel of 7 DNA damage and repair pathway markers, including phosphorylated Chk1 (Ser 345), Chk2 (Thr68), H2A.X (Ser139), and p53 (Ser15) as well as total protein levels of ATR, MDM2, and p21. Following 24 h exposure to PM, SAEC were lysed, and protein was collected using mammalian protein extraction reagent (MPER, Thermo Fisher) according to the manufacturer's protocol. Protein extracts were diluted to 1 mg/mL and analyzed according to the assay protocol. The Median Fluorescence Intensity (MFI) was measured on a Luminex Flexmap 3D system. Triplicate readings were blank-corrected and averaged for each control and sample.

Cytokine analysis

Cytokines were detected and quantified in media collected from SAEC following 24 h exposure to PM using the Quantibody® Human Cytokine Array (QAH-CYT-1) full testing ELISA service provided by Raybiotech Life, Inc. (Peachtree Corners, GA). Media samples were centrifuged at 250 × g for 1 min prior to cytokine analysis. A panel of 20 cytokines, including IL-1α, IL-1β, IL-2, IL-4, IL-5, IL-6, IL-8, IL-10, IL-12p70, IL-13, GM-CSF, GRO, IFNg, MCP-1, MIP-1α, MIP-1β, MMP-9, RANTES, TNFα, and VEGF, were analyzed. Quantibody® employs matched pairs of antibodies for target protein detection in which multiple capture antibody arrays are printed on a standard slide. After blocking, unknown samples are incubated with the arrays, followed by a wash step to remove non-specific protein binding. A cocktail of biotinylated detection antibodies was then added to the array along with streptavidin-conjugated fluorescent reagents that were subsequently detected using a fluorescence laser scanner. Array-specific predetermined protein standards were utilized to generate an 8-point standard curve of each target protein. Concentrations of each cytokine were calculated in unknown samples using the standard curve and Q analyzer software.

Metabolite profiling, sample preparation, and extraction

Protein removal and sample extraction were performed by adding 500 mL of methanol to 200 mL of cell supernatant. Solutions were vortexed and centrifuged at 16,000 g for 8 min. The supernatants were transferred to separate vials and evaporated to dryness in a vacuum concentrator. The dried polar fractions were reconstituted in 60 mL of diluent composed of 95% water and 5% acetonitrile, containing 0.1% formic acid.

High performance liquid chromatography-mass spectrometry (HPLC-MS) and bioinformatic analyses

HPLC-MS and bioinformatic analyses were performed as described in our previous publication (20). Separations were performed on an Agilent 1,290 system (Palo Alto, CA), with a mobile phase flow rate of 0.45 mL/min. The metabolites were assayed using a Waters HSS T3 column (1.8 µm, 2.1 × 100 mm), where the mobile phases were A (0.1% formic acid in ddH2O) and B (0.1% formic acid in acetonitrile). Initial conditions were 100:0 A:B, held for 1 min, followed by a linear gradient of 80:20 at 16 min, then 5:95 at 21 min, held for 1.5 min. Column re-equilibration was performed by returning to 100:0 A:B at 23.5 min and holding until 28.5 min. The mass analysis was obtained in positive ionization mode using an Agilent 6,545 Q-TOF mass spectrometer with ESI capillary voltage +3.5 kV, nitrogen gas temperature 325°C, drying gas flow rate 8.0 L/min, nebulizer gas pressure 30 psig, fragmentor voltage 135 V, skimmer 45 V, and OCT RF 750 V. Mass data (from m/z 70–1,000) were collected using Agilent MassHunter Acquisition software (v. B.06). Mass accuracy was improved by infusing Agilent Reference Mass Correction Solution (G1969-85001). MS/MS was performed in a data dependent acquisition mode. Peak picking and annotation was performed using MS-DIAL (v. 4.7).[1] Adduct ions selected were [M + H]+, [M + Na]+, [2 M + H]+, [2 M + Na]+. After blank peak removal, 1,141 sample related peaks were observed. Peak annotations were performed using the MassBank of North America metabolomics MS/MS library, based on authentic standards (v. 16).[2] Mass tolerances were 0.005 Da for MS1 and 0.01 Da for MS2. Statistical analysis was performed using MetaboAnalyst 5.0.[3] Data imputation, normalization, and comparisons were made with significance threshold set at $p < 0.05$.

Pathway analysis

For each condition, a 4-column table of m/z features, *p*-values, *t* scores, and retention time was inputted into the MS Peaks to Pathways

1 http://prime.psc.riken.jp/compms/msdial/main.html
2 http://prime.psc.riken.jp/compms/msdial/main.html#MSP
3 https://www.metaboanalyst.ca/

TABLE 2 Characteristics of collected PM when submerged in SAEC media as measured by dynamic light scattering (DLS).

Sample location	Z-average (nm)	Polydispersity index (PDI)	Zeta potential (mV)
Control room	261.21 ± 24.52	0.546 ± 0.11	−21.556 ± 0.86
Printer room during ABS printing	1269.26 ± 33.02	0.444 ± 0.12	−18.824 ± 3.44
Printer room during PLA printing	1515.85 ± 205.53	0.502 ± 0.092	−13.411 ± 5.89

module on MetaboAnalyst 5.0 (see text footnote 3). The Mummichog algorithm was selected as the analysis parameter, and the human KEGG pathway library was selected. Significantly enriched pathways were selected with an adjusted $p < 0.05$.

Statistical analysis

Results obtained from the MTS, DNA, and cytokine assays were assessed for statistical significance using one-way ANOVA followed by a Dunnett's post-hoc analysis using GraphPad Prism version 10.1.2 (Boston, Massachusetts, United States) to compare each treatment group to the untreated negative control (NC). For metabolomics, all statistical analyses were performed using MetaboAnalyst 5.0 (see text footnote 3). The level of statistical significance was $p < 0.05$ for all analyses. HCA heatmaps were made using MetaboAnalyst 5.0. Venn diagrams were made using Venn Diagram Plotter version 1.6.7458.[4] All other graphs were made using GraphPad Prism version 10.1.2.

Results

Indoor aerosol characterization and dosimetry

Aerosol characteristics, estimated inhaled and *in vitro* dose are described in Table 1. Details of particle number distribution are shown in Supplementary Figure S1. Particles emitted during ABS printing fell within the nanoscale range and were smaller, but more concentrated relative to particles in the control room. The estimated inhaled and *in vitro* deposited doses were smaller for ABS-emitted particles compared to particles in the control room, and this was likely because smaller-sized particles contributed to less mass deposition. On the other hand, particles in the PLA printing room were slightly larger and more concentrated than particles in the control room. The size, average concentration, and estimated inhaled and *in vitro* deposited doses of particles emitted in the printer room during ABS printing were consistently lower than the corresponding characteristics of particles emitted during PLA printing. This could be due to a combination of variables such as printer emission rate, local ventilation conditions, occupancy, and in-room activities that likely differed during the dates of sampling.

4 https://github.com/PNNL-Comp-Mass-Spec/Venn-Diagram-Plotter/releases

Size, polydispersity, and surface charge of submerged PM samples

We performed dynamic light scattering (DLS) to assess the physical properties of PM upon submersion in cell culture media (Table 2). The size of PM from all sampling locations increased upon submersion in media, as indicated by hydrodynamic diameter or z-averages relative to the count median diameters summarized in Table 1. PLA PM had a greater hydrodynamic diameter compared to ABS PM. Additionally, PM from all sample locations had similar polydispersity, with control room PM being the most polydisperse. Finally, the surface charge of all PM was negative, with control room being the most negatively charged, followed by ABS, and then PLA.

Effect of 3D printer emissions on cellular viability

The MTS assay was used to determine the metabolic capacity and viability of SAEC after 24 h of exposure to PM emitted during 3D printing (Figure 1A). 5 μg/mL and 10 μg/mL PM were used as the administered concentrations to cover the range of extrapolated *in vitro* doses described in Table 1 and to identify the biologically effective dose. Cells exposed to extracts from blank filters did not display decreased viability (data not shown). In comparison to untreated cells, cells exposed to control room PM did not experience significant reductions in cellular viability (Figure 1A). Exposure to 10 μg/mL PM emitted during printing with ABS significantly reduced cellular viability to 51%, while exposure to 5 μg/mL had a slight but non-significant effect (74.1% viability). Exposure to both doses of PM emitted during printing with PLA also significantly reduced cell viability. Specifically, cells exposed to 5 μg/mL and 10 μg/mL PLA were 44 and 59% viable, respectively. We also confirmed that SAEC lysates contained minimal levels of endotoxin. These levels were not significantly different from levels in negative control cells and are below the available FDA limits for sterile water and medical device eluates (0.25 and 0.5 EU/mL, respectively). Therefore, bacterial contamination had a minimal effect on the toxicological endpoints measured (Supplementary Figure S2).

Genotoxicity of 3D printer emissions

To explore the potential genotoxicity of ABS and PLA emissions, we measured a panel of seven DNA damage and repair pathway proteins in SAEC after 24 h of exposure to 5 μg/mL and 10 μg/mL doses of PM emitted during 3D printing (Figure 1B). Although most

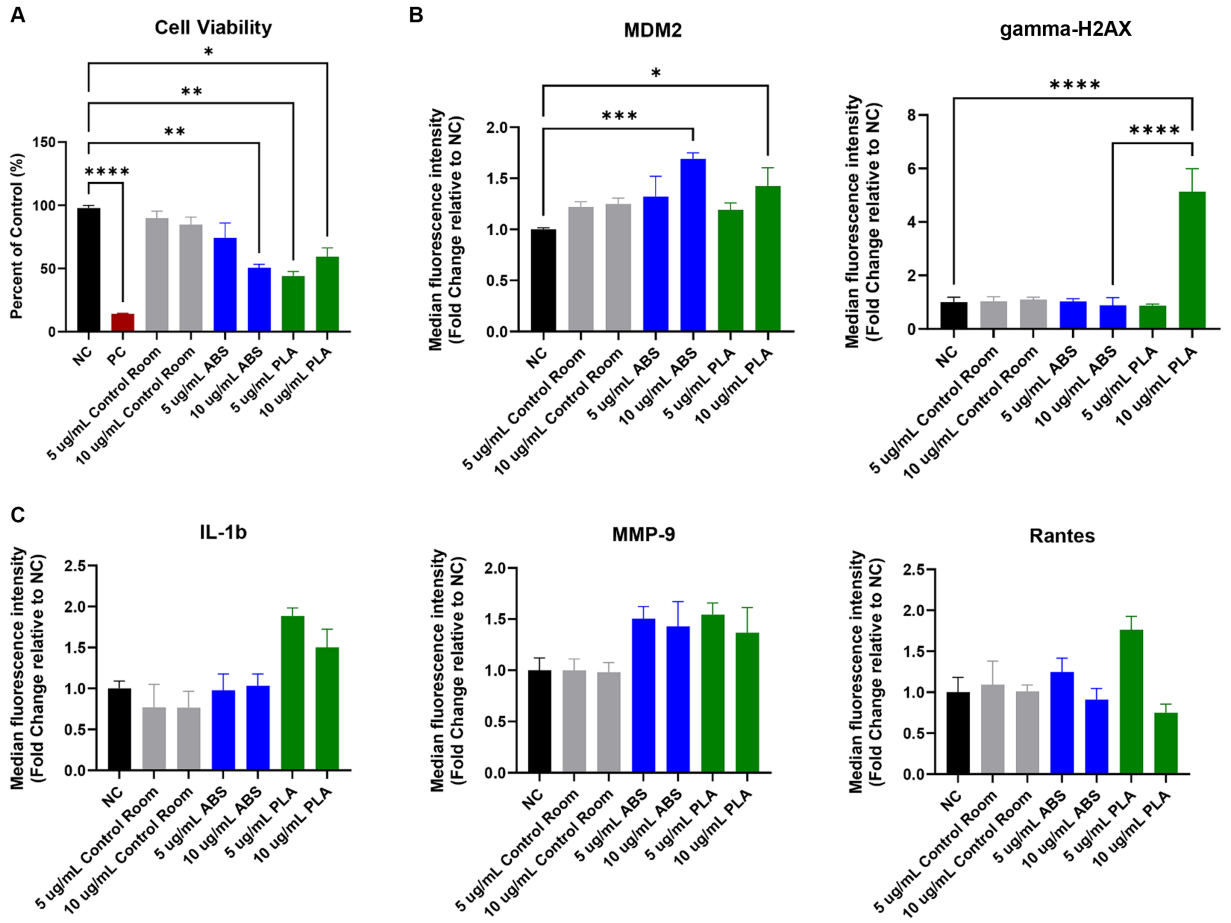

FIGURE 1
Toxicological effects of 24 h exposure to PM emitted during 3 h of 3D printing in SAEC. Each graph represents the effect of exposure to 5 μg/mL and 10 μg/mL PM collected during printing with ABS, PM collected during printing with PLA, or PM collected from the control room on **(A)** SAEC cell viability as measured by the MTS assay; **(B)** expression of DNA damage and repair markers; and **(C)** release of pro-inflammatory cytokines. Error bars represent the standard error of the mean. $n = 3–4$. *$p < 0.05$, **$p < 0.01$, ***$p < 0.001$, ****$p < 0.0001$ relative to untreated negative control cells (NC).

proteins did not change significantly in response to ABS or PLA emissions at either dose, murine double minute clone 2 (MDM2) increased upon exposure to ABS and PLA-emitted PM at 10 μg/mL. Additionally, gamma-H2AX increased in response to 10 μg/mL PM collected during PLA printing.

Effect of 3D printer emissions on release of pro-inflammatory factors

To determine the effect of exposure to PM emitted during 3D printing on inflammation, we measured a panel of 20 cytokines, chemokines, and other pro-inflammatory factors in SAEC supernatants. Exposure to ABS and PLA emissions increased the release of some pro-inflammatory cytokines relative to untreated cells, although these increases did not reach statistical significance. Specifically, exposure to PM emitted during printing with PLA increased IL-1β at both doses (Figure 1C). Exposure to PM emitted during printing with ABS and PLA at both doses increased MMP-9 release. Finally, exposure to ABS and PLA at 5 μg/mL elevated RANTES.

Effect of 3D printer emissions on the metabolome

Using HPLC MS/MS, we characterized the metabolites released by SAEC exposed to ABS, PLA, and control classroom emissions, alongside untreated negative control (NC) cells (Figure 2). Hierarchical clustering analysis (HCA) of all detected metabolites yielded separate clusters for NC, cells exposed to control classroom PM, and cells exposed to 3D printer emissions (Figure 2A). This was the case for both low (5 μg/mL) and high (10 μg/mL) exposures. This suggests that 3D printer emissions and ambient classroom air both have distinct effects on cellular metabolic profiles. Notably, in the high dose exposure, ABS and PLA-exposed cells were not clustered separately from one another, suggesting that at higher doses, printer filament types may differ less in terms of their effects on cellular metabolism.

To further examine the metabolomic responses revealed by the HCA, we identified metabolites that were significantly altered relative to NC cells at each dose for each treatment group (Figure 2B; Supplementary Tables S1–S6). SAEC exposed to PLA emissions yielded the highest number of significantly altered metabolites at both

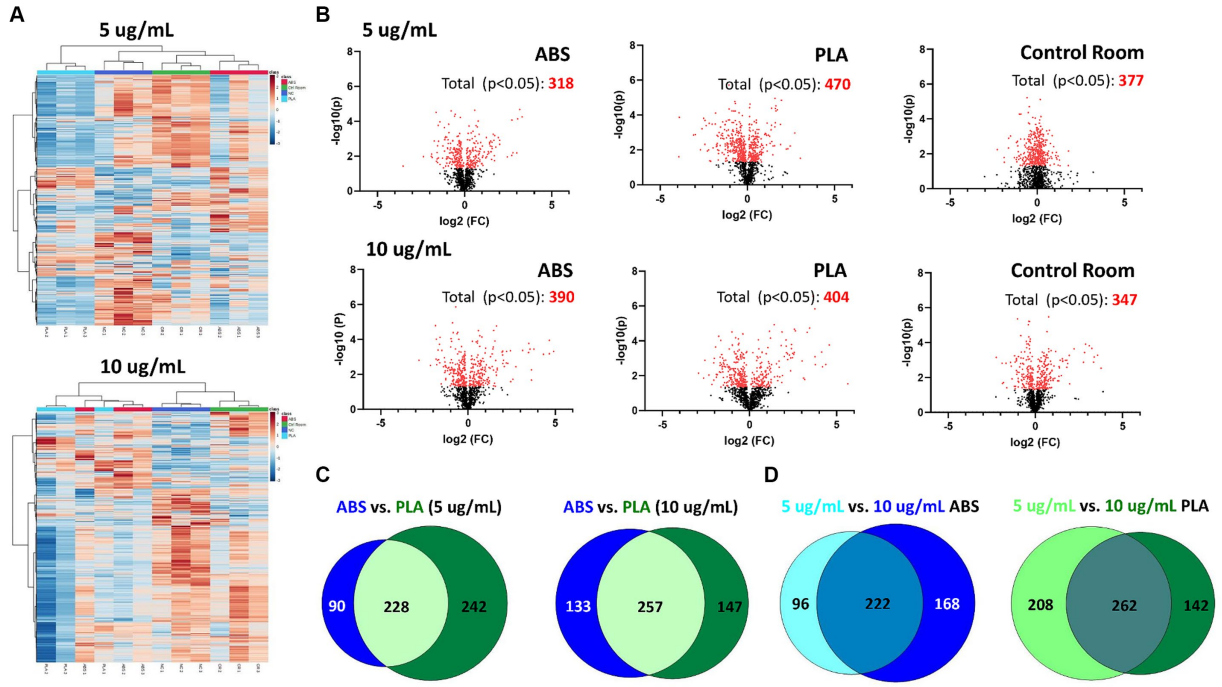

FIGURE 2
Metabolic changes in SAEC exposed to low (5 μg/mL) and high (10 μg/mL) doses of PM collected during 3D printing. **(A)** Heatmaps depict HCA of all metabolic features detected in cells exposed to ABS emissions (red), PLA emissions (light blue), control room PM (green), and untreated (NC) cells (dark blue). **(B)** Volcano plots depict the significantly altered metabolites for each exposure ($p < 0.05$ relative to NC). Venn diagrams compare the significantly altered metabolites ($p < 0.05$ relative to NC) between **(C)** each filament for a given dose and **(D)** between doses for a given filament.

the low ($n = 470$) and high ($n = 404$) dose (Figure 2B). For the low dose exposure group, this was followed by cells exposed to the control room emissions ($n = 377$) and then ABS emissions ($n = 318$). For the high dose exposure group, this was followed by cells exposed to ABS emissions ($n = 390$) and then control room emissions ($n = 347$).

We also compared the overlap in significantly altered metabolites across filaments and doses (Figures 2C,D). Although ABS and PLA-exposed cells shared 228 and 257 significantly altered metabolites at low and high doses respectively, we still identified metabolites that were uniquely altered for each filament type (Figure 2C). Additionally, 222 metabolites were shared between low and high doses for ABS, and 262 metabolites were shared between low and high doses for PLA (Figure 2D).

Pathway analysis of metabolic changes

To determine the biological significance of the metabolic changes noted above, we used the MS Peaks to Pathways module on Metaboanalyst to identify metabolic pathways that were significantly enriched in SAECs exposed to ABS emissions and PLA emissions relative to untreated negative control (NC) cells (Supplementary Tables S7–S12). Next, we compared the overlap in significantly enriched pathways between ABS and PLA filaments at each tested dose (5 μg/mL and 10 μg/mL, respectively) (Figure 3). Although ABS and PLA-exposed cells shared some significantly enriched pathways at each dose (Figures 3A,C), we also identified pathways that were uniquely enriched for each filament type (Figure 3B). At the low dose, ABS-enriched pathways were primarily related to carbohydrate metabolism, whereas PLA-enriched pathways were related to metabolism of cofactors and vitamins and amino acid metabolism (Figure 3B; Supplementary Tables S8, S9). Conversely, for the high dose exposure, ABS-enriched pathways were primarily related to amino acid metabolism, whereas PLA-enriched pathways were primarily related to carbohydrate metabolism (Figure 3B; Supplementary Tables S11, S12). These results support our differential metabolomics data by suggesting that ABS and PLA have distinct effects on cellular metabolism, this time at the pathway level.

To distinguish the effect of dose on metabolic pathway enrichment, we compared the pathways that were significantly enriched for both low and high doses of a given filament (Figure 4). Specifically, six pathways were shared between both doses for ABS (Figures 4A,C) and seven pathways were shared between both doses for PLA (Figures 4B,D), suggesting that the effects of a given 3D printer filament exposure on metabolic pathways vary greatly depending on the dose.

Discussion

In this study, we characterized and sampled particulates emitted from ABS and PLA filaments during 3 h 3D printer operation at a high school. We also exposed small airway epithelial cells (SAEC) to the sampled emissions and studied effects on cell viability, DNA damage, inflammation, and cellular metabolomics after 24 h of exposure. By evaluating a single classroom exposure and comparing across different doses, this field investigation builds on previous

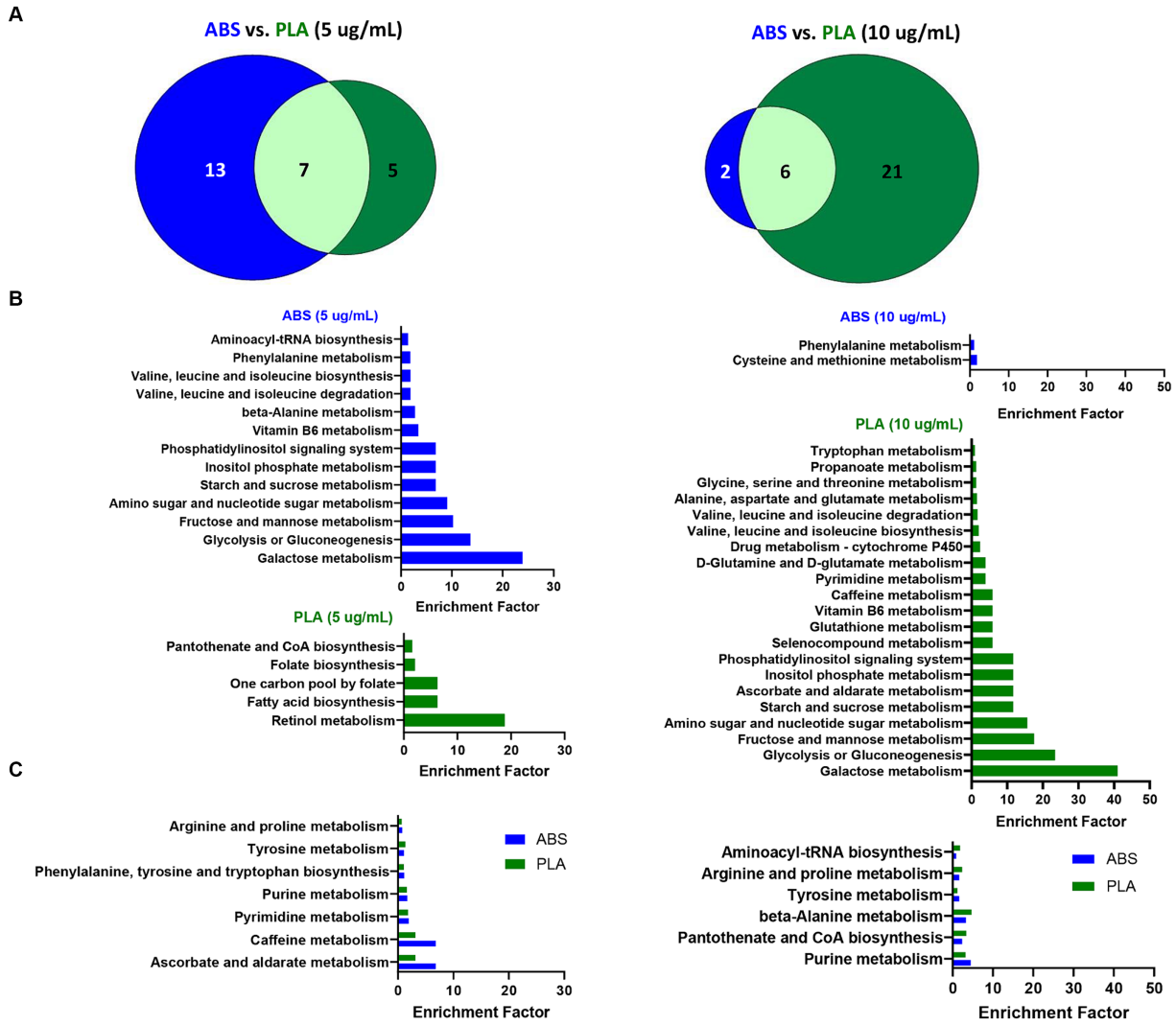

FIGURE 3
Metabolic pathways altered by ABS vs. PLA emissions at each dose. **(A)** Venn diagrams depict the overlap between significantly enriched pathways ($p < 0.05$ relative to NC cells) in ABS and PLA-exposed cells. Histograms list the significantly enriched pathways ($p < 0.05$ relative to NC cells) that were **(B)** unique to ABS or PLA and **(C)** shared between ABS and PLA.

metabolomics studies conducted in laboratory settings (20). In doing so, it reveals important insights into the potential respiratory consequences of 3D printing exposure and the metabolic changes that govern these effects.

Our toxicological data suggests that ABS and PLA-emitted PM are potentially cytotoxic and genotoxic. Specifically, exposure to emissions from both filament types reduced airway epithelial cell viability, which was previously observed in laboratory studies (16, 17, 20, 21). In addition to impacting cell viability, exposure to PM emitted from both ABS and PLA filaments increased levels of murine double minute clone 2 (MDM2), which is observed in different types of cancers and promotes genomic instability (22). Specifically, increased MDM2 can negatively regulate p53 in order to reduce DNA repair activity. Although p53 did not decrease in the present study, MDM2 can also function independently of p53 to inhibit DNA breakage repair through associating with the Mre11/Rad50/Nbs1 DNA repair complex (22). Future studies should explore the impact of ABS and PLA- emitted PM on these different mechanisms of MDM2-mediated genomic instability.

Additionally, we found that exposure to PM emitted during 3D printing with PLA filaments, but not ABS filaments, induced DNA damage in SAEC as measured by increased gamma-H2AX. Formation of gamma-H2AX occurs upon phosphorylation of the Ser-139 residue of the histone variant H2AX and is an early response to DNA double-strand breakage that recruits DNA repair proteins (23). Given that DNA damage and reduced DNA repair capacity are both involved in asthma development (24, 25), these findings reveal potential mechanisms that mediate the development of asthma-like symptoms in 3D printer users (26, 27).

In support of our toxicological data, several metabolic pathways that function during DNA damage and repair were perturbed in cells exposed to ABS and PLA-emitted PM. Specifically, purine and pyrimidine metabolism, amino sugar and nucleotide sugar metabolism, and intermediates from glucose,

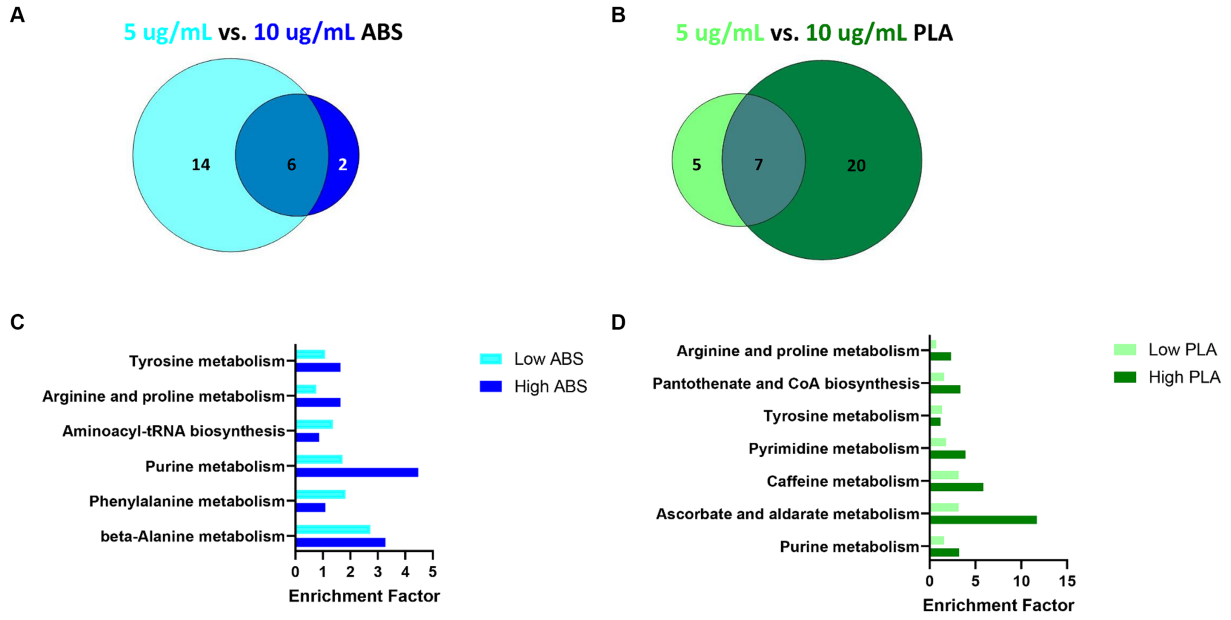

FIGURE 4
Metabolic pathways altered by low (5 μg/mL) vs. high (10 μg/mL) doses for a given filament. Venn diagrams depict the overlap between significantly enriched pathways ($p < 0.05$ relative to NC cells) in **(A)** ABS-exposed cells at each dose and **(B)** PLA-exposed cells at each dose. Histograms depict the enrichment factor for significantly enriched pathways ($p < 0.05$ relative to NC cells) that were shared between high and low doses for **(C)** ABS-exposed cells and **(D)** PLA-exposed cells.

glutamine, and aspartate metabolisms were perturbed by 3D printer filament exposure in the present study. Importantly, these metabolic pathways function to regulate the pool of nucleotides available for DNA repair (28). Additionally, ABS and PLA-emitted PM disrupted cysteine metabolism and glutathione metabolism, respectively, at the high dose, suggesting that 3D printer emissions may additionally induce genotoxicity through de-regulating redox homeostasis (28). Taken together, these results provide additional support for the potential genotoxicity of ABS and PLA-emitted PM at the level of cellular metabolism.

Additionally, exposure to 3D printer-emitted PM altered several metabolites and pathways that are implicated in respiratory disease. Specifically analysis of the serum, plasma, blood, urine, and exhaled breath condensate of asthma patients have observed dysregulated tyrosine, arginine, purine, and phenylalanine metabolites (29, 30). Arginine and phenylalanine are also dysregulated in COPD patients (31). According to an additional study, arginine expression was elevated in the plasma of patients with chronic obstructive pulmonary disease (COPD) compared to the healthy population and was further elevated in acute exacerbation of COPD (AECOPD) (32). Furthermore, pathway analysis of altered metabolites in serum samples collected from patients with allergic rhinitis revealed that purine metabolism was enriched relative to healthy controls and that the associated metabolites hypoxanthine and urate could be potential biomarkers (33). Therefore, the metabolic changes noted in this study provide early indicators that 3D printer-emitted PM may induce adverse respiratory consequences.

Moreover, several pathways that were altered by 3D printer-emitted PM in this study were also associated with PM exposure from ambient air pollution, indoor classroom air, and occupational exposures in other studies. Specifically, in patients with silicosis, arginine and proline metabolism was the major perturbed pathway relative to healthy controls (34). Furthermore, the abundance of L-arginine was negatively correlated with the predicted percentage of forced vital capacity in these patients, which is a measure of lung function. In children exposed to ambient classroom air, both $PM_{0.5}$ exposure and decreased pulmonary function were associated with dysregulated purine metabolism (35). In plasma from patients with COPD, arginine and proline metabolism was affected by $PM_{2.5}$ exposure, and arginine was positively associated with acute exacerbation of COPD (AECOPD). Taken together, these findings suggest that perturbed amino acid metabolism and purine metabolism may play a role in the adverse respiratory effects associated with 3D printer emissions exposures.

We previously found that exposure to ABS and PLA-emitted PM triggered formation of reactive oxygen species (ROS), increased total glutathione, and release of pro-inflammatory cytokines in airway epithelial cells (4, 20). Although we did not measure oxidative stress in the present study, ABS and PLA emissions exposures perturbed metabolic pathways that have previously been observed alongside PM-induced oxidative stress and inflammation, which are key events responsible for the increased risk of COPD, asthma, and other lung diseases associated with PM exposure (36, 37). Specifically, tyrosine metabolism was enriched in blood from healthy volunteers 2 h following exposure to ambient air pollution. In the same cohort, tyrosine levels correlated with fibrinogen levels, which increase in the presence of inflammation (38). Altered purine metabolism was observed alongside disrupted pro-oxidant/antioxidant balance in rodents exposed to $PM_{2.5}$ via intratracheal instillation (39). Purine metabolism was also altered in mice with $PM_{2.5}$ exposure-induced asthma. Furthermore, five inflammatory cytokines (IL-4, IL-5, IL-13, IL-1β, IL-8) were positively correlated

with levels of uric acid, which is a product of purine metabolism (40). Additionally, exposure to $PM_{2.5}$ perturbed purine metabolism and arginine and proline metabolism in BEAS-2B cells. This was coupled with significant increases in oxidative stress markers including reactive oxygen species (ROS), malondialdehyde (MDA), and nitric oxide (NO) pro-inflammatory cytokines (TNF-α, IL-6 and IL-1β), and metabolic reprogramming from oxidative phosphorylation to glycolysis (41). Furthermore, in two studies, purine metabolism and pyrimidine metabolism were enriched alongside increased alongside increases in gamma-H2AX in rats exposed to long-term low-level $PM_{2.5}$ and O_3 through ambient air pollution. Results also showed that the DNA damage biomarker gamma-H2AX in the lungs was positively correlated with ADP and N-acetyl-D-glucosamine, which are two serum metabolites involved in these pathways (42, 43). Given that 3D printers emit fine and ultrafine particles, the above studies reveal how the metabolic changes noted in this study may be mechanistically linked to respiratory symptoms reported by occupational users of 3D printers.

Our data additionally suggest that the toxicological and metabolic effects of 3D printer emissions differ depending on the filament used, with PLA impacting more of the endpoints studied. For example, although both ABS and PLA-emitted PM impacted cell viability, MDM2, and increased MMP-9, only PLA increased gamma-H2AX, IL-1β and RANTES. The metabolomic alterations observed in this study additionally support this. Specifically, PLA exposure resulted in larger numbers of significantly altered metabolites relative to ABS at both tested doses. Pathway analysis further revealed that ABS primarily altered pathways related to carbohydrate metabolism at the low dose and amino acid metabolism at the high dose. Conversely, PLA exposure altered pathways related to cofactor and vitamin metabolism at the low dose and carbohydrate metabolism at the high dose. Taken together, these results agree with our previous finding that ABS and PLA exposure perturbed different metabolic pathways (20).

A combination of physical and chemical properties of 3D printer-emitted particles was likely responsible for the filament-specific differences in cellular outcomes. PLA-emitted PM potentially produced more toxicological effects and altered more metabolites in the present study because of particle kinetics that caused a larger effective dose relative to ABS-emitted particles. Specifically, our aerosol characterization data predicted higher deposition of PLA-emitted PM relative to ABS, which was likely due to the larger size of PLA-emitted particles. In addition to size, differences in the effective density of ABS and PLA-emitted PM may have increased the effective dose of PLA-emitted PM relative to ABS when particles were dispersed in cell culture media. Specifically, particles with effective densities lower than the cell culture media will exhibit buoyancy, which may alter particle deposition and dose–response relationship (44). To support this, the raw material density of PLA is higher than the density of cell culture media ($1.25\ g/cm^3$ vs. ~$1.0\ g/cm^3$) (44–46). Conversely, ABS PM may float or settle at a lower rate in cell culture media due to a similar density ($1.05\ g/cm^3$) (47), which may have contributed to certain differences found in genotoxicity and metabolic profiling. Therefore, future studies should measure the physicochemical properties of 3D printer emissions including effective density alongside markers of genotoxicity to distinguish which filament and PM properties produce these effects.

It is important to note that this study is not without limitations. First, we were unable to control for other sources of particulate emissions in the printer room that could have resulted from classroom activities. Second, due to scheduled classroom activities, we were only allowed to sample and collect PM on restricted occasions for each experimental group. Future studies should consider more sampling occasions and duplicates to better monitor the environments. Third, we did not characterize the chemical composition of 3D printer emissions. Although we previously characterized VOCs and metals present in ABS and PLA 3D printer emissions (4, 20), future studies should measure physical and chemical properties of emissions alongside toxicological outcomes to distinguish their contributions to toxicity. Fourth, as discussed above, SAEC were exposed to PM in a submerged format, which may have altered the particle kinetics and cellular uptake of PM despite equivalent administered doses. Notably, we addressed this limitation, as well as the potential for external sources of PM in ambient air, in a previously published laboratory study by measuring metabolomic responses in cells cultured in air-liquid interface in real-time during 3D printing (20). Furthermore, SAEC were exposed to PM after sampling and extraction from filters, which raises the possibility of particle alterations due to the solvent extraction method employed. As the present study is a field study conducted in a non-laboratory setting, this limitation was unavoidable. Finally, because particulates were sampled outside of a laboratory setting, SAEC may have been subjected to bacterial contamination. To address this, we confirmed that the endotoxin levels in cells exposed to PM were below FDA limits and were not significantly different from the levels detected in untreated negative control cells. Therefore, the toxicological and metabolic changes observed in this study were likely due to PM exposure rather than due to bacterial contamination.

Conclusion

The data presented here suggest that after a single printing job in a high school classroom, 3D-printers emit fine and ultrafine particles, which may compromise cellular viability and induce genotoxic effects in airway epithelial cells. Furthermore, to determine molecular mechanisms governing these effects, we measured metabolic responses to 3D printer emissions exposure in SAEC, which varied depending on the filament used. Although SAEC metabolic responses also varied depending on the dose, we identified metabolic pathways that were enriched across both doses for a given filament. Importantly, some of these pathways play known roles in oxidative stress, DNA damage, and inflammation induced by PM exposures and are implicated in respiratory diseases such as asthma, allergic rhinitis, and COPD. Taken together, these results reveal early molecular events that may drive 3D printer-induced respiratory toxicity.

Data availability statement

The original contributions presented in the study are included in the article/Supplementary material, further inquiries can be directed to the corresponding author.

Ethics statement

Ethical approval was not required for the studies on humans in accordance with the local legislation and institutional requirements because only commercially available established cell lines were used. Ethical approval was not required for the studies on animals in accordance with the local legislation and institutional requirements because only commercially available established cell lines were used.

Author contributions

LB: Formal analysis, Investigation, Visualization, Writing – original draft, Writing – review & editing. QZ: Formal analysis, Investigation, Writing – review & editing. SS: Investigation, Visualization, Writing – review & editing. SA: Formal analysis, Investigation, Writing – review & editing. JS: Writing – review & editing, Conceptualization, Formal analysis, Investigation. MB: Writing – review & editing. CW: Conceptualization, Investigation, Supervision, Writing – review & editing.

Funding

The author(s) declare that no financial support was received for the research, authorship, and/or publication of this article.

Acknowledgments

The authors would like to acknowledge the support of the Purdue Metabolite Profiling Facility for their technical support in generating the data presented with the manuscript.

Conflict of interest

The authors declare that the research was conducted in the absence of any commercial or financial relationships that could be construed as a potential conflict of interest.

Publisher's note

All claims expressed in this article are solely those of the authors and do not necessarily represent those of their affiliated organizations, or those of the publisher, the editors and the reviewers. Any product that may be evaluated in this article, or claim that may be made by its manufacturer, is not guaranteed or endorsed by the publisher.

Supplementary material

The Supplementary material for this article can be found online at: https://www.frontiersin.org/articles/10.3389/fpubh.2024.1408842/full#supplementary-material

References

1. Kim Y, Yoon C, Ham S, Park J, Kim S, Kwon O, et al. Emissions of nanoparticles and gaseous material from 3D printer operation. *Environ Sci Technol*. (2015) 49:12044–53. doi: 10.1021/acs.est.5b02805

2. Azimi P, Zhao D, Pouzet C, Crain NE, Stephens B. Emissions of ultrafine particles and volatile organic compounds from commercially available desktop three-dimensional printers with multiple filaments. *Environ Sci Technol*. (2016) 50:1260–8. doi: 10.1021/acs.est.5b04983

3. Yi J, LeBouf RF, Duling MG, Nurkiewicz T, Chen BT, Schwegler-Berry D, et al. Emission of particulate matter from a desktop three-dimensional (3D) printer. *J Toxic Environ Health A*. (2016) 79:453–65. doi: 10.1080/15287394.2016.1166467

4. Zhang Q, Pardo M, Rudich Y, Kaplan-Ashiri I, Wong JPS, Davis AY, et al. Chemical composition and toxicity of particles emitted from a consumer-level 3D printer using various materials. *Environ Sci Technol*. (2019) 53:12054–61. doi: 10.1021/acs.est.9b04168

5. Kwon H-S, Ryu MH, Carlsten C. Ultrafine particles: unique physicochemical properties relevant to health and disease. *Exp Mol Med*. (2020) 52:318–28. doi: 10.1038/s12276-020-0405-1

6. Stefaniak AB, LeBouf RF, Yi J, Ham J, Nurkewicz T, Schwegler-Berry DE, et al. Characterization of chemical contaminants generated by a desktop fused deposition modeling 3-dimensional printer. *J Occup Environ Hyg*. (2017) 14:540–50. doi: 10.1080/15459624.2017.1302589

7. Zhang Q, Weber RJ, Luxton TP, Peloquin DM, Baumann EJ, Black MS. Metal compositions of particle emissions from material extrusion 3D printing: emission sources and indoor exposure modeling. *Sci Total Environ*. (2023) 860:160512. doi: 10.1016/j.scitotenv.2022.160512

8. Tedla G, Jarabek AM, Byrley P, Boyes W, Rogers K. Human exposure to metals in consumer-focused fused filament fabrication (FFF)/3D printing processes. *Sci Total Environ*. (2022) 814:152622. doi: 10.1016/j.scitotenv.2021.152622

9. Davis A., Black M, Zhang Q, Wong J, Weber R. Fine particulate and chemical emissions from desktop 3D printers. In NIP & Digital Fabrication Conference. (2016). Society for Imaging Science and Technology Virginia, VA, USA.

10. Davis AY, Zhang Q, Wong JPS, Weber RJ, Black MS. Characterization of volatile organic compound emissions from consumer level material extrusion 3D printers. *Build Environ*. (2019) 160:106209. doi: 10.1016/j.buildenv.2019.106209

11. Azimi P, Fazli T, Stephens B. Predicting concentrations of ultrafine particles and volatile organic compounds resulting from desktop 3D printer operation and the impact of potential control strategies. *J Ind Ecol*. (2017) 21:S107–19. doi: 10.1111/jiec.12578

12. Zhang Q, Black MS. Exposure hazards of particles and volatile organic compounds emitted from material extrusion 3D printing: Consolidation of chamber study data. *Environ Int*. (2023) 182:108316. doi: 10.1016/j.envint.2023.108316

13. Byrley P, George BJ, Boyes WK, Rogers K. Particle emissions from fused deposition modeling 3D printers: evaluation and meta-analysis. *Sci Total Environ*. (2019) 655:395–407. doi: 10.1016/j.scitotenv.2018.11.070

14. Vance ME, Pegues V, van Montfrans S, Leng W, Marr LC. Aerosol emissions from fuse-deposition modeling 3D printers in a chamber and in real indoor environments. *Environ Sci Technol*. (2017) 51:9516–23. doi: 10.1021/acs.est.7b01546

15. Jeon H, Park J, Kim S, Park K, Yoon C. Effect of nozzle temperature on the emission rate of ultrafine particles during 3D printing. *Indoor Air*. (2020) 30:306–14. doi: 10.1111/ina.12624

16. Zhang Q, Wong JPS, Davis AY, Black MS, Weber RJ. Characterization of particle emissions from consumer fused deposition modeling 3D printers. *Aerosol Sci Technol*. (2017) 51:1275–86. doi: 10.1080/02786826.2017.1342029

17. Farcas MT, Stefaniak AB, Knepp AK, Bowers L, Mandler WK, Kashon M, et al. Acrylonitrile butadiene styrene (ABS) and polycarbonate (PC) filaments three-dimensional (3-D) printer emissions-induced cell toxicity. *Toxicol Lett*. (2019) 317:1–12. doi: 10.1016/j.toxlet.2019.09.013

18. Stefaniak A, LeBouf RF, Duling MG, Yi J, Abukabda AB, McBride CR, et al. Inhalation exposure to three-dimensional printer emissions stimulates acute hypertension and microvascular dysfunction. *Toxicol Appl Pharmacol*. (2017) 335:1–5. doi: 10.1016/j.taap.2017.09.016

19. Chan F, House R, Kudla I, Lipszyc JC, Rajaram N, Tarlo SM. Health survey of employees regularly using 3D printers. *Occup Med*. (2018) 68:211–4. doi: 10.1093/occmed/kqy042

20. He X, Barnett LM, Jeon J, Zhang Q, Alqahtani S, Black M, et al. Real-time exposure to 3D-printing emissions elicits metabolic and pro-inflammatory responses in human airway epithelial cells. *Toxics*. (2024) 12:67. doi: 10.3390/toxics12010067

21. Fang R, Mohammed AN, Yadav JS, Wang J. Cytotoxicity and characterization of ultrafine particles from desktop three-dimensional printers with multiple filaments. *Toxics*. (2023) 11:720. doi: 10.3390/toxics11090720

22. Zhao Y, Yu H, Hu W. The regulation of MDM2 oncogene and its impact on human cancers. *Acta Biochim Biophys Sin*. (2014) 46:180–9. doi: 10.1093/abbs/gmt147

23. Valdiglesias V, Giunta S, Fenech M, Neri M, Bonassi S. γH2AX as a marker of DNA double strand breaks and genomic instability in human population studies. *Mutat Res*. (2013) 753:24–40. doi: 10.1016/j.mrrev.2013.02.001

24. Chan TK, Loh XY, Tan DWS, Engelward BP, Wong FWS. O21-the role of DNA damage and repair in allergic airway inflammation. *Clin Transl Allergy*. (2014) 4:1. doi: 10.1186/2045-7022-4-S1-O21

25. Chan TK, Loh XY, Peh HY, Tan WNF, Tan WSD, Li N, et al. House dust mite–induced asthma causes oxidative damage and DNA double-strand breaks in the lungs. *J Allergy Clin Immunol*. (2016) 138:84–96.e1. e1. doi: 10.1016/j.jaci.2016.02.017

26. Gümperlein I, Fischer E, Dietrich-Gümperlein G, Karrasch S, Nowak D, Jörres RA, et al. Acute health effects of desktop 3D printing (fused deposition modeling) using acrylonitrile butadiene styrene and polylactic acid materials: an experimental exposure study in human volunteers. *Indoor Air*. (2018) 28:611–23. doi: 10.1111/ina.12458

27. House R, Rajaram N, Tarlo S. Case report of asthma associated with 3D printing. *Occup Med*. (2017) 67:652–4. doi: 10.1093/occmed/kqx129

28. Turgeon M-O, Perry NJ, Poulogiannis G. DNA damage, repair, and cancer metabolism. *Front Oncol*. (2018) 8:15. doi: 10.3389/fonc.2018.00015

29. Pite H, Aguiar L, Morello J, Monteiro E, Alves AC, Bourbon M, et al. Metabolic dysfunction and asthma: current perspectives. *J Asthma Allergy*. (2020) 13:237–47. doi: 10.2147/JAA.S208823

30. Wang C, Jiang S, Zhang S, Ouyang Z, Wang G, Wang F. Research progress of metabolomics in asthma. *Meta*. (2021) 11:567. doi: 10.3390/metabo11090567

31. Ran N, Pang Z, Gu Y, Pan H, Zuo X, Guan X, et al. An updated overview of metabolomic profile changes in chronic obstructive pulmonary disease. *Meta*. (2019) 9:111. doi: 10.3390/metabo9060111

32. Yu T, Wu H, Huang Q, Dong F, Li X, Zhang Y, et al. Outdoor particulate matter exposure affects metabolome in chronic obstructive pulmonary disease: preliminary study. *Front Public Health*. (2023) 11:1069906. doi: 10.3389/fpubh.2023.1069906

33. Ma GC, Wang TS, Wang J, Ma ZJ, Pu SB. Serum metabolomics study of patients with allergic rhinitis. *Biomed Chromatogr*. (2020) 34:e4739. doi: 10.1002/bmc.4739

34. Xue C, Wu N, Fan Y, Ma J, Ye Q. Distinct metabolic features in the plasma of patients with silicosis and dust-exposed workers in China: a case–control study. *BMC Pulm Med*. (2021) 21:1–10. doi: 10.1186/s12890-021-01462-1

35. Liu S, Huang Q, Chen C, Song Y, Zhang X, Dong W, et al. Joint effect of indoor size-fractioned particulate matters and black carbon on cardiopulmonary function and relevant metabolic mechanism: a panel study among school children. *Environ Pollut*. (2022) 307:119533. doi: 10.1016/j.envpol.2022.119533

36. Thangavel P, Park D, Lee Y-C. Recent insights into particulate matter (PM2. 5)-mediated toxicity in humans: an overview. *Int J Environ Res Public Health*. (2022) 19:7511. doi: 10.3390/ijerph19127511

37. Valavanidis A, Vlachogianni T, Fiotakis K, Loridas S. Pulmonary oxidative stress, inflammation and cancer: respirable particulate matter, fibrous dusts and ozone as major causes of lung carcinogenesis through reactive oxygen species mechanisms. *Int J Environ Res Public Health*. (2013) 10:3886–907. doi: 10.3390/ijerph10093886

38. Vlaanderen J, Janssen NA, Hoek G, Keski-Rahkonen P, Barupal DK, Cassee FR, et al. The impact of ambient air pollution on the human blood metabolome. *Environ Res*. (2017) 156:341–8. doi: 10.1016/j.envres.2017.03.042

39. Wang X, Jiang S, Liu Y, du X, Zhang W, Zhang J, et al. Comprehensive pulmonary metabolome responses to intratracheal instillation of airborne fine particulate matter in rats. *Sci Total Environ*. (2017) 592:41–50. doi: 10.1016/j.scitotenv.2017.03.064

40. Wang Z, Gao S, Xie J, Li R. Identification of multiple dysregulated metabolic pathways by GC-MS-based profiling of lung tissue in mice with PM2. 5-induced asthma. *Chemosphere*. (2019) 220:1–10. doi: 10.1016/j.chemosphere.2018.12.092

41. Song Y, Li R, Zhang Y, Wei J, Chen W, Chung CKA, et al. Mass spectrometry-based metabolomics reveals the mechanism of ambient fine particulate matter and its components on energy metabolic reprogramming in BEAS-2B cells. *Sci Total Environ*. (2019) 651:3139–50. doi: 10.1016/j.scitotenv.2018.10.171

42. Xu J, Zhang Q, Su Z, Liu Y, Yan T, Zhang Y, et al. Genetic damage and potential mechanism exploration under different air pollution patterns by multi-omics. *Environ Int*. (2022) 170:107636. doi: 10.1016/j.envint.2022.107636

43. Xu J, Liu Y, Zhang Q, Su Z, Yan T, Zhou S, et al. DNA damage, serum metabolomic alteration and carcinogenic risk associated with low-level air pollution. *Environ Pollut*. (2022) 297:118763. doi: 10.1016/j.envpol.2021.118763

44. Watson C, DeLoid GM, Pal A, Demokritou P. Buoyant nanoparticles: implications for nano-biointeractions in cellular studies. *Small*. (2016) 12:3172–80. doi: 10.1002/smll.201600314

45. Poon C. Measuring the density and viscosity of culture media for optimized computational fluid dynamics analysis of in vitro devices. *J Mech Behav Biomed Mater*. (2022) 126:105024. doi: 10.1016/j.jmbbm.2021.105024

46. Farah S, Anderson DG, Langer R. Physical and mechanical properties of PLA, and their functions in widespread applications—a comprehensive review. *Adv Drug Deliv Rev*. (2016) 107:367–92. doi: 10.1016/j.addr.2016.06.012

47. Schmitz D, Ecco LG, Dul S, Pereira ECL, Soares BG, Barra GMO, et al. Electromagnetic interference shielding effectiveness of ABS carbon-based composites manufactured via fused deposition modelling. *Mater Today Commun*. (2018) 15:70–80. doi: 10.1016/j.mtcomm.2018.02.034

frontiers | Frontiers in Public Health

TYPE Review
PUBLISHED 15 July 2024
DOI 10.3389/fpubh.2024.1390099

OPEN ACCESS

EDITED BY
Annangi Balasubramanyam,
Autonomous University of Barcelona, Spain

REVIEWED BY
Becky Hess,
Pacific Northwest National Laboratory (DOE), United States
Shamali De Silva,
Environmental Protectio Authority (EPA), Australia
Yi Gao,
Shanxi Medical University, China

*CORRESPONDENCE
Gang Zhang
✉ zhanggangbbmm@126.com
Xiangming Huang
✉ 13607717704@163.com
Peizheng Xiong
✉ xiongpeizheng@cdutcm.edu.cn

†These authors have contributed equally to this work

RECEIVED 22 February 2024
ACCEPTED 03 July 2024
PUBLISHED 15 July 2024

CITATION
Wang F, Zhou L, Mu D, Zhang H, Zhang G, Huang X and Xiong P (2024) Current research on ecotoxicity of metal-based nanoparticles: from exposure pathways, ecotoxicological effects to toxicity mechanisms.
Front. Public Health 12:1390099.
doi: 10.3389/fpubh.2024.1390099

Current research on ecotoxicity of metal-based nanoparticles: from exposure pathways, ecotoxicological effects to toxicity mechanisms

Fang Wang[1†], Li Zhou[2†], Dehong Mu[2], Hui Zhang[2], Gang Zhang[3*], Xiangming Huang[4*] and Peizheng Xiong[2*]

[1]Department of Ophthalmology, Chengdu First People's Hospital, Chengdu, China, [2]Department of Torhinolaryngology, Hospital of Chengdu University of Traditional Chinese Medicine, Chengdu, China, [3]Department of Oncology, Chengdu Second People's Hospital, Chengdu, China, [4]Department of Otorhinolaryngology, The First Affiliated Hospital of Guangxi University of Traditional Chinese Medicine, Nanning, China

Metal-based nanoparticles have garnered significant usage across industries, spanning catalysis, optoelectronics, and drug delivery, owing to their diverse applications. However, their potential ecological toxicity remains a crucial area of research interest. This paper offers a comprehensive review of recent advancements in studying the ecotoxicity of these nanoparticles, encompassing exposure pathways, toxic effects, and toxicity mechanisms. Furthermore, it delves into the challenges and future prospects in this research domain. While some progress has been made in addressing this issue, there is still a need for more comprehensive assessments to fully understand the implications of metal-based nanoparticles on the environment and human well-being.

KEYWORDS

metal-based NPs, exposure pathway, toxic effects, toxicity mechanisms, review

1 Introduction

Metal-based nanoparticles (NPs) are metal-based particles with nanometric dimensions. Due to their exceptionally large specific surface area, these particles possess exceptional physicochemical properties, including catalysis, light absorption and magnetic properties (1–3). Metal-based NPs have diverse applications in electronic devices, energy storage, and conversion (4–6). For example, FeN_4 graphite nanosheets show promise for improving oxygen electrocatalytic activity and durability in zinc-air batteries (7); and gold NPs (AuNPs), for the photothermal enhancement of tumor vascular destruction (8). Copper sulfide NPs are an inexpensive and widely available plasma material that exhibits high photothermal conversion efficiency, making it suitable for solar evaporation and water purification applications (9). Fe_7Se_8 NPs supported on nitrogen-doped carbon nanofibers are utilized as a high-rate anode material for sodium ion batteries (10).

However, there are also potential risks to the environment and human well-being associated with the widespread use of metal-based NPs. Metal-based NPs can be released into the environment during manufacture, use and disposal and then cause ecotoxicity through various exposure pathways (11). The ecotoxicity of metal-based NPs refers to their adverse

effects on the survival, growth, and reproduction of organisms in the environment, including microorganisms, plants, and animals. The mechanisms of ecotoxicity include physical and chemical effects such as oxidative stress, DNA damage, and Cell membrane damage (12, 13). Research on the ecotoxicity of metal-based NPs is still in its infancy, and there are many challenges in the research process. The first challenge is how to measure the exposure of metal-based NPs to organisms. Metal-based NPs are difficult to measure due to their small size and aggregation properties. The second challenge is how to accurately assess the toxicity of metal-based NPs. Metal-based NPs have different toxicities in different organisms and under different conditions. Therefore, it is necessary to conduct toxicological experiments under controlled conditions to obtain accurate toxicity data.

In this review, we summarize recent advances in ecotoxicity studies of metal-based NPs, including their exposure pathways, ecotoxicological effects and toxicity mechanisms. For metal-based NPs of natural origin, their toxicity may differ from that of synthetic NPs. Naturally occurring NPs are often encapsulated or stabilized by other substances found in nature, which may affect their biological activity and toxicity. In addition, natural NPs are often less concentrated and have evolved and dispersed in the environment over a long period of time, which may have reduced their potential toxicity. Since there are relatively few toxicity studies on natural metal-based NPs, we focus on the ecotoxicity of engineered metal-based NPs. We also discuss the challenges and prospects for ecotoxicity studies of metal-based NPs and how to comprehensively assess the impact of metal-based NPs on the environment and human health (Figure 1).

2 Exposure pathways to metal-based NPs

Due to the distinctive characteristics of NPs, their impact on organisms is expected to manifest through various exposure pathways (14). NPs are small in size and can thus pass through the cell membrane, cytoplasm, and nucleus, entering directly into the cell interior, making its mode of exposure significantly different from that of other particles (15–17). Generally, NPs enter the organism through absorption, diffusion, contact, and binding. This exposure mode can largely reflect the direct effects of NPs on organisms.

2.1 Exposure pathways of aquatic organisms enrichment

The enrichment exposure pathway of metal-based NPs in aquatic ecosystems is a matter of great concern. These NPs may have far-reaching effects on aquatic organisms and the entire ecosystem due to their unique physical and chemical properties.

First, metal-based NPs can enter aquatic organisms through direct contact. Metal-based NPs enter freshwater ecosystems through wastewater discharges and agricultural runoff. These NPs, such as copper and gold, can be taken up by tissues within aquatic organisms and accumulate, leading to the transfer of metals from aquatic to terrestrial ecosystems (Figure 2) (18). In addition, the presence of organic matter can influence the behavior and toxicity of metal-based NPs, for example, it can reduce the toxicity of AgNPs to bacteria and protozoa (19). This suggests that the bioaccumulation process of metal-based NPs is influenced by organic matter in the environment.

Metal-based NPs can also spread in aquatic ecosystems through biotransfer mechanisms. Biotransfer is the process by which one organism transfers substances from the environment to another organism (20). For example, AgNPs can be transferred and biomagnified to Tetrahymena thermophila through the food chain (19). In addition, the transformation, bioavailability, and toxic effects of metal-oxide-based NPs in fresh water on invertebrates suggest a potential risk of their delivery in the food chain (21).

Finally, the ability of metal-based NPs to bioaccumulate and biomagnify depends on a variety of factors, including the physicochemical properties of the NPs, the physiological properties of the organism, and environmental conditions. For example, studies of the accumulation dynamics of silver NPs with different coatings in simple freshwater food chains have shown that diet is the main uptake pathway for silver NPs (22). The ability of marine invertebrates to bioaccumulate heavy metals is also influenced by their physiological and biochemical processes.

2.2 Exposure pathways of plant enrichment

The pathways of plant uptake of metal-based NPs mainly include roots, leaves and other ways, which are affected by various factors such as the physicochemical properties of metal-based NPs, environmental conditions, and plant species and size.

2.2.1 Absorption of metal-based NPs by leaves

Metal-based NPs can enter the plant through adsorption and penetration on the leaf surface. For example, studies on gold NPs (AuNPs) have shown that smaller-sized AuNPs (3, 10 nm) adhere more readily to leaf surfaces and are able to penetrate more efficiently through the epidermal layer into the plant compared to polyvinylpyrrolidone (PVP) coatings (23). In addition, the physicochemical properties of the NPs, such as size, surface charge, and chemical composition, affect their uptake and transport in the leaf (Figure 3) (24).

2.2.2 Uptake of metal-based NPs by plant roots

Plant roots are another important pathway for metal-based NPs to enter the plant. The Fe(II) transporter protein encoded by the iron-regulated transporter (IRT1) gene was found in *Arabidopsis thaliana*, suggesting that plants can take up divalent Fe ions from roots via specific transporter proteins (24). In addition, some metal-based NPs, such as AgNPs, can also enter the plant via root uptake and may affect the physiological activity of the plant (25).

2.2.3 Translocation of metal-based NPs in the plant vascular system

Once metal-based NPs enter the plant, they can be translocated through the plant's vascular system. Studies have shown that metal-based NPs can be efficiently translocated from leaves to other parts of the plant, such as shoots and roots (23). This process may involve complex mechanisms within the plant, including metal transport involving organic molecules (26).

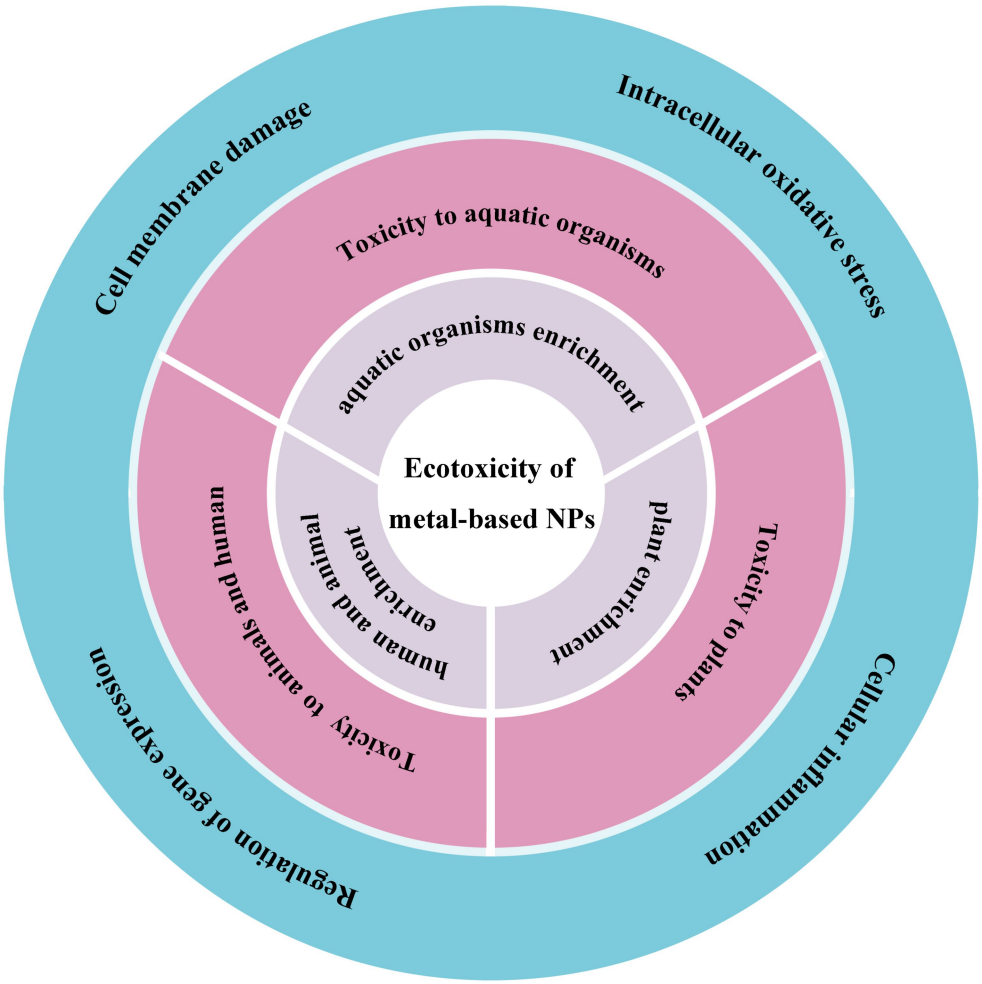

FIGURE 1
The schematic shows the ecotoxicity induced by metal-based NPs from the exposure pathways (grey), ecotoxicological effects (pink) to toxicity mechanisms (blue).

2.3 Exposure pathways of human and animal enrichment

Animals are exposed to metal-based NPs in a variety of ways, including inhalation, oral and dermal contact. These exposure modes reflect the behavior of NPs in the environment and their migration pathways within the organism, as well as their potential impact on the health of the organism. Therefore, these different exposure pathways need to be considered when assessing the effects of NPs on animal health.

2.3.1 Inhalation exposure to metal-based NPs

Inhalation is a primary means of exposure to metal-based NPs, particularly in occupational settings or laboratories, where individuals may inhale them through respiration (27). Inhalation toxicity is mainly dependent on the physical and chemical properties of NPs, such as particle size, shape, surface chemistry, and biological activity (28, 29). The inhalation toxicity of metal-based NPs is closely related to their particle size, as demonstrated by inhalation toxicity studies. Generally, NPs with smaller particle sizes are more likely to penetrate the cell membrane and enter the cell interior, thus causing greater harm to the human body. Here, we summarize the inhalation exposure to some metal-based NPs (Table 1).

For instance, Zhu et al. (37) compared the toxic effects of iron oxide NPs of different sizes on the lungs and found that nanosized Fe_2O_3 particles increased the microvascular permeability and cell lysis in the lung epithelium and significantly interfered with coagulation parameters compared with submicron Fe_2O_3 particles. Another study found that the deposition distribution of AuNPs in the lungs was age independent, that AuNPs was mainly deposited in the lung bases and cleared by mucus, and that in the long term, the clearance of AuNPs in the lungs and secondary organs was mainly mediated by macrophages (38).

The production of industrially manufactured TiO_2 NPs is on the rise, posing a growing threat of inhalation exposure to professionals and consumers. Kreyling et al. (39) investigated the 28-day biokinetic pattern of the inhaled nanoparticulate material TiO_2 NPs and found that NPs are redistributed within the alveoli over a long period through alveolar macrophage-mediated scavenging and reentry into alveolar epithelial cells. In addition, significant time-dependent differences were found in the accumulation and clearance process of TiO_2 NPs *in vivo* compared with aerosol particles of the same size.

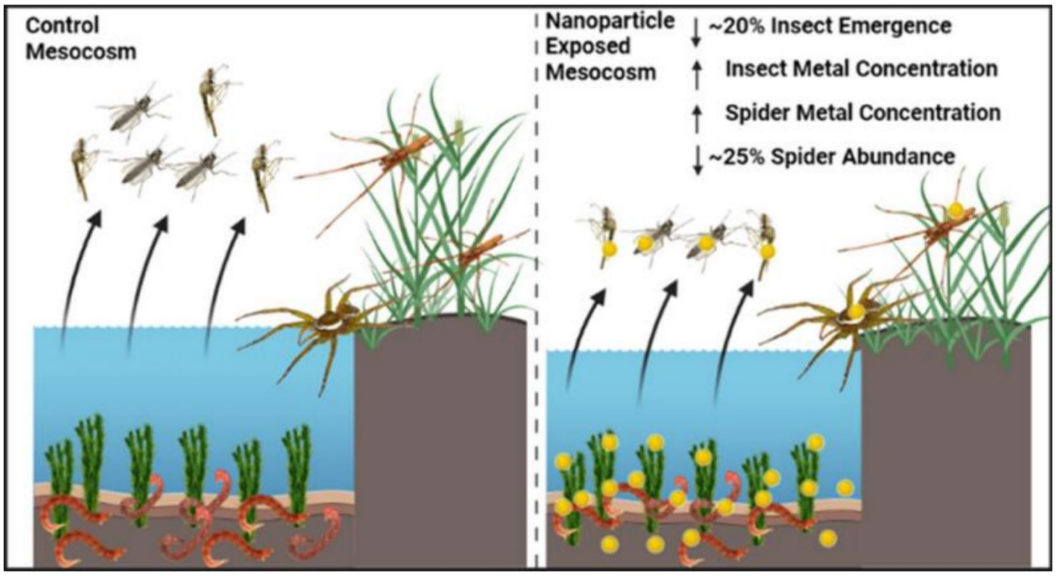

FIGURE 2
Schematic representation of the transfer of metal-based NPs from aquatic to terrestrial ecosystems (18). Copyright 2023, American chemical society.

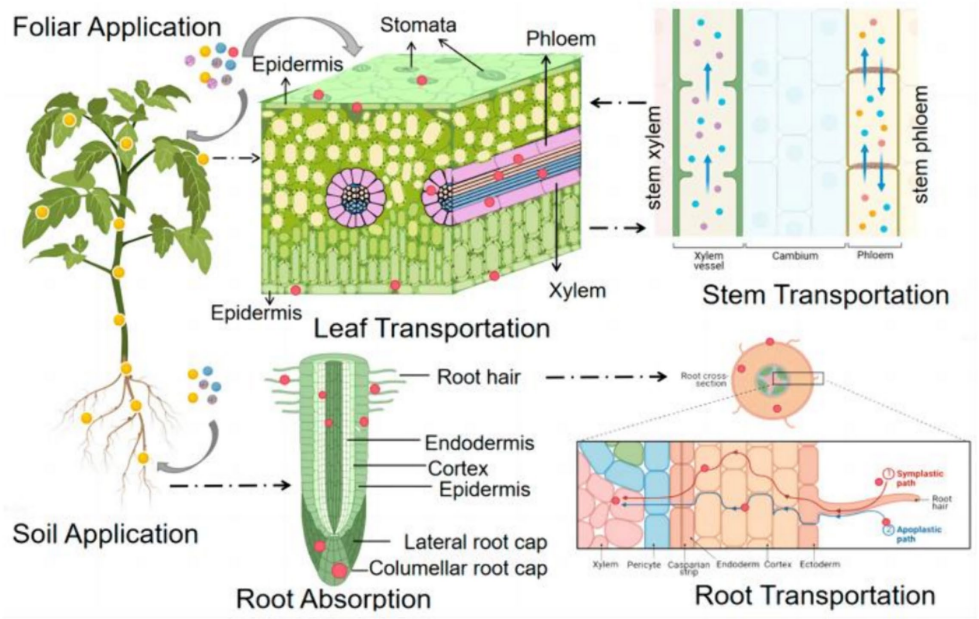

FIGURE 3
A schematic diagram of the uptake and translocation of NPs in plants through foliar application or root exposure treatment (24). Copyright 2023, Molecular Diversity Preservation International (MDPI).

In addition, Kim et al. (40) conducted research on inhaled nanomixes and found that the removal of Silver NPs (AgNPs) followed a two-phase model with rapid and slow dissolution rates, while the removal of AuNPs could be described by a single-phase model with a longer half-life. When exposed to both AuNPs and AgNPs, it was observed that the removal of AgNPs was affected by the presence of AuNPs. This change may be due to various interactions between AgNPs and AuNPs that influenced the solubilization and/or mechanical removal of AgNPs *in vivo*. After inhalation exposure, a minor proportion of the inhaled AgNPs dose that reaches the lungs is rapidly eliminated within the initial 72 h. The remaining portion of the dose is then slowly excreted. It appears that the inhaled dose cleared from the lungs is transferred to the body's circulation between 48 and 72 h after inhalation (41).

2.3.2 Oral ingestion exposure to metal-based NPs

Metal-based NPs may be ingested during production and use, especially in food and pharmaceuticals. After oral ingestion of

TABLE 1 Inhalation exposure to some metal-based NPs.

Materials	Dose (mg)	Model	Typical effects	Ref.
In_2O_3	0.05–0.6	Rats	Lung damage	(30)
ZnO	0–1	Monkeys	Pulmonary inflammatory	(31)
La_2O_3	0.5–10	Rats	Alveolar proteinosis	(32)
NiO	0.1, 0.2	Rats	Alveolar macrophages damage	(33)
WC	10	Rats	Pulmonary toxicity	(34)
MnO_2	15, 30	Rats	Altered spontaneous cortical activity	(35)
Fe_2O_3	0.014–0.128	Mice	DNA strand breaks	(36)

metal-based NPs, they may adhere to the gastrointestinal tract mucosa, causing local inflammation, ulcers, and other adverse reactions, and enter the blood system, causing damage to other organs and tissues (42–44). For example, some studies have shown that oral administration of TiO_2 NPs, which are commonly used as food additives in candies, chocolates, and beverages, can affect the course of acute colitis and exacerbate the onset, prolong the course, and inhibit the recovery of ulcerative colitis (Figure 4) (45).

By contrast, Jones et al. (46) examined the gastrointestinal absorption of NPs in humans and *in vitro* using titanium dioxide as a model compound. They compared the behavior of NPs with larger particles and found no evidence that TiO_2 NPs were more easily absorbed into the gut than micron-sized particles. Tang et al. (47) compared the detailed toxicity of copper NPs with $CuCl_2•2H_2O$ (copper ions) *in vivo*. They also examined the oral toxicity of four sizes of copper particles (30 n, 50 nm, 80 nm, and 1 μm) in rats. The researchers compared acute LD50 values of $CuCl_2•2H_2O$ and other copper materials under acute exposure. After administering a single equivalent dose (200 mg/kg) of five copper materials, researchers evaluated the kinetics of copper and found that the acute toxic effects produced by Cu NPs were strongly associated with particle size. Furthermore, repeated exposure to copper NPs produced toxic effects that differed from those observed with single exposure. The size of the NPs may be responsible for the organ-targeting effects. This could explain the observed differences in organ-specific accumulation. Here, we summarize the Oral ingestion exposure to some metal-based NPs (Table 2).

2.4 Dermal exposure to metal-based NPs

Metal-based NPs may have irritating effects on the skin and cause skin inflammation and allergic reactions. Some studies have shown that these NPs may adhere to the skin surface, have toxic effects on skin cells, and induce skin inflammation and allergic reactions. In addition, metal-based NPs may enter the body through broken skin and cause damage and irritation to deeper skin cells and tissues (52, 53). AuNPs are used for many applications, but available data are lacking on their dermal absorption. Filon et al. (54) conducted experiments utilizing the Franz diffusion cell technique to examine the penetration of intact and compromised human skin by AuNPs. Their findings revealed that AuNPs are capable of permeating human skin in an *in vitro* diffusion cell system. The growing utilization of palladium NPs (PdNPs) in various chemical processes, jewelry production, electronic gadgets, automotive catalytic converters, and medical uses has resulted in a notable rise in palladium exposure. Exposure of the skin to palladium can lead to allergic contact dermatitis. For example, Filon et al. (55) found that PdNPs can significantly penetrate the skin.

3 Toxic effects of metal-based NPs

The widespread use of metal-based NPs has also led to their potential toxic effects on organisms. Such ecotoxicity effects are closely related to factors such as the type, size, surface properties, and concentration and exposure duration of NPs. Herein, we summarize various ecotoxicity effects such as toxicity to aquatic organisms, plants, animals and human.

3.1 Toxicity of metal-based NPs to aquatic organisms

In recent years, scholars have begun to focus on the toxic effects of metal-based NPs on aquatic organisms, and have achieved certain results. Current studies have mainly concentrated on the toxic effects of metal-based NPs on aquatic animals. However, research has shown that these NPs have various effects on aquatic organisms (56–58). The toxic effects of metal-based NPs on aquatic organisms are complex and diverse. The degree of toxicity varies depending on the type of metal-based NPs, with each type possessing unique physical, chemical, morphological, and biological characteristics that influence their impact on aquatic organisms.

3.1.1 Toxicity to fish

Studies have shown that the amount of NPs in the water column and the form in which they are present in the water column can have an effect on fish. Marinho et al. (59) conducted an analysis on the impact of exposure to various AgNPs concentrations on zebrafish tissues, discovering a substantial reduction in acetylcholinesterase (AChE) activities in both the brain and muscle. Another study observed that exposure to AgNPs decreased levels of l-histidine, l-isoleucine, and l-phenylalanine, crucial amino acids in fish gills. This suggests that AgNPs may disrupt amino acid metabolism, potentially affecting fish health and function. Furthermore, AgNPs altered citric acid levels, possibly disrupting the citrate cycle, essential for energy production. This disruption could lead to decreased energy production and metabolic dysfunction in fish gills. The present findings stress the potential consequences of AgNPs on fish metabolism, emphasizing the requirement for more research on the

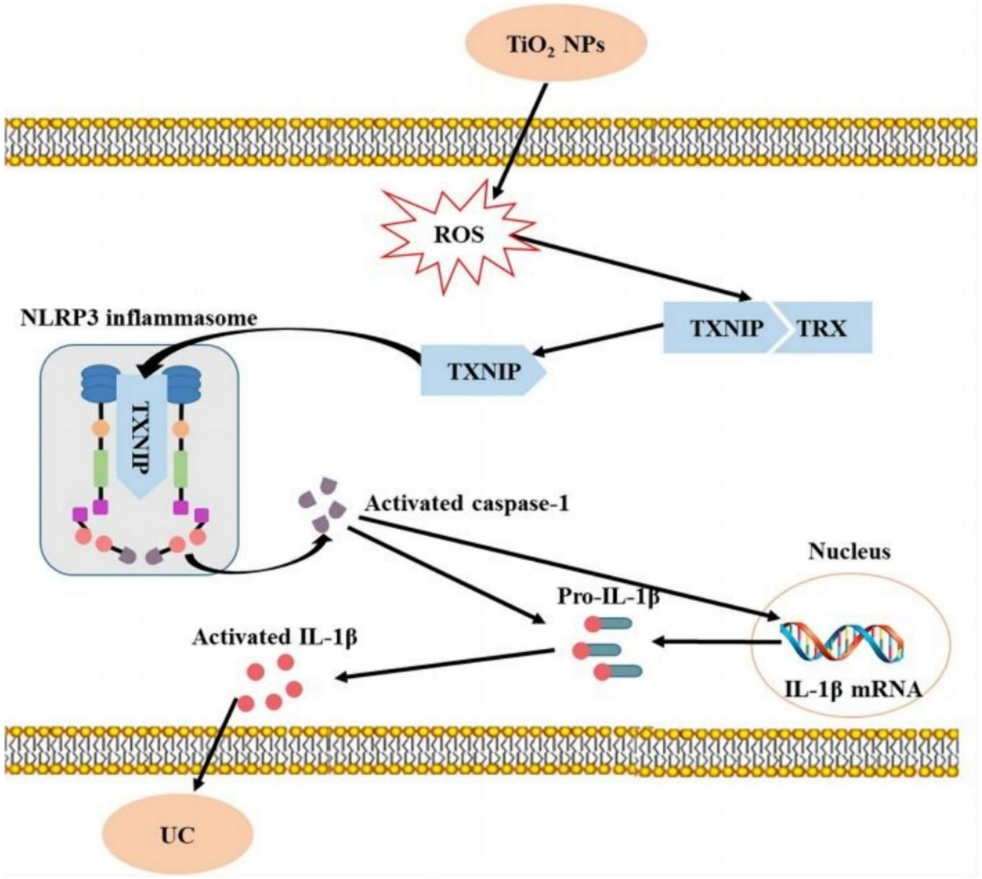

FIGURE 4
Short-term intake of TiO_2 NPs induces mild colitis and exacerbates the development of ulcerative colitis (45). Copyright 2023, Springer Nature.

TABLE 2 Oral ingestion exposure to some metal-based NPs.

Materials	Dose (mg)	Model	Typical effects	Ref.
TiO_2	0–300	Mice	Prolonging the UC course	(45)
Cu	60–180	Rats	Fetal development	(48)
MgO	250–1,000	Rats	Genotoxicity	(49)
Y_2O_3	30–480	Rats	Apparent genotoxicity	(50)
NiO	500–1,000	Rats	Metabolic abnormality	(51)

effects of NP exposure on aquatic lifeforms (Figure 5) (60). Another study on TiO_2 NPs revealed that the treatment dose of these NPs was directly linked to increased motility and bacterial population in water. Notably, the zebrafish exhibited a significant rise in the bacterial load in its gills and caudal fins (61).

3.1.2 Toxicity to shellfish

As an important component of aquatic animals, the health status of shellfish is of great significance in maintaining the stability of the entire ecosystem. Shellfish have a strong bioconcentration effect on heavy metals and other pollutants and show different degrees of enrichment patterns in different sea areas. Elevated levels of ZnO NPs had a significant impact on various physiological parameters in the thick-shelled mussel, *Mytilus coruscus*. These effects included a decrease in total hematocrit, phagocytosis, esterase, and lysosomal contents, as well as an increase in hematocrit and ROS levels. Furthermore, the combination of high ZnO NPs concentrations and low pH had a negative synergistic effect on the mussels (62). AgNPs are frequently used in consumer products due to their antimicrobial and exceptional properties, leading to increasing concerns about their potential impact on aquatic ecosystems. Duroudier et al. (62) found that PVP/PEI-coated AgNPs ingested through the food web accumulated significantly in mussel tissues and adversely affected cell and tissue levels in autumn and spring. Furthermore, the total hematocrit, phagocytosis, esterase, and lysosomal contents of mussels were found to decrease at low pH and elevated concentrations of TiO_2 NPs. Conversely, the hematocrit and ROS levels were observed to increase with increasing TiO_2 NPs concentration under low pH conditions (63). The majority of recent studies have primarily concentrated on the toxic effects of individual metal NPs on mussels. However, further research is required to comprehensively examine the toxic impact of metal NPs on mussels as a whole.

3.2 Toxicity of metal-based NPs to plants

In recent years, the ecotoxicological response of plants to NPs has gradually become a research topic. The toxicity of metal-based NPs to

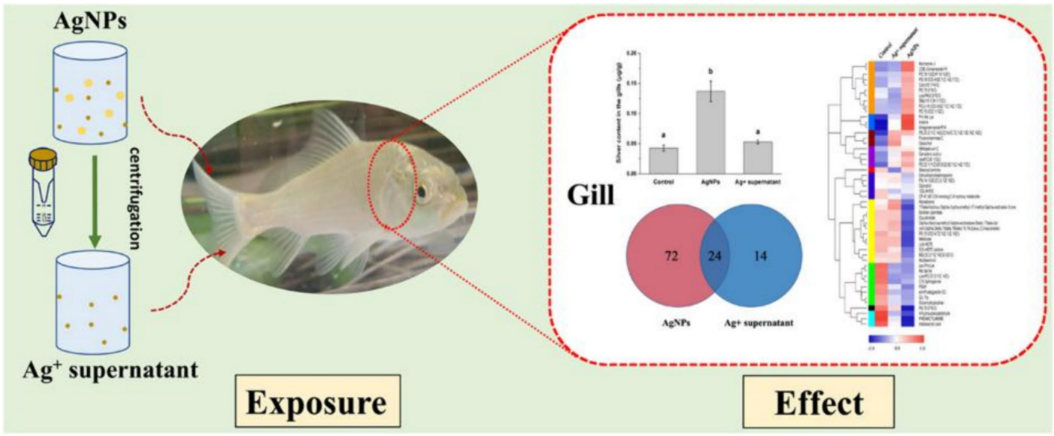

FIGURE 5
Schematic diagram of nano-silver toxicity in carp gills (60). Copyright 2021, Elsevier.

plants is mainly manifested in two aspects: plant growth inhibition and the influence of plant metabolic processes.

3.2.1 Plant growth inhibition

Plant growth is affected by several factors, including soil, temperature, moisture, and light. Although soil is the most significant factor impacting plant growth, certain NPs can also exhibit inhibitory effects on plants. During the early growth stage, the inhibitory effect of NPs on plants is primarily manifest as a suppression of germination and seedling development (64, 65). For example, Zhang et al. (66) carried out research into the influence of ZnO NPs on the germination of seeds and the growth of roots in maize and cucumber. Their findings indicated that the inhibitory effect of ZnO NPs on root growth in maize was predominantly attributed to the NPs, as opposed to the Zn^{2+} ions. Conversely, the Zn ions released from ZnO only inhibited root elongation in cucumber. The toxicity level of ZnO NPs was found to be dependent on its concentration (67). The phytotoxicity ranking shows that CuO NPs have the highest toxicity, followed by the binary mixture (CuO + ZnO) NPs, and then ZnO NPs. This significant toxicity and uptake in germinating seedlings is observed when exposure concentrations exceed 10 mg/L (Figure 6) (68).

3.2.2 Influence on plant metabolic processes

When metal-based NPs are introduced into plants, they enter the cell and affect plant metabolic processes by altering the intracellular environment. Chloroplasts, mitochondria, and peroxisomes, which have high oxidative metabolic activity and electron flow rates, are the primary sources of ROS in plant cells. The production of ROS by these organelles can lead to lipid peroxidation, membrane fluidity and permeability changes, and nutrient acquisition difficulties, ultimately impeding overall plant growth and development. NPs can also affect these processes, causing further damage to plant cells (69). In addition, metal-based NPs can affect the metabolites of secondary metabolites such as amino acids (Figure 7) (70). NPs have the potential to induce DNA damage, including DNA mismatch damage, DNA strand breaks, and chromosome damage. TiO_2 NPs are known to be especially detrimental in this regard (70).

3.3 Toxicity of metal-based NPs to animals

The toxicity of NPs can be attributed to their physicochemical properties, such as size, surface chemistry, and redox potential, and is associated with the dissolution and release of toxic metals. Metal-based NPs are significantly toxic to human, including to the immune system (48, 71, 72).

For example, metal-based NPs can cause structural and functional damages to the ovary and testis. One research study discovered that Cu NPs induced both intrinsic and extrinsic apoptotic pathways in oxidative stress-induced ovarian dysfunction and controlled important ovarian genes, leading to harm to ovarian tissue (73). Subsequent study has shown that Cu NPs are a greater threat to reproduction than copper particles. This is due to the direct damage caused by Cu NPs to the ovary and their impact on ovarian hormone metabolism (74). Yang et al. (75) discovered that exposure to CdSe/ZnS quantum dots impairs the repair of double-strand breaks in spermatocytes, disrupts meiotic progression, and causes apoptosis and reduced sperm production.

Indeed, the potential for NPs to cross the alveolar-capillary barrier and enter the bloodstream, thereby reaching other organs, is a legitimate concern. For example, Nemmar et al. (76) discovered that mice exposed to CeO_2 NPs exhibited a dose-dependent infiltration of inflammatory cells, including macrophages and neutrophils, in their lung sections. These findings suggest that acute lung exposure to CeO_2 NPs triggers pulmonary and systemic inflammation, oxidative stress, and promotes *in vivo* thrombus formation. Similarly, TiO_2 NPs exhibit size-dependent genotoxicity, with smaller particles being more significantly toxic (77). Kim et al. (30) found that a single inhalation exposure to anosized indium oxide (In_3O_2) resulted in worsening of lung damage such as chronic active inflammation, foamy macrophage infiltration, and granulomas. Early-onset and persistent pulmonary alveolar proteosis, even at very low doses, indicates an urgent need to reassess occupationally recommended exposure limits for In_3O_2 NPs to protect workers.

Compared with ordinary metal ions, metal-based NPs are more likely to penetrate into cell membranes or cells, causing excessive generation of intracellular superoxide anions, damaging membrane integrity and thus causing oxidative damage leading to cell death, and resulting in toxic effects on the digestive and nervous systems, among others (78, 79).

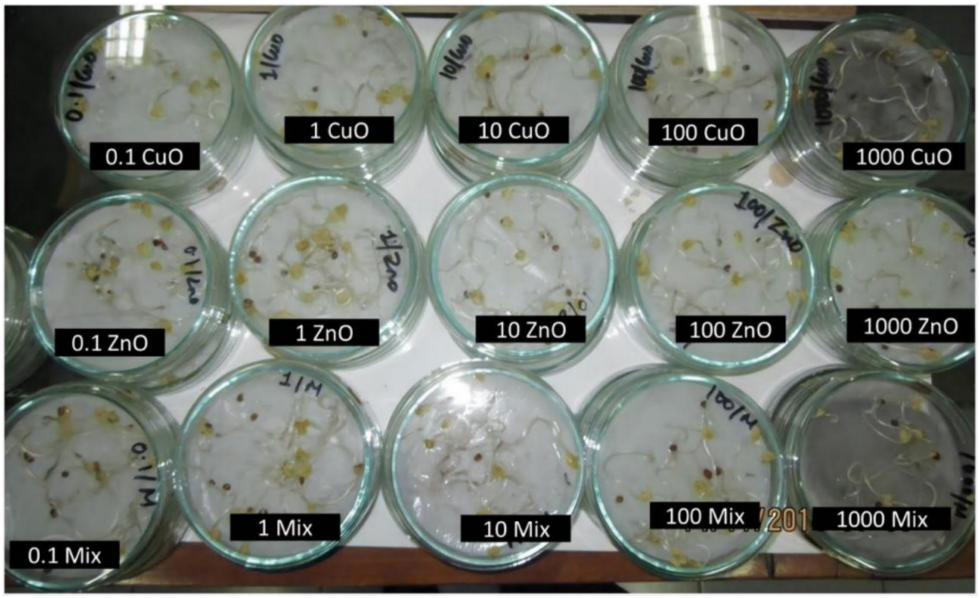

FIGURE 6
Images showing radish seedlings exposed to varying concentrations of different NPs (68). Copyright 2019, Springer Nature.

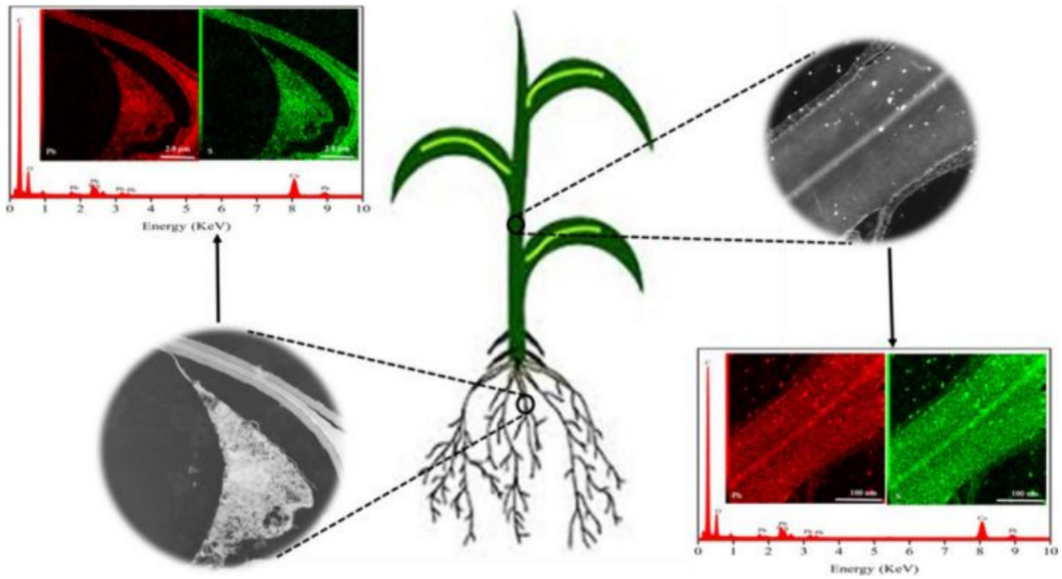

FIGURE 7
Diagram of the uptake of PbS NPs in plants (70). Copyright 2020, Elsevier.

3.4 Toxicity of metal-based NPs to human

These metal-based NPs, particularly noble metals such as gold, silver and platinum, have shown significant potential in the treatment of various diseases, including cancer, pneumonia and Parkinson's disease, due to their unique optoelectronic properties and ease of surface functionalisation (80, 81).

However, metal-based NPs can enter the human body through multiple pathways and affect different tissues and systems. Its toxic effects are multifaceted and include effects on the immune system, cytotoxicity and genotoxicity. For example, copper oxide NPs are able to activate the production of reactive oxygen species and pro-inflammatory cytokines in human lung epithelial cells (82), whereas silver, gold, and platinum NPs can enter the human body through therapeutic applications and cause damage to erythrocytes, including hemolysis, agglutination, and membrane damage (83). In addition, metal-based NPs can affect the systemic system by being deposited through the respiratory tract and taken up by phagocytes in

the lung (84). It can enter the human body through skin exposure, and although the skin barrier prevent the penetration of NPs to some extent, it has been shown that NPs are able to cross the skin barrier under certain conditions (85, 86).

Notably, the morphology of metal-based nanoparticles has a significant effect on the toxicity of skin pathogens and HaCaT keratinocytes. It was shown that the toxicity of different shapes of AgNPs to bacteria and HaCaT cells varied, with truncated plate-shaped AgNPs showing the highest cytotoxicity (87). The biodistribution and metabolic consequences of metal-based NPs have also been the focus of research. Several studies have shown that metal-based NPs can migrate *in vivo* to locations far from the site of administration, requiring careful monitoring of their migration pathways and potential toxic effects (88). For example, inhaled ultrafine manganese oxide NPs can migrate to the central nervous system via the olfactory nerve pathway, causing inflammatory changes (89).

For human exposure assessment of metal-based NPs, a comprehensive approach is needed to consider their safety. For example, a study of Italian nanomaterials workers developed a human biomonitoring method based on single-particle inductively coupled plasma mass spectrometry to assess the level of NPs exposure in the workplace (Figure 8) (90).

4 Toxicity mechanisms of metal-based NPs

The mechanism of toxicity for metal-based NPs is multifaceted and intricate. In terms of the interaction between NPs and living organisms, the size and shape of metal-based NPs have a significant impact on their interactions with cells. For instance, smaller NPs tend to accumulate more easily in cells, potentially causing damage to cellular structures and disrupting normal cell function. Furthermore, the surface properties of metal-based NPs can influence their interactions with proteins and other biomolecules, leading to adverse effects on cell health. Therefore, a better understanding of the mechanisms underlying the toxicity of metal-based NPs is essential for the development of effective safety measures and the design of more biocompatible materials (91, 92).

4.1 Cell membrane damage

The cell membrane is a barrier for the exchange of substances inside and outside the cell, preventing harmful substances from entering the cell and protecting the internal structure of the cell. Studies have shown that metal-based NPs may cause direct damage to the cell membrane, resulting in altered cell membrane permeability (93), the disruption of cell membrane integrity (94), and the alteration of cell membrane structure (95), among others. For example, zinc oxide NPs induce toxicity by affecting cell wall integrity pathways, mitochondrial function, and lipid homeostasis in *Saccharomyces cerevisiae* (96). Chen et al. (12) studied the biological effects of TiO_2 NPs on the unicellular green alga *Chlamydomonas reinhardtii*. The cell surface morphology of *Chlamydomonas reinhardtii* was found to be altered on scanning electron microscopy, indicating that photocatalytic TiO_2 NPs disrupted the cell surface.

4.2 Intracellular oxidative stress

In a normal environment, intracellular ROS are generated at a low production rate and rapidly eliminated by antioxidant defense systems such as glutathione and antioxidant enzymes, thus maintaining cellular redox balance. However, when ROS are overproduced, the redox reaction becomes unbalanced, triggering a series of biochemical reactions that lead to cellular damage (97, 98). The mechanism of action of metal-based NPs is, on the one hand, to increase the production of ROS, and the generation of excess ROS is the precursor to oxidative damage effects. Direct contact of NPs with the mitochondria or storage

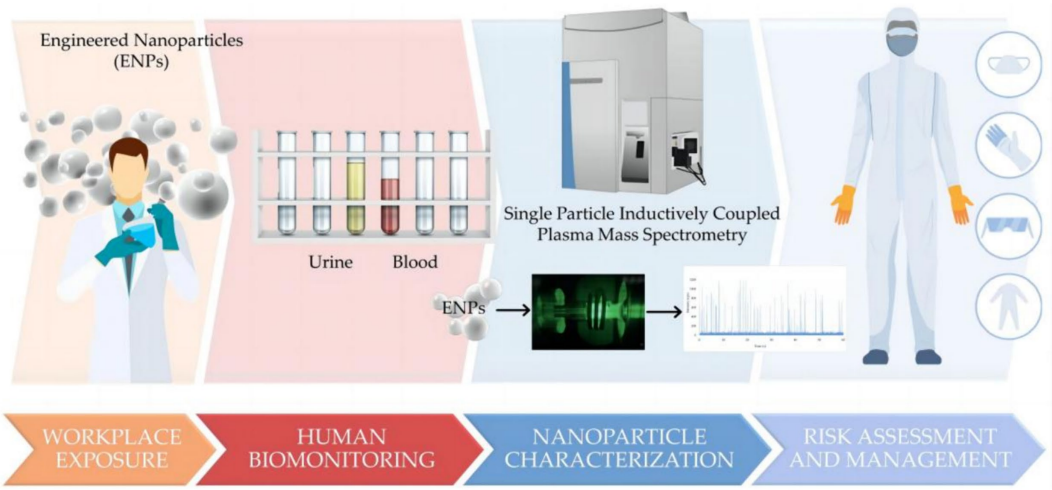

FIGURE 8
A human biomonitoring method based on single particle inductively coupled plasma mass spectrometry (90). Copyright 2023, Molecular Diversity Preservation International (MDPI).

in the acidic environment of lysosomes allows for the direct cellular production of ROS (99, 100). On the other hand, metal-based NPs cause the intracellular antioxidant enzyme system to be underproduced. The antioxidant enzyme system includes superoxide dismutase, catalase, and glutathione peroxidase (101, 102). For example, when Ag NPs are used as a stressor, *Cryptobacterium hidradii* nematodes can regulate oxidative stress through the p38 MAPK pathway (103).

4.3 Cellular inflammation

NF-κB-regulated inflammatory response plays an important role in the differentiation, value addition, and expression of biological proteins and biological enzymes. When mouse hearts were exposed to TiO_2 NPs, cardiomyocyte swelling and inflammatory cell infiltration were observed, as a significant increase in NF-κB promoted the expression of IL-1β and TNF-α (104). Another study revealed that ZnO NPs play an important role in regulating the inflammatory response of vascular endothelial cells through NF-κB signaling, which may be important for the treatment of vascular diseases (105). The inflammatory response of ZnO NPs was also confirmed in another study (106). In addition, metal oxide NPs can activate human lung epithelial cells to produce ROS and pro-inflammatory cytokines such as interleukin 8 and granulocyte-macrophage colony-stimulating factor, which activate and recruit immune cells (82).

4.4 Regulation of gene expression

Abnormalities in gene expression levels can be caused by mutations, environmental factors, or dysregulation of intracellular regulatory mechanisms (107, 108). For example, metal-based NPs may interfere with gene transcription, affecting the binding of DNA to RNA polymerase, leading to abnormal gene transcription, which in turn affects protein expression and function (109). Alternatively, they may affect the DNA methylation status, which in turn affects the regulation of gene expression. Methylation is an important mode of gene expression regulation, and metal-based NPs may affect gene expression and function by altering the DNA methylation state (13).

5 Challenges and prospects for the ecotoxicity of metal-based NPs

Some progress has been made in the research on the ecotoxicity of metal-based NPs, but there are still many challenges and problems to be solved. First, the ecotoxicity assessment of metal-based NPs requires an integrated assessment approach. Integrated biomarker response has been shown to be an effective tool for assessing the toxic effects of metal-based NPs on environmental biomass. In addition, computational toxicology applications such as quantitative structure–activity relationships and read across techniques are important for predicting nanotoxicity and filling data gaps. Second, it is necessary to strengthen the research on the interactions and mechanisms between metal-based NPs and living organisms, including their direct effects on living organisms and potential risks. In addition, experimental studies and field investigations should be actively conducted to assess the potential impacts of metal-based NPs on the environment and human health.

In order to manage the ecotoxicity risks of metal-based NPs, appropriate regulatory measures need to be developed. This includes the classification and labelling of nanomaterials and the setting of hazard threshold levels for human health and the environment. Furthermore, research should focus on increasing the body's resistance to the harmful effects of metal-based nanoparticles in order to mitigate their potential toxic effects.

To achieve this goal, interdisciplinary collaboration is essential, involving researchers from a wide range of fields, including chemistry, physics, biology, and environmental sciences, to promote the in-depth development of ecotoxicity research on metal-based NPs. Looking ahead, with continuous progress and innovation in science and technology, we are confident that the impacts of metal-based NPs on the environment and human health can be better understood and controlled. At the same time, there is a need to strengthen public education on scientific literacy, improve public awareness and understanding of nanotechnology, and promote the sustainable development and application of nanotechnology.

Author contributions

FW: Formal analysis, Investigation, Writing – review & editing, Writing – original draft. LZ: Data curation, Resources, Writing – review & editing, Writing – original draft. DM: Data curation, Writing – review & editing. HZ: Formal analysis, Writing – review & editing. GZ: Conceptualization, Resources, Writing – review & editing. XH: Conceptualization, Resources, Writing – review & editing. PX: Conceptualization, Resources, Writing – review & editing, Writing – original draft.

Funding

The author(s) declare financial support was received for the research, authorship, and/or publication of this article. This study is jointly supported by funding from (1) the National Natural Science Foundation of China (52102340); (2) Xinglin Talent Program of Chengdu University of TCM (330023085); (3) Scientific Project of Hospital of Chengdu University of Traditional Chinese Medicine (No. 21ZL01); and (4) Sichuan Provincial Administration of Traditional Chinese Medicine Research Project (2023MS300).

Conflict of interest

The authors declare that the research was conducted in the absence of any commercial or financial relationships that could be construed as a potential conflict of interest.

Publisher's note

References

1. Liu J, Huang J, Zhang L, Lei J. Multifunctional metal-organic framework heterostructures for enhanced cancer therapy. *Chem Soc Rev*. (2021) 50:1188–218. doi: 10.1039/d0cs00178c

2. Wu D, Kusada K, Yamamoto T, Toriyama T, Matsumura S, Kawaguchi S, et al. Platinum-group-metal high-entropy-alloy nanoparticles. *J Am Chem Soc*. (2020) 142:13833–8. doi: 10.1021/jacs.0c04807

3. Rezania S, Kamboh MA, Arian SS, Al-Dhabi NA, Arasu MV, Esmail GA, et al. Conversion of waste frying oil into biodiesel using recoverable nanocatalyst based on magnetic graphene oxide supported ternary mixed metal oxide nanoparticles. *Bioresour Technol*. (2021) 323:124561. doi: 10.1016/j.biortech.2020.124561

4. Wang Y, Lin Z, Ma J, Wu Y, Yuan H, Cui D, et al. Multifunctional solar-blind ultraviolet photodetectors based on p-PCDTBT/n-Ga2O3 heterojunction with high photoresponse. *InfoMat*. (2023) 6:e12503. doi: 10.1002/inf2.12503

5. Yan X, Zhang Y, Fang Z, Sun Y, Liu P, Sun J, et al. A multimode-fused sensory memory system based on a robust self-assembly nanoscaffolded BaTiO3:Eu2O3 memristor. *InfoMat*. (2023) 5:e12429. doi: 10.1002/inf2.12429

6. Xiong P, Huang X, Ye N, Lu Q, Zhang G, Peng S, et al. Cytotoxicity of metal-based nanoparticles: from mechanisms and methods of evaluation to pathological manifestations. *Adv Sci*. (2022) 9:2106049. doi: 10.1002/advs.202106049

7. Xiao M, Xing Z, Jin Z, Liu C, Ge J, Zhu J, et al. Preferentially engineering FeN(4) edge sites onto graphitic Nanosheets for highly active and durable oxygen Electrocatalysis in rechargeable Zn-air batteries. *Adv Mater*. (2020) 32:e2004900. doi: 10.1002/adma.202004900

8. Hong S, Zheng D, Zhang C, Huang Q, Cheng S, Zhang X. Vascular disrupting agent induced aggregation of gold nanoparticles for photothermally enhanced tumor vascular disruption. *Sci Adv*. (2020) 6:eabb0020. doi: 10.1126/sciadv.abb0020

9. Zhang Q, Yin X, Zhang C, Li Y, Xiang K, Luo W, et al. Self-assembled Supercrystals enhance the Photothermal conversion for solar evaporation and water purification. *Small*. (2022) 18:e2202867. doi: 10.1002/smll.202202867

10. Zhang DM, Jia JH, Yang CC, Jiang Q. Fe7Se8 nanoparticles anchored on N-doped carbon nanofibers as high-rate anode for sodium-ion batteries. *Energy Storage Mater*. (2019) 24:439–49. doi: 10.1016/j.ensm.2019.07.017

11. Santos J, Barreto A, Fernandes C, Silva ARR, Cardoso DN, Pinto E, et al. A comprehensive Ecotoxicity study of molybdenum disulfide Nanosheets versus bulk form in soil organisms. *Nano*. (2023) 13:3163. doi: 10.3390/nano13243163

12. Chen X, Lu R, Liu P, Li X. Effects of Nano-TiO2 on *Chlamydomonas reinhardtii* cell surface under UV,Natural light conditions. *J Wuhan Univ Technol*. (2017) 32:6. doi: 10.1007/s11595-017-1583-0

13. Patil NA, Gade WN, Deobagkar DD. Epigenetic modulation upon exposure of lung fibroblasts to TiO_2 and ZnO nanoparticles: alterations in DNA methylation. *Int J Nanomedicine*. (2016) 11:4509–19. doi: 10.2147/IJN.S110390

14. Sharma VK, Filip J, Zboril R, Varma RS. Natural inorganic nanoparticles--formation, fate, and toxicity in the environment. *Chem Soc Rev*. (2015) 44:8410–23. doi: 10.1039/c5cs00236b

15. Panja P, Jana NR. Arginine-terminated nanoparticles of <10 nm size for direct membrane penetration and protein delivery for straight access to cytosol and nucleus. *J Phys Chem Lett*. (2020) 11:2363–8. doi: 10.1021/acs.jpclett.0c00176

16. Hollóczki O, Gehrke S. Can Nanoplastics Alter cell membranes? *ChemPhysChem*. (2020) 21:9–12. doi: 10.1002/cphc.201900481

17. Yong X, Du K. Effects of shape on interaction dynamics of tetrahedral Nanoplastics and the cell membrane. *J Phys Chem B*. (2023) 127:1652–63. doi: 10.1021/acs.jpcb.2c07460

18. Perrotta BG, Simonin M, Colman BP, Anderson SM, Baruch E, Castellon BT, et al. Chronic engineered nanoparticle additions Alter insect emergence and result in metal flux from aquatic ecosystems into riparian food webs. *Environ Sci Technol*. (2023) 57:8085–95. doi: 10.1021/acs.est.3c00620

19. Liang D, Fan W, Wu Y, Wang Y. Effect of organic matter on the trophic transfer of silver nanoparticles in an aquatic food chain. *J Hazard Mater*. (2022) 438:129521. doi: 10.1016/j.jhazmat.2022.129521

20. Peng C, Zhang W, Gao H, Li Y, Tong X, Li K, et al. Behavior and potential impacts of metal-based engineered nanoparticles in aquatic environments. *Nano*. (2017) 7:21. doi: 10.3390/nano7010021

21. Wang T, Liu W. Emerging investigator series: metal nanoparticles in freshwater: transformation, bioavailability and effects on invertebrates. *Environ Sci Nano*. (2022) 9:2237–63. doi: 10.1039/d2en00052k

22. Kalman J, Paul KB, Khan FR, Stone V, Fernandes TF. Characterisation of bioaccumulation dynamics of three differently coated silver nanoparticles and aqueous silver in a simple freshwater food chain. *Environ Chem*. (2015) 12:662. doi: 10.1071/en15035

23. Avellan A, Yun J, Zhang Y, Spielman-Sun E, Unrine JM, Thieme J, et al. Nanoparticle size and coating chemistry control foliar uptake pathways, translocation, and leaf-to-rhizosphere transport in wheat. *ACS Nano*. (2019) 13:5291–305. doi: 10.1021/acsnano.8b09781

24. Wang X, Xie H, Wang P, Yin H. Nanoparticles in plants: uptake, transport and physiological activity in leaf and root. *Materials*. (2023) 16:3097. doi: 10.3390/ma16083097

25. Levard C, Hotze EM, Lowry GV, Brown GEJ. Environmental transformations of silver nanoparticles: impact on stability and toxicity. *Environ Sci Technol*. (2012) 46:6900–14. doi: 10.1021/es2037405

26. Alvarez-Fernández A, Díaz-Benito P, Abadía A, López-Millán A, Abadía J. Metal species involved in long distance metal transport in plants. *Front Plant Sci*. (2014) 5:105. doi: 10.3389/fpls.2014.00105

27. Landsiedel R, Ma-Hock L, Hofmann T, Wiemann M, Strauss V, Treumann S, et al. Application of short-term inhalation studies to assess the inhalation toxicity of nanomaterials. *Part Fibre Toxicol*. (2014) 11:16. doi: 10.1186/1743-8977-11-16

28. Kreyling WG, Holzwarth U, Hirn S, Schleh C, Wenk A, Schäffler M, et al. Quantitative biokinetics over a 28 day period of freshly generated, pristine, 20 nm silver nanoparticle aerosols in healthy adult rats after a single 1½-hour inhalation exposure. *Part Fibre Toxicol*. (2020) 17:21. doi: 10.1186/s12989-020-00347-1

29. Park JD, Kim JK, Jo MS, Kim YH, Jeon KS, Lee JH, et al. Lobar evenness of deposition/retention in rat lungs of inhaled silver nanoparticles: an approach for reducing animal use while maximizing endpoints. *Part Fibre Toxicol*. (2019) 16:2. doi: 10.1186/s12989-018-0286-9

30. Kim S, Jeon S, Lee D, Lee S, Jeong J, Kim JS, et al. The early onset and persistent worsening pulmonary alveolar proteinosis in rats by indium oxide nanoparticles. *Nanotoxicology*. (2020) 14:468–78. doi: 10.1080/17435390.2019.1694184

31. Park E, Kim SN, Yoon C, Cho J, Lee G, Kim D, et al. Repeated intratracheal instillation of zinc oxide nanoparticles induced pulmonary damage and a systemic inflammatory response in cynomolgus monkeys. *Nanotoxicology*. (2021) 15:621–35. doi: 10.1080/17435390.2021.1905899

32. Shin S, Lim C, Kim Y, Lee Y, Kim S, Kim J. Twenty-eight-day repeated inhalation toxicity study of nano-sized lanthanum oxide in male Sprague-dawley rats. *Environ Toxicol*. (2017) 32:1226–40. doi: 10.1002/tox.22319

33. Nishi K, Kadoya C, Ogami A, Oyabu T, Morimoto Y, Ueno S, et al. Changes over time in pulmonary inflammatory response in rat lungs after intratracheal instillation of nickel oxide nanoparticles. *J Occup Health*. (2020) 62:e12162. doi: 10.1002/1348-9585.12162

34. Zhou P, Pan Y, Yuan B, Zhou J, Jiang J. Organ distribution of Nano-WC particles after repeated intratracheal instillation into the lungs of SD rats and subsequent organ injury. *Biochem Biophys Res Commun*. (2023) 653:38–46. doi: 10.1016/j.bbrc.2023.02.059

35. Máté Z, Horváth E, Kozma G, Simon T, Kónya Z, Paulik E, et al. Size-dependent toxicity differences of Intratracheally instilled manganese oxide nanoparticles: conclusions of a subacute animal experiment. *Biol Trace Elem Res*. (2016) 171:156–66. doi: 10.1007/s12011-015-0508-z

36. Hadrup N, Saber AT, Kyjovska ZO, Jacobsen NR, Vippola M, Sarlin E, et al. Pulmonary toxicity of Fe(2)O(3), ZnFe(2)O(4), NiFe(2)O(4) and NiZnFe(4)O(8) nanomaterials: inflammation and DNA strand breaks. *Environ Toxicol Phar*. (2020) 74:103303. doi: 10.1016/j.etap.2019.103303

37. Zhu M, Feng W, Wang B, Wang T, Gu Y, Wang M, et al. Comparative study of pulmonary responses to nano- and submicron-sized ferric oxide in rats. *Toxicology*. (2008) 247:102–11. doi: 10.1016/j.tox.2008.02.011

38. Kreyling WG, Möller W, Holzwarth U, Hirn S, Wenk A, Schleh C, et al. Age-dependent rat lung deposition patterns of inhaled 20 nanometer gold nanoparticles and their quantitative biokinetics in adult rats. *ACS Nano*. (2018) 12:7771–90. doi: 10.1021/acsnano.8b01826

39. Kreyling WG, Holzwarth U, Schleh C, Hirn S, Wenk A, Schäffler M, et al. Quantitative biokinetics over a 28 day period of freshly generated, pristine, 20 nm titanium dioxide nanoparticle aerosols in healthy adult rats after a single two-hour inhalation exposure. *Part Fibre Toxicol*. (2019) 16:29. doi: 10.1186/s12989-019-0303-7

40. Kim JK, Kim HP, Park JD, Ahn K, Kim WY, Gulumian M, et al. Lung retention and particokinetics of silver and gold nanoparticles in rats following subacute inhalation co-exposure. *Part Fibre Toxicol*. (2021) 18:5. doi: 10.1186/s12989-021-00397-z

41. Andriamasinoro SN, Dieme D, Marie-Desvergne C, Serventi AM, Debia M, Haddad S, et al. Kinetic time courses of inhaled silver nanoparticles in rats. *Arch Toxicol*. (2022) 96:487–98. doi: 10.1007/s00204-021-03191-0

42. Golasik M, Herman M, Olbert M, Librowski T, Szklarzewicz J, Piekoszewski W. Toxicokinetics and tissue distribution of titanium in ionic form after intravenous and oral administration. *Toxicol Lett*. (2016) 247:56–61. doi: 10.1016/j.toxlet.2016.02.009

43. Brand W, Peters RJB, Braakhuis HM, Maślankiewicz L, Oomen AG. Possible effects of titanium dioxide particles on human liver, intestinal tissue, spleen and kidney after oral exposure. *Nanotoxicology*. (2020) 14:985–1007. doi: 10.1080/17435390.2020.1778809

44. Rolo D, Assunção R, Ventura C, Alvito P, Gonçalves L, Martins C, et al. Adverse outcome pathways associated with the ingestion of titanium dioxide nanoparticles-a systematic review. *Nano*. (2022) 12:3275. doi: 10.3390/nano12193275

45. Duan S, Wang H, Gao Y, Wang X, Lyu L, Wang Y. Oral intake of titanium dioxide nanoparticles affect the course and prognosis of ulcerative colitis in mice: involvement

of the ROS-TXNIP-NLRP3 inflammasome pathway. *Part Fibre Toxicol*. (2023) 20:24. doi: 10.1186/s12989-023-00535-9

46. Jones K, Morton J, Smith I, Jurkschat K, Harding A, Evans G. Human in vivo and in vitro studies on gastrointestinal absorption of titanium dioxide nanoparticles. *Toxicol Lett*. (2015) 233:95–101. doi: 10.1016/j.toxlet.2014.12.005

47. Tang H, Xu M, Zhou X, Zhang Y, Zhao L, Ye G, et al. Acute toxicity and biodistribution of different sized copper nano-particles in rats after oral administration. *Mater Sci Eng C Mater Biol Appl*. (2018) 93:649–63. doi: 10.1016/j.msec.2018.08.032

48. Luo J, Hao S, Zhao L, Shi F, Ye G, He C, et al. Oral exposure of pregnant rats to copper nanoparticles caused nutritional imbalance and liver dysfunction in fetus. *Ecotoxicol Environ Saf*. (2020) 206:111206. doi: 10.1016/j.ecoenv.2020.111206

49. Mangalampalli B, Dumala N, Perumalla Venkata R, Grover P. Genotoxicity, biochemical, and biodistribution studies of magnesium oxide nano and microparticles in albino wistar rats after 28-day repeated oral exposure. *Environ Toxicol*. (2018) 33:396–410. doi: 10.1002/tox.22526

50. Panyala A, Chinde S, Kumari SI, Rahman MF, Mahboob M, Kumar JM, et al. Comparative study of toxicological assessment of yttrium oxide nano- and microparticles in Wistar rats after 28 days of repeated oral administration. *Mutagenesis*. (2019) 34:181–201. doi: 10.1093/mutage/gey044

51. Ali AA. Evaluation of some biological, biochemical, and hematological aspects in male albino rats after acute exposure to the nano-structured oxides of nickel and cobalt. *Environ Sci Pollut R*. (2019) 26:17407–17. doi: 10.1007/s11356-019-05093-2

52. Aarzoo N, Samim M. Palladium nanoparticles as emerging pollutants from motor vehicles: an in-depth review on distribution, uptake and toxicological effects in occupational and living environment. *Sci Total Environ*. (2022) 823:153787. doi: 10.1016/j.scitotenv.2022.153787

53. Crosera M, Adami G, Mauro M, Bovenzi M, Baracchini E, Larese FF. In vitro dermal penetration of nickel nanoparticles. *Chemosphere*. (2016) 145:301–6. doi: 10.1016/j.chemosphere.2015.11.076

54. Filon FL, Crosera M, Adami G, Bovenzi M, Rossi F, Maina G. Human skin penetration of gold nanoparticles through intact and damaged skin. *Nanotoxicology*. (2011) 5:493–501. doi: 10.3109/17435390.2010.551428

55. Larese Filon F, Crosera M, Mauro M, Baracchini E, Bovenzi M, Montini T, et al. Palladium nanoparticles exposure: evaluation of permeation through damaged and intact human skin. *Environ Pollut*. (2016) 214:497–503. doi: 10.1016/j.envpol.2016.04.077

56. Mittal K, Rahim AA, George S, Ghoshal S, Basu N. Characterizing the effects of titanium dioxide and silver nanoparticles released from painted surfaces due to weathering on zebrafish (*Danio rerio*). *Nanotoxicology*. (2021) 15:527–41. doi: 10.1080/17435390.2021.1897173

57. Lacave JM, Vicario-Parés U, Bilbao E, Gilliland D, Mura F, Dini L, et al. Waterborne exposure of adult zebrafish to silver nanoparticles and to ionic silver results in differential silver accumulation and effects at cellular and molecular levels. *Sci Total Environ*. (2018) 642:1209–20. doi: 10.1016/j.scitotenv.2018.06.128

58. Lee WS, Kim E, Cho H, Kang T, Kim B, Kim MY, et al. The relationship between dissolution behavior and the toxicity of silver nanoparticles on zebrafish embryos in different ionic environments. *Nano*. (2018) 8:652. doi: 10.3390/nano8090652

59. Marinho CS, Matias MVF, Toledo EKM, Smaniotto S, Ximenes-da-Silva A, Tonholo J, et al. Toxicity of silver nanoparticles on different tissues in adult *Danio rerio*. *Fish Physiol Biochem*. (2021) 47:239–49. doi: 10.1007/s10695-020-00909-2

60. Li Q, Xiang Q, Lian L, Chen Z, Luo X, Ding C, et al. Metabolic profiling of nanosilver toxicity in the gills of common carp. *Ecotoxicol Environ Saf*. (2021) 222:112548. doi: 10.1016/j.ecoenv.2021.112548

61. Huang C, Yu W, Liu G, Hung S, Chang J, Chang J, et al. Opportunistic gill infection is associated with TiO2 nanoparticle-induced mortality in zebrafish. *PLoS One*. (2021) 16:e0247859. doi: 10.1371/journal.pone.0247859

62. Wu F, Cui S, Sun M, Xie Z, Huang W, Huang X, et al. Combined effects of ZnO NPs and seawater acidification on the haemocyte parameters of thick shell mussel Mytilus coruscus. *Sci Total Environ*. (2018) 624:820–30. doi: 10.1016/j.scitotenv.2017.12.168

63. Huang X, Lin D, Ning K, Sui Y, Hu M, Lu W, et al. Hemocyte responses of the thick shell mussel Mytilus coruscus exposed to nano-TiO_2 and seawater acidification. *Aquat Toxicol*. (2016) 180:1–10. doi: 10.1016/j.aquatox.2016.09.008

64. Wang W, Ren Y, He J, Zhang L, Wang X, Cui Z. Impact of copper oxide nanoparticles on the germination, seedling growth, and physiological responses in *Brassica pekinensis* L. *Environ Sci Pollut R*. (2020) 27:31505–15. doi: 10.1007/s11356-020-09338-3

65. Doğaroğlu ZG, Eren A, Baran MF. Effects of ZnO nanoparticles and Ethylenediamine-N,N'-Disuccinic acid on seed germination of four different plants. *Glob Chall*. (2019) 3:1800111. doi: 10.1002/gch2.201800111

66. Zhang R, Zhang H, Tu C, Hu X, Li L, Luo Y, et al. Phytotoxicity of ZnO nanoparticles and the released Zn(II) ion to corn (*Zea mays* L.) and cucumber (*Cucumis sativus* L.) during germination. *Environ Sci Pollut R*. (2015) 22:11109–17. doi: 10.1007/s11356-015-4325-x

67. Tymoszuk A, Wojnarowicz J. Zinc oxide and zinc oxide nanoparticles impact on in vitro germination and seedling growth in *Allium cepa* L. *Materials*. (2020) 13:2784. doi: 10.3390/ma13122784

68. Singh D, Kumar A. Assessment of toxic interaction of nano zinc oxide and nano copper oxide on germination of *Raphanus sativus* seeds. *Environ Monit Assess*. (2019) 191:703. doi: 10.1007/s10661-019-7902-5

69. Ahmed B, Rizvi A, Zaidi A, Khan MS, Musarrat J. Understanding the phyto-interaction of heavy metal oxide bulk and nanoparticles: evaluation of seed germination, growth, bioaccumulation, and metallothionein production. *RSC Adv*. (2019) 9:4210–25. doi: 10.1039/c8ra09305a

70. Ullah H, Li X, Peng L, Cai Y, Mielke HW. In vivo phytotoxicity, uptake, and translocation of PbS nanoparticles in maize (*Zea mays* L.) plants. *Sci Total Environ*. (2020) 737:139558. doi: 10.1016/j.scitotenv.2020.139558

71. Wang Z, Wang Z. Nanoparticles induced embryo-fetal toxicity. *Toxicol Ind Health*. (2020) 36:181–213. doi: 10.1177/0748233720918689

72. Xu M, Tang H, Zhou X, Chen H, Dong Q, Zhang Y, et al. Effects and mechanisms of sub-chronic exposure to copper nanoparticles on renal cytochrome P450 enzymes in rats. *Environ Toxicol Phar*. (2018) 63:135–46. doi: 10.1016/j.etap.2018.08.004

73. Yang J, Hu S, Rao M, Hu L, Lei H, Wu Y, et al. Copper nanoparticle-induced ovarian injury, follicular atresia, apoptosis, and gene expression alterations in female rats. *Int J Nanomedicine*. (2017) 12:5959–71. doi: 10.2147/IJN.S139215

74. Luo J, Zhang M, Deng Y, Li H, Bu Q, Liu R, et al. Copper nanoparticles lead to reproductive dysfunction by affecting key enzymes of ovarian hormone synthesis and metabolism in female rats. *Ecotoxicol Environ Saf*. (2023) 254:114704. doi: 10.1016/j.ecoenv.2023.114704

75. Yang Q, Li F, Miao Y, Luo X, Dai S, Liu J, et al. CdSe/ZnS quantum dots induced spermatogenesis dysfunction via autophagy activation. *J Hazard Mater*. (2020) 398:122327. doi: 10.1016/j.jhazmat.2020.122327

76. Nemmar A, Al-Salam S, Beegam S, Yuvaraju P, Ali BH. The acute pulmonary and thrombotic effects of cerium oxide nanoparticles after intratracheal instillation in mice. *Int J Nanomedicine*. (2017) 12:2913–22. doi: 10.2147/IJN.S127180

77. Wang J, Wang J, Liu Y, Nie Y, Si B, Wang T, et al. Aging-independent and size-dependent genotoxic response induced by titanium dioxide nanoparticles in mammalian cells. *J Environ Sci*. (2019) 85:94–106. doi: 10.1016/j.jes.2019.04.024

78. Li L, Lin X, Chen T, Liu K, Chen Y, Yang Z, et al. Systematic evaluation of CdSe/ZnS quantum dots toxicity on the reproduction and offspring health in male BALB/c mice. *Ecotoxicol Environ Saf*. (2021) 211:111946. doi: 10.1016/j.ecoenv.2021.111946

79. Bai C, Tang M. Progress on the toxicity of quantum dots to model organism-zebrafish. *J Appl Toxicol*. (2023) 43:89–106. doi: 10.1002/jat.4333

80. da Silva PB, Araújo VHS, Fonseca-Santos B, Solcia MC, Ribeiro CM, da Silva IC, et al. Highlights regarding the use of metallic nanoparticles against pathogens considered a priority by the World Health Organization. *Curr Med Chem*. (2021) 28:1906–56. doi: 10.2174/0929867327666200513080719

81. Li H, Duan S, Li L, Zhao G, Wei L, Zhang B, et al. Bio-responsive sliver peroxide-Nanocarrier serves as broad-Spectrum Metallo-β-lactamase inhibitor for combating severe pneumonia. *Adv Mater*. (2024) 36:e2310532. doi: 10.1002/adma.202310532

82. Elfsmark L, Ekstrand-Hammarström B, Forsgren N, Lejon C, Hägglund L, Wingfors H. Characterization of toxicological effects of complex nano-sized metal particles using in vitro human cell and whole blood model systems. *J Appl Toxicol*. (2022) 42:203–15. doi: 10.1002/jat.4202

83. Asharani PV, Sethu S, Vadukumpully S, Zhong S, Lim CT, Hande MP, et al. Investigations on the structural damage in human erythrocytes exposed to silver, gold, and platinum nanoparticles. *Adv Funct Mater*. (2010) 20:1233–42. doi: 10.1002/adfm.200901846

84. Katsnelson BA, Privalova LI, Sutunkova MP, Gurvich VB, Loginova NV, Minigalieva IA, et al. Some inferences from in vivo experiments with metal and metal oxide nanoparticles: the pulmonary phagocytosis response, subchronic systemic toxicity and genotoxicity, regulatory proposals, searching for bioprotectors (a self-overview). *Int J Nanomedicine*. (2015) 10:3013–29. doi: 10.2147/IJN.S80843

85. Wang M, Lai X, Shao L, Li L. Evaluation of immunoresponses and cytotoxicity from skin exposure to metallic nanoparticles. *Int J Nanomedicine*. (2018) 13:4445–59. doi: 10.2147/IJN.S170745

86. Zanoni I, Crosera M, Ortelli S, Blosi M, Adami G, Larese Filon F, et al. CuO nanoparticle penetration through intact and damaged human skin. *New J Chem*. (2019) 43:17033–9. doi: 10.1039/c9nj03373d

87. Holmes AM, Lim J, Studier H, Roberts MS. Varying the morphology of silver nanoparticles results in differential toxicity against micro-organisms, HaCaT keratinocytes and affects skin deposition. *Nanotoxicology*. (2016) 10:1503–14. doi: 10.1080/17435390.2016.1236993

88. Crane JK. Metal nanoparticles in infection and immunity. *Immunol Investig*. (2020) 49:794–807. doi: 10.1080/08820139.2020.1776724

89. Elder A, Gelein R, Silva V, Feikert T, Opanashuk L, Carter J, et al. Translocation of inhaled ultrafine manganese oxide particles to the central nervous system. *Environ Health Perspect*. (2006) 114:1172–8. doi: 10.1289/ehp.9030

90. Bocca B, Battistini B, Leso V, Fontana L, Caimi S, Fedele M, et al. Occupational exposure to metal engineered nanoparticles: a human biomonitoring pilot study involving Italian nanomaterial workers. *Toxics*. (2023) 11:11. doi: 10.3390/toxics11020120

91. Li M, Xu G, Yang X, Zeng Y, Yu Y. Metal oxide nanoparticles facilitate the accumulation of bifenthrin in earthworms by causing damage to body cavity. *Environ Pollut*. (2020) 263:114629. doi: 10.1016/j.envpol.2020.114629

92. Liu H, Lai W, Liu X, Yang H, Fang Y, Tian L, et al. Exposure to copper oxide nanoparticles triggers oxidative stress and endoplasmic reticulum (ER)-stress induced toxicology and apoptosis in male rat liver and BRL-3A cell. *J Hazard Mater*. (2021) 401:123349. doi: 10.1016/j.jhazmat.2020.123349

93. Wang J, Zhao G, Shu Z, Zhou P, Cao Y, Gao D. Effect of iron oxide nanoparticles on the permeability properties of Sf21 cells. *Cryobiology*. (2016) 72:21–6. doi: 10.1016/j.cryobiol.2015.12.002

94. Huerta-García E, Zepeda-Quiroz I, Sánchez-Barrera H, Colín-Val Z, Alfaro-Moreno E, Ramos-Godinez MDP, et al. Internalization of titanium dioxide nanoparticles is cytotoxic for H9c2 rat Cardiomyoblasts. *Molecules*. (2018) 23:23. doi: 10.3390/molecules23081955

95. Hong F, Li W, Ji J, Ze X, Diao E. Nanostructured titanium dioxide (TiO_2) reduces sperm concentration involving disorder of meiosis and signal pathway. *J Biomed Nanotechnol*. (2020) 16:659–71. doi: 10.1166/jbn.2020.2926

96. Babele PK, Thakre PK, Kumawat R, Tomar RS. Zinc oxide nanoparticles induce toxicity by affecting cell wall integrity pathway, mitochondrial function and lipid homeostasis in *Saccharomyces cerevisiae*. *Chemosphere*. (2018) 213:65–75. doi: 10.1016/j.chemosphere.2018.09.028

97. Lee J, Kim J, Lee R, Lee E, Choi TG, Lee AS, et al. Therapeutic strategies for liver diseases based on redox control systems. *Biomed Pharmacother*. (2022) 156:113764. doi: 10.1016/j.biopha.2022.113764

98. Ramakrishnan M, Papolu PK, Satish L, Vinod KK, Wei Q, Sharma A, et al. Redox status of the plant cell determines epigenetic modifications under abiotic stress conditions and during developmental processes. *J Adv Res*. (2022) 42:99–116. doi: 10.1016/j.jare.2022.04.007

99. Liu Z, Zhang M, Han X, Xu H, Zhang B, Yu Q, et al. TiO2 nanoparticles cause cell damage independent of apoptosis and autophagy by impairing the ROS-scavenging system in Pichia pastoris. *Chem Biol Interact*. (2016) 252:9–18. doi: 10.1016/j.cbi.2016.03.029

100. Wang J, Jia Y, Whalen JK, McShane H, Driscoll BT, Sunahara GI. Evidence that nano-TiO(2) induces acute cytotoxicity to the agronomically beneficial nitrogen-fixing bacteria *Sinorhizobium meliloti*. *Can J Microbiol*. (2021) 13:1–6. doi: 10.1139/cjm-2021-0124

101. Sheng L, Wang X, Sang X, Ze Y, Zhao X, Liu D, et al. Cardiac oxidative damage in mice following exposure to nanoparticulate titanium dioxide. *J Biomed Mater Res A*. (2013) 101:3238–46. doi: 10.1002/jbm.a.34634

102. González-Esquivel AE, Charles-Niño CL, Pacheco-Moisés FP, Ortiz GG, Jaramillo-Juárez F, Rincón-Sánchez AR. Beneficial effects of quercetin on oxidative stress in liver and kidney induced by titanium dioxide (TiO_2) nanoparticles in rats. *Toxicol Mech Methods*. (2015) 25:166–75. doi: 10.3109/15376516.2015.1006491

103. Lim D, Roh J, Eom H, Choi J, Hyun J, Choi J. Oxidative stress-related PMK-1 P38 MAPK activation as a mechanism for toxicity of silver nanoparticles to reproduction in the nematode *Caenorhabditis elegans*. *Environ Toxicol Chem*. (2012) 31:585–92. doi: 10.1002/etc.1706

104. Hong F, Wang L, Yu X, Zhou Y, Hong J, Sheng L. Toxicological effect of TiO2 nanoparticle-induced myocarditis in mice. *Nanoscale Res Lett*. (2015) 10:1029. doi: 10.1186/s11671-015-1029-6

105. Tsou T, Yeh S, Tsai F, Lin H, Cheng T, Chao H, et al. Zinc oxide particles induce inflammatory responses in vascular endothelial cells via NF-κB signaling. *J Hazard Mater*. (2010) 183:182–8. doi: 10.1016/j.jhazmat.2010.07.010

106. Monsé C, Raulf M, Jettkant B, van Kampen V, Kendzia B, Schürmeyer L, et al. Health effects after inhalation of micro- and nano-sized zinc oxide particles in human volunteers. *Arch Toxicol*. (2021) 95:53–65. doi: 10.1007/s00204-020-02923-y

107. Ndika J, Seemab U, Poon W, Fortino V, El-Nezami H, Karisola P, et al. Silver, titanium dioxide, and zinc oxide nanoparticles trigger miRNA/isomiR expression changes in THP-1 cells that are proportional to their health hazard potential. *Nanotoxicology*. (2019) 13:1380–95. doi: 10.1080/17435390.2019.1661040

108. Ng CT, Yong LQ, Hande MP, Ong CN, Yu LE, Bay BH, et al. Zinc oxide nanoparticles exhibit cytotoxicity and genotoxicity through oxidative stress responses in human lung fibroblasts and *Drosophila melanogaster*. *Int J Nanomedicine*. (2017) 12:1621–37. doi: 10.2147/IJN.S124403

109. Zhang X, Song Y, Wang J, Wu C, Xiang H, Hu J, et al. Chronic exposure to titanium dioxide nanoparticles induces deficits of locomotor behavior by disrupting the development of NMJ in Drosophila. *Sci Total Environ*. (2023) 888:164076. doi: 10.1016/j.scitotenv.2023.164076

frontiers | Frontiers in Public Health

TYPE Original Research
PUBLISHED 25 July 2024
DOI 10.3389/fpubh.2024.1415028

OPEN ACCESS

EDITED BY
Giovanna Deiana,
University of Sassari, Italy

REVIEWED BY
Octavio Jiménez-Garza,
University of Guanajuato, Mexico
Nasser Hatamzadeh,
Ahvaz Jundishapur University of Medical Sciences, Iran

*CORRESPONDENCE
Jinwei He
✉ hotred_714@163.com

RECEIVED 09 April 2024
ACCEPTED 15 July 2024
PUBLISHED 25 July 2024

CITATION
Gu J, Li J, Liu L, Cao M, Tian X, Wang Z and He J (2024) Exploring the association between atmospheric pollutants and preterm birth risk in a river valley city.
Front. Public Health 12:1415028.
doi: 10.3389/fpubh.2024.1415028

Exploring the association between atmospheric pollutants and preterm birth risk in a river valley city

Jiajia Gu, Jimin Li, Lang Liu, Meiying Cao, Xi Tian, Zeqi Wang and Jinwei He*

Medical School of Yan'an University, Yan'an, China

Objective: To investigate the association between exposure to atmospheric pollutants and preterm birth in a river valley-type city and its critical exposure windows.

Methods: A retrospective cohort study was used to collect data from the medical records of preterm and full-term deliveries in two hospitals in urban areas of a typical river valley-type city from January 2018 to December 2019. A total of 7,288 cases were included in the study with general information such as pregnancy times, the number of cesarean sections, occupation, season of conception and regularity of the menstrual cycle. And confounding factors affecting preterm birth were inferred using the chi-square test. The effects of exposure to each pollutant, including particulate matter 2.5 ($PM_{2.5}$), particulate matter 10 (PM_{10}), nitrogen dioxide (NO_2), sulfur dioxide (SO_2), carbon monoxide (CO) and ozone (O_3), during pregnancy on preterm birth and the main exposure windows were explored by establishing a logistic regression model with pollutants introduced as continuous variables.

Results: Maternal age, pregnancy times, number of births, number of cesarean sections, season of conception, complications diseases, comorbidities diseases, hypertension disorder of pregnancy and neonatal low birth weight of the newborn were significantly different between preterm and term pregnant women. Logistic regression analysis after adjusting for the above confounders showed that the risk of preterm birth increases by 0.9, 0.6, 2.4% in T_2 and by 1.0, 0.9, 2.5% in T_3 for each 10 $\mu g/m^3$ increase in $PM_{2.5}$, PM_{10}, NO_2 concentrations, respectively. The risk of preterm birth increases by 4.3% in T_2 for each 10 $\mu g/m^3$ increase in SO_2 concentrations. The risk of preterm birth increases by 123.5% in T_2 and increases by 188.5% in T_3 for each 10 mg/m^3 increase in CO concentrations.

Conclusion: Maternal exposure to $PM_{2.5}$, PM_{10}, NO_2, CO was associated with increased risk on preterm birth in mid-pregnancy (T_2) and late pregnancy (T_3), SO_2 exposure was associated with increased risk on preterm birth in mid-pregnancy (T_2).

KEYWORDS

preterm birth, air pollution, environmental exposure, risk assessment, public health

1 Introduction

There are approximately 13.4 million preterm births globally in 2020, accounting for more than one-tenth of all newborns (1). Although the number of preterm births has declined compared to 2010, there has been no measurable change in the global preterm birth rate during this decade (1). In China, the status of preterm birth is not encouraging. Research data show that China's preterm birth rate is 12.0% in 2014, the second highest in the world (2). With the opening of China's two-child policy in 2016, the preterm birth rate has shown a trend of gradual increase (3), and the incidence is not balanced between regions (4).

Rising rates of preterm birth are accompanied by an increase in the number of children under the age of five who die from preterm birth complications, with statistics indicating that approximately 900,000 children worldwide have died from preterm birth complications in 2019 (5). The infants who survive from preterm birth events also face great risks, such as lifelong disabilities, and these surviving preterm infants are prone to comorbidities such as cerebral palsy, progressive developmental lag, chronic lung disease or neurological sequelae (6, 7), which can impose a heavy burden on both families and society in terms of mental and economic aspects. Preterm labor is considered to be triggered by multiple mechanisms, including infection or inflammation, uteroplacental ischemia or hemorrhage, uterine overstretching, stress, oxidative stress, and other immune-mediated processes (8, 9). Besides, there is evidence that preterm birth is the result of the interaction of multiple risk factors (10), and in addition to well-known risk factors such as maternal demographics (11, 12), psychological characteristics (13), pregnancy comorbidities (14), and genetic characteristics (15), epidemiological studies have suggested that preterm birth is associated with atmospheric pollutants (16–18).

In China, with the rapid economic development of industrialization and urbanization in the past decades, environmental problems have become increasingly serious (19). These are dominated by increasing atmospheric pollution and particulate matter in the environment, with $PM_{2.5}$, PM_{10}, SO_2, O_3, NO_2 and CO being the main air pollutants. A study on air pollutants conducted in 2015 found that the rate of air pollution and persistent air pollution in northern China is much higher than that in the south, especially in cities in the Bohai Rim and Xinjiang Province (20). It can be seen that there is spatial heterogeneity in air pollutant levels in different cities, especially in the northern cities of China. Therefore, a typical river valley city located in Northwest China was selected for this study, which develops on the axis of the Weihe Plain and is dominated by mountains and hills, with a slightly more complex geological structure than other surrounding cities. The city has a long heating period due to cold winters, which increases the amount of coal and carbon consumed, and the pollutants released from coal combustion are not easily dispersed due to the unique geographic characteristics of the city. It is also due to the frequent occurrence of unfavorable weather such as fog and inversions, which further contribute to the increase in pollutant concentrations.

This study investigates the association between exposure to pollutants and the occurrence of preterm birth in river basin cities and the main exposure windows, with a view to inform potential risk factors of preterm births.

2 Materials and methods

2.1 Study participants

We collect information on all pregnant women with preterm and full-term births from January 2018 to December 2019 from two hospitals in Baoji city. This includes general maternal information (name, age, date of admission, occupation, gestational address), current pregnancy (pregnancy times, number of births, number of cesarean sections, last menstrual period, season, regularity of menstrual cycle, mode of delivery in this case), pregnancy outcome, neonatal information [neonatal date of birth, gestational age (gestational age was usually calculated from the first day of the mother's last menstrual period), weight (g), number of births], complications diseases, hypertensive disorder of pregnancy, comorbidity diseases and passive smoking.

Pregnancy comorbidities are a condition in which a pregnant woman develops other diseases in addition to the symptoms associated with pregnancy, i.e., a state in which a pregnant woman is comorbid with one or more diseases. Including combined cardiovascular disease, combined hematological disease, combined respiratory disease, combined gastrointestinal disease, combined urological disease, combined endocrine disease, combined infectious disease and combined neoplasm.

Pregnancy complications refer to a variety of conditions that occur during pregnancy that may have some impact on the health of the mother and the births. These include placenta previa, placental abruption, premature rupture of membranes, low amniotic fluid, fetal distress and so on.

Inclusion criteria: ① local residence for more than 1 year and detailed address; ② no assisted conception (exclusion of fertility achieved through unnatural conception and with the help of medical technology); ③ age greater than 18 years old; ④ no acute or chronic diseases; ⑤ the births was born as a single live birth; ⑥ no communication barriers (communication barriers, including hearing or visual impairments, neurological disorders or psychological disorders, etc.). Exclusion criteria: ① not residing in Baoji city during pregnancy or residing locally for less than 1 year; ② assisted conception (e.g., *in vitro* fertilization (IVF)); ③ unmarried women; ④ ectopic pregnancy; ⑤ births born as twin or multiple births.

In the case information collected in this retrospective cohort study, a total of 7,288 cases were included in the study, of which 372 cases were preterm pregnant women and 6,916 cases were full-term pregnant women. Preterm births were selected from those delivered at 28 weeks to less than 37 weeks of gestation from the first day of the last menstrual period, and term births were selected from those delivered at 37 weeks of gestation.

The questionnaire used to collect information on maternity was designed with a clear research objective combined with existing research findings and expertise. A small-scale pre-test was conducted before its official use, and the questionnaire was further revised and improved based on the test results. Validity analyses were also conducted to assess the reasonableness of the questionnaire design as well as to verify the reliability of the questionnaire through reliability analyses. Finally, in order to ensure the high quality of the information collected, all investigators were required to receive professional training before entering the above hospitals, obtaining the case records of all participants, and completing the questionnaire.

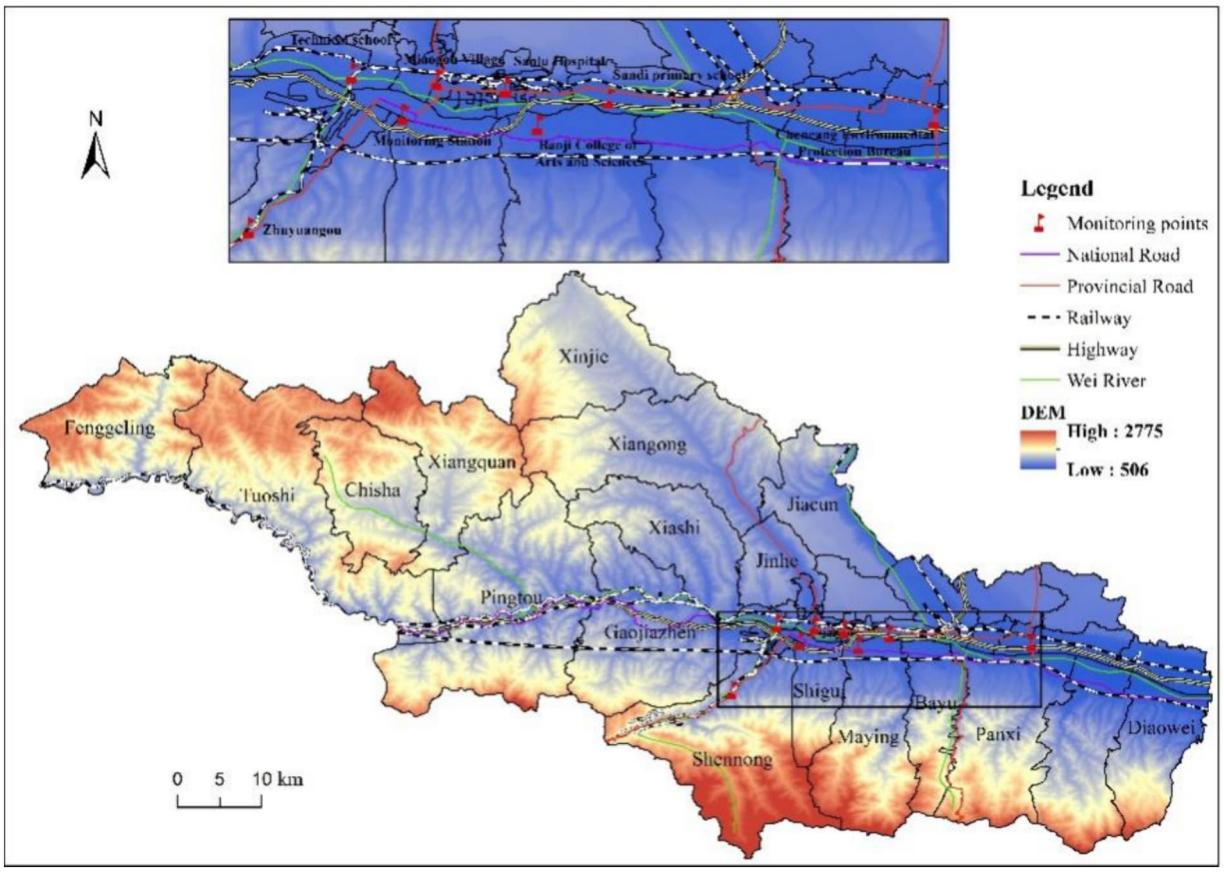

FIGURE 1
Distribution of air quality monitoring stations and topographic map of Baoji city.

2.2 Methods

2.2.1 Air pollutant exposure assessment

A total of 7 air monitoring stations have been set up in Baoji city, the distribution of which can be seen at Figure 1. The actual straight-line distance between the pregnant women eventually included in the study and each of the above air monitoring stations was calculated based on the latitude and longitude of their main residential address during pregnancy, and then the nearest monitoring station to each of the pregnant women's residential address was selected. The air pollutant concentrations monitored at that station were used as the exposure of air pollutants for that pregnant woman during her pregnancy period. The air pollutant data was obtained from the National Urban Air Quality Real-Time Distribution System (https://air.cnemc.cn:18007/) of the China Environmental Monitoring General Station of the Ministry of Environmental Protection (MEP), and included the concentrations of six pollutants, namely, $PM_{2.5}$, PM_{10}, O_3, SO_2, CO and NO_2. The $PM_{2.5}$, PM_{10}, SO_2, CO and NO_2 are 24 h moving averages, and O_3 is the maximum 8 h moving average. To determine the pollutant exposure window, we divided the course of pregnancy into three stages: 0–12 weeks of gestation was defined as early pregnancy (T_1), 13–27 weeks as mid-pregnancy (T_2), and 28 weeks to the end of pregnancy as late pregnancy (T_3) (21, 22). According to the time period corresponding to the different exposure windows of each pregnant women, the daily moving average of each pollutant in that time period was found separately, and after averaging, the air pollutant exposure level of the pregnant women in a certain exposure window was modelled accordingly, so as to determine the susceptibility windows for various air pollutants during pregnancy.

2.2.2 Statistical methods

Data was collated using Excel and analyzed using SPSS 20.0. Normality test was performed for pollutants and the levels of exposure to pollutants in different exposure windows were described using mean, standard deviation (SD), median, and interquartile range (IQR). General maternal data was compared using one-way chi-square test to determine whether there is a difference between pregnant women with preterm versus term births. If they do, they can be considered and evaluated as potential confounders and were introduced as covariates in the subsequent logistic regression model. After the test, confounding factors are maternal age, pregnancy times, number of births, number of cesarean sections, season of conception, complications disease, comorbidity diseases, hypertensive disorder complicating pregnancy and low birth weight. For missing data, it was treated as discrete missing values 999 in SPSS software. The relationship between each pollutant and preterm birth and the main exposure windows were explored by logistic regression modelling, adjusting

for confounding factors after introducing the pollutant as a continuous variable ($\alpha = 0.05$).

3 Results

3.1 General description of air pollution in Baoji city 2017–2019

The air pollutant exposure window for some of the pregnant women who gave birth in 2018 was in 2017, so 2017 was included when describing the air pollution profile. And we compared the concentration of each pollutant with the national secondary standard (Level II), respectively. The national secondary standards of $PM_{2.5}$, PM_{10}, SO_2, NO_2, CO and O_3 are respectively 35 μg/m^3, 70μg/m^3, 60μg/m^3, 40μg/m^3, 4mg/m^3, 200μg/m^3 (Table 1). During the period of 2017–2019, $PM_{2.5}$ and PM_{10} concentrations were significantly higher than the national secondary standards most of the time; SO_2 and CO concentrations were always lower than the national secondary standards; NO_2 concentrations showed an unstable situation of being sometimes higher and sometimes lower than the national secondary standards; and O_3 concentrations, although they were almost always lower than the national secondary standards, showed a different pattern from the other pollutants: with peaks in the summer and drops in the winter (Figure 2).

3.2 Comparative analysis of general maternal information

Analysis of the general data of pregnant women revealed that: pregnant women older than 30 years are more likely to have preterm births; pregnant women with more than one pregnancy times, births and cesarean sections are prone to have preterm births; compared with full-term pregnant women, season of conception of preterm pregnant women is concentrated in winter (29.3%) and spring (27.7%); the proportion of preterm pregnant women suffering from pregnancy complications (93.3%), hypertensive disorders of pregnancy (18.8%), and pregnancy comorbidities (77.7%) is higher than that of full-term pregnant women. At the same time, preterm births are more likely to result in low birth weight (46.2%).

Maternal age, pregnancy times, number of births, number of cesarean sections, season of conception, complications diseases, comorbidities diseases, hypertension disorder of pregnancy, and neonatal low birth weight of the newborn were significantly ($P < 0.05$)

TABLE 1 Description of exposure levels in preterm and term women across exposure windows in 2017–2019.

Pollutants	Preterm birth				Full term birth				China ambient air quality standards GB 3095–2012
	Mean	SD	Median	IQR	Mean	SD	Median	IQR	
Trimester 1									Level II
$PM_{2.5}$ (μg/m^3)	54.67	24.82	47.29	46.88	53.79	24.18	46.82	45.14	35
PM_{10} (μg/m^3)	100.71	31.16	103.37	56.59	99.48	31.37	100.89	61.32	70
SO_2 (μg/m^3)	8.81	3.99	7.56	4.31	8.83	4.06	7.85	4.25	60
NO_2 (μg/m^3)	37.13	8.06	35.84	14.12	37.29	8.14	35.98	14.19	40
CO (mg/m^3)	0.88	0.23	0.8	0.42	0.87	0.23	0.79	0.41	4
O_3 (μg/m^3)	86.03	32.85	90.65	56.51	85.22	35.15	89.64	60.57	200
Trimester 2									#
$PM_{2.5}$ (μg/m^3)	50.88	25.48	41.88	45.02	54.51	25.36	49.19	47.64	#
PM_{10} (μg/m^3)	94.64	34.06	91.49	62.68	99.50	32.96	102.93	61.39	#
SO_2 (μg/m^3)	8.52	4.37	6.97	4.85	8.80	4.24	7.59	4.86	#
NO_2 (μg/m^3)	35.73	9.46	34.52	15.77	36.96	9.06	36.81	14.55	#
CO (mg/m^3)	0.83	0.28	0.71	0.43	0.86	0.26	0.84	0.46	#
O_3 (μg/m^3)	83.80	33.46	96.1	57.69	80.44	32.19	85.39	57.24	#
Trimester 3									#
$PM_{2.5}$ (μg/m^3)	52.17	28.51	42.82	51.69	53.63	27.45	43.64	51.32	#
PM_{10} (μg/m^3)	95.42	39.42	93.73	74.95	97.62	36.45	98.64	69.04	#
SO_2 (μg/m^3)	8.71	4.75	6.93	4.72	8.77	4.49	7.35	4.76	#
NO_2 (μg/m^3)	35.97	10.36	35.82	17.45	36.25	9.65	35.66	16.38	#
CO (mg/m^3)	0.80	0.30	0.69	0.44	0.82	0.29	0.69	0.46	#
O_3 (μg/m^3)	82.79	31.85	88.48	53.67	83.23	30.87	90.25	52.72	#

0–12 weeks of gestation was defined as early pregnancy (T_1), 13–27 weeks as mid-pregnancy (T_2), and 28 weeks to the end of pregnancy as late pregnancy (T_3). #: No data or information at this location. Level II is a standard, which means acceptable air quality, but some pollutants may have a weak impact on the health of a very small number of unusually sensitive people.

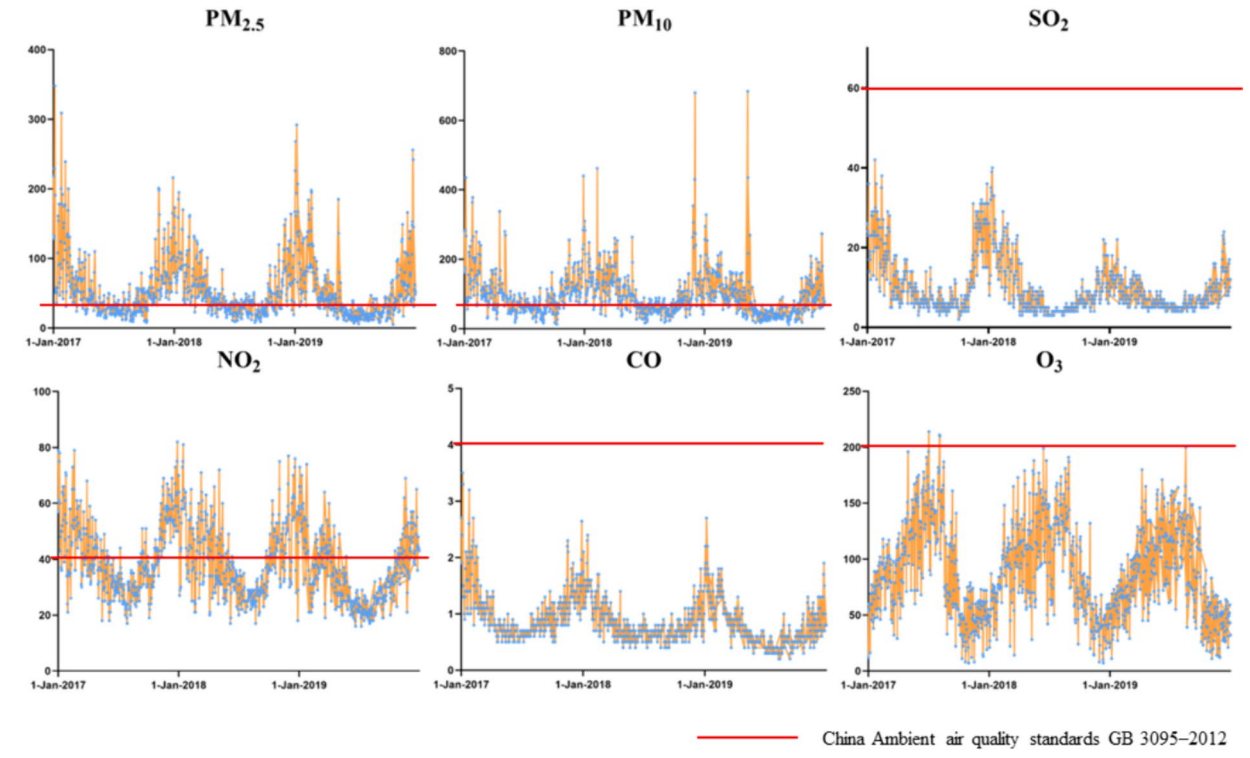

FIGURE 2
Daily variation of air pollutant concentrations in Baoji city, 2017–2019.

different between preterm and term pregnant women. Maternal occupation, regularity of the menstrual cycle and passive smoking did not differ significantly between preterm and term pregnant women. And we did not model newborn sex and other variables, such as mother's education and maternal smoking during pregnancy, because of the difficulty to obtain the data in retrospective cohort study and large number of missing values (Table 2).

3.3 Comparison of pollutant exposure concentrations in preterm pregnant women versus term pregnant women

In early pregnancy, mid-pregnancy and late pregnancy, the mean levels of exposure concentrations of $PM_{2.5}$ and PM_{10} for preterm and full-term pregnant women were higher than the national secondary standard (Level II), while the concentrations of other pollutants were lower than the national secondary standard.

In early pregnancy, the mean levels of $PM_{2.5}$, PM_{10}, CO and O_3 exposure of preterm pregnant women were 54.67 μg/m^3, 100.71 μg/m^3, 0.88 mg/m^3 and 86.03 μg/m^3, respectively, which were slightly higher than those of term pregnant women. The mean levels of SO_2 and NO_2 exposure were higher in term than in preterm women. In mid-pregnancy, the mean levels of $PM_{2.5}$, PM_{10}, SO_2, NO_2 and CO exposure for preterm pregnant women were lower than those for term pregnant women, and only the mean level of O_3 exposure was higher than that for term pregnant women, at 83.80 μg/m^3. In the late pregnancy, the mean levels of $PM_{2.5}$, PM_{10}, SO_2, NO_2, CO and O_3 exposure of preterm women were all lower than those of term pregnant women. Differences in pollutant exposure levels in the three exposure windows between the two groups may be due to the fact that full-term pregnant women are generally exposed for a longer period of time in late pregnancy than preterm pregnant women, which results in higher exposure levels of each pollutant for full-term pregnant women than for preterm pregnant women in late pregnancy (Table 1).

3.4 Logistic regression analysis of preterm birth

Before adjustment, only $PM_{2.5}$, $PM_{10,}$ NO_2, CO exposure was associated with increased risk on preterm birth in mid-pregnancy, and exposure to the other pollutants had no association with preterm birth in each exposure window. In multivariate analyses of single-pollutant models, exposure to $PM_{2.5}$, $PM_{10,}$ NO_2, CO was associated with increased risk on preterm birth in mid-pregnancy (T_2) and late pregnancy (T_3), SO_2 exposure was associated with increased risk on preterm birth in mid-pregnancy (T_2). The risk of preterm birth increased by 0.9, 0.6, 2.4% in T_2 and by 1.0, 0.9, 2.5% in T_3 for each 10 μg/m^3 increase in $PM_{2.5}$, PM_{10}, NO_2 concentrations, respectively. The risk of preterm birth increased by 4.3% in T_2 for each 10 μg/m^3 increase in SO_2. The risk of preterm birth increased by 123.5% in T_2 and by 188.5% in T_3 for each 10 mg/m^3 increase in CO concentrations. Other pollutants were not associated with increased risk on preterm birth in 3 exposure windows (Table 3).

10.3389/fpubh.2024.1415028

TABLE 2 Comparative analysis of the general data of preterm and term pregnant women.

Covariates		Preterm birth (n = 372)		Full term birth (n = 6,916)		p
		N	P (%)	N	P (%)	
Mean maternal age		30.07		29.29		#
Maternal age range		20–43		18–46		#
Maternal age (years)	18–19	0	0.0	22	0.3	0.007
	20–24	40	10.8	795	11.5	
	25–29	144	38.7	3,089	44.7	
	30–34	123	33.1	2,201	31.8	
	35	65	17.5	809	11.7	
Pregnancy times	1	102	27.4	2,436	35.2	0.002
	>1	270	72.6	4,478	64.7	
Number of births	≤1	174	46.8	3,789	54.8	0.002
	>1	198	53.2	3,118	45.1	
Number of cesarean sections	≤1	280	75.3	5,587	80.8	0.008
	>1	92	24.7	1,326	19.2	
Occupation	National civil servants	4	1.1	117	1.7	0.373
	Professional and technical staff	58	15.6	1,162	16.8	
	Business and services	84	22.6	1,241	17.9	
	Agriculture	63	16.9	1,338	19.3	
	Production and transport	8	2.2	164	2.4	
	Other special occupations	66	17.7	1,163	16.8	
	Unemployed	73	19.6	1,312	19	
Season of conception	Spring	103	27.7	1,712	24.8	0.034
	Summer	85	22.8	1,774	25.7	
	Fall	75	20.2	1,726	25	
	Winter	109	29.3	1,704	24.6	
Regularity of the menstrual cycle	Regularity	366	98.4	6,791	98.2	0.601
	Irregularity	4	1.1	97	1.4	
Pregnancy complications	Yes	347	93.3	6,077	87.9	0.002
	No	25	6.7	839	12.1	
Hypertensive disorder of pregnancy	Yes	70	18.8	353	5.1	0.000
	No	261	70.2	5,751	83.2	
Pregnancy comorbidities	Yes	289	77.7	4,804	69.5	0.001
	No	83	22.3	2,112	30.5	
Low birth weight	≥2,500 g	197	53	6,808	98.4	0.000
	<2,500 g	172	46.2	84	1.2	
Passive smoking	Yes	10	2.7	160	2.3	0.769
	No	274	73.7	4,833	69.9	

P (%) means percentage of the number of people with each categorical factor in the preterm and term birth groups, respectively. p-value comes from the chi-square test, at the significance level of $\alpha = 0.05$, the smaller the p-value, the more reason there is to believe that a factor differs between the two groups of pregnant women. Pregnancy times include the current pregnancy. Pregnancy comorbidities are a condition in which a pregnant woman develops other diseases in addition to the symptoms associated with pregnancy. Pregnancy complications refer to a variety of conditions that occur during pregnancy that may have some impact on the health of the mother and the births. #: No data or information at this location.

4 Discussion

In this retrospective cohort study, we investigated the association between air pollutants and preterm birth in Baoji city in 2018–2019. The study showed that preterm births were conceived more often in spring and winter compared to full-term births. This may be due to the fact that Baoji city has a warm-temperate monsoon climate with cold and dry winters, so coal combustion increases during the collective heating phase and pollutants are released, which results in higher concentrations of air pollutants in spring and winter than in other seasons. There were

10.3389/fpubh.2024.1415028

TABLE 3 Associations between pollutants and preterm birth.

Pollutants	Unadjusted			Adjusted		
	OR	95% CI	*p*	OR	95% CI	*p*
Trimester 1						
$PM_{2.5}$ (μg/m^3)	0.999	0.994–1.003	0.495	0.991	0.983–0.999	0.034
PM_{10} (μg/m^3)	0.999	0.995–1.002	0.463	0.993	0.987–0.999	0.023
SO_2 (μg/m^3)	1.002	0.976–1.028	0.904	0.984	0.947–1.023	0.426
NO_2 (μg/m^3)	1.003	0.990–1.016	0.701	0.994	0.972–1.015	0.553
CO (mg/m^3)	0.911	0.582–1.425	0.683	0.730	0.335–1.588	0.427
O_3 (μg/m^3)	0.999	0.996–1.002	0.667	0.999	0.994–1.004	0.674
Trimester 2						
$PM_{2.5}$ (μg/m^3)	1.006	1.002–1.010	0.007	1.009	1.003–1.014	0.001
PM_{10} (μg/m^3)	1.004	1.001–1.008	0.006	1.006	1.002–1.010	0.002
SO_2 (μg/m^3)	1.016	0.991–1.043	0.210	1.043	1.009–1.077	0.011
NO_2 (μg/m^3)	1.015	1.003–1.027	0.011	1.024	1.009–1.038	0.002
CO (mg/m^3)	1.743	1.167–2.603	0.007	2.235	1.358–3.678	0.002
O_3 (μg/m^3)	0.997	0.993–1.000	0.051	0.992	0.987–0.996	0.000
Trimester 3						
$PM_{2.5}$ (μg/m^3)	1.002	0.998–1.006	0.319	1.010	1.002–1.018	0.011
PM_{10} (μg/m^3)	1.002	0.999–1.005	0.260	1.009	1.003–1.015	0.002
SO_2 (μg/m^3)	1.003	0.980–1.027	0.806	1.061	0.999–1.126	0.053
NO_2 (μg/m^3)	1.003	0.992–1.014	0.589	1.025	1.001–1.051	0.044
CO (mg/m^3)	1.324	0.919–1.907	0.131	2.885	1.377–6.042	0.005
O_3 (μg/m^3)	1.000	0.997–1.004	0.790	1.001	0.994–1.008	0.770

What increase in pollutant are the results reported for "per 10 μg/m^3" or "per 10 mg/m^3." Adjustment factors: maternal age, pregnancy times, number of births, number of cesarean sections, season of conception, complications disease, comorbidity diseases, hypertensive disorder of pregnancy, low birth weight.

significant differences between preterm births and full-term births with respect to maternal age, pregnancy times, number of births, number of cesarean sections, season of conception, complications diseases, comorbidities diseases, hypertension disorder of pregnancy and neonatal low birth weight. In multivariate single pollutant models, exposure to $PM_{2.5}$, $PM_{10,}$ NO_2, CO was associated with increased risk on preterm birth in mid-pregnancy and late pregnancy, and SO_2 exposure was associated with increased risk on preterm birth in mid-pregnancy. The risk of preterm birth increased by 0.9, 0.6, 2.4% in T_2 and by 1.0, 0.9, 2.5% in T_3 for each 10 μg/m^3 increase in $PM_{2.5}$, $PM_{10,}$ NO_2 concentrations, respectively. The risk of preterm birth increased by 4.3% in T_2 for each 10 μg/m^3 increase in SO_2. The risk of preterm birth increased by 123.5% in T_2 and by 188.5% in T_3 for each 10 mg/m^3 increase in CO concentrations. There was no association between exposure to O_3 and preterm birth in any stage of pregnancy.

These results are consistent with findings from other studies. The exposure of $PM_{2.5}$ in T_1, T_2, T_3 and E can increase the risk of preterm birth (23). And the strongest association was observed in the second trimester (24). Exposure to high concentrations of PM_{10} increases the risk of preterm birth (25, 26), the study (25) also suggested that the risk may vary according to the clinical subtypes of preterm birth and the time window of exposure. Significant association was found between NO_2 exposure and preterm birth (27, 28) and NO_2 exposure in only the 3rd trimester was positively associated with PTB (29). It is showed that (30) exposure to $PM_{2.5}$, PM_{10}, and NO_2 for 1 week prior to delivery increased the risk of preterm birth. One study (31), also conducted in a river valley type city, showed that PM_{10}, O_3 exposure in late pregnancy, SO_2 in mid pregnancy, and SO_2 exposure in late pregnancy were all likely to increase the risk of preterm birth. Although the above studies have shown that exposure to $PM_{2.5}$, $PM_{10,}$ NO_2, CO and SO_2 during pregnancy increases the risk of preterm birth, the key exposure windows and associated intensities are not the same, which may be attributed to different pollution levels, specific study periods and study populations, or other factors.

In our study, we did not observe any association for O_3, however other studies showed that O_3 was associated with preterm birth. A study (32) showed that exposure to O_3 during pregnancy increased the risk of preterm birth. Another study in China (33) also illustrated that O_3 was one of the risk factors for the occurrence of preterm birth, and the susceptibility window was late in pregnancy at T_3. These inconsistencies may be due to differences in the locations of the studies, differences in the experimental design of the studies, or differences in the methods of exposure assessment and statistical analyses.

Although this study showed that exposures to certain pollutants in later pregnancy is associated with preterm birth, there is no clear understanding of the molecular mechanism of the occurrence of preterm birth induced by air pollutants. It has been suggested that it is fetal growth and development within the placenta that is more sensitive and vulnerable to exposure to air pollutants (34), thereby predisposing to preterm birth or other adverse pregnancy outcomes. Prenatal exposure to air pollution has also been found to be associated with nitrosative stress and epigenetic alterations in the placenta (35). Air

pollution particles may be transferred into and across the placental barrier, leading to placental oxidative and nitrosative stress due to the ability of pollution particles to produce reactive oxygen species/reactive nitrogen species (ROS/RNS) in a direct or indirect manner; another important target of the early life effects of air pollution is the induction of epigenetic alterations of the placenta, including DNA methylation, histone and noncoding RNA modifications, and changes in chromatin remodeling. The Developmental Origins of Health and Disease (DOHaD) hypothesis similarly suggests an association between perinatal complications induced by prenatal exposure to air pollutants (preterm birth or fetal growth restriction), and placental epigenomics (36). In contrast, another study found that the onset of preterm birth inversely enhances the toxicity of air pollutants through oxidative stress and placental function (37), which means that air pollution particles affect the anatomical structure and/or physiological function of the developing lungs and related systems through oxidative stress, which also contributes to placental aging leading to preterm birth, and that the occurrence of preterm birth during this critical period may further enhance the ensuing alterations in lung function and physiology.

The strength of this study is that all data was collected from two of the largest hospitals in the city, which are the top hospitals in China's healthcare system, with a high level of medical technology and quality of service. As a result, large amounts of medical data can be collected and the data tends to be more accurate and reliable, contributing to more accurate conclusions. This study also has some limitations. First, using ambient monitoring data, we could not account for the differences in pollutant concentrations between the daily living and working environments of the study subjects. And assessing pollutant exposure levels of the study subjects based only on their home addresses may lead to some errors and may bias the association; Secondly, although the nearest monitoring site method is able to obtain more accurate data than the global average method used in previous studies, it still has some limitations. For example, in some cases, the quality of data collected may be poor due to errors in monitoring equipment, improper maintenance, etc., affecting the accuracy of the analyzed results. In addition, the large number of missing important confounders, such as child sex, maternal education level, and marital status is an important limitation of this study.

5 Conclusion

In conclusion, we observed an association between exposures to $PM_{2.5}$, PM_{10}, NO_2, CO in mid-pregnancy and late pregnancy and increased risk on preterm birth, but little evidence of associations with O_3.

In light of importance of air quality on maternal health and birth outcomes, measures to improve air quality, its monitoring and health educations for women especially in reiver valley cities need to be public health priorities.

Data availability statement

The original contributions presented in the study are included in the article/supplementary material, further inquiries can be directed to the corresponding author.

Ethics statement

The studies involving humans were approved by Medical School of Yan'an University. The studies were conducted in accordance with the local legislation and institutional requirements. The participants provided their written informed consent to participate in this study. Written informed consent was obtained from the individual(s) for the publication of any potentially identifiable images or data included in this article.

Author contributions

JG: Conceptualization, Data curation, Formal analysis, Investigation, Methodology, Project administration, Writing – original draft, Writing – review & editing. JL: Conceptualization, Formal analysis, Investigation, Methodology, Writing – original draft, Writing – review & editing. LL: Investigation, Methodology, Project administration, Software, Writing – original draft, Writing – review & editing. MC: Investigation, Methodology, Project administration, Software, Writing – original draft, Writing – review & editing. XT: Data curation, Methodology, Writing – original draft, Writing – review & editing. ZW: Data curation, Methodology, Writing – original draft, Writing – review & editing. JH: Funding acquisition, Supervision, Writing – original draft, Writing – review & editing.

Funding

The author(s) declare that financial support was received for the research, authorship, and/or publication of this article. This work was supported by the National Natural Science Foundation of China (No. 41761100); and the Natural Science Basic Research Program of Shaanxi (No. 2018JQ4013); and the 2022 National Innovation and Entrepreneurship Training Program for College Students of Yan'an University (No. 202210719043).

Acknowledgments

The authors thank the National Natural Science Foundation of China (41761100), the Natural Science Basic Research Program of Shaanxi (2018JQ4013).

Conflict of interest

The authors declare that the research was conducted in the absence of any commercial or financial relationships that could be construed as a potential conflict of interest.

Publisher's note

References

1. Ohuma EO, Moller AB, Bradley E, Chakwera S, Hussain-Alkhateeb L, Lewin A, et al. National, regional, and global estimates of preterm birth in 2020, with trends from 2010: a systematic analysis. *Lancet*. (2023) 402:1261–71. doi: 10.1016/S0140-6736(23)00878-4

2. Chawanpaiboon S, Vogel JP, Moller AB, Lumbiganon P, Petzold M, Hogan D, et al. Global, regional, and national estimates of levels of preterm birth in 2014: a systematic review and modelling analysis. *Lancet Glob Health*. (2019) 7:e37–46. doi: 10.1016/S2214-109X(18)30451-0

3. Deng K, Liang J, Mu Y, Liu Z, Wang Y, Li M, et al. Preterm births in China between 2012 and 2018: an observational study of more than 9 million women. *Lancet Glob Health*. (2021) 9:e1226–41. doi: 10.1016/S2214-109X(21)00298-9

4. Zou L, Wang X, Ruan Y, Li G, Chen Y, Zhang W. Preterm birth and neonatal mortality in China in 2011. *Int J Gynaecol Obstet*. (2014) 127:243–7. doi: 10.1016/j.ijgo.2014.06.018

5. Perin J, Mulick A, Yeung D, Villavicencio F, Lopez G, Strong KL, et al. Global, regional, and national causes of under-5 mortality in 2000-19: an updated systematic analysis with implications for the sustainable development goals. *Lancet Child Adolesc Health*. (2022) 6:106–15. doi: 10.1016/S2352-4642(21)00311-4

6. Liu L, Johnson HL, Cousens S, Perin J, Scott S, Lawn JE, et al. Global, regional, and national causes of child mortality: an updated systematic analysis for 2010 with time trends since 2000. *Lancet*. (2012) 379:2151–61. doi: 10.1016/S0140-6736(12)60560-1

7. Mwaniki MK, Atieno M, Lawn JE, Newton CR. Long-term neurodevelopmental outcomes after intrauterine and neonatal insults: a systematic review. *Lancet*. (2012) 379:445–52. doi: 10.1016/S0140-6736(11)61577-8

8. Burris HH, Baccarelli AA, Wright RO, Wright RJ. Epigenetics: linking social and environmental exposures to preterm birth. *Pediatr Res*. (2016) 79:136–40. doi: 10.1038/pr.2015.191

9. Proietti E, Röösli M, Frey U, Latzin P. Air pollution during pregnancy and neonatal outcome: a review. *J Aerosol Med Pulm Drug Deliv*. (2013) 26:9–23. doi: 10.1089/jamp.2011.0932

10. Goldenberg RL, Culhane JF, Iams JD, Romero R. Epidemiology and causes of preterm birth. *Lancet*. (2008) 371:75–84. doi: 10.1016/S0140-6736(08)60074-4

11. Torchin H, Ancel PY. Epidemiology and risk factors of preterm birth. *J Gynecol Obstet Biol Reprod*. (2016) 45:1213–30. doi: 10.1016/j.jgyn.2016.09.013

12. Ye CX, Chen SB, Wang TT, Zhang SM, Qin JB, Chen LZ. Risk factors for preterm birth: a prospective cohort study. *Zhongguo Dang Dai Er Ke Za Zhi*. (2021) 23:1242–9. doi: 10.7499/j.issn.1008-8830.2108015

13. Barfield WD. Public health implications of very preterm birth. *Clin Perinatol*. (2018) 45:565–77. doi: 10.1016/j.clp.2018.05.007

14. Jiang M, Mishu MM, Lu D, Yin X. A case control study of risk factors and neonatal outcomes of preterm birth. *Taiwan J Obstet Gynecol*. (2018) 57:814–8. doi: 10.1016/j.tjog.2018.10.008

15. Crawford N, Prendergast D, Oehlert JW, Shaw GM, Stevenson DK, Rappaport N, et al. Divergent patterns of mitochondrial and nuclear ancestry are associated with the risk for preterm birth. *J Pediatr*. (2018) 194:40–46.e4. doi: 10.1016/j.jpeds.2017.10.052

16. Alman BL, Stingone JA, Yazdy M, Botto LD, Desrosiers TA, Pruitt S, et al. Associations between $PM_{2.5}$ and risk of preterm birth among liveborn infants. *Ann Epidemiol*. (2019) 39:46–53.e2. doi: 10.1016/j.annepidem.2019.09.008

17. Hansen C, Neller A, Williams G, Simpson R. Maternal exposure to low levels of ambient air pollution and preterm birth in Brisbane, Australia. *BJOG*. (2006) 113:935–41. doi: 10.1111/j.1471-0528.2006.01010.x

18. Wilhelm M, Ritz B. Local variations in CO and particulate air pollution and adverse birth outcomes in Los Angeles County, California, USA. *Environ Health Perspect*. (2005) 113:1212–21. doi: 10.1289/ehp.7751

19. Hu LW, Lawrence WR, Liu Y, Yang BY, Zeng XW, Chen W, et al. Ambient air pollution and morbidity in Chinese. *Adv Exp Med Biol*. (2017) 1017:123–51. doi: 10.1007/978-981-10-5657-4_6

20. Zhan D, Kwan MP, Zhang W, Wang S, Yu J. Spatiotemporal variations and driving factors of air pollution in China. *Int J Environ Res Public Health*. (2017) 14:1538. doi: 10.3390/ijerph14121538

21. Chen Q, Ren Z, Liu Y, Qiu Y, Yang H, Zhou Y, et al. The association between preterm birth and ambient air pollution exposure in Shiyan, China, 2015–2017. *Int J Environ Res Public Health*. (2021) 18:4326. doi: 10.3390/ijerph18084326

22. Ha S, Hu H, Roussos-Ross D, Haidong K, Roth J, Xu X. The effects of air pollution on adverse birth outcomes. *Environ Res*. (2014) 134:198–204. doi: 10.1016/j.envres.2014.08.002

23. Zhang X, Fan C, Ren Z, Feng H, Zuo S, Hao J, et al. Maternal $PM_{2.5}$ exposure triggers preterm birth: a cross-sectional study in Wuhan, China. *Glob Health Res. Policy*. (2020) 5:17. doi: 10.1186/s41256-020-00144-5

24. Jiang P, Li Y, Tong MK, Ha S, Gaw E, Nie J, et al. Wildfire particulate exposure and risks of preterm birth and low birth weight in the Southwestern United States. *Public Health*. (2024) 230:81–8. doi: 10.1016/j.puhe.2024.02.016

25. Zhao N, Qiu J, Zhang Y, He X, Zhou M, Li M, et al. Ambient air pollutant PM_{10} and risk of preterm birth in Lanzhou, China. *Environ Int*. (2015) 76:71–7. doi: 10.1016/j.envint.2014.12.009

26. Han Y, Jiang P, Dong T, Ding X, Chen T, Villanger GD, et al. Maternal air pollution exposure and preterm birth in Wuxi, China: effect modification by maternal age. *Ecotoxicol Environ Saf*. (2018) 157:457–62. doi: 10.1016/j.ecoenv.2018.04.002

27. Bhardwaj N, Nigam A, De A, Gupta N. Ambient air pollution: a new intrauterine environmental toxin for preterm birth and low birth weight. *J Obstet Gynaecol India*. (2023) 73:25–9. doi: 10.1007/s13224-023-01790-8

28. Ahn TG, Kim YJ, Lee G, You YA, Kim SM, Chae R, et al. Association between individual air pollution (PM_{10}, $PM_{2.5}$) exposure and adverse pregnancy outcomes in Korea: a multicenter prospective cohort, air pollution on pregnancy outcome (APPO) study. *J Korean Med Sci*. (2024) 39:e131. doi: 10.3346/jkms.2024.39.e131

29. Ju L, Li C, Yang M, Sun S, Zhang Q, Cao J, et al. Maternal air pollution exposure increases the risk of preterm birth: evidence from the meta-analysis of cohort studies. *Environ Res*. (2021) 202:111654. doi: 10.1016/j.envres.2021.111654

30. Siddika N, Rantala AK, Antikainen H, Balogun H, Amegah AK, Ryti NRI, et al. Short-term prenatal exposure to ambient air pollution and risk of preterm birth—a population-based cohort study in Finland. *Environ Res*. (2020) 184:109290. doi: 10.1016/j.envres.2020.109290

31. He J, Cao N, Hei J, Wang H, He J, Liu Y, et al. Relationship between ambient air pollution and preterm birth: a retrospective birth cohort study in Yan'an, China. *Environ Sci Pollut Res Int*. (2022) 29:73271–81. doi: 10.1007/s11356-022-20852-4

32. Siddika N, Rantala AK, Antikainen H, Balogun H, Amegah AK, Ryti NRI, et al. Synergistic effects of prenatal exposure to fine particulate matter ($PM_{2.5}$) and ozone (O_3) on the risk of preterm birth: a population-based cohort study. *Environ Res*. (2019) 176:108549. doi: 10.1016/j.envres.2019.108549

33. Wang X, Wang X, Gao C, Xu X, Li L, Liu Y, et al. Relationship between outdoor air pollutant exposure and premature delivery in China-systematic review and meta-analysis. *Int J Public Health*. (2023) 68:1606226. doi: 10.3389/ijph.2023.1606226

34. Tosevska A, Ghosh S, Ganguly A, Cappelletti M, Kallapur SG, Pellegrini M, et al. Integrated analysis of an in vivo model of intra-nasal exposure to instilled air pollutants reveals cell-type specific responses in the placenta. *Sci Rep*. (2022) 12:8438. doi: 10.1038/s41598-022-12340-z

35. Saenen ND, Martens DS, Neven KY, Alfano R, Bové H, Janssen BG, et al. Air pollution-induced placental alterations: an interplay of oxidative stress, epigenetics, and the aging phenotype? *Clin Epigenetics*. (2019) 11:124. doi: 10.1186/s13148-019-0688-z

36. Lapehn S, Paquette AG. The placental epigenome as a molecular link between prenatal exposures and Fetal health outcomes through the DOHaD hypothesis. *Curr Environ Health Rep*. (2022) 9:490–501. doi: 10.1007/s40572-022-00354-8

37. Wright RJ. Preterm birth enhances ambient pollution toxicity: oxidative stress and placental function. *Am J Respir Crit Care Med*. (2022) 205:10–2. doi: 10.1164/rccm.202110-2338ED

frontiers | Frontiers in Public Health

TYPE Original Research
PUBLISHED 01 August 2024
DOI 10.3389/fpubh.2024.1401034

OPEN ACCESS

EDITED BY
Yizhong Yan,
Shihezi University, China

REVIEWED BY
Rossanna Rodriguez-Canul,
Center for Research and Advanced Studies – Mérida Unit, Mexico
Aziz-Ur-Rahim Bacha,
Harbin Institute of Technology, Shenzhen, China
Mohd Kamil Hussain,
Govt. Raza Post Graduate College, Rampur, India

*CORRESPONDENCE
Qinghua Qiu
✉ qinghuaqiu@163.com

†These authors have contributed equally to this work

RECEIVED 14 March 2024
ACCEPTED 18 July 2024
PUBLISHED 01 August 2024

CITATION
Meng C, Gu C, Cai C, He S, Lai D and Qiu Q (2024) Associations of heavy metal exposure with diabetic retinopathy in the U.S. diabetic population: a cross-sectional study. *Front. Public Health* 12:1401034. doi: 10.3389/fpubh.2024.1401034

Associations of heavy metal exposure with diabetic retinopathy in the U.S. diabetic population: a cross-sectional study

Chunren Meng[1,2†], Chufeng Gu[2,3†], Chunyang Cai[1,2], Shuai He[1,2], Dongwei Lai[1,2] and Qinghua Qiu[1,2,4,5*]

[1]Department of Ophthalmology, Tong Ren Hospital, Shanghai Jiao Tong University School of Medicine, Shanghai, China, [2]Department of Ophthalmology, Shanghai General Hospital, Shanghai Jiao Tong University School of Medicine, National Clinical Research Center for Eye Diseases; Shanghai Clinical Research Center for Eye Diseases, Shanghai, China, [3]Department of Ophthalmology, Fuzhou University Affiliated Provincial Hospital, Fuzhou, Fujian, China, [4]Department of Ophthalmology, Shigatse People's Hospital, Shigatse, Xizang, China, [5]High Altitude Ocular Disease Research Center of Shigatse People's Hospital and Tongren Hospital Affiliated to Shanghai Jiao Tong University School of Medicine, Shanghai, China

Background: Mounting evidence suggests a correlation between heavy metals exposure and diabetes. Diabetic retinopathy (DR) is a prevalent and irreversible complication of diabetes that can result in blindness. However, studies focusing on the effects of exposure to heavy metals on DR remain scarce. Thus, this study aimed to investigate the potential correlation between heavy metals exposure and DR.

Methods: A total of 1,146 diabetics from the National Health and Nutrition Examination Survey (NHANES) between 2005 and 2018 were included in this study. Heavy metal levels were measured via urine testing. Weighted logistic regression, Bayesian kernel machine regression (BKMR), weighted quantile sum (WQS) regression, and restricted cubic spline (RCS) were utilized to investigate the potential relationships between exposure to 10 heavy metals and DR. Finally, subgroup analysis was conducted based on the glycemic control status.

Results: Among the 1,146 participants, 239 (20.86%) were diagnosed with DR. Those with DR had worse glycemic control and a higher prevalence of chronic kidney disease compared to those without DR. Moreover, both the WQS regression and BKMR models demonstrated a positive relationship between exposure to mixed heavy metals and the risk of DR. The results of weighted logistic regression revealed a positive correlation between cobalt (Co) and antimony (Sb) exposure and the risk of DR (OR = 1.489, 95%CI: 1.064–2.082, p = 0.021; OR = 1.475, 95% CI: 1.084–2.008, p = 0.014), while mercury (Hg) exposure was found to promote DR exclusively in the group with good glycemic control (OR = 1.509, 95% CI: 1.157–1.967, p = 0.003). These findings were corroborated by the results of the RCS analysis.

Conclusion: Heavy metal exposure is associated with an increased risk of DR, especially Sb, Co, and Hg exposure. Nevertheless, well-designed prospective studies are warranted to validate these findings.

KEYWORDS

heavy metal exposure, diabetic retinopathy, public health, NHANES, risk factors

1 Introduction

Diabetic retinopathy (DR) is a prevalent microvascular complication of diabetes mellitus that affects approximately one-third of diabetic patients (1). It causes varying degrees of visual impairment (2), which significantly impacts the quality of life of patients and imposes substantial economic burdens on society (3). Notably, its pathogenesis is complex and multifaceted, including oxidative stress, inflammation, and mitochondrial disorders, among others (4). At present, there is a pressing need to identify the risk factors and intervention strategies for DR in order to enhance the prognosis of patients with DR.

As is well documented, heavy metals are ubiquitously present in the air, soil, water, food, and manufactured products (5–9). Exposure to heavy metals may increase the risk of various ocular diseases, including DR, age-related macular degeneration (AMD), glaucoma, and cataracts (10–13). Zhu et al. demonstrated that the accumulation of serum cesium (Cs) and cadmium (Cd) was significantly correlated with the risk of developing DR (10). Similarly, the findings of Li et al. indicated that exposure to certain heavy metals, including lithium (Li), Cd, strontium (Sr), and magnesium (Mg), may increase the risk of developing proliferative DR, whereas selenium (Se) appears to be a protective factor (14). Zhang et al. observed a significant negative correlation between serum manganese (Mn) levels and DR prevalence in individuals with type 2 diabetes mellitus in the United States (15). However, the correlation between serum Cd, mercury (Hg), and lead (Pb), and DR was not statistically significant (15). Other studies have determined a potential association between cobalt (Co), barium (Ba), molybdenum (Mo), antimony (Sb), thallium (Tl), and tungsten (Tu) and the risk of diabetes (16–18), but their relationship with DR remains elusive. Although previous studies have preliminarily explored the link between heavy metals and DR, certain limitations remain. For instance, earlier studies exclusively investigated the association between the levels of serum heavy metals and DR risk, with a lack of research on the effect of urinary heavy metals on DR. Serum heavy metal levels may correlate with recent exposure, whereas urine heavy metal concentrations reflect long-term exposure (19). Furthermore, heavy metals are frequently co-exposed in the environment, and interactions between metals may also have an impact on human health (20, 21). However, studies on co-exposure to heavy metals and DR risk are lacking. Additionally, there is a lack of epidemiological studies to elucidate the effects of other heavy metals, such as Co and Sb, on the risk of developing DR.

The present study extracted U.S. demographic data from the National Health and Nutrition Examination Survey (NHANES) between 2005 and 2018 to investigate the relationship between heavy metals and the risk of DR. A total of 10 urinary heavy metals, namely Ba, Cd, Co, Cs, Mo, Pb, Sb, Tl, Tu, and Hg were analyzed. The effect of single and multiple metals on DR risk was evaluated using weighted logistic regression analysis. Furthermore, weighted quantile sum (WQS) regression and Bayesian kernel machine regression (BKMR) model were applied to investigate the relationship between heavy metals co-exposure and DR. In addition, dose–response relationships between heavy metals and DR were explored using restricted cubic spline (RCS) regression. Lastly, subgroup analysis was conducted based on glycemic control levels. Our findings are anticipated to provide new epidemiological evidence to enhance the understanding of the correlation between heavy metals and DR and assist in the prevention of DR.

2 Materials and methods

2.1 Study design

2.1.1 Participants

The NHANES aimed to assess the health and nutritional status of the US population. By employing a complex multistage probability sampling technique, the NHANES collects information on the nation's civilian population every 2 years (22). In the current study, data derived from NHANES between 2005 and 2018 (seven NHANES cycles) were analyzed, given that participants underwent relatively comprehensive urine testing for heavy metals during these cycles. NHANES was approved by the Ethics Review Committee at the National Center for Health Statistics, and all participants provided informed consent. Among the 70,190 participants across the NHANES cycles conducted between 2005 and 2018, several groups were excluded according to the following criteria: (1) participants who were pregnant or lacked data on diabetes ($n = 3,744$); (2) participants with incomplete urinary metal levels ($n = 48,050$); (3) participants who had missing covariate data ($n = 8,806$); (4) non-diabetic individuals ($n = 7,852$); and (5) participants with other missing information on diabetic retinopathy ($n = 592$). The final study cohort comprised 1,146 subjects, as illustrated in Figure 1.

2.1.2 Definitions of diabetes and DR

Diagnostic criteria for diabetes comprised any of the following: (1) diagnosis by medical professionals during a non-gestational period, (2) hemoglobin A1c level (HbA1c) (%) $\geq$ 6.5, (3) fasting plasma glucose level (FPG) $\geq$ 7.0 mmol/L, (4) random blood glucose level $\geq$ 11.1 mmol/L, (5) 2-h oral glucose tolerance test (OGTT) blood glucose $\geq$11.1 mmol/L, and (6) receiving anti-diabetic medication (23). DR was determined through self-report using a dichotomous approach. Participants were informed by medical professionals that diabetes had affected their eyes (24).

2.2 Metal measurement

Between 2005 and 2018, the levels of 10 heavy metals, namely Ba, Cd, Co, Cs, Mo, Pb, Sb, Tl, Tu, and Hg, were detected in urine samples. The NHANES website provides all laboratory methods and quality control information. Briefly, the concentration of 10 urinary metals was determined using inductively coupled plasma-mass spectrometry (ICP-MS). If the metal concentration was below the limit of detection (LOD), the LOD divided by the square root of two was used as the surrogate. In addition, all urinary metal levels were normalized to urinary creatinine and reported as μg/g creatinine (25).

2.3 Covariates

Demographic characteristics [gender, age, ethnicity, educational background, and family poverty income ratio (PIR)], along with data on body mass index (BMI), HbA1c levels, history of hypertension

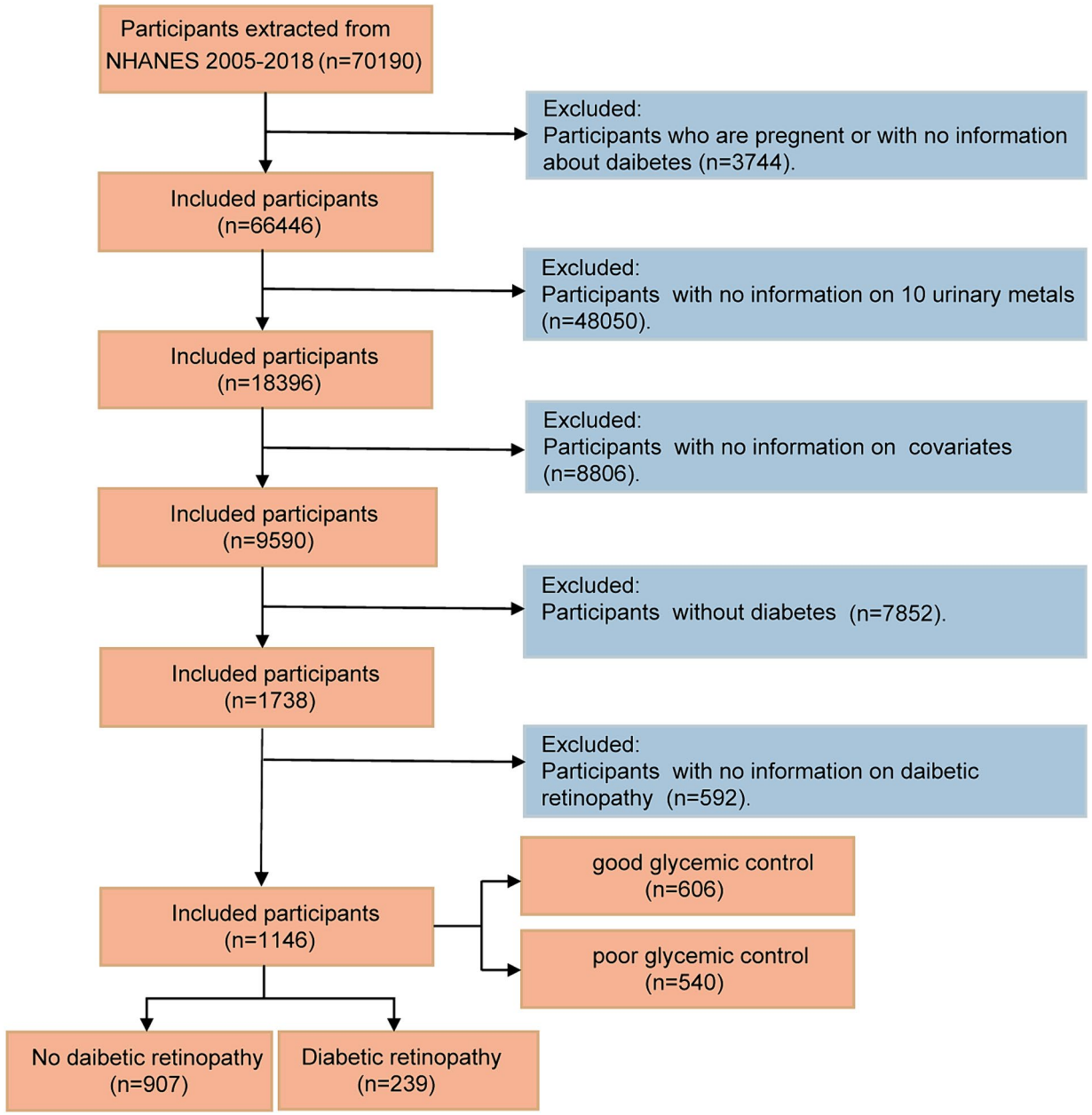

FIGURE 1
Flow diagram of the screening and enrollment of study participants.

and chronic kidney disease (CKD), smoking status, and drinking habits, were acquired through either home interviews or laboratory assessments. Ethnicity was classified into five groups: non-Hispanic white, non-Hispanic black, Mexican American, other Hispanic, and other race/multiracial. PIR was categorized into three levels: <1.30, 1.30–3.5, and ≥3.5 (21). Similarly, BMI was divided into three levels: <25, 25–30, and >30 kg/m^2. Glycemic control was classified as well (HbA1c < 7%) and poor (HbA1c ≥7%). Drinking status was self-reported by the participants. Smoking status was determined through the evaluation of serum cotinine levels, with a cutoff value of ≤0.011 ng/mL for nonsmokers and higher levels indicating smoking status for both active and second-hand smokers (26). Hypertension was defined as any of the following: self-reported hypertension, ever or currently taking anti-hypertensive drugs, a systolic blood pressure over 140 mmHg, or a diastolic blood pressure exceeding 90 mmHg. CKD was defined as any of the following: an estimated glomerular filtration rate (eGFR) < 60 mL/min/1.73 m^2 or the presence of elevated albuminuria (urine albumin creatinine ratio ≥ 30 mg/g) (27).

2.4 Statistical analysis

WTSA2YR is considered the appropriate NHANES sampling weight to analyze data on urinary heavy metals. Given the complex sampling design of NHANES, weights (1/7 * WTSA2YR) were constructed in accordance with the analytic guidelines of

NHANES. Weighted means (standard errors) were employed to present continuous variables, while unweighted frequencies (weighted percentages) were utilized to present categorical variables. Baseline comparisons were made based on DR status stratification. The *t*-test was used to compare continuous variables, whereas the chi-square test was used to compare categorical variables. Given the upward trend in heavy metal concentration in the human body, an Ln transformation was performed on heavy metal concentration data to approximate a normal distribution (continuous variable) and divided the heavy metal concentration data into quartiles. The relationships between the concentrations of the 10 metals were determined using Pearson correlation analysis.

First and foremost, weighted logistic regression was employed to explore the impact of each metal on the risk of DR. The reference group was set as the first quartile (Q1), and the results were expressed as odds ratios (ORs) and their corresponding 95% confidence intervals (CIs). All covariates, including age, gender, ethnicity, educational background, PIR, glycemic control, smoking and drinking status, BMI, hypertension, and CKD, were adjusted. Furthermore, a weighted logistic regression analysis encompassing all heavy metals was conducted to adjust for the effects of other metals.

Secondly, to assess the combined effect of exposure to multiple metals on DR risk, a WQS regression analysis was carried out. This method was selected owing to its effective characterization of environmental mixtures (28). The R package ("gWQS") was utilized to compute the WQS index, which is a weighted sum of the concentrations of individual heavy metals (21). The WQS index (ranging from 0 to 1) indicated the level of mixed exposure to the 10 heavy metals. The weight of each metal reflected its relative importance for the risk of DR. The WQS analysis results provided information about the concurrent influence of adding a quartile to heavy metals mixtures on DR risk.

BKMR is a developing statistical method that utilizes kernel functions to effectively model the individual and joint impacts of mixture exposure on health results (29). The common influences of heavy metal mixtures on DR were examined by analyzing the DR estimates for every 5 percent increase/decrease in the median concentration of metal mixtures (reference) (25). The posterior probability of inclusion (PIP) was calculated with a threshold of 0.5 to assess the relative contribution of each metal component to the outcome (30). The BKMR model was generated via the R package "bkmr" through 10,000 iterations (31).

Subsequently, an RCS regression analysis was conducted using the R package "rms" to investigate the dose–response association of heavy metal exposure with DR risk. RCS regression was used to analyze both the linear and nonlinear relationships between heavy metals levels and DR risk (32). The number of nodes was selected to maintain the best fit and prevent overfitting the principal spline, with a range of 3–7 nodes considered according to the minimum absolute value of Akaike's information criterion (33). Finally, the 3 knots corresponding to the 10th, 50th, and 90th percentiles were chosen.

Finally, the same statistical analysis procedures previously outlined were applied to the subgroups based on glycemic control (well-controlled group: HbA1c value <7%, poorly-controlled group: HbA1c value ≥7%).

Statistical analyses were performed using R software (v4.3.1), with *p*-values less than 0.05 considered statistically significant.

3 Results

3.1 Study population characteristics

This study included 1,146 participants from seven NHANES cycles, comprising 550 women (weighted survey sample of 7,898,021) and 596 men (weighted survey sample of 8,162,870). Among them, 239 (20.86%) were diagnosed with DR, including 134 males and 105 females. Table 1 presents a summary of the baseline characteristics of the study participants with and without DR. Consistent with the findings of previously published studies, our study confirmed that participants with DR exhibited poorer glycemic control than those with diabetes without DR. Furthermore, the prevalence of CKD was higher in individuals with DR compared to those without DR. The two groups were comparable in age, gender, ethnicity, educational background, PIR, BMI, drinking and smoking status, and prevalence of hypertension.

3.2 Distributions and correlations of the 10 heavy metals

Supplementary Table 1 lists the distribution of concentrations for 10 heavy metals, with detection rates exceeding 93.0% for each metal. Interestingly, Mo was the most metal with the highest level. Additionally, patients with DR had significantly higher levels of Sb compared to those without DR ($p = 0.021$). The correlations between the 10 heavy metals are detailed in Supplementary Figure 1. Co and Tl ($r = 0.58$), Co and Ba ($r = 0.43$), Cs and Ba ($r = 0.35$), Co and Cs ($r = 0.34$), Tu and Mo ($r = 0.34$), and Tl and Ba ($r = 0.31$) exhibited positive correlations. Other metals had relatively weak correlations.

3.3 Association of heavy metals with DR risk evaluated by weighted logistic regression

As displayed in Table 2, weighted logistic regression was applied to analyze the association between each metal and DR risk after adjusting for all covariates. When considering the concentrations of Co and Sb as continuous variables, an increase of one unit in Ln-Co and Ln-Sb concentrations resulted in a 48.9 and 47.5% increase in the risk of DR, respectively (all $p < 0.05$). In addition, a positive correlation was observed between Sb and DR when metal concentrations were divided into quartiles (p for trend = 0.036). Notably, there was a significantly positive correlation found between DR risk and Hg concentration in the third quartile (Q3) (OR = 2.322, 95% CI: 1.158–4.655, $p = 0.018$), whereas no significant correlation was detected for concentrations in the highest quartile (Q4).

Subgroup analysis based on the level of glycemic control was also performed (Table 2). In the poorly-controlled group, Sb exerted the most significant effect (OR = 1.596, 95% CI: 1.022–2.493, $p = 0.04$), but this relationship was not significantly different from that in the well-controlled group. In the well-controlled group, Ba concentration in Q3 (OR = 0.274, 95% CI: 0.120–0.627, $p = 0.003$) was significantly and negatively correlated with DR risk, but Ba concentration in Q4 did not. Both Hg concentrations in Q4 and Ln-Hg significantly increased the

10.3389/fpubh.2024.1401034

TABLE 1 Baseline characteristics of study population by DR status.

Variable	Total (*N* = 1,146)	Non-DR (*N* = 907)	DR (*N* = 239)	*p* value
Age, years	58.514 (0.549)	58.745 (0.606)	57.578 (1.183)	0.378
Sex, *n* (%)				0.342
Female	550 (49.175)	445 (50.328)	105 (44.502)	
Male	596 (50.825)	462 (49.672)	134 (55.498)	
Ethnicity, *n* (%)				0.473
Mexican American	217 (9.219)	173 (9.275)	44 (8.991)	
Non-Hispanic Black	275 (13.323)	221 (13.453)	54 (12.796)	
Non-Hispanic White	425 (64.961)	344 (65.232)	81 (63.861)	
Other Hispanic	120 (5.651)	91 (5.847)	29 (4.855)	
Other race	109 (6.846)	78 (6.192)	31 (9.496)	
Education, *n* (%)				0.79
Greater than high school	478 (49.391)	378 (49.696)	100 (48.154)	
High school or below	668 (50.609)	529 (50.304)	139 (51.846)	
BMI (kg/m^2), *n* (%)				0.82
<25	141 (10.047)	103 (9.666)	38 (11.590)	
25–30	320 (26.132)	253 (26.098)	67 (26.271)	
≥30	685 (63.821)	551 (64.236)	134 (62.139)	
PIR, *n* (%)				0.481
≤1.30	408 (24.080)	310 (23.297)	98 (27.255)	
1.30–3.50	473 (41.302)	386 (42.522)	87 (36.355)	
>3.50	265 (34.619)	211 (34.181)	54 (36.390)	
Drinking, *n* (%)				0.088
Never	204 (15.090)	149 (13.444)	55 (21.764)	
Former	302 (22.077)	235 (22.170)	67 (21.699)	
Now	640 (62.833)	523 (64.386)	117 (56.537)	
Smoking, *n* (%)				0.833
Non-smoker	314 (30.365)	247 (30.624)	67 (29.313)	
Smoker	832 (69.635)	660 (69.376)	172 (70.687)	
Glycemic control, *n* (%)				**<0.0001**
Well-controlled	606 (56.183)	511 (60.711)	95 (37.829)	
Poorly controlled	540 (43.817)	396 (39.289)	144 (62.171)	
Hypertension, *n* (%)				0.346
No	301 (27.458)	242 (28.240)	59 (24.287)	
Yes	845 (72.542)	665 (71.760)	180 (75.713)	
CKD, *n* (%)				**0.002**
No	681 (64.623)	574 (67.894)	107 (51.365)	
Yes	465 (35.377)	333 (32.106)	132 (48.635)	

Continuous variables were presented as weighted means (standard errors) and categorical variables are expressed as unweighted numbers (weighted percentages). DR, diabetic retinopathy; BMI, body mass index; N, numbers of subject; %, weighted percentage; NHANES, National Health and Nutrition Examination Survey; PIR, Poverty Income Ratio; CKD, chronic kidney disease. *P* value was calculated by chi-squared test and Student's t-test. Bold: $p < 0.05$.

risk of DR (OR = 3.608, 95% CI: 1.695–7.681, $p = 0.001$; OR = 1.509, 95% CI: 1.157–1.967, $p = 0.003$) in the well-controlled group. Other metals have not been shown to have a meaningful association with DR.

To account for the potential influence of other heavy metals, weighted logistic regression models that considered all heavy metals were applied. As demonstrated in Supplementary Table 2, Hg concentration in Q3 significantly increased the risk of DR (OR = 2.407, 95% CI: 1.264–4.585, $p = 0.008$). Additionally, each per-unit increase in Ln-Co and Ln-Sb concentrations led to a 62.7 and 42.7% higher risk of DR, respectively (all $p < 0.05$).

TABLE 2 Associations of single urinary metals with DR risk in the study population.

Metal (μg/g creatinine)	Continuous		Q1	Q2		Q3		Q4		*p* for trend
	OR (95% CI)	*p* value	OR (95% CI)	OR (95% CI)	*p* value	OR (95% CI)	*p* value	OR (95% CI)	*p* value	
Ba										
Total	0.974 (0.809, 1.171)	0.773	ref	0.574 (0.336, 0.980)	0.042	0.836 (0.472, 1.482)	0.536	0.914 (0.504, 1.655)	0.763	0.868
Well-controlled	0.872 (0.671, 1.133)	0.301	ref	0.712 (0.326, 1.552)	0.387	**0.274 (0.120, 0.627)**	**0.003**	0.840 (0.349, 2.021)	0.693	0.537
Poorly controlled	1.083 (0.854, 1.374)	0.506	ref	**0.441 (0.215, 0.906)**	**0.027**	1.411 (0.671, 2.968)	0.359	1.007 (0.465, 2.178)	0.986	0.359
Co										
Total	**1.489 (1.064, 2.082)**	**0.021**	ref	0.917 (0.529, 1.589)	0.755	1.021 (0.602, 1.733)	0.937	1.547 (0.849, 2.819)	0.152	0.145
Well-controlled	1.508 (0.956, 2.377)	0.076	ref	0.717 (0.334, 1.539)	0.388	0.761 (0.359, 1.613)	0.472	1.798 (0.829, 3.901)	0.135	0.129
Poorly controlled	1.427 (0.940, 2.167)	0.094	ref	0.994 (0.464, 2.130)	0.988	1.190 (0.551, 2.569)	0.654	1.318 (0.503, 3.454)	0.569	0.494
Cs										
Total	1.294 (0.799, 2.096)	0.292	ref	0.696 (0.368, 1.316)	0.261	0.934 (0.502, 1.737)	0.827	1.281 (0.668, 2.458)	0.452	0.317
Well-controlled	0.790 (0.467, 1.336)	0.374	ref	0.616 (0.256, 1.483)	0.276	0.461 (0.184, 1.157)	0.098	0.802 (0.408, 1.576)	0.517	0.457
Poorly controlled	1.751 (0.948, 3.231)	0.073	ref	0.666 (0.269, 1.649)	0.374	1.722 (0.788, 3.765)	0.170	1.755 (0.694, 4.437)	0.231	0.106
Mo										
Total	0.947 (0.651, 1.376)	0.771	ref	1.015 (0.502, 2.053)	0.967	0.901 (0.439, 1.853)	0.775	1.073 (0.555, 2.075)	0.832	0.945
Well-controlled	1.505 (0.764, 2.965)	0.233		1.219 (0.386, 3.853)	0.732	1.828 (0.564, 5.923)	0.310	2.457 (0.802, 7.528)	0.114	0.092
Poorly controlled	0.630 (0.393, 1.009)	0.055	ref	0.870 (0.357, 2.120)	0.756	0.542 (0.188, 1.565)	0.253	0.562 (0.249, 1.272)	0.164	0.12
Sb										
Total	**1.475 (1.084, 2.008)**	**0.014**	ref	0.799 (0.426, 1.500)	0.481	1.471 (0.770, 2.809)	0.239	1.685 (0.948, 2.992)	0.075	**0.036**
Well-controlled	1.442 (0.961, 2.165)	0.077	ref	0.586 (0.258, 1.330)	0.198	1.566 (0.646, 3.798)	0.316	1.749 (0.747, 4.093)	0.194	0.094
Poorly controlled	**1.596 (1.022, 2.493)**	**0.040**	ref	0.837 (0.346, 2.026)	0.690	1.479 (0.617, 3.549)	0.375	1.632 (0.747, 3.561)	0.215	0.121
Tu										
Total	1.101 (0.807, 1.502)	0.538	ref	**0.485 (0.264, 0.891)**	**0.02**	1.169 (0.619, 2.210)	0.627	1.148 (0.598, 2.202)	0.675	0.299
Well-controlled	1.643 (0.999, 2.703)	0.051	ref	0.573 (0.260, 1.265)	0.165	**2.405 (1.075, 5.381)**	**0.033**	2.065 (0.802, 5.315)	0.131	**0.031**
Poorly controlled	0.850 (0.572, 1.262)	0.414	ref	0.474 (0.216, 1.041)	0.062	0.760 (0.303, 1.908)	0.554	0.832 (0.337, 2.052)	0.685	0.861
Tl										
Total	1.091 (0.737, 1.617)	0.442	ref	1.087 (0.621, 1.902)	0.768	0.849 (0.455, 1.583)	0.603	1.053 (0.619, 1.792)	0.848	0.838
Well-controlled	1.068 (0.605, 1.884)	0.818	ref	1.089 (0.558, 2.124)	0.801	0.921 (0.356, 2.380)	0.863	0.780 (0.371, 1.639)	0.507	0.461
Poorly controlled	1.050 (0.652, 1.690)	0.838	ref	1.155 (0.497, 2.688)	0.734	0.834 (0.361, 1.925)	0.666	1.280 (0.626, 2.617)	0.493	0.742

(Continued)

10.3389/fpubh.2024.1401034

10.3389/fpubh.2024.1401034

TABLE 2 (Continued)

Metal (μg/g creatinine)	Continuous		Q1	Q2		Q3		Q4		*p* for trend
	OR (95% CI)	*p* value	OR (95% CI)	OR (95% CI)	*p* value	OR (95% CI)	*p* value	OR (95% CI)	*p* value	
Pb										
Total	1.235 (0.914, 1.668)	0.167	ref	1.202 (0.658, 2.198)	0.545	1.236 (0.599, 2.551)	0.562	1.744 (0.954, 3.191)	0.07	0.116
Well-controlled	1.253 (0.827, 1.900)	0.283	ref	1.188 (0.463, 3.048)	0.717	1.614 (0.680, 3.831)	0.274	1.546 (0.631, 3.789)	0.336	0.219
Poorly controlled	1.229 (0.790, 1.910)	0.355	ref	1.249 (0.560, 2.786)	0.581	1.081 (0.429, 2.722)	0.868	2.099 (0.890, 4.951)	0.089	0.215
Cd										
Total	0.882 (0.639, 1.218)	0.441	ref	0.921 (0.454, 1.866)	0.816	1.046 (0.524, 2.091)	0.897	0.829 (0.423, 1.628)	0.583	0.714
Well-controlled	0.846 (0.543, 1.318)	0.455	ref	0.953 (0.351, 2.585)	0.924	0.540 (0.215, 1.351)	0.185	0.683 (0.279, 1.670)	0.398	0.237
Poorly controlled	0.896 (0.593, 1.353)	0.595	ref	0.951 (0.375, 2.411)	0.915	1.520 (0.625, 3.699)	0.351	0.949 (0.368, 2.446)	0.913	0.779
Hg										
Total	1.110 (0.909, 1.356)	0.302	ref	1.605 (0.794, 3.248)	0.190	**2.322 (1.158, 4.655)**	**0.018**	1.539 (0.727, 3.259)	0.256	0.13
Well-controlled	**1.509 (1.157, 1.967)**	**0.003**	ref	1.638 (0.596, 4.503)	0.334	**3.213 (1.377, 7.498)**	**0.008**	**3.608 (1.695, 7.681)**	**0.001**	**<0.001**
Poorly controlled	0.904 (0.694, 1.177)	0.447	ref	1.773 (0.709, 4.431)	0.216	2.329 (0.958, 5.658)	0.062	0.742 (0.263, 2.091)	0.567	0.731

Models were adjusted for age, sex, ethnicity, education, poverty income ratio, body mass index, drinking alcohol status, smoking status, glycemic control, hypertension and CKD. Continuous, Ln-transformed concentration of metal; CI, confidence interval; OR, odds ratio; Q, quartile; Ref, reference. *p* value was calculated by weighted logistic regression. Bold: $p < 0.05$.

3.4 Associations between heavy metal mixtures and DR risk evaluated by WQS regression

WQS regression was conducted to investigate the correlation between heavy metal mixtures and DR risk while adjusting for all covariates. In our study, the WQS index was positively correlated with DR risk (OR = 1.5, 95%CI: 1.07–2.10, $p = 0.019$). In the subgroup analysis stratified by glycemic control, the correlation between exposure to heavy metals and DR risk was not statistically significant in either the well-controlled or poorly-controlled group (all $p > 0.05$). Among the 10 heavy metals, Pb, Mo, Hg, Sb, and Co exhibited the highest weight in the whole population (Figure 2A). In the well-controlled group, Sb was determined to be the highest weighted metal (Figure 2B), whereas Cs and Co were the most heavily weighted metals in the poorly-controlled group (Figure 2C).

3.5 Associations between heavy metal mixtures and DR risk evaluated by the BKMR model

Although no statistically significant effect was observed, there was a discernible increase in the risk of DR when heavy metal mixture concentrations were at or exceeded the 60th percentile (Figure 3A). Similar associations were observed in both the well-controlled and poorly-controlled groups, as depicted in Figure 3A. When concentrations of other metals were fixed at the 25th, 50th, and 75th percentiles, Co, Mo, Sb, Tu, Pb, and Hg concentrations all displayed a positive correlation with DR risk, with PIP values exceeding 0.55 (Figure 3B and Supplementary Table 3). Similar trends were observed in both the well-controlled and poorly-controlled groups, although the correlations were not statistically significant, as delineated in Figure 3B. The univariate exposure-response relationship exhibited a monotonic upward trend between DR and Co, Sb, Tu, and Pb concentrations when the other metals were fixed at the median level. However, Ba, Tl, and Cd displayed a monotonic downward trend (Supplementary Figure 2). Based on the moderate correlations between some metals, the interactions among the 10 heavy metals were separately analyzed, revealing underlying interactions between specific heavy metals. Supplementary Figure 3 delineates that Co interacts with Cs, Sb, Tl, Hg, and Pb, whilst Sb interacts with Tu, Cd, and Hg, and Hg interacts with most metals.

3.6 Associations between concentrations of heavy metals and DR risk in the RCS analysis

Co, Sb, and Hg concentrations, which were closely related to DR risk, were further analyzed. The dose–response relationships were evaluated in the RCS analysis (Figure 4). Linear and positive associations with DR risk were identified for the Ln-transformed concentrations of Co and Sb (all $p_{nonlinearity} > 0.05$, all $p_{overall} < 0.05$), except for Hg ($p_{nonlinearity} = 7e\text{-}04$). In both the well-controlled and poorly-controlled groups, Co and Sb concentrations had a linear relationship with DR risk. In the well-controlled group, the risk of DR generally increased with increasing Co concentration ($p_{overall} = 0.011$, $p_{nonlinearity} = 0.262$). Conversely, in the

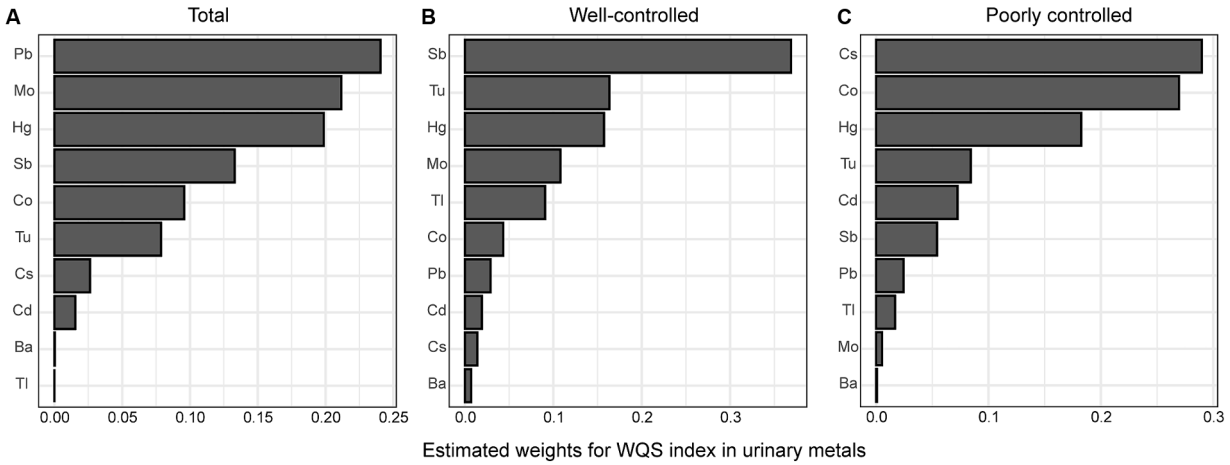

FIGURE 2
Estimated weights of heavy metals for DR by WQS models were adjusted for age, sex, ethnicity, education, poverty income ratio, body mass index, drinking alcohol status, smoking status, glycemic control, hypertension and CKD. **(A)** total population, **(B)** good glycemic control group, **(C)** poor glycemic control group. Ba, Barium; Cd, Cadmium; Co, Cobalt; Cs, Cesium; Mo, Molybdenum; Pb, lead; Sb, Antimony; Tl, Thallium; Tu, Tungsten; lead, Pb; mercury, Hg.

poorly-controlled group, a positive linear dose correlation between Sb concentrations and DR risk was noted ($p_{overall} = 0.045$, $p_{nonlinearity} = 0.790$). Finally, a linear and positive correlation between Hg concentrations and the risk of DR was observed solely in the well-controlled group ($p_{overall} = 0.01$, $p_{nonlinearity} = 0.385$).

4 Discussion

To the best of our knowledge, this is the first cross-sectional study to investigate the effects of urinary heavy metals on the risk of DR in a substantial, nationally representative sample utilizing various statistical techniques. Herein, the results of weighted logistic regression demonstrated that Co, Sb, and Hg were associated with DR risk in the single-metal model, and this association was also observed in the multi-metal model. Both the WQS and BMKR models suggested that mixed exposure to these 10 heavy metals was positively associated with DR risk. Furthermore, the results of the RCS regression displayed a linear and positive correlation between Co and Sb and DR risk but a non-linear correlation between Hg concentrations and DR risk. The results of the subgroup analyses signaled that the aforementioned associations appeared to be more pronounced in the poorly-controlled group.

Co is widely distributed in nature. Humans are commonly exposed to Co through multiple routes, including food, environmental pollution, occupational exposure, and medical interventions (34). Besides, it is an essential element for human health, serving as the metallic component of vitamin B12 (35). Despite its vital importance, its potential toxicity can elicit adverse health effects after prolonged exposure. A cross-sectional study identified a positive correlation between diabetes and urinary Co concentrations (16). Consistently, a study discovered a strong correlation between elevated urinary Co levels and increased levels of FPG and HbA1c in male participants (36). At the same time, Cancarini et al. concluded that the Co concentration in the tear film of diabetic patients was higher than that in the control group (37). This increase may be attributed to the rise in conjunctival vascular permeability caused by diabetes, similar to the increase in retinal vascular permeability driven by diabetes (a characteristic of DR) (38). In our study, diabetic patients with higher urinary concentrations of Co were more likely to develop DR. This may be ascribed to the oxidizing effect of Co promoting the formation of free radicals, inducing oxidative stress responses, and contributing to mitochondrial dysfunction (39). Of note, accumulating evidence suggests that oxidative damage and mitochondrial dysfunction promote the development of DR (40, 41).

Sb is a toxic heavy metal to which humans are primarily exposed through the consumption of food and air, soil, and water exposure. Numerous studies have demonstrated that it exerts various toxic effects on vital organs, including but not limited to the pancreas, liver, lungs, intestines, and spleen (42). A cross-sectional study conducted in the USA demonstrated an association between urine Sb concentrations and insulin resistance (16). Likewise, a cross-sectional study conducted in China found that urinary Sb levels are linked to an increased risk of increased FPG levels, impaired fasting glucose, and diabetes (18). Furthermore, a prospective study indicated that pregnant women with higher exposure to Sb may face an increased risk of gestational diabetes mellitus (43). Xiao et al. reported that elevated urinary Sb concentrations are linked to a higher incidence of type 2 diabetes, and this process is partially implicated in oxidative DNA damage (44). These studies collectively imply that Sb exposure may contribute to the development of diabetes. However, to date, there has been no report on the correlation between Sb levels and DR. Our study uncovered that diabetic patients with elevated urinary Sb levels have a significantly increased risk of developing DR, especially in those with poor glycemic control.

Hg is a highly toxic heavy metal that can cause significant harm to numerous organs in the human body (45). Currently, research on the relationship between Hg levels and diabetes risk remains inconclusive. Earlier studies found no significant association between blood or urine Hg concentrations and an increased risk of diabetes in adults (46–48). However, Tsai et al. observed a significant increase in Hg levels in the red blood cells of type 2 diabetes patients compared to those without the condition (49). A large prospective cohort study determined that people with high Hg exposure during early adulthood

10.3389/fpubh.2024.1401034

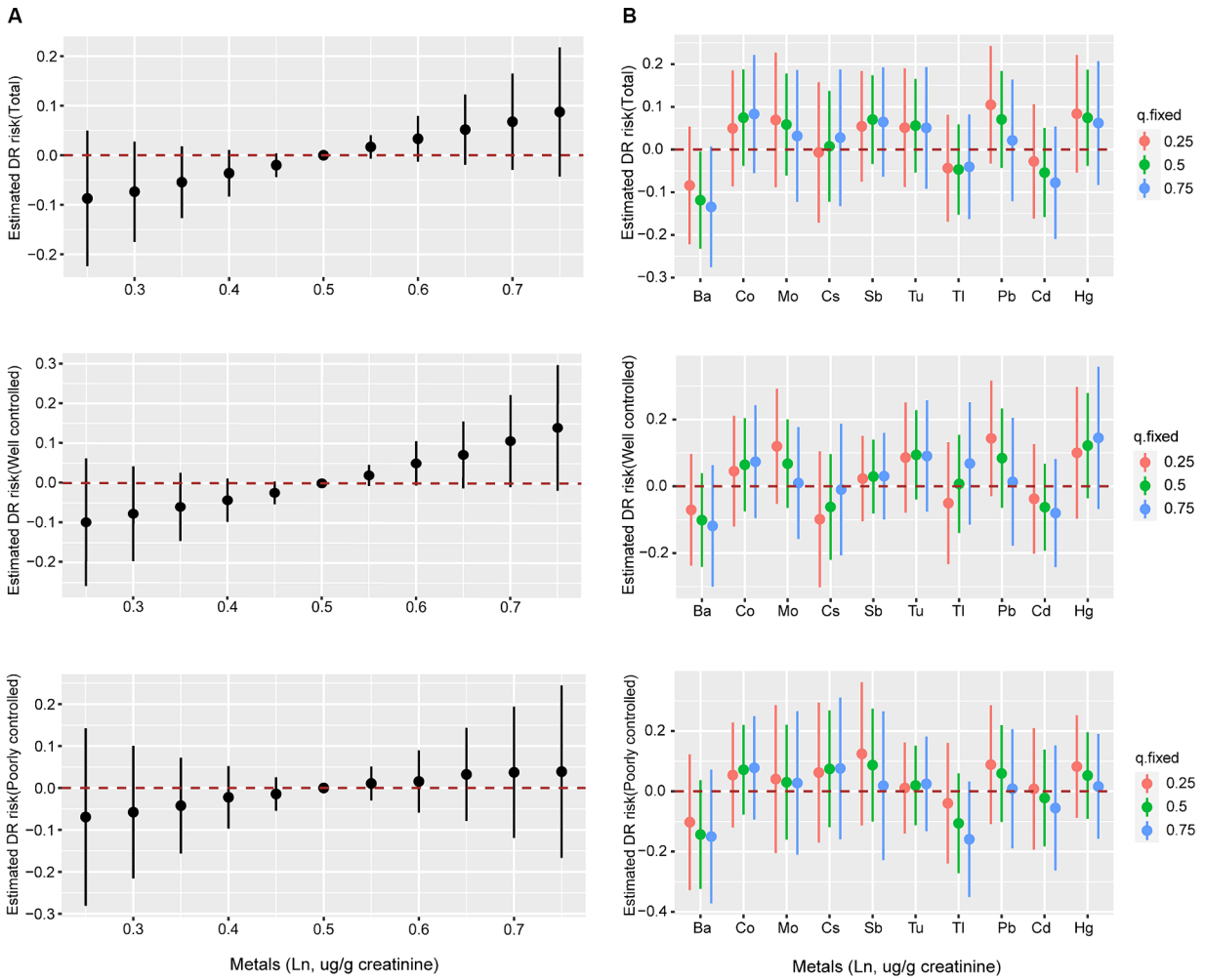

FIGURE 3
The associations of metal mixtures and DR risk evaluated by BKMR model. **(A)** The joint effects of heavy metal mixtures on DR risk were estimated by BKMR models in total population and subgroups, when all the metals at particular percentiles were compared to all the metals at their 50th percentile. **(B)** Associations of single heavy metals with DR risk were estimated by BKMR models in total population and subgroups, when other all metals were held at their corresponding 25th (red), 50th (green) or 75th (blue) percentile, respectively. Models were adjusted for age, sex, ethnicity, education, poverty income ratio, body mass index, drinking alcohol status, smoking status, glycemic control, hypertension and CKD. Ba, Barium; Cd, Cadmium; Co, Cobalt; Cs, Cesium; Mo, Molybdenum; Pb, lead; Sb, Antimony; Tl, Thallium; Tu, Tungsten; lead, Pb; mercury, Hg.

were at a higher risk of developing diabetes in the future (50). Furthermore, research has demonstrated that Hg can selectively affect β cells in the pancreas, resulting in cellular dysfunction and apoptosis (51). In this study, urine Hg levels among diabetes patients with DR were higher compared to those without DR, although the difference was not statistically significant. Additionally, a clear non-monotonic relationship was identified between Hg levels and the risk of DR. This may be due to the fact that the chief source of human exposure to Hg is the consumption of marine fish, which are rich in omega-3 fatty acids that counteract the toxicity of Hg (52, 53). A significant positive correlation was observed between Hg concentrations and DR risk only in the well-controlled group, warranting further investigation.

Heavy metals stimulate reactive oxygen species production, leading to oxidative damage, which is one of the mechanisms involved in disease development (54). The retina is a high-oxygen-consuming tissue that is highly susceptible to damage from oxidative stress. Previous studies have shown a robust correlation between oxidative stress and retinal vascular impairment under hyperglycemic conditions (55). However, the role of heavy metals in DR development via oxidative stress mechanisms remains unclear. Thus, further experimental validation is necessary.

This study has several advantages. Firstly, it is the first study that investigated the correlation between urinary heavy metals and DR risk, considering both the single and co-exposure effects of heavy metals. In contrast, Zhang et al. focused on the relationship between blood heavy metals and DR risk without exploring the combined effects of heavy metals on DR (15). Furthermore, our study included a higher number of metals than those conducted by Zhang et al. (15) and reported for the first time that urinary levels of Co, Sb, and Hg may be associated with DR risk. Secondly, weighted logistic regression, WQS regression model, BMKR model, and RCS regression were employed to investigate the correlation between heavy metals and DR risk in a diabetes population from multiple perspectives. These statistical methods have been extensively utilized to explore the effects of heavy metals on diabetes and hypertension (21, 56). Finally, previous

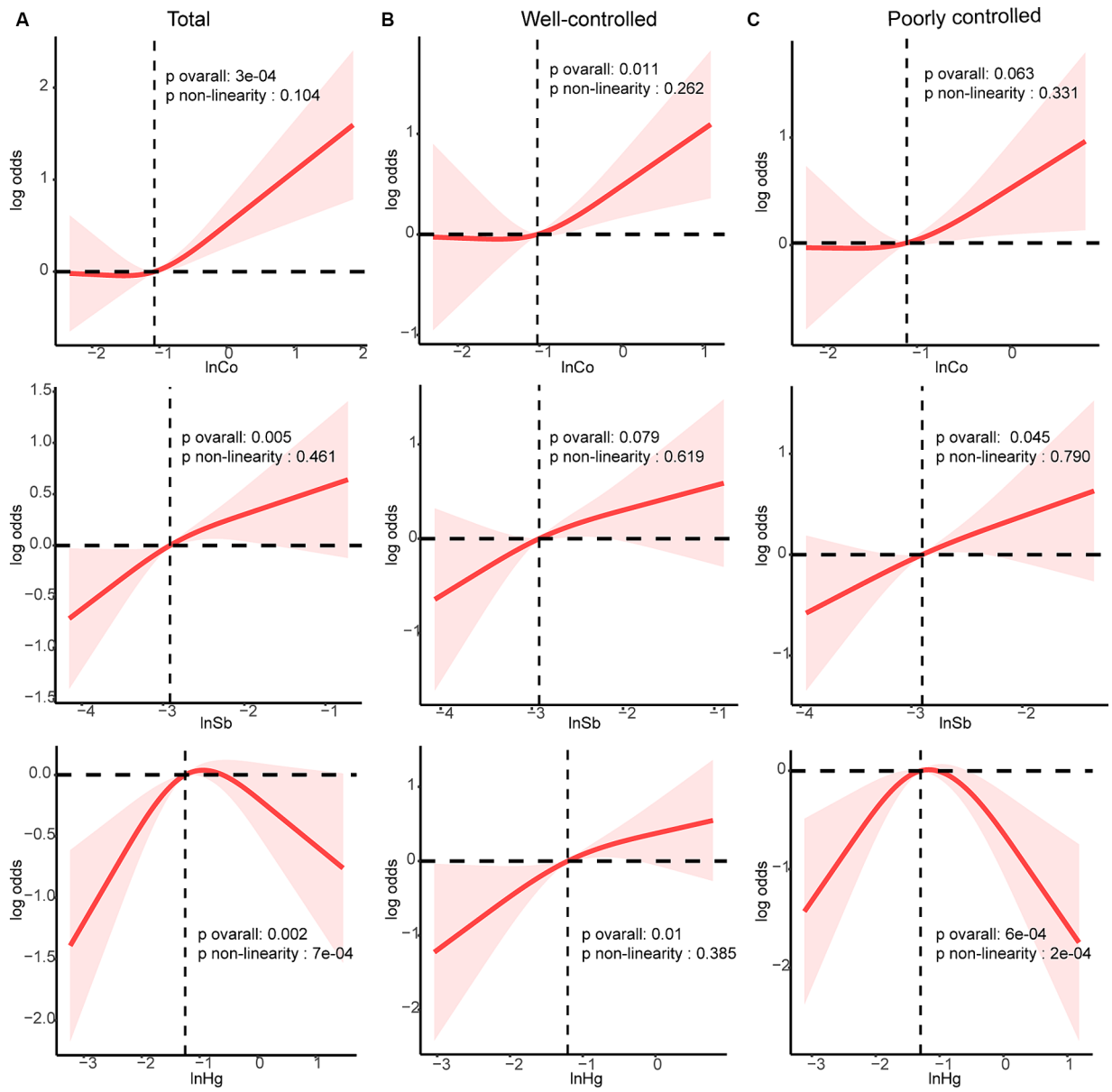

FIGURE 4
Dose–response relationship between Sb, Co and Hg with DR risk were estimated by RCS models in total population and subgroups. Models were adjusted for age, sex, ethnicity, education, poverty income ratio, body mass index, drinking alcohol status, smoking status, glycemic control, hypertension and CKD. **(A)** total population, **(B)** good glycemic control group, **(C)** poor glycemic control group. Solid line, odds ratios; red-shade, 95% CI.

research has demonstrated a correlation between heavy metal exposure and HbA1c levels. High HbA1c level has been established as a risk factor for DR. Therefore, subgroup analysis was initially conducted based on glycemic control (determined by HbA1c value) to investigate the correlation between urine levels of heavy metals and DR risk.

Nevertheless, some limitations of this study merit acknowledgment. Given the inherent shortcomings of cross-sectional studies (57), this study could not establish a causal relationship between metal exposure and the risk of DR. Furthermore, relying on self-report questionnaires for DR diagnosis may introduce recall bias. In addition, the dataset lacked precise information regarding retinopathy severity, thereby limiting further analysis. The concentrations of heavy metals in urine are affected by various factors, not all of which were accounted for in this study, potentially compromising the reliability of the results. Additionally, selection bias selection bias may be present due to missing data and the exclusion of participants with incomplete information. Therefore, further studies are necessitated to corroborate our findings and to investigate the relationship between metal concentrations and DR severity, as well as to elucidate the underlying mechanisms by which metals affect DR.

5 Conclusion

Overall, our cross-sectional study demonstrated that several heavy metals, including Co, Sb, and Hg, were significantly associated with an elevated risk of DR. Furthermore, a linear and positive correlation

was observed between the concentrations of Co and Sb and the risk of DR, while a non-linear correlation was identified between Hg levels and DR risk. The results of the subgroup analyses signaled that the aforementioned associations appeared to be more pronounced in the poorly-controlled group. The results of the mixture exposure analysis indicated a positive association between mixed metal exposure and the risk of DR. This association was observed in both the well-controlled group and the poorly-controlled group. Due to the limitations of the present study, subsequent investigations are required to substantiate these findings and to clarify the mechanisms by which heavy metals affect DR.

Data availability statement

The original contributions presented in the study are included in the article/Supplementary material, further inquiries can be directed to the corresponding author.

Author contributions

CM: Conceptualization, Formal analysis, Methodology, Writing – original draft, Writing – review & editing. CG: Data curation, Formal analysis, Methodology, Writing – original draft, Writing – review & editing. CC: Formal analysis, Methodology, Writing – review & editing. SH: Formal analysis, Methodology, Writing – original draft. DL: Data curation, Methodology, Writing – original draft. QQ: Conceptualization, Supervision, Writing – review & editing.

Funding

The author(s) declare that financial support was received for the research, authorship, and/or publication of this article. This work has been supported by the National Natural Science Foundation of China (82371072).

Conflict of interest

The authors declare that the research was conducted in the absence of any commercial or financial relationships that could be construed as a potential conflict of interest.

Publisher's note

Supplementary material

The Supplementary material for this article can be found online at: https://www.frontiersin.org/articles/10.3389/fpubh.2024.1401034/full#supplementary-material

References

1. Yau JW, Rogers SL, Kawasaki R, Lamoureux EL, Kowalski JW, Bek T, et al. Global prevalence and major risk factors of diabetic retinopathy. *Diabetes Care*. (2012) 35:556–64. doi: 10.2337/dc11-1909

2. Zhou C, Li S, Ye L, Chen C, Liu S, Yang H, et al. Visual impairment and blindness caused by retinal diseases: a nationwide register-based study. *J Glob Health*. (2023) 13:04126. doi: 10.7189/jogh.13.04126

3. Marques AP, Ramke J, Cairns J, Butt T, Zhang JH, Jones I, et al. The economics of vision impairment and its leading causes: a systematic review. *EClinicalMedicine*. (2022) 46:101354. doi: 10.1016/j.eclinm.2022.101354

4. Li H, Liu X, Zhong H, Fang J, Li X, Shi R, et al. Research progress on the pathogenesis of diabetic retinopathy. *BMC Ophthalmol*. (2023) 23:372. doi: 10.1186/s12886-023-03118-6

5. Wang X, Mukherjee B, Park SK. Associations of cumulative exposure to heavy metal mixtures with obesity and its comorbidities among U.S. adults in NHANES 2003-2014. *Environ Int*. (2018) 121:683–94. doi: 10.1016/j.envint.2018.09.035

6. Fatma UK, Nizami G, Ahamad S, Saquib M, Hussain MK. Activated green tamarind pulp (Agtp) as an efficient adsorbent for removal of Pb2+, Cu2+, Zn2+ & Ni2+ from contaminated water. *J Water Proc Eng*. (2024) 59:105048. doi: 10.1016/j.jwpe.2024.105048

7. Fatma UK, Nizami G, Ahamad S, Hussain MK. Efficient removal of Pb2+, Cu2+ and Zn2+ by waste tea-derived cost-effective bioadsorbent. *ChemistrySelect*. (2023) 8:e202300944. doi: 10.1002/slct.202300944

8. Alloway BJ. Sources of heavy metals and metalloids in soils In: BJ Alloway, editor. Heavy metals in soils: trace metals and metalloids in soils and their bioavailability. Dordrecht: Springer Netherlands (2013). 11–50.

9. Bosch AC, O'Neill B, Sigge GO, Kerwath SE, Hoffman LC. Heavy metals in marine fish meat and consumer health: a review. *J Sci Food Agric*. (2016) 96:32–48. doi: 10.1002/jsfa.7360

10. Zhu X, Hua R. Serum essential trace elements and toxic metals in Chinese diabetic re tinopathy patients. *Medicine*. (2020) 99:e23141. doi: 10.1097/MD.0000000000023141

11. Park SJ, Lee JH, Woo SJ, Kang SW, Park KHEpidemiologic Survey Committee of Korean Ophthalmologic Society. Five heavy metallic elements and age-related macular degeneration: Korean National Health and Nutrition Examination Survey, 2008-2011. *Ophthalmology*. (2015) 122:129–37. doi: 10.1016/j.ophtha.2014.07.039

12. Vennam S, Georgoulas S, Khawaja A, Chua S, Strouthidis NG, Foster PJ. Heavy metal toxicity and the aetiology of Glaucoma. *Eye*. (2020) 34:129–37. doi: 10.1038/s41433-019-0672-z

13. Wang W, Schaumberg DA, Park SK. Cadmium and lead exposure and risk of cataract surgery in U.S. adults. *Int J Hyg Environ Health*. (2016) 219:850–6. doi: 10.1016/j.ijheh.2016.07.012

14. Li Y-Q, Zhang S-T, Ke N-Y, Fang Y-C, Hu W-L, Li G-A, et al. The impact of multiple metals exposure on the risk of developing proli ferative diabetic retinopathy in Anhui, China: a case-control study. *Environ Sci Pollut Res Int*. (2023) 30:112132–43. doi: 10.1007/s11356-023-30294-1

15. Zhang Y, Liu X, Zhang X, Li L, Li Q, Geng H, et al. Association between serum heavy metal levels and diabetic retinopathy in NHANES 2011-2020. *Sci Rep*. (2024) 14:1268. doi: 10.1038/s41598-024-51749-6

16. Menke A, Guallar E, Cowie CC. Metals in urine and diabetes in U.S. adults. *Diabetes*. (2016) 65:164–71. doi: 10.2337/db15-0316

17. Hendryx M, Luo J, Chojenta C, Byles JE. Exposure to heavy metals from point pollution sources and risk of incident type 2 diabetes among women: a prospective cohort analysis. *Int J Environ Health Res*. (2021) 31:453–64. doi: 10.1080/09603123.2019.1668545

18. Feng W, Cui X, Liu B, Liu C, Xiao Y, Lu W, et al. Association of urinary metal profiles with altered glucose levels and diabetes risk: a population-based study in China. *PLoS One*. (2015) 10:e0123742. doi: 10.1371/journal.pone.0123742

19. Wilhelm M, Müller F, Idel H. Biological monitoring of mercury vapour exposure by scalp hair analysis in comparison to blood and urine. *Toxicol Lett*. (1996) 88:221–6. doi: 10.1016/0378-4274(96)03741-1

20. Chen L, Sun Q, Peng S, Tan T, Mei G, Chen H, et al. Associations of blood and urinary heavy metals with rheumatoid arthritis risk among adults in NHANES, 1999-2018. *Chemosphere*. (2022) 289:133147. doi: 10.1016/j.chemosphere.2021.133147

21. Wu Z, Guan T, Cai D, Su G. Exposure to multiple metals in adults and diabetes mellitus: a cross-sectional analysis. *Environ Geochem Health*. (2023) 45:3251–61. doi: 10.1007/s10653-022-01411-9

22. Kim D, Lee S, Choi J-Y, Lee J, Lee H-J, Min J-Y, et al. Association of A-klotho and lead and cadmium: a cross-sectional study. *Sci Total Environ*. (2022) 843:156938. doi: 10.1016/j.scitotenv.2022.156938

23. American Diabetes Association. 2. Classification and diagnosis of diabetes: standards of medical care in diabetes—2018. *Diabetes Care*. (2018, 2018) 41:S13–27. doi: 10.2337/dc18-S002

24. Xu H, Dong X, Wang J, Cheng X, Qu S, Jia T, et al. Association of calcium, magnesium, zinc, and copper intakes with diabetic retinopathy in diabetics: National Health and Nutrition Examination Survey, 2007–2018. *Curr Eye Res*. (2023, 2023) 48:485–91. doi: 10.1080/02713683.2023.2165105

25. Chen Y, Pan Z, Shen J, Wu Y, Fang L, Xu S, et al. Associations of exposure to blood and urinary heavy metal mixtures wit H psoriasis risk among U.S. adults: a cross-sectional study. *Sci Total Environ*. (2023) 887:164133. doi: 10.1016/j.scitotenv.2023.164133

26. Xu C, Liang J, Xu S, Liu Q, Xu J, Gu A. Increased serum levels of aldehydes are associated with cardiovascular disease and cardiovascular risk factors in adults. *J Hazard Mater*. (2020) 400:123134. doi: 10.1016/j.jhazmat.2020.123134

27. Webster AC, Nagler EV, Morton RL, Masson P. Chronic kidney disease. *Lancet*. (2017) 389:1238–52. doi: 10.1016/s0140-6736(16)32064-5

28. Carrico C, Gennings C, Wheeler DC, Factor-Litvak P. Characterization of weighted quantile sum regression for highly correlated data in a risk analysis setting. *J Agric Biol Environ Stat*. (2015) 20:100–20. doi: 10.1007/s13253-014-0180-3

29. Bobb JF, Valeri L, Claus Henn B, Christiani DC, Wright RO, Mazumdar M, et al. Bayesian kernel machine regression for estimating the health effects of multi-pollutant mixtures. *Biostatistics*. (2015) 16:493–508. doi: 10.1093/biostatistics/kxu058

30. Ma Y, Hu Q, Yang D, Zhao Y, Bai J, Mubarik S, et al. Combined exposure to multiple metals on serum uric acid in NHANES under three statistical models. *Chemosphere*. (2022) 301:134416. doi: 10.1016/j.chemosphere.2022.134416

31. Weng X, Tan Y, Fei Q, Yao H, Fu Y, Wu X, et al. Association between mixed exposure of phthalates and cognitive function among the U.S. elderly from NHANES 2011-2014: three statistical models. *Sci Total Environ*. (2022) 828:154362. doi: 10.1016/j.scitotenv.2022.154362

32. Desquilbet L, Mariotti F. Dose-response analyses using restricted cubic spline functions in public health research. *Stat Med*. (2010) 29:1037–57. doi: 10.1002/sim.3841

33. Johannesen CDL, Langsted A, Mortensen MB, Nordestgaard BG. Association between low density lipoprotein and all cause and cause specific mortality in Denmark: prospective cohort study. *BMJ*. (2020) 371:m4266. doi: 10.1136/bmj.m4266

34. Tvermoes BE, Unice KM, Paustenbach DJ, Finley BL, Otani JM, Galbraith DA. Effects and blood concentrations of cobalt after ingestion of 1 mg/d by human volunteers for 90 d. *Am J Clin Nutr*. (2014) 99:632–46. doi: 10.3945/ajcn.113.071449

35. Reynolds E. Vitamin B12, folic acid, and the nervous system. *Lancet Neurol*. (2006) 5:949–60. doi: 10.1016/S1474-4422(06)70598-1

36. Yang J, Lu Y, Bai Y, Cheng Z. Sex-specific and dose-response relationships of urinary cobalt and molybdenum levels with glucose levels and insulin resistance in U.S. adults. *J Environ Sci*. (2023) 124:42–9. doi: 10.1016/j.jes.2021.10.023

37. Cancarini A, Fostinelli J, Napoli L, Gilberti ME, Apostoli P, Semeraro F. Trace elements and diabetes: assessment of levels in tears and serum. *Exp Eye Res*. (2017) 154:47–52. doi: 10.1016/j.exer.2016.10.020

38. Rudraraju M, Narayanan SP, Somanath PR. Regulation of blood-retinal barrier cell-junctions in diabetic retinopathy. *Pharmacol Res*. (2020) 161:105115. doi: 10.1016/j.phrs.2020.105115

39. Karovic O, Tonazzini I, Rebola N, Edström E, Lövdahl C, Fredholm BB, et al. Toxic effects of cobalt in primary cultures of mouse astrocytes. *Biochem Pharmacol*. (2007) 73:694–708. doi: 10.1016/j.bcp.2006.11.008

40. Kang Q, Yang C. Oxidative stress and diabetic retinopathy: molecular mechanisms, pathogenetic role and therapeutic implications. *Redox Biol*. (2020) 37:101799. doi: 10.1016/j.redox.2020.101799

41. Wu M-Y, Yiang G-T, Lai T-T, Li C-J. The oxidative stress and mitochondrial dysfunction during the pathogenesis of diabetic retinopathy. *Oxidative Med Cell Longev*. (2018) 2018:3420187. doi: 10.1155/2018/3420187

42. Coelho DR, Miranda ES, Saint?Pierre TD, Paumgartten FJR. Tissue distribution of residual antimony in rats treated with multiple doses of meglumine antimoniate. *Mem Inst Oswaldo Cruz*. (2014) 109:420–7. doi: 10.1590/0074-0276140030

43. Zhang G, Wang X, Zhang X, Li Q, Xu S, Huang L, et al. Antimony in urine during early pregnancy correlates with increased risk of gestational diabetes mellitus: a prospective cohort study. *Environ Int*. (2019) 123:164–70. doi: 10.1016/j.envint.2018.11.072

44. Xiao L, Zhou Y, Ma J, Sun W, Cao L, Wang B, et al. Oxidative DNA damage mediates the association between urinary metals and prevalence of type 2 diabetes mellitus in Chinese adults. *Sci Total Environ*. (2018) 627:1327–33. doi: 10.1016/j.scitotenv.2018.01.317

45. Rice KM, Walker EM Jr, Wu M, Gillette C, Blough ER. Environmental mercury and its toxic effects. *J Prev Med Public Health*. (2014) 47:74–83. doi: 10.3961/jpmph.2014.47.2.74

46. Moon MK, Lee I, Lee A, Park H, Kim MJ, Kim S, et al. Lead, mercury, and cadmium exposures are associated with obesity but not with diabetes mellitus: Korean National Environmental Health Survey (KONEHS) 2015-2017. *Environ Res*. (2022) 204:111888. doi: 10.1016/j.envres.2021.111888

47. Ghorbani Nejad B, Raeisi T, Janmohammadi P, Mehravar F, Zarei M, Dehghani A, et al. Mercury exposure and risk of type 2 diabetes: a systematic review and meta-analysis. *Int J Clin Pract*. (2022) 2022:1–13. doi: 10.1155/2022/7640227

48. Moon SS. Association of lead, mercury and cadmium with diabetes in the Korean population: the Korea National Health and Nutrition Examination Survey (KNHANES) 2009-2010. *Diabet Med*. (2013) 30:e143–8. doi: 10.1111/dme.12103

49. Tsai T-L, Kuo C-C, Pan W-H, Wu T-N, Lin P, Wang S-L. Type 2 diabetes occurrence and mercury exposure – from the National Nutrition and Health Survey in Taiwan. *Environ Int*. (2019) 126:260–7. doi: 10.1016/j.envint.2019.02.038

50. He K, Xun P, Liu K, Morris S, Reis J, Guallar E. Mercury exposure in young adulthood and incidence of diabetes later in life: the cardia trace element study. *Diabetes Care*. (2013) 36:1584–9. doi: 10.2337/dc12-1842

51. Yang C-Y, Liu S-H, Su C-C, Fang K-M, Yang T-Y, Liu J-M, et al. Methylmercury induces mitochondria-and endoplasmic reticulum stress-D ependent pancreatic B-cell apoptosis via an oxidative stress-mediated JNK signaling pathway. *Int J Mol Sci*. (2022) 23:2858. doi: 10.3390/ijms23052858

52. Karapehlivan M, Ogun M, Kaya I, Ozen H, Deveci HA, Karaman M. Protective effect of omega-3 fatty acid against mercury chloride intoxication in mice. *J Trace Elem Med Biol*. (2014) 28:94–9. doi: 10.1016/j.jtemb.2013.08.004

53. Smith KL, Guentzel JL. Mercury concentrations and omega-3 fatty acids in fish and shrimp: preferential consumption for maximum health benefits. *Mar Pollut Bull*. (2010) 60:1615–8. doi: 10.1016/j.marpolbul.2010.06.045

54. Rehman K, Fatima F, Waheed I, Akash MSH. Prevalence of exposure of heavy metals and their impact on health consequences. *J Cell Biochem*. (2018) 119:157–84. doi: 10.1002/jcb.26234

55. Kruk J, Kubasik-Kladna K, Aboul-Enein HY. The role oxidative stress in the pathogenesis of eye diseases: current status and a dual role of physical activity. *Mini Rev Med Chem*. (2015) 16:241–57. doi: 10.2174/1389557516666151120114605

56. Zhao S, Fan L, Wang Y, Dong S, Han M, Qin Y, et al. Combined exposure to multiple metals on hypertension in NHANES under four statistical models. *Environ Sci Pollut Res Int*. (2023) 30:92937–49. doi: 10.1007/s11356-023-28902-1

57. Wang X, Cheng Z. Cross-sectional studies: strengths, weaknesses, and recommendations. *Chest*. (2020) 158:S65–71. doi: 10.1016/j.chest.2020.03.012

frontiers | Frontiers in Public Health

TYPE Original Research
PUBLISHED 01 August 2024
DOI 10.3389/fpubh.2024.1369698

OPEN ACCESS

EDITED BY
Catherine Bulka,
University of South Florida, United States

REVIEWED BY
Suzana M. Blesic,
University of Belgrade, Serbia
Timoteo Marchini,
University Heart Center Freiburg, Germany

*CORRESPONDENCE
David Q. Rich
david_rich@urmc.rochester.edu

RECEIVED 12 January 2024
ACCEPTED 18 July 2024
PUBLISHED 01 August 2024

CITATION
Zhao T, Hopke PK, Utell MJ, Croft DP, Thurston SW, Lin S, Ling FS, Chen Y, Yount CS and Rich DQ (2024) A case-crossover study of ST-elevation myocardial infarction and organic carbon and source-specific $PM_{2.5}$ concentrations in Monroe County, New York.
Front. Public Health 12:1369698.
doi: 10.3389/fpubh.2024.1369698

A case-crossover study of ST-elevation myocardial infarction and organic carbon and source-specific $PM_{2.5}$ concentrations in Monroe County, New York

Tianming Zhao[1], Philip K. Hopke[1,2], Mark J. Utell[3,4], Daniel P. Croft[3], Sally W. Thurston[4,5], Shao Lin[6], Frederick S. Ling[7], Yunle Chen[1], Catherine S. Yount[1] and David Q. Rich[1,3,4]*

[1]Department of Public Health Sciences, University of Rochester Medical Center, Rochester, NY, United States, [2]Center for Air and Aquatic Resources Engineering and Sciences, Clarkson University, Potsdam, NY, United States, [3]Division of Pulmonary and Critical Care, Department of Medicine, University of Rochester Medical Center, Rochester, NY, United States, [4]Department of Environmental Medicine, University of Rochester Medical Center, Rochester, NY, United States, [5]Department of Biostatistics and Computational Biology, University of Rochester Medical Center, Rochester, NY, United States, [6]Department of Environmental Health, University at Albany School of Public Health, State University of New York, Rensselaer, NY, United States, [7]Division of Cardiology, Department of Medicine, University of Rochester Medical Center, Rochester, NY, United States

Background: Previous work reported increased rates of cardiovascular hospitalizations associated with increased source-specific $PM_{2.5}$ concentrations in New York State, despite decreased $PM_{2.5}$ concentrations. We also found increased rates of ST elevation myocardial infarction (STEMI) associated with short-term increases in concentrations of ultrafine particles and other traffic-related pollutants in the 2014–2016 period, but not during 2017–2019 in Rochester. Changes in $PM_{2.5}$ composition and sources resulting from air quality policies (e.g., Tier 3 light-duty vehicles) may explain the differences. Thus, this study aimed to estimate whether rates of STEMI were associated with organic carbon and source-specific $PM_{2.5}$ concentrations.

Methods: Using STEMI patients treated at the University of Rochester Medical Center, compositional and source-apportioned $PM_{2.5}$ concentrations measured in Rochester, a time-stratified case-crossover design, and conditional logistic regression models, we estimated the rate of STEMI associated with increases in mean primary organic carbon (POC), secondary organic carbon (SOC), and source-specific $PM_{2.5}$ concentrations on lag days 0, 0–3, and 0–6 during 2014–2019.

Results: The associations of an increased rate of STEMI with interquartile range (IQR) increases in spark-ignition emissions (GAS) and diesel (DIE) concentrations in the previous few days were not found from 2014 to 2019. However, IQR increases in GAS concentrations were associated with an increased rate of STEMI on the same day in the 2014–2016 period (Rate ratio [RR] = 1.69; 95% CI = 0.98, 2.94; 1.73 $\mu g/m^3$). In addition, each IQR increase in mean SOC concentration in the previous 6 days was associated with an increased rate of STEMI, despite imprecision (RR = 1.14; 95% CI = 0.89, 1.45; 0.42 $\mu g/m^3$).

Conclusion: Increased SOC concentrations may be associated with increased rates of STEMI, while there seems to be a declining trend in adverse effects of GAS on triggering of STEMI. These changes could be attributed to changes in $PM_{2.5}$ composition and sources following the Tier 3 vehicle introduction.

KEYWORDS

myocardial infarction, air pollution, $PM_{2.5}$, source apportionment, organic carbon, case-crossover

Introduction

Ambient air pollution is a growing global public health concern (1), particularly fine particulate matter (<2.5 μm; $PM_{2.5}$), which is the fifth-ranking global risk factor for mortality (2). Previous studies have demonstrated that elevations in $PM_{2.5}$ concentrations increase the risk of cardiovascular events, partially attributable to the development of cardiometabolic risk factors (3–5). Further, some reported associations between increased ambient $PM_{2.5}$ concentrations over the previous hours and days and the onset of myocardial infarctions (6–9). Our group and others have reported triggering of ST-elevation myocardial infarction (STEMI) by ambient pollutant concentrations (including $PM_{2.5}$) in the previous few hours and days in some analyses (7, 8, 10–12), but not others (13, 14), suggesting work is needed to know what components or sources of PM may be driving any associations with STEMI.

$PM_{2.5}$ is a complex mixture that includes organic compounds, elemental carbon, ions, and metal oxides, indicating $PM_{2.5}$ components from various sources with different physicochemical characteristics and toxicological effects (15). Rich et al. observed larger odds of myocardial infarction associated with increased mass fractions of sulfate, nitrate, and ammonium and a lower elemental carbon mass fraction (16). Some reported an increased risk of cardiovascular admissions and mortality associated with short-term increases in elemental carbon and organic carbon concentrations (17–19), especially ischemic heart disease admissions (18). Our prior studies (13, 14) revealed increased STEMI rates associated with increases in ultrafine particles and black carbon concentrations in the previous hour. Thus, short-term changes in the concentration of specific PM components may trigger cardiovascular events including STEMI.

Organic carbon is classified as either primary organic carbon (POC) or secondary organic carbon (SOC), based on whether the constituent organic matter is generated from other compounds released into the atmosphere. POC is produced mostly from combustion processes, whereas SOC is formed through the oxidation of volatile organic compounds (VOCs) (20) and contains reactive oxygen species (10, 21, 22) that may induce oxidative stress and systemic inflammation, contributing to acute cardiovascular events (23, 24). To our knowledge, this work is the first epidemiological study to examine triggering of STEMI by short-term increases in SOC and POC concentrations.

$PM_{2.5}$ sources emit particles with specific chemical characteristics that allow the identification and apportionment of PM to these sources. Previously, we employed source apportionment analyses to examine whether individual $PM_{2.5}$ sources were associated with acute cardiovascular hospitalizations (25) and hospitalizations and emergency department (ED) visits for respiratory infections (26) and diseases (27) in adults across New York State from 2005 to 2016. Positive matrix factorization (PMF) was used to estimate the mass concentrations of particles corresponding to specific pollution sources at six urban sites (Buffalo, Rochester, Albany, Bronx, Manhattan, and Queens) in New York (28). There were 12 $PM_{2.5}$ sources identified, including secondary sulfate (SS), secondary nitrate (SN), biomass burning (BB), diesel (DIE), spark-ignition emissions (GAS), pyrolyzed organic rich (OP), road dust (RD), aged sea salt (AGS), fresh sea salt (FSS), residual oil (RO), road salt (RS), and industrial (IND). Rich et al. reported that interquartile range (IQR) increases in GAS concentrations were associated with increased rates of hospitalization for cardiac arrhythmia and ischemic stroke on the same day, while IQR elevations in DIE concentrations were associated with elevated rates of hospitalization due to congestive heart failure and ischemic heart disease on the same day (25). Increased acute cardiovascular hospitalization rates were also associated with increased concentrations of RD, RO, and SN over the previous 1, 4, and 7 days.

Over the last decade, air quality in New York State has changed resulting from the reduction in sulfur concentrations in fuels, the closure of upwind coal-fired power plants, the energy transition from coal to natural gas, emissions controls on heavy-duty diesel vehicles, the Cross-State Air Pollution Rule, and the phase-out of residual oil for space heating in New York City. Furthermore, economic factors including the 2008 recession and the shift in the cost of natural gas relative to coal and oil, drove changes in electricity-generating unit technologies as well as air quality (29, 30). These changes resulted in substantial decreases in $PM_{2.5}$ concentrations across New York State from 2005 to 2019 (29, 30), but compositional particle changes also occurred. We found that SS and SN concentrations decreased across New York State during 2005–2019, while GAS concentrations increased over this period (31, 32). We also observed decreased POC concentrations between 2005 and 2016, and an increase in SOC concentrations during 2014–2016 after a decline in the early years of the 2005–2013 period (28). In 2017, new regulations for Tier 3 light-duty vehicles began in New York State to improve emissions, and specifically to have lower SOC formation. These Tier 3 emission controls were only included in vehicles starting in 2017 and are not mandated for all vehicles until 2025. Any resulting reduction in emissions from these vehicles provided an opportunity to explore if the associations between the rates of STEMI and $PM_{2.5}$ components and sources changed after their introduction in 2017 (i.e., early implementation period).

Using a dataset of patients whose STEMI was treated at the University of Rochester Medical Center (URMC) and ambient air pollutant concentrations from the monitoring station in Rochester

from 2014 to 2019, we hypothesized that increases in concentrations of $PM_{2.5}$ from motor vehicle and diesel sources (i.e., GAS and DIE) as well as SOC would be associated with an increased rate of STEMI. We also explored whether the introduction of Tier 3 light-duty vehicles from 2017 to 2019 (early Tier 3 implementation period) would lead to a reduced rate of STEMI associated with these specific $PM_{2.5}$ sources/components, compared to the 2014–2016 period.

Methods

Study Population and Outcome Assessment: This study included STEMI patients treated at the Cardiac Catheterization Laboratory (Cath Lab) at URMC in Rochester, New York from January 1, 2014 to December 31, 2019, who lived within 15 miles of the pollution monitoring site in Rochester. According to the American College of Cardiology (ACC)/American Heart Association (AHA) guidelines, a STEMI was defined as a myocardial infarction with an ST-segment elevation of >1 mm in two or more contiguous precordial leads, two or more adjacent limb leads, or a new or presumed new left bundle branch block in the presence of angina or angina equivalent on the presenting electrocardiogram (33). All STEMI events were diagnosed at the time of admission, with symptom onset date and time self-reported by each patient. If patients were unable to communicate, we obtained the information from their relatives. In terms of patients who experienced multiple STEMIs during the study period, if the subsequent STEMI event occurred ≥72 h after the previous one, it was counted as an additional event. In addition, demographic and clinical characteristics of patients were obtained from medical history and chart review. This study was approved by the University of Rochester Medical Center Research Subjects Review Board.

Air Pollution and Meteorology Measurements: $PM_{2.5}$ compositional data was obtained from the U.S. Environmental Protection Agency (EPA) Chemical Speciation Network.[1] Daily samples were collected and analyzed every third day in Rochester, and organic carbon, including primary organic carbon (POC) and secondary organic carbon (SOC), was measured using thermo-optical analysis. More details of the sampling methods, analytical protocols, and quality assurance and control were described previously (34). $PM_{2.5}$ sources were identified using EPA positive matrix factorization (PMF) version 5, with further information on these analyses provided previously (28, 32). Eight $PM_{2.5}$ sources identified in Rochester were used in this study, including secondary sulfate (SS), secondary nitrate (SN), spark-ignition emissions (GAS), diesel (DIE), road dust (RD), biomass burning (BB), pyrolyzed organic rich (OP), and road salt (RS). Daily ambient temperature and relative humidity in Rochester were measured at the Rochester International Airport and obtained from the National Weather Service (National Climate Data Center).[2]

Study Design and Statistical Analyses: We used a modified time-stratified case-crossover study design to estimate the rate of STEMI associated with each interquartile range increase in SOC, POC, and source-specific $PM_{2.5}$ concentration in the previous 1, 3, and 6 days. For each STEMI, the standard time-stratified design (35, 36) would include the day of STEMI symptom onset as the case day (e.g., Wednesday July 12, 2023), and then use all of the same weekdays in the same calendar month (i.e., Wednesdays July 5, 19, and 26, 2023) as control days. All case and control days would be 7 days apart, and air pollutant concentrations (e.g., $PM_{2.5}$ available for every day of the study period) would then be matched to each case and control day in the dataset for analysis. This time-stratified case-crossover design controls for non-time-varying potential confounders such as underlying medical conditions, long-term time trends, season, and weekday by design. Thus, we would not need to control for weekday in our conditional logistic regression models since each case and control day have the same value of weekday.

However, for our SOC, POC, and source-specific $PM_{2.5}$ data (32) which were only available every 3rd day, there would be very few complete sets of case and control days for analysis using this standard time-stratified design (where case and referent days are 7 days apart). Therefore, we used a modified time-stratified design, where the day of STEMI symptom onset was again the case day (e.g., Wednesday July 12, 2023), but control days were now all the 6 days intervals before and after the case day within the same calendar month (e.g., Thursday July 6, 2023; Tuesday July 18, 2023; Monday July 24, 2023; Sunday July 30, 2023). Non-time varying potential confounders, such as underlying medical conditions, long-term time trends, and season, are still controlled by design. However, weekday is not, since case and referent days are no longer the same weekday. Further, air pollutant concentrations vary by weekday (28), and weekday has been included in acute health effect studies of air pollution and cardiorespiratory health events as a potential confounder (37–39). Therefore, using a conditional logistic regression model, stratified by each case–control set, we regressed case–control status (i.e., case = 1; control = 0) against the mean SOC concentration on lag day 0, adjusting for the mean residual $PM_{2.5}$ concentration (i.e., residual $PM_{2.5}$ = $PM_{2.5}$–SOC; to control for potential confounding by non-SOC $PM_{2.5}$), weekday, holidays, temperature (natural spline with 4 degrees of freed(39)om [df]), and relative humidity (linear term) on the same case and control days. We also separately re-ran this set of models for the mean SOC concentration on lag days 0–3 and 0–6. We then re-ran this set of model analyses for POC (including residual $PM_{2.5}$ = $PM_{2.5}$–POC) and each $PM_{2.5}$ source in the same manner (residual $PM_{2.5}$ = $PM_{2.5}$–source-specific $PM_{2.5}$ concentration [e.g., $PM_{2.5}$–GAS]). For each model, we estimated the rate of STEMI associated with each interquartile range (IQR) increase in the specific pollutant concentration, and its 95% confidence interval (CI).

Next, we examined whether the rates of STEMI associated with each IQR increase in POC, SOC, and each $PM_{2.5}$ source concentration differed between the 2014–2016 and 2017–2019 periods by adding an interaction term (e.g., SOC * 2017–2019_Period) to the model. Since we examined three lag times for each pollutant, statistical significance was defined as $p < 0.017$ (0.05/3). All data management and analyses were performed using SAS version 9.4 (©SAS Institute Inc., Cary, NC) and R version 4.2.3.

Results

The demographic characteristics of the 186 patients with 188 STEMI events during the study period are provided in Table 1. The majority of these subjects were male (72.3%), white (83.4%), and

1 www.epa.gov/aqs

2 https://www.ncdc.noaa.gov/cdo-web/datatools/lcd

10.3389/fpubh.2024.1369698

TABLE 1 Characteristics of STEMI patients by period.

Characteristics	2014–2016 (*N* = 76)[a] n (%)	2017–2019 (*N* = 122)[a] n (%)
Age (years)		
<50	12 (15.8)	14 (12.5)
50–59	26 (34.2)	30 (26.8)
60–69	25 (32.9)	36 (32.1)
70–79	10 (13.2)	15 (13.4)
≥80	3 (3.9)	17 (15.2)
Mean ± SD	60.6 ± 10.8	64.4 ± 13.0
Sex		
Female	18 (23.7)	34 (30.4)
Male	58 (76.3)	78 (69.6)
Race		
Missing	0	1
Caucasian	63 (82.9)	93 (83.8)
African American	10 (13.2)	13 (11.7)
Asian	2 (2.6)	5 (4.5)
Others	1 (1.3)	0 (0)
Ethnicity		
Missing	1	0
Non-Hispanic	71 (94.7)	108 (96.4)
Hispanic/Latino	4 (5.3)	4 (3.6)
Body Mass Index (kg/m^2)		
Normal (<25)	15 (19.7)	31 (27.7)
Overweight (25 ≤ ~ <30)	36 (47.4)	40 (35.7)
Obesity (30 ≤ ~ <35)	15 (19.7)	32 (28.6)
Severe Obesity (≥35)	10 (13.2)	9 (8.0)
Mean ± SD	28.8 ± 4.9	28.4 ± 5.6
Smoking		
Missing	0	12
Yes	27 (35.5)	45 (45.0)
No	49 (64.5)	55 (55.0)
Health Insurance		
Missing	6	2
Private	60 (85.7)	67 (60.9)
Medicare	3 (4.3)	31 (28.2)
Medicaid	3 (4.3)	12 (10.9)
No insurance	3 (4.3)	0 (0)
Other (military, non-US)	1 (1.4)	0 (0)
Clinical Presentation		
Prior Myocardial Infarction	7 (9.2)	20 (17.9)
Prior Percutaneous Coronary Intervention	7 (9.2)	14 (12.5)
Prior Coronary Artery Bypass Graft	4 (5.3)	3 (2.7)
Cardiovascular Disease	5 (6.6)	9 (8.0)
Hypertension[b]	53 (69.7)	75 (84.3)

(Continued)

TABLE 1 (Continued)

Characteristics	2014–2016 (*N* = 76)[a] n (%)	2017–2019 (*N* = 122)[a] n (%)
Dyslipidemia	42 (55.3)	55 (49.1)
Diabetes	21 (27.6)	25 (22.3)
Prior Heart Failure	1 (1.3)	4 (3.6)
Family History Coronary Artery Disease	16 (21.1)	20 (17.9)
Prior Peripheral Arterial Disease[b]	3 (4.0)	3 (2.7)
Current Dialysis	1 (1.3)	0 (0)
Chronic Lung Disease	8 (10.5)	9 (8.0)
Length of Stay (days)[c] Mean ± SD	5.2 ± 12.5	4.2 ± 4.3

For any given characteristic, the denominator of percentage is the number of STEMIs events with available data on that characteristic. SD, Standard Deviation.
[a]Ns were the number of STEMI events. There was a total of 188 STEMI events among 186 patients.
[b]The variable of hypertension had 23 missing values in the period of 2017–2019. The variable of prior peripheral arterial disease had one missing value in the 2014–2016 period.
[c]One outlier (length of stay = 347 days) removed from the period of 2014–2016.

non-Hispanic (94.7%) with a mean age of 62.8 years (standard deviation [SD]: 10.8 years). Compared to the 2014–2016 period, STEMI patients in the 2017–2019 period were older (64.4 ± 13.0 vs. 60.6 ± 10.8 years) and more likely to be smokers (45.0% vs. 35.5%). They were also less likely to be male (69.6% vs. 76.3%). More subjects had Medicare (28.2% vs. 4.3%) and Medicaid (10.9% vs. 4.3%) in the 2017–2019 period than those in the 2014–2016 period. Furthermore, a prior history of myocardial infarction and hypertension was more prevalent, and diabetes and dyslipidemia were less common among the participants in the 2017–2019 period relative to the 2014–2016 period. Participants in the 2017–2019 period stayed in the hospital for 4.2 days on average (SD = 4.3 days), shorter than the 2014–2016 period (Mean ± SD: 5.2 ± 12.5 days).

Daily concentrations of POC, SOC, and $PM_{2.5}$ sources are summarized in Table 2. From the 2014–2016 period to the 2017–2019 period, the median concentration of POC and SOC increased by 34.4% (2014–2016: 0.32 μg/m^3; 2017–2019: 0.43 μg/m^3) and 41.8% (2014–2016: 0.55 μg/m^3; 2017–2019: 0.78 μg/m^3), respectively. In terms of $PM_{2.5}$ sources, there were substantial increases in median concentrations of SN (100%; 2014–2016: 0.15 μg/m^3; 2017–2019: 0.30 μg/m^3), GAS (125%; 2014–2016: 0.96 μg/m^3; 2017–2019: 2.16 μg/m^3), and OP (71.4%; 2014–2016: 0.21 μg/m^3; 2017–2019: 0.36 μg/m^3). There were large decreases in median concentrations of SS (48%; 2014–2016: 1.13 μg/m^3; 2017–2019: 0.59 μg/m^3) and BB (59%; 2014–2016: 0.44 μg/m^3; 2017–2019: 0.18 μg/m^3), but little to no change in $PM_{2.5}$, DIE, RD, and RS concentrations. SOC was moderately correlated with $PM_{2.5}$ (r = 0.53) and POC (r = 0.51; Table 3), while SS was moderately correlated with $PM_{2.5}$ (r = 0.64) and OP (r = 0.58). SN was negatively correlated with temperature (r = −0.55). DIE was positively correlated with RD (r = 0.14) and OP (r = 0.03), but negatively correlated with other $PM_{2.5}$ sources (SS: r = −0.14; SN: r = −0.06; GAS: r = −0.12; BB: r = −0.23; RS: −0.14), although these correlations were weak.

Inconsistent with our *a priori* hypothesis, interquartile range (IQR) increases in mean SOC concentrations on the same day, and previous 3 and 6 days, were not associated with increased rates of STEMI (Table 4). However, each IQR increase in mean SOC concentration in the previous 6 days was associated with an imprecise, but suggestive 14% increased rate of STEMI (Rate ratio [RR] = 1.14; 95% CI = 0.89, 1.45). Similarly, inconsistent with our *a priori* hypotheses, IQR increases in GAS and DIE on the same day, and previous 3 and 6 days, were not associated with increased rates of STEMI. There were no increased rates of STEMI associated with POC or any other source specific $PM_{2.5}$ concentration at any lag time (Table 4).

We also explored whether rates of STEMI were separately associated with increased SOC, POC, and source-specific $PM_{2.5}$ concentrations in 2014–2016 and 2017–2019 and whether these period-specific rate ratios were different (Table 5). Although increased SOC, POC, and source-specific $PM_{2.5}$ concentrations were not associated with increased rates of STEMI during either period at any lag time, each IQR increase in SS on lag day 0 was associated with a decreased rate of STEMI (RR = 0.63; 95% CI = 0.40, 0.98) during 2017–2019. Further, although imprecise, rate ratios were substantially greater than 1.0 for POC, SOC, SS, and GAS for most lag times in 2014–2016.

Next, there were significant differences (p < 0.017) in period specific rate ratios for SS on lag day 0 (2014–2016: RR = 1.22, 95% CI = 0.90, 1.65; 2017–2019: RR = 0.63, 95% CI = 0.40, 0.98) and GAS on lag day 0 (2014–2016: RR = 1.69, 95% CI = 0.98, 2.94; 2017–2019: RR = 0.79, 95% CI = 0.55, 1.13; Table 5). Although not statistically significant, there were substantial differences in rate ratios for POC on lag day 0 (2014–2016: RR = 1.20, 95% CI = 0.90, 1.60; 2017–2019: RR = 0.79, 95% CI = 0.60, 1.03) and lag day 6 (2014–2016: RR = 1.79, 95% CI = 0.83, 3.86; 2017–2019: RR = 0.69, 95% CI = 0.43, 1.12), and GAS on lag day 6 (2014–2016: RR = 1.63, 95% CI = 0.87, 3.04; 2017–2019: RR = 0.70, 95% CI = 0.42, 1.17).

Discussion

Inconsistent with our *a priori* hypothesis, we did not observe an increase in rates of STEMI associated with increased $PM_{2.5}$ concentrations from GAS and DIE sources (i.e., markers of traffic pollution) in Rochester, New York, from 2014 to 2019. However, an increase in GAS concentrations was associated with the increased rate of STEMI on the same day in the 2014–2016 period, but not in the 2017–2019 period. In addition, each IQR increase in

10.3389/fpubh.2024.1369698

TABLE 2 Distribution of daily concentrations ($\mu g/m^3$) of organic carbon and $PM_{2.5}$ sources and weather characteristics by period[a].

	N	Mean	Min	P5	P25	Median	P75	P95	Max	IQR
$PM_{2.5}$ – From composition measurements										
All years	716	6.90	−0.73	1.81	3.48	5.72	7.95	12.65	88.11	4.47
2014–2016	288	8.02	−0.73	1.64	3.51	5.69	8.78	13.27	88.11	5.27
2017–2019	428	6.13	0.18	1.88	3.48	5.74	7.60	12.49	21.73	4.13
Primary Organic Carbon (POC)										
All years	716	0.56	−0.47	0.00	0.19	0.37	0.70	1.72	3.74	0.51
2014–2016	288	0.47	0.00	0.00	0.17	0.32	0.54	1.33	3.74	0.37
2017–2019	428	0.63	−0.47	0.00	0.23	0.43	0.79	2.13	3.57	0.55
Secondary Organic Carbon (SOC)										
All years	716	0.83	0.00	0.10	0.42	0.71	1.06	1.61	11.63	0.65
2014–2016	288	0.83	0.00	0.00	0.30	0.55	1.06	1.74	11.63	0.76
2017–2019	428	0.83	0.13	0.21	0.51	0.78	1.06	1.56	2.62	0.56
$PM_{2.5}$ – From source measurements										
All years	716	6.5	0.9	2.2	3.8	6.0	8.2	12.8	21.7	4.4
2014–2016	288	6.7	1.0	2.1	3.8	6.0	8.5	13.5	20.1	4.7
2017–2019	428	6.4	0.9	2.2	3.8	6.0	7.7	12.5	21.7	3.9
Secondary Sulfate (SS)										
All years	716	1.33	−1.29	−0.40	0.15	0.78	2.06	4.91	11.48	1.90
2014–2016	288	1.92	−0.75	−0.25	0.17	1.13	3.12	6.29	11.48	2.96
2017–2019	428	0.99	−1.29	−0.54	0.11	0.59	1.41	4.20	5.72	1.30
Secondary Nitrate (SN)										
All years	716	0.89	−0.55	−0.19	0.01	0.26	1.14	4.19	10.55	1.12
2014–2016	288	0.67	−0.40	−0.29	−0.03	0.15	0.98	2.90	7.92	1.01
2017–2019	428	1.02	−0.55	−0.17	0.02	0.30	1.19	4.73	10.55	1.17
Spark-ignition Emissions (GAS)										
All years	716	1.99	−0.16	−0.03	0.96	1.79	2.68	4.60	8.05	1.73
2014–2016	288	1.28	−0.16	−0.06	0.42	0.96	1.91	4.01	5.07	1.48
2017–2019	428	2.41	−0.10	0.77	1.42	2.16	2.99	5.00	8.05	1.56
Diesel (DIE)										
All years	716	0.61	−0.29	0.05	0.34	0.60	0.81	1.19	2.43	0.47
2014–2016	288	0.61	−0.12	0.09	0.33	0.60	0.79	1.25	2.10	0.46
2017–2019	428	0.61	−0.29	0.02	0.35	0.60	0.83	1.19	2.43	0.49
Road Dust (RD)										
All years	716	0.21	−0.12	−0.02	0.07	0.16	0.32	0.61	1.65	0.25
2014–2016	288	0.24	−0.07	0.01	0.09	0.18	0.34	0.61	1.65	0.25
2017–2019	428	0.20	−0.12	−0.04	0.06	0.15	0.30	0.54	1.18	0.24
Biomass Burning (BB)										
All years	716	0.42	−0.24	−0.09	0.00	0.25	0.63	1.47	3.23	0.63
2014–2016	288	0.58	−0.24	−0.02	0.16	0.44	0.78	1.90	3.23	0.62
2017–2019	428	0.32	−0.23	−0.12	−0.05	0.18	0.53	1.25	2.09	0.58
Road Salt (RS)										
All years	716	0.07	−0.06	−0.02	0.00	0.01	0.03	0.36	1.89	0.03
2014–2016	288	0.10	−0.03	−0.01	0.00	0.01	0.04	0.56	1.89	0.04
2017–2019	428	0.05	−0.06	−0.02	0.00	0.01	0.03	0.25	1.62	0.03

(Continued)

TABLE 2 (Continued)

	N	Mean	Min	P5	P25	Median	P75	P95	Max	IQR
Pyrolyzed Organic Rich (OP)										
All years	716	0.38	−0.21	−0.02	0.14	0.33	0.55	0.99	2.47	0.41
2014–2016	288	0.33	−0.12	−0.02	0.08	0.21	0.53	1.11	1.59	0.45
2017–2019	428	0.41	−0.21	−0.02	0.22	0.36	0.56	0.95	2.47	0.34
Temperature (°C)										
All years	716	12.47	−13.97	−5.61	4.55	13.93	20.67	26.03	29.46	−1.65
2014–2016	288	13.81	−11.64	−6.01	7.49	16.00	21.24	27.83	28.83	−4.03
2017–2019	428	11.55	−13.97	−5.00	2.74	12.69	20.42	25.49	29.46	−0.10
Relative Humidity (%)										
All years	716	67.02	30.33	45.46	58.08	66.33	75.85	89.56	98.25	17.77
2014–2016	288	62.97	30.33	42.98	54.38	61.75	71.17	86.37	96.00	16.79
2017–2019	428	69.78	31.26	50.63	60.25	71.29	78.46	90.37	98.25	18.21

Min, Minimum; P5, 5th Percentile; P25, 25th Percentile; P75, 75th Percentile; P95, 95th Percentile; Max, Maximum; IQR, Interquartile Range.[a]Data on control periods and lag day 0 were used.

TABLE 3 Pearson correlation coefficients between daily pollutant concentrations (μg/m^3) and weather measurements during 2014–2019[a].

Compositional $PM_{2.5}$ Measurements											
	$PM_{2.5}$	**POC**	**SOC**	**Temp**	**RH**						
$PM_{2.5}$	1.00										
POC	0.34	1.00									
SOC	0.53	0.51	1.00								
Temp	0.19	0.47	0.24	1.00							
RH	−0.06	−0.11	−0.09	−0.13	1.00						
Source-specific $PM_{2.5}$ Measurements											
	$PM_{2.5}$	**SS**	**SN**	**GAS**	**DIE**	**RD**	**BB**	**RS**	**OP**	**Temp**	**RH**
$PM_{2.5}$	1.00										
SS	0.64	1.00									
SN	0.39	−0.08	1.00								
GAS	0.48	0.16	−0.12	1.00							
DIE	−0.14	−0.14	−0.06	−0.12	1.00						
RD	0.15	0.23	−0.03	−0.06	0.14	1.00					
BB	0.45	0.32	0.33	0.03	−0.23	0.16	1.00				
RS	0.15	0.00	0.34	−0.13	−0.14	0.04	0.22	1.00			
OP	0.45	0.58	−0.15	0.31	0.03	0.13	−0.01	−0.15	1.00		
Temp	0.22	0.39	−0.55	0.40	0.15	0.11	−0.19	−0.32	0.44	1.00	
RH	−0.02	−0.11	0.13	−0.08	0.11	−0.27	−0.08	0.01	−0.04	−0.13	1.00

POC, primary organic carbon; SOC, secondary organic carbon; SS, secondary sulfate; SN, secondary nitrate; GAS, spark-ignition emissions; DIE, diesel; RD, road dust; BB, biomass burning; RS, road salt; OP, pyrolyzed organic rich; Temp, temperature (°C); RH, relative humidity (%).[a]Data on control periods and lag day 0 were used.

mean SOC concentration in the previous 6 days was associated with an increased rate of STEMI in 2014–2016, despite the lack of precision. Similarly, we generally did not find increased rates of STEMI associated with increased POC or any other source-specific $PM_{2.5}$ concentrations. In the exploratory analysis by period, we found a negative association between SS concentration on the same day and the rate of STEMI during 2017–2019 (i.e., after Tier 3 vehicle introduction). In addition, even in this early Tier 3 implementation period (2017–2019), there were significant differences in the rates of STEMI associated with SS and GAS on lag day 0 between the 2014–2016 and 2017–2019 periods. Further work will be needed to examine full implementation of Tier 3 through 2025.

This finding of a decreased rate of STEMI associated with increased SS concentrations in 2017–2019 may be spurious, and just a result of an examining effect modification of an overall null association in secondary analyses. In this case, the overall effect across the 2014–2019 period is null (i.e., RR = 1.0) and we find an increased

10.3389/fpubh.2024.1369698

TABLE 4 Rates of STEMI associated with each interquartile range increase in concentrations (μg/m³) of organic carbon and $PM_{2.5}$ sources in a multivariable model[a].

Lag day	IQR[b]	N of STEMI	OR	95% CI	*p*-value
Primary Organic Carbon (POC)					
0	0.51	180	0.94	0.77, 1.15	0.565
0–3	0.53	177	0.89	0.63, 1.26	0.527
0–6	0.55	182	0.87	0.57, 1.34	0.527
Secondary Organic Carbon (SOC)					
0	0.65	180	1.00	0.88, 1.14	0.950
0–3	0.45	177	1.06	0.84, 1.33	0.640
0–6	0.42	182	1.14	0.89, 1.45	0.306
Secondary Sulfate (SS)					
0	1.90	170	1.00	0.77, 1.31	0.972
0–3	1.51	146	1.18	0.88, 1.59	0.226
0–6	1.61	161	0.99	0.70, 1.42	0.969
Secondary Nitrate (SN)					
0	1.12	170	0.95	0.79, 1.13	0.530
0–3	1.18	146	0.90	0.68, 1.19	0.467
0–6	1.24	161	0.93	0.64, 1.34	0.687
Spark-ignition Emissions (GAS)					
0	1.73	170	0.97	0.72, 1.31	0.828
0–3	1.52	146	0.92	0.62, 1.36	0.681
0–6	1.33	161	0.96	0.63, 1.46	0.849
Diesel (DIE)					
0	0.47	170	0.86	0.66, 1.12	0.254
0–3	0.36	146	0.89	0.63, 1.25	0.492
0–6	0.34	161	1.06	0.72, 1.56	0.765
Road Dust (RD)					
0	0.25	170	0.99	0.77, 1.28	0.941
0–3	0.18	146	0.96	0.71, 1.31	0.809
0–6	0.18	161	1.01	0.72, 1.42	0.944
Biomass Burning (BB)					
0	0.63	170	0.88	0.67, 1.15	0.335
0–3	0.47	146	1.00	0.72, 1.39	0.977
0–6	0.46	161	0.76	0.54, 1.06	0.104
Road Salt (RS)					
0	0.03	170	0.99	0.95, 1.02	0.418
0–3	0.04	146	0.98	0.90, 1.07	0.687
0–6	0.04	161	1.00	0.93, 1.09	0.931
Pyrolyzed Organic Rich (OP)					
0	0.41	170	1.03	0.79, 1.34	0.833
0–3	0.34	146	0.99	0.69, 1.43	0.972
0–6	0.31	161	1.08	0.73, 1.61	0.687

STEMI, ST-elevation myocardial infarction; IQR, interquartile range; OR, odds ratio; CI, confidence interval.[a]For organic carbons, adjustments included the residuals between $PM_{2.5}$ (from composition measurements) and POC or SOC for the corresponding lag day, weekday, holidays, and temperature (a natural spline with 4 degrees of freedom) and relative humidity (a linear term) for the corresponding lag day. For PM2.5 sources, adjustments included the residuals between $PM_{2.5}$ (from source measurements) and specific $PM_{2.5}$ source for the corresponding lag day, weekday, holidays, and temperature (a natural spline with 4 degrees of freedom) and relative humidity (a linear term) for the corresponding lag day.
[b]The IQR for the corresponding pollutant and lag day was calculated using data from the control periods during all years.

10.3389/fpubh.2024.1369698

TABLE 5 Rates of STEMI associated with each interquartile range in concentrations (μg/m^3) of organic carbon and $PM_{2.5}$ sources by period, from a model including the interaction between pollutant concentrations and period[a].

Lag day	IQR[b]	2014–2016				2017–2019				Period Interaction *p*-value
		N of STEMI	OR	95% CI	*p*-value	N of STEMI	OR	95% CI	*p*-value	
Primary Organic Carbon (POC)										
0	0.51	74	1.20	0.90, 1.60	0.219	106	0.79	0.60, 1.03	0.083	0.023
0–3	0.53	72	1.48	0.79, 2.78	0.226	105	0.78	0.52, 1.15	0.202	0.066
0–6	0.55	74	1.79	0.83, 3.86	0.139	108	0.69	0.43, 1.12	0.130	0.028
Secondary Organic Carbon (SOC)										
0	0.65	74	1.02	0.90, 1.15	0.769	106	0.83	0.57, 1.21	0.335	0.294
0–3	0.45	72	1.13	0.88, 1.44	0.350	105	0.90	0.62, 1.30	0.569	0.274
0–6	0.42	74	1.27	0.96, 1.67	0.092	108	0.84	0.54, 1.30	0.431	0.103
Secondary Sulfate (SS)										
0	1.90	67	1.22	0.90, 1.65	0.203	103	0.63	0.40, 0.98	0.040	**0.006**
0–3	1.51	50	1.30	0.93, 1.80	0.120	96	0.90	0.55, 1.48	0.675	0.170
0–6	1.61	59	1.16	0.80, 1.69	0.426	102	0.60	0.33, 1.09	0.093	0.039
Secondary Nitrate (SN)										
0	1.12	67	0.60	0.38, 0.97	0.037	103	1.01	0.85, 1.21	0.908	0.039
0–3	1.18	50	0.73	0.35, 1.53	0.406	96	0.93	0.69, 1.24	0.616	0.546
0–6	1.24	59	0.47	0.19, 1.11	0.086	102	1.10	0.74, 1.64	0.649	0.071
Spark-ignition Emissions (GAS)										
0	1.73	67	1.69	0.98, 2.94	0.061	103	0.79	0.55, 1.13	0.199	**0.016**
0–3	1.52	50	1.42	0.74, 2.72	0.295	96	0.75	0.47, 1.21	0.240	0.109
0–6	1.33	59	1.63	0.87, 3.04	0.125	102	0.70	0.42, 1.17	0.173	0.028
Diesel (DIE)										
0	0.47	67	0.67	0.41, 1.07	0.096	103	0.97	0.70, 1.33	0.834	0.196
0–3	0.36	50	0.75	0.42, 1.34	0.326	96	0.97	0.64, 1.47	0.884	0.471
0–6	0.34	59	0.93	0.52, 1.66	0.809	102	1.16	0.71, 1.88	0.551	0.554
Road Dust (RD)										
0	0.25	67	0.91	0.63, 1.32	0.635	103	1.07	0.75, 1.51	0.718	0.539
0–3	0.18	50	0.84	0.52, 1.35	0.464	96	1.06	0.72, 1.55	0.775	0.428
0–6	0.18	59	0.77	0.47, 1.25	0.291	102	1.33	0.84, 2.11	0.227	0.097
Biomass Burning (BB)										
0	0.63	67	1.05	0.74, 1.48	0.797	103	0.70	0.47, 1.05	0.084	0.125
0–3	0.47	50	1.15	0.74, 1.79	0.522	96	0.86	0.54, 1.37	0.537	0.352
0–6	0.46	59	0.83	0.54, 1.28	0.405	102	0.66	0.40, 1.11	0.118	0.500
Road Salt (RS)										
0	0.03	67	0.98	0.94, 1.03	0.490	103	0.99	0.94, 1.04	0.663	0.882
0–3	0.04	50	1.01	0.90, 1.14	0.811	96	0.95	0.84, 1.08	0.413	0.443
0–6	0.04	59	0.99	0.90, 1.09	0.846	102	1.03	0.90, 1.19	0.649	0.627
Pyrolyzed Organic Rich (OP)										
0	0.41	67	1.33	0.91, 1.94	0.143	103	0.86	0.61, 1.21	0.395	0.070
0–3	0.34	50	1.32	0.70, 2.50	0.396	96	0.91	0.61, 1.36	0.653	0.289
0–6	0.31	59	1.49	0.83, 2.70	0.184	102	0.92	0.58, 1.45	0.707	0.150

STEMI, ST-elevation myocardial infarction; IQR, interquartile range; OR, odds ratio; CI, confidence interval.[a]For organic carbons, adjustments included the residuals between $PM_{2.5}$ (from composition measurements) and POC or SOC for the corresponding lag day, weekday, holidays, and temperature (a natural spline with 4 degrees of freedom) and relative humidity (a linear term) for the corresponding lag day. For $PM_{2.5}$ sources, adjustments included the residuals between $PM_{2.5}$ (from source measurements) and specific $PM_{2.5}$ source for the corresponding lag day, weekday, holidays, and temperature (a natural spline with 4 degrees of freedom) and relative humidity (a linear term) for the corresponding lag day.
[b]The IQR for the corresponding pollutant and lag day was calculated using data from the control periods during all years.

rate ratio in 2014–2016, so there must be a decreased rate ratio in 2017–2019. Two prior studies, also using STEMI data from the Cath Lab, air pollution data from the Rochester monitoring station, and the same analysis methods, found no associations between the rate of STEMI and $PM_{2.5}$ concentration in the previous few hours and days in Rochester during the 2005–2016 (13) and 2014–2019 periods (14). Our null findings with $PM_{2.5}$ sources and components over 2014–2019 are consistent with these analyses.

However, there were also studies suggesting positive associations using earlier data from the same sources and the same analysis methods (7, 8). After rescaling effects with the same IQR (4.47 μg/m^3) for $PM_{2.5}$ used in our analysis, Evans et al. reported a 10% increase in the rate of STEMI associated with each 4.47 μg/m^3 increase in $PM_{2.5}$ concentration in the previous hour (RR = 1.10, 95% CI = 0.99, 1.23) during 2007–2012 (8). A similar result (IQR = 4.47 μg/m^3, RR = 1.11, 95% CI = 1.01, 1.22) was also found by Gardner et al. using data from 2007 to 2010 (7). Some, but not all, other case-crossover studies also reported that increased $PM_{2.5}$ concentrations were associated with an increased risk of STEMI. For example, each 4.47 μg/m^3 increase in $PM_{2.5}$ concentration was associated with estimated RRs of 1.06 (95% CI = 1.01, 1.12) in Utah, United States, between 1993 and 2014 (10), 1.02 (95% CI = 1.00, 1.05) in Beijing in 2014 (12), and 1.72 (95% CI = 1.00, 2.19) in Suzhou, China, from 2013 to 2016 (11). The discrepancy in these results is likely due to different study locations and changes in PM composition over time. However, it could also be due to differences in STEMI patient characteristics over time and differences in lag patterns of associations.

Although this study did not find associations between GAS and DIE sources and the rates of STEMI during the entire period (2014–2019), each 1.73 μg/m^3 increase in $PM_{2.5}$ concentration from the GAS source was associated with an increased rate of STEMI on lag day 0 in the 2014–2016 period (RR = 1.69; 95% CI = 0.98, 2.94), but not in the 2017–2019 period (RR = 0.79; 95% CI = 0.55, 1.13). This can perhaps be explained, in part, by our recent study (32). We found that although the monotonic trend in GAS over the period of 2010 to 2019 was positive and significant, the piecewise analysis found a breakpoint occurring around the middle of 2017 and a small downward trend to the end of 2019 suggesting changing GAS emissions during this period (Figure 1) (32). Alternatively, DIE remained constant according to the monotonic trend, but was decreasing slowly from the middle of 2012 according to the breakpoint analysis. Consistent with our study, Rich et al. reported an increased excess rate of hospitalizations for myocardial infarction (MI) associated with increased concentrations of $PM_{2.5}$ from the GAS source on lag day 0 in New York State from 2005 and 2016 (2.3%; 95% CI = 0.1, 4.5%; IQR = 2.56 μg/m^3), but not from the DIE source (0.4%; 95% CI = −0.5, 1.2%; IQR = 0.53 μg/m^3) (25). They also found increased GAS concentrations associated with increased hospitalizations for ischemic stroke (excess rate = 3.5%; 95% CI = 1.0, 6.0%; IQR = 2.56 μg/m^3) and an increase in DIE source (IQR = 0.53 μg/m^3) associated with increased excess rates of congestive heart failure (0.7%; 95% CI = 0.2, 1.3%) and ischemic heart disease (0.6%; 95% CI = 0.1, 1.1%) hospitalizations on lag day 0. In addition, Sarnat et al. observed that cardiovascular emergency department (ED) visits were positively associated with same-day $PM_{2.5}$ concentrations from mobile sources (RR range, 1.018–1.025) in Atlanta from 1998 to 2002 (40). In contrast, another Atlanta study (41) accounting for the uncertainty of source apportionment methods, reported no associations between mobile source $PM_{2.5}$ (diesel- and gasoline-fueled vehicles) and ED visits for ischemic heart disease during 1998–2010. A possible mechanism for traffic $PM_{2.5}$ sources associated with an increased risk of cardiovascular events is that traffic-related particles could contribute to both exogenous and endogenous reactive oxygen species (ROS).

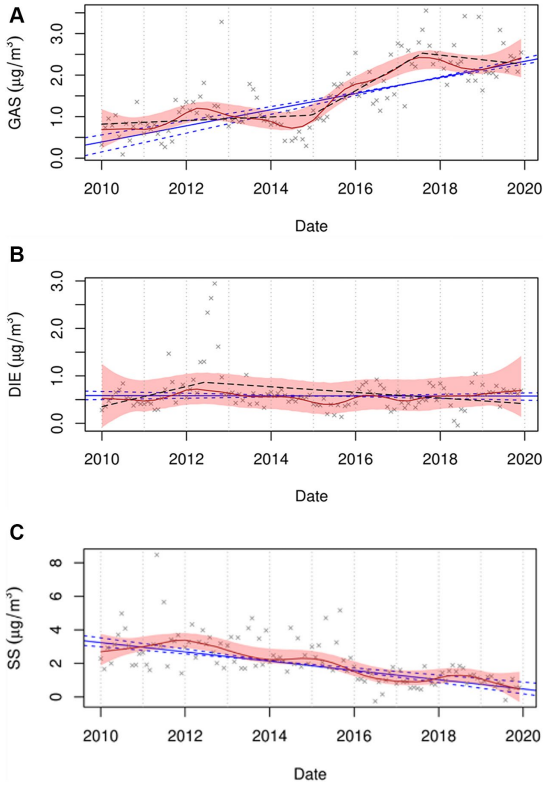

FIGURE 1
Trend plots for GAS **(A)**, DIE **(B)**, and SS **(C)** for the period of 2010 to 2019. The red line represents the seasonal by loess trends (STL), with 95% confidence bound as a shaded area. The blue line represents the Thiel-Sen monotonic trend, with a 95% confidence interval as dashed lines. The black dashed line represents the piecewise trend. GAS, DIE, and SS represent spark-ignition emissions, diesel, and secondary sulfate, respectively. (Figures from the supplemental material of Chen et al. (32)).

Multiple prior studies have examined associations between organic carbon (OC) and adverse cardiovascular outcomes, with both positive (19, 42, 43) and negative (44–46) results reported. In addition, the long-term associations between SOC and cardiovascular events have been explored and their results were inconsistent (47, 48). However, current evidence about the short-term association is limited. Pennington et al. found each 1 μg/m^3 increase in SOC concentrations was associated with ED visits for ischemic heart disease on lag day 0 (RR = 1.003; 95% CI = 0.997, 1.009) in Atlanta from 1998 to 2010 (41). Similarly, despite imprecision, our finding indicated a suggestive increased rate of STEMI associated with an increase in SOC concentration on lag day 0–6 (RR = 1.14; 95% CI = 0.89, 1.45; IQR = 0.42 μg/m^3). The possible mechanism for the association between SOC and STEMI is likely related to the formation of secondary PM species including SOC, alongside the identification of increased $PM_{2.5}$ toxicity, resulting in an increased risk of cardiovascular events (16, 49). SOC formation can result in concurrent oxidant species, and the related oxidative stress and inflammation could

be potential drivers of adverse cardiovascular outcomes (22, 25). The imprecision in this study could be attributable to the limited sample size of the present study. Another possible factor to be considered is that the same pollutant values from one monitoring site were assigned for each subject on a specific day, regardless of how far they lived from the monitoring site, which likely cause underestimated effects.

Rather than single components being considered as causal, the combined effects of multiple constituents that possibly interact with environmental factors or combine with socioeconomic and biological characteristics may have substantial impacts on cardiac health (3). Secondary organic aerosol (SOA), derived from volatile organic compounds, is one such component. Fresh SOA is considered to contain peroxy radicals and peroxides and be strongly oxidizing (21, 22, 25, 50). Further, traffic PM sources may not only contribute to increased SOC concentrations (25, 26, 31, 49) but are also an important source of SOA and its precursors (3, 25, 51, 52).

A recent study (53) examined the association between SOA concentrations and cardiorespiratory disease mortality in the United States in 2016. It demonstrated that annual average SOA concentrations were strongly associated with county-level cardiorespiratory death rates, with a larger association per unit mass ($\beta = 8.9$ additional deaths per 100,000; 95% CI = 6.0, 12.0) than total $PM_{2.5}$ ($\beta = 1.4$ additional deaths per 100,000; 95% CI = 0.5, 2.3). They considered that prior inconsistent results about associations of OC with adverse health outcomes could be, in part, explained by total OC lacking the distinction between primary organic aerosol (POA) and SOA (53). Although ambient $PM_{2.5}$ concentrations are expected to decline in the future with strict air quality policies, SOA levels may relatively increase, resulting in increased health consequences per unit mass (49). Thus, future research should focus on the health effects of different PM components, including SOA and its constituents.

We did not observe increased rates of STEMI associated with SS, SN, RD, BB, OP, and RS. Similarly, Rich et al. reported no obvious associations of MI hospitalizations with SS, RD, BB, OP, and RS, while they found an association with SN (excess rate = 1.7%; 95% CI = 0.4, 3.0%; IQR = 1.53 μg/m^3) on lag day 0–3 (25). Another study reported no clear associations between MI mortality and SS, SN, and BB (54). SS and SN, being unreactive particles, would not provide oxidative potential or the resulting reactive oxygen species and oxidative stress (25, 26). OP is thought to represent more aged SOA that has been transported into the area with little associated ROS (25, 55–57). As a result, the absence of OP association might reflect its low ROS concentration. Our null findings about RD and BB may be related to their heterogeneities. RD, representing non-exhaust traffic emissions, contains deposited soil and road surface material. Its effects on STEMI may differ by deposition rates, variability in reactivity, and environmental factors. Likewise, BB could have different PM compositional patterns due to various biofuels. RS does not generally include strongly oxidizing constituents.

Interestingly, although the difference in the association between SOC and the rate of STEMI between the two periods was not found, we observed that SS and GAS concentrations on lag day 0 associated with the rates of STEMI were different between the 2014–2016 and 2017–2019 periods, and their adverse effects on the triggering of STEMI might have a declining trend. Concentrations of sulfur-containing pollutants have been decreasing (58, 59) due to the implementation of air quality policies in New York State, such as particle traps required on heavy-duty diesel trucks and reductions in the sulfur content of diesel and home heating fuels. Also in Figure 1, SS shows a steady monotonic downward trend with only minor deviations showing the impacts of coal-fired power plant closures and reduced fuel sulfur concentrations. Consistent with our finding, Yount et al. (14) found that increased rates of STEMI were associated with increases in SO_2 concentrations in previous 120 h (RR = 1.26; 95% CI = 1.03, 1.55; IQR = 0.59 ppb) during 2014–2016, but not in the 2017–2019 period (RR = 1.21; 95% CI = 0.87, 1.68). Our finding regarding GAS is also similar to our previous study (14), which showed an increased rate of STEMI associated with an increase in concentrations of black carbon, a marker of traffic pollution, in the previous hour (RR = 1.16; 95% CI = 0.99, 1.34; IQR = 0.30 μg/m^3) in the 2014–2016 period instead of the 2017–2019 period (RR = 0.85; 95% CI = 0.72, 1.01). The reduction in the impact of GAS may be due to changes in PM components and/or PM mixtures resulting from air pollution regulations, including the introduction of Tier 3 light-duty vehicles. Inconsistent with our exception, we did not observe changes in the rate of STEMI associated with SOC after the Tier 3 regulation was implemented. It is estimated that only 36% of vehicles registered in New York State were Tier 3 in 2020 (14). Thus, the null finding of SOC is possibly attributed to the limited penetration of Tier 3 vehicles in the early Tier 3 implementation period (2017–2019). Consequently, the magnitude of the association between SOC and STEMI is not strong enough to be observed. In addition, when accounting for these results, some other possible reasons should be considered, such as healthcare improvements, public awareness and behavioral changes, and differences in study populations, as well as greater access to health care and medical insurance over the study period.

This study has several strengths, including the use of a well-defined STEMI study population treated at the Cath Lab in Rochester and the use of a case-crossover study design to control for non-time-varying factors and interactions between them, thereby reducing confounding by these factors. However, there are several limitations to be considered when interpreting our results. First, since $PM_{2.5}$ sources and components were only measured every 3rd or 6th day, the number of subjects for whom exposure data were available largely decreased, thus reducing statistical power and precision. Second, all cases were assigned the same values of $PM_{2.5}$ sources and components for a specific day from a single monitoring site without considering individual-specific differences, such as the distance from the emission source and/or the monitoring site, outdoor exposure duration, and protective measures. This assumption likely led to non-differential exposure misclassification and underestimated effects. Third, it is difficult for case-crossover designs combined with conditional logistic regression to fully adjust for possible overdispersion (60), which may cause larger confidence intervals than reported. Last, the 2014–2016 and 2017–2019 periods were selected based on the implementation timing of the new policy for Tier 3 light-duty vehicles. However, given that 2017–2019 is the early Tier 3 implementation period and the interventions generally phase in and take time to be effective, there are actually no well-defined time windows for the policies and emission changes. Therefore, the actual impact of this new policy should be further evaluated after the full implementation of Tier 3 through 2025.

Conclusion

We used data on STEMI events treated at the University of Rochester Medical Center from 2014 to 2019, as well as the

concentrations of $PM_{2.5}$ sources and organic carbon measured in Rochester, NY. Inconsistent with our *a priori* hypothesis, increased rates of STEMI were not associated with increased GAS and DIE concentrations in the previous few days. However, in the 2014–2016 period, increased $PM_{2.5}$ concentrations from the GAS source were associated with an increased rate of STEMI on the same day, which was not observed in the 2017–2019 period. Despite imprecision, our finding suggested that a short-term increase in SOC concentration might be associated with an increased rate of STEMI. We also found no association between rates of STEMI and POC or any other source-specific $PM_{2.5}$ concentration. These negative results may be due to the potential changes in traffic emissions as well as the reduced statistical power and precision resulting from our limited sample size and potential exposure misclassification and effect underestimation. Furthermore, we observed significant differences in period-specific rate ratios for SS and GAS on the same day between the 2014–2016 and 2017–2019 periods, with a declining trend regarding adverse effects on the triggering of STEMI. This finding may be related to the changes in PM components and/or PM mixtures. Future work will be needed to further examine the effects of PM components and sources on triggering MI using a large sample after the Tier 3 light-duty vehicle policy is fully implemented in New York State.

Data availability statement

The datasets presented in this article are not readily available because they contain protected health information and the authors are thus not permitted to release the data.

Ethics statement

The studies involving humans were approved by University of Rochester Research Subjects Review Board. The studies were conducted in accordance with the local legislation and institutional requirements. The ethics committee/institutional review board waived the requirement of written informed consent for participation from the participants or the participants' legal guardians/next of kin because the research involved no more than minimal risk to study subjects, the research could not be carried out without the waiver, and the waiver was judged not to adversely affect the rights and welfare of the subjects.

Author contributions

TZ: Formal analysis, Writing – original draft. PH: Funding acquisition, Project administration, Conceptualization, Data curation, Formal analysis, Methodology, Supervision, Writing – review & editing. MU: Conceptualization, Funding acquisition, Writing – review & editing. DC: Funding acquisition, Conceptualization, Investigation, Writing – review & editing. ST: Funding acquisition, Conceptualization, Methodology, Writing – review & editing. SL: Funding acquisition, Project administration, Conceptualization, Methodology, Writing – review & editing. FL: Conceptualization, Data curation, Writing – review & editing. YC: Data curation, Formal analysis, Writing – review & editing. CY: Formal analysis, Writing – review & editing. DR: Conceptualization, Data curation, Formal analysis, Funding acquisition, Methodology, Project administration, Supervision, Writing – review & editing.

Funding

The author(s) declare that financial support was received for the research, authorship, and/or publication of this article. This work was supported by the New York State Energy Research and Development Authority (Contract #'s 125993 and 156226) and the National Institute of Environmental Health Sciences (Grant # P30ES001247).

Conflict of interest

The authors declare that the research was conducted in the absence of any commercial or financial relationships that could be construed as a potential conflict of interest.

The author(s) declared that they were an editorial board member of Frontiers, at the time of submission. This had no impact on the peer review process and the final decision.

Publisher's note

References

1. Fuller R, Landrigan PJ, Balakrishnan K, Bathan G, Bose-O'Reilly S, Brauer M, et al. Pollution and health: a progress update. *Lancet Planet Health*. (2022) 6:e535–47. doi: 10.1016/S2542-5196(22)00090-0

2. Cohen AJ, Brauer M, Burnett R, Anderson HR, Frostad J, Estep K, et al. Estimates and 25-year trends of the global burden of disease attributable to ambient air pollution: an analysis of data from the global burden of diseases study 2015. *Lancet*. (2017) 389:1907–18. doi: 10.1016/S0140-6736(17)30505-6

3. Al-Kindi SG, Brook RD, Biswal S, Rajagopalan S. Environmental determinants of cardiovascular disease: lessons learned from air pollution. *Nat Rev Cardiol*. (2020) 17:656–72. doi: 10.1038/s41569-020-0371-2

4. Brauer M, Casadei B, Harrington RA, Kovacs R, Sliwa K. Taking a stand against air pollution-the impact on cardiovascular disease: a joint opinion from the world heart federation, American College of Cardiology, American Heart Association, and the European Society of Cardiology. *Circulation*. (2021) 143:e800–4. doi: 10.1161/CIRCULATIONAHA.120.052666

5. Rajagopalan S, Al-Kindi SG, Brook RD. Air pollution and cardiovascular disease: JACC state-of-the-art review. *J Am Coll Cardiol*. (2018) 72:2054–70. doi: 10.1016/j.jacc.2018.07.099

6. Mustafic H, Jabre P, Caussin C, Murad MH, Escolano S, Tafflet M, et al. Main air pollutants and myocardial infarction: a systematic review and meta-analysis. *JAMA*. (2012) 307:713–21. doi: 10.1001/jama.2012.126

7. Gardner B, Ling F, Hopke PK, Frampton MW, Utell MJ, Zareba W, et al. Ambient fine particulate air pollution triggers ST-elevation myocardial infarction, but not non-ST elevation myocardial infarction: a case-crossover study. *Part Fibre Toxicol*. (2014) 11:1. doi: 10.1186/1743-8977-11-1

8. Evans KA, Hopke PK, Utell MJ, Kane C, Thurston SW, Ling FS, et al. Triggering of ST-elevation myocardial infarction by ambient wood smoke and other particulate and gaseous pollutants. *J Expo Sci Environ Epidemiol*. (2017) 27:198–206. doi: 10.1038/jes.2016.15

9. Cheng J, Tong S, Su H, Xu Z. Hourly air pollution exposure and emergency department visit for acute myocardial infarction: vulnerable populations and susceptible time window. *Environ Pollut*. (2021) 288:117806. doi: 10.1016/j.envpol.2021.117806

10. Pope CA III, Muhlestein JB, Anderson JL, Cannon JB, Hales NM, Meredith KG, et al. Short-term exposure to fine particulate matter air pollution is preferentially

associated with the risk of ST-segment elevation acute coronary events. *J Am Heart Assoc*. (2015) 4:e002506. doi: 10.1161/JAHA.115.002506

11. Sun Q, Cao B, Jiang Y, Zhuang J, Zhang C, Jiang B. Association between ambient particulate matter (PM2. 5/PM10) and first incident ST-elevation myocardial infarction in Suzhou, China. *Environ Sci Pollut Res*. (2022) 29:62690–7. doi: 10.1007/s11356-022-20150-z

12. Zhang Q, Qi W, Yao W, Wang M, Chen Y, Zhou Y. Ambient particulate matter (PM2. 5/PM10) exposure and emergency department visits for acute myocardial infarction in Chaoyang District, Beijing, China during 2014: a case-crossover study. *J Epidemiol*. (2016) 26:538–45. doi: 10.2188/jea.JE20150209

13. Wang M, Hopke PK, Masiol M, Thurston SW, Cameron S, Ling F, et al. Changes in triggering of ST-elevation myocardial infarction by particulate air pollution in Monroe County, New York over time: a case-crossover study. *Environ Health*. (2019) 18:82. doi: 10.1186/s12940-019-0521-3

14. Yount CS, Utell MJ, Hopke PK, Thurston SW, Lin S, Ling FS, et al. Triggering of ST-elevation myocardial infarction by ultrafine particles in New York: changes following tier 3 vehicle introduction. *Environ Res*. (2023) 216:114445. doi: 10.1016/j.envres.2022.114445

15. Nassan FL, Wang C, Kelly RS, Lasky-Su JA, Vokonas PS, Koutrakis P, et al. Ambient PM(2.5) species and ultrafine particle exposure and their differential metabolomic signatures. *Environ Int*. (2021) 151:106447. doi: 10.1016/j.envint.2021.106447

16. Rich DQ, Ozkaynak H, Crooks J, Baxter L, Burke J, Ohman-Strickland P, et al. The triggering of myocardial infarction by fine particles is enhanced when particles are enriched in secondary species. *Environ Sci Technol*. (2013) 47:9414–23. doi: 10.1021/es4027248

17. Peng RD, Bell ML, Geyh AS, McDermott A, Zeger SL, Samet JM, et al. Emergency admissions for cardiovascular and respiratory diseases and the chemical composition of fine particle air pollution. *Environ Health Perspect*. (2009) 117:957–63. doi: 10.1289/ehp.0800185

18. Kim SY, Peel JL, Hannigan MP, Dutton SJ, Sheppard L, Clark ML, et al. The temporal lag structure of short-term associations of fine particulate matter chemical constituents and cardiovascular and respiratory hospitalizations. *Environ Health Perspect*. (2012) 120:1094–9. doi: 10.1289/ehp.1104721

19. Ito K, Mathes R, Ross Z, Nádas A, Thurston G, Matte T. Fine particulate matter constituents associated with cardiovascular hospitalizations and mortality in new York City. *Environ Health Perspect*. (2011) 119:467–73. doi: 10.1289/ehp.1002667

20. Ziemann PJ, Atkinson R. Kinetics, products, and mechanisms of secondary organic aerosol formation. *Chem Soc Rev*. (2012) 41:6582–605. doi: 10.1039/c2cs35122f

21. Docherty KS, Wu W, Lim YB, Ziemann PJ. Contributions of organic peroxides to secondary aerosol formed from reactions of monoterpenes with O3. *Environ Sci Technol*. (2005) 39:4049–59. doi: 10.1021/es050228s

22. Chen X, Hopke PK, Carter WP. Secondary organic aerosol from ozonolysis of biogenic volatile organic compounds: chamber studies of particle and reactive oxygen species formation. *Environ Sci Technol*. (2011) 45:276–82. doi: 10.1021/es102166c

23. Münzel T, Sørensen M, Gori T, Schmidt FP, Rao X, Brook FR, et al. Environmental stressors and cardio-metabolic disease: part II-mechanistic insights. *Eur Heart J*. (2017) 38:557–64. doi: 10.1093/eurheartj/ehw294

24. Marchini T. Redox and inflammatory mechanisms linking air pollution particulate matter with cardiometabolic derangements. *Free Radic Biol Med*. (2023) 209:320–41. doi: 10.1016/j.freeradbiomed.2023.10.396

25. Rich DQ, Zhang W, Lin S, Squizzato S, Thurston SW, van Wijngaarden E, et al. Triggering of cardiovascular hospital admissions by source specific fine particle concentrations in urban centers of New York state. *Environ Int*. (2019) 126:387–94. doi: 10.1016/j.envint.2019.02.018

26. Croft DP, Zhang W, Lin S, Thurston SW, Hopke PK, van Wijngaarden E, et al. Associations between source-specific particulate matter and respiratory infections in New York state adults. *Environ Sci Technol*. (2020) 54:975–84. doi: 10.1021/acs.est.9b04295

27. Hopke PK, Croft DP, Zhang W, Lin S, Masiol M, Squizzato S, et al. Changes in the hospitalization and ED visit rates for respiratory diseases associated with source-specific PM(2.5) in New York state from 2005 to 2016. *Environ Res*. (2020) 181:108912. doi: 10.1016/j.envres.2019.108912

28. Squizzato S, Masiol M, Rich DQ, Hopke PK. A long-term source apportionment of PM2. 5 in New York state during 2005–2016. *Atmos Environ*. (2018) 192:35–47. doi: 10.1016/j.atmosenv.2018.08.044

29. Squizzato S, Masiol M, Rich DQ, Hopke PK. PM2.5 and gaseous pollutants in New York state during 2005–2016: spatial variability, temporal trends, and economic influences. *Atmos Environ*. (2018) 183:209–24. doi: 10.1016/j.atmosenv.2018.03.045

30. Chen Y, Rich DQ, Masiol M, Hopke PK. Changes in ambient air pollutants in New York state from 2005 to 2019: effects of policy implementations and economic and technological changes. *Atmos Environ*. (2023) 311:119996. doi: 10.1016/j.atmosenv.2023.119996

31. Masiol M, Squizzato S, Rich DQ, Hopke PK. Long-term trends (2005–2016) of source apportioned PM2. 5 across New York state. *Atmos Environ*. (2019) 201:110–20. doi: 10.1016/j.atmosenv.2018.12.038

32. Chen Y, Rich DQ, Masiol M, Hopke PK. Changes in source specific PM2.5 from 2010 to 2019 in New York and New Jersey identified by dispersion normalized PMF. *Atmos Res*. (2024) 304:107353. doi: 10.1016/j.atmosres.2024.107353

33. O'Gara PT, Kushner FG, Ascheim DD, Casey DE Jr, Chung MK, de Lemos JA, et al. 2013 ACCF/AHA guideline for the management of ST-elevation myocardial infarction: a report of the American College of Cardiology Foundation/American Heart Association task force on practice guidelines. *Circulation*. (2013) 127:e362–425. doi: 10.1161/CIR.0b013e3182742cf6

34. Solomon PA, Crumpler D, Flanagan JB, Jayanty R, Rickman EE, McDade CE. US national PM2. 5 chemical speciation monitoring networks—CSN and IMPROVE: description of networks. *J Air Waste Manage Assoc*. (2014) 64:1410–38. doi: 10.1080/10962247.2014.956904

35. Maclure M. The case-crossover design: a method for studying transient effects on the risk of acute events. *Am J Epidemiol*. (1991) 133:144–53. doi: 10.1093/oxfordjournals.aje.a115853

36. Levy D, Lumley T, Sheppard L, Kaufman J, Checkoway H. Referent selection in case-crossover analyses of acute health effects of air pollution. *Epidemiology*. (2001) 12:186–92. doi: 10.1097/00001648-200103000-00010

37. Byrne CP, Bennett KE, Hickey A, Kavanagh P, Broderick B, O'Mahony M, et al. Short-term air pollution as a risk for stroke admission: a time-series analysis. *Cerebrovasc Dis*. (2020) 49:404–11. doi: 10.1159/000510080

38. Chen H, Cheng Z, Li M, Luo P, Duan Y, Fan J, et al. Ambient air pollution and hospitalizations for ischemic stroke: a time series analysis using a distributed lag nonlinear model in Chongqing. *China Front Public Health*. (2021) 9:762597. doi: 10.3389/fpubh.2021.762597

39. Liu C, Chen R, Sera F, Vicedo-Cabrera AM, Guo Y, Tong S, et al. Ambient particulate air pollution and daily mortality in 652 cities. *N Engl J Med*. (2019) 381:705–15. doi: 10.1056/NEJMoa1817364

40. Sarnat JA, Marmur A, Klein M, Kim E, Russell AG, Sarnat SE, et al. Fine particle sources and cardiorespiratory morbidity: an application of chemical mass balance and factor analytical source-apportionment methods. *Environ Health Perspect*. (2008) 116:459–66. doi: 10.1289/ehp.10873

41. Pennington AF, Strickland MJ, Gass K, Klein M, Sarnat SE, Tolbert PE, et al. Source-apportioned PM2.5 and cardiorespiratory emergency department visits: accounting for source contribution uncertainty. *Epidemiology*. (2019) 30:789–98. doi: 10.1097/EDE.0000000000001089

42. Lin H, Tao J, Du Y, Liu T, Qian Z, Tian L, et al. Particle size and chemical constituents of ambient particulate pollution associated with cardiovascular mortality in Guangzhou. *China Environ Pollution*. (2016) 208:758–66. doi: 10.1016/j.envpol.2015.10.056

43. Atkinson RW, Mills IC, Walton HA, Anderson HR. Fine particle components and health—a systematic review and meta-analysis of epidemiological time series studies of daily mortality and hospital admissions. *J Expo Sci Environ Epidemiol*. (2015) 25:208–14. doi: 10.1038/jes.2014.63

44. Son J-Y, Lee J-T, Kim K-H, Jung K, Bell ML. Characterization of fine particulate matter and associations between particulate chemical constituents and mortality in Seoul. *Korea Environ Health Perspect*. (2012) 120:872–8. doi: 10.1289/ehp.1104316

45. Chen C, Xu D, He MZ, Wang Y, Du Z, Du Y, et al. Fine particle constituents and mortality: a time-series study in Beijing. *China Environ Sci Technol*. (2018) 52:11378–86. doi: 10.1021/acs.est.8b00424

46. Bell ML, Ebisu K, Peng RD, Samet JM, Dominici F. Hospital admissions and chemical composition of fine particle air pollution. *Am J Respir Crit Care Med*. (2009) 179:1115–20. doi: 10.1164/rccm.200808-1240OC

47. Walsh A, Russell AG, Weaver AM, Moyer J, Wyatt L, Ward-Caviness CK. Associations between source-apportioned PM2. 5 and 30-day readmissions in heart failure patients. *Environ Res*. (2023) 228:115839. doi: 10.1016/j.envres.2023.115839

48. Slawsky E, Ward-Caviness CK, Neas L, Devlin RB, Cascio WE, Russell AG, et al. Evaluation of PM(2.5) air pollution sources and cardiovascular health. *Environ Epidemiol*. (2021) 5:e157. doi: 10.1097/EE9.0000000000000157

49. Zhang W, Lin S, Hopke PK, Thurston SW, van Wijngaarden E, Croft D, et al. Triggering of cardiovascular hospital admissions by fine particle concentrations in New York state: before, during, and after implementation of multiple environmental policies and a recession. *Environ Pollut*. (2018) 242:1404–16. doi: 10.1016/j.envpol.2018.08.030

50. Hopke PK. Reactive ambient particles In: SS Nadadur and JW Hollingsworth, editors. Air pollution and health effects. London: Springer (2015). 1–24.

51. Zhao Y, Nguyen NT, Presto AA, Hennigan CJ, May AA, Robinson AL. Intermediate volatility organic compound emissions from on-road gasoline vehicles and small off-road gasoline engines. *Environ Sci Technol*. (2016) 50:4554–63. doi: 10.1021/acs.est.5b06247

52. Zhao Y, Lambe AT, Saleh R, Saliba G, Robinson AL. Secondary organic aerosol production from gasoline vehicle exhaust: effects of engine technology, cold start, and emission certification standard. *Environ Sci Technol*. (2018) 52:1253–61. doi: 10.1021/acs.est.7b05045

53. Pye HOT, Ward-Caviness CK, Murphy BN, Appel KW, Seltzer KM. Secondary organic aerosol association with cardiorespiratory disease mortality in the United States. *Nat Commun*. (2021) 12:7215. doi: 10.1038/s41467-021-27484-1

54. Berger K, Malig BJ, Hasheminassab S, Pearson DL, Sioutas C, Ostro B, et al. Associations of source-apportioned fine particles with cause-specific mortality in California. *Epidemiology*. (2018) 29:639–48. doi: 10.1097/EDE.0000000000000873

55. Kim E, Hopke PK. Source apportionment of fine particles in Washington, DC, utilizing temperature-resolved carbon fractions. *J Air Waste Manage Assoc*. (2004) 54:773–85. doi: 10.1080/10473289.2004.10470948

56. Kim E, Hopke PK, Edgerton ES. Improving source identification of Atlanta aerosol using temperature resolved carbon fractions in positive matrix factorization. *Atmos Environ*. (2004) 38:3349–62. doi: 10.1016/j.atmosenv.2004.03.012

57. Kim E, Hopke PK. Improving source identification of fine particles in a rural northeastern US area utilizing temperature-resolved carbon fractions. *J Geophys Res Atmos*. (2004) 109:D09204. doi: 10.1029/2003JD004199

58. Emami F, Masiol M, Hopke PK. Air pollution at Rochester, NY: long-term trends and multivariate analysis of upwind SO2 source impacts. *Sci Total Environ*. (2018) 612:1506–15. doi: 10.1016/j.scitotenv.2017.09.026

59. Rattigan OV, Civerolo KL, Felton HD, Schwab JJ, Demerjian KL. Long term trends in New York: PM2. 5 mass and particle components. Aerosol and air quality. *Demogr Res*. (2016) 16:1191–205. doi: 10.4209/aaqr.2015.05.0319

60. Armstrong BG, Gasparrini A, Tobias A. Conditional Poisson models: a flexible alternative to conditional logistic case cross-over analysis. *BMC Med Res Methodol*. (2014) 14:122. doi: 10.1186/1471-2288-14-122

frontiers | Frontiers in Public Health

TYPE Original Research
PUBLISHED 21 August 2024
DOI 10.3389/fpubh.2024.1427905

OPEN ACCESS

EDITED BY
Dimirios Nikolopoulos,
University of West Attica, Greece

REVIEWED BY
Natasa Krsto Rancic,
University of Nis, Serbia
Nadia Mahmoud Tawfiq Jebril,
University of Babylon, Iraq

*CORRESPONDENCE
Yu Zhang
✉ 25457057@qq.com
Shaohe Chen
✉ bebigcrane@163.com

†These authors have contributed equally to this work and share first authorship

RECEIVED 05 May 2024
ACCEPTED 07 August 2024
PUBLISHED 21 August 2024

CITATION
Chen F, Lin H, Zhang Y, Zhang Y and Chen S (2024) Investigating how blood cadmium levels influence cardiovascular health scores across sexes and dose responses.
Front. Public Health 12:1427905.
doi: 10.3389/fpubh.2024.1427905

Investigating how blood cadmium levels influence cardiovascular health scores across sexes and dose responses

Feng Chen[1,2†], Hao Lin[3†], Yuansi Zhang[4†], Yu Zhang[1*] and Shaohe Chen[1*]

[1]Department of Child Healthcare, Wenzhou People's Hospital, Wenzhou, China, [2]Children's Heart Center, The Second Affiliated Hospital and Yuying Children's Hospital, Institute of Cardiovascular Development and Translational Medicine, Wenzhou Medical University, Wenzhou, China, [3]Department of Gastroenterology, Pingyang Affiliated Hospital of Wenzhou Medical University, Wenzhou, China, [4]Department of Traditional Chinese Medicine, Wenzhou Yebo Proctology Hospital, Wenzhou, China

Background: The association between exposure to cadmium (Cd) and cardiovascular health (CVH) has received considerable scientific interest. However, findings thus far have been inconclusive, particularly regarding sex-specific effects and dose–response relationships. The aim of our study was to investigate the relationships of blood Cd levels with the overall and component CVH scores.

Methods: We used data from the 2011–2018 NHANES to assess CVH using indicators such as BMI, blood pressure, lipid profiles, glucose levels, diet, physical activity, nicotine use, and sleep quality, each rated on a 0–100 scale. The overall CVH score was calculated as the average of these indicators. We employed both multiple linear and restricted cubic spline analyses to examine the relationship between blood Cd levels and CVH scores, including nonlinear patterns and subgroup-specific effects.

Results: Our analysis revealed that higher blood Cd levels were associated with lower overall CVH, nicotine exposure, sleep, and diet scores, with nonlinear decreases observed in overall CVH and nicotine exposure scores at specific thresholds (–1.447 and –1.752 log μg/dL, respectively). Notably, sex differences were evident; females experienced more adverse effects of Cd on CVH and lipid scores, while in males, Cd exposure was positively correlated with BMI, a link not observed in females.

Conclusion: Our study highlights the complex interplay between blood Cd levels and various aspects of CVH, revealing significant dose–response relationships and sex disparities. These findings enhance our understanding of the biobehavioral mechanisms linking Cd exposure to cardiovascular risk.

KEYWORDS

cadmium, cardiovascular health, sex factors, risk factors, NHANES

1 Introduction

Cardiovascular disease (CVD) is the leading cause of death worldwide and has a major impact on both global health and the economy (1). In 2019, an estimated 523 million people were affected by CVD, resulting in 18.6 million deaths (2). As the incidence of CVD increases, effective prevention and management strategies are vital. In 2010, the American

Heart Association (AHA) implemented the "Life's Simple 7" (LS7) scoring system to measure cardiovascular health (CVH) based on seven essential components: body mass index, smoking status, diet, cholesterol levels, blood pressure, blood glucose levels, and physical activity (3). The scores from these components are combined to classify individuals into three CVH categories: poor, intermediate, or ideal. Research has consistently shown that higher CVH scores are associated with a lower incidence of CVD complications and mortality (4–7). In 2022, the AHA updated the LS7 to include sleep health, refining the scoring system to better reflect contemporary health challenges (8).

Recent research has also highlighted the significant role of environmental factors, such as cadmium (Cd) exposure, in CVD development (9). Cd, a common heavy metal detectable in blood, enters the human body through water, food, and air (10, 11). Recent studies have further emphasized the association between blood Cd levels and cardiovascular health outcomes. For instance, a comprehensive review indicates that elevated blood Cd levels are significantly associated with increased incidence and mortality rates of CVD, coronary artery disease, and stroke (12). Another study reported that higher blood Cd levels were associated with increased all-cause and cardiovascular mortality in patients with hypertension (13). Despite extensive studies, the relationship between Cd exposure and CVD remains unclear, particularly regarding sex-specific effects (14, 15). To address this research gap, we utilized the extensive data from the National Health and Nutrition Examination Survey (NHANES) spanning 2011 to 2018, setting clear research objectives. The primary goal is to thoroughly investigate the relationships between blood Cd levels and both overall and specific cardiovascular health scores. The secondary goal is to examine the potential influence of sex differences within these relationships. Our findings can inform more targeted and effective CVD prevention and management strategies.

2 Materials and methods

2.1 Study population

We used data from the National Health and Nutrition Examination Survey (NHANES), which was conducted by the Centers for Disease Control and Prevention (CDC). The NHANES aims to assess the health and nutritional status of the U.S. population through interviews, biological samples, and physical exams. This comprehensive survey encompasses various aspects, such as interviews, biological sample collection, and physical examinations, to gather diverse health and nutrition-related data. Every individual involved in the study gave their informed consent, and the Institutional Review Board of the National Center for Health Statistics (NCHS) approved the research. Our analysis included data from three consecutive NHANES cycles (2013–2018), totaling 29,400 participants. We excluded individuals under 20 years old ($n = 12,343$), those missing key CVH component data ($n = 14,460$), and those lacking blood Cd measurements ($n = 939$). Our final sample consisted of 1,658 adults aged 20 and older with complete datasets for CVH score calculation and blood Cd levels (Figure 1). This sample includes both healthy individuals and those with various health conditions, reflecting a broad spectrum of cardiovascular health statuses.

2.2 Measurement of Cd

Blood Cd levels were measured using inductively coupled plasma mass spectrometry (ICP-MS) at the CDC's National Center for Environmental Health. Samples were diluted with a solution containing tetramethylammonium hydroxide, EDTA, and other stabilizers, then atomized and ionized at high temperatures to quantify trace elements based on their mass-to-charge ratios. The detection limit was managed precisely, and for elements below this limit, values were imputed as the detection limit divided by the square root of two. Rigorous quality assurance protocols were followed to ensure the accuracy of the results.

2.3 CVH scores

CVH scores were based on eight components: blood pressure, BMI, blood glucose levels, blood lipid levels, physical activity, sleep duration, nicotine exposure, and diet. Each component was assessed on a 0–100 scale, as detailed in Supplementary Table S1 and the 2022 AHA Presidential Advisory (8). The composite CVH score aggregates these individual scores, categorizing CVH status into three levels: high (80–100), moderate (50–79), and low (0–49).

2.4 Covariates

Covariates were based on previous literature and assumptions related to CVH and included several factors (16–18): age, sex (female, male), race/ethnicity (Mexican American, non-Hispanic Black, non-Hispanic White, other race), educational attainment (less than high school, high school graduate, college or above), marital status (married/living with partner, divorced/widowed/separated, never married), poverty income ratio (PIR) (<1.3, ≥ 1.3), alcohol consumption status (<12 drinks/year, ≥ 12 drinks/year), waist circumference, and estimated glomerular filtration rate (eGFR). These variables were obtained through direct interviews or assessments of biological indicators. Alcohol consumption status was defined based on the question "Do you consume at least 12 alcoholic beverages per year?" The eGFR was calculated using the Chronic Kidney Disease Epidemiology Collaboration equation (19).

2.5 Statistical analyses

Descriptive statistics are presented as the mean ± standard deviation or median (interquartile range) for skewed distributions such as blood Cd, which were logarithmically transformed to achieve normality. Baseline characteristics across CVH categories and between sexes were compared using *t*-tests or Mann–Whitney U tests for continuous variables and chi–square tests for categorical variables. Both univariate and multivariate linear regression analyses explored the associations between blood Cd levels and CVH scores. Restricted cubic spline (RCS) curves were used to assess dose–response relationships, and threshold effect analysis was used to identify inflection points. Covariates adjusted in the models included sex, age, race, PIR, education, alcohol consumption, marital status, waist circumference, and eGFR. Sensitivity analyses, including subgroup

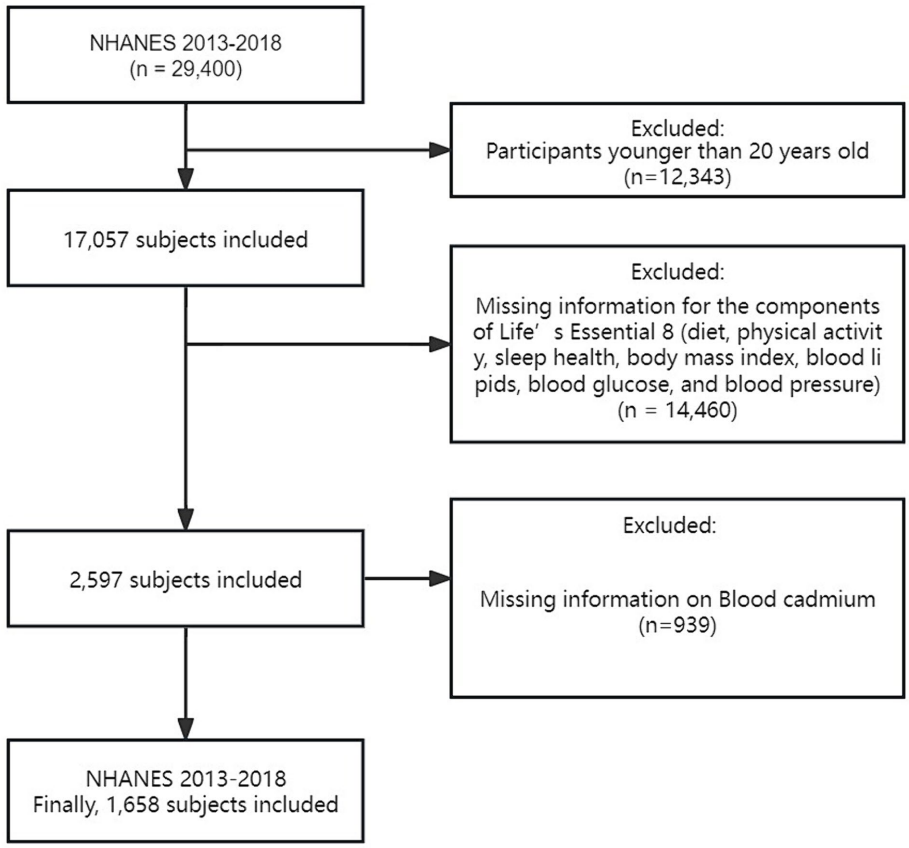

FIGURE 1
The study's flow diagram.

analyses presented in forest plots and reanalyzes excluding participants with a history of CVD (n = 183), were conducted to confirm the robustness of our findings.

All analyses were performed using R Statistical Software (Version 4.3.1, The R Foundation)[1] and the Free Statistical analysis platform (Version 1.9, Beijing, China). A two-tailed test was used, and a result was considered statistically significant when the *p*-value was <0.05.

3 Results

3.1 Population characteristics

Table 1 presents the basic characteristics of the study population classified by CVH. The study involved 1,658 individuals, with an average age of 49.5 ± 17.4 years. Among them, 61.9% were male, and 38.1% were female. Male sex, higher economic income and education levels, non-Hispanic white race, married/cohabitating status, a higher eGFR, and a smaller waist circumference were associated with a higher CVH score. Importantly, participants with high CVH scores had lower blood Cd concentrations ($p < 0.05$). Additionally, we compared baseline data between different sexes. Compared to male participants, female participants exhibited higher blood Cd concentrations ($p < 0.05$) (Supplementary Table S3).

3.2 Associations between overall and component CVH scores and blood Cd concentrations

The linear model relationships between the overall and component CVH scores and the ln-transformed blood Cd concentrations (continuous and categorized) are presented in Table 2. According to the adjusted multivariate model, the ln-transformed blood Cd concentration was negatively associated with the overall score, nicotine exposure score, sleep score, and diet score (overall score: β = −3.32, 95% CI: −3.97 to −2.67; nicotine exposure score: β = −19.41, 95% CI: −20.94 to-17.88; sleep score: β = −1.99, 95% CI: −3.5 to −0.47; diet score: β = −5.65, 95% CI: −8.02 to −3.27). When blood Cd concentrations were converted into four categorical variables using the first quartile as the reference and adjusted for multiple variables, consistent results were observed, confirming the impact of excessive Cd levels on the overall and component CVH scores.

In addition, RCS curves demonstrated the dose–response relationship between the overall and component CVH scores and

1 http://www.R-project.org

TABLE 1 Baseline characteristics of participants classified by their overall CVH score.

Characteristic	Total (*n* = 1,658)	Low CVH (*n* = 163)	Moderate CVH (*n* = 1,232)	High CVH (*n* = 263)	*p*-value
Sex[a]					< 0.001
Male	1,026 (61.9)	96 (58.9)	793 (64.4)	137 (52.1)	
Female	632 (38.1)	67 (41.1)	439 (35.6)	126 (47.9)	
Age[a], years	49.5 ± 17.4	48.5 ± 14.5	49.8 ± 17.6	48.7 ± 18.0	0.471
Race[a]					< 0.001
Mexican American	160 (9.7)	17 (10.4)	128 (10.4)	15 (5.7)	
Non-Hispanic White	764 (46.1)	58 (35.6)	569 (46.2)	137 (52.1)	
Non-Hispanic Black	351 (21.2)	55 (33.7)	271 (22)	25 (9.5)	
Other race	383 (23.1)	33 (20.2)	264 (21.4)	86 (32.7)	
Family poverty-income ratio[a]					< 0.001
<1.3	432 (26.1)	58 (35.6)	340 (27.6)	34 (12.9)	
≥1.3	1,226 (73.9)	105 (64.4)	892 (72.4)	229 (87.1)	
Educational level[a]					< 0.001
Below high school	265 (16.0)	35 (21.5)	204 (16.6)	26 (9.9)	
High-school graduate	392 (23.6)	55 (33.7)	301 (24.4)	36 (13.7)	
College or above	1,001 (60.4)	73 (44.8)	727 (59)	201 (76.4)	
MS, (%)[a]					0.012
Married/living with partner	967 (58.3)	88 (54)	700 (56.8)	179 (68.1)	
Widowed/divorced/separated	378 (22.8)	40 (24.5)	293 (23.8)	45 (17.1)	
Never married	313 (18.9)	35 (21.5)	239 (19.4)	39 (14.8)	
Drinking status, (%)[a]					0.33
No	776 (53.3)	65 (48.5)	576 (53.2)	135 (56.5)	
Yes	680 (46.7)	69 (51.5)	507 (46.8)	104 (43.5)	
Waist circumference, cm[a]	100.0 ± 16.1	113.5 ± 16.9	100.7 ± 15.3	88.5 ± 10.4	< 0.001
eGFR, mL/min/1.73 m^{2a}	96.7 ± 22.9	97.6 ± 22.4	95.8 ± 23.1	100.6 ± 21.6	0.007
log Cd, log μg/dL[a]	−0.8 ± 0.9	−0.5 ± 0.9	−0.8 ± 0.9	−1.1 ± 0.8	< 0.001

CVH, cardiovascular health; Low CVH 0–49; Moderate CVH 50–79; High CVH 80–100.
[a]Continuous variables are presented as mean ± SD; categorical variables are presented as N(%).

blood Cd concentrations (Figure 2). We found a nonlinear correlation between the blood Cd concentration and the overall score and between the blood Cd concentration and the nicotine exposure score (p for nonlinearity <0.05). Threshold effect analysis indicated that when the blood Cd concentration reached approximately −1.447 log μg/dL, the CVH rapidly decreased, and when the blood Cd concentration reached approximately −1.752 log μg/dL, the nicotine exposure score also rapidly decreased (Supplementary Tables S4, S5).

3.3 Sensitivity analyses

Figure 3 shows consistent correlations between blood Cd concentrations, CVH scores, and various subscale scores across age, race, education level, income, marital status, and alcohol consumption. However, there was a significant interaction effect among sex groups. Specifically, among females, the ln-transformed blood Cd levels and the total CVH score and lipid score displayed stronger negative correlations. On the other hand, ln-transformed blood Cd levels were positively correlated with BMI in males but not in females (Supplementary Figures S1, S2).

Additionally, after excluding individuals with a history of CVD, the associations between the blood Pb level and the overall CVH score remained consistent, while other results showed a similar impact of blood Cd levels on CVH scores (Supplementary Table S6).

4 Discussion

In this study, we utilized NHANES data from 2011 to 2018 waves to investigate the relationships between the blood concentrations of Cd and overall and component CVH scores. We found a complex and rational relationship among them. Additionally, we observed sex differences in the effects of Cd exposure.

Over the past century, we have observed a notable increase in environmental pollution and consequent human exposure to Cd (20). The most common sources of Cd contamination are waste, industrial emissions, and soil, which lead to ingestion via food, tobacco smoke, and occupational hazards (11). Prospective studies have established a

10.3389/fpubh.2024.1427905

TABLE 2 Association between the blood Cd concentrations and CVH scores.

		CVH		Body mass index		Blood pressure		Blood lipids		Blood glucose		Physical activity		Nicotine exposure		Sleep health		Diet	
		Model 1	Model 2	Model 1	Model 2	Model 1	Model 2	Model 1	Model 2	Model 1	Model 2	Model 1	Model 2	Model 1	Model 2	Model 1	Model 2	Model 1	Model 2
Cd																			
Continuous	1,658	−2.95 (−3.66 ~ −2.25)*	−3.32 (−3.97 ~ −2.67)*	3.43 (1.58 ~ 5.27)*	0.19 (−0.92 ~ 1.29)	0.48 (−1.43 ~ 2.39)	0.35 (−1.54 ~ 2.23)	0.13 (−1.57 ~ 1.83)	−1.28 (−3.12 ~ 0.56)	1.41 (−0.08 ~ 2.9)	0.53 (−0.9 ~ 1.97)	−0.21 (−1.22 ~ 0.8)	0.67 (−0.46 ~ 1.79)	−20.3 (−21.98 ~ −18.62)*	−19.41 (−20.94 ~ −17.88)*	−2.67 (−4.04 ~ −1.31)*	−1.99 (−3.5 ~ −0.47)*	−5.89 (−8.16 ~ −3.62)*	−5.65 (−8.02 ~ −3.27)*
Q1	398	Ref	Ref	Ref	Ref	Ref	Ref	Ref	Ref	Ref	Ref	Ref	Ref	Ref	Ref	Ref	Ref	Ref	Ref
Q2	413	0.19 (−1.54 ~ 1.92)	−1.25 (−2.78 ~ 0.28)	2.61 (−1.95 ~ 7.18)	−0.24 (−2.84 ~ 2.35)	0.99 (−3.73 ~ 5.72)	3.77 (−0.66 ~ 8.21)	−0.9 (−5.1 ~ 3.31)	−0.82 (−5.15 ~ 3.52)	−1.45 (−5.12 ~ 2.23)	0.47 (−2.92 ~ 3.85)	−1.14 (−3.64 ~ 1.36)	−0.95 (−3.6 ~ 1.7)	−7.2 (−11.27 ~ −3.13)	−14.07 (−17.67 ~ −10.48)*	2.01 (−1.36 ~ 5.39)	0.61 (−2.97 ~ 4.18)	6.55 (0.98 ~ 12.13)*	1.22 (−4.38 ~ 6.81)
Q3	430	−2.39 (−4.1 ~ −0.68)*	−4.33 (−5.89 ~ −2.77)*	6.67 (2.15 ~ 11.19)*	−1.16 (−3.8 ~ 1.48)	−1.7 (−6.38 ~ 2.97)	0.34 (−4.17 ~ 4.86)	1.64 (−2.52 ~ 5.81)	0.34 (−4.07 ~ 4.75)	1.08 (−2.55 ~ 4.72)	1.95 (−1.49 ~ 5.39)	−0.26 (−2.74 ~ 2.21)	0.04 (−2.66 ~ 2.73)	−21.19 (−25.22 ~ −17.16)*	−25.78 (−29.44 ~ −22.11)*	−2.31 (−5.65 ~ 1.03)	−3.43 (−7.07 ~ 0.21)	−3.05 (−8.57 ~ 2.47)	−6.94 (−12.64 ~ −1.25)*
Q4	417	−6.69 (−8.42 ~ −4.97)*	−7.67 (−9.26 ~ −6.08)*	7.84 (3.29 ~ 12.39)*	0.43 (−2.27 ~ 3.13)	2.21 (−2.51 ~ 6.92)	0.97 (−3.65 ~ 5.59)	−0.03 (−4.23 ~ 4.16)	−3.75 (−8.26 ~ 0.76)	3.49 (−0.18 ~ 7.15)	0.85 (−2.66 ~ 4.37)	−0.78 (−3.28 ~ 1.71)	1.11 (−1.64 ~ 3.87)	−48.68 (−52.74 ~ −44.62)*	−46.29 (−50.03 ~ −42.55)*	−5.02 (−8.39 ~ −1.65)*	−3.36 (−7.08 ~ 0.36)	−12.55 (−18.11 ~ −6.99)*	−11.32 (−17.14 ~ −5.5)*

CVH, cardiovascular health; Model 1 was crude model; Model 2 was adjusted for age, sex, race, family PIR, educational level, marital status, drinking status, waist circumference, and eGFR. *$P < 0.05$.

link between Cd concentrations and adverse CVD outcomes (21–23), supported by evidence that Cd-induced endothelial dysfunction could accelerate atherosclerosis (24). Our findings align with these scholarly insights (25–27), emphasizing the need for stringent monitoring of environmental Cd. Intriguingly, we identified a nonlinear relationship between blood Cd levels and overall CVH scores, with a marked decline in overall CVH scores at a blood Cd concentration of-1.447 log μg/dL, akin to the findings of Tellez-Plaza et al. (21). They found that urinary Cd levels above 0.57 μg/g were associated with increased CVD mortality. Another study found that the exposure-response relationship between blood Cd levels and acute coronary events appears to be relatively linear up to a blood Cd level of 1 μg/L, after which it levels off (28), suggesting a potential benchmark for safe blood Cd ranges. We corroborated this threshold and recommend that it be considered in future health guidelines. The biological effects of Cd indicate that at low exposure levels, the body might mitigate oxidative stress through natural antioxidant systems, thereby not exhibiting significant toxic effects. However, when Cd exposure exceeds the processing capacity of the body's antioxidant systems, these systems may be overwhelmed, leading to a sharp increase in intracellular oxidative stress and consequently causing extensive damage to cell structure and function (29).

Additionally, our subgroup analysis showed significant sex differences in the association between blood Cd levels and CVH scores, with a stronger negative association observed in females. This finding is consistent with existing research, where multiple studies have shown correlations between Cd concentrations in the blood and urine of adult females and increased incidences of peripheral arterial disease, myocardial infarction, and increased intima-media thickness of the carotid arteries, whereas these correlations were not found in males (24, 30, 31). Studies suggest that females generally have higher levels of Cd in their bodies (32). Women might absorb more Cd through the gastrointestinal tract, where Cd enters the body, binds with metallothionein, and then accumulates in other significant organs and tissues, eliciting a more intense inflammatory response (33, 34). In addition to increased bodily Cd levels, females may exhibit increased expression of the metallothionein IIA gene (35). Animal studies have shown that Cd exposure increases the reactivity of male rats' blood vessels to norepinephrine, leading to elevated blood pressure (36). Another study revealed that Cd had a reduced lethal effect on ovariectomized female rats, indicating that estrogen plays a role in the response to Cd exposure (37), which might explain the differences in Cd toxicity related to cardiovascular health between males and females. However, other scholars have reached differing conclusions, with environmental Cd exposure correlating with increased CVD mortality rates in males but not in females (22). Another study indicated that blood Cd levels are positively correlated with the 10-year risk score for atherosclerotic cardiovascular disease (ASCVD), with the risk significantly increasing in populations with higher blood Cd levels, particularly among men (38). Therefore, future research needs to further explore how sex differences affect the impact of Cd exposure on cardiovascular health. We also found that blood Cd levels were negatively correlated with nicotine exposure, sleep, and diet. This is likely because smoking is a primary pathway for Cd exposure (39). Moreover, recent research has shown that Cd can disrupt sleep patterns by causing sleep interruptions and decreasing the length of rapid eye movement (REM) sleep stages (40). Research by Unno et al. has shown that Cd in drinking water induces oxidative stress, resulting in an elevation of non-REM sleep levels and a reduction in rhythmic physical

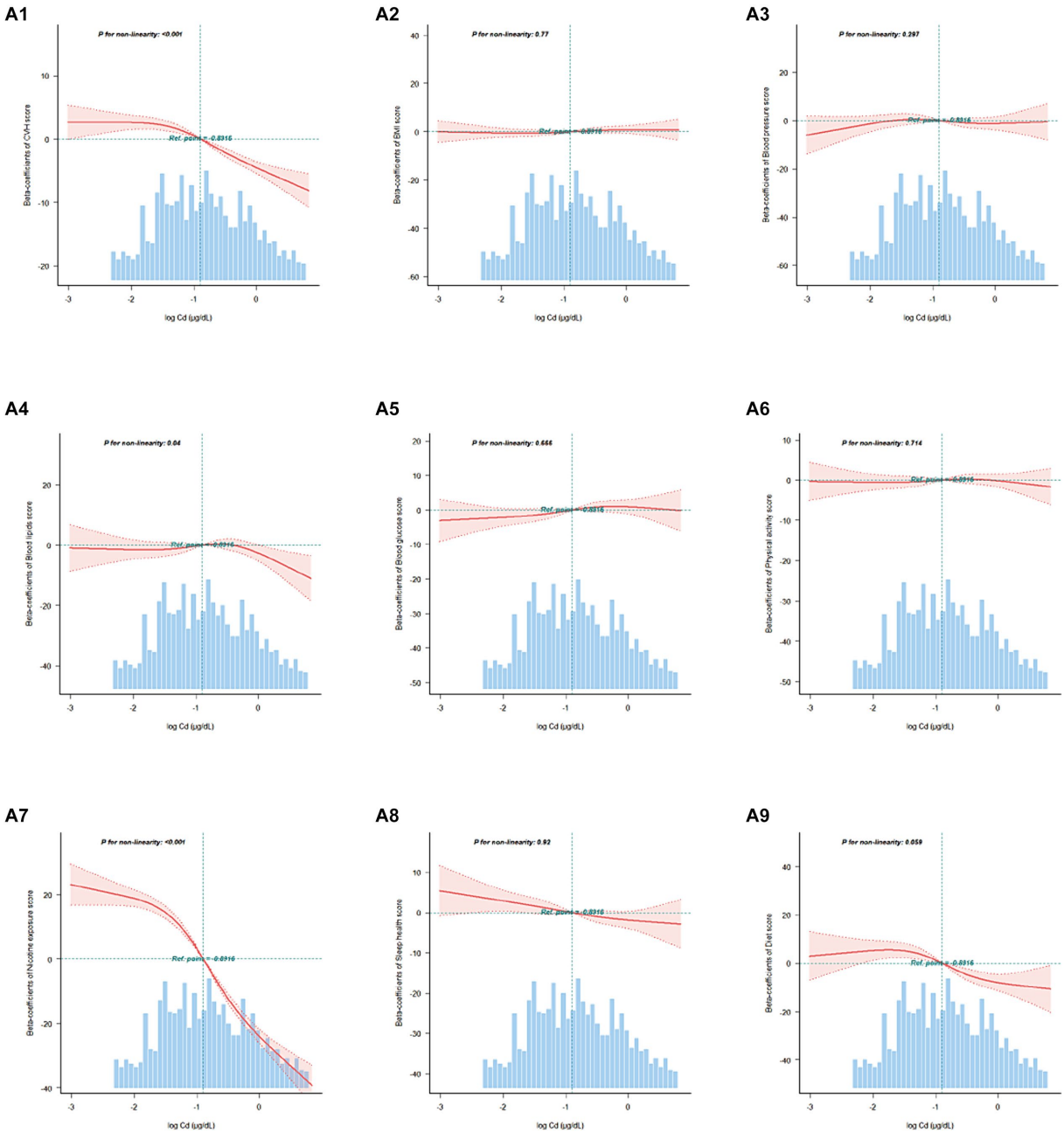

FIGURE 2
Association between the overall and component CVH scores and blood Cd levels beta-coefficients. Solid and dashed lines represent the predicted value and 95% confidence intervals. The models were adjusted for age, sex, race, family PIR, educational level, marital status, drinking status, waist circumference, and eGFR. A1, CVH scores; A2, Body mass index scores; A3, Blood pressure scores; A4, Blood lipids scores; A5, Blood glucose scores; A6, Physical activity scores; A7, Nicotine exposure scores; A8, Sleep health scores; A9, Diet scores.

activity (41). Thus, the findings of previous studies confirming the impact of Cd on overall sleep quality are consistent with our findings. Additionally, Cd is commonly found in staple foods such as leafy vegetables and grains (11). Participants with higher blood Cd levels tended to have a diet richer in refined grains, which can reasonably explain our conclusions (Supplementary Table S7). Although no correlation was found between blood Cd levels and lipid scores in the overall population, our subgroup analysis revealed a significant negative correlation between these variables in female participants—a rare observation. This finding contrasts with studies that did not stratify by sex and found no correlation between low-level Cd exposure and lipid levels (42). A previous study involving Korean adults revealed that the blood Cd concentration was positively correlated with the risk of low-density lipoprotein cholesterol in a dose-dependent manner (43). The sex differences were notable: for males, high blood Cd was associated with an increased risk of low HDL-C and a high triglyceride-to-HDL-C ratio; for females, this association was weaker, potentially due to ethnic differences. Further research is required to confirm these findings. Another significant observation is that blood Cd levels in males were positively correlated with BMI, indicating a connection

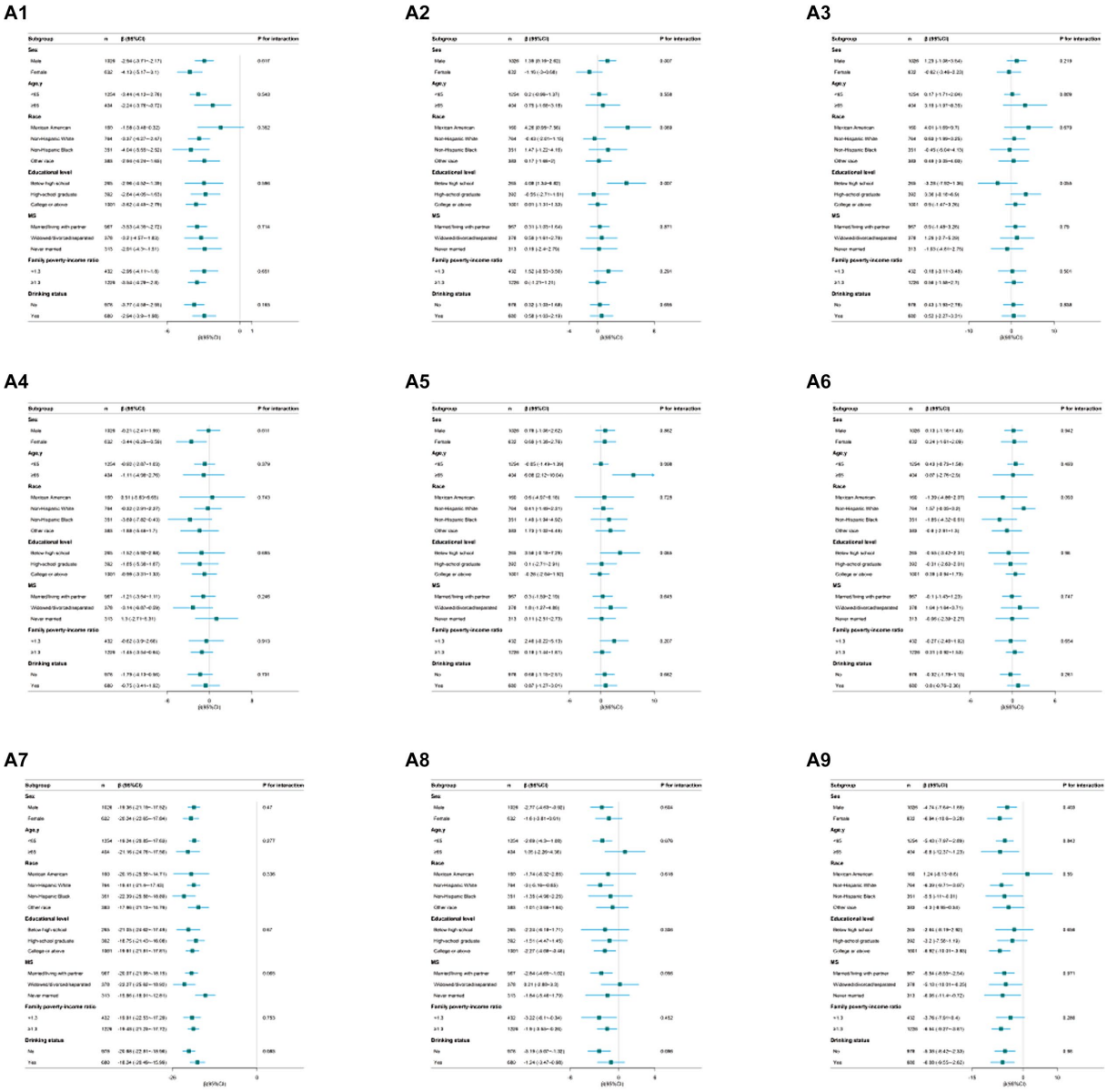

FIGURE 3
Subgroup analysis of the association between the overall and component CVH scores and blood Cd levels. Each stratification was adjusted for age, sex, race, family PIR, educational level, marital status, drinking status, waist circumference, and eGFR. A1, CVH scores; A2, Body mass index scores; A3, Blood pressure scores; A4, Blood lipids scores; A5, Blood glucose scores; A6, Physical activity scores; A7, Nicotine exposure scores; A8, Sleep health scores; A9, Diet scores. Except the stratification factor itself. Squares indicate β, with horizontal lines indicating 95% CIs.

between higher Cd levels and lower BMI—this was not observed in females. A study on Chinese adults revealed that blood Cd concentrations were negatively associated with overweight status, with no sex differences observed (44). Another prospective cohort study in Mexico revealed that the effects of prenatal exposure to Cd continues into adolescence, affecting obesity, and this relationship was observed only in girls, not boys (45). The differences in outcomes might be related to Cd's endocrine-disrupting properties affecting fat distribution. Laboratory studies have revealed interactions between Cd and estrogen and between Cd and androgen receptors, which activate estrogen receptor alpha (46). The lipid mobilization and fat breakdown in the body are regulated by hormone receptors (47), and this estrogenic effect might account for the inverse relationship with body fat seen in females. Conversely, exposure to Cd in males was linked to reduced levels of estradiol and testosterone in circulation, potentially elucidating the sex-specific outcomes (48). Therefore, when assessing the impact of blood Cd on body weight, these sex differences should be considered.

Our study has several advantages. First, the NHANES database contains a large amount of detailed information about a diverse population in the United States. The database is maintained with consistent data collection techniques and rigorous quality control measures to guarantee the precision and dependability of the data. Second, the latest CVH scores include behaviors and factors that impact CVH. These scores are currently the most advanced, and through our comprehensive evaluation, they have promoted new

perspectives for understanding the effects of Cd on CVH. Several limitations must be taken into account. First, the cross-sectional nature of this database prevents us from establishing causal relationships; we can only infer correlations. Second, despite controlling for various confounding variables, there may still be unmeasurable factors that could confound the results. Third, due to potential variations in Cd exposure environments and differences in dietary and lifestyle habits among different countries and populations, our conclusions may not be generalizable to other countries or populations.

5 Conclusion

In conclusion, our research revealed complex and multifaceted associations of blood Cd levels with overall and component CVH scores. Notably, we identified nonlinear correlations of blood Cd levels with the overall CVH score and nicotine exposure score, with critical thresholds. Furthermore, sex differences were observed in the effects on blood Cd levels. Subsequent studies might also explore potential preventive and therapeutic interventions, refine risk assessment models, and extend these findings to broader populations to cement our understanding of these relationships.

Data availability statement

Publicly available datasets were analyzed in this study. This data can be found at: https://wwwn.cdc.gov/nchs/nhanes/Default.aspx.

Ethics statement

The survey protocol (Protocol #2011–17, Continuation of Protocol #2011–17) received approval from both the National Center for Health Statistics (NCHS) Ethics Review Board and the Centers for Disease Control and Prevention (CDC). The studies were conducted in accordance with the local legislation and institutional requirements. Written informed consent for participation in this study was provided by the participants' legal guardians/next of kin.

Author contributions

FC: Conceptualization, Data curation, Formal analysis, Investigation, Methodology, Supervision, Validation, Visualization, Writing – original draft, Writing – review & editing. HL: Conceptualization, Data curation, Formal analysis, Methodology, Supervision, Visualization, Writing – original draft. YuaZ: Data curation, Methodology, Software, Supervision, Validation, Visualization, Writing – original draft. YuZ: Conceptualization, Investigation, Methodology, Project administration, Software, Supervision, Validation, Writing – review & editing. SC: Conceptualization, Formal analysis, Investigation, Methodology, Software, Supervision, Validation, Visualization, Writing – review & editing.

Funding

The author(s) declare that no financial support was received for the research, authorship, and/or publication of this article.

Conflict of interest

The authors declare that the research was conducted in the absence of any commercial or financial relationships that could be construed as a potential conflict of interest.

Publisher's note

Supplementary material

The Supplementary material for this article can be found online at: https://www.frontiersin.org/articles/10.3389/fpubh.2024.1427905/full#supplementary-material

SUPPLEMENTARY FIGURE S1
Association between the male overall and component CVH scores and blood Cd levels beta-coefficients. Solid and dashed lines represent the predicted value and 95% confidence intervals. The models were adjusted for age, sex, race, family PIR, educational level, marital status, drinking status, waist circumference, and eGFR. A1, CVH scores; A2, Body mass index scores; A3, Blood pressure scores; A4, Blood lipids scores; A5, Blood glucose scores; A6, Physical activity scores; A7, Nicotine exposure scores; A8, Sleep health scores; A9, Diet scores.

SUPPLEMENTARY FIGURE S2
Association between the female overall and component CVH scores and blood Cd levels beta-coefficients. Solid and dashed lines represent the predicted value and 95% confidence intervals. The models were adjusted for age, sex, race, family PIR, educational level, marital status, drinking status, waist circumference, and eGFR. A1, CVH scores; A2, Body mass index scores; A3, Blood pressure scores; A4, Blood lipids scores; A5, Blood glucose scores; A6, Physical activity scores; A7, Nicotine exposure scores; A8, Sleep health scores; A9, Diet scores.

References

1. Roth GA, Johnson C, Abajobir A, Abd-Allah F, Abera SF, Abyu G, et al. Global, regional, and National Burden of cardiovascular diseases for 10 causes, 1990 to 2015. *J Am Coll Cardiol.* (2017) 70:1–25. doi: 10.1016/j.jacc.2017.04.052

2. Roth GA, Mensah GA, Johnson CO, Addolorato G, Ammirati E, Baddour LM, et al. Global burden of cardiovascular diseases and risk factors, 1990-2019: update from the GBD 2019 study. *J Am Coll Cardiol.* (2020) 76:2982–3021. doi: 10.1016/j.jacc.2020.11.010

3. Lloyd-Jones DM, Hong Y, Labarthe D, Mozaffarian D, Appel LJ, Van Horn L, et al. Defining and setting national goals for cardiovascular health promotion and disease reduction: the American Heart Association's strategic impact goal through

2020 and beyond. *Circulation*. (2010) 121:586–613. doi: 10.1161/CIRCULATIONAHA.109.192703

4. Yang Q, Cogswell ME, Flanders WD, Hong Y, Zhang Z, Loustalot F, et al. Trends in cardiovascular health metrics and associations with all-cause and CVD mortality among US adults. *JAMA*. (2012) 307:1273–83. doi: 10.1001/jama.2012.339

5. Ford ES, Greenlund KJ, Hong Y. Ideal cardiovascular health and mortality from all causes and diseases of the circulatory system among adults in the United States. *Circulation*. (2012) 125:987–95. doi: 10.1161/CIRCULATIONAHA.111.049122

6. Hwang SJ, Onuma O, Massaro JM, Zhang X, Fu YP, Hoffmann U, et al. Maintenance of ideal cardiovascular health and coronary artery calcium progression in low-risk men and women in the Framingham heart study. *Circ Cardiovasc Imaging*. (2018) 11:e006209. doi: 10.1161/CIRCIMAGING.117.006209

7. Li Y, Pan A, Wang DD, Liu X, Dhana K, Franco OH, et al. Impact of healthy lifestyle factors on life expectancies in the US population. *Circulation*. (2018) 138:345–55. doi: 10.1161/CIRCULATIONAHA.117.032047

8. Lloyd-Jones DM, Allen NB, Anderson CAM, Black T, Brewer LC, Foraker RE, et al. Life's essential 8: updating and enhancing the American Heart Association's construct of cardiovascular health: a presidential advisory from the American Heart Association. *Circulation*. (2022) 146:e18–43. doi: 10.1161/CIR.0000000000001078

9. Bhatnagar A. Environmental cardiology: studying mechanistic links between pollution and heart disease. *Circ Res*. (2006) 99:692–705. doi: 10.1161/01.RES.0000243586.99701.cf

10. González-Villalva A, Colín-Barenque L, Bizarro-Nevares P, Rojas-Lemus M, Rodríguez-Lara V, García-Pelaez I, et al. Pollution by metals: is there a relationship in glycemic control? *Environ Toxicol Pharmacol*. (2016) 46:337–43. doi: 10.1016/j.etap.2016.06.023

11. Järup L, Akesson A. Current status of cadmium as an environmental health problem. *Toxicol Appl Pharmacol*. (2009) 238:201–8. doi: 10.1016/j.taap.2009.04.020

12. Lamas GA, Ujueta F, Navas-Acien A. Lead and cadmium as cardiovascular risk factors: the burden of proof has been met. *J Am Heart Assoc*. (2021) 10:e018692. doi: 10.1161/JAHA.120.018692

13. Chen S, Shen R, Shen J, Lyu L, Wei T. Association of blood cadmium with all-cause and cause-specific mortality in patients with hypertension. *Front Public Health*. (2023) 11:1106732. doi: 10.3389/fpubh.2023.1106732

14. Hecht EM, Hlaing WWM. Association between cadmium and cardiovascular outcomes by gender. *Ann Epidemiol*. (2015) 25:707. doi: 10.1016/j.annepidem.2015.06.028

15. Newson L. Menopause and cardiovascular disease. *Post Reprod Health*. (2018) 24:44–9. doi: 10.1177/2053369117749675

16. Guo X, Li N, Wang H, Su W, Song Q, Liang Q, et al. Combined exposure to multiple metals on cardiovascular disease in NHANES under five statistical models. *Environ Res*. (2022) 215:114435. doi: 10.1016/j.envres.2022.114435

17. Duan W, Xu C, Liu Q, Xu J, Weng Z, Zhang X, et al. Levels of a mixture of heavy metals in blood and urine and all-cause, cardiovascular disease and cancer mortality: a population-based cohort study. *Environ Pollut*. (2020) 263:114630. doi: 10.1016/j.envpol.2020.114630

18. Liang JH, Pu YQ, Liu ML, Hu LX, Bao WW, Zhang YS, et al. Joint effect of whole blood metals exposure with dyslipidemia in representative US adults in NHANES 2011-2020. *Environ Sci Pollut Res Int*. (2023) 30:96604–16. doi: 10.1007/s11356-023-28903-0

19. Levey AS, Stevens LA, Schmid CH, Zhang YL, Castro AF 3rd, Feldman HI, et al. A new equation to estimate glomerular filtration rate. *Ann Intern Med*. (2009) 150:604–12. doi: 10.7326/0003-4819-150-9-200905050-00006

20. Nriagu JO, Pacyna JM. Quantitative assessment of worldwide contamination of air, water and soils by trace metals. *Nature*. (1988) 333:134–9. doi: 10.1038/333134a0

21. Tellez-Plaza M, Navas-Acien A, Menke A, Crainiceanu CM, Pastor-Barriuso R, Guallar E. Cadmium exposure and all-cause and cardiovascular mortality in the U.S. general population. *Environ Health Perspect*. (2012) 120:1017–22. doi: 10.1289/ehp.1104352

22. Menke A, Muntner P, Silbergeld EK, Platz EA, Guallar E. Cadmium levels in urine and mortality among U.S. adults. *Environ Health Perspect*. (2009) 117:190–6. doi: 10.1289/ehp.11236

23. Nawrot TS, Van Hecke E, Thijs L, Richart T, Kuznetsova T, Jin Y, et al. Cadmium-related mortality and long-term secular trends in the cadmium body burden of an environmentally exposed population. *Environ Health Perspect*. (2008) 116:1620–8. doi: 10.1289/ehp.11667

24. Messner B, Knoflach M, Seubert A, Ritsch A, Pfaller K, Henderson B, et al. Cadmium is a novel and independent risk factor for early atherosclerosis mechanisms and in vivo relevance. *Arterioscler Thromb Vasc Biol*. (2009) 29:1392–8. doi: 10.1161/ATVBAHA.109.190082

25. Ma S, Zhang J, Xu C, Da M, Xu Y, Chen Y, et al. Increased serum levels of cadmium are associated with an elevated risk of cardiovascular disease in adults. *Environ Sci Pollut Res Int*. (2022) 29:1836–44. doi: 10.1007/s11356-021-15732-2

26. Tellez-Plaza M, Guallar E, Howard BV, Umans JG, Francesconi KA, Goessler W, et al. Cadmium exposure and incident cardiovascular disease. *Epidemiology*. (2013) 24:421–9. doi: 10.1097/EDE.0b013e31828b0631

27. Chowdhury R, Ramond A, O'Keeffe LM, Shahzad S, Kunutsor SK, Muka T, et al. Environmental toxic metal contaminants and risk of cardiovascular disease: systematic review and meta-analysis. *BMJ*. (2018) 362:k3310. doi: 10.1136/bmj.k3310

28. Barregard L, Sallsten G, Fagerberg B, Borné Y, Persson M, Hedblad B, et al. Blood cadmium levels and incident cardiovascular events during follow-up in a population-based cohort of Swedish adults: the Malmö diet and Cancer study. *Environ Health Perspect*. (2016) 124:594–600. doi: 10.1289/ehp.1509735

29. Sandra Concepcion D, Hamda A-N. Cadmium toxicity: oxidative stress, inflammation and tissue injury. *Occupat Dis Environ Med*. (2019) 17:144–63. doi: 10.4236/odem.2019.74012

30. Tellez-Plaza M, Navas-Acien A, Crainiceanu CM, Sharrett AR, Guallar E. Cadmium and peripheral arterial disease: gender differences in the 1999-2004 US National Health and nutrition examination survey. *Am J Epidemiol*. (2010) 172:671–81. doi: 10.1093/aje/kwq172

31. Everett CJ, Frithsen IL. Association of urinary cadmium and myocardial infarction. *Environ Res*. (2008) 106:284–6. doi: 10.1016/j.envres.2007.10.009

32. Vahter M, Akesson A, Lidén C, Ceccatelli S, Berglund M. Gender differences in the disposition and toxicity of metals. *Environ Res*. (2007) 104:85–95. doi: 10.1016/j.envres.2006.08.003

33. Huang YH, Shih CM, Huang CJ, Lin CM, Chou CM, Tsai ML, et al. Effects of cadmium on structure and enzymatic activity of cu,Zn-SOD and oxidative status in neural cells. *J Cell Biochem*. (2006) 98:577–89. doi: 10.1002/jcb.20772

34. Kataranovski M, Janković S, Kataranovski D, Stosić J, Bogojević D. Gender differences in acute cadmium-induced systemic inflammation in rats. *Biomed Environ Sci*. (2009) 22:1–7. doi: 10.1016/S0895-3988(09)60014-3

35. Kwon CS, Kountouri AM, Mayer C, Gordon MJ, Kwun IS, Beattie JH. Mononuclear cell metallothionein mRNA levels in human subjects with poor zinc nutrition. *Br J Nutr*. (2007) 97:247–54. doi: 10.1017/S0007114507328614

36. Almenara CC, Broseghini-Filho GB, Vescovi MV, Angeli JK, Faria Tde O, Stefanon I, et al. Chronic cadmium treatment promotes oxidative stress and endothelial damage in isolated rat aorta. *PLoS One*. (2013) 8:e68418. doi: 10.1371/journal.pone.0068418

37. de Oliveira TF, Rossi EM, da Costa CS, Graceli JB, Krause M, Carneiro M, et al. Sex-dependent vascular effects of cadmium sub-chronic exposure on rats. *Biometals*. (2023) 36:189–99. doi: 10.1007/s10534-022-00470-w

38. Choi S, Kwon J, Kwon P, Lee C, Jang SI. Association between blood heavy metal levels and predicted 10-year risk for a first atherosclerosis cardiovascular disease in the general Korean population. *Int J Environ Res Public Health*. (2020) 17:2134. doi: 10.3390/ijerph17062134

39. Fireman Klein E, Klein I, Ephrat O, Dekel Y, Kessel A, Adir Y. Trajectory of inhaled cadmium ultrafine particles in smokers. *BMJ Open Respir Res*. (2021) 8:e001000. doi: 10.1136/bmjresp-2021-001000

40. Frosztega W, Wieckiewicz M, Gac P, Lachowicz G, Poreba R, Mazur G, et al. The effect of cadmium on sleep parameters assessed in polysomnographic studies: a case-control study. *J Clin Med*. (2023) 12. doi: 10.3390/jcm12123899

41. Unno K, Yamoto K, Takeuchi K, Kataoka A, Ozaki T, Mochizuki T, et al. Acute enhancement of non-rapid eye movement sleep in rats after drinking water contaminated with cadmium chloride. *J Appl Toxicol*. (2014) 34:205–13. doi: 10.1002/jat.2853

42. Xu H, Mao Y, Xu B, Hu Y. Low-level environmental lead and cadmium exposures and dyslipidemia in adults: findings from the NHANES 2005-2016. *J Trace Elements Med Biol*. (2021) 63:126651. doi: 10.1016/j.jtemb.2020.126651

43. Kim K. Blood cadmium concentration and lipid profile in Korean adults. *Environ Res*. (2012) 112:225–9. doi: 10.1016/j.envres.2011.12.008

44. Nie X, Wang N, Chen Y, Chen C, Han B, Zhu C, et al. Blood cadmium in Chinese adults and its relationships with diabetes and obesity. *Environ Sci Pollut Res Int*. (2016) 23:18714–23. doi: 10.1007/s11356-016-7078-2

45. Moynihan M, Telléz-Rojo MM, Colacino J, Jones A, Song PXK, Cantoral A, et al. Prenatal cadmium exposure is negatively associated with adiposity in girls not boys during adolescence. *Front Public Health*. (2019) 7:61. doi: 10.3389/fpubh.2019.00061

46. Stoica A, Katzenellenbogen BS, Martin MB. Activation of estrogen receptor-alpha by the heavy metal cadmium. *Mol Endocrinol*. (2000) 14:545–53. doi: 10.1210/mend.14.4.0441

47. Hackney AC, Muoio D, Meyer WR. The effect of sex steroid hormones on substrate oxidation during prolonged submaximal exercise in women. *Jpn J Physiol*. (2000) 50:489–94. doi: 10.2170/jjphysiol.50.489

48. Dhooge W, den Hond E, Koppen G, Bruckers L, Nelen V, van de Mieroop E, et al. Internal exposure to pollutants and sex hormone levels in Flemish male adolescents in a cross-sectional study: associations and dose-response relationships. *J Expo Sci Environ Epidemiol*. (2011) 21:106–13. doi: 10.1038/jes.2009.63

frontiers | Frontiers in Public Health

TYPE Original Research
PUBLISHED 21 August 2024
DOI 10.3389/fpubh.2024.1397236

OPEN ACCESS

EDITED BY
João Cavaleiro Rufo,
University Porto, Portugal

REVIEWED BY
Penghao Ye,
Hainan University, China
Tomoya Harada,
Tottori University Hospital, Japan

*CORRESPONDENCE
Paulo Moreira
✉ jpm2030@outlook.com
Dou Mei
✉ doumei@qdu.edu.cn

†These authors share first authorship

RECEIVED 07 March 2024
ACCEPTED 22 July 2024
PUBLISHED 21 August 2024

CITATION
Yang L, Xinting C, Aie Z, Ruiqi X, Moreira P and Mei D (2024) Insights into uncovered public health risks. The case of asthma attacks among archival workers: a cross-sectional study.
Front. Public Health 12:1397236.
doi: 10.3389/fpubh.2024.1397236

Insights into uncovered public health risks. The case of asthma attacks among archival workers: a cross-sectional study

Liu Yang[1†], Chen Xinting[2†], Zhang Aie[3], Xu Ruiqi[2], Paulo Moreira[4,5,6*] and Dou Mei[2,7*]

[1]Shandong Provincial Chronic Disease Hospital, Qingdao, China, [2]School of Public Health, Qingdao University, Qingdao, China, [3]Qilu Hospital, Shandong University, Jinan, China, [4]The First Affiliated Hospital of Shandong First Medical University & Shandong Provincial Qianfoshan Hospital, International Healthcare Management Research and Development Centre (IHM-RDC), Jinan, China, [5]Henan Normal University, School of Social Affairs, Xinxiang, China, [6]Atlantica Instituto Universitario, Gestao em Saude, Oeiras, Portugal, [7]Qingdao University Archives, Qingdao, China

Objective: To ascertain the prevalence of asthma attacks among archivists and identify the associated occupational factors in this understudied professional population.

Methods: We conducted a cross-sectional, questionnaire-based study among 1,002 archival workers. A multiple logistic regression was conducted to identify the association between asthma attacks and occupational exposures. The Strobe Protocol was applied.

Results: 999 workers were included in the final analysis with the asthma prevalence of 33.3%. Main factors associated with asthma attacks (OR [95% CI]) were the presence of chemically irritating odors (2.152 [1.532–3.024]), mold odors (1.747 [1.148–2.658]), and insects (1.409[1.041–1.907]). A significant synergistic effect was observed between chemical irritants and mold, the odds ratio was 7.098 (95% CI, 4.752–10.603).

Conclusion: There was a high prevalence of asthma attacks among archival workers, an under-studied population. Chemical irritants, molds and insects were associated with their asthma attacks. Notably, this study's data analysis has revealed a strong synergy (OR = 7.098) between chemical odors and molds in the workplace. While the existing international literature on this specific interaction remains somewhat limited, previous studies have already demonstrated the potential for chemical irritants, such as sulfur dioxide and ozone, to synergistically interact with inhalable allergens, including fungi, molds and dust mites. Consequently, this interaction seems to exacerbate asthma symptoms and perpetuate untreated exposure. Furthermore, in damp and damaged buildings, the presence of microbial components, such as cellular debris or spores released during fungal growth can trigger an inflammatory response, potentially served as a shared pathway for the development of asthma among individuals exposed to these hazardous factors.

KEYWORDS

public health, asthma attacks, archival workers, chemical irritants, molds

1 Introduction

Asthma is a heterogeneous clinical syndrome that affects approximately 360 million people worldwide. Studies have found that up to 25% of adult asthma cases are work-related (1). The incidence does not appear to be decreasing (2), which leading to significant social and economic burdens. Recently, new cases of work related asthma due to workplace exposures in many sectors have been reported (3–5). Among all the workplaces, offices are not frequently associated with common agents for occupational asthma, office workers consequently remain a low risk of contracting occupational asthma (6, 7). Among all the workplaces, with relatively few exposure conditions associated with the incidence of occupational asthma, the risk of occupational asthma in the offices is low. However, A prevalence study conducted among office workers found totally 9.6% had doctor-diagnosed asthma (8). Anderson et al. (9) found that administrative support workers, including clerical workers and health service workers had significantly higher prevalence ratios (PR 1.5, 95%CI 1.2–1.9) of current asthma than prevalence in all industries. Thus, attention should be paid to the more specific occupational groups used to be simply classified as office workers.

Asthma can be triggered by factors such as exposure to allergens or irritants (10). A positive association between HDM allergens, dust, indoor air, mold, solvents and respiratory symptoms in office workers was reported (8, 11).

Related studies have shown a positive correlation between HDM allergens, dust, indoor air, mold, solvents and respiratory symptoms in office workers. The influencing factors of asthma are intricate, mainly attributed to genetic and environmental factors (12). Some researches have pointed out that there is also a certain amount of fungal pollution in different working environments, such as hospitals, nursing homes, museums and so on (13–15). When the fungus is exposed to a certain concentration it can cause asthma attacks in residents or staff (16, 17). Among them, archivists are susceptible to asthma due to the influence of working area and working mode.

Archive workers, a more specific occupational group as part of the office workers, besides dealing with relevant works in the office, closely expose to archive documents and document storage environment resulting. Most documents and files deposited in archives are made of paper, which are susceptible to chemical and biological damage. As a consequence of the exposed items degradation, VOCs can be formed from the paper itself (18), including acetic acid, formic acid, furfural, furfural, 4-hydroxy benzoic acid, 4-hydroxy acetophenone (19). Cladosporium, Aspergillus, and Penicillium species are almost ubiquitous in the archives (20), which induces allergic reactions and further developing of asthma (1, 21, 22). Exposure to biological allergens such as insect and microorganism is another crucial potential risk factor associated with incidence of asthma (23, 24). To the best of our knowledge, no studies have investigated asthma among archive workers.

Therefore, we sought to identify the prevalence and factors associated with asthma attacks in archival workers. In this study, a questionnaire-based study was conducted among archivists to investigate the associated factors concerning asthma attacks, and concurrently assessed potential interactions that may augment the risk of asthma attacks.

1.1 Contribution to the field

The evidence generated in this study suggests the need to further study and protect archivists as there is a strong synergy between chemical odors and molds in interaction with the potential of chemical irritants, such as sulfur dioxide and ozone, to synergistically interact with inhalable allergens, including fungi, molds and dust mites. Consequently, this interaction seems to exacerbate asthma symptom, perpetuate untreated exposure and trigger an inflammatory response potentially serving as a shared pathway for the development of asthma among individuals exposed to these hazardous factors (add here one more paragraph or two clarifying what can this paper contribute to knowledge and unknown aspects associated with the topic and the population under study, to be arranged in an independent section).

Additionally, the occupational health of archivists, who are the participants and executors of the preservation of important historical materials in countries and organizations, affects the sustainable development of archival undertakings. Archival workers often need to deal with all kinds of archival materials, including photo archives, physical archives and paper archives, etc., which plays a key role in the archives management work. These files may contain a variety of pathogenic microorganisms, such as bacteria, viruses, fungi and parasites, which may pose a potential risk of pathogenic infection to the archivists. A large number of occupational health studies have found that the human body will develop allergy symptoms, respiratory diseases and other health problems in the poor indoor environment.

At present, there are many studies based on the correlation between asthma and other occupations, but few studies on occupational risk factors for archivists, especially for the prevalence of asthma attacks in archivists, no evidence or correlation studies have been found. Therefore, the study of occupational hazard factors for archivists concerned in this study is a critical and ongoing topic, and its related research is of great significance for the protection of the health and safety of archival professionals.

2 Subjects and methods

2.1 Subjects

This cross-sectional, questionnaire-based study was conducted at the archives nationwide in China in a multi-center setting, including archives of enterprises and institutions (74.78%), national comprehensive archives (23.22%) and specialized archives (2.10%). Individuals who were currently employed in archive setting were included in the study. The questionnaire is available as Supplementary material.

2.1.1 Sample size calculation

The results of the total work-life microsimulation conducted by Laditka (25) showed that 14.9% (CI 13.4–16.3) of those with low trigger exposure risk reported asthma at least once. We classified archivists as having a low risk of triggering asthma exposure and considered the prevalence of asthma among archivists to be approximately 14.9%, calculated according to the PASS software. Based on $\alpha = 0.05$, $\delta = 0.03$, $p = 0.149$, the total sample size required was calculated to be 573 cases. Considering the possibility of invalid

samples in the questionnaire, the final sample size required was calculated to be 717 cases.

2.2 Methods

2.2.1 Questionnaire

The questionnaires were sent to all eligible archivists in February 2022, and archivists were requested to fill out the questionnaires within 10 days. Here, we define "asthma attacks and exacerbation of asthma attacks among archivists after work" as asthma attacks. Data on the following personal factors were collected: sex (male, female), age (20–30 years, 31–40 years,41–50 years,51–65 years), education (below bachelor degree, bachelor, master's degree or above), duration of employment (≤5 years,6–10 years,11–20 years, ≥21 years) and family history of the respiratory system. In order to explore archivists' knowledge of occupational hazard factors, we also collected the data: whether knowing the effective protection measures to risk factors in the archival profession and well protection in work according to the professional protection files? The response to each is either "yes" or "no." Furthermore, work-related factors were gathered: archivists' average frequency of contacting paper files at work (times per day) ≤1, 1–2, 3–4, ≥5. And the strict separation of the working areas from archives warehouses, dampness in the working area, chemically irritating odor in working areas, mold odor in working areas, insects (roaches, ants, tobacco beetle and dust mite etc.) in working area. The answer options in each question are dichotomous (yes or no). To further adjust for confounding factors, the self-administered questionnaire asked about the protection to adverse factors related to archival work, i.e., legislation of protective measures of risk factors in the archival profession, having equipment for occupational protection, training on occupational protections of archives. Finally, subjects were asked to answer if they had asthma or more frequent asthma attacks at work (especially when in contact with archival entities), including questions about asthma symptoms, namely wheezing, chest tightness or shortness of breath which were questions in questionnaire. Responses range from always, frequently, occasionally, never. The data collected were conducted in an anonymous fashion. Ethical approval was obtained from XXX [Anonymized by request from JOEM]. Electronic informed consent was obtained for each participant.

2.3 Statistical analysis

All statistical analysis was performed using SPSS 26.0. Initially, associations between personal factors (age, sex, duration of employment, family history) and asthma attacks were analyzed by Chi-square test or the Mann–Whitney-U test. Next, the association between the related factors in archival work, i.e., strict separation of working areas from archives warehouses, ventilation and its average time in warehouse, temperature and humidity of the warehouse in summer, chemically irritating odor, mold odor and insects (roaches, ants, tobacco beetle and dust mite etc) in working areas and asthma attacks were also assessed by Chi-square test. Thereby, logistic regression was conducted according to the p value. For the first selection of associated factors, univariate logistic regression analysis was performed. Subsequently, multiple logistic regression analysis was performed to assess independent association, in which the presence of asthma attacks was the objective variable and the associated factors that showed significant associations in the univariate analysis were the explanation variables. For the variables with a p value <0.05 in the univariable analysis were entered into the multiple logistic regression model. The interaction between the chemically irritating odors and mold odors was examined in the logistic regression model. Statistical significance was set at $p < 0.05$.

The Strobe Protocol for Cross-Sectional studies was applied.

3 Results

3.1 Basic characteristics of the subjects

A total of 1,002 people submitted questionnaires, of which 999 were valid and included in the final analysis, with an effective rate of 99.7%. The gender, age, education, and duration of employment of the respondents substantially matched the statistics of the National Bureau of Statistics 2021. As shown in Table 1, individuals with asthma attacks accounted for 33%, of which 67% were female. Duration of employment were less than 10 years for 45% ($n = 453$) of subjects and 11 years or more for 55% ($n = 556$). Approximately 66% of those archivists with family history of the respiratory system had asthma attacks (Table 1).

3.2 Work-related factors

Archive's daily sanitary measures and status in terms of asthma attacks in archivists are shown in Table 2. The archivists who have strict separation of the working areas from archives' warehouses tended to respond that they suffered less asthma attacks, and many individuals respond that the occurrence of dampness, pungent chemical odor, mold odor as well as the harmful insects in the working area were significantly associated with the asthma attacks among them. Archives' protective measures thought to be associated with asthma attacks were also assessed, the results of which were shown in Table 3. Those archivists having documentation of archival occupational risk factors in the workplace and achieving standardized protection at work were prone to have a lower prevalence of asthma attacks. As archival workers are exposed to various hazards in the workplace, it is essential for them to take appropriate protective measures. However, many archives fail to raise awareness of the dangers present in the workplace. Only 135 archivists participating in the study have had professional protection protocols in place. This study data indicates that chemically irritating odors, mold odors, and insects in the workplace are correlated with asthma attacks amongst the population studied. Therefore, it suggests that the workplace environment plays a key role in the occurrence of asthma attacks, and achieving standardized protection at work is prone to promote a lower prevalence of asthma attacks in the context studied.

3.3 Factors associated with asthma attacks

The univariate and multivariate analysis are summarized in Table 4. In the multivariate logistic regression analysis, sex, working years, strict separation of the working areas from archives, mold odor,

TABLE 1 Basic characteristics of the subjects by asthma attacks (n = 999) [n (%)].

	Total (n = 999)	Non-asthma attacks (n = 666)	Asthma attacks (n = 333)	p-value
Gender				
Female	722	499 (74.9)	223 (67)	0.008
Male	277	167 (25.1)	110 (33)	
Age (years)				0.008[a]
≤40	286	211 (31.7)	75 (22.5)	
41–50	413	265 (39.8)	148 (44.4)	
≥51	300	190 (28.5)	110 (33.0)	
Education				0.515
Below bachelor degree	157	106 (15.9)	51 (15.3)	
Bachelor	631	413 (62.0)	218 (65.5)	
Master's degree or above	211	147 (22.1)	64 (19.2)	
Duration of employment (years)				
≤5	273	208 (31.2)	65 (19.5)	<0.001
6–10	180	124 (18.6)	56 (16.8)	
11–20	274	176 (26.4)	98 (29.4)	
≥21	272	158 (23.7)	114 (34.2)	
The average frequency of contacting paper files at work (times/day)				
≤1	154	110 (16.5)	44 (13.2)	0.031
1–2	313	208 (31.2)	105 (31.5)	
3–4	220	158 (23.7)	62 (18.6)	
≥5	312	190 (28.5)	122 (36.6)	
Family history of the respiratory system	41	14 (2.1)	27 (8.1)	<0.001
Exercise regularly	673	452 (67.9)	221 (66.4)	0.633

[a]Mann–Whitney test.

chemically irritating odor and insects in the workplaces were significantly associated with the incidence of asthma attacks ($p < 0.05$). Workers who had work experiences≥21 years (OR, 95%CI: 2.116, 1.420 ~ 3.153) had the odds of developing asthma attacks 1.1 times more than workers who had work experiences between 6 and 10 years. Workers without strict separation of the working areas from archives warehouses were 0.522 times more likely to develop asthma attacks (OR, 95%CI: 1.522, 1.096 ~ 2.113). Workers who found mold odor in working areas as well as warehouses had a higher risk of developing asthma attacks (OR, 95%CI: 1.747, 1.148 ~ 2.658; 1.666, 1.084 ~ 2.561 separately). Workers who found chemically irritating odor in working areas were 1.152 times more likely to develop asthma attacks (OR, 95%CI: 2.152, 1.532 ~ 3.024). Workers who found insects in working areas were 0.409 times more likely to develop asthma attacks (OR, 95%CI: 1.409, 1.041 ~ 1.907).

Table 5 shows the results of analysis in which we tested for interactions between chemically irritating odor and mold odor in working areas for asthma attacks. A significant synergistic effect was observed between chemical irritants and molds, the odds ratio was 7.098 (95% CI, 4.752–10.603). A program flowchart is presented in Figure 1.

4 Discussion

This study found that the prevalence of asthma attacks was 33.3%, higher among male archivists. The existence of chemically irritating odors and moldy smells within the work environment were associated with higher asthma attacks. We also found a significant synergistic effect between the two risk factors. To the best of our knowledge, this is the first multicenter study focusing specifically on the risk factors related to asthma in archivists and provides a fresh perspective on occupational asthma.

The present study identified a significant association between the presence of chemically irritating odors in archival workplaces and high asthma attacks among archivists. Occupational hazards for archivists primarily stem from indoor air pollution, including conventional indoor chemical pollutants such as formaldehyde, sulfur dioxide, volatile organic compound (26). Additionally, there are archival-specific chemical pollutants such as acetic acid, hydrogen sulfide, ethylene oxide, sulfuryl fluoride, furfural, and other compounds (19). It has been reported that exposure to ozone and sulfur dioxide has deleterious effects on immune competent cells and airway responsiveness (27). Owing to its potential to sensitize airway inflammation, ozone exhibits a propensity to induce various respiratory ailments, encompassing coughing and wheezing (28). It has been extensively elucidated that elevated ozone levels have an inflammatory impact on the respiratory system, thereby contributing to the progression of asthma (29). Interestingly, a study revealed a negative correlation between low-to-moderate atmospheric ozone levels and hospital visits by asthma patients (30). However, the measured median ozone concentration in office environments is 9.04 μg/m^3 (31), which were consistent with this study's results. A noteworthy association between the frequency of printer usage (exceeding seven times per day) and the occurrence of asthma attack was demonstrated in our study. A study conducted in Estonia, with participation from over 50,000 adults, have revealed a significant association between exposure ranging from low to moderate levels of indoor air pollutants and asthma (OR = 1.88, 95%CI 1.48 ~ 2.37) (22). Inhalation of VOCs, in particular, has been implicated in various adverse health effects (32), and their role in triggering asthma is well-documented. VOCs can activate the immune system, cause oxidative stress, and interact with some allergens (33). Metabolites of VOCs have also been found to be correlated with markers of oxidative stress, which are associated with lung function parameters (33–35). Furthermore, multiple studies have reported a connection between exposure to formaldehyde and the development of asthma and asthma symptoms in adults. Formaldehyde, as a respiratory irritant, exerts its effects by inducing inflammation of the airway mucosa and eliciting an inflammatory response via cytokines produced by Th2 cells (34).

TABLE 2 Worker-related factors in archival work [*n* (%)].

	Non-asthma attacks (*n* = 666)	Asthma attacks (*n* = 333)	*p*-value
Frequency of cleaning in warehouses (times/month)			0.039
<1	139 (20.9)	74 (22.2)	
1	196 (29.4)	92 (27.6)	
2–3	177 (26.6)	67 (20.1)	
≥4	154 (23.1)	100 (30.0)	
Strict separation of the working areas from archives warehouses	530 (79.6)	230 (69.1)	<0.001
dampness in the working area	340 (51.1)	229 (68.8)	<0.001
Ventilation in warehouses			0.407
Power ventilation	184 (27.6)	105 (31.5)	
Natural ventilation	372 (55.9)	179 (53.8)	
Power and natural ventilation	110 (16.5)	49 (14.7)	
Average ventilation time of warehouses (hour/day)			0.184
Never	132 (19.8)	76 (22.8)	
1	210 (31.5)	83 (24.9)	
1–2	147 (22.1)	79 (23.7)	
≥2	177 (26.6)	95 (28.5)	
Warehouse temperature in summer (°C)			0.147
14–24	491 (73.7)	231 (69.4)	
>24	175 (26.3)	102 (30.6)	
Warehouse humidity in summer (%)			0.684
<45%	225 (33.8)	119 (35.7)	
45–60%	395 (59.3)	195 (58.6)	
>60%	46 (6.9)	19 (5.7)	
Pungent chemical odor in working areas	96 (14.4)	118 (35.4)	<0.001
Mold odor in working areas (except warehouses)	263 (39.5)	226 (67.9)	<0.001
Mold odor in archives warehouses	294 (44.1)	241 (72.4)	<0.001
Insects in working area	257 (38.6)	192 (57.7)	<0.001

TABLE 3 Protection to adverse factors related to archival work (*n* = 999) [*n* (%)].

	Non-asthma (*n*%)	Asthma (*n* %)	*p*-value
Legislation of protective measures of risk factors in the archival profession	117 (17.6)	42 (12.6)	0.044
Knowing the effective protection measures to risk factors in the archival profession	314 (47.1)	136 (40.8)	0.059
Well protection in work according to the professional protection files*	105 (89.7)	30 (71.4)	0.004

*Archivists whose workplace have professional protection files.

Additionally, transient decreases in lung function have been attributed to formaldehyde exposure (36).

In addition, this study has indicated mold as an associated factor for asthma among archivists, exhibiting a correlated escalation of 65.1 and 73.8% in warehouses and workplaces, respectively. Molds, being a potent allergens, can trigger allergic reactions, provoke inflammatory responses and augment the susceptibility to asthma via the emission of VOCs (26). A study has revealed a pronounced elevation of Asthma-COPD Overlap Syndrome (ACOS) associated with occupational exposure to mold odor, with an odds ratio (OR) of 3.43(95%CI 1.04–11.29) (37). Although limited research has been conducted among office workers, previous studies have consistently reported a positive correlation between mold odor and adult individuals in residential settings (38–40). Furthermore, a heightened susceptibility to asthma was detected in relation to occupational exposure to mold odor, as opposed to exposure within the confines of one's abode (37). This could be potentially elucidated by the more pervasive prevalence of mold issues in archives, coupled with a tendency for individuals to expeditiously remedy any mold-related

TABLE 4 Factors associated with asthma attacks among archivists in univariate and multivariable analyses.

Characteristic	Univariable			Multivariable		
	Odds radio	95%CI	*p*-value	Odds radio	95%CI	*p*-value
Gender						
Female	Ref			Ref		
Male	1.474	1.105–1.966	0.008	1.665	1.211–2.289	0.002
Family history of respiratory system	4.109	1.909–8.030	<0.001	3.928	1.908–8.085	<0.001
Working years in archives Department (years)			<0.001			0.003
≤5	Ref			Ref		
6–10	1.445	0.949–2.201	0.086	1.315	0.835–2.071	0.238
11–20	1.782	1.228–2.585	0.002	1.522	1.018–2.276	0.041
≥21	2.309	1.598–3.337	<0.001	2.115	1.419–3.152	<0.001
Strict separation of the working areas from archives warehouses	0.573	1.294–2.354	<0.001	1.523	1.097–2.115	0.012
Mold odor in working areas (except warehouses)	3.236	2.452–4.272	<0.001	1.738	1.14–2.65	0.010
Mold odor in archives warehouses	3.315	2.493–4.407	<0.001	1.651	1.068–2.553	0.024
Chemical irritating odor in working areas	3.259	2.386–4.451	<0.001	2.145	1.526–3.017	<0.001
Insects in working area	2.167	1.658–2.832	<0.001	1.395	1.019–1.909	0.038
Dampness in the working area	2.111	1.600–2.785	<0.001	1.042	0.743–1.461	0.813

TABLE 5 The interaction analysis between the pungent chemical odor and mold in working areas.

Factors	Number of subjects	Odds radio	95%CI	*p*-value
Chemically irritating odor (−) and mold odor (−)	451	Ref		
Chemically irritating odor (−) and mold odor (+)	59	2.345	1.310–4.199	0.004
Chemically irritating odor (+) and mold odor (−)	334	2.671	1.935–3.685	<0.001
Chemically irritating odor (+) and mold odor (+)	155	7.098	4.752–10.603	<0.001

problems within their own dwellings. Another biological factor encountered in the workplace, i.e., dust mites and cockroaches, may contribute to an elevated risk of asthma by 39.5%. A recent study revealed that dust mite allergen concentration of 10 μg g-1 has been proposed as the threshold for asthma development. While the levels of Der p 1 and Der f 1 allergens in dust samples collected from offices in Malaysia were found to be as high as 556 ng/g and 658 ng/g, respectively (8). Our findings align with the previous study, as we have observed an increased asthma attacks in connection with exposure to dust mites and cockroaches (41). Hence, it is crucial to accord primacy to the eradication of dust particles and the implementation of sterilization protocols within archival repositories.

Notably, our data analysis has revealed a strong synergy (OR = 7.098) between chemical odors and molds in the workplace. While the existing literature on this specific interaction remains somewhat limited, previous studies have already demonstrated the potential for chemical irritants, such as sulfur dioxide and ozone, to synergistically interact with inhalable allergens, including fungi, molds and dust mites. Consequently, this interaction serves to exacerbate asthma symptoms and perpetuate untreated exposure (42). Furthermore, in damp and damaged buildings, the presence of microbial components, such as cellular debris or spores released during fungal growth can trigger an inflammatory response, potentially served as a shared pathway for the development of asthma among individuals exposed to these hazardous factors.

Interestingly, contrary to findings from other studies that reported a higher prevalence of asthma among women than men, this study revealed that the prevalence of asthma among archivists was

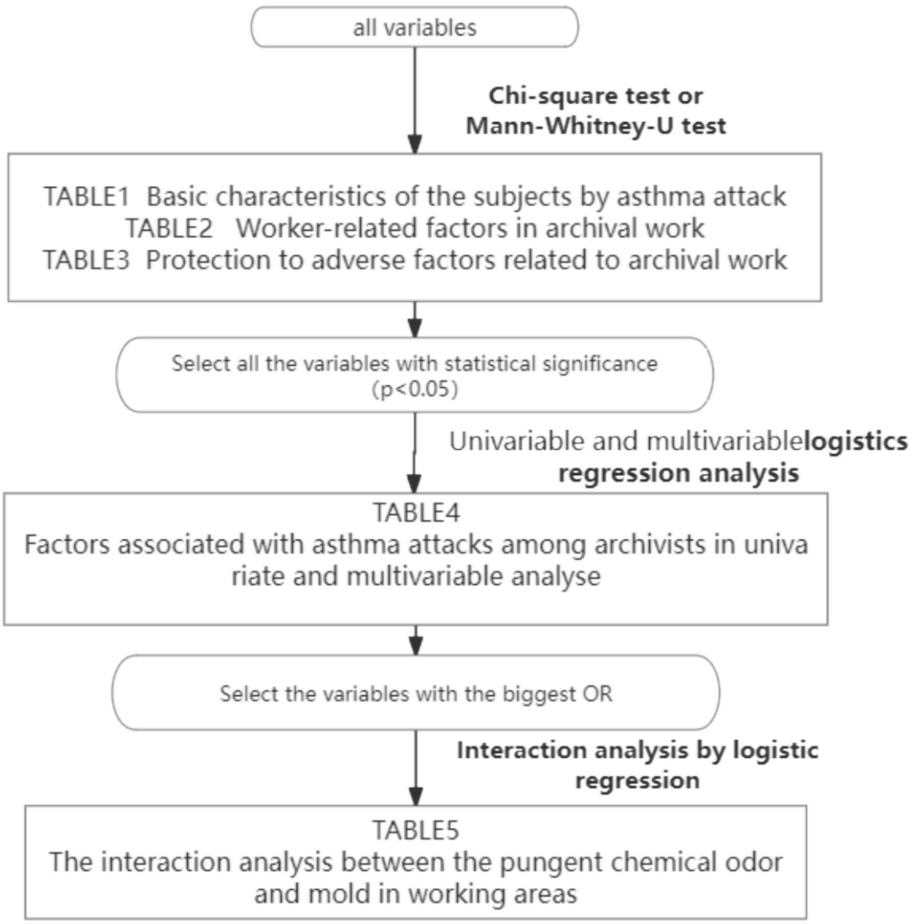

FIGURE 1
Program flowchart.

1.28 times higher among male workers. Stratified analysis by gender demonstrates significantly higher odds ratios (ORs) for males in both chemical and biological factors. More precisely, the presence of chemically irritating odors and biological agents, such as molds and dust mites, in the archival work environment is more robustly correlated with declining pulmonary function in males. This finding in concordance with a previous study carried out in Italy (43).

In conclusion, this survey revealed that approximately one-third of archivists experienced asthma attacks. Chemically irritating odor, Mold odor and insects in the workplaces are associated with asthma attacks. Moreover, chemically irritating gases and molds in the archival workplace were highly associated with asthma attack, with a significant interaction between them. However, the health relevance and mechanism of the work-related exposure in archives need to be further explored by more detailed assessments.

4.1 Strengths and limitations

There are several strengths in this study. First, the participation of archivists from various types of archives nationwide, who exhibit higher levels of compliance and consistency in their education and job type, significantly enhances the credibility and generalizability of our findings. Consequently, it is reasonable to extrapolate the results to a broader population of office workers. Second, given the intricate compositions, relatively low concentrations and inherent difficulty in precise measurement of various factors within the work environment, pertinent information was gathered through the employment of a questionnaire-based approach. Hence, employing a questionnaire to gauge the overall extent of exposure among archivists represents a judicious methodology within this framework. The study revised and adopted recent trends in healthcare research and related challenges (44–68).

Also, there are some limitations. First, as was the case for most of the previous studies, this was a cross-sectional study. Therefore, the causality between the asthma attacks and the associated factors were not clarified in this study. Second, current study surveyed subjects via a self-administered questionnaire, but the reliability and validity of this questionnaire was not tested. Second, the lack of quantification pertaining to the exposures presents a notable challenge in elucidating potential mechanisms of action or dose–response relationships. Third, similar to other large-scale population-based surveys, the diagnosis of asthma was based mainly on a standardized questionnaire, which could potentially have led to the misclassification of some pulmonary diseases.

4.2 Further research

Current study surveyed subjects via a self-administered questionnaire, but the reliability and validity of this questionnaire

were not tested, especially the diagnosis of asthma. Therefore, future research is expected to add some questions, such as the doctor diagnosed asthma, asthma medication, etc. In addition, as mentioned above, the causality between asthma attacks and the associated factors was not clarified in this study. Clearly, future longitudinal studies are necessary to address this issue. Finally, concerning measurement of exposure-related factors. Microorganisms, dust particles, etc. in the archive working environment can be measured using more accurate measurement techniques or culture methods.

Data availability statement

The original contributions presented in the study are included in the article/Supplementary material, further inquiries can be directed to the corresponding authors.

Author contributions

LY: Conceptualization, Investigation, Writing – original draft. CX: Methodology, Writing – original draft. ZA: Formal analysis, Writing – original draft. XR: Data curation, Writing – original draft. PM: Validation, Writing – review & editing. DM: Funding acquisition, Supervision, Validation, Writing – original draft.

Funding

The author(s) declare financial support was received for the research, authorship, and/or publication of this article. Study on the correlation between multiple physical discomforts and working environment of archivists" (Project No: 2021-B-16) of the Science and Technology Project of the National Archives Administration of China. This work was supported by "Research on the Cultural Communication Strategies and Paths of Memory of the Archives: Based on the Oral Archives Construction" (Project No: QDSKL2301266) of Qingdao Planning Project for Philosophy and Social Sciences in 2023.

Conflict of interest

The authors declare that the research was conducted in the absence of any commercial or financial relationships that could be construed as a potential conflict of interest.

Publisher's note

All claims expressed in this article are solely those of the authors and do not necessarily represent those of their affiliated organizations, or those of the publisher, the editors and the reviewers. Any product that may be evaluated in this article, or claim that may be made by its manufacturer, is not guaranteed or endorsed by the publisher.

Supplementary material

The Supplementary material for this article can be found online at: https://www.frontiersin.org/articles/10.3389/fpubh.2024.1397236/full#supplementary-material

References

1. Karvala K, Toskala E, Luukkonen R, Lappalainen S, Uitti J, Nordman H. New-onset adult asthma in relation to damp and moldy workplaces. *Int Arch Occup Environ Health*. (2010) 83:855–65. doi: 10.1007/s00420-010-0507-5

2. Jo W, Seo KW, Jung HS, Park CY, Kang BJ, Kang HH, et al. Clinical importance of work-exacerbated asthma: findings from a prospective asthma cohort in a highly Industrialized City in Korea. *Allergy Asthma Immunol Res*. (2021) 13:256–70. doi: 10.4168/aair.2021.13.2.256

3. Reilly MJ, Wang L, Rosenman KD. The burden of work-related asthma in Michigan, 1988-2018. *Ann Am Thorac Soc*. (2020) 17:284–92. doi: 10.1513/AnnalsATS.201905-401OC

4. Jouneau S, Chapron A, Ropars C, Marette S, Robert AM, Gouyet T, et al. Prevalence and risk factors of asthma in dairy farmers: ancillary analysis of AIRBAg. *Environ Res*. (2022) 214:114145. doi: 10.1016/j.envres.2022.114145

5. Lagiso ZA, Mekonnen WT, Abaya SW, Takele AK, Workneh HM. Chronic respiratory symptoms, lung function and associated factors among flour mill factory workers in Hawassa city, southern Ethiopia: "comparative cross-sectional study". *BMC Public Health*. (2020) 20:909. doi: 10.1186/s12889-020-08950-9

6. Huntley CC, Burge PS, Moore VC, Robertson AS, Walters GI. Occupational asthma in office workers. *Occup Med*. (2022) 72:411–4. doi: 10.1093/occmed/kqac023

7. Wang L, Rosenman K. Adverse health outcomes among industrial and occupational sectors in Michigan. *Prev Chronic Dis*. (2018) 15:E102. doi: 10.5888/pcd15.170487

8. Lim FL, Hashim Z, Than LT, Md Said S, Hisham Hashim J, Norbäck D. Asthma, airway symptoms and rhinitis in Office Workers in Malaysia: associations with house dust mite (HDM) allergy, cat allergy and levels of house dust mite allergens in office dust. *PLoS One*. (2015) 10:e0124905. doi: 10.1371/journal.pone.0124905

9. Anderson NJ, Fan ZJ, Reeb-Whitaker C, Bonauto DK, Rauser E. Distribution of asthma by occupation: Washington state behavioral risk factor surveillance system data, 2006-2009. *J Asthma*. (2014) 51:1035–42. doi: 10.3109/02770903.2014.939282

10. Papi A, Brightling C, Pedersen SE, Reddel HK. Asthma. *Lancet*. (2018) 391:783–800. doi: 10.1016/S0140-6736(17)33311-1

11. Fletcher AM, London MA, Gelberg KH, Grey AJ. Characteristics of patients with work-related asthma seen in the New York state occupational health clinics. *J Occup Environ Med*. (2006) 48:1203–11. doi: 10.1097/01.jom.0000245920.87676.7b

12. Zhang J. A study of the relationship between asthma and blood lipids. *J Inner Mongol Med*. (2016) 44:129–32. In Chinese

13. Gheith S, Ranque S, Bannour W, Ben Youssef Y, Khelif A, Ben Said M, et al. Hospital environment fungal contamination and aspergillosis risk in acute Leukaemia patients in Sousse (Tunisia). *Mycoses*. (2015) 58:337–42. doi: 10.1111/myc.12320

14. Lu R, Tendal K, Frederiksen MW, Uhrbrand K, Li Y, Madsen AM. Strong variance in the inflammatory and cytotoxic potentials of Penicillium and aspergillus species from cleaning workers' exposure in nursing homes. *Sci Total Environ*. (2020) 724:138231. doi: 10.1016/j.scitotenv.2020.138231

15. Awad AHA, Saeed Y, Shakour AA, Abdellatif NM, Ibrahim YH, Elghanam M, et al. Indoor air fungal pollution of a historical museum, Egypt: A case study. *Aerobiologia*. (2020) 36:197–209. doi: 10.1007/s10453-019-09623-w

16. Baxi SN, Portnoy JM, Larenas-Linnemann D, Phipatanakul W, Workgroup EA. Exposure and health effects of Fungi on humans. *J Allergy Clin Immunol Pract*. (2016) 4:396–404. doi: 10.1016/j.jaip.2016.01.008

17. Belizario JA, Lopes LG, Pires RH. Fungi in the indoor air of critical hospital areas: A review. *Aerobiologia*. (2021) 37:379–94. doi: 10.1007/s10453-021-09706-7

18. Cincinelli A, Martellini T, Amore A, Dei L, Marrazza G, Carretti E, et al. Measurement of volatile organic compounds (VOCs) in libraries and archives in Florence (Italy). *Sci Total Environ*. (2016) 572:333–9. doi: 10.1016/j.scitotenv.2016.07.201

19. Salthammer T, Mentese S, Marutzky R. Formaldehyde in the indoor environment. *Chem Rev*. (2010) 110:2536–72. doi: 10.1021/cr800399g

20. Pinheiro AC, Sequeira SO, Macedo MF. Fungi in archives, libraries, and museums: a review on paper conservation and human health. *Crit Rev Microbiol*. (2019) 45:686–700. doi: 10.1080/1040841X.2019.1690420

21. Peel AM, Wilkinson M, Sinha A, Loke YK, Fowler SJ, Wilson AM. Volatile organic compounds associated with diagnosis and disease characteristics in asthma—A systematic review. *Respir Med*. (2020) 169:105984. doi: 10.1016/j.rmed.2020.105984

22. Maestrelli P, Henneberger PK, Tarlo S, Mason P, Boschetto P. Causes and phenotypes of work-related asthma. *Int J Environ Res Public Health*. (2020) 17:4713. doi: 10.3390/ijerph17134713

23. Savoldelli S, Cattò C, Villa F, Saracchi M, Troiano F, Cortesi P, et al. Biological risk assessment in the history and historical documentation library of the University of Milan. *Sci Total Environ*. (2021) 790:148204. doi: 10.1016/j.scitotenv.2021.148204

24. Baldacci S, Maio S, Cerrai S, Sarno G, Baïz N, Simoni M, et al. Allergy and asthma: effects of the exposure to particulate matter and biological allergens. *Respir Med*. (2015) 109:1089–104. doi: 10.1016/j.rmed.2015.05.017

25. Laditka JN, Laditka SB, Arif AA, Hoyle JN. Work-related asthma in the USA: nationally representative estimates with extended follow-up. *Occup Environ Med*. (2020) 77:617–22. doi: 10.1136/oemed-2019-106121

26. Mu L, Liu L, Niu R, Zhao B, Shi J, Li Y, et al. Indoor air pollution and risk of lung cancer among Chinese female non-smokers. *Cancer Causes Control*. (2013) 24:439–50. doi: 10.1007/s10552-012-0130-8

27. Delfino RJ, Chang J, Wu J, Ren C, Tjoa T, Nickerson B, et al. Repeated hospital encounters for asthma in children and exposure to traffic-related air pollution near the home. *Ann Allergy Asthma Immunol*. (2009) 102:138–44. doi: 10.1016/S1081-1206(10)60244-X

28. Xu F, Yan S, Wu M, Li F, Xu X, Song W, et al. Ambient ozone pollution as a risk factor for skin disorders. *Br J Dermatol*. (2011) 165:224–5. doi: 10.1111/j.1365-2133.2011.10349.x

29. Paulin LM, Gassett AJ, Alexis NE, Kirwa K, Kanner RE, Peters S, et al. Association of Long-term Ambient Ozone Exposure with Respiratory Morbidity in smokers. *JAMA Intern Med*. (2020) 180:106. doi: 10.1001/jamainternmed.2019.5498

30. Lee S, Lee M. Low-to-moderate atmospheric ozone levels are negatively correlated with hospital visits by asthma patients. *Medicine*. (2022) 101:e31737. doi: 10.1097/MD.0000000000031737

31. Salonen H, Salthammer T, Morawska L. Human exposure to ozone in school and office indoor environments. *Environ Int*. (2018) 119:503–14. doi: 10.1016/j.envint.2018.07.012

32. Maung TZ, Bishop JE, Holt E, Turner AM, Pfrang C. Indoor air pollution and the health of vulnerable groups: a systematic review focused on particulate matter (PM), volatile organic compounds (VOCs) and their effects on children and people with pre-existing lung disease. *Int J Environ Res Public Health*. (2022) 19:8752. doi: 10.3390/ijerph19148752

33. Tischer C, Karvonen AM, Kirjavainen PV, Flexeder C, Roponen M, Hyvärinen A, et al. Early age exposure to moisture and mould is related to FeNO at the age of 6 years. *Pediatr Allergy Immunol*. (2021) 32:1226–37. doi: 10.1111/pai.13526

34. Ren B, Wu Q, Muskhelishvili L, Davis K, Wang Y, Rua D, et al. Evaluating the sub-acute toxicity of formaldehyde fumes in an in vitro human airway epithelial tissue model. *Int J Mol Sci*. (2022) 23:2593. doi: 10.3390/ijms23052593

35. Yeatts KB, el-Sadig M, Leith D, Kalsbeek W, al-Maskari F, Couper D, et al. Indoor air pollutants and health in the United Arab Emirates. *Environ Health Perspect*. (2012) 120:687–94. doi: 10.1289/ehp.1104090

36. Herbert FA, Hessel PA, Melenka LS, Yoshida K, Nakaza M. Respiratory consequences of exposure to wood dust and formaldehyde of workers manufacturing oriented Strand board. *Arch Environ Health*. (1994) 49:465–70. doi: 10.1080/00039896.1994.9955002

37. Jaakkola MS, Lajunen TK, Jaakkola JJK. Indoor mold odor in the workplace increases the risk of asthma-COPD overlap syndrome: a population-based incident case–control study. *Clin Transl Allergy*. (2020) 10:3. doi: 10.1186/s13601-019-0307-2

38. Husman T. Health effects of indoor-air microorganisms. *Scand J Work Environ Health*. (1996) 22:5–13. doi: 10.5271/sjweh.103

39. Shiue I. Indoor mildew odour in old housing was associated with adult allergic symptoms, asthma, chronic bronchitis, vision, sleep and self-rated health: USA NHANES, 2005–2006. *Environ Sci Pollut Res*. (2015) 22:14234–40. doi: 10.1007/s11356-015-4671-8

40. Zhang X, Norbäck D, Fan Q, Bai X, Li T, Zhang Y, et al. Dampness and mold in homes across China: associations with rhinitis, ocular, throat and dermal symptoms, headache and fatigue among adults. *Indoor Air*. (2018) 29:30–42. doi: 10.1111/ina.12517

41. Ghaemmaghami AM, Shakib F. Human T cells that have been conditioned by the proteolytic activity of the major dust mite allergen Der p 1 trigger enhanced immunoglobulin E synthesis by B cells. *Clin Exp Allergy*. (2002) 32:728–32. doi: 10.1046/j.1365-2222.2002.01374.x

42. Sokol K, Sur S, Ameredes BT. Inhaled environmental allergens and toxicants as determinants of the asthma phenotype. *Heterogen Asthma*. (2014):43–73. doi: 10.1007/978-1-4614-8603-9_4

43. Moscato G, Apfelbacher C, Brockow K, Eberle C, Genuneit J, Mortz CG, et al. Gender and occupational allergy: report from the task force of the EAACI environmental and occupational allergy interest group. *Allergy*. (2020) 75:2753–63. doi: 10.1111/all.14317

44. Antunes V. On nursing research and evidence-based practice: topics for researchers and practitioners. *Int Healthc Rev*. (2022) 1:12. doi: 10.56226/ihr.v1i1.12

45. Chen S, Qin Y. On ethics, biomedical education and health promotion: international and Chinese perspectives. *Int Healthc Rev*. (2023). doi: 10.56226/46

46. Chen Y, Moreira P, Liu W, Monachino M, Nguyen TLH, Wang A. Is there a gap between artificial intelligence applications and priorities in health care and nursing management? *J Nurs Manag*. (2022) 30:3736–42. doi: 10.1111/jonm.13851

47. Dsouza B. On sustainable health systems: a research emergency in pandemic times. *Int Healthc Rev*. (2022) 1. doi: 10.56226/ihr.v1i1.7

48. Dsouza B, Prabhu R, Unnikrishnan B, Ballal S, Mundkur SC, Chandra Sekaran V, et al. Effect of educational intervention on knowledge and level of adherence among hemodialysis patients: A randomized controlled trial. *Glob Health Epidemiol Genom*. (2023) 2023:4295613. doi: 10.1155/2023/4295613

49. Ferreira J, Horta P, Geada F. Internal audit process in eHealth: A case study. *Int Healthc Rev*. (2023). doi: 10.56226/50

50. Han T, Han M, Moreira P, Song H, Li P, Zhang Z. Association between specific social activities and depressive symptoms among older adults: A study of urban-rural differences in China. *Front Public Health*. (2023) 11:1099260. doi: 10.3389/fpubh.2023.1099260

51. Jacennik B, Zawadzka-Gosk E, Moreira JP, Glinkowski WM. Evaluating patients' experiences with healthcare services: extracting domain and language-specific information from free-text narratives. *Int J Environ Res Public Health*. (2022) 19:10182. doi: 10.3390/ijerph191610182

52. Gao Y, Zhang S, Zhao Y, Yang T, Moreira P, Sun G. Reduction of retinal vessel density in non-exudative macular neovascularization: a retrospective study. *Front Med*. (2024) 10:1219423. doi: 10.3389/fmed.2023.1219423

53. Jia X, Tang X, Li Y. And Paulo Moreira (2023) update of dialysis initiation timing in end stage kidney disease patients: is it a resolved question? A systematic literature review. *BMC Nephrol*. (2023) 24:162. doi: 10.1186/s12882-023-03184-4

54. Kehinde O, Dixon-Lawson K, Mendelsohn A. On community pharmacists and promotion of lifestyle modification in adults with hypertension: practice protocol. *Int Healthc Rev*. (2023). doi: 10.56226/49

55. Li N, Guo M, You S, Ji H. On patient readiness for hospital discharge: an update on recent evidence. *Int Healthc Rev*. (2022). doi: 10.56226/ihr.v1i2.30

56. Lloyd Williams D. On healthcare research priorities in the USA: from long COVID to precision health, what else is new? *Int Healthc Rev*. (2022) 1. doi: 10.56226/ihr.v1i1.14

57. Loureiro Pais Batista SM, Pereira Gaspar AC, Madeira dos Santos B, da Cunha Silva F, Fonseca Marta F, Pinto Pedrosa I, et al. Nurses' knowledge of patients'' swallowing ability: a cross sectional study in Portugal. *Int Healthc Rev*. (2023). doi: 10.56226/64

58. Monachino M. On healthcare research for disease prevention: critical knowledge gaps in European public health. *Int Healthc Rev*. (2022) 1. doi: 10.56226/ihr.v1i1.6

59. Moreira P. On new clinical research methods and technologies: from decentralised designs to artificial intelligence. *Int Healthc Rev*. (2022) 1. doi: 10.56226/ihr.v1i1.11

60. Nguyen TLH. On improving healthcare with a world perspective: evidence for Global Health programs. *Int Healthc Rev*. (2022) 1. doi: 10.56226/ihr.v1i1.10

61. Niu M. On planning and designing general hospitals in smart technology contexts. *Int Healthc Rev*. (2023). doi: 10.56226/59

62. Song C, Xie H. On disparities in breast Cancer screening: an analysis of behavioral risk factor surveillance survey data related to racial/ ethnic characteristics. *Int Healthc Rev*. (2023). doi: 10.56226/53

63. Sun P, Li Z, Guo W, Moreira P. Evidence on the need for early identification of asymptomatic true abdominal aortic aneurysm in pregnancy: A case report. *SAGE Open Med Case Rep*. (2023) 11:11. doi: 10.1177/2050313X231173789

64. Tian M, Li X, Zhou F, Wang Y, Wang Q, Pan N, et al. On the psychological experiences of hematopoietic stem cell donors: an update on international evidence. *Int Healthc Rev*. (2023). doi: 10.56226/31

65. Wei L, Xue J. A longitudinal study on the emotional support mechanism of the mental health of empty nesters: recent evidence from China National Health and retirement survey. *Int Healthc Rev*. (2022). doi: 10.56226/37

66. Wang M, Yang Q, Chen Y. International comparison of the financing mechanism of basic medical insurance and its implications for China. *Int Healthc Rev*. (2024). doi: 10.56226/63

67. Zhang B, Li Y, Cao M, Xu C. On workplace bullying in nursing: findings from a rapid review of the literature. *Int Healthc Rev*. (2023). doi: 10.56226/51

68. Zhang L, Lei J, Zhang J, Yin L, Chen Y, Xi Y, et al. Undiagnosed long COVID-19 in China among non-vaccinated individuals: identifying persistent symptoms and impacts on Patients' health-related quality of life. *J Epidemiol Glob Health*. (2022) 12:560–71. doi: 10.1007/s44197-022-00079-9

69. Wei Y. Opportunities and challenges in cross-border healthcare: A case study based on the court of justice of the European Union. *Int Healthc Rev*. (2023). doi: 10.56226/65

70. Zhang Y, Zhang Y, Ren M, Xue M, Chunying H, Hou Y, et al. Atrial standstill associated with Lamin A/C mutation: a case report. *SAGE Open Med Case Rep*. (2023) 11:11. doi: 10.1177/2050313X231179810

frontiers | Frontiers in Public Health

TYPE Original Research
PUBLISHED 29 August 2024
DOI 10.3389/fpubh.2024.1418134

OPEN ACCESS

EDITED BY
Bin Wang,
Huazhong University of Science and Technology, China

REVIEWED BY
Zygmunt F. Dembek,
Battelle, United States
Pramita Sharma,
University of Burdwan, India

*CORRESPONDENCE
Xiao Li
lixiao617@hotmail.com

†These authors share first authorship

RECEIVED 16 April 2024
ACCEPTED 14 August 2024
PUBLISHED 29 August 2024

CITATION
Zong S, Wang L, Wang S, Wang Y, Jiang Y, Sun L, Zong Y and Li X (2024) Exposure to per- and polyfluoroalkyl substances is associated with impaired cardiovascular health: a cross-sectional study. *Front. Public Health* 12:1418134. doi: 10.3389/fpubh.2024.1418134

Exposure to per- and polyfluoroalkyl substances is associated with impaired cardiovascular health: a cross-sectional study

Shuli Zong[1†], Lin Wang[1†], Sutong Wang[1], Yongcheng Wang[2], Yuehua Jiang[3], Liping Sun[4], Yingying Zong[5] and Xiao Li[2*]

[1]First Clinical Medical College, Shandong University of Traditional Chinese Medicine, Jinan, China, [2]Department of Cardiovascular Diseases, Shandong University of Traditional Chinese Medicine Affiliated Hospital, Jinan, China, [3]Central Laboratory, Shandong University of Traditional Chinese Medicine Affiliated Hospital, Jinan, China, [4]Department of Endocrine Tumor Intervention, Central Hospital Affiliated to Shandong First Medical University, Jinan, China, [5]Department of Business Administration, Shandong Yingcai University, Jinan, China

Background: Per- and polyfluoroalkyl substance (PFAS) exposure and cardiovascular disease are controversial. We aimed to assess the association between serum PFAS exposure and cardiovascular health (CVH) in U.S. adults.

Methods: We analyzed serum PFAS concentration data of U.S. adults reported in the National Health and Nutrition Examination Survey (NHANES) study (2005–2018). We employed two weighted logistic regression models and a restricted cubic spline (RCS) to examine the association between each PFAS and impaired CVH (defined as moderate and low CVH). Quantile g-computation (Qgcomp) and weighted quantile sum (WQS) analysis were used to estimate the effects of mixed exposures to PFASs on impaired CVH.

Results: PFAS were associated with an increased risk of impaired CVH (OR_{PFNA}: 1.40, 95% CI: 1.09, 1.80; OR_{PFOA}: 1.44, 95% CI: 1.10, 1.88; OR_{PFOS}: 1.62, 95% CI: 1.25, 2.11). PFOA and PFOS exhibited nonlinear relationships with impaired CVH. Significant interactions were observed for impaired CVH between race/ethnicity and PFHxS ($p = 0.02$), marital status and PFOA ($p = 0.03$), and both marital status and race/ethnicity with PFOS ($p = 0.01$ and $p = 0.02$, respectively). Analysis via WQS and Qgcomp revealed that the mixture of PFAS was positively associated with an increased risk of impaired CVH.

Conclusion: PFNA, PFOA, and PFOS exposure are associated with an increased risk of impaired CVH in U.S. adults. Race/ethnicity and marital status may influence CVH. Reducing PFAS exposure could alleviate the burden of disease associated with impaired CVH.

KEYWORDS

cardiovascular health, perfluoroalkyl and polyfluoroalkyl substances, NHANES, Life's essential 8, cross-sectional study

1 Introduction

Cardiovascular disease (CVD) constitutes a significant global health burden, exhibiting a rising incidence and a trend towards affecting younger individuals (1). The 2024 US Heart Disease and Stroke Statistics Report revealed that approximately 127.9 million Americans aged ≥20 years (48.6%) are afflicted by CVD, resulting in an average annual cost of 42.23 billion dollars (2). The American Heart Association (AHA) reported that a substantial number of CVDs stem from health and behavioral factors. To address this, they developed Life's Essential 8 (LE8), which emphasizes eight critical aspects of cardiovascular health (CVH). These include four health behaviors [diet, physical activity (PA), tobacco/nicotine exposure, and sleep health] and four health factors [body mass index (BMI), lipids, blood glucose, and blood pressure (BP)] (3). Research indicates that maintaining high CVH is linked with reducing the risk of multiple health risks (4, 5). Despite implementing various public health and healthcare policies and programs in the U.S. aimed at preventing CVD, the overall CVH scores for U.S. adults have remained largely unchanged over the past decade (6).

In parallel with ongoing efforts to manage CVD, emerging concerns about environmental contaminants, such as per—and polyfluoroalkyl substances (PFASs), have gained attention. PFASs are synthetic compounds that are found in humans and animals worldwide. Characterized by their distinctive chemical structure and properties, PFASs are commonly used in various industries, such as surfactants, food packaging, waterproof coatings, and nonstick coatings on cookware (7). The half-life of long-chain PFASs can range from 3 years to decades, so even a single serum measurement can represent long-term exposure to PFASs (8, 9). Owing to their resistance to biodegradation, PFAS tend to accumulate in the biosphere through the food chain. This results in persistent health effects, including endocrine disruption, immune-inflammatory responses, and cytotoxicity (10–12). Previous studies linked PFAS exposure to an array of CVDs, and a cross-sectional study in the U.S. revealed that the risk of total CVD increased with increasing levels of PFAS, with the highest quartile of PFAS levels increasing the risk of CVD by 45% compared with the lowest quartile (13). Furthermore, another study showed that higher levels of perfluorooctanesulfonic acid (PFOS) and perfluorononanoic acid (PFNA) were associated with an increased risk of stroke in U.S. adults, in addition to an increased risk of coronary heart disease with elevated PFNA levels (14). PFASs have also been associated with cardiovascular risk factors such as insulin resistance, metabolic syndrome, and dyslipidemia, and in these high-risk populations, PFAS exposure may exacerbate adverse cardiovascular events (12, 15, 16). A prospective study of 666 pre-diabetic adults revealed that increased PFAS exposure was associated with an increased risk of coronary and thoracic aortic calcification (17). However, these studies focused primarily on the prevalence of CVD rather than CVH status. Recent evidence has challenged the traditional view. Two independent Swedish population-based cohort studies reported no statistically significant associations between PFAS levels and CVD incidence, and a meta-analysis of results from five independent cohort studies revealed a modest inverse association between perfluorooctanoic acid (PFOA) levels and CVD incidence (18). These conflicting findings suggest a multifaceted and complex relationship between PFAS exposure and CVD. Thus, exploring the direct link between PFASs and CVH may lead to a deeper understanding of the systemic effects of PFASs, thereby enabling the development of more effective preventive and intervention strategies.

In this study, we used the LE8 score to assess CVH and a cross-sectional approach to examine the relationship between PFAS exposure and CVH in U.S. adults based on nationally representative National Health and Nutrition Examination Survey (NHANES) data. Additionally, we analyzed the associations between PFAS exposure and CVH in different subpopulations.

2 Methods

2.1 Study design and population

The NHANES is conducted by the National Center for Health Statistics (NCHS) in the U.S. and is a biennial survey of representative data on demographics, socioeconomic status, health, and nutrition using a stratified multistage probability sampling design. The NHANES datasets are publicly available on the official website. This study used data from seven NHANES cycles from 2005 to 2018 in a cross-sectional design. A total of 15,868 participants were subjected to PFAS measurements over the seven survey cycles. We first excluded 3,461 adolescents under 20 to focus on the adult population. We subsequently excluded another 3,671 participants who lacked complete LE8 data. Furthermore, we excluded participants with incomplete covariate information ($n = 1,371$) and those lacking complete PFAS data ($n = 181$), resulting in a final analysis of 7,184 participants (Supplementary Figure S1). The study was approved by the NCHS Institutional Review Board, and all participants provided written informed consent. It was also conducted under the Strengthening the Reporting of Observational Studies in Epidemiology (STROBE) guidelines (Supplementary Table S6) (19).

2.2 Measurement of serum PFAS exposure

Our study focused on four PFAS substances, perfluorohexane sulfonic acid (PFHxS), PFOS, PFOA, and PFNA, as their detection rates exceeded 90% in all analyzed samples from the NHANES (2005–2018). According to the NHANES data description document, in the 2005–2012 cycles, NHANES directly quantified these four PFAS, whereas in the 2013–2018 cycles, a quantitative analysis of four different structural isomers of PFOS and PFOA was performed. The NHANES survey analysis guidelines suggest that the total PFOS concentration includes linear PFOS (n-PFOS) and the monomethyl branched isomers of PFOS (Sm-PFOS), whereas the total PFOA concentration is derived by combining linear PFOA (n-PFOA) and the branched isomer of PFOA (Sb-PFOA). Samples falling below the limit of detection were recorded as the limit of detection divided by the square root of 2 (20).

2.3 Assessment of CVH

The LE8 score was used to assess CVH and consisted of two main components: four health behaviors and four health factors. For diet scores, the Healthy Eating Index 2015 (HEI-2015) was calculated from

24-h dietary recall data collected through interviews and phone follow-ups and analyzed with the United States Department of Agriculture's Food Patterns Equivalents Database. The total reported weekly duration of moderate or greater activities was used for the PA scores. For nicotine exposure scores, questionnaires assessed the use of combustible cigarettes, e-cigarettes, other tobacco products, and household secondhand smoke exposure. For sleep health scores, self-reported sleep duration was used. For health factors, BMI scores were calculated from weight and height measurements taken by trained researchers at the Mobile Examination Center (MEC). For BP scores, measurements were taken by trained personnel on the MEC, with additional data on antihypertensive medication use obtained from questionnaires. For lipid scores, blood samples collected from the MEC were analysed in a central laboratory, where non-HDL cholesterol was calculated by subtracting HDL cholesterol from total cholesterol, with information on lipid-lowering medication use gathered from questionnaires. For blood glucose scores, fasting blood samples were tested for fasting glucose or HbA1c in a central laboratory, and data on diabetes history and glucose-lowering medication use were obtained via questionnaires. Each component was rigorously scored from 0 to 100 according to AHA guidelines, and the total LE8 score was computed as the unweighted average of these scores. Based on the total score, CVH was categorized as low (0–49), moderate (50–79), or high (80–100). Impaired CVH was defined as moderate and low levels of CVH. Details of the LE8 score were shown in Supplementary Table S1.

2.4 Assessment of covariates

Information on demographic and health-related factors, including age, sex, race/ethnicity, education level, marital status, poverty income ratio (PIR), health insurance, medical history, and alcohol consumption, was collected via standardized questionnaires. In detail, race/ethnicity was divided into non-Hispanic whites, non-Hispanic blacks, Mexican Americans, and others. Marital status was divided into coupled (defined as married or living with a partner) and single or separated. Education level was divided into three categories: high school or less, some college or associate degree, and college graduate degree or above. Health insurance status was recorded as yes or no (21). Alcohol consumption was obtained via 24-h dietary recall and categorized according to intake (22). Depression was assessed via the PHQ9 scale, with a score of 10 or higher considered indicative of depression. Diabetes diagnosis was based on medical and medication history and blood glucose levels. The glomerular filtration rate (eGFR) was estimated via the CKD-EPI Formula (23). The urinary albumin-to-creatinine ratio (uACR) and the use of antihypertensive and antidiabetic medications were also included in the analysis.

2.5 Statistical methods

To ensure the national representativeness of the research, we followed NHANES guidelines and considered the complex sampling design of the survey. Continuous variables that followed a normal distribution were compared between groups via *t*-tests and are expressed as the means and standard errors. Non-normally distributed continuous variables were compared via Wilcoxon tests and are expressed as medians (interquartile ranges). Categorical variables were analyzed via chi-square tests, and the data are presented as frequencies and weighted percentages (%).

We employed weighted multifactor logistic regression to investigate the correlation of each PFAS with impaired CVH. To improve the model fit, we log-transformed the concentrations of each PFAS (24). We also included the PFAS quartiles in the analysis as categorical variables, with the Q1 group (low) as the control, and calculated odds ratios (ORs) and their corresponding 95% confidence intervals (95% CIs). Two different statistical models were used: the crude model without adjustment for any variables and Model 1, which accounted for age, sex, race/ethnicity, education level, marital status, PIR, alcohol consumption, health insurance, diabetes, depression, antihypertensive or lipid-lowering medication, CVD, eGFR, and the uACR.

We implemented RCS regression model, adjusting for the covariates described in Model 1 to further investigate the potential relationship between PFASs and impaired CVH. To ensure the representativeness of the results for the U.S. population, RCS modelling was performed with NHANES sample weights. The number and placement of knots in the RCS model were determined based on the Akaike information criterion (AIC) to achieve an optimal balance between model fit and avoiding overfitting. In constructing the RCS model for PFHxS and PFNA, three knots were positioned at the 10th, 50th, and 90th percentiles of their respective distributions, with the medians used as reference points. In the RCS model for PFOA and PFOS, four knots were placed at the 5th, 35th, 65th, and 95th percentiles of their distributions, with the inflexion points serving as reference points. Moreover, subgroup analyses of age, sex, race/ethnicity, PIR, education level, marital status, and health insurance status were performed to identify potential subgroups and to perform interaction tests.

Additionally, we used quantile g-computation (Qgcomp) and weighted quantile sum (WQS) analysis to test the association of mixed PFAS exposure with impaired CVH (25). To increase the reliability of our findings, we performed a sensitivity analysis and re-evaluated the associations via weighted multifactorial logistic regression after excluding participants with CVD, diabetes, or depression.

All the statistical procedures were conducted via version 4.3.2 of the R software. All the statistical tests were two-sided, with p values less than 0.05 indicating statistical significance.

3 Results

3.1 Population characteristics

The participants were categorized into groups with high CVH and impaired CVH. As shown in Table 1, the study included 7,184 participants, with a mean age of 47.97 years. Female participants outnumbered male participants (51.27% vs. 48.73%). The average LE8 score was 68.39, with most participants being non-Hispanic white, possessing high school or less, being coupled, enjoying good economic status, being mild drinkers, and having health insurance. Overall, 12.05% of the participants had diabetes, 8.03% had CVD, and 32.89% were prescribed medication for hypertension or lowering lipids. A total of 5,802 individuals exhibited impaired CVH. Compared with those in the high-CVH group, those with impaired CVH tended to be older, male, non-Hispanic black, with high school education or less, single or separated, economically disadvantaged, former drinkers, no

10.3389/fpubh.2024.1418134

TABLE 1 Baseline characteristics of the study population according to high CVH and impaired CVH.

Variable	Total (n = 7,184)	High CVH (n = 1,382)	Impaired CVH (n = 5,802)	p-value
Age (years)	47.97 ± 0.33	42.47 ± 0.56	49.63 ± 0.34	< 0.0001
Age group (n, %)				< 0.0001
20–39	2,282 (33.84)	709 (49.38)	1,573 (29.14)	
40–59	2,512 (40.29)	409 (34.80)	2,103 (41.95)	
>=60	2,390 (25.87)	264 (15.82)	2,126 (28.91)	
Gender (n, %)				< 0.0001
Female	3,672 (51.27)	833 (59.72)	2,839 (48.72)	
Male	3,512 (48.73)	549 (40.28)	2,963 (51.28)	
Race/ethnicity (n, %)				< 0.0001
Non-Hispanic Black	1,457 (9.80)	161 (5.06)	1,296 (11.24)	
Non-Hispanic white	3,397 (71.55)	707 (75.29)	2,690 (70.42)	
Mexican American	1,029 (7.32)	180 (6.63)	849 (7.53)	
Other	1,301 (11.32)	334 (13.02)	967 (10.81)	
Education level (n, %)				< 0.0001
High school or less	3,154 (35.84)	333 (17.19)	2,821 (41.48)	
Some college or associate degree	2,185 (31.42)	389 (26.73)	1,796 (32.84)	
College graduate or above	1,845 (32.74)	660 (56.08)	1,185 (25.68)	
Marital status (n, %)				0.03
Coupled	4,430 (65.75)	899 (69.07)	3,531 (64.74)	
Single or separated	2,754 (34.25)	483 (30.93)	2,271 (35.26)	
PIR (n, %)				< 0.0001
<1.3	2,061 (18.47)	276 (12.29)	1,785 (20.34)	
1.3–3.5	2,692 (35.13)	464 (29.26)	2,228 (36.91)	
>3.5	2,431 (46.40)	642 (58.45)	1,789 (42.75)	
Alcohol consumption status (n, %)				< 0.0001
Never	912 (9.63)	213 (11.38)	699 (9.10)	
Former	1,207 (13.71)	125 (7.50)	1,082 (15.59)	
Mild	2,562 (38.81)	549 (42.77)	2,013 (37.61)	
Moderate	1,132 (17.91)	264 (21.79)	868 (16.74)	
Heavy	1,371 (19.93)	231 (16.56)	1,140 (20.96)	
Health insurance (n, %)				< 0.001
No	1,386 (15.17)	237 (11.84)	1,149 (16.18)	
Yes	5,798 (84.83)	1,145 (88.16)	4,653 (83.82)	
Diabetes (n, %)				< 0.0001
No	6,050 (87.95)	1,352 (98.00)	4,698 (84.92)	
Yes	1,134 (12.05)	30 (2.00)	1,104 (15.08)	
Depression (n, %)				< 0.0001
No	6,577 (92.96)	1,339 (97.64)	5,238 (91.55)	
Yes	607 (7.04)	43 (2.36)	564 (8.45)	
CVD (n, %)				< 0.0001
No	6,436 (91.97)	1,325 (97.27)	5,111 (90.37)	
Yes	748 (8.03)	57 (2.73)	691 (9.63)	
Take anti-hypertensive or lipid-lowering medication (n, %)				< 0.0001
No	4,557 (67.11)	1,186 (86.47)	3,371 (61.25)	

(Continued)

TABLE 1 (Continued)

Variable	Total (n = 7,184)	High CVH (n = 1,382)	Impaired CVH (n = 5,802)	p-value
Yes	2,627 (32.89)	196 (13.53)	2,431 (38.75)	
eGFR (mL/min/1.73 m^2)	93.49 ± 0.42	97.74 ± 0.72	92.21 ± 0.43	< 0.0001
uACR (mg/g)	30.36 ± 2.92	12.76 ± 1.38	35.69 ± 3.75	< 0.0001
LE8	68.39 ± 0.31	86.76 ± 0.20	62.84 ± 0.23	< 0.0001
Diet score	38.95 ± 0.60	59.15 ± 1.05	32.85 ± 0.57	< 0.0001
Physical activity score	72.11 ± 0.69	94.41 ± 0.58	65.37 ± 0.77	< 0.0001
Nicotine exposure score	71.67 ± 0.74	92.73 ± 0.61	65.31 ± 0.86	< 0.0001
Sleep health score	83.93 ± 0.43	92.83 ± 0.46	81.24 ± 0.50	< 0.0001
Body mass index score	60.41 ± 0.64	84.95 ± 0.76	52.99 ± 0.64	< 0.0001
Blood lipids score	63.78 ± 0.53	82.29 ± 0.80	58.18 ± 0.60	< 0.0001
Blood glucose score	86.25 ± 0.34	97.12 ± 0.42	82.96 ± 0.40	< 0.0001
Blood pressure score	69.96 ± 0.55	90.35 ± 0.60	63.79 ± 0.62	< 0.0001

NHANES 2005–2018. CVH, cardiovascular health; LE8, Life's Essential 8; PIR, the ratio of family income to poverty; CVD, cardiovascular diseases; eGFR, estimated glomerular filtration rate; uACR, urinary albumin, and creatinine.

TABLE 2 Distribution of PFAS concentrations by cardiovascular health status.

PFAS (ng/mL)	Total	Detection Rate[a]	High CVH	Impaired CVH	p-value
PFHxS Median (IQR)	1.50 (0.89, 2.60)	98.51%	1.37 (0.75, 2.35)	1.50 (0.90, 2.70)	< 0.0001
PFNA Median (IQR)	0.90 (0.52, 1.39)	98.30%	0.80 (0.50, 1.23)	0.90 (0.57, 1.40)	< 0.001
PFOA Median (IQR)	2.57 (1.57, 4.20)	100%	2.40 (1.47, 3.70)	2.63 (1.60, 4.30)	< 0.001
PFOS Median (IQR)	8.40 (4.60, 14.90)	99.80%	6.94 (4.00, 12.00)	9.00 (4.80, 15.90)	< 0.0001

[a]Detection rates for PFOA and PFOS were calculated for 2005–2012 cycles, because in cycles 2013–2018 PFOA and PFOS were measured as isomers. PFOA, perfluorooctanoic acid; PFOS, perfluorooctane sulfonic acid; PFNA, perfluorononanoic acid; PFHxS, perfluorohexane sulfonic acid.

health insurance, diabetic, depressed, and on antihypertensive or lipid-lowering medication. Additionally, these participants also presented lower eGFRs and higher uACR values.

3.2 PFAS concentration distribution

Table 2 shows the distribution of PFAS concentrations. All PFAS compounds investigated had detection rates above 98%, with PFOS being the highest at 100%. PFOS had the highest median serum concentration at 8.40 ng/mL, whereas PFNA had the lowest at 0.90 ng/mL. The median concentrations of PFNA and PFOA were 1.50 ng/mL and 2.57 ng/mL, respectively. The concentrations of PFAS were lower in individuals with high CVH than in those with impaired CVH ($p < 0.001$). Supplementary Table S2 lists the minimum detection concentrations for each PFAS. Additionally, a noticeable downward trend in the median concentrations of each PFAS over the years was observed ($p < 0.001$), as detailed in Supplementary Table S3. Figure 1 shows the results of the Spearman rank correlation analysis, with correlation coefficients ranging from 0.45 to 0.71 for the four PFASs.

3.3 PFAS exposure and impaired CVH

Table 3 shows weighted logistic regression analyses for variables related to impaired CVH. Age was positively associated with impaired CVH. Men were 56% more likely to have impaired CVH than women were. (OR: 1.56; 95% CI: 1.34, 1.82). There were notable racial differences, with non-Hispanic white, Mexican American, and other individuals showing lower odds of impaired CVH than non-Hispanic black individuals. An inverse relationship between education level and impaired CVH was demonstrated. Lifestyle factors also showed significant associations, with former drinkers and uninsured individuals being at greater risk. Health conditions such as diabetes, depression, and CVD are linked to an increased likelihood of impaired CVH. In particular, each unit increase in the eGFR was shown to have a protective effect against impaired CVH.

Table 4 shows the results of weighted logistic regression analyses for each PFAS compound on impaired CVH. In the crude model, the continuous variables PFHxS, PFNA, PFOA, and PFOS were positively associated with impaired CVH ($OR_{ln\text{-}PFHxS}$: 1.18, 95% CI: 1.10, 1.27; $OR_{ln\text{-}PFNA}$: 1.22, 95% CI: 1.10, 1.35; $OR_{ln\text{-}PFOA}$: 1.21, 95% CI: 1.09, 1.33; $OR_{ln\text{-}PFOS}$: 1.30, 95% CI: 1.20, 1.41). Categorizations of PFAS with Q1 as a reference revealed that higher quartiles, especially Q4, were associated with an increased risk of impaired CVH, trend test $p < 0.001$ (OR_{PFHxS}: 1.63, 95% CI: 1.33, 1.99; OR_{PFNA}: 1.54, 95% CI: 1.21, 1.96; OR_{PFOA}: 1.56, 95% CI: 1.24, 1.95; OR_{PFOS}: 2.20, 95% CI: 1.72, 2.81).

3.4 Dose–response relationship between PFAS and impaired CVH

Figure 2 shows the RCS curves for each PFAS in relation to impaired CVH, adjusting for the covariates described in Model 1.

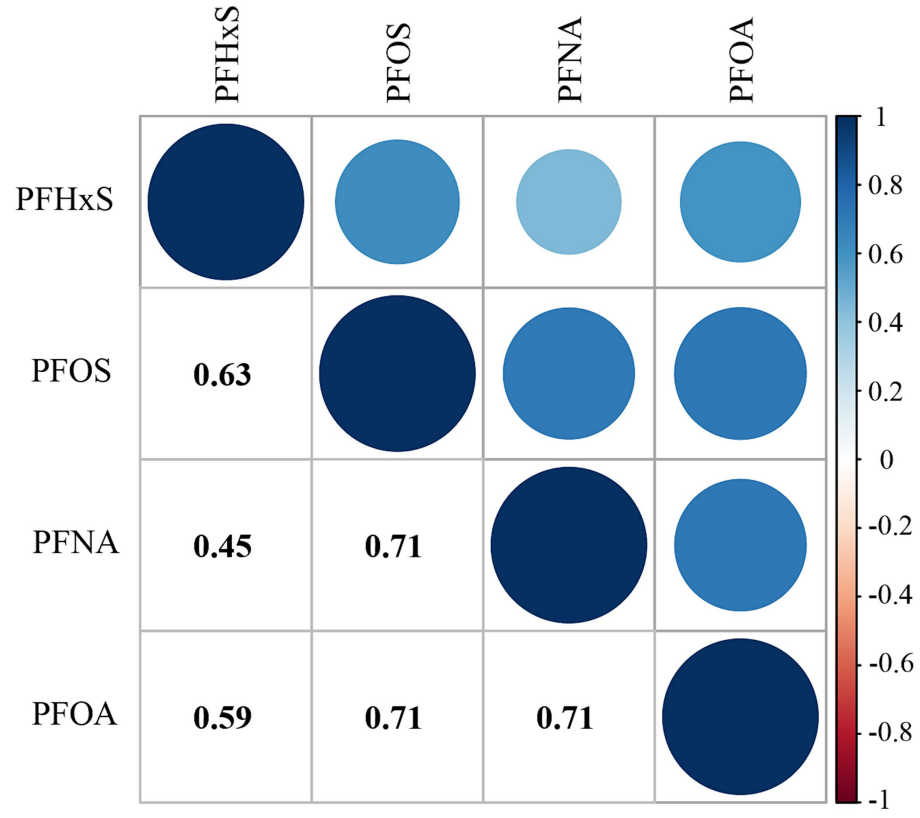

FIGURE 1
Correlations among the serum PFAS concentrations.

There was a linear relationship between PFNA levels and impaired CVH ($p = 0.001$; p for nonlinearity = 0.179). In contrast, the serum PFOA and PFOS levels exhibited a nonlinear relationship with impaired CVH (p for nonlinearity = 0.015 and p for nonlinearity <0.001, respectively). The minimum thresholds for a favorable association were identified at 1.61 ng/mL for PFOA and 5.24 ng/mL for PFOS.

3.5 Subgroup analysis

Supplementary Figures S2–S5 show the subgroup analysis results. A positive association was noted between each PFAS exposure and impaired CVH in the 20–39 age cohort. In the 40–59 age group, PFHxS, PFOA, and PFOS were all positively associated with impaired CVH, whereas in the 60+ age group, PFOS exposure was of particular concern. Among males, PFNA and PFOS exposure were positively associated with impaired CVH, with similar caution advised for females regarding PFOS. Non-Hispanic white individuals were positively associated with impaired CVH for all four PFAS compounds, and among Mexican Americans, PFHxS, PFNA, and PFOS were all positively associated with CVH impairment. In terms of education, PFOS exposure was consistently associated with impaired CVH across all levels of education, with notable concern also directed at PFHxS exposure among those with less than a high school education and a college degree or above and PFOA and PFNA exposure among those with a college degree or above. With respect to economic status, as measured by PIR, serum PFAS levels were predominantly associated with impaired CVH at 1.3–3.5 and 3.5 above the PIR range. For marital status, all four PFAS compounds were associated with a greater risk of impaired CVH in coupled individuals, a trend also observed among those with health insurance. Interaction analyses revealed that race/ethnicity influenced the associations between PFHxS and PFOS exposure and impaired CVH. Marital status influenced the associations between PFOA and PFOS exposure and impaired CVH.

3.6 WQS and Qgcomp analysis

Figure 3 shows the results of the analysis of the WQS model. The results of the WQS via a positive model revealed that each quartile increase in mixed PFASs was associated with an increased risk of impaired CVH (OR: 1.15, 95% CI: 1.06, 1.25), with PFOS having the largest positive weight (0.86). In contrast to WQS, Qgcomp allows weights to move in either direction, reflecting the complex interplay within the mixture. The analysis conducted by Qgcomp revealed that each quantile increase in the serum concentration of all PFASs was associated with increased odds of impaired CVH (OR: 1.10, 95% CI: 1.02, 1.19). In particular, PFOS and PFNA contributed the main positive weights to the outcome, with PFOS having the largest positive weight (0.61) and PFNA following 0.39; PFHxS and PFOA had negative weights, with PFHxS having the largest negative weight at 0.93 and PFOA having a negative weight of 0.07 (Supplementary Figure S6).

10.3389/fpubh.2024.1418134

TABLE 3 Weighted univariate logistic regression analyses of variables associated with impaired CVH.

Variable	OR	95% CI	*p*-value
Age (years)	1.03	1.03 (1.02, 1.03)	<0.0001
Gender			
Female	Reference	Reference	Reference
Male	1.56	1.56 (1.34, 1.82)	<0.0001
Race/ethnicity			
Non-Hispanic Black	Reference	Reference	Reference
Non-Hispanic white	0.42	0.42 (0.35, 0.51)	<0.0001
Mexican American	0.51	0.51 (0.40, 0.66)	<0.0001
Other	0.37	0.37 (0.29, 0.48)	<0.0001
Education levels			
High school or less	Reference	Reference	Reference
Some college or associate degree	0.51	0.51 (0.41, 0.63)	<0.0001
College graduate or above	0.19	0.19 (0.15, 0.23)	<0.0001
Marital status			
Coupled	Reference	Reference	Reference
Single or separated	1.22	1.22 (1.02, 1.44)	0.03
PIR			
<1.3	Reference	Reference	Reference
1.3–3.5	0.76	0.76 (0.62, 0.94)	0.01
>3.5	0.44	0.44 (0.36, 0.54)	<0.0001
Alcohol intake status			
Never	Reference	Reference	Reference
Former	2.6	2.60 (1.97, 3.44)	<0.0001
Mild	1.1	1.10 (0.88, 1.37)	0.40
Moderate	0.96	0.96 (0.74, 1.26)	0.77
Heavy	1.58	1.58 (1.18, 2.11)	0.002
Health insurance			
No	Reference	Reference	Reference
Yes	0.7	0.70 (0.57, 0.85)	<0.001
Diabetes			
No	Reference	Reference	Reference
Yes	8.68	8.68 (4.94, 15.26)	<0.0001
Depression			
No	Reference	Reference	Reference
Yes	3.83	3.83 (2.51, 5.84)	<0.0001
CVD			
No	Reference	Reference	Reference
Yes	3.8	3.80 (2.74, 5.28)	<0.0001
Take anti-hypertensive or lipid-lowering medication			
No	Reference	Reference	Reference
Yes	4.04	4.04 (3.29, 4.96)	<0.0001
eGFR (mL/min/1.73 m^2)	0.99	0.99 (0.98, 0.99)	<0.0001
uACR (mg/g)	1	1.00 (1.00, 1.01)	0.05

CVH, cardiovascular health; PIR, the ratio of family income to poverty; CVD, cardiovascular diseases; eGFR, estimated glomerular filtration rate; uACR, urinary albumin and creatinine.

10.3389/fpubh.2024.1418134

TABLE 4 Results of weighted multivariable logistic regression analyses for PFAS compounds and impaired CVH.

PFAS exposure (ng/ml)	Crude model			Model 1		
	OR	95% CI	*P*-value	OR	95% CI	*P*-value
PFHxS						
ln-PFHxS	1.18	1.10, 1.27	<0.0001	1.07	0.99, 1.17	0.09
Q1 (low)	1	Reference		1	Reference	
Q2	1.48	1.20, 1.83	<0.001	1.33	1.05, 1.69	0.02
Q3	1.38	1.10, 1.73	0.01	1.09	0.85, 1.40	0.49
Q4 (high)	1.63	1.33, 1.99	<0.0001	1.21	0.95, 1.54	0.13
p for trend			<0.0001			0.33
PFNA						
ln-PFNA	1.22	1.10, 1.35	<0.001	1.14	1.02, 1.28	0.03
Q1 (low)	1	Reference		1	Reference	
Q2	1.08	0.89, 1.32	0.41	1.13	0.91, 1.39	0.28
Q3	1.30	1.04, 1.62	0.02	1.22	0.97, 1.54	0.09
Q4 (high)	1.54	1.21, 1.96	<0.001	1.40	1.09, 1.80	0.01
p for trend			<0.001			0.01
PFOA						
ln-PFOA	1.21	1.09, 1.33	<0.001	1.15	1.02, 1.29	0.02
Q1 (low)	1	Reference		1	Reference	
Q2	1.14	0.93, 1.40	0.2	1.13	0.91, 1.41	0.25
Q3	1.18	0.94, 1.48	0.15	1.14	0.88, 1.49	0.32
Q4 (high)	1.56	1.24, 1.95	<0.001	1.44	1.10, 1.88	0.01
p for trend			<0.001			0.02
PFOS						
ln-PFOS	1.30	1.20, 1.41	<0.0001	1.18	1.08, 1.30	<0.001
Q1 (low)	1	Reference		1	reference	
Q2	1.07	0.85, 1.34	0.58	0.98	0.78, 1.24	0.86
Q3	1.44	1.14, 1.81	0.002	1.27	1.01, 1.59	0.04
Q4 (high)	2.20	1.72, 2.81	<0.0001	1.62	1.25, 2.11	<0.001
p for trend			<0.0001			<0.0001

Crude model: no covariates were adjusted. Model 1: age (as a continuous variable), gender, race/ethnicity, educational level, marital status, PIR, alcohol consumption, health insurance, diabetes, depression, take anti-hypertensive or lipid-lowering medication, cardiovascular disease, eGFR, and UACR. PFOA, perfluorooctanoic acid; PFOS, perfluorooctane sulfonic acid; PFNA, perfluorononanoic acid; PFHxS, perfluorohexane sulfonic acid. OR, odds ratio; 95% CI, confidence intervals.

3.7 Sensitivity analysis

Supplementary Table S4 shows the outcomes of the sensitivity analysis. The exposure levels of PFNA, PFOA, and PFOS in the highest quartile were still positively associated with impaired CVH (OR_{PFNA}: 1.49, 95% CI: 1.14, 1.94; OR_{PFOA}: 1.50, 95% CI: 1.13, 1.98; OR_{PFOS}: 1.74, 95% CI: 1.30, 2.33). Similarly, ln-PFNA, ln-PFOA, and ln-PFOS were found to be associated with an increased risk of impaired CVH ($OR_{ln\text{-}PFNA}$: 1.18, 95% CI: 1.04, 1.33; $OR_{ln\text{-}PFOA}$: 1.17, 95% CI: 1.03, 1.32; $OR_{ln\text{-}PFOS}$: 1.21, 95% CI: 1.09, 1.34).

4 Discussions

In this nationally representative study, we determined that PFAS were associated with a greater risk of impaired CVH. After controlling for covariates, the risk of impaired CVH was increased by 40, 10, and 25% for PFNA, PFOA, and PFOS, respectively, in the highest group compared with the lowest group. Similar statistical results were obtained when PFAS was used as a continuous variable. Trend tests validated the persistence of the positive relationships, and subgroup analysis results underscored the universality of this association across different subpopulations. The sensitivity analysis reinforced the robustness of the statistical results. The RCS curve revealed that PFNA maintains a positive linear relationship with impaired CVH, whereas PFOS and PFOA exhibit a nonlinear relationship with impaired CVH. The results of the Qgcomp analysis and WQS model revealed that mixed exposure to PFASs is linked to impaired CVH. PFOS had the most positive weight, as did PFHxS, which had the largest negative weight.

Previous studies have linked serum PFAS exposure and CVD, such as coronary heart disease, stroke, carotid artery thickness, and lower limb arterial occlusion (11, 26). These investigations relied primarily on medical history for diagnosis and lacked a direct focus on CVH. Given that young people have a lower risk of CVD, we used

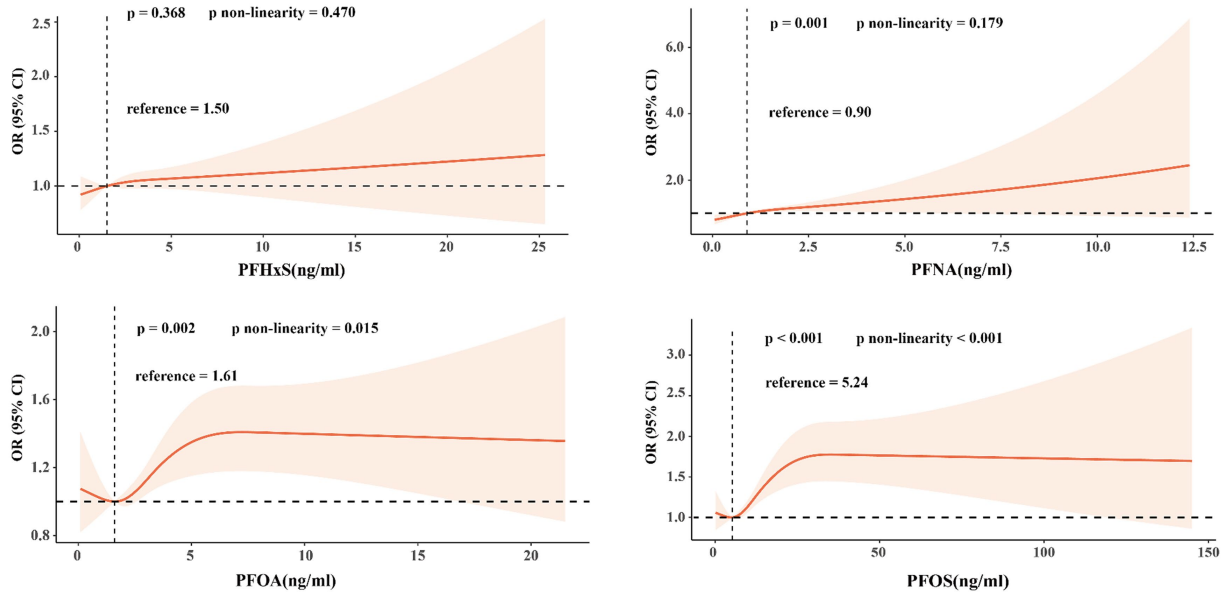

FIGURE 2
Restricted cubic splines were used to determine the relationship between PFAS exposure concentration and the risk of impaired CVH in adults.

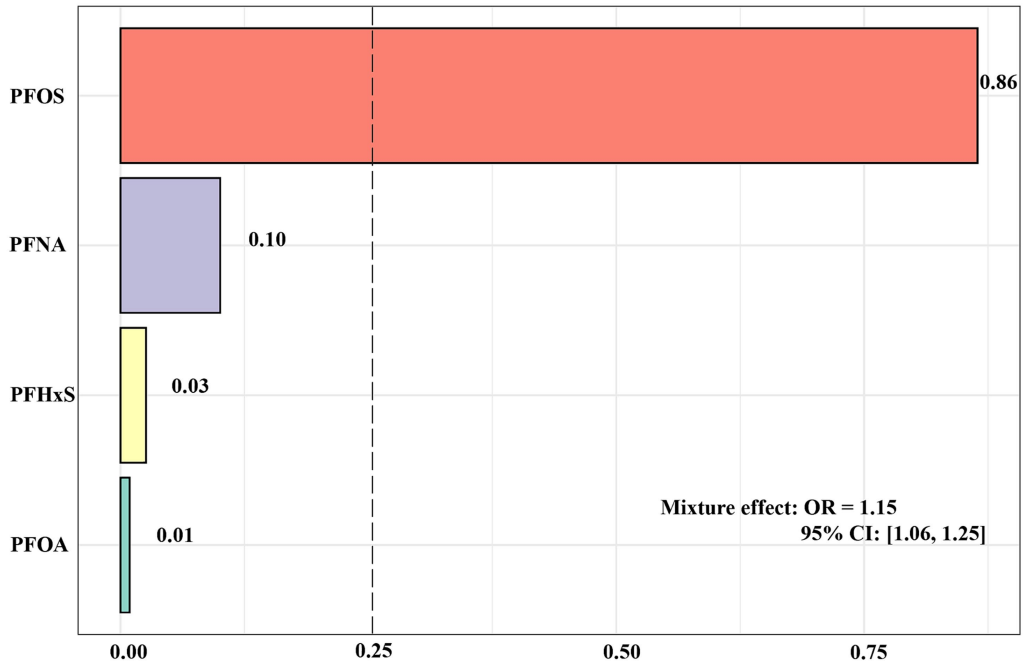

FIGURE 3
WQS regression index weights for each PFAS in the PFAS mixture.

LE8 to examine the associations between PFASs and CVH and included a wider range of health indicators.

In the present study, exposure to almost all PFOS was positively associated with impaired CVH in the young and middle-aged groups. The association was particularly significant in the middle-aged group. This possibly reflects the cumulative effect of chronic exposure with age, as confirmed by Supplementary Table S5, which shows the cumulative effect of increasing PFAS concentrations with age. In contrast, for older adults aged 60 years and older, despite having longer cumulative exposure concentrations, only the presence of an effect of PFOS exposure on impaired CVH was found, hinting at a potential relevance of age, which is in line with the findings of a previous German study that reported that, relative to older adults, PFAS have a greater risk of increasing cardiometabolic outcomes in people younger than 54 years

(16). Although the physiological mechanisms are not understood, multiple CVH risk factors are already present in older adults, including metabolic abnormalities, medications, and ageing; these issues increase the degree of competing risk and may mask the independent effects of PFASs. Our finding that exposure to PFNA and PFOS was more significantly associated with impaired CVH in males than in females suggests that there may be biological or environmental factors that increase the susceptibility of males to the negative effects of these chemicals on CVH. Consistent with our results, Sun and colleagues reported higher serum PFAS concentrations in men than in women (25). Pan and colleagues reported that males exposed to PFNA, PFOA, and PFOS have a greater risk of hypertension than females do, which may be influenced by differences in hormone levels and body clearance by sex (27). Non-Hispanic whites and Mexican Americans are more susceptible to PFAS for CVH. According to Liddie et al. (28), the detection of PFASs in community water systems in the U.S. was positively associated with the number of sources of PFASs and the proportion of people of color served by these water systems, highlighting the role of race in environmental health inequities. Additionally, our study revealed a linear relationship between PFNA levels and impaired CVH, suggesting that the risk increases with increasing exposure. In contrast, there was a nonlinear trend for PFOA and PFOS, with the ratio of impaired CVH increasing as concentrations reached a certain threshold, beyond which the risk stabilized. These findings suggest that complex biological mechanisms may reduce risk at higher exposures. Individuals who are coupled have an increased risk of impaired CVH risk following exposure to four PFASs, and further research may be needed to investigate the relationships between different lifestyles and environmental factors and PFASs and CVH. Given the cross-sectional study design, it is important to consider that high CVH might enhance PFAS elimination. The HOME study involving 166 mother–child pairs revealed that physical exercise modified the impact of PFOA exposure on cardiac metabolic risk scores, visceral fat area, and insulin resistance, suggesting that lifestyle interventions could mitigate some adverse effects of PFAS exposure (29).

The mechanism by which PFASs affect CVH is not fully understood. Previous evidence has suggested that PFAS may be associated with the aggravation of CVD risk factors and events through endocrine disruption and possibly a direct vascular toxic effect (30). Endothelial dysfunction is widely recognized as a foundational pathology of various CVDs. Earlier experimental research suggested that PFAS exposure can induce inflammation, initiate the generation of reactive oxygen species, increase endothelial cell permeability, and increase the expression of adhesion molecules, such as intercellular adhesion molecule-1, thus attracting monocytes to atherosclerotic lesions and exacerbating atherosclerosis (31, 32). Omoike et al. (33) reported that PFAS exposure was linked to increased serum markers of chronic inflammation and oxidative stress, such as lymphocyte count, serum iron, albumin, and bilirubin. In animal experiments, PFAS has been found to cause cardiotoxicity in rats by increasing cell apoptosis and proinflammatory cytokine expression (34). DNA methylation, an important epigenetic modification predominantly occurring on cytosine–phosphate–guanine islands in gene promoter regions and regulated by DNA methyltransferases, has recently been connected to the expression of genes linked to CVD (35). Research indicates that PFAS exposure is correlated with epigenetic alterations, including DNA methylation, in adults and birth cohorts (36, 37). Lin's study revealed an association between PFOS exposure and elevated 5mdC/dG levels, highlighting the potential relevance of DNA methylation in the pathophysiology of PFOS-related atherosclerosis (38). Another potential pathway involves PPAR receptor activation, which is crucial for fatty acid and metabolism regulation and is a potential drug target for reducing atherosclerosis risk; however, this pathway is associated with increased cardiovascular events (39, 40). PFAS interaction with PPARs has been shown to lead to hypertension (41). Additionally, PFOS preferentially accumulates in platelets, affecting the stability of the plasma membrane and altering membrane fluidity, which affects platelet activation and aggregation, leading to thrombosis (42).

This study is the first to measure and diagnose impaired CVH risk associated with PFASs via the LE8 score. This method has several advantages. First, we use NHANES data to ensure data quality and national representativeness by adjusting for appropriate weights and confounders. Second, the LE8 score is employed as a comprehensive CVH assessment criterion. Directly linking PFAS exposure to quantifiable changes in CVH facilitates early identification of at-risk individuals. Third, applying multiple statistical analysis techniques strengthens the robustness of the findings by identifying specific subpopulations and elucidating complex relationships.

Our study has several clear limitations. First, we only analyzed data from a single measurement of serum PFAS concentrations rather than from repeated measurements, which would be more appropriate for estimating the cumulative effects of PFAS exposure over many years. Second, since certain metrics are derived from self-report questionnaires, this may introduce potential biases. Third, although our study controlled for a wide range of confounding factors, there are still potential confounding factors that could affect the results. Finally, we cannot determine the inherent causal relationships given the limitations of the study type.

5 Conclusion

In summary, our research revealed a significant association between PFAS exposure and elevated risk of impaired CVH, with almost consistent results across diverse subpopulations. These findings contribute to the advancement of understanding PFAS risks in public health and environmental studies, to identify individuals at risk before major health events occur and potentially alleviate the overall burden of diseases in the population. Furthermore, there is a pressing need for future longitudinal studies on populations with high PFAS exposure and emerging PFAS compounds to confirm the current findings. Finally, in-depth experimental research is essential to uncover the potential mechanisms behind this association.

Data availability statement

Publicly available datasets were analyzed in this study. This data can be found at: https://wwwn.cdc.gov/nchs/nhanes/continuousnhanes/default.aspx.

Ethics statement

The study was approved by the NCHS Institutional Review Board and all participants provided written informed consent.

The studies were conducted in accordance with the local legislation and institutional requirements. The participants provided their written informed consent to participate in this study. Written informed consent was obtained from the individual(s) for the publication of any potentially identifiable images or data included in this article.

Author contributions

SZ: Conceptualization, Methodology, Visualization, Writing – original draft. LW: Methodology, Software, Writing – review & editing. SW: Conceptualization, Software, Validation, Writing – review & editing. YW: Formal analysis, Methodology, Software, Writing – review & editing. YJ: Supervision, Writing – review & editing. LS: Conceptualization, Project administration, Writing – review & editing. YZ: Methodology, Visualization, Writing – original draft. XL: Data curation, Funding acquisition, Supervision, Writing – review & editing.

Funding

The author(s) declare that financial support was received for the research, authorship, and/or publication of this article. Grants supported this study from the National Natural Science Foundation of China (Nos. 82074388 and 82274477). The funder had no influence on the study design or the interpretation of the results.

Acknowledgments

The author extends sincere gratitude to all individuals who made invaluable contributions to this research.

Conflict of interest

The authors declare that the research was conducted in the absence of any commercial or financial relationships that could be construed as a potential conflict of interest.

Publisher's note

Supplementary material

The Supplementary material for this article can be found online at: https://www.frontiersin.org/articles/10.3389/fpubh.2024.1418134/full#supplementary-material

References

1. Roth GA, Mensah GA, Johnson CO, Addolorato G, Ammirati E, Baddour LM, et al. Global burden of cardiovascular diseases and risk factors, 1990-2019: update from the GBD 2019 study. *J Am Coll Cardiol.* (2020) 76:2982–3021. doi: 10.1016/j.jacc.2020.11.010

2. Martin SS, Aday AW, Almarzooq ZI, Anderson CAM, Arora P, Avery CL, et al. 2024 heart disease and stroke statistics: a report of US and global data from the American Heart Association. *Circulation.* (2024) 149:e347–913. doi: 10.1161/CIR.0000000000001209

3. Lloyd-Jones DM, Allen NB, Anderson CAM, Black T, Brewer LC, Foraker RE, et al. Life's essential 8: updating and enhancing the American Heart Association's construct of cardiovascular health: a presidential advisory from the American Heart Association. *Circulation.* (2022) 146:e18–43. doi: 10.1161/CIR.0000000000001078

4. Sun J, Li Y, Zhao M, Yu X, Zhang C, Magnussen CG, et al. Association of the American Heart Association's new "Life's essential 8" with all-cause and cardiovascular disease-specific mortality: prospective cohort study. *BMC Med.* (2023) 21:116. doi: 10.1186/s12916-023-02824-8

5. Zhang Y, Sun M, Wang Y, Xu T, Ning N, Tong L, et al. Association of cardiovascular health using Life's essential 8 with noncommunicable disease multimorbidity. *Prev Med.* (2023) 174:107607. doi: 10.1016/j.ypmed.2023.107607

6. Li C, Li Y, Zhao M, Zhang C, Bovet P, Xi B. Using the new "Life's essential 8" metrics to evaluate trends in cardiovascular health among US adults from 2005 to 2018: analysis of serial cross-sectional studies. *JMIR Public Health Surveill.* (2023) 9:e45521. doi: 10.2196/45521

7. Brunn H, Arnold G, Körner W, Rippen G, Steinhäuser KG, Valentin I. PFAS: forever chemicals—persistent, bioaccumulative and mobile. Reviewing the status and the need for their phase out and remediation of contaminated sites. Environmental sciences. *Europe.* (2023) 35:20. doi: 10.1186/s12302-023-00721-8

8. Xu Y, Fletcher T, Pineda D, Lindh CH, Nilsson C, Glynn A, et al. Serum half-lives for short- and Long-chain Perfluoroalkyl acids after ceasing exposure from drinking water contaminated by firefighting foam. *Environ Health Perspect.* (2020) 128:77004. doi: 10.1289/EHP6785

9. Batzella E, Rosato I, Pitter G, Da Re F, Russo F, Canova C, et al. Determinants of PFOA serum half-life after end of exposure: a longitudinal study on highly exposed subjects in the Veneto region. *Environ Health Perspect.* (2024) 132:27002. doi: 10.1289/EHP13152

10. Barton KE, Zell-Baran LM, DeWitt JC, Brindley S, McDonough CA, Higgins CP, et al. Cross-sectional associations between serum PFASs and inflammatory biomarkers in a population exposed to AFFF-contaminated drinking water. *Int J Hyg Environ Health.* (2022) 240:113905. doi: 10.1016/j.ijheh.2021.113905

11. Meneguzzi A, Fava C, Castelli M, Minuz P. Exposure to Perfluoroalkyl chemicals and cardiovascular disease: experimental and epidemiological evidence. *Front Endocrinol.* (2021) 12:706352. doi: 10.3389/fendo.2021.706352

12. Zhang Y-T, Zeeshan M, Su F, Qian Z-M, Dee Geiger S, Edward McMillin S, et al. Associations between both legacy and alternative per- and polyfluoroalkyl substances and glucose-homeostasis: the isomers of C8 health project in China. *Environ Int.* (2022) 158:106913. doi: 10.1016/j.envint.2021.106913

13. Huang M, Jiao J, Zhuang P, Chen X, Wang J, Zhang Y. Serum polyfluoroalkyl chemicals are associated with risk of cardiovascular diseases in national US population. *Environ Int.* (2018) 119:37–46. doi: 10.1016/j.envint.2018.05.051

14. Feng X, Long G, Zeng G, Zhang Q, Song B, Wu K-H. Association of increased risk of cardiovascular diseases with higher levels of perfluoroalkylated substances in the serum of adults. *Environ Sci Pollut Res.* (2022) 29:89081–92. doi: 10.1007/s11356-022-22021-z

15. Wu M, Zhu Z, Wan R, Xu J. Exposure to per- and polyfluoroalkyl substance and metabolic syndrome: a nationally representative cross-sectional study from NHANES, 2003-2018. *Environ Pollut.* (2024) 346:123615. doi: 10.1016/j.envpol.2024.123615

16. Faquih TO, Landstra EN, van Hylckama Vlieg A, Aziz NA, Li-Gao R, de Mutsert R, et al. Per- and Polyfluoroalkyl Substances Concentrations are Associated with an Unfavorable Cardio-Metabolic Risk Profile: Findings from Two Population-Based Cohort Studies. *Expo Health.* (2024). doi: 10.1007/s12403-023-00622-4

17. Osorio-Yáñez C, Sanchez-Guerra M, Cardenas A, Lin P-ID, Hauser R, Gold DR, et al. Per- and polyfluoroalkyl substances and calcifications of the coronary and aortic arteries in adults with prediabetes: results from the diabetes prevention program outcomes study. *Environ Int.* (2021) 151:106446. doi: 10.1016/j.envint.2021.106446

18. Dunder L, Salihovic S, Varotsis G, Lind P, Elmståhl S, Lind L. Plasma levels of per- and polyfluoroalkyl substances (PFAS) and cardiovascular disease - results from two independent population-based cohorts and a meta-analysis. *Environ Int.* (2023) 181:108250. doi: 10.1016/j.envint.2023.108250

19. von Elm E, Altman DG, Egger M, Pocock SJ, Gøtzsche PC, Vandenbroucke JP, et al. The strengthening the reporting of observational studies in epidemiology (STROBE) statement: guidelines for reporting observational studies. *Lancet.* (2007) 370:1453–7. doi: 10.1016/S0140-6736(07)61602-X

20. Boss J, Mukherjee B, Ferguson KK, Aker A, Alshawabkeh AN, Cordero JF, et al. Estimating outcome-exposure associations when exposure biomarker detection limits vary across batches. *Epidemiology*. (2019) 30:746–55. doi: 10.1097/EDE.0000000000001052

21. Wang L, Wang S, Wang Y, Zong S, Li Z, Jiang Y, et al. Association between dietary live microbe intake and Life's essential 8 in US adults: a cross-sectional study of NHANES 2005–2018. *Front Nutr*. (2024) 11:1340028. doi: 10.3389/fnut.2024.1340028

22. Rattan P, Penrice DD, Ahn JC, Ferrer A, Patnaik M, Shah VH, et al. Inverse Association of Telomere Length with Liver Disease and Mortality in the US population. *Hepatol Commun*. (2022) 6:399–410. doi: 10.1002/hep4.1803

23. Levey AS, Stevens LA, Schmid CH, Zhang YL, Castro AF, Feldman HI, et al. A new equation to estimate glomerular filtration rate. *Ann Intern Med*. (2009) 150:604–12. doi: 10.7326/0003-4819-150-9-200905050-00006

24. Zhang Y, Mustieles V, Wang YX, Sun Y, Agudelo J, Bibi Z, et al. Folate concentrations and serum perfluoroalkyl and polyfluoroalkyl substance concentrations in adolescents and adults in the USA (National Health and nutrition examination study 2003–16): an observational study. *Lancet Planet Health*. (2023) 7:e449–58. doi: 10.1016/S2542-5196(23)00088-8

25. Sun X, Yang X, Zhang Y, Liu Y, Xiao F, Guo H, et al. Correlation analysis between per-fluoroalkyl and poly-fluoroalkyl substances exposure and depressive symptoms in adults: NHANES 2005–2018. *Sci Total Environ*. (2024) 906:167639. doi: 10.1016/j.scitotenv.2023.167639

26. Lin CY, Lin LY, Wen T-W, Lien G-W, Chien K-L, Hsu SHJ, et al. Association between levels of serum perfluorooctane sulfate and carotid artery intima-media thickness in adolescents and young adults. *Int J Cardiol*. (2013) 168:3309–16. doi: 10.1016/j.ijcard.2013.04.042

27. Pan K, Xu J, Long X, Yang L, Huang Z, Yu J. The relationship between perfluoroalkyl substances and hypertension: a systematic review and meta-analysis. *Environ Res*. (2023) 232:116362. doi: 10.1016/j.envres.2023.116362

28. Liddie JM, Schaider LA, Sunderland EM. Sociodemographic factors are associated with the abundance of PFAS sources and detection in U.S. community water systems. *Environ Sci Technol*. (2023) 57:7902–12. doi: 10.1021/acs.est.2c07255

29. Braun JM, Papandonatos GD, Li N, Sears CG, Buckley JP, Cecil KM, et al. Physical activity modifies the relation between gestational perfluorooctanoic acid exposure and adolescent cardiometabolic risk. *Environ Res*. (2022) 214:114021. doi: 10.1016/j.envres.2022.114021

30. Wen Z-J, Wei Y-J, Zhang Y-F, Zhang Y-F. A review of cardiovascular effects and underlying mechanisms of legacy and emerging per- and polyfluoroalkyl substances (PFAS). *Arch Toxicol*. (2023) 97:1195–245. doi: 10.1007/s00204-023-03477-5

31. Qian Y, Ducatman A, Ward R, Leonard S, Bukowski V, Lan Guo N, et al. Perfluorooctane sulfonate (PFOS) induces reactive oxygen species (ROS) production in human microvascular endothelial cells: role in endothelial permeability. *J Toxic Environ Health A*. (2010) 73:819–36. doi: 10.1080/15287391003689317

32. Wittkopp S, Wu F, Windheim J, Robinson M, Kannan K, Katz SD, et al. Vascular endothelium as a target for perfluroalkyl substances (PFAs). *Environ Res*. (2022) 212:113339. doi: 10.1016/j.envres.2022.113339

33. Omoike OE, Pack RP, Mamudu HM, Liu Y, Strasser S, Zheng S, et al. Association between per and polyfluoroalkyl substances and markers of inflammation and oxidative stress. *Environ Res*. (2021) 196:110361. doi: 10.1016/j.envres.2020.110361

34. Xu D, Li L, Tang L, Guo M, Yang J. Perfluorooctane sulfonate induces heart toxicity involving cardiac apoptosis and inflammation in rats. *Exp Ther Med*. (2022) 23:14. doi: 10.3892/etm.2021.10936

35. di A, Sabovic I, Valente U, Tescari S, Rocca MS, Guidolin D, et al. Endocrine disruption of androgenic activity by Perfluoroalkyl substances: clinical and experimental evidence. *J Clin Endocrinol Metabol*. (2019) 104:1259–71. doi: 10.1210/jc.2018-01855

36. Kim S, Thapar I, Brooks BW. Epigenetic changes by per- and polyfluoroalkyl substances (PFAS). *Environ Pollut*. (2021) 279:116929. doi: 10.1016/j.envpol.2021.116929

37. Leung Y-K, Ouyang B, Niu L, Xie C, Ying J, Medvedovic M, et al. Identification of sex-specific DNA methylation changes driven by specific chemicals in cord blood in a Faroese birth cohort. *Epigenetics*. (2018) 13:290–300. doi: 10.1080/15592294.2018.1445901

38. Lin C-Y, Lee H-L, Chen C-W, Wang C, Sung F-C, Su T-C. Global DNA methylation mediates the association between serum perfluorooctane sulfonate and carotid intima-media thickness in young and middle-aged Taiwanese populations. *Ecotoxicol Environ Saf*. (2022) 241:113782. doi: 10.1016/j.ecoenv.2022.113782

39. Ivanova EA, Myasoedova VA, Melnichenko AA, Orekhov AN. Peroxisome proliferator-activated receptor (PPAR) gamma agonists as therapeutic agents for cardiovascular disorders: focus on atherosclerosis. *CPD*. (2017) 23:1119–24. doi: 10.2174/1381612823666161118145850

40. Usuda D, Kanda T. Peroxisome proliferator-activated receptors for hypertension. *World J Cardiol*. (2014) 6:744–54. doi: 10.4330/wjc.v6.i8.744

41. Lin N, Zhang Y, Su S, Feng Y, Wang B, Li Z. Exposure characteristics of legacy and novel per- and polyfluoroalkyl substances in blood and association with hypertension among low-exposure population. *J Hazard Mater*. (2023) 459:132185. doi: 10.1016/j.jhazmat.2023.132185

42. De Toni L, Radu CM, Sabovic I, Di Nisio A, Dall'Acqua S, Guidolin D, et al. Increased cardiovascular risk associated with chemical sensitivity to Perfluoro-Octanoic acid: role of impaired platelet aggregation. *Int J Mol Sci*. (2020) 21:399. doi: 10.3390/ijms21020399

frontiers | Frontiers in Public Health

TYPE Original Research
PUBLISHED 02 October 2024
DOI 10.3389/fpubh.2024.1468384

OPEN ACCESS

EDITED BY
Pu Xia,
University of Birmingham, United Kingdom

REVIEWED BY
Jianghua Yang,
Nanjing University, China
Sai Wang,
Hainan University, China

*CORRESPONDENCE
Fengru Zhang
✉ zhangfengru@126.com
Shuangxin Wu
✉ 409794313@qq.com

RECEIVED 22 July 2024
ACCEPTED 09 September 2024
PUBLISHED 02 October 2024

CITATION
Wei F, Gu W, Zhang F and Wu S (2024) Paralysis caused by dinotefuran at environmental concentration via interfering the Ca^{2+}–ROS–mitochondria pathway in *Chironomus kiiensis*. *Front. Public Health* 12:1468384. doi: 10.3389/fpubh.2024.1468384

Paralysis caused by dinotefuran at environmental concentration via interfering the Ca^{2+}–ROS–mitochondria pathway in *Chironomus kiiensis*

Fenghua Wei[1], Weiwen Gu[1], Fengru Zhang[1]* and Shuangxin Wu[2]*

[1]School of Chemistry and Environment, Jiaying University, Meizhou, China, [2]School of Physics and Electrical Engineering, Jiaying University, Meizhou, China

Introduction: Dinotefuran as the third-generation of neonicotinoid insecticides is extensively used in agriculture worldwide, posing a potential toxic threat to non-target animals and humans. However, the chronic toxicity mechanism related to mitochondria damage of dinotefuran to non-target animals at environmental concentration is unclear.

Methods: In this study, the mitochondria damage and oxidative stress of dinotefuran on *Chironomus kiiensis* were investigated at environmental concentrations by long-term exposure. At the same time, relevant gene expressions of these toxicity indexes were measured as sensitive ecotoxicity biomarkers to reflect the toxic effects of dinotefuran on Chironomidae.

Results: Our present study showed that chronic exposure to environmental concentrations of dinotefuran resulted in behavioral inhibition in the larvae of Chironomidae. For burrowing inhibition of 10 days, the lowest observed-effect concentration (LOEC) and 50% inhibitory concentration (IC_{50}) were 0.01 (0.01–0.04) and 0.60 (0.44–0.82) μg/L, respectively. Dinotefuran promoted the release of intracellular calcium ions (Ca^{2+}) in Chironomidae via dysregulating the gene expressions of *atp2b*, *camk ii*, and *calm*. Subsequently, the disruption of the Ca^{2+} signaling pathway induced oxidative stress by raising reactive oxygen species (ROS), hydrogen peroxide (H_2O_2), and malonaldehyde (MDA) levels. Thus, the over-release of Ca^{2+} and ROS disordered the normal functioning of mitochondrial-related pathways by dysregulating the expressions of mitochondria-related genes of *atpef0a*, *sdha*, and *cyt b*.

Conclusion: Our findings showed that low environmental concentrations of dinotefuran caused paralysis of the midge via interfering the Ca^{2+}–ROS–mitochondria pathway. These results provided data support for assessing the potential environmental risk of dinotefuran.

KEYWORDS

neonicotinoid insecticides, long-term exposure, mitochondria, Chironomidae, environmental dose

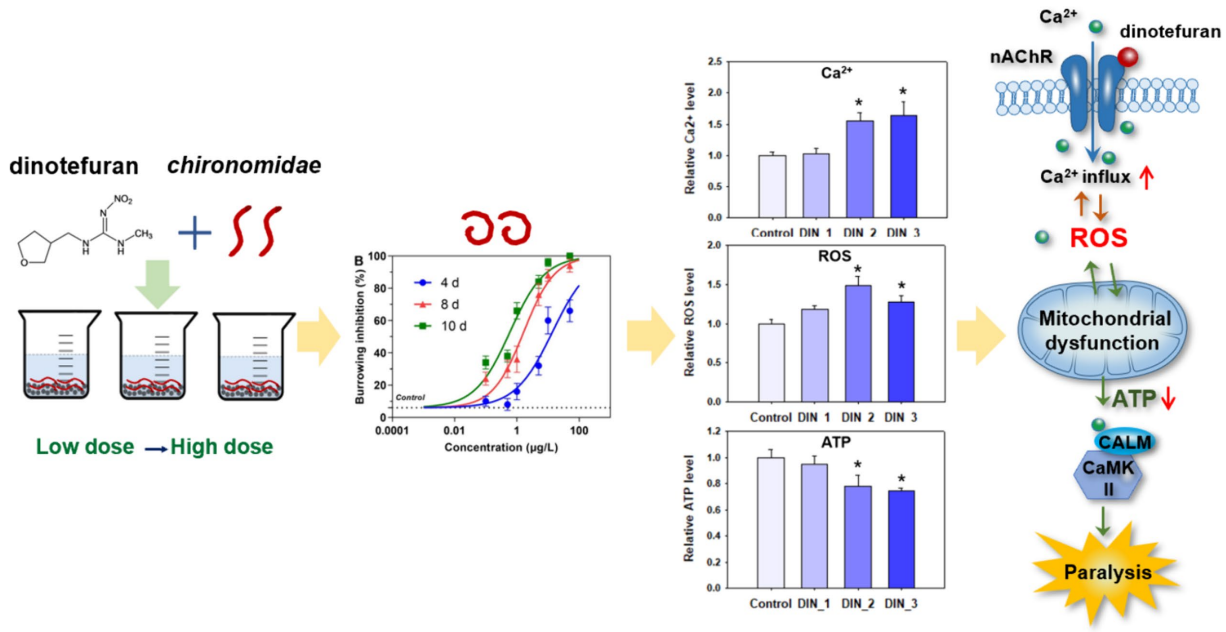

GRAPHICAL ABSTRACT

1 Introduction

Neonicotinoid insecticides are the fastest-growing systemic pesticides in the world due to being considered to be less toxic to mammalian species than traditional insecticide classes, such as organochlorines and organophosphates (1). Dinotefuran, which is a third-generation neonicotinoid insecticide, has a tetrahydrofuran ring but no halogen elements of other neonicotinoids (2). It has more excellent properties than first-and second-generation neonicotinoids, such as higher insecticidal activity, quicker uptake, smaller resistance, broader spectrum, and safer for the environment and humans (3). Nowadays, dinotefuran has been widely used, accounting for more than 25% of the global pesticides used (4). Excessive use and high water solubility of dinotefuran unavoidably remained in residues in surface waters, causing harm to aquatic organisms and humans (5).

Dinotefuran was less studied in previous reports compared with the other neonicotinoid insecticides. A few studies reported the detection of waterborne dinotefuran in various regions. Xiong et al. (6) detected neonicotinoid insecticides from a paddy field to receiving waters in the Poyang Lake basin of China, showing that dinotefuran was the dominant neonicotinoid with a mean concentration of 200 ± 296 ng/L and the maximum concentration of 802 ± 139 ng/L. Dinotefuran was detected with a concentration of 12.7–75.5 ng/L in rivers near maize fields in Ontario, Canada (7) and 1.60–134 ng/L in streams across the United States (8). Putri et al. (9) analyzed neonicotinoid occurrence in tropical environmental waters of Indonesia, the highest concentration of dinotefuran was 23.12 ng/L in estuaries and mangrove areas. Thompson et al. (10) investigated neonicotinoid insecticides in well tap water and human urine samples in eastern Iowa, the max concentration of dinotefuran was 3.9 ng/L in groundwater samples and 2.9 μg/g in urine samples.

It is well known that the toxicity target of neonicotinoids is the nicotinic acetylcholine receptors (nAChRs) of insects. They act on nAChRs and disrupt the central nervous system of insects, thus, insects become paralyzed and even die due to overexcitement (11). Even so, numerous recent reports have found neonicotinoids could cause unintended toxic effects on non-target organisms, even humans. Therefore, the exploration of their additional toxic mechanism has become the emerging focus of public attention. Although the toxicity of dinotefuran is low, the toxicity to non-target organisms cannot be ignored. Liu et al. (12) showed that more than 1.0 mg/kg of dinotefuran caused oxidative stress and genetic toxicity in earthworms (*Eisenia fetida*) during the 28 d exposure. Dinotefuran (0.1, 0.5, and 2.0 mg/L) induced oxidative stress and DNA damage in juvenile Chinese rare minnows (*Gobiocypris rarus*) after 60 d exposure (13). Though these toxicities of dinotefuran have been studied in some organisms, little is known about Chironomidae, especially for environmental concentrations and long-term exposure. Chironomid larvae are the main invertebrates in freshwater ecosystems and play important ecological functions because they are natural baits for many other aquatic organisms (14). In addition, Chironomidae are more sensitive to neonicotinoids compared with a lot of other aquatic invertebrates (5). Therefore, it is necessary to study the chronic toxicity mechanism of dinotefuran to Chironomidae as representative organisms at environmental concentrations. In addition, as the experimental animal chironomid is a lower invertebrate and belongs to the class of insects of the invertebrate phylum, therefore no ethical review is required.

In this study, *Chironomus kiiensis* was chosen as the test organism. Compared to the commonly used *Chironomus dilutus* (approximately 60 days), the life cycle of *Chironomus kiiensis* is shorter, only approximately 23 days, which is more time-saving on biological tests. The mitochondria damage and oxidative stress of dinotefuran on *Chironomus kiiensis* were investigated at environmental concentrations by long-term exposure. At the same time, relevant gene expressions of these toxicity indexes were measured as sensitive ecotoxicity biomarkers to reflect the toxic effects of dinotefuran on Chironomidae. These results will improve our understanding of the potential toxic mechanisms of dinotefuran to

Chironomidae and provide data support for assessing neonicotinoid insecticides' potential environmental risks.

2 Materials and methods

2.1 Materials

Dinotefuran (CAS: 165252-70-0), thiamethoxam-d_3 (internal standard), and imidacloprid-d_4 (surrogate standard) were purchased from Dr. Ehrenstorfer GmbH (Augsburg, Germany) with purity >98%. The midges, *Chironomus kiiensis* (*C. kiiensis*) were cultured in Jiaying University according to the standard protocol of USEPA2000 proposed by the U.S. Environmental Protection Agency.

2.2 Toxicological assay

Test water was freshly prepared by a range of concentrations (0.1, 0.5, 1, 5, 10, and 50 μg/L) of dinotefuran (DIN_1, DIN_2, DIN_3, DIN_4, DIN_5, and DIN_6) into reconstituted moderately hard water. Negative control and solvent control were tested in the meantime. A 0.5 cm layer of quartz sand and 200 mL of testing solution were introduced into each 500 mL beaker. Ten 1st instar larvae of *C. kiiensis* were randomly added into each beaker with 3–5 replicates per treatment group or control group. The entire exposure period ended until the first pupa appeared (approximately 10 days). The test solution was changed once on day 5. The organisms were fed ground fish food every 2 days per beaker. Water quality parameters (i.e., conductivity, pH, temperature, and dissolved oxygen) in the test solution were monitored every day and ammonia nitrogen was monitored on days 0, 5, and 10. At the end of the exposure period, the survival larvae were evaluated for a series of toxicity indexes, including lethality, burrowing inhibition, cellular responses, and the corresponding gene expressions. For burrowing inhibition, under normal circumstances, a larva of Chironomidae burrows into sand for nesting. If more than half of its body fails to burrow successfully, burrowing behavior is considered inhibited. The exposed solution was sampled at 5 and 10 days in three replicates and analyzed for dinotefuran actual concentrations using HPLC-MS/MS following a previously developed method by Wei et al. (15). More details on the quantification of dinotefuran are shown in the Supplementary material and qualification parameters for the analyte are listed in Supplementary Table S1.

2.3 Intracellular calcium ion level

Survival organisms in each group of control and three treat groups (DIN_1, DIN_2, and DIN_3) were used to measure the content of the intracellular Ca^{2+}. The concentration of Ca^{2+} was measured using a Fura-2/AM probe (Beyotime, Haimen, China). Survival midge larvae were homogenized in 3 mL of phosphate buffer solution (PBS) using a glass homogenizer and sieved with a 75 μm cell strainer. The homogenate was centrifuged twice for washing purposes at 1000 g and 4°C. The cell precipitate was resuspended in PBS. The cell suspension was preloaded with 2 μmol/L Fura-2/AM at 37°C for 30 min and was centrifugated at 1000 g for 5 min after being washed in PBS solution. Then the cells were resuspended in PBS and moved into 6-well plates (1×10^5 cells/well). The fluorescent signal was measured using a microplate spectrophotometer (Biotek, Synergy H1, United States) with emission wavelength at 510 nm and excitation wavelength at 340 and 380 nm. The relative amount of Ca^{2+} was calculated as the ratio of F340/F380 relative to control.

2.4 Oxidative stress indexes

Survival larvae in control and three treat groups (DIN_1, DIN_2, and DIN_3) were homogenized in 1 mL PBS for 3 min and the solution was centrifuged at 10,000 g at 4°C for 10 min. The supernatants were used for measuring protein content, hydrogen peroxide (H_2O_2) concentration, and malondialdehyde (MDA) content using commercial assay kits according to the manufacturer's protocols (Beyotime).

For H_2O_2 levels, 50 μL of supernatant sample or standard was added to the test well followed by 100 μL of H_2O_2 detection reagent to each well. The mixture solution was gently shaken and remained at room temperature for 30 min and immediately determined 560 nm. The concentration of H_2O_2 was calculated according to the standard curve.

For the MDA content, 100 μL of the standard products with different concentrations or 100 μL of the supernatant sample were added to the centrifuge tube. Then 200 μL of MDA detection fluid was added. The mixture was heated in a boiling water bath for 15 min and cooled to room temperature. After centrifugation at 1000 g for 10 min at room temperature, 200 μL of supernatant was added to the 96-well plate, and then the absorbance was measured at 532 nm.

ROS levels were measured using a commercial ROS assay kit (Beyotime) following the manufacturer's protocol. Surviving midge larvae were cut into small pieces with scissors. The fragment of tissue was gently rubbed on the 300 mesh nylon net which was put on the small test tube. Cell suspension was collected, and centrifuged at 500 g for 10 min, then the supernatant was removed. The cell precipitation was washed with PBS 1–2 times. The cell suspension was suspended in the DCFH-DA probe and incubated in a cell incubator at 37°C for 20 min. Subsequently, the mixture was inverted and mixed every 3–5 min so that the probe was in full contact with the cells. The cells were washed three times with serum-free cell culture solution to fully remove DCFH-DA that did not enter the cells. The concentration of ROS was detected at 488 nm excitation wavelength and 525 nm emission wavelength.

2.5 Mitochondria indexes

Mitochondrial membrane potential (MMP) was measured using a commercial MMP assay kit with JC-1 (Beyotime) following the standard procedure by the manufacturer's protocols. Mitochondrial depolarization was measured by the relative ratio of red to green fluorescence on a multifunctional microplate reader. Red fluorescence was detected at excitation light 525 nm and emission light 590 nm. Green fluorescence was detected at excitation light 490 nm and emission light 530 nm.

Adenosine triphosphate (ATP) level was measured using a commercial ATP assay kit (Beyotime) according to the manufacturer's protocols. A total of 100 μL of ATP test fluid was added to the test tube, which was placed at room temperature for 3–5 min, so that all the background ATP was consumed, thereby reducing the background. A total of 20 μL of sample or standard was introduced in the detection tube and mixed quickly, and the response by the chemiluminescence mode was measured after at least 2 s.

2.6 Measurements of gene levels

Survived larvae (DIN_1, DIN_2, and DIN_3) were immediately frozen with liquid nitrogen before use. Total RNA was isolated using an RNeasy Mini Kit (Qiagen, Hilden, Germany) according to the manufacturer's protocol. Expressions of 9 genes (Supplementary Table S2) were quantified using a real-time quantitative polymerase chain reaction (RT-qPCR) according to the method of the previous study by Wei et al. (15). In brief, β-actin was chosen as an internal control. The RNA samples were reversely transcribed into cDNA by using a Bestar™ qPCR-RT Kit (DBI-2220, German). RT-qPCR was performed in an ABI 7500 fluorescence quantitative PCR instrument (ThermoFisher, United States). The fold changes of the target genes were calculated using a $2^{-\Delta\Delta CT}$ method.

2.7 Statistical analysis

The concentration-effect curve was fitted by the GraphPad Prism 5.0 software (San Diego, CA, United States). Differences among the treatments were analyzed with one-way ANOVA by SPSS 17.0 software (SPSS Inc., Chicago, Ill., United States). The p-value <0.05 was considered statistically significant.

3 Results

3.1 Phenotypic toxicity

Dinotefuran concentrations in exposure solutions varied little under the experiment duration (Supplementary Table S3). Survival and burrowing behavior of the larva were impaired by dinotefuran in a concentration-dependent manner at 4, 8, and 10 days (Figures 1A,B and Supplementary Table S4). There was no significant difference in larva lethality between negative control and solvent control (Supplementary Figure S1). For lethality of 4 days, the lowest observed-effect concentration (LOEC), and 10 and 50% lethal concentrations (LC_{10} and LC_{50}) were 0.46 (0.15–1.61), 1.40 (0.55–3.25), and 36.4 (21.5–61.6) μg/L (mean (95% confidence interval)), respectively (Table 1). For burrowing inhibition of 4 days, LOEC, and 10 and 50% inhibitory concentrations (IC_{10} and IC_{50}) were 0.24 (0.07–0.93), 0.66 (0.24–1.72), and 13.9 (8.6–22.5) μg/L, respectively (Table 1). For lethality of 8 days, the LOEC, LC_{10}, and LC_{50} were 0.09 (0.02–0.43), 0.38 (0.12–1.06), and 23.3 (13.0–41.6) μg/L, respectively (Table 1). For burrowing inhibition of 8 days, LOEC, IC_{10}, and IC_{50} were 0.06 (0.02–0.17), 0.13 (0.06–0.29), and 1.66 (1.16–2.37) μg/L, respectively (Table 1). For lethality of 10 days, the LOEC, LC_{10}, and LC_{50} were 0.01 (0.002–0.12), 0.08 (0.02–0.33), and 13.4 (6.7–26.8) μg/L, respectively (Table 1). For burrowing inhibition of 10 days, LOEC, IC_{10}, and IC_{50} were 0.01 (0.01–0.04), 0.04 (0.02–0.08), and 0.60 (0.44–0.82) μg/L, respectively (Table 1).

3.2 Intracellular Ca^{2+} concentration

Dinotefuran significantly stimulated the release of intracellular Ca^{2+} concentrations of the midges above concentrations of 0.5 μg/L (DIN_2-DIN_3) after 10 d exposure ($p < 0.05$) (Figure 2A and Supplementary Table S5). The gene expressions of *atp2b* (Ca^{2+} transporting ATPase plasma membrane), *camk ii* (calcium/calmodulin-dependent protein kinase II), and *calm* (calmodulin) related to the calcium pathway were significantly upregulated after exposure to dinotefuran above the concentrations of 0.1 μg/L (DIN_1-DIN_3) or 0.5 μg/L (DIN_2-DIN_3) (Figures 3A–C and Supplementary Table S6).

3.3 Oxidative stress

The levels of ROS were significantly increased after 10 d exposure to dinotefuran at 0.5–1 μg/L (DIN_2-DIN_3) in larva (Figure 2B). The H_2O_2 levels were significantly upraised at 0.1 and 1 μg/L (DIN_1 and DIN_3) by dinotefuran (Figure 2C) but except for 0.5 μg/L (DIN_2). Similarly, the MDA contents were significantly increased at 0.1–1 μg/L (DIN_1-DIN_3) of dinotefuran (Figure 2D). The gene expressions of *cat* (catalase) and *sod* (superoxide dismutase) related to oxidative stress were significantly upregulated relative to the control group at DIN_1-DIN_3 and DIN_2-DIN_3 groups, respectively

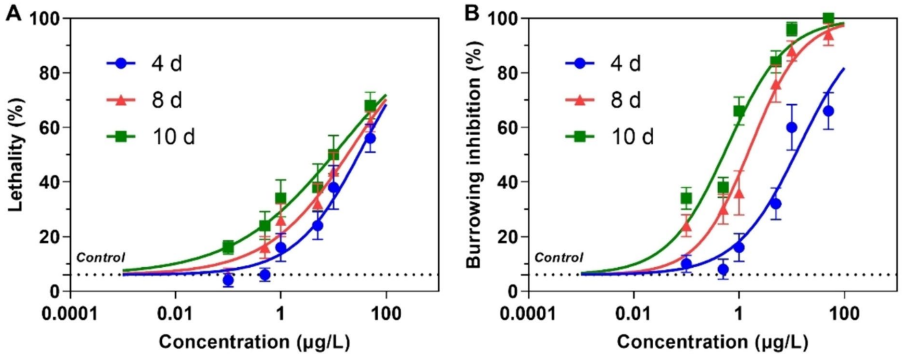

FIGURE 1
Lethality **(A)** and burrowing inhibition **(B)** of the larva of *Chironomus kiiensis* after exposure to dinotefuran. Data are expressed as mean ± standard error ($n = 5$). The dotted line represents solvent control.

TABLE 1 Effect concentrations (μg/L) of dinotefuran exposed to 1st instar larva of *Chironomus kiiensis* (Data are expressed as mean±standard error (*n*=5)).

Toxicity index	Effect concentration	4 d	8 d	10 d
Lethality (mean (95% confidence interval))	LOEC[a]	0.46 (0.15–1.61)	0.09 (0.02–0.43)	0.01 (0.002–0.12)
	LC_{10}[b]	1.40 (0.55–3.25)	0.38 (0.12–1.06)	0.08 (0.02–0.33)
	LC_{50}[c]	36.4 (21.5–61.6)	23.3 (13.0–41.6)	13.4 (6.7–26.8)
Burrowing inhibition (mean (95% confidence interval))	LOEC	0.24 (0.07–0.93)	0.06 (0.02–0.17)	0.01 (0.01–0.04)
	IC_{10}[d]	0.66 (0.24–1.72)	0.13 (0.06–0.29)	0.04 (0.02–0.08)
	IC_{50}[e]	13.9 (8.6–22.5)	1.66 (1.16–2.37)	0.60 (0.44–0.82)

[a]LOEC, lowest observed-effect concentration.
[b]LC_{10}, 10% lethal concentration.
[c]LC_{50}, median lethal concentrations.
[d]IC_{10}, 10% inhibitory concentration.
[e]IC_{50}, median inhibitory concentration.

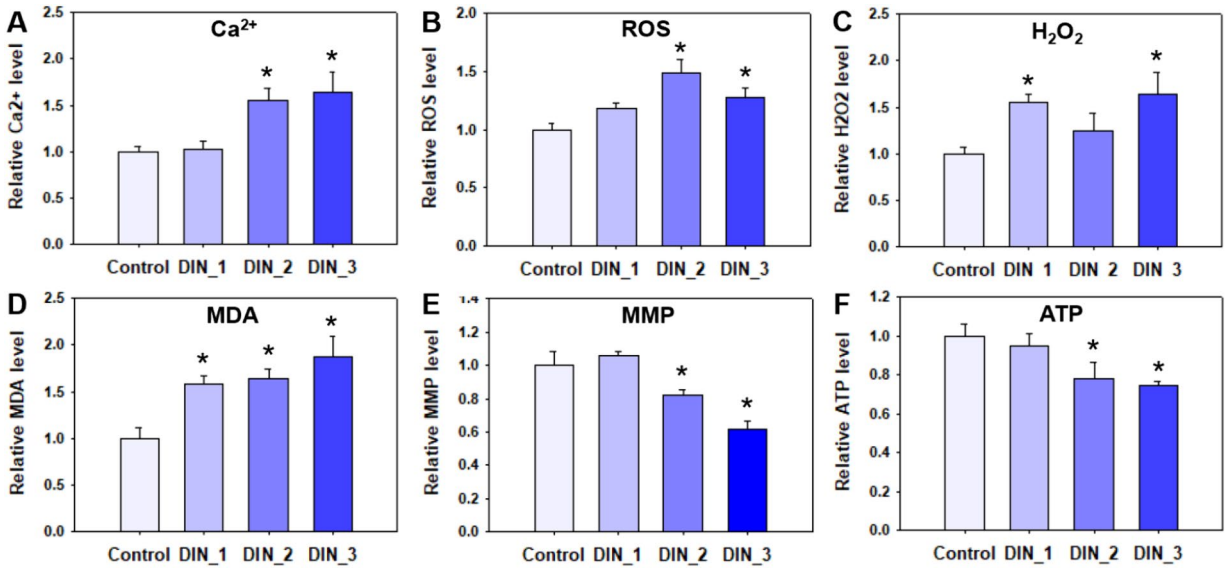

FIGURE 2
Intracellular calcium ion **(A)**, oxidative stress **(B–D)**, and mitochondria **(E,F)** indexes in 1st instar larva after exposure to dinotefuran until the first pupa appears. Data are expressed as mean ± standard error ($n = 3$). The asterisk denotes a significant difference from the solvent control ($p < 0.05$). ROS, reactive oxygen species; H_2O_2, hydrogen peroxide; MDA, malondialdehyde; MMP, mitochondrial membrane potential; ATP, adenosine triphosphate.

(Figures 3D,E). Conversely, the gene expressions of *akt* (RAC serine/threonine-protein kinase) were significantly downregulated at DIN_1–DIN_3 groups relative to the control group (Figure 3F).

3.4 Mitochondrial dysfunction

The levels of MMP and ATP were decreased after exposure to dinotefuran (Figures 2E,F). Significant reduction ($p < 0.05$) was observed at concentrations of 0.5 and 1 μg/L (DIN_2–DIN_3). In addition, the related gene expressions of *atpef0a* (F-type H^+-transporting ATPase subunit a) were significantly downregulated at 0.1–1 μg/L of dinotefuran (DIN_1–DIN_3) (Figure 4A). Other important genes, *sdha* (succinate dehydrogenase (ubiquinone) flavoprotein subunit) and *cyt b* (cytochrome b) were significantly downregulated at 0.5–1 μg/L of dinotefuran (DIN_2–DIN_3) (Figures 4B,C).

4 Discussion

Neonicotinoid insecticides are widely used as alternatives to traditional pesticides due to less toxic to mammals. They were usually detected in the environment (source water, tap water, fruit, and vegetable), even in human samples (16–19). Dinotefuran, as the third generation of neonicotinoid insecticides, was more safe for the environment and humans (3). However, our present study demonstrated that chronic (10 days) exposure to environmental concentrations (0.1–1 μg/L) of dinotefuran resulted in behavioral inhibition of the larvae, even death. Xiong et al. (6) reported that dinotefuran was detected with a mean concentration of 200 ± 296 ng/L and a maximum concentration of 802 ± 139 ng/L from a paddy field to receiving waters in the Poyang Lake basin of China. Meanwhile, dinotefuran was detected with a concentration of 12.7–75.5 ng/L in rivers near maize fields in Ontario, Canada (7) and 1.60–134 ng/L in streams across the United States (8). Our present report revealed that the LC_{10} values (0.38 (0.12–1.06) and 0.08 (0.02–0.33) μg/L) of dinotefuran after 8 and 10 days exposure to 1st instar larva of *C. kiiensis*

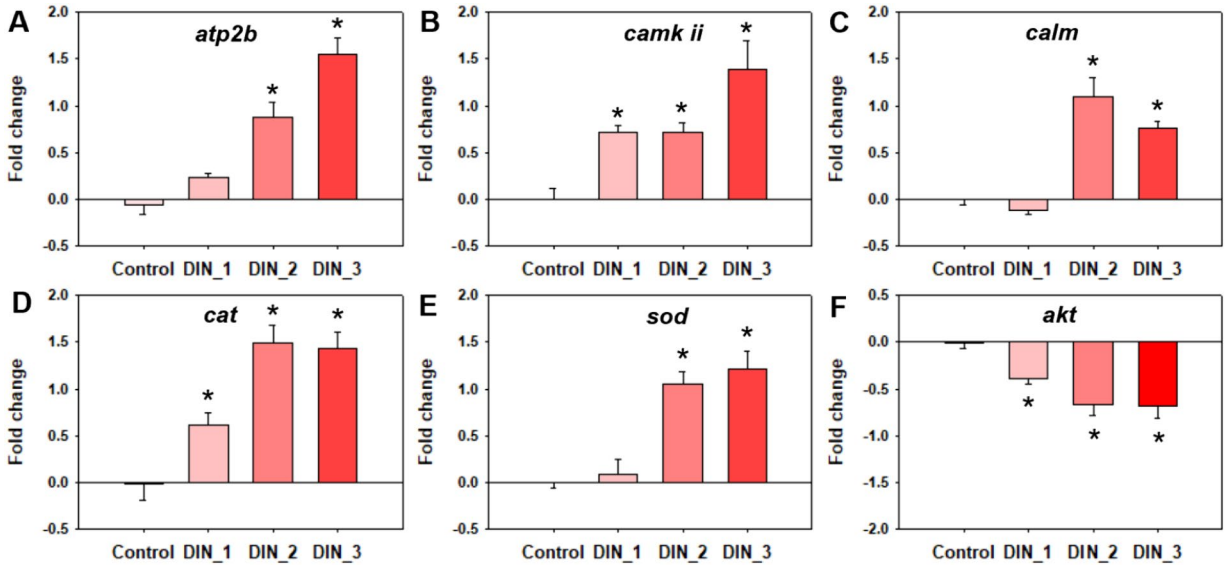

FIGURE 3
Genes expressions related to calcium ion **(A–C)** and oxidative stress **(D–F)** in 1st instar larva after exposure to dinotefuran until the first pupa appears. Data are expressed as mean ± standard error ($n = 3$). The asterisk denotes a significant difference with $p < 0.05$ compared with the solvent control.

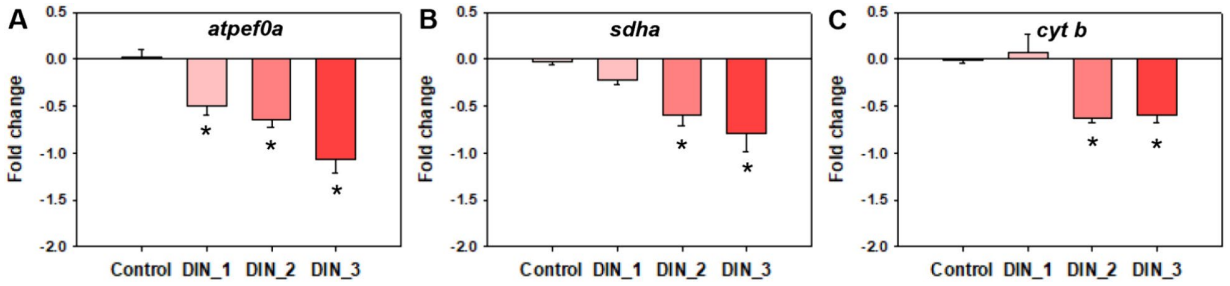

FIGURE 4
Genes expressions related to mitochondrial function **(A–C)** in 1st instar larva after exposure to dinotefuran until the first pupa appears. Data are expressed as mean ± standard error ($n = 3$). The asterisk denotes a significant difference with $p < 0.05$ compared with the solvent control.

were lower than the environmental concentrations (0.1–0.8 μg/L) (6, 8). Moreover, after 10 d exposure, the behavioral inhibition effect IC_{50} (0.60 (0.44–0.82) μg/L) was also lower than the environmental concentrations. These results suggested that choric exposure to dinotefuran in actual environment could cause lethality and paralysis to Chironomidae, even other aquatic organisms.

The toxicity target of neonicotinoids is the nAChRs of insects. First, they activate the nAChRs, then interfere with the central nervous system of insects, leading to overstimulation. Thus, insects become paralyzed and even die (11). Although the main modes of action (MoAs) of neonicotinoids to target species have been well characterized, numerous recent reports have found the unintended toxic effects of neonicotinoids on non-target organisms, even humans. Therefore, the exploration of their additional toxic mechanism has become the emerging focus of public attention. The nAChRs are pentameric ligand-gated ion channels selective for cations, including permeable to Ca^{2+}. The entry of Ca^{2+} through nAChR channels has been demonstrated to regulate Ca^{2+}-dependent cellular processes, such as the release of many neurotransmitters (20). Calcium is essential to adjust a large number of neuronal processes. Our present study demonstrated that dinotefuran enhanced Ca^{2+} influx via dysregulating the gene expressions of *atp2b*, *camk ii*, and *calm* at environmental concentrations. The gene *atp2b* is related to Ca^{2+} transporting ATPase plasma membrane. ATPase pumps played an important role in Ca^{2+} transporting (21). The gene *calm* is related to the protein Calmodulin is the predominant intracellular receptor of Ca^{2+} and is a highly conserved Ca^{2+} sensor, which is ubiquitously expressed in mammalian cells (22). The two genes *calm* and *camk ii* were involved in the synthesis of calcium ion regulatory proteins. Our previous studies also revealed that imidacloprid significantly interfered with the expressions of these genes and related proteins (15). Similarly, neonicotinoid insecticides (dinotefuran, nitenpyram, and acetamiprid) amplified Ca^{2+} influx via activating the store-operated Ca^{2+} entry (SOCE) in mice liver (23). Intracellular calcium signaling through nAChRs was activated by imidacloprid (10–100 μmol/L) in the dopaminergic Lund human mesencephalic (LUHMES) cell line (24). Imidacloprid overloaded Ca^{2+} influx by activating the nAChRs (25). However, most of the current studies did not take into account the reality of environmental concentrations, therefore most of the studies were

conducted at high concentrations of acute exposure. Given this, we selected from low to high concentrations (0.1–1 μg/L) of dinotefuran for long-term exposure to chironomids. Our results revealed that dinotefuran under environmental concentrations (0.5–1 μg/L) and 10 d exposure, disrupted the calcium signaling pathway of midge by increasing the Ca^{2+} levels. Guzman-Vallejos et al. (26) revealed that 250–500 μmol/L of imidacloprid evoked more calcium changes in differentiated human neuroblastoma cells SH-SY5Y neurons by molecular docking analysis. Taha et al. (27) reported that neonicotinoid insecticides may be involved in a CaMKK/AMPK pathway in the regulation of neuron nAChRs, meanwhile, the calcium-calmodulin-dependent protein kinase inhibitor, STO-609, inhibited currents induced by neonicotinoids and the increase of intracellular calcium. To sum up, the genes, *atp2b*, *calm*, and *camk ii* of the calcium pathway might be the key biomarkers for dinotefuran.

The increase of intracellular Ca^{2+} was closely related to the overproduction of ROS. Our results suggested that dinotefuran increased ROS levels, along with the increase of H_2O_2 and MDA concentrations. ROS are highly active radicals formed upon unpaired electrons of oxygen (e.g., hydroxyl radical (•OH) and superoxide ($•O_2^-$)). Excessive ROS in biological systems could induce oxidative stress, which is closely related to physiological and pathological processes, such as aging and the development of cancer (28). When ROS levels exceed antioxidant defense capabilities, lipids, and proteins damage would be triggered, leading to lipid peroxidation (29). Accordingly, our study found that the MDA level of the midge, an indicator for lipid peroxidation, was significantly increased after exposure to dinotefuran. Meanwhile, the expressions of three key genes (*akt*, *cat*, and *sod*) of midge were altered exposed to above 0.1 μg/L of dinotefuran. A previous study reported the disorder of calcium signaling overproduced ROS concentration (30). Li et al. (23) reported that Ca^{2+} overload caused by dinotefuran was associated with the overproduction of ROS through the manipulation of SOCE protein expression because ROS scavenger n-acetylcysteine could attenuate Ca^{2+} overload induced by neonicotinoid insecticides. Previous reports found that AKT, as the key protein of oxidative stress, was also affected by neonicotinoid insecticides. For example, the phosphorylation of AKT (p-AKT) was reduced by imidacloprid in mice and human cells (31). Imidacloprid significantly decreased the ratio of p-AKT/AKT in the SH-SY5Y cells (15). Similarly, Wang et al. (38) revealed that intracellular ROS levels were markedly raised, and the activity of the cellular antioxidant enzymes (CAT, SOD, and GPx) was diminished when chicken lymphocyte lines were exposed to 110 μg/mL imidacloprid for 24 h.

The mitochondrion is a major producer of ROS in cells. In the present study, long-term exposure to dinotefuran reduced the levels of MMP and ATP of the larva, suggesting the mitochondrial dysfunction of the larva. Ca^{2+} overload is sufficient to induce the mitochondrial permeability transition (MPT), which is important in necrosis and apoptosis (32). The opening of mitochondrial membrane permeability transport pores can cause the breakdown of MMP. The reduction of MMP which was the key factor of mitochondrial homeostasis and oxidative phosphorylation, could induce the deficiency of ATP production. Mitochondrial damage can cause an imbalance between ROS production and removal, resulting in net ROS production. Inversely, increasing ROS or decreasing ATP necessary for repair, may exacerbate mitochondrial dysfunction (33). Some previous reports revealed that mitochondria are important neonicotinoid targets (34). After exposure to environmental-related concentrations (5 and 50 μg/L) of dinotefuran for 21 days, mitochondria fusion of *Xenopus laevis* tadpoles was excessively manifested and the mitochondrial respiratory chain was also disturbed, which brought about the rise of ROS production and a reduction of the ATP levels (35). Thus, cardiotoxicity associated with mitochondrial disorders was induced by dinotefuran. Neonicotinoid insecticides imidacloprid also led to mitochondrial damage via inhibiting FoF1-ATPase activity in rats (36). The concentrations of imidacloprid in the human urinary were significantly correlative with the mitochondrial DNA copy number, suggesting the possibility of dose-dependent mitochondrial damage (37). In the present study, the expressions of mitochondria-related genes of *atpef0*a, *sdha*, and *cyt b* were significantly downregulated in exposure groups, indicating the potential biomarkers for dinotefuran. These results suggested that dinotefuran disrupted the mitochondrial electron transport chains (ETCs). *In vitro* assays based on SH-SY5Y cells, neonicotinoid inhibited the expressions of these genes encoding mitochondrial oxidative phosphorylation complexes I and III (e.g., CytB, and CYC1), while increasing the production of ROS (37). Our previous study has revealed that imidacloprid significantly decreased the expression of important genes, *atpef0a/d*, *atpev1g*, and *cox2* related to the mitochondrial pathway in larvae of *C. dilutus* (15). Additionally, 110 mg/L imidacloprid upregulated the gene expressions of mitochondrial apoptosis (*Caspase 3*, *Caspase 9*, *Bax*, and *Cyt-c*) and necroptosis (*Caspase 8*, *RIPK1*, *RIPK3*, and *MLKL*) related factors of chicken lymphocyte lines (38). Thus, the disruption of the Ca^{2+} signal pathway and mitochondrial dysfunction disrupted the nerve system by interdicting normal neurotransmission, inhibiting behaviors, and eventually leading to the death of the midge.

In summary, calcium signaling was the key biomarker for dinotefuran. The excess Ca^{2+} influx led to the ROS overproduction. The interference of the Ca^{2+}–ROS pathway would damage the mitochondrial function. Meanwhile, mitochondria are the sites of ROS production, the mitochondrial dysfunction would affect the production of ROS. Thus,

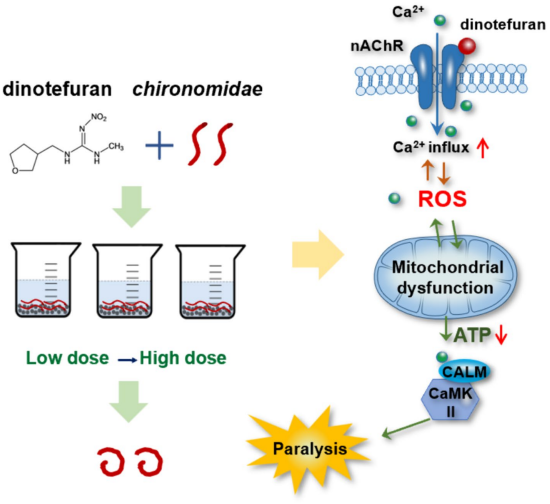

FIGURE 5
Toxicity pathway of dinotefuran acted on chironomid larvae.

the neurotransmission depended on Ca^{2+}/calmodulin-mediated signal transduction was intercepted, triggering aberrant behaviors of the midge larva (Figure 5). Meanwhile, dysregulated genes (*atp2b*, *calm*, *camk ii*, *atpef0*a, *sdha*, and *cyt b*) in these response pathways at environmental concentrations may be important early biomarkers of dinotefuran.

5 Conclusion

The mechanism by which neonicotinoids cause behavioral inhibition and thus death in insects via acting on targets has been well known. However, the discovery of a large number of new toxicities, especially for non-target organisms, has stimulated the exploration of new toxicity mechanisms. In addition, most of the past toxicity reports were based on acute toxicity studies at high concentrations. However, the environmental concentrations of neonicotinoids are relatively low. At environmental concentrations, some studies have shown neonicotinoids negatively impact the health of aquatic organisms, even humans. Therefore, it is urgent to explore the mechanism of chronic toxicity at environmental concentrations. Our present study showed that long-term (10 days) exposure to environmental concentrations of dinotefuran resulted in behavioral inhibition of the larvae, even death of the Chironomidae larvae. Dinotefuran promoted the release of intracellular Ca^{2+} in Chironomidae. Subsequently, the disruption of the calcium signaling pathway induced oxidative stress by ROS overproduction, Thus, the over-release of Ca^{2+} and ROS disordered the mitochondrial-related pathway by dysregulating the expressions of mitochondria-related genes. Our findings showed low environmental concentrations of dinotefuran caused paralysis of the midge via interfering the Ca^{2+}–ROS–mitochondria pathway. Dysregulated genes (*atp2b*, *calm*, *camk ii*, *atpef0*a, *sdha*, and *cyt b*) in these response pathways at environmental concentrations may be important early biomarkers of dinotefuran. However, more validation is necessary to support the current results. Calcium signaling and mitochondrial dysfunction were identified as the potential early warning responses for neonicotinoids, providing key biomarkers for aquatic risk assessment.

Data availability statement

All datasets generated for this study are included in the article/Supplementary material. More detailed data are available on request to the corresponding author.

Ethics statement

The manuscript presents research on animals that do not require ethical approval for their study.

Author contributions

FW: Conceptualization, Data curation, Funding acquisition, Methodology, Visualization, Writing – original draft. WG: Data curation, Investigation, Writing – original draft. FZ: Conceptualization, Supervision, Writing – review & editing. SW: Conceptualization, Investigation, Supervision, Writing – review & editing.

Funding

The author(s) declare financial support was received for the research, authorship, and/or publication of this article. This work was supported by the Natural Science Foundation of China (No. 42307369), Department of Education of Guangdong Province (No. 2021KQNCX087) and research project of Jiaying University (2021KJZ03).

Conflict of interest

The authors declare that the research was conducted in the absence of any commercial or financial relationships that could be construed as a potential conflict of interest.

Publisher's note

All claims expressed in this article are solely those of the authors and do not necessarily represent those of their affiliated organizations, or those of the publisher, the editors and the reviewers. Any product that may be evaluated in this article, or claim that may be made by its manufacturer, is not guaranteed or endorsed by the publisher.

Supplementary material

The Supplementary material for this article can be found online at: https://www.frontiersin.org/articles/10.3389/fpubh.2024.1468384/full#supplementary-material

References

1. Wang Z, Brooks BW, Zeng EY, You J. Comparative mammalian hazards of neonicotinoid insecticides among exposure durations. *Environ Int.* (2019) 125:9–24. doi: 10.1016/j.envint.2019.01.040

2. Chen X, Dong F, Liu X, Xu J, Li J, Li Y, et al. Enantioselective separation and determination of the dinotefuran enantiomers in rice, tomato and apple by HPLC. *J Sep Sci.* (2015) 35:200–5. doi: 10.1002/jssc.201100823

3. Hem L, Abd El-Aty AM, Park J-H, Shim J-H. Determination of dinotefuran in pepper using liquid chromatography: contribution to safety evaluation. *J Korean Soc Appl B.* (2012) 55:765–8. doi: 10.1007/s13765-012-2140-3

4. Sluijs JPVD, Simon-Delso N, Goulson D, Maxim L, Bonmatin JM, Belzunces LP. Neonicotinoids, bee disorders and the sustainability of pollinator services. *Curr Opin Env Sust.* (2013) 5:293–305. doi: 10.1016/j.cosust.2013.05.007

5. Morrissey CA, Mineau P, Devries JH, Sanchez-Bayo F, Liess M, Cavallaro MC, et al. Neonicotinoid contamination of global surface waters and associated risk to aquatic invertebrates: a review. *Environ Int.* (2015) 74:291–303. doi: 10.1016/j.envint.2014.10.024

6. Xiong JJ, Tan BX, Ma X, Li HZ, You J. Tracing neonicotinoid insecticides and their transformation products from paddy field to receiving waters using polar organic chemical integrative samplers. *J. Hazard. Mater.* (2021) 413:125421. doi: 10.1016/j.jhazmat.2021.125421

7. Schaafsma A, Limay-Rios V, Baute T, Smith J, Xue YG. Neonicotinoid insecticide residues in surface water and soil associated with commercial maize (corn) fields in southwestern Ontario. *PLoS One*. (2015) 10:e0118139. doi: 10.1371/journal.pone.0118139

8. Hladik ML, Kolpin DW. First national-scale reconnaissance of neonicotinoid insecticides in streams across the USA. *Environ Chem*. (2016) 13:12–20. doi: 10.1071/EN15061

9. Putri ZS, Sato T, Yamamuro M. Neonicotinoid occurrence and its potential toxicity level in tropical environmental waters of Indonesia. *Limnology*. (2023) 24:205–15. doi: 10.1007/s10201-023-00718-5

10. Thompson DA, Kolpin DW, Hladik ML, Lehmler HJ, Meppelink SM, Poch MC, et al. Prevalence of neonicotinoid insecticides in paired private-well tap water and human urine samples in a region of intense agriculture overlying vulnerable aquifers in eastern Iowa. *Chemosphere*. (2023) 319:137904. doi: 10.1016/j.chemosphere.2023.137904

11. Matsuda K, Buckingham SD, Kleier D, Rauh JJ, Grauso M, Sattelle DB. Neonicotinoids: insecticides acting on insect nicotinic acetylcholine receptors. *Trends Pharmacol Sci*. (2001) 22:573–80. doi: 10.1016/S0165-6147(00)01820-4

12. Liu T, Wang X, Xu J, You X, Chen D, Wang F, et al. Biochemical and genetic toxicity of dinotefuran on earthworms (*Eisenia fetida*). *Chemosphere*. (2017) 176:156–64. doi: 10.1016/j.chemosphere.2017.02.113

13. Tian X, Hong X, Yan S, Li X, Wu H, Lin A, et al. Neonicotinoids caused oxidative stress and DNA damage in juvenile Chinese rare minnows (*Gobiocypris rarus*). *Ecotox Environ Safe*. (2020) 197:110566. doi: 10.1016/j.ecoenv.2020.110566

14. Taenzler V, Bruns E, Dorgerloh M, Pfeifle V, Weltje L. Chironomids: suitable test organisms for risk assessment investigations on the potential endocrine disrupting properties of pesticides. *Ecotoxicology*. (2007) 16:221–30. doi: 10.1007/s10646-006-0117-x

15. Wei FH, Wang DL, Li HZ, Xia P, Ran Y, You J. Toxicogenomics provides insights to toxicity pathways of neonicotinoids to aquatic insect. *Environ Pollut*. (2020) 260:114011. doi: 10.1016/j.envpol.2020.114011

16. Luo XY, Zeng X, Wei DD, Ma CC, Li JH, Guo XH, et al. Pesticide residues in common fruits and vegetables in Henan Province. *China Food Addit Contam B*. (2023) 16:244–52. doi: 10.1080/19393210.2023.2214797

17. Qu YJ, Li AJ, Liu XQ, Lin S, Bloom MS, Wang XM, et al. Maternal serum neonicotinoids during early-mid pregnancy and congenital heart diseases in offspring: an exploratory study. *Environ Pollut*. (2023) 342:123046. doi: 10.1016/j.envpol.2023.123046

18. Wang YP, Gesang YZ, Wang Y, Yang ZC, Zhao K, Liu JQ, et al. Source and health risk of urinary neonicotinoids in Tibetan pregnant women. *Chemosphere*. (2024) 349:140774. doi: 10.1016/j.chemosphere.2023.140774

19. Xiong ZH, Wu Y, Zhou Y, He SH, Huang DY, Zhang MS, et al. Rapid determination and health risk assessment of neonicotinoids in source water and tap water of the tropical Hainan Island, China. *Environ. Sci. Pollut. R*. (2023) 23:e27026. doi: 10.1007/s11356-023-27026-w

20. Fucile S. Ca^{2+} permeability of nicotinic acetylcholine receptors. *Cell Calcium*. (2004) 35:1–8. doi: 10.1016/j.ceca.2003.08.006

21. Clapham DE. Calcium signaling. *Cell*. (2007) 131:1047–58. doi: 10.1016/j.cell.2007.11.028

22. Yamauchi T. Neuronal Ca^{2+}/Calmodulin-dependent protein kinase II—discovery, Progress in a quarter of a century, and perspective: implication for learning and memory. *Biol Pharm Bull*. (2005) 28:1342–54. doi: 10.1248/bpb.28.1342

23. Li SE, Cao Y, Pan QG, Xiao YW, Wang YL, Wang XL, et al. Neonicotinoid insecticides triggers mitochondrial bioenergetic dysfunction via manipulating ros-calcium influx pathway in the liver. *Ecotox. Environ. Safe*. (2021) 224:112690. doi: 10.1016/j.ecoenv.2021.112690

24. Loser D, Grillberger K, Hinojosa MG, Blum J, Haufe Y, Danker T, et al. Acute effects of the imidacloprid metabolite desnitro-imidacloprid on human nACh receptors relevant for neuronal signaling. *Arch Toxicol*. (2021) 95:3695–716. doi: 10.1007/s00204-021-03168-z

25. Wang X, Anadon A, Wu Q, Qiao F, Ares I, Martinez-Larranaga M-R, et al. Mechanism of neonicotinoid toxicity: impact on oxidative stress and metabolism. *Annu Rev Pharmacol Toxicol*. (2018) 58:471–507. doi: 10.1146/annurev-pharmtox-010617-052429

26. Guzman-Vallejos MS, Ramirez-Cando LJ, Aguayo L, Ballaz SJ. Molecular docking analysis at the human α7-nAChR and proliferative and evoked-calcium changes in SH-SY5Y cells by imidacloprid and acetamiprid insecticides. *Neurotox Res*. (2024) 42:12640. doi: 10.1007/s12640-024-00697-0

27. Taha M, Houchat JN, Taillebois E, Thany SH. The calcium-calmodulin-dependent protein kinase inhibitor, STO-609, inhibits nicotine-induced currents and intracellular calcium increase in insect neurosecretory cells. *J Neurochem*. (2024) 168:1281–96. doi: 10.1111/jnc.16077

28. Zhang CY, Wang X, Du JF, Gu ZJ, Zhao YL. Reactive oxygen species-regulating strategies based on nanomaterials for disease treatment. *Adv Sci*. (2021) 8:2002797. doi: 10.1002/advs.202002797

29. Schieber M, Chandel NS. ROS function in redox signaling and oxidative stress. *Curr Biol*. (2014) 24:R453–62. doi: 10.1016/j.cub.2014.03.034

30. Peng TI, Jou MJ. Oxidative stress caused by mitochondrial calcium overload. *Ann N Y Acad Sci*. (2010) 1201:183–8. doi: 10.1111/j.1749-6632.2010.05634.x

31. Kim J, Park Y, Yoon KS, Clark JM, Park Y. Imidacloprid, a neonicotinoid insecticide, induces insulin resistance. *J Toxicol Sci*. (2013) 38:655–60. doi: 10.2131/jts.38.655

32. Lemasters J, Theruvath TP, Zhong Z, Nieminen AL. Mitochondrial calcium and the permeability transition in cell death. *BBA-Bioenergetics*. (2009) 1787:1395–401. doi: 10.1016/j.bbabio.2009.06.009

33. Lin MT, Beal MF. Mitochondrial dysfunction and oxidative stress in neurodegenerative diseases. *Nature*. (2006) 443:787–95. doi: 10.1038/nature05292

34. Xu X, Wang X, Yang Y, Ares I, Martínez M, Lopez-Torres B, et al. Neonicotinoids: mechanisms of systemic toxicity based on oxidative stress-mitochondrial damage. *Arch Toxicol*. (2022) 96:1493–520. doi: 10.1007/s00204-022-03267-5

35. Zhu JP, Tao Q, Du GY, Huang L, Li M, Wang MC, et al. Mitochondrial dynamics disruption: unraveling Dinotefuran's impact on cardiotoxicity. *Environ Pollut*. (2024) 343:123238. doi: 10.1016/j.envpol.2023.123238

36. Bizerra PF, Guimaraes AR, Maioli MA, Mingatto FE. Imidacloprid affects rat liver mitochondrial bioenergetics by inhibiting FoF1-ATP synthase activity. *J Toxicol Env Heal A*. (2018) 81:229–39. doi: 10.1080/15287394.2018.1437581

37. Gu SJ, Fu LL, Wang J, Sun XH, Wang XM, Lou J, et al. MtDNA copy number in oral epithelial cells serves as a potential biomarker of mitochondrial damage by neonicotinoid exposure: a cross-sectional study. *Environ Sci Technol*. (2023) 57:15816–24. doi: 10.1021/acs.est.3c03835

38. Wang XD, Sun JT, Xu T, Lei YT, Gao MC, Lin HJ. Resveratrol alleviates imidacloprid-induced mitochondrial apoptosis, necroptosis, and immune dysfunction in chicken lymphocyte lines by inhibiting the ROS/MAPK signaling pathway. *Environ Toxicol*. (2024) 39:2052–63. doi: 10.1002/tox.24097

frontiers | Frontiers in Public Health

TYPE Mini Review
PUBLISHED 04 October 2024
DOI 10.3389/fpubh.2024.1465837

OPEN ACCESS

EDITED BY
Pu Xia,
University of Birmingham, United Kingdom

REVIEWED BY
Gaetano Settimo,
Istituto Superiore di Sanità, Italy

*CORRESPONDENCE
Katherine Simbaña-Rivera
✉ katherine.simbana101@alu.ulpgc.es

RECEIVED 16 July 2024
ACCEPTED 23 September 2024
PUBLISHED 04 October 2024

CITATION
Boada LD, Simbaña-Rivera K, Rodríguez-Pérez C, Fuentes-Ferrer M, Henríquez-Hernández LA, López-Villarrubia E and Alvarez-León EE (2024) Assessing the hidden dangers of volcanic CO_2 exposure: a critical review of health impacts.
Front. Public Health 12:1465837.
doi: 10.3389/fpubh.2024.1465837

Assessing the hidden dangers of volcanic CO_2 exposure: a critical review of health impacts

Luis D. Boada[1], Katherine Simbaña-Rivera[1,2]*, C. Rodríguez-Pérez[3], M. Fuentes-Ferrer[3], Luis Alberto Henríquez-Hernández[1], E. López-Villarrubia[4,5] and E. E. Alvarez-León[6,7]

[1]Toxicology Unit, Research Institute of Biomedical and Health Sciences (IUIBS), University of Las Palmas de Gran Canaria (ULPGC), Las Palmas de Gran Canaria, Spain, [2]Centro de Investigación para la Salud en América Latina (CISeAL), Facultad de Medicina, Pontificia Universidad Católica del Ecuador (PUCE), Quito, Ecuador, [3]Canary Health Service, University Hospital Nuestra Señora de Candelaria and Primary Care Authority of Tenerife, Santa Cruz de Tenerife, Spain, [4]General Public Health Directorate, Canarian Health Service, Las Palmas de Gran Canaria, Spain, [5]Spanish Consortium for Research on Epidemiology and Public Health (CIBERESP), Instituto de Salud Carlos III, Madrid, Spain, [6]Preventive Medicine Service, Complejo Hospitalario Universitario Insular Materno Infantil, Canary Health Service, Las Palmas de Gran Canaria, Spain, [7]Instituto Ramón y Cajal de Investigación Sanitaria (IRYCIS), Madrid, Spain

Volcanic eruptions pose significant health risks to inhabitants of affected regions, with volcanic gases, including carbon dioxide (CO_2), being a notable concern. This review examines the implications of long-term exposure to volcanic CO_2 emissions on public health, highlighting the shift in understanding from acute to chronic health effects. Recent studies have underscored the need to reevaluate the adverse health impacts of CO_2 beyond acute toxicity symptoms. While previous guidelines deemed an indoor (residential) acceptable long-term exposure range (ALTER) of ≤3,000 parts per million (ppm) in residential housing areas, emerging evidence suggests that even concentrations within the range of 3,000 to 1,000 ppm may induce deleterious health effects. International agencies now advocate for lower safe indoor CO_2 levels (600–1,000 ppm), necessitating a reassessment of public health strategies in volcanic areas. This review argues for increased awareness among local and public health authorities about the chronic toxicity of CO_2 exposure and emphasizes the importance of safeguarding populations from the adverse health effects induced by CO_2 exposure.

KEYWORDS

volcanic CO2 emissions, health risks, chronic exposure, public health, mitigation strategies

1 Introduction

Volcanism stands as one of the most potent geological phenomena, exemplifying the dynamic activity within the Earth's interior and the shifts of its crust (1). During volcanic eruptions, vast quantities of pyroclastic material, ashes, and gases are expelled, often projected over considerable distances (2). Intriguingly, around 500 million people globally reside within potential exposure zones of volcanoes, which can also induce climatic changes with global ripple effects (3, 4).

Among the array of volcanic gases, carbon dioxide (CO_2) is notably prevalent in volcanic and geothermal regions worldwide (5). It is emitted in substantial quantities by soils around

active and post-eruptive volcanoes (6, 7). While CO2, a naturally occurring trace gas in the atmosphere, is involved in essential processes such as cellular respiration, organic matter fermentation, and the combustion of fossil fuels, its elevated concentrations can be hazardous (8). The current atmospheric concentration of CO_2 is approximately 412 parts per million (ppm), or about 0.04% (9). Elevated levels of CO_2 can lead to intoxication by impacting oxygen and serum bicarbonate levels (10), and it is classified as an asphyxiant by international standards (11).

The implications of CO_2 on human health extend beyond asphyxiation (12); it poses significant risks to human health, manifesting both acute and chronic adverse effects (13). Considering that volcanic zones may continuously emit CO_2 across vast areas over extended periods, it becomes imperative to assess the health risks for potentially exposed populations (14). This exposure is notably prevalent in occupational settings such as metallurgy, welding, and the production of carbonated beverages, where CO_2 is commonly encountered (15, 16).

From a toxicological view, CO_2 is absorbed passively through the lungs and is primarily excreted via the lungs after being transported in the blood as bicarbonate, a process facilitated by the enzyme carbonic anhydrase (17).

Cases of CO_2 poisoning have been documented in medical literature since the 1950s (18), often resulting from accidental exposure to CO_2 from sources such as dry ice, fermentation, or inadvertently opened liquid CO_2 tanks (19). Additionally, cases of CO_2 poisoning stemming from suicide attempts or even homicides have been reported (20). Notably, fatalities from asphyxiation due to the accumulation of CO_2 from volcanic sources have also been recorded (3, 5, 21).

Populations residing in volcanic regions, whether active or dormant, face significant risks from diffuse CO_2 emissions. Anomalous gas emissions are a common occurrence in areas with recent volcanic activity (7, 22, 23). Particularly vulnerable are areas where residential and tourist activities converge near emission sites, such as Colli Albani (Italy), and Stromboli and Vulcano Islands (Aeolian Archipelago, Italy) (23, 24), Rotorua city in New Zealand (25), La Palma Island in the Canary Islands (Spain) (26), and Sao Miguel Island in Azores Archipelago (Portugal) (27). Some of these areas feature sites of continuous high gas emission, with intermittent periods of increased release.

Considering these factors, the aim of this study is to assess the adverse effects experienced by populations inadvertently exposed to volcanic CO_2. Given the scarcity of comprehensive data on health risks associated with volcanic CO_2 exposure beyond its fatal outcomes, this critical review synthesizes both scientific and gray literature to assess the chronic and acute health risks to populations exposed to variable CO_2 concentrations.

Abbreviations: CO2, carbon dioxide; ppm, parts per million; WHO, World Health Organization; ILO, International Labor Organization; OECD, Organization for Economic Co-operation and Development; OSHA, Occupational Safety and Health Administration; NIOSH, National Institute for Occupational Safety & Health; CDC, Centers for Disease Control and Prevention; ALTER, acceptable long-term exposure range; TWA, time-weighted average; EPA, Environmental Protection Agency.

2 Toxic effects of CO_2: current understanding

As previously discussed, CO_2 is not inherently toxic, although it could also act as a toxicant. It constitutes a component of air (412 ppm), and it is generated and employed in many human processes.

The gas's odorless and colorless nature renders detection without specific testing devices impossible, and its high density in comparison to oxygen and nitrogen results in high concentrations being condensed in the lower layers of both indoor and outdoor air, heightening its danger. CO_2 may accumulate in lower spaces, leading to oxygen deficiency. Consequently, CO_2 concentrations tend to be higher in environments such as mines, sugar refineries, distilleries, grain silos, and drains (28).

Although CO_2 emissions from volcanic sites can indeed be fatal, such incidents are rare. However, it is crucial to remember that CO_2 was implicated in the deaths of approximately 1,700 people in Cameroon, West Africa, in 1986 (as well as a similar event at Lake Monoun, also in Cameroon, in 1984) following a massive release of gas from these volcanic crater lakes (29, 30). Similarly, on February 20, 1979, in Dieng Plateau (Indonesia), 149 people perished and 1,000 others were injured after being enveloped in a gas cloud produced by a phreatic eruption (24, 31).

In addition to these major incidents, recent fatal accidents in Western countries have also been attributed to exposure to high concentrations of volcanic-origin CO_2. Notably, during a period of significant degassing at La Fossa crater in the 1980s, two children and numerous small wild animals lost their lives on Vulcano Island, Italy. During this time, emissions reached up to 1,350 tons per day, with outdoor CO_2 concentrations recorded as high as 9.8% (98,000 ppm) (32). Moreover, D'Alessandro and Kyriakopoulos (2013) reported three additional fatalities in the 1990s linked to CO_2 accumulation in the Pausanias thermal baths on the northern coast of the Methana Peninsula (Greece) (14). In 1992, two fatalities were reported in the Azores archipelago, Portugal, inside a lava cave where diffusely released CO_2 reached indoor concentrations of 10% (100,000 ppm) (21). Furthermore, in 1998, other fatality was reported in Mammoth Mountain (California, United States) when a cross-country skier fell into a snow well where CO_2 concentration soared to 70% (33). Interestingly, in some of these cases, the recorded CO_2 concentrations were not excessively high, suggesting that even initial exposure to low concentrations can be hazardous. This is attributed to the fact that exposure to gradually increasing CO_2 concentrations, starting from atmospheric levels, can induce unconsciousness due to the narcotic properties of CO_2, often without the victims perceiving any imminent danger (34, 35).

Additionally, the significant tourist activity in volcanic regions and geothermal fields globally necessitates attention to the risks faced by tourists in degassing zones. This is particularly crucial in coastal areas where tourists might be sunbathing close to the ground, a position that increases the risk of inhaling concentrated CO_2 in the absence of wind. Monitoring activities that could lead to exposure to high CO_2 concentrations is therefore essential for the safety of visiting tourists. Notably, cases of intoxication among tourists have been documented in volcanic regions. Documented cases of CO_2 intoxication among tourists in volcanic regions underscore this risk. For instance, in April 2015, a 9-year-old French child experienced severe intoxication from gases emitted by an undersea vent near the

shoreline on Vulcano Island, Italy (36). In 2019, three fatalities were reported among tourists visiting the "Solfatara," geothermal area near Naples, Italy (37). Moreover, tourists in Sao Miguel (Azores Islands, Portugal), Hawaii (Hawaiian Islands, United States), and Mammoth Mountain (California, United States) have also suffered adverse health effects due to CO_2 exposure (38–41).

The intoxications mentioned above can be attributed to the fact that CO_2 poisoning typically involves life-threatening hypoxia and hypercapnia, resulting in varying levels of consciousness impairment ranging from drowsiness and confusion to deep coma and respiratory acidosis. In cases of inadvertent exposure to increasing CO_2 levels, severe hypercapnia can lead to cerebral edema and respiratory center paralysis. Podlewski et al. have stated that CO_2 concentrations of up to 1% (10,000 ppm) may induce drowsiness in some individuals, while concentrations above 3% (30,000 ppm) can disrupt gas exchange at the pulmonary membrane, altering pH and causing hypercapnia associated with brain damage and loss of consciousness. Breathing air with CO_2 concentrations exceeding 5% (50,000 ppm) can lead to breathlessness, anxiety, and stimulation of the respiratory center. At levels between 7 and 10%, individuals may experience dizziness, headaches, visual and auditory impairments, and may rapidly become unconscious. It has been documented that CO_2 concentrations of 9% inhaled for more than 10 min, and higher concentrations inhaled for less than 10 min, are poorly tolerated or not tolerated at all due to symptoms including exhaustion, anxiety, dissociation, or acidosis (pH < 7.2), despite normal oxygenation (42). Concentrations exceeding 10% are known to cause hallucinations and significantly impaired consciousness, potentially resulting in coma and convulsions. Furthermore, exposure to concentrations above 20% (200,000 ppm) typically results in death within minutes, while levels exceeding 30% (300,000 ppm) lead to instantaneous death (43). Acute effects of CO_2 intoxication are shown in Table 1.

International recommendations and occupational guidelines regarding indoor CO_2 levels suggest a time-weighted average (TWA) of 5,000 ppm (0.5%; for an 8-h weighted average) or a short-term TWA (15 min) of 30,000 ppm (44, 45). However, considering that elevated CO_2 levels may disrupt placental development, it is essential to provide specific protection for pregnant women. Consequently, the US Navy's toxicity experts have lowered short-term exposure limits and 24-h emergency exposure limits for submarines with female crew members to 0.8% (8,000 ppm) (46). In fact, most countries have set references values between 1,000 ppm to 1800 ppm in school, and working environments (47).

TABLE 1 Short-term effects based on CO_2 concentration levels.

CO_2 concentration (ppm)	Short-term effects
1,000–10,000	Drowsiness, headache, fatigue, concentration difficulties
10,000–30,000	Dizziness, headache, visual and auditory impairments, rapid onset of unconsciousness
30,000–50,000	Severe hypercapnia, breathlessness, anxiety, stimulation of the respiratory center
50,000–98,000	Increased risk of unconsciousness, severe intoxication symptoms (e.g., exhaustion, anxiety, dissociation, acidosis with intact oxygenation)
>100,000	Hallucinations, impaired consciousness, coma, convulsions
>200,000	Death within minutes
>300,000	Instant death

ppm, parts per million.

Although low levels of CO_2 have long been regarded as a toxicant with no immediate lethal effects, recent studies have sparked interest in its potential health implications, particularly concerning chronic and/or intermittent long-term exposure. Such exposure has been associated with pathological conditions, including DNA alterations, nasal inflammation, and pulmonary inflammation (48). Notably, during the SARS-CoV-2 pandemic, the wearing of face masks has contributed to increased resistance and dead space volume, resulting in the re-breathing of CO_2. Elevated blood CO_2 levels are a key feature of the *Mask-Induced Exhaustion Syndrome* (49). In addition, rising indoor CO_2 concentrations have been associated with symptoms characteristic of *Sick Building Syndrome*. These symptoms include headache, drowsiness, lethargy, tiredness, mental fatigue, reduction in decision-making performance, dizziness, as well as upper respiratory and mucosal symptoms, and skin irritation, such as itching, stinging, or dryness (50–52).

Nevertheless, given the current global trend of rising outdoor atmospheric CO_2 concentrations, it is imperative to re-evaluate the effects of low-level CO_2 exposure on human health. Indeed, it has been documented that CO_2 can produce various hazardous health effects even at relatively low concentrations (13, 51). Long-term exposure to air polluted with CO_2 from soil diffuse degassing sites has been linked to an increased risk of developing pulmonary restrictive diseases and exacerbating chronic obstructive pulmonary diseases, particularly among asthmatic and older adults (53). Residents of volcanic areas chronically exposed to high concentrations of CO_2, such as Furnas in the Azores Islands, Portugal, exhibit a high incidence of chronic bronchitis and other respiratory disorders (54). Likewise, a high prevalence of non-infectious respiratory diseases has been observed among residents living in geothermal areas, such as Rotorua, New Zealand (25). Even more so, recent studies suggest that increased CO_2 exposure may contribute to obesity, potentially playing a role in the rising trends of obesity and diabetes after chronic exposures to around 500 ppm CO_2 (55–57).

Considering these findings, it is worth noting that while an acceptable long-term exposure range (ALTER) of ≤3,000 ppm for CO_2 in residential indoor air had initially been established (58), Satish reported that even indoor concentrations ranging from 3,000 to 1,000 ppm may lead to deleterious health effects. These effects include mucous membrane or respiratory symptoms, decreased test performance, and neurophysiological symptoms (e.g., headache, fatigue) (51). Gall et al. define a level of concern for CO_2 exposure, particularly regarding adverse cognitive impacts, as average personal exposure exceeding 1,000 ppm for exposures greater than 2.5 h (59). Consequently, international agencies have adopted an acceptable long-term exposure range (ALTER) of ≤1,000 ppm for CO_2 in residential indoor air (54, 56).

Furthermore, although not directly related to the harmful effects of CO_2, it is pertinent to note that CO_2 naturally carries radioactive radon gas, a well-known carcinogen (60). Long-term

inhalation exposure to radon has been linked to respiratory disorders and lung cancer (61, 62). Higher cancer incidence rates have been reported in volcanic areas compared to non-volcanic areas, with CO_2 potentially acting as a carrier for radon gas (63). Populations residing in volcanic areas with chronic exposure to environmental factors resulting from volcanic activity show a higher risk of certain cancers, such as lip, oral cavity, pharynx, and breast cancers (64). Indeed, biomonitoring studies in the Azores Islands, Portugal, have revealed a higher incidence of micronucleated cells in oral epithelium (a recognized predictive biomarker of cancer risk) in individuals inhabiting volcanically active environments, suggesting an increased risk of cancer (65), thus underscoring the need for further investigation into the health effects of low levels of CO_2 long-term exposure. Potential adverse health effects related to long-term CO_2 exposure are summarized in Table 2.

3 Discussion

In light of these considerations, akin to urban populations residing in highly polluted regions, it is evident that safeguarding the inhabitants of volcanic areas from the adverse effects associated with relatively low-dose/long-term CO_2 inadvertent exposure is imperative.

In volcanic regions featuring degassing sites, all the subtle/chronic effects of CO_2 must be duly considered by Public Health Authorities when implementing measures aimed at reducing gas concentrations and mitigating the associated health risks. While ventilation with ambient air is a common strategy for reducing indoor CO_2 levels, it may not always be suitable in volcanic degassing sites where outdoor CO_2 levels are also elevated. Consequently, in such instances, evacuating volcanic/geothermal areas may be necessary, mirroring the evacuation ordered in the Port of Volcano (Volcano Island, Italy) in 2021 when outdoor CO_2 levels of approximately 12.5% (125.000 ppm) were recorded (66). This proactive approach should be prioritized by Public Health Authorities in volcanic regions where sporadic and unpredictable releases of CO_2 may occur, resulting in inadvertent population exposure to escalating CO_2 levels (27).

Moreover, the existence of population subgroups more susceptible to the toxic effects of CO_2 must also be taken into consideration. For instance, the exposure of older adults, pregnant women, cardiac or pulmonary patients, and children to CO_2 warrants careful oversight (46, 49).

TABLE 2 Potential chronic adverse health effects related to long-term (chronic/intermittent) CO_2 exposure.

Mental fatigue, impaired work performance, decrements in decision-making performance
Development of restrictive lung diseases,
Exacerbation of chronic obstructive pulmonary diseases
Increased incidence of chronic bronchitis
Potential contribution to obesity and diabetes
DNA damage
Elevated cancer risk
Lung cancer

DNA, Deoxyribonucleic Acid.

In this scenario, in volcanic regions it would be necessary to be able to set dangerous levels at which chronic CO_2 exposure capable of producing subtle health effects is occurring. Unfortunately, measurement of bicarbonate levels or blood pH in populations chronically exposed to increasing CO_2 concentrations is neither useful, nor possible, as arterial blood gasometry tests are invasive and cannot be repeated continuously for an individual tracking. Similarly, while the quantification of exhaled CO_2 through capnography is valuable for assessing hypoventilation, there is no scientific evidence supporting its efficacy in diagnosing CO_2 intoxication or exposure. In fact, to diagnose chronic or even acute CO_2 intoxication, exposure to this gas must be confirmed in a manner akin to practices in forensic and occupational medicine (15, 19), namely, by quantifying the CO2 levels in the suspected area. In any case, in long-term exposures, it may be possible to rely on the presence of neurophysiological symptoms, (e.g., headache, or fatigue), and to perform decision-making tests, as described by Satish et al.

Implementing measures to protect the population from anthropogenic high indoor CO_2 levels is feasible, given the extensive regulations and recommendations governing indoor CO_2 exposure levels both internationally and occupationally. However, mitigating the effects or controlling emissions from outdoor CO_2 sources poses significant challenges, being enormously complex and often hardly feasible.

Indeed, outdoor CO_2 concentrations are not typically regulated, and research into the toxic effects of CO_2 in open environments remains scarce. In the context of volcanic degassing sites, Public Health faces several challenges. These include the inability to control emission sources, which often produce unpredictable peaks of extremely high CO_2 levels, and the absence of regulatory thresholds. This is due to limited evidence on the health effects of CO_2 exposure on the general population, both short- and long-term, which complicates decision-making processes.

Further prospective studies are warranted to advance our understanding of the chronic health effects of volcanic emissions, including gases like CO_2, as well as aerosols and ashes. Ongoing studies, such as the studies on the island of La Palma (Spain), could be instrumental in defining safe versus dangerous concentrations of CO_2 for the population (65, 66). This would enable International Agencies and institutions to establish guidelines and recommendations for protecting health in outdoor areas affected by volcanic gas emissions. Such insights would be invaluable for Local Authorities in conducting health impact assessments and making informed planning decisions, especially concerning the placement of human settlements in volcanic zones.

In summary, although the scientific evidence on lethal incidents due to CO_2 degassing in volcanic zones is generally limited, the potential for such incidents cannot be ignored, particularly in active volcanic areas where extraordinarily high concentrations of CO_2 have been recorded both indoors and outdoors. This is particularly concerning in areas with significant residential and tourist activity.

Considering the "precautionary principle" in health impact assessments, which emphasizes the avoidance of unnecessary risks to population health (67). In case of population exposed to volcanic emissions, Public Health Authorities have adopted several measures to prevent or minimize individual hazards. These measures included: (a) Establishing a sensor network to continuously monitor CO_2 concentrations indoors and outdoors (68); (b) Strictly controlling

access to areas with the highest CO_2 concentrations to mitigate the risk of accidental exposures in areas with elevated (potentially lethal) CO_2 levels (66); (c) Prioritizing efforts to keep vulnerable populations (children, older adults, pregnant women, individuals with pre-existing respiratory or cardiovascular conditions) away from such areas (49); (d) Enhancing information dissemination to affected populations (including tourists) through informative meetings to foster cooperation and shared responsibility for the implemented measures (40). Thus, raising awareness and disseminating information about the "hidden" dangers of CO_2 is essential.

Finally, as highlighted by Pefferkorn et al., it is crucial not to overlook the importance of adhering to safety protocols and utilizing appropriate respiratory protection near eruptive zones, even in open environments, due to the potential invisible dangers posed by volcanic areas (69).

Author contributions

LB: Conceptualization, Formal analysis, Investigation, Methodology, Project administration, Supervision, Validation, Visualization, Writing – original draft, Writing – review & editing. KS-R: Formal analysis, Funding acquisition, Investigation, Methodology, Supervision, Validation, Visualization, Writing – original draft, Writing – review & editing. CR-P: Writing – original draft, Writing – review & editing. MF-F: Writing – original draft, Writing – review & editing. LH-H: Writing – original draft, Writing – review & editing. EL-V: Writing – original draft, Writing – review & editing. EA-L: Writing – original draft, Writing – review & editing.

Funding

The authors declare that no financial support was received for the research and authorship. However, the publication fees related to this manuscript was financed by Pontificia Universidad Católica del Ecuador (PUCE).

Conflict of interest

The authors declare that this research was carried out in the absence of any commercial or financial relationships that could be perceived as a potential conflict of interest.

Publisher's note

References

1. Fabricio Neta A d B, do Nascimento CWA, Biondi CM, van Straaten P, Bittar SMB. Natural concentrations and reference values for trace elements in soils of a tropical volcanic archipelago. *Environ Geochem Health*. (2018) 40:163–73. doi: 10.1007/s10653-016-9890-5

2. Ruggieri F, Saavedra J, Fernandez-Turiel JL, Gimeno D, Garcia-Valles M. Environmental geochemistry of ancient volcanic ashes. *J Hazard Mater*. (2010) 183:353–65. doi: 10.1016/j.jhazmat.2010.07.032

3. Hansell AL, Horwell CJ, Oppenheimer C. The health hazards of volcanoes and geothermal areas. *Occup Environ Med*. (2006) 63:149–25. doi: 10.1136/oem.2005.022459

4. Sasidharan S, Dhillon HS. Health hazards from a volcano eruption. *Am J Emerg Med*. (2022) 56:254–6. doi: 10.1016/j.ajem.2021.06.063

5. Hansell A, Oppenheimer C. Health hazards from volcanic gases: a systematic literature review. *Archives Environ Heal: Int J*. (2004) 59:628–39. doi: 10.1080/00039890409602947

6. Allard P, Carbonnelle J, Dajlevic D, Bronec JL, Morel P, Robe MC, et al. Eruptive and diffuse emissions of CO2 from Mount Etna. *Nature*. (1991) 351:387–91. doi: 10.1038/351387a0

7. Chiodini G, Cioni R, Guidi M, Raco B, Marini L. Soil CO2 flux measurements in volcanic and geothermal areas. *Appl Geochem*. (1998) 13:543–52. doi: 10.1016/S0883-2927(97)00076-0

8. International volcanic health Hazard network (IVHHN). Health impacts of volcanic gases. (2020). Available from: https://www.ivhhn.org/information/health-impacts-volcanic-gases (Accessed on 2024 Feb 26)

9. Cui Y, Schubert BA, Jahren AH. A 23 m.y. record of low atmospheric CO2. *Geology*. (2020) 48:888–92. doi: 10.1130/G47681.1

10. Dunford JV, Lucas J, Vent N, Clark RF, Cantrell FL. Asphyxiation due to dry ice in a walk-in freezer. *J Emerg Med*. (2009) 36:353–6. doi: 10.1016/j.jemermed.2008.02.051

11. Organisation for economic co-operation and development (OECD). Guidelines for the testing of chemicals. (2023). Available from: https://www.oecd.org/chemicalsafety/testing/oecdguidelinesforthetestingofchemicals.htm (Accessed on 2024 Feb 26)

12. Permentier K, Vercammen S, Soetaert S, Schellemans C. Carbon dioxide poisoning: a literature review of an often forgotten cause of intoxication in the emergency department. *Int J Emerg Med*. (2017) 10:14. doi: 10.1186/s12245-017-0142-y

13. Azuma K, Kagi N, Yanagi U, Osawa H. Effects of low-level inhalation exposure to carbon dioxide in indoor environments: a short review on human health and psychomotor performance. *Environ Int*. (2018) 121:51–6. doi: 10.1016/j.envint.2018.08.059

14. D'Alessandro W, Kyriakopoulos K. Preliminary gas hazard evaluation in Greece. *Nat Hazards*. (2013) 69:1987–2004. doi: 10.1007/s11069-013-0789-5

15. Oyama I, Tajima Y, Ojima T, Iida A. Exposure to high concentrations of carbon dioxide during transporting a cadaver preserved with dry ice inside an ambulance vehicle. *Forensic Toxicol*. (2023) 41:179–82. doi: 10.1007/s11419-022-00644-8

16. Kettner M, Ramsthaler F, Juhnke C, Bux R, Schmidt P. A fatal case ofCO2Intoxication in a fermentation tank. *J Forensic Sci*. (2013) 58:556–8. doi: 10.1111/1556-4029.12058

17. Langford NJ. Carbon dioxide poisoning. *Toxicol Rev*. (2005) 24:229–35. doi: 10.2165/00139709-200524040-00003

18. Williams HI. Carbon dioxide poisoning. *Br Med J*. (1958) 2:1012–4. doi: 10.1136/bmj.2.5103.1012

19. Scott JL, Kraemer DG, Keller RJ. Occupational hazards of carbon dioxide exposure. *J Chem Health Saf*. (2009) 16:18–22. doi: 10.1016/j.jchas.2008.06.003

20. Sautter J, Gapert R, Tsokos M, Oesterhelweg L. Murder-suicide by carbon dioxide (CO2) poisoning: a family case from Berlin, Germany. *Forensic Sci Med Pathol*. (2014) 10:97–102. doi: 10.1007/s12024-013-9495-6

21. Viveiros F, Gaspar JL, Ferreira T, Silva C. Hazardous indoor CO2 concentrations in volcanic environments. *Environ Pollut*. (2016) 214:776–86. doi: 10.1016/j.envpol.2016.04.086

22. Barberi F, Carapezza ML. Helium and CO2 soil gas emission from Santorini (Greece). *Bull Volcanol*. (1994) 56:335–42. doi: 10.1007/BF00326460

23. Carapezza ML, Badalamenti B, Cavarra L, Scalzo A. Gas hazard assessment in a densely inhabited area of Colli Albani volcano (cava Dei Selci, Roma). *J Volcanol Geotherm Res*. (2003) 123:81–94. doi: 10.1016/S0377-0273(03)00029-5

24. Madonia P, Cangemi M, Colajanni M, Winkler A. Atmospheric concentration of CO2 and PM2.5 at Salina, Stromboli, and Vulcano Islands (Italy): how anthropogenic sources, ordinary volcanic activity and unrests affect air quality. *Int J Environ Res Public Health*. (2022) 19:4833. doi: 10.3390/ijerph19084833

25. Durand M, Wilson JG. Spatial analysis of respiratory disease on an urbanized geothermal field. *Environ Res*. (2006) 101:238–45. doi: 10.1016/j.envres.2005.08.006

26. Padilla GD, Barrancos J, Hernández PA, Díaz AJÁ, Pérez NM, Pérez AMG, et al. Air CO2 monitoring network in the urban areas of Puerto naos and La Bombilla, La Palma, Canary Islands. Copernicus Meetings; (2023). Available from: https://meetingorganizer.copernicus.org/EGU23/EGU23-4188.html (Accessed on 2024 Mar 12)

27. Viveiros F, Gaspar JL, Ferreira T, Silva C, Marcos M, Hipólito A. Chapter 14 mapping of soil CO2diffuse degassing at São Miguel Island and its public health implications. *Geol Soc Lond Mem*. (2015) 44:185–95. doi: 10.1144/M44.14

28. World Health Organization/International Labour Organization (WHO/ILO). International Chemical Safety Cards, Card 0021: carbon dioxide. (2018). Available from: https://www.ilo.org/dyn/icsc/showcard.display?p_lang=en&p_card_id=0021&p_version=2 (Accessed on 2024 Feb 26)

29. Baxter PJ, Kapila M, Mfonfu D. Lake Nyos disaster, Cameroon, 1986: the medical effects of large scale emission of carbon dioxide? *BMJ*. (1989) 298:1437–41. doi: 10.1136/bmj.298.6685.1437

30. Baxter PJ, Tedesco D, Miele G, Baubron JC, Cliff K. Health hazards of volcanic gases. *Lancet*. (1990) 336:176. doi: 10.1016/0140-6736(90)91695-7

31. International volcanic health Hazard network (IVHHN). Volcanic gases and aerosols guidelines. (2022). Available from: https://www.ivhhn.org/images/pdf/gas_guidelines.pdf (Accessed on 2024 Mar 12)

32. Carapezza ML, Barberi F, Ranaldi M, Ricci T, Tarchini L, Barrancos J, et al. Diffuse CO2 soil degassing and CO2 and H2S concentrations in air and related hazards at Vulcano Island (Aeolian arc, Italy). *J Volcanol Geotherm Res*. (2011) 207:130–44. doi: 10.1016/j.jvolgeores.2011.06.010

33. Hill PM. Possible asphyxiation from carbon dioxide of a cross-country skier in eastern California: a deadly volcanic hazard. *Wilderness Environ Med*. (2000) 11:192–5. doi: 10.1580/1080-6032(2000)011[0192:PAFCDO]2.3.CO;2

34. Seevers M. The narcotic properties of carbon dioxide. *NY State J Med*. (1944) 44:597–602.

35. Gill M, Natoli MJ, Vacchiano C, MacLeod DB, Ikeda K, Qin M, et al. Effects of elevated oxygen and carbon dioxide partial pressures on respiratory function and cognitive performance. *J Appl Physiol*. (2014) 117:406–12. doi: 10.1152/japplphysiol.00995.2013

36. Diliberto IS, Cangemi M, Gagliano AL, Inguaggiato S, Jacome Paz MP, Madonia P, et al. Volcanic gas Hazard assessment in the Baia di Levante area (Vulcano Island, Italy) inferred by geochemical investigation of passive fluid degassing. *Geosciences*. (2021) 11:478. doi: 10.3390/geosciences11110478

37. Carfora A, Campobasso CP, Cassandro P, la Sala F, Maiellaro A, Perna A, et al. Fatal inhalation of volcanic gases in three tourists of a geothermal area. *Forensic Sci Int*. (2019) 297:e1–7. doi: 10.1016/j.forsciint.2019.01.044

38. Sorey ML, Evans WC, Kennedy BM, Farrar CD, Hainsworth LJ, Hausback B. Carbon dioxide and helium emissions from a reservoir of magmatic gas beneath Mammoth Mountain, California. *J Geophys Res Solid Earth*. (1998) 103:15303–23. doi: 10.1029/98JB01389

39. Baxter PJ, Baubron JC, Coutinho R. Health hazards and disaster potential of ground gas emissions at Furnas volcano, São Miguel, Azores. *J Volcanol Geotherm Res*. (1999) 92:95–106. doi: 10.1016/S0377-0273(99)00070-0

40. Heggie TW. Reported fatal and non-fatal incidents involving tourists in Hawaii volcanoes National Park, 1992–2002. *Travel Med Infect Dis*. (2005) 3:123–31. doi: 10.1016/j.tmaid.2004.09.004

41. Heggie TW. Geotourism and volcanoes: health hazards facing tourists at volcanic and geothermal destinations. *Travel Med Infect Dis*. (2009) 7:257–61. doi: 10.1016/j.tmaid.2009.06.002

42. van der Schrier R, van Velzen M, Roozekrans M, Sarton E, Olofsen E, Niesters M, et al. Carbon dioxide tolerability and toxicity in rat and man: a translational study. *Front Toxicol*. (2022) 4:1001709. doi: 10.3389/ftox.2022.1001709

43. Podlewski R, Płotek W, Grześkowiak M, Małkiewicz T, Frydrysiak K, Żaba Z. Carbon dioxide as a potential danger to medical rescue teams at work–a case study. *Med Pr*. (2017) 68:135–8. doi: 10.13075/mp.5893.00408

44. Occupational safety and health administration (OSHA). Permissible Exposure Limits. (2019). Available from: https://www.osha.gov/annotated-pels/table-z-1 (Accessed on 2024 Mar 12)

45. Centers for Disease Control and Prevention (CDC). National Institute for Occupational Safety and Health (NIOSH) - pocket guide to chemical hazards - carbon dioxide. (2019). Available from: https://www.cdc.gov/niosh/npg/npgd0103.html (Accessed on 2024 Mar 12)

46. Howard WR, Wong B, Yeager KSB, Stump DG, Edwards T, Arden James R, et al. Submarine exposure guideline recommendations for carbon dioxide based on the prenatal developmental effects of exposure in rats. *Birth Defects Res*. (2019) 111:26–33. doi: 10.1002/bdr2.1417

47. Settimo G, Yu Y, Gola M, Buffoli M, Capolongo S. Challenges in IAQ for indoor spaces: a comparison of the reference guideline values of indoor air pollutants from the governments and international institutions. *Atmosfera*. (2023) 14:633. doi: 10.3390/atmos14040633

48. Guais A, Brand G, Jacquot L, Karrer M, Dukan S, Grévillot G, et al. Toxicity of carbon dioxide: a review. *Chem Res Toxicol*. (2011) 24:2061–70. doi: 10.1021/tx200220r

49. Kisielinski K, Wagner S, Hirsch O, Klosterhalfen B, Prescher A. Possible toxicity of chronic carbon dioxide exposure associated with face mask use, particularly in pregnant women, children and adolescents – a scoping review. *Heliyon*. (2023) 9:e14117. doi: 10.1016/j.heliyon.2023.e14117

50. Apte MG, Fisk WJ, Daisey JM. Associations between indoor CO2Concentrations and sick building syndrome symptoms in U.S. office buildings: an analysis of the 1994-1996 BASE study data. *Indoor Air*. (2000) 10:246–57. doi: 10.1034/j.1600-0668.2000.010004246.x

51. Satish U, Mendell MJ, Shekhar K, Hotchi T, Sullivan D, Streufert S, et al. Is CO2 an indoor pollutant? Direct effects of low-to-moderate CO2 concentrations on human decision-making performance. *Environ Health Perspect*. (2012) 120:1671–7. doi: 10.1289/ehp.1104789

52. Tsai DH, Lin JS, Chan CC. Office workers' sick building syndrome and indoor carbon dioxide concentrations. *J Occup Environ Hyg*. (2012) 9:345–51. doi: 10.1080/15459624.2012.675291

53. Linhares D, Garcia PV, Viveiros F, Ferreira T. Air pollution by hydrothermal volcanism and human pulmonary function. *Biomed Res Int*. (2015) 2015:e326794:1–9. doi: 10.1155/2015/326794

54. Navarro-Sempere A, Segovia Y, Rodrigues AS, Garcia PV, Camarinho R, García M. First record on mercury accumulation in mice brain living in active volcanic environments: a cytochemical approach. *Environ Geochem Health*. (2021) 43:171–83. doi: 10.1007/s10653-020-00690-4

55. Hersoug LG, Sjödin A, Astrup A. A proposed potential role for increasing atmospheric CO2 as a promoter of weight gain and obesity. *Nutr & Diabetes*. (2012) 2:e31–1. doi: 10.1038/nutd.2012.2

56. Zheutlin AR, Adar SD, Park SK. Carbon dioxide emissions and change in prevalence of obesity and diabetes in the United States: an ecological study. *Environ Int*. (2014) 73:111–6. doi: 10.1016/j.envint.2014.07.012

57. Chen JK, Wu C, Su TC. Positive association between indoor gaseous air pollution and obesity: an observational study in 60 households. *Int J Environ Res Public Health*. (2021) 18:11447. doi: 10.3390/ijerph182111447

58. Health Canada. Government of Canada. (2021). Residential indoor air quality guidelines: Carbon dioxide. Available from: https://www.canada.ca/en/health-canada/services/publications/healthy-living/residential-indoor-air-quality-guidelines-carbon-dioxide.html (Accessed on 2024 Mar 12)

59. Gall E, Cheung T, Luhung I, Schiavon S, Nazaroff W. Real-time monitoring of personal exposures to carbon dioxide. *Build Environ*. (2016) 104:59–67. doi: 10.1016/j.buildenv.2016.04.021

60. Sóki E, Gyila S, Csige I. Origin and transport of radon in a dry and in a wet mofette of COVASNA, Romania. *J Environ Radioact*. (2022) 251:106962. doi: 10.1016/j.jenvrad.2022.106962

61. Field RW, Steck DJ, Smith BJ, Brus CP, Fisher EL, Neuberger JS, et al. Residential radon gas exposure and lung Cancer: the Iowa radon lung Cancer study. *Am J Epidemiol*. (2000) 151:1091–102. doi: 10.1093/oxfordjournals.aje.a010153

62. Field RW, Steck DJ, Smith BJ, Brus CP, Fisher EF, Neuberger JS, et al. The Iowa radon lung cancer study — phase I: residential radon gas exposure and lung cancer. *Sci Total Environ*. (2001) 272:67–72. doi: 10.1016/S0048-9697(01)00666-0

63. Putri RGP, Ysrafil Y, Awisarita W. Cancer incidence in volcanic areas: a systematic review. *Asian Pac J Cancer Prev*. (2022) 23:1817–26. doi: 10.31557/APJCP.2022.23.6.1817

64. Amaral A, Rodrigues V, Oliveira J, Pinto C, Carneiro V, Sanbento R, et al. Chronic exposure to volcanic environments and cancer incidence in the Azores, Portugal. *Sci Total Environ*. (2006) 367:123–8. doi: 10.1016/j.scitotenv.2006.01.024

65. Rodrigues AS, Arruda MSC, Garcia PV. Evidence of DNA damage in humans inhabiting a volcanically active environment: a useful tool for biomonitoring. *Environ Int*. (2012) 49:51–6. doi: 10.1016/j.envint.2012.08.008

66. Inguaggiato S, Vita F, Diliberto IS, Inguaggiato C, Mazot A, Cangemi M, et al. The volcanic activity changes occurred in the 2021–2022 at Vulcano island (Italy), inferred by the abrupt variations of soil CO2 output. *Sci Rep*. (2022) 12:21166. doi: 10.1038/s41598-022-25435-4

67. Environmental Protection Agency (EPA). Emisiones de dióxido de carbono. (2021). Available from: https://espanol.epa.gov/la-energia-y-el-medioambiente/emisiones-de-dioxido-de-carbono (Accessed on 2024 Mar 13)

68. Viveiros F, Silva C, Pacheco J, Moreno L, Ferreira T, Gaspar JL. "A permanent indoor CO2 monitoring system installed in a degassing area of the Azores archipelago." In: *International conference on urban risks (ICUR2016)*. Lisboa; (2016). 907–914.

69. Pefferkorn E, Lossois M, Le Gallo A, Loire C, Bascou A, Berthezène JM. Forensic diagnostic approach of peri-volcanic area fatalities: about two cases at piton de la Fournaise. *J Forensic Sci*. (2022) 67:2497–503. doi: 10.1111/1556-4029.15111

frontiers | Frontiers in Public Health

TYPE Review
PUBLISHED 08 October 2024
DOI 10.3389/fpubh.2024.1420933

OPEN ACCESS

EDITED BY
Arpit Bhargava,
Ram Krishna Dharmarth Foundation University, India

REVIEWED BY
Peifen Zhang,
Sun Yat-sen University Cancer Center (SYSUCC), China
Sina Azadnajafabad,
Washington University in St. Louis, United States

*CORRESPONDENCE
Guanghui Huang
✉ ghhuang1@must.edu.mo
Zheng Li
✉ lizhengcpu@163.com
Qibiao Wu
✉ qbwu@must.edu.mo
Jue Wang
✉ wangjue@must.edu.mo

†These authors have contributed equally to this work

RECEIVED 21 April 2024
ACCEPTED 30 September 2024
PUBLISHED 08 October 2024

CITATION
Zhang A, Luo X, Li Y, Yan L, Lai X, Yang Q, Zhao Z, Huang G, Li Z, Wu Q and Wang J (2024) Epigenetic changes driven by environmental pollutants in lung carcinogenesis: a comprehensive review. *Front. Public Health* 12:1420933. doi: 10.3389/fpubh.2024.1420933

Epigenetic changes driven by environmental pollutants in lung carcinogenesis: a comprehensive review

Aijia Zhang[1†], Xuexing Luo[1†], Yu Li[2,3†], Lunchun Yan[3,4†], Xin Lai[5], Qianxu Yang[6], Ziming Zhao[2,3], Guanghui Huang[1*], Zheng Li[7,8*], Qibiao Wu[2,3,9*] and Jue Wang[2,3,9*]

[1]Faculty of Humanities and Arts, Macau University of Science and Technology, Taipa, Macau SAR, China, [2]State Key Laboratory of Quality Research in Chinese Medicines, Macau University of Science and Technology, Taipa, Macau SAR, China, [3]Faculty of Chinese Medicine, Macau University of Science and Technology, Taipa, Macau SAR, China, [4]Department of Comprehensive Surgery, Hengqin Hospital, The First Affiliated Hospital of Guangzhou Medical University, Guangdong-Macao in-Depth Cooperation Zone in Hengqin, Hengqin, China, [5]Department of Traditional Chinese Medicine, The Sixth Affiliated Hospital, Sun Yat-sen University, Guangzhou, China, [6]Centre for Epidemiology and Evidence-Based Practice, Department of Social and Preventive Medicine, Faculty of Medicine, University of Malaya, Kuala Lumpur, Malaysia, [7]Jiangsu Engineering Research Center of Cardiovascular Drugs Targeting Endothelial Cells, College of Health Sciences, School of Life Sciences, Jiangsu Normal University, Xuzhou, Jiangsu Province, China, [8]State Key Laboratory of Natural and Biomimetic Drugs, Peking University, Beijing, China, [9]Guangdong-Hong Kong-Macao Joint Laboratory for Contaminants Exposure and Health, Guangzhou, Guangdong Province, China

Lung cancer remains the leading cause of cancer-related mortality globally, with environmental pollutants identified as significant risk factors, especially for nonsmokers. The intersection of these pollutants with epigenetic mechanisms has emerged as a critical area of interest for understanding the etiology and progression of lung cancer. Epigenetic changes, including DNA methylation, histone modifications, and non-coding RNAs, can induce alterations in gene expression without affecting the DNA sequence and are influenced by environmental factors, contributing to the transformation of normal cells into malignant cells. This review assessed the literature on the influence of environmental pollutants on lung cancer epigenetics. A comprehensive search across databases such as PubMed, Web of Science, Cochrane Library, and Embase yielded 3,254 publications, with 22 high-quality papers included for in-depth analysis. These studies demonstrated the role of epigenetic markers, such as DNA methylation patterns of genes like F2RL3 and AHRR and alterations in the miRNA expression profiles, as potential biomarkers for lung cancer diagnosis and treatment. The review highlights the need to expand research beyond homogenous adult male groups typically found in high-risk occupational environments to broader population demographics. Such diversification can reduce biases and enhance the relevance of findings to various clinical contexts, fostering the development of personalized preventive and therapeutic measures. In conclusion, our findings underscore the potential of innovative epigenetic therapies, such as DNA demethylating drugs and histone modification agents, to counter environmental toxins' carcinogenic effects. The growing interest in miRNA therapies and studies aiming to correct aberrant methylation patterns indicate significant strides toward better lung cancer management and a healthier future for global communities.

KEYWORDS

epigenetics, lung cancer, DNA methylation, environment pollution, miRNA

1 Introduction

Lung cancer is the most prevalent malignant tumor afflicting humanity, consistently occupying the highest rank in both global cancer incidence and mortality rates (1–3). According to GLOBOCAN estimates of incidence and mortality for 36 cancers in 185 countries worldwide, lung cancer is the most commonly diagnosed cancer in 2022, with nearly 2.5 million new cases and accounting for one in eight cancers worldwide (4). In our country, including the Macao Special Administrative Region, lung cancer ranks first in incidence and mortality rates among all malignant tumors (3, 5). Non-small cell lung cancer (NSCLC) comprises approximately 85% of all cases and includes adenocarcinoma, squamous cell carcinoma, and large cell carcinoma, among others (2, 6). Although smoking is a recognized primary risk factor for lung cancer, a significant number of lung cancer cases, particularly among Asian women who have never smoked, are associated with air pollution and environmental pollutants (7–9). These pollutants, including particulate matter, toxic metals, and nitrogen oxides, threaten everyone's health (10–12). These pollutants penetrate the human respiratory system, potentially inducing epigenetic changes that lead to the transformation of normal cells into cancerous cells (13–16).

Due to the insidious onset of lung cancer, most patients are diagnosed at an advanced stage, missing the best opportunity for surgical treatment. Chemotherapy and targeted therapy are the main treatments for these patients. Chemotherapy often comes with many adverse reactions, and targeted therapy frequently leads to issues such as drug resistance, which results in many patients being unable to tolerate the drug treatment (10–12, 17). Over the past two decades, epigenetic research has advanced by leaps and bounds, offering a glimmer of hope for novel diagnostics and treatments of lung cancer. Epigenetics orchestrates the regulation of gene expression without altering the DNA sequence itself, thus revealing the intricate process of lung cancer formation from a genetic perspective. Alterations in epigenetics have been identified as crucial prognostic elements and potential therapeutic targets, with studies indicating that methylation patterns of specific genes, such as RASSF1A and RUNX3, are correlated with the prognosis and recurrence of lung cancer (16, 18). Epigenetic modifications, such as DNA methylation, histone modification, and non-coding RNAs, play a pivotal role in the onset and progression of lung cancer by regulating gene expression, impacting cell cycles, genomic imprinting, and X-chromosome inactivation (19–22). A deeper understanding of the underlying biological pathways elucidates how environmental pollutants induce such epigenetic changes. For instance, the p16INK4a pathway, often silenced by promoter hypermethylation, is crucial for cell cycle regulation and is frequently altered in lung carcinogenesis. Similarly, the PI3K/AKT signaling pathway can be activated by the demethylation of certain genes, contributing to tumorigenesis. Mediators such as reactive oxygen species (ROS) generated by pollutants can lead to oxidative stress, subsequently causing DNA damage and altered methylation patterns. Additionally, histone deacetylases (HDACs) and DNA methyltransferases (DNMTs) have been identified as critical enzymes that mediate these epigenetic changes, making them potential targets for therapeutic interventions. Hence, contemporary etiological studies of lung cancer are also focusing on the intersection of environmental pollutants and epigenetic mechanisms. An in-depth examination of these mechanisms provides novel strategies for treating lung cancer (23–25).

As industrialization accelerates, the incidence and mortality rates of lung cancer have surged dramatically, necessitating the implementation of urgent public health measures and innovative research to prevent and combat this disease (26–28). This article encapsulates the impact of environmental pollutants on the epigenetic alterations associated with lung cancer, and the underlying physiological mechanisms induced by these contaminants (Figure 1). Understanding the molecular mechanics of epigenetic changes and their correlation with environmental pollutants can pave the way for the development of novel therapeutics and preventive measures for lung cancer, ultimately enhancing patient survival quality and prognosis, and prolonging patient lifespan (29–32).

2 Methods

2.1 Search strategy

Utilizing the electronic databases PubMed, Web of Science, Cochrane Library, and Embase, we carried out an exhaustive literature search for publications released prior to November 2023. The search was conducted using key terms that encompass the following: 1: environmental pollution (environmental biomarkers, air pollution, radiation, tobacco smoke pollution, aromatic hydrocarbons); 2: epigenetics (DNA methylation, histone, non-coding RNA); 3: lung cancer (primary bronchogenic carcinoma, non-small cell lung cancer, small cell lung cancer). The schema for the search is depicted in Table 1. Additionally, manual searches were also performed within the bibliographies of published articles and reviews. Adhering to the inclusion criteria, we discussed 22 high-quality papers from the initial pool of 3,254. The outcome of the search and the inclusion and exclusion process are shown in Figure 2.

2.2 Inclusion and exclusion criteria

The criteria for inclusion of literature were as follows: (1) Studies that exclusively investigate primary bronchogenic carcinoma; (2) Research defining air pollution factors according to the "Environmental Health" (33) criteria established by the World Health Organization, which includes environmental biomarkers, air pollution, radiation, tobacco smoke pollution, and aromatic hydrocarbons; (3) Studies involving any epigenetic mechanisms, inclusive of DNA methylation, histone modifications, and non-coding RNA; (4) Research conducted in human subjects; (5) The study designs included analyses of cohort, cross-sectional and longitudinal studies, as well as randomized, non-randomized and semi-randomized studies.

Exclusion criteria were: (1) Literature pertaining to metastatic lung cancer or studies not concerning lung cancer; (2) Studies without relevant environmental pollutant exposure; (3) Research lacking examination of epigenetic mechanisms; (4) Animal studies; (5) Academic theses, conference abstracts, books, reports, or non-empirical articles.

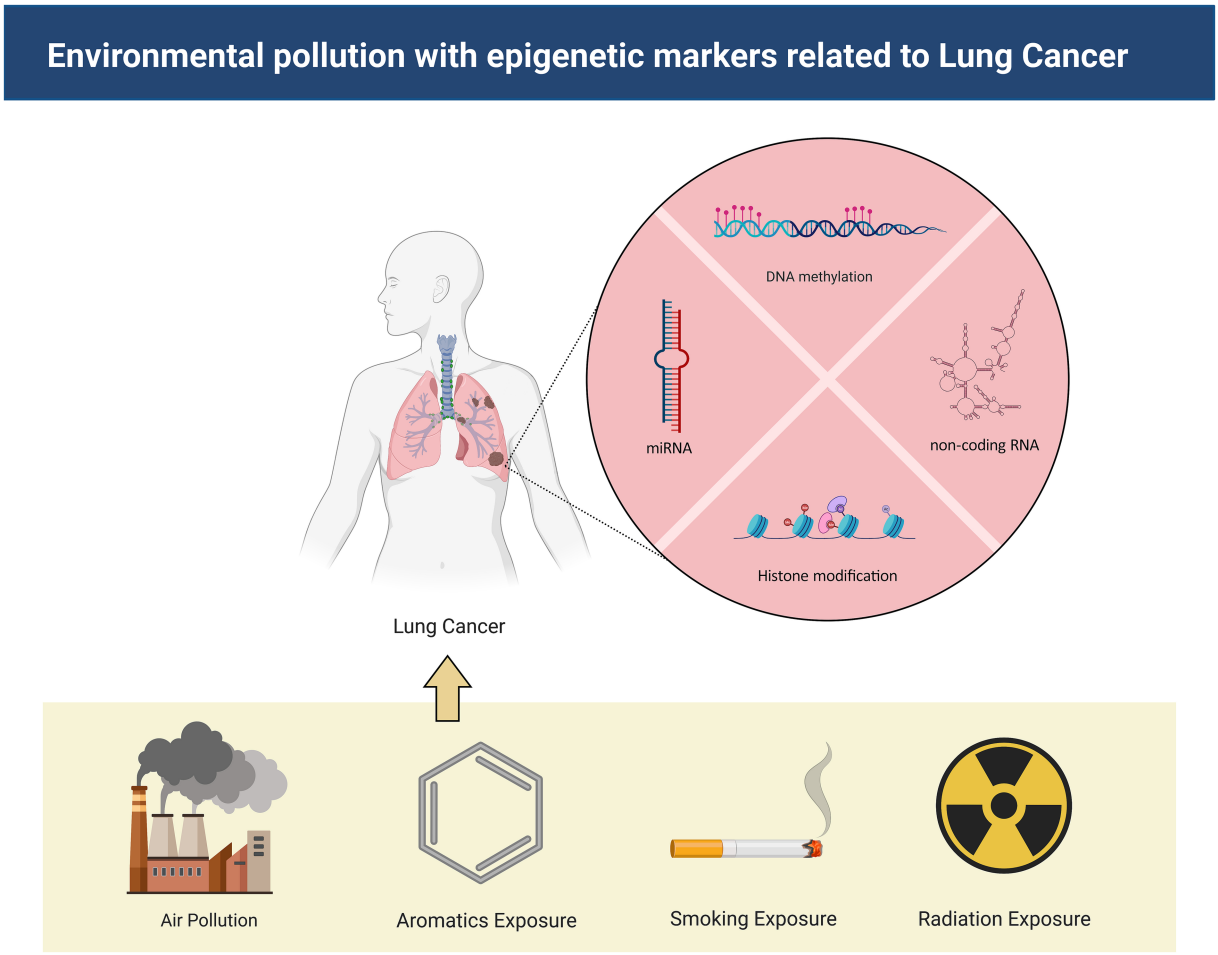

FIGURE 1
The mechanisms by which environmental pollutants lead to lung cancer. Environmental contaminants exert influence on non-coding RNA, DNA methylation, and histone modification, thereby instigating the onset of lung cancer.

2.3 Data extraction

Two reviewers, A.J. Zhang and X.X. Luo, independently screened the titles, abstracts, and full texts of the retrieved articles, and sorted out the studies that met the inclusion criteria. Any disagreements between reviewers were resolved by discussion and reaching a consensus, with the contribution of a third independent reviewer, Y. Li, made the final decision when necessary.

Data were extracted from the included literature using a standardized data extraction form. The collected information included: (1) Basic details: author's name, year of publication, region of publication, and number of cases included; (2) Type of study; (3) Clinical and pathological data of participants; (4) Experimental methods; (5) Outcome measures.

2.4 Assessment of evidence quality

As the included articles employed disparate methodological approaches, we employed a multi-method quality framework to assess the quality of the articles according to standardized criteria (34). The framework was categorized into four main quality categories: truth value, applicability, consistency and neutrality. In addition, we considered the context of the study, potential benefits and harms, and patient value systems when interpreting the results. A score was assigned to each category, with the average score across the four categories indicating that the overall quality of the article was rated as robust, high, moderate, low, or very low.

3 Results

The search terms identified a total of 3,254 articles. A rigorous selection process led to the exclusion of some studies: 10 concerning metastatic lung cancer or not involving lung cancer, 7 with undefined types of environmental pollutants, 15 lacking examinations of epigenetic mechanisms, 14 based on non-human subjects, and 11 non-empirical articles. Ultimately, 22 published studies met the predetermined inclusion criteria (Table 2).

3.1 Characteristics of the included studies

Tables 2, 3 summarize the detailed characteristics of the included studies. According to quality assessment standards, six studies were of

TABLE 1 Search strategies for English databases or Chinese databases.

Number	Search terms
#1	Environmental Pollution [MeSH]
#2	Environmental Biomarkers [MeSH]
#3	Air Pollution [MeSH]
#4	Air Pollution, Radioactive [MeSH]
#5	Air Pollution, Indoor [MeSH]
#6	Tobacco Smoke Pollution [MeSH]
#7	Radiation [MeSH]
#8	Hydrocarbons, Aromatic [MeSH]
#9	#1 OR #2 OR #3 OR #4 OR #5 OR #6 OR #7 OR #8
#10	Epigenomics [MeSH]
#11	DNA Methylation [MeSH]
#12	#10 OR #11
#13	Lung Neoplasms [MeSH]
#14	Small Cell Lung Carcinoma (SCLC) [MeSH]
#15	Non small cell lung cancer (NSCLC) [MeSH]
#16	Lung Cancer Cell Lines[MeSH]
#17	#13 OR #14 OR #15 OR #16
#18	#9 AND #12 AND #17
#19	#9 keywords translated into Chinese
#20	#12 keywords translated into Chinese
#21	#17 keywords translated into Chinese
#22	#19 AND #20 AND #21

MeSH, Medical Subject Headings; The formular of Search by PubMed with: ("Environmental Pollution"[Mesh]) OR "(Environmental Biomarkers"[Mesh]) OR ("Air Pollution"[Mesh] OR "Air Pollution, Indoor"[Mesh] OR "Air Pollution, Radioactive"[Mesh]) OR "(Tobacco Smoke Pollution"[Mesh]) OR "(Radiation"[Mesh]) OR "(Hydrocarbons, Aromatic"[Mesh]) AND "(Epigenomics"[Mesh]) OR "(DNA Methylation"[Mesh]) AND "(Lung Neoplasms"[Mesh]) OR "(Small Cell Lung Carcinoma"[Mesh]) OR "(Carcinoma, Non-Small-Cell Lung"[Mesh]) OR "Lung Cancer Cell Lines"[Mesh].

good quality, and 16 were of moderate quality. The identified research employed a variety of methods to detect alterations in lung cancer epigenetics: 16 studies conducted assays of specific candidate genes as shown in Table 4, which included *F2RL3* and *AHRR* (35–38), CDKN2A, DLEC1, CDH1, DAPK, RUNX3, APC, WIF1, and MGMT (39), SATα, NBL2, and D4Z4 (40, 41), DNMT1, DNMT3a, DNMT3b, TET1, TET2, TET3 (42), L3MBTL1, NNAT, PEG10, GNAS Ex1A, MCTS2, SNURF/SNRPN, IGF2R, RB1, and CYP1B1 (43), CYP1A1 (44), miRNA (45–50). Additionally, some studies assessed the impact of environmental pollutants using different mediators, such as raised levels of DNA methyltransferase enzyme (DNA MTase) (51) and chemical modifications 5mC and 5hmC (52); 1 study conducted a whole-genome DNA methylation analysis using the Illumina Infinium HumanMethylation450 platform (36); 4 studies reviewed the effect of environmental pollutants on epigenetics (53–56).

3.2 Participant demographics

The inquiries predominantly explored the demographic of male adults, with a preponderance of professions including drivers and laborers. These investigations unveiled a considerable overlap in samples, as three studies (40, 41, 52) recruited truck drivers from China for analysis. The pathological phenotypes were most frequently assessed through DNA methylation patterns, some of which involved levels of gene expression. However, other epigenetic pathways, such as histone modifications or non-coding RNAs, have yet to be thoroughly examined.

3.3 Types of pertinent environmental pollutants

According to the research conducted by Xue et al. (57), environmental pollutants associated with lung cancer are categorized into two types: outdoor and indoor air pollutants (Table 5).

3.3.1 Outdoor air pollutants

Eight studies identified within the pertinent body of research analyzed the hazards posed by outdoor environmental pollutants, focusing primarily on particulate matter (PMs) and polycyclic aromatic hydrocarbons (PAHs) (35, 40, 41, 43, 45, 52, 53, 58). The composition of atmospheric particulates is complex, encompassing organic compounds (such as polycyclic aromatic hydrocarbons, dioxins, and benzene) and inorganic substances (like carbon, chlorides, nitrates, and sulfates) and metals. Due to their substantial surface area and robust adsorption capacity, PMs not only carry toxic metals and organic constituents but can also adsorb bacteria and virus (59). These pollutants enter the lungs via the respiratory system and could potentially elevate the risk of developing lung cancer.

3.3.2 Indoor air pollutants

An additional 10 studies discussed the possibility of indoor environmental pollutants—including tobacco smoke and coal for curing—inducing epigenetic modifications associated with lung cancer (36–39, 44, 46, 48–51). Indoor smoking and exposure to secondhand smoke are significant risk factors for lung cancer. Long-term exposure to environmental tobacco smoke, including secondhand aerosols from tobacco or electronic cigarettes, increases the risk of lung cancer (49, 51). Moreover, some reports suggest that the cumulative toxicity of co-existing air pollutants is an important consideration to take into account (57).

3.4 Alterations in the epigenetics of lung cancer

Epigenetic alterations—including changes in microRNAs (miRNAs), DNA methylation, and histone modifications—are major determinants in the development of disease phenotypes following exposure to air pollution (53, 55). The different types of lung cancer driven by epigenetic changes driven by environmental pollutants are shown in Figure 3.

3.4.1 The mechanisms of DNA methylation in driving lung cancer

DNA methylation represents a significant epigenetic change underlying the pathogenic mechanisms induced by air pollution (55).

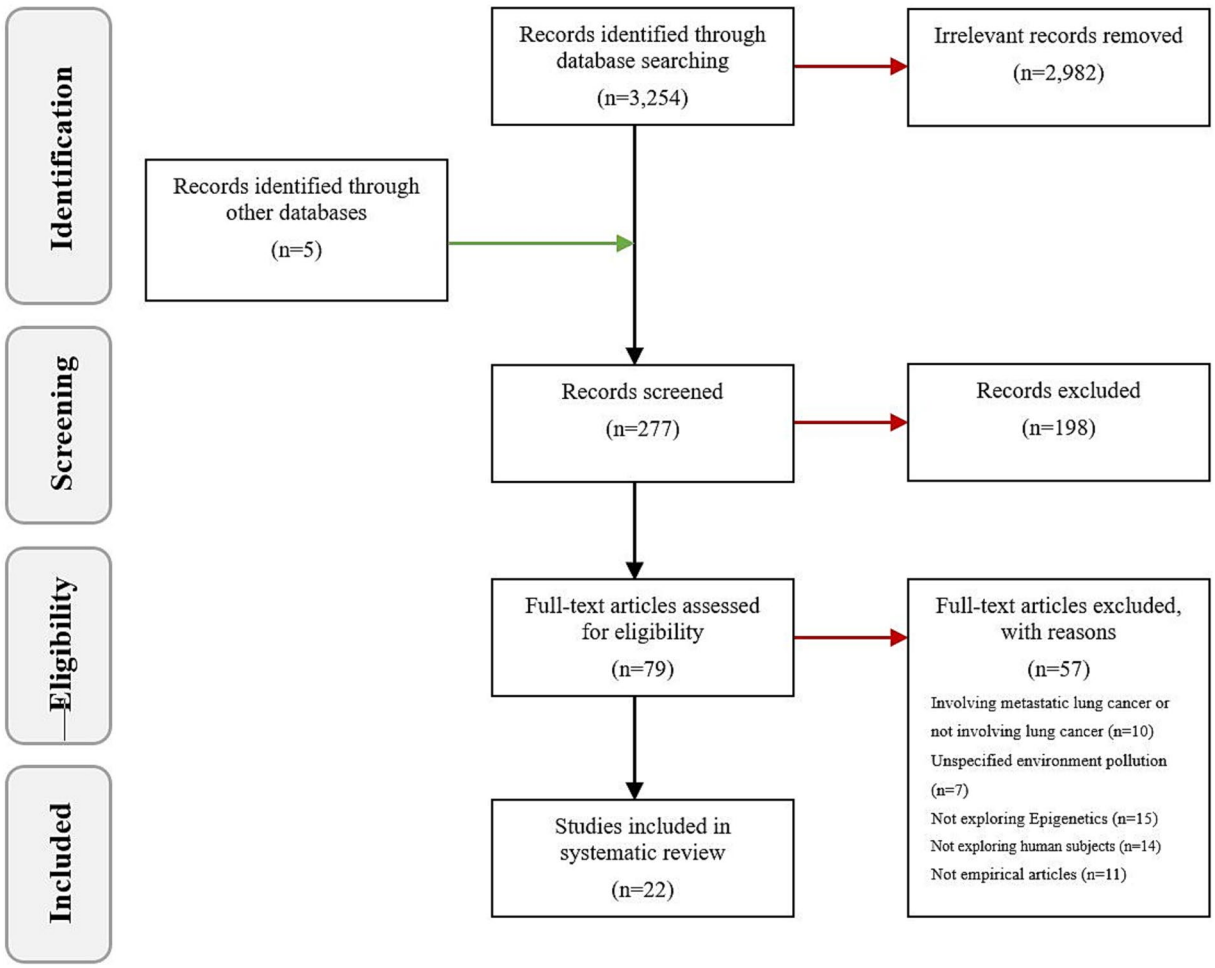

FIGURE 2
Flow diagram for the included and excluded articles.

Changes in DNA methylation occurred after exposure to PMs (56). PM2.5 exposure suppresses p53 expression through promoter hypermethylation mediated by the ROS-protein kinase B (Akt)-DNMT3B pathway, suggesting that PM2.5 exposure could increase the risk of lung cancer (53). Furthermore, compounds produced by smoking (36–38) and perfluoroalkyl substances [PFAS, (42)] have been shown to affect gene expression in lung cancer cells by altering DNA methylation patterns. This alteration may lead to dysregulation of the cell cycle and apoptosis pathways, thereby promoting the onset and progression of lung cancer. The A549 lung cancer cell line serves as a research model, providing crucial experimental evidence for understanding how these environmental factors impact lung cancer (42, 44).

3.4.2 The mechanisms of histone modifications in driving lung cancer

Some studies also show that differential histone modifications involve PM-induced inflammatory responses and oxidative stress, particularly leading to pulmonary diseases (53). Long-term exposure to PM2.5 downregulates the expression of histone demethylase Kdm6a in lung macrophages, which may result in increased methylation of H3K4 and H3K9 in the promoter regions of IL-6 and IFN-β. Exposure to cigarette smoke reduces the activity of histone deacetylases (HDACs) and decreases the expression of HDAC1, HDAC2, and HDAC3 in macrophages, resulting in an inflammatory response. Exposure to particulates leads to an imbalance in the expression of histone acetyltransferases (HATs) and HDACs in human bronchial epithelial cells, as well as an increase in the acetylation of certain histones, such as H4, which in turn triggers inflammation (55).

3.4.3 The mechanisms of miRNAs in driving lung cancer

Sima et al. (47) analyzed the expression of miRNAs associated with exposure to air pollutants and lung cancer. Twenty-five miRNAs were correlated with exposure to air pollution and lung cancer, with miR-222, miR-21, miR-126-3p, miR-155, and miR-425 being the most significant. They play pivotal roles in promoting or inhibiting angiogenesis, inflammation, and the progression of lung cancer. Additionally, a specific set of upregulated or downregulated miRNAs was observed in the progression of bronchogenic carcinoma in smokers, ranging from normal lung to hyperplasia, metaplasia, carcinoma *in situ*, and finally, to lung squamous cell carcinoma (LUSC) (46). Exposure to cigarette smoke leads to an early, pronounced reduction in the

TABLE 2 Record of citation analyses and full texts reviewed.

Name	Region/ Country	Types	Participants	Exposure	Methodology	Analysis	Results
Alhamdow et al. (35)	Sweden	Research article	151 chimney sweeps, 19 creosote-exposed workers and 152 unexposed workers (controls), all men	PAHs	Measured monohydroxylated metabolites of phenanthrene and fluorene in urine using liquid chromatography-mass spectrometry.	Unadjusted and multivariable linear regression models were fit to evaluate associations.	Increasing fluorene exposure, among chimney sweeps, was associated with lower DNA methylation of *F2RL3* and *AHRR*, markers for increased lung cancer risk.
Baglietto, et al. (36)	France	Research article	Participants were from the EPIC-Italy cohort and the MCCS cohort, including cases of lung cancer and controls, with over 700 case–control pairs in total.	Tobacco	Used Illumina Infinium HumanMethylation450 array to measure DNA methylation in pre-diagnostic blood samples.	Conditional logistic regression models, stratified by smoking status, and fixed effect models for pooled ORs.	Identified six CpGs associated with lung cancer risk, hypomethylation observed in current smokers, and increased methylation post-quitting.
Fasanelli et al. (37)	Italy	Research article	132 case–control pairs in the NOWAC cohort and an additional 664 case–control pairs tightly matched for smoking from the MCCS, NSHDS and EPIC HD cohorts.	Tobacco	Genome-wide DNA methylation analyses were performed on pre-diagnostic blood samples using the Illumina Infinium HumanMethylation450 platform.	Performed mediation analysis to assess whether methylation of cg05575921 (AHRR) and cg03636183 (F2RL3).	The most significant associations with lung cancer risk are for cg05575921 in *AHRR* and cg03636183 in *F2RL3*, previously shown to be strongly hypomethylated in smokers. These associations remain significant after adjustment for smoking.
Guo et al. (40)	China	Review article	Truck drivers and office workers in Beijing	PMs	Multilevel mixed-effect regression models	The data were analyzed using multilevel mixed-effect regression models to account for the lack of independence between repeated measures.	Interquartile increases in personal PM2.5 and ambient PM10 levels were associated with significant covariate-adjusted decreases in SATa methylation.
Guo et al. (53)	China	Review article	N/A	PM2.5	Epidemiological and toxicological studies, biomarker investigations.	N/A	Results indicate PM2.5 exposure is associated with oxidative stress, inflammation, DNA damage, and epigenetic changes, potentially leading to respiratory diseases.
Hammons et al. (51)	USA	Research article	55 human donors (smokers and nonsmokers)	Tobacco	RT-PCR analysis, DNA MTase enzyme assay	Data were analyzed statistically by ANOVA using Sigma-Stat software, with Tukey test evaluating differences between means.	DNA MTase mRNA levels were significantly higher in smokers.
Hou et al. (41)	China	Research article	60 truck drivers and 60 office workers in Beijing	PM	Blood DNA methylation measured, personal exposure assessment	GEE models adjusted for covariates, FDR applied	Positive associations between PM elemental components and DNA methylation changes in a Beijing population, with NBL2 methylation linked to silicon (Si) and calcium (Ca) in truck drivers, and SATa methylation linked to sulfur (S) in office workers.

(Continued)

10.3389/fpubh.2024.1420933

TABLE 2 (Continued)

Name	Region/ Country	Types	Participants	Exposure	Methodology	Analysis	Results
Huang et al. (39)	China	Research article	87 lung cancer patients and 31 healthy subjects	Smoky coals	Genomic DNA extracted from tissues and plasma; candidate gene promoter methylation status determined using Nested Methylation-Specific PCR (nMSP).	Sanger sequencing verified nMSP results; methylation frequencies compared across tissue and plasma samples.	Seven of eight genes showed high methylation frequencies in tissues (39–74%). Methylation in plasma was detected for five genes with frequencies of 45% for CDKN2A, 48% for DLEC1, 76% for CDH1, 14% for DAPK, and 29% for RUNX3. Healthy controls showed no methylation.
Jabeen, M et al. (42)	USA	Research article	A549 lung carcinoma cells	10-, 200-, and 400 μM concentrations of PFAS	Cell culture, MTT assay, qRT-PCR, UPLC-MS, HS-DFM.	Used GraphPad Software for statistical tests and analysis.	Exposure to per- and polyfluoroalkyl substances (PFAS) can cause epigenetic modifications in A549 lung cancer cells. Lower doses of PFAS compounds promote cell proliferation, whereas higher concentrations induce apoptosis, potentially impacting patients with pre-existing lung conditions or contributing to lung carcinogenesis.
Lee et al. (38)	South Korea	Research article	330 adults (46 to 87 years of age)	Tobacco	Pyrosequencing was performed to measure DNA methylation of AHRR and F2RL3.	The Kruskal-Wallis ANOVA test was used to compare data. Pearson tests were performed to assess any correlation between methylation values.	AHRR and F2RL3 genes were significantly hypomethylated in current smokers. AHRR methylation is significantly associated with the risk of lung cancer (OR = 0.96, $p = 0.011$).
Li et al. (54)	China	Review article	N/A	PMs	English-language publications focusing on PM, epigenetic changes, and lung cancer were reviewed.	Reviewing English-language publications and conducting a comprehensive comparison approach.	PM2.5 is associated with the increased lung cancer risk and mortality. PM-induced epigenetic changes may play important roles in the pathogenesis of lung cancer.
Liang et al. (43)	China	Research article	19–23 years old students	PM2.5	Mixed-effects models were used to evaluate the influence of PM2.5 and its constituent exposure on DNAm while controlling for potential confounders.	Used MethylTarget to determine and analyze DNAm of imprinted genes in blood samples. Statistical analysis included natural logarithmic transformation of methylation data and mixed-effects models.	No significant correlation between DNAm and personal PM2.5 exposure mass. However, DNAm changes in eight imprinted control regions (ICRs) and a non-imprinted gene were significantly associated with PM2.5 constituents.
Mukherjee et al. (55)	India	Review article	N/A	Air pollution	Literature review and analysis of 235 articles	N/A	DNA methylation represents the most prominent epigenetic alteration underlying the air pollution-induced pathogenic mechanism. Several other types of epigenetic changes, such as histone modifications, miRNA, and non-coding RNA expression, have also been found to have been linked with air pollution.

(Continued)

10.3389/fpubh.2024.1420933

TABLE 2 (Continued)

Name	Region/ Country	Types	Participants	Exposure	Methodology	Analysis	Results
Pan et al. (45)	China	Research article	105 patients with untreated lung adenocarcinoma (AD) or squamous cell carcinoma (SCC)	Smoky coals	MicroRNA microarray analysis, quantitative RT-PCR, cell culture assays, luciferase reporter assays, animal studies	Volcano Plot filtering, Median normalization, Student's t-test, Pearson correlation analysis	miR-144 was significantly down-regulated in NSCLCs from HPR; miR-144 targets oncogene Zeb1; overexpression of miR-144 inhibits NSCLC cell migration and tumor progression.
Sanchez-Guerra et al. (52)	USA	Review article	60 truck drivers, 60 office workers in Beijing	PMs	ELISA for global 5mC and 5hmC; mixed-effects regression models	Adjusted mixed-effects regression models were used to evaluate associations.	PM10 exposure associated with increased 5hmC levels, no correlation with 5mC.
Sato & Ishigami (44)	Japan	Review article	Human lung adenocarcinoma (A549) cells	HTPs, RC	Cell treatment with aerosol extracts, global DNA methylation analysis, gene expression profiling.	Cell culture treated with aerosol extracts, followed by various assays (dot blot, RRBS, DNA microarray, RT-qPCR).	The HTP extract affected gene expression. In particular, the HTP extract markedly affected the mRNA expression and promoter methylation of cytochrome P450 family 1 subfamily A member 1 (CYP1A1), which is associated with carcinogenic risk.
Schembri et al. (46)	USA	Research article	20 volunteers (10 current smokers, 10 never smokers)	Tobacco	The methodological approach of the study involved microarray profiling of miRNAs and mRNAs, *in vitro* transfections to modulate miRNA levels, and real-time PCR validations to assess the effects on gene expression changes in response to cigarette smoke exposure.	The article analyzed data using microarray preprocessing, normalization, Welch's t-test, and Pearson correlation, followed by GSEA and hierarchical clustering.	The study found 28 miRNAs differentially expressed in smokers, with mir-218 significantly down-regulated, which modulates airway epithelial gene expression response to cigarette smoke.
Sima et al. (47)	Czech Republic	Review article	N/A	Air pollution	Literature review, data synthesis, and analysis of miRNA deregulation in relation to air pollution and lung cancer.	Data analysis involved literature search, miRNA pattern comparison, and identification of commonalities in miRNA deregulation.	Detected a total of25 miRNAs meeting the criteria, among them, miR-222, miR-21, miR-126-3p, miR-155 and miR-425 being the most prominent.
Tellez et al. (48)	USA	Research article	Immortalized human bronchial epithelial cells (HBEC)	Tobacco	*In vitro* model, gene expression analysis, immunoblot, chromatin immunoprecipitation assay.	qRT-PCR, immunoblot, chromatin immunoprecipitation, bisulfite sequencing, statistical analysis using Pearson correlation and t-tests.	Carcinogen exposure induces EMT and stem cell-like properties in HBECs through epigenetic silencing of miR-200 and miR-205.

(Continued)

10.3389/fpubh.2024.1420933

TABLE 2 (Continued)

Name	Region/ Country	Types	Participants	Exposure	Methodology	Analysis	Results
Wang et al. (49)	USA	Research article	Healthy nonsmokers and healthy smokers	Tobacco	miRNA microarray analysis, qRT-PCR validation, bioinformatics tools	Processed Affymetrix miRNA array data using Partek, performed two-way ANOVA, and validated with qRT-PCR.	The study found that smoking induces persistent dysregulation of 12 miRNAs in the small airway epithelium even after smoking cessation, which may contribute to the increased risk of COPD and lung cancer in former smokers.
Wu et al. (56)	China	Systematic review and meta-analysis	38 articles were included in this study: 16 using global methylation, 18 using candidate genes, and 11 using EWAS, with 7 studies using more than one approach.	Air pollution	Systematic search, meta-analysis, and candidate-gene, epigenome-wide association studies (EWAS)	Meta-analysis, heterogeneity assessed with Cochran Q test and I^2 statistic, sensitivity and publication bias tests using R Studio and Stata.	Imprecise inverse association between PM2.5 and global DNA methylation; candidate-gene results suggest hypermethylation in ERCC3 with benzene and SOX2 with PM2.5 exposure; 201 CpG sites and 148 differentially methylated regions associated with air pollution.
Xi et al. (50)	USA	Research article	Normal human respiratory epithelial cells and lung cancer cells	Tobacco	Array techniques, qRT-PCR, Ago-CLIP, luciferase assays, ChIP, MeDIP, MNase protection	Methodology for data analysis includes qRT-PCR, Western blot, Ago-CLIP, luciferase reporter assays, ChIP, MeDIP, MNase protection assays, and statistical tests.	These findings indicate that miR-487b is a tumor suppressor microRNA silenced by epigenetic mechanisms during tobacco-induced pulmonary carcinogenesis and suggest that DNA demethylating agents may be useful for activating miR-487b for lung cancer therapy.

PAHs, polycyclic aromatic hydrocarbons; PMs, particulate matter; HTPs, Aerosol extracts of heated tobacco products; RC, reference cigarette.

10.3389/fpubh.2024.1420933

TABLE 3 Record of citation score.

	Validate	Suitability	Therapeutic	Consistency	Overall score
Alhamdow et al. (35)	5	5	4	5	Good (5)
Baglietto, et al. (36)	4	4	3	4	Moderate (4)
Fasanelli et al. (37)	4	5	3	4	Moderate (4)
Guo et al. (40)	3	3	2	4	Moderate (3)
Guo et al. (53)	5	5	4	4	Good (5)
Hammons et al. (51)	5	5	4	5	Good (5)
Hou et al. (41)	3	3	2	4	Moderate (3)
Huang et al. (39)	5	4	3	4	Moderate (4)
Jabeen, M et al. (42)	4	5	3	4	Moderate (4)
Lee et al. (38)	5	5	4	5	Good (5)
Li et al. (54)	4	5	3	4	Moderate (4)
Liang et al. (43)	4	4	3	4	Moderate (4)
Mukherjee et al. (55)	5	5	4	5	Good (5)
Pan et al. (45)	4	4	4	5	Moderate (4)
Sanchez-Guerra et al. (52)	3	2	3	3	Moderate (3)
Sato & Ishigami (44)	4	4	3	4	Moderate (4)
Schembri et al. (46)	4	3	3	4	Moderate (4)
Sima et al. (47)	4	4	2	3	Moderate (3)
Tellez et al. (48)	4	3	3	3	Moderate (3)
Wang et al. (86)	5	5	4	5	Good (5)
Wu et al. (56)	4	3	3	3	Moderate (3)
Xi et al. (50)	4	4	5	4	Moderate (4)

expression of the tumor-suppressor miR-487b through promoter methylation, thereby facilitating lung oncogenesis through Wnt signaling (50). Similarly, tumor suppressor miR-196b is silenced early through promoter methylation in the same experimental model, giving a selective growth advantage to precancerous cells. A case–control study showed a strong correlation between methylation of miR-196b in sputum and the occurrence of lung cancer (48).

4 Discussion

Epigenetic characteristics mirror the shifts in cellular environments and are also discernible within the human circulatory system across a spectrum of diseases (60, 61). Exploration of these epigenetic attributes may lead to the identification of sensitive biomarkers, which hold promise for the early screening of lung cancer as well as the monitoring of the clinical treatment outcomes. This study is dedicated to revisiting the extensive interplay between environmental pollutants and lung cancer, with a comprehensive analysis of current research highlighting the crucial role that epigenetic modifications play in the etiology of lung cancer. Specifically, DNA methylation of genes such as F2RL3 and AHRR is accentuated (62–65), aberrant miRNA expression patterns stand out as additional key epigenetic markers (49, 66–68). In the future, these could serve as potential targets for diagnosing and treating lung cancer. However, such studies are predominantly confined to specific demographics, primarily consisting of adult males exposed to highly polluted environments, which may introduce biases and affect the objectivity of the data.

Corresponding research indicates that the impact of environmental pollutants on diverse populations is multifaceted, with contributing factors encompassing genetic characteristics, occupation, lifestyle choices, and socioeconomic status (69). In particular, alterations in DNA methylation at specific genomic loci constitute a fundamental aspect of the initiation and progression of lung cancer (70–73). Epigenetic variations observed within the CDKN2A gene, engendered by exogenous environmental elements, exemplify the paradigmatic mechanisms of tumor formation instigated by external environmental factors through the genesis of heterotypic cells (74).

The horizon of avant-garde therapeutic approaches brims with potential. Although minimization of exposure remains an unwavering pillar, the advent of molecular treatment regimens, ingeniously devised to rectify epigenetic aberrations, heralds a significant leap forward in therapeutic innovation. Pertaining to DNA demethylation (75–77), histone modification pharmacologic (75, 78, 79) and miRNA therapeutic interventions (54, 80, 81). Research into histone-modifying drugs and miRNA therapies may revolutionize the treatment approaches for individuals exposed to environmental toxins, heralding a paradigm shift in managing pollution-related lung cancer. The development of these treatments necessitates rigorous

TABLE 4 The types of candidate genes for detecting alterations in lung cancer epigenetics.

Candidate gene type	Authors	Exposure	General characteristics of epigenetic changes
F2RL3, AHRR	Alhamdow et al. (35)	PAHs	DNA methylation
	Baglietto, et al. (36)	Tobacco	
	Fasanelli et al. (37)	Tobacco	
	Lee et al. (38)	Tobacco	
CDKN 2A, DLEC 1, CDH 1, DAPK, RUNX 3, APC, WIF 1 and MGMT	Huang et al. (39)	Smoky coals	
SATα, NBL2 and D4Z4	Guo et al. (40)	PMs	
	Hou et al. (41)	PM	
DNMT1, DNMT3a, DNMT3b, TET1, TET2, TET3	Jabeen et al. (42)	10-, 200-, and 400 μM concentrations of PFAS	
L3MBTL1, NNAT, PEG10, GNAS, Ex1A, MCTS2, SNURF/ SNRPN, IGF2R, RB1 and CYP1B1	Liang et al. (43)	PM2.5	
CYP1A1	Sato & Ishigami, (44)	HTPs, RC	
HATs and HDACs	Guo et al. (53)	PM2.5	Histone modifications
Kdm6a	(55)	Air pollution	
miRNA	Guo et al. (53)	PM2.5	microRNAs
miRNA	Li et al. (54)	PM	
miR-144	Pan et al. (45)	Smoky coals	
mir-218	Schembri et al. (46)	Tobacco	
miR-222, miR-21, miR-126-3p, miR-155, and miR-425	Sima et al. (47)	Air pollution	
miR-196b, miR-200, and miR-205	Tellez et al. (48)	Tobacco	
miRNA	Wang et al. (49)	Tobacco	
miR-487b	Xi et al. (50)	Tobacco	

PAHs, polycyclic aromatic hydrocarbons; PMs, particulate matter; HTPs, Aerosol extracts of heated tobacco products; RC, reference cigarette.

investigations to ascertain their safety and efficacy. Clinical trials examining the effectiveness of agents like azacitidine in correcting methylation patterns associated with pollution-induced lung malignancies are imperative (82, 83), as well as clinical trials evaluating the effectiveness of drugs like azacitidine in correcting methylation patterns in pollution-related lung cancers. Further assessment of the anti-inflammatory properties of HDAC inhibitors is also imperative (84, 85). Such endeavors in therapeutic experimentation bear the potential to catalyze transformative changes in care for individuals plagued by environmental toxins. Consequently, the research must be conducted meticulously to ensure beneficial outcomes.

4.1 Limitations

The limitations of our review merit recognition and warrant attention. Initially, the caliber of evidence extracted from the 18 documents included was heterogeneous, with some studies potentially needing more rigorous methodological design, comprehensive data collection, or extensive peer-review processes. Such imperfections in quality may impinge upon the reliability and universality of the research findings, as lower quality investigations could introduce biases or overlook critical variables, our literature search was confined solely to published articles in English, introducing a language bias that may have excluded pertinent studies published in other tongues, which could provide insights into the epigenetic impacts of environmental pollutants on lung cancer. Consequently, our findings do not encompass the complete scope of global research and may lead to an incomplete understanding of the subject matter.

The robustness of the discussions presented might also be questioned, as they may not have considered all alternative explanations, counterarguments, or the full breadth of complex interactions between environmental pollutants and genetic susceptibility across different populations. The discussions may also need more comprehensiveness in resolving the heterogeneity of the study populations and methodologies, potentially limiting the strength of the conclusions drawn.

These limitations underscore the necessity for a cautious interpretation of the review outcomes. Future research should strive to include a broader scope of studies, encompassing multiple languages and more diverse populations, to offer a more comprehensive understanding of the effects of environmental pollutants on lung cancer through epigenetic alterations. Furthermore, ensuring that discussions in future reviews are grounded in extensive consideration of all pertinent factors and opposing viewpoints will enhance the research findings' validity and practical applicability.

5 Conclusion

The current review delves into an increasing body of evidence that underscores how environmental pollutants act as catalysts for

TABLE 5 Types of environmental pollutants that trigger epigenetic changes in lung cancer.

Type	Authors	Environmental pollutants	Epigenetic changes in lung cancer
Outdoor Air Pollutants	Alhamdow et al. (35)	PAHs	PAHs induced hypomethylation of F2RL3 and AHRR, epigenetic changes linked to lung cancer risk.
	Hou et al. (41)	PM	PM exposure induced hypomethylation in tandem repeats SATa and NBL2 among study participants, potentially impacting lung cancer risk.
	Guo et al. (40)	PMs	PM exposure is linked to hypomethylation of tandem repeats SATa, NBL2, and D4Z4, potentially impacting lung cancer risk.
	Guo et al. (53)	PM2.5	PMs induces epigenetic alterations such as DNA methylation, histone modification, and miRNA dysregulation, contributing to lung carcinogenesis.
	Li et al. (54)	PM	
	Sanchez-Guerra et al. (52)	PMs	PM10 exposure linked to increased blood 5-hydroxymethylcytosine (5hmC), indicative of epigenetic changes in lung cancer risk.
	Liang et al. (43)	PM2.5	PM2.5 exposure induced changes in DNA methylation of imprinted genes, potentially affecting lung cancer pathways and susceptibility.
Indoor Air Pollutants	Baglietto, et al. (36)	Tobacco	Smoking exposure induced hypomethylation of AHRR and F2RL3, associated with increased lung cancer risk.
	Fasanelli et al. (37)	Tobacco	
	Lee et al. (38)	Tobacco	
	Hammons et al. (51)	Tobacco	Tobacco was associated with increased expression of hepatic DNA methyltransferase, which indicate a greater susceptibility to cancer.
	Schembri et al. (46)	Tobacco	Tobacco induce down-regulation of miR-144, affecting Zeb1 expression and promoting epithelial-mesenchymal transition in lung cancer cells.
	Sato & Ishigami (44)	HTPs, RC	RC reduced 5-mC and 5-hmC; HTPs altered CpG, affecting CYP1A1 mRNA and methylation, linked to cancer risk.
	Tellez et al. (48)	Tobacco	Tobacco induces epigenetic changes including promoter hypermethylation and H3K27me3 enrichment, leading to silencing of tumor-suppressive miRNAs.
	Wang et al. (86)	Tobacco	Tobacco induces epigenetic repression of miR-487b and alters microRNA expression, contributing to lung carcinogenesis.
	Xi et al. (50)	Tobacco	Tobacco induces demethylation of miR-487b, alters nucleosome positioning, and increases DNA methylation, leading to its repression and lung cancer progression.
	Huang et al. (39)	Smoky coals	Smoky coals induced aberrant methylation in promoters of lung cancer-related genes, potentially serving as epigenetic biomarkers for early detection.
	Pan et al. (45)	Smoky coals	Smoky coals induced down-regulation of miR-144, associated with increased Zeb1 expression and EMT phenotype in lung cancer.

HTPs, Aerosol extracts of heated tobacco products; RC, reference cigarette.

carcinogenesis within pulmonary tissues, focusing on epigenetic mechanisms. Studies on epigenetic markers—particularly DNA methylation of pivotal genes such as F2RL3 and AHRR, as well as alterations in miRNA profiles affecting gene expression—have emerged as significant indicators for diagnosing and treating lung cancer. However, focusing solely on homogenous male adult populations within specific high-risk occupational environments may fall short of a comprehensive picture, as it fails to encapsulate the demographic and occupational diversity prevalent in a broader population base. Additionally, as suggested by prior comprehensive reviews, these epigenetic characteristics may extend beyond the biomarkers for lung cancer, representing the organism's response to environmental stressors.

In light of these findings, it is imperative to expand the research scope to include more diverse population groups, thereby mitigating the risk of biased data that may not represent the entirety of vulnerable cohorts. Widening the demographic reach of these studies can greatly enhance the validity of research outcomes and facilitate their application across varied clinical settings. Moreover, it allows for formulating of personalized preventive measures and interventions, considering the intricate interplay products between unique epigenomic landscapes, environmental exposures, lifestyles, and genetic susceptibilities.

Looking ahead, the pursuit of innovative treatments such as drugs targeting DNA demethylation and histone modification offers new avenues for combatting pollution-induced malignancies.

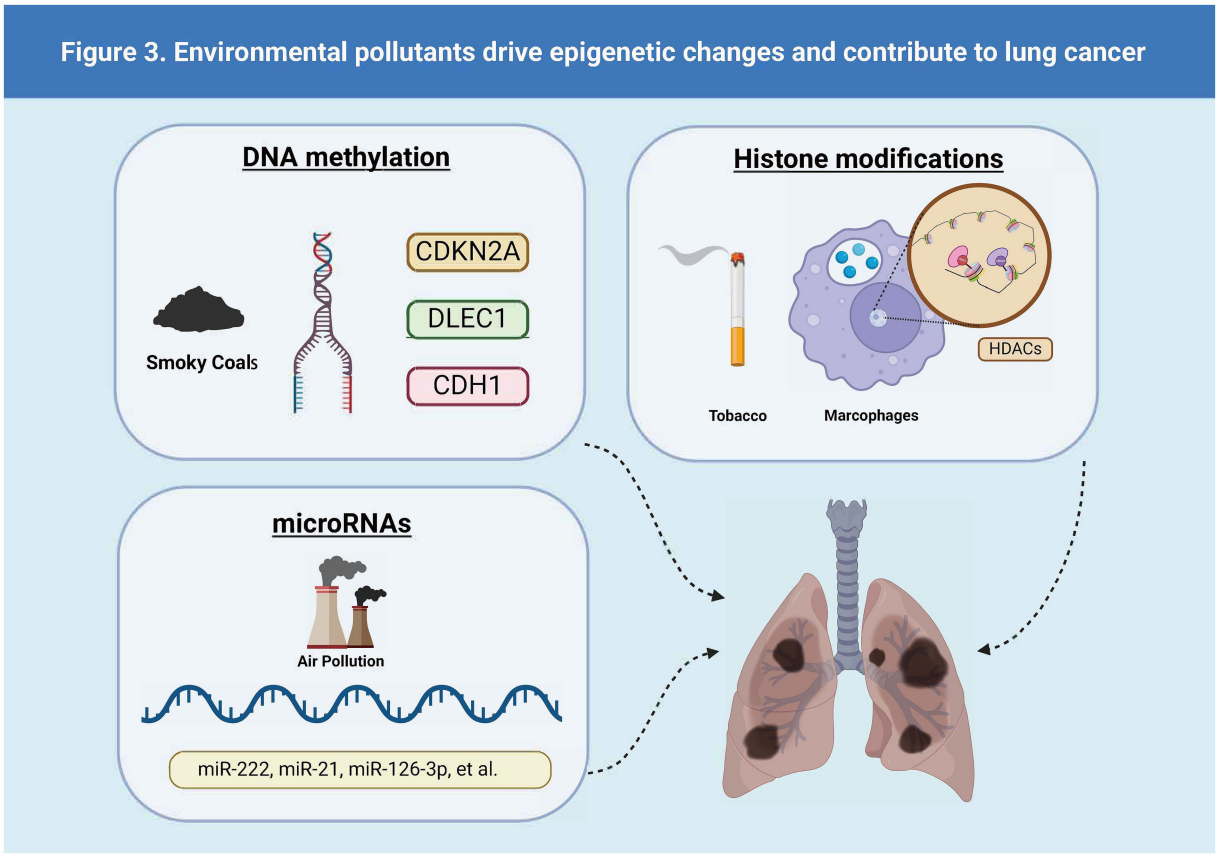

FIGURE 3
Environmental pollutants drive epigenetic changes and contribute to lung cancer.

Rigorous scrutiny and clinical trials of these emerging therapeutic modalities, coupled with the burgeoning interest in miRNA therapies, highlight their potential to significantly impact on individuals affected by the deleterious effects of environmental toxins. Research aimed at correcting aberrant methylation patterns with drugs like azacitidine, as well as exploring the anti-inflammatory properties of HDAC inhibitors represent scientific endeavors and steps toward a healthier future for the global community.

Author contributions

AZ: Conceptualization, Data curation, Methodology, Writing – original draft. XL: Conceptualization, Investigation, Writing – original draft. YL: Conceptualization, Methodology, Writing – review & editing. LY: Conceptualization, Data curation, Writing – original draft. XiL: Data curation, Writing – review & editing. QY: Investigation, Writing – review & editing. ZZ: Data curation, Writing – review & editing. GH: Resources, Supervision, Validation, Writing – review & editing. ZL: Project administration, Supervision, Validation, Writing – review & editing. QW: Funding acquisition, Project administration, Supervision, Validation, Writing – review & editing. JW: Project administration, Supervision, Validation, Writing – review & editing.

Funding

The author(s) declare that financial support was received for the research, authorship, and/or publication of this article. This work was supported by grants from the Science and Technology Development Fund, Macau SAR (File No. 0098/2021/A2 and 0048/2023/AFJ), Macau University of Science and Technology's Faculty Research Grant (No. FRG-23-003-FC, FRG-24-049-FA) and Open funding of Guangdong-Hong Kong-Macao Joint Laboratory for Contaminants Exposure and Health (No. GHMJLCEH-09).

Conflict of interest

The authors declare that the research was conducted in the absence of any commercial or financial relationships that could be construed as a potential conflict of interest.

Publisher's note

References

1. Bray F, Ferlay J, Soerjomataram I, Siegel RL, Torre LA, Jemal A. Global cancer statistics 2018: GLOBOCAN estimates of incidence and mortality worldwide for 36 cancers in 185 countries. *CA Cancer J Clin*. (2018) 68:394–424. doi: 10.3322/caac.21492

2. Jonna S, Subramaniam DS. Molecular diagnostics and targeted therapies in non-small cell lung cancer (NSCLC): an update. *Discov Med*. (2019) 27:167–70.

3. Xia C, Dong X, Li H, Cao M, Sun D, He S, et al. Cancer statistics in China and United States, 2022: profiles, trends, and determinants. *Chin Med J*. (2022) 135:584–90. doi: 10.1097/CM9.0000000000002108

4. Bray F, Laversanne M, Sung H, Ferlay J, Siegel RL, Soerjomataram I, et al. Global cancer statistics 2022: GLOBOCAN estimates of incidence and mortality worldwide for 36 cancers in 185 countries. *CA Cancer J Clin*. (2024) 74:229–63. doi: 10.3322/caac.21834

5. Taskforce for Annual Report of Macao Cancer Registry. (2020). 2020 Annual Report of Macao Cancer Registry. Available at: https://ssm.gov.mo/docs/25291/25291_83af9211caf1406abead778c4f9b9574_000.pdf (Accessed August 1, 2022).

6. Ettinger DS, Wood DE, Akerley W, Bazhenova LA, Borghaei H, Camidge DR, et al. Non-small cell lung Cancer, version 6.2015. *J National Comprehensive Cancer Network: JNCCN*. (2015) 13:515–24. doi: 10.6004/jnccn.2015.0071

7. Tseng C-H, Tsuang B-J, Chiang C-J, Ku K-C, Tseng J-S, Yang T-Y, et al. The relationship between air pollution and lung Cancer in nonsmokers in Taiwan. *J Thoracic Oncol: Official Pub Int Association For the Study of Lung Cancer*. (2019) 14:784–92. doi: 10.1016/j.jtho.2018.12.033

8. Wang N, Mengersen K, Tong S, Kimlin M, Zhou M, Wang L, et al. Short-term association between ambient air pollution and lung cancer mortality. *Environ Res*. (2019) 179:108748. doi: 10.1016/j.envres.2019.108748

9. Xing DF, Xu CD, Liao XY, Xing TY, Cheng SP, Hu MG, et al. Spatial association between outdoor air pollution and lung cancer incidence in China. *BMC Public Health*. (2019) 19:1377. doi: 10.1186/s12889-019-7740-y

10. Aokage K, Yoshida J, Hishida T, Tsuboi M, Saji H, Okada M, et al. Limited resection for early-stage non-small cell lung cancer as function-preserving radical surgery: a review. *Jpn J Clin Oncol*. (2017) 47:7–11. doi: 10.1093/jjco/hyw148

11. Donington JS, Koo CW, Ballas MS. Novel therapies for non-small cell lung cancer. *J Thorac Imaging*. (2011) 26:175–85. doi: 10.1097/RTI.0b013e3182161709

12. Hirsch FR, Scagliotti GV, Mulshine JL, Kwon R, Curran WJ, Wu Y-L, et al. Lung cancer: current therapies and new targeted treatments. *Lancet (London, England)*. (2017) 389:299–311. doi: 10.1016/S0140-6736(16)30958-8

13. Kato A, Shimizu K, Shimoichi Y, Fujii H, Honoki K, Tsujiuchi T. Aberrant DNA methylation of E-cadherin and p16 genes in rat lung adenocarcinomas induced by N-nitrosobis(2-hydroxypropyl)amine. *Mol Carcinog*. (2006) 45:106–11. doi: 10.1002/mc.20162

14. Shimizu K, Kato A, Shigemura M, Fujii H, Honoki K, Tsujiuchi T. Aberrant methylation patterns of the Rassf1a gene in rat lung adenocarcinomas induced by N-nitrosobis(2-hydroxypropyl)amine. *Mol Carcinog*. (2006) 45:112–7. doi: 10.1002/mc.20173

15. Shimizu K, Shigemura M, Fujii H, Honoki K, Tsujiuchi T. Reduced expression of the Connexin26 gene and its aberrant DNA methylation in rat lung adenocarcinomas induced by N-nitrosobis(2-hydroxypropyl)amine. *Mol Carcinog*. (2006) 45:710–4. doi: 10.1002/mc.20207

16. Yanagawa N, Tamura G, Oizumi H, Kanauchi N, Endoh M, Sadahiro M, et al. Promoter hypermethylation of RASSF1A and RUNX3 genes as an independent prognostic prediction marker in surgically resected non-small cell lung cancers. *Lung Cancer (Amsterdam, Netherlands)*. (2007) 58:131–8. doi: 10.1016/j.lungcan.2007.05.011

17. Duma N, Santana-Davila R, Molina JR. Non-small cell lung Cancer: epidemiology, screening, diagnosis, and treatment. *Mayo Clin Proc*. (2019) 94:1623–40. doi: 10.1016/j.mayocp.2019.01.013

18. Brock MV, Hooker CM, Ota-Machida E, Han Y, Guo M, Ames S, et al. DNA methylation markers and early recurrence in stage I lung cancer. *N Engl J Med*. (2008) 358:1118–28. doi: 10.1056/NEJMoa0706550

19. Christiani DC. Ambient air pollution and lung Cancer: nature and nurture. *Am J Respir Crit Care Med*. (2021) 204:752–3. doi: 10.1164/rccm.202107-1576ED

20. Orru H, Ebi KL, Forsberg B. The interplay of climate change and air pollution on health. *Current Environ Health Reports*. (2017) 4:504–13. doi: 10.1007/s40572-017-0168-6

21. Tang W, Pei Y, Zheng H, Zhao Y, Shu L, Zhang H. Twenty years of China's water pollution control: experiences and challenges. *Chemosphere*. (2022) 295:133875. doi: 10.1016/j.chemosphere.2022.133875

22. The L. UK air pollution and public health. *Lancet (London, England)*. (2017) 389:1860. doi: 10.1016/S0140-6736(17)31271-0

23. Hascher A, Haase A-K, Hebestreit K, Rohde C, Klein H-U, Rius M, et al. DNA methyltransferase inhibition reverses epigenetically embedded phenotypes in lung cancer preferentially affecting polycomb target genes. *Clin Cancer Res: Official J American Association For Cancer Res*. (2014) 20:814–26. doi: 10.1158/1078-0432.CCR-13-1483

24. Lantuéjoul S, Salameire D, Salon C, Brambilla E. Pulmonary preneoplasia--sequential molecular carcinogenetic events. *Histopathology*. (2009) 54:43–54. doi: 10.1111/j.1365-2559.2008.03182.x

25. Wistuba II, Gazdar AF. Lung cancer preneoplasia. *Annu Rev Pathol*. (2006) 1:331–48. doi: 10.1146/annurev.pathol.1.110304.100103

26. Chen W, Zheng R, Baade PD, Zhang S, Zeng H, Bray F, et al. Cancer statistics in China, 2015. *CA Cancer J Clin*. (2016) 66:115–32. doi: 10.3322/caac.21338

27. Jemal A, Bray F, Center MM, Ferlay J, Ward E, Forman D. Global cancer statistics. *CA Cancer J Clin*. (2011) 61:69–90. doi: 10.3322/caac.20107

28. Siegel RL, Miller KD, Jemal A. Cancer statistics, 2016. *CA Cancer J Clin*. (2016) 66:7–30. doi: 10.3322/caac.21332

29. Duan J, Zhong B, Fan Z, Zhang H, Xu M, Zhang X, et al. DNA methylation in pulmonary fibrosis and lung cancer. *Expert Rev Respir Med*. (2022) 16:519–28. doi: 10.1080/17476348.2022.2085091

30. Liang W, Zhao Y, Huang W, Gao Y, Xu W, Tao J, et al. Non-invasive diagnosis of early-stage lung cancer using high-throughput targeted DNA methylation sequencing of circulating tumor DNA (ctDNA). *Theranostics*. (2019) 9:2056–70. doi: 10.7150/thno.28119

31. Tsujiuchi T, Masaoka T, Sugata E, Onishi M, Fujii H, Shimizu K, et al. Hypermethylation of the dal-1 gene in lung adenocarcinomas induced by N-nitrosobis(2-hydroxypropyl)amine in rats. *Mol Carcinog*. (2007) 46:819–23. doi: 10.1002/mc.20316

32. Yang Z, Qi W, Sun L, Zhou H, Zhou B, Hu Y. DNA methylation analysis of selected genes for the detection of early-stage lung cancer using circulating cell-free DNA. *Advan Clin Experimental Med: Official Organ Wroclaw Medical University*. (2019) 28:355–60. doi: 10.17219/acem/84935

33. The World Health Organization (WHO). (2023). Ambient air pollution data [database]. Home/data/GHO/themes/air pollution data portal/ambient air pollution data. Retrieved from https://www.who.int/data/gho/data/themes/air-pollution/ambient-air-pollution (Accessed on December 1, 2023)

34. Attard A, Larkin M. Art therapy for people with psychosis: a narrative review of the literature. *Lancet Psychiatry*. (2016) 3:1067–78. doi: 10.1016/S2215-0366(16)30146-8

35. Alhamdow A, Essig YJ, Krais AM, Gustavsson P, Tinnerberg H, Lindh CH, et al. Fluorene exposure among PAH-exposed workers is associated with epigenetic markers related to lung cancer. *Occup Environ Med*. (2020) 77:488–95. doi: 10.1136/oemed-2020-106413

36. Baglietto L, Ponzi E, Haycock P, Hodge A, Bianca Assumma M, Jung CH, et al. DNA methylation changes measured in pre-diagnostic peripheral blood samples are associated with smoking and lung cancer risk. *Int J Cancer*. (2017) 140:50–61. doi: 10.1002/ijc.30431

37. Fasanelli F, Baglietto L, Ponzi E, Guida F, Campanella G, Johansson M, et al. Hypomethylation of smoking-related genes is associated with future lung cancer in four prospective cohorts. *Nat Commun*. (2015) 6:10192. doi: 10.1038/ncomms10192

38. Lee DH, Hwang SH, Lim MK, Oh JK, Song DY, Yun EH, et al. Performance of urine cotinine and hypomethylation of AHRR and F2RL3 as biomarkers for smoking exposure in a population-based cohort. *PLoS One*. (2017) 12:e0176783. doi: 10.1371/journal.pone.0176783

39. Huang X, Wu C, Fu Y, Guo L, Kong X, Cai H. Methylation analysis for multiple gene promoters in non-small cell lung cancers in high indoor air pollution region in China. *Bull Cancer*. (2018) 105:746–54. doi: 10.1016/j.bulcan.2018.05.004

40. Guo L, Byun HM, Zhong J, Motta V, Barupal J, Zheng Y, et al. Effects of short-term exposure to inhalable particulate matter on DNA methylation of tandem repeats. *Environ Mol Mutagen*. (2014) 55:322–35. doi: 10.1002/em.21838

41. Hou L, Zhang X, Zheng Y, Wang S, Dou C, Guo L, et al. Altered methylation in tandem repeat element and elemental component levels in inhalable air particles. *Environ Mol Mutagen*. (2014) 55:256–65. doi: 10.1002/em.21829

42. Jabeen M, Fayyaz M, Irudayaraj J. Epigenetic modifications, and alterations in cell cycle and apoptosis pathway in A549 lung carcinoma cell line upon exposure to perfluoroalkyl substances. *Toxics*. (2020) 8:112. doi: 10.3390/toxics8040112

43. Liang Y, Hu L, Li J, Liu F, Jones KC, Li D, et al. Short-term personal PM2. 5 exposure and change in DNA methylation of imprinted genes: panel study of healthy young adults in Guangzhou city, China. *Environ Pollut*. (2021) 275:116601. doi: 10.1016/j.envpol.2021.116601

44. Sato A, Ishigami A. Effects of heated tobacco product aerosol extracts on DNA methylation and gene transcription in lung epithelial cells. *Toxicol Appl Pharmacol*. (2023) 475:116637. doi: 10.1016/j.taap.2023.116637

45. Pan HL, Wen ZS, Huang YC, Cheng X, Wang GZ, Zhou YC, et al. Down-regulation of microRNA-144 in air pollution-related lung cancer. *Sci Rep*. (2015) 5:14331. doi: 10.1038/srep14331

46. Schembri F, Sridhar S, Perdomo C, Gustafson AM, Zhang X, Ergun A, et al. MicroRNAs as modulators of smoking-induced gene expression changes in human airway epithelium. *Proc Natl Acad Sci*. (2009) 106:2319–24. doi: 10.1073/pnas.0806383106

47. Sima M, Rossnerova A, Simova Z, Rossner P Jr. The impact of air pollution exposure on the MicroRNA machinery and lung cancer development. *J Personalized Med*. (2021) 11:60. doi: 10.3390/jpm11010060

48. Tellez CS, Juri DE, Do K, Bernauer AM, Thomas CL, Damiani LA, et al. EMT and stem cell–like properties associated with miR-205 and miR-200 epigenetic silencing are early manifestations during carcinogen-induced transformation of human lung epithelial cells. *Cancer Res*. (2011) 71:3087–97. doi: 10.1158/0008-5472.CAN-10-3035

49. Wang G, Wang R, Strulovici-Barel Y, Salit J, Staudt MR, Ahmed J, et al. Persistence of smoking-induced dysregulation of miRNA expression in the small airway epithelium despite smoking cessation. *PLoS One*. (2015) 10:e0120824. doi: 10.1371/journal.pone.0120824

50. Xi S, Xu H, Shan J, Tao Y, Hong JA, Inchauste S, et al. Cigarette smoke mediates epigenetic repression of miR-487b during pulmonary carcinogenesis. *J Clin Invest*. (2013) 123:1241–61. doi: 10.1172/JCI61271

51. Hammons GJ, Yan Y, Lopatina NG, Jin B, Wise C, Blann EB, et al. Increased expression of hepatic DNA methyltransferase in smokers. *Cell Biol Toxicol*. (1999) 15:389–94. doi: 10.1023/A:1007658000971

52. Sanchez-Guerra M, Zheng Y, Osorio-Yanez C, Zhong J, Chervona Y, Wang S, et al. Effects of particulate matter exposure on blood 5-hydroxymethylation: results from the Beijing truck driver air pollution study. *Epigenetics*. (2015) 10:633–42. doi: 10.1080/15592294.2015.1050174

53. Guo C, Lv S, Liu Y, Li Y. Biomarkers for the adverse effects on respiratory system health associated with atmospheric particulate matter exposure. *J Hazard Mater*. (2022) 421:126760. doi: 10.1016/j.jhazmat.2021.126760

54. Li G, Fang J, Wang Y, Wang H, Sun CC. MiRNA-based therapeutic strategy in lung cancer. *Curr Pharm Des*. (2017) 23:6011–8. doi: 10.2174/1381612823666170725141954

55. Mukherjee S, Dasgupta S, Mishra PK, Chaudhury K. Air pollution-induced epigenetic changes: disease development and a possible link with hypersensitivity pneumonitis. *Environ Sci Pollut Res*. (2021) 28:55981–6002. doi: 10.1007/s11356-021-16056-x

56. Wu Y, Qie R, Cheng M, Zeng Y, Huang S, Guo C, et al. Air pollution and DNA methylation in adults: a systematic review and meta-analysis of observational studies. *Environ Pollut*. (2021) 284:117152. doi: 10.1016/j.envpol.2021.117152

57. Xue Y, Wang L, Zhang Y, Zhao Y, Liu Y. Air pollution: a culprit of lung cancer. *J Hazard Mater*. (2022) 434:128937. doi: 10.1016/j.jhazmat.2022.128937

58. Li J, Li WX, Bai C, Song Y. Particulate matter-induced epigenetic changes and lung cancer. *Clin Respir J*. (2017) 11:539–46. doi: 10.1111/crj.12389

59. Liu J, Chen Y, Cao H, Zhang A. Burden of typical diseases attributed to the sources of PM2. 5-bound toxic metals in Beijing: an integrated approach to source apportionment and QALYs. *Environ Int*. (2019) 131:105041. doi: 10.1016/j.envint.2019.105041

60. Bhargava A, Bunkar N, Aglawe A, Pandey KC, Tiwari R, Chaudhury K, et al. Epigenetic biomarkers for risk assessment of particulate matter associated lung cancer. *Curr Drug Targets*. (2018) 19:1127–47. doi: 10.2174/1389450118666170911114342

61. Ladd-Acosta C. Epigenetic signatures as biomarkers of exposure. *Current environmental health reports*. (2015) 2:117–25. doi: 10.1007/s40572-015-0051-2

62. Hong Y, Kim WJ. DNA methylation markers in lung cancer. *Curr Genomics*. (2021) 22:79–87. doi: 10.2174/1389202921999201013164110

63. Nikolaidis G, Raji OY, Markopoulou S, Gosney JR, Bryan J, Warburton C, et al. DNA methylation biomarkers offer improved diagnostic efficiency in lung cancer. *Cancer Res*. (2012) 72:5692–701. doi: 10.1158/0008-5472.CAN-12-2309

64. Tsou JA, Hagen JA, Carpenter CL, Laird-Offringa IA. DNA methylation analysis: a powerful new tool for lung cancer diagnosis. *Oncogene*. (2002) 21:5450–61. doi: 10.1038/sj.onc.1205605

65. Wei B, Wu F, Xing W, Sun H, Yan C, Zhao C, et al. A panel of DNA methylation biomarkers for detection and improving diagnostic efficiency of lung cancer. *Sci Rep*. (2021) 11:16782. doi: 10.1038/S41598-021-96242-6

66. Del Vescovo V, Grasso M, Barbareschi M, Denti MA. MicroRNAs as lung cancer biomarkers. *World J Clinical Oncol*. (2014) 5:604–20. doi: 10.5306/wjco.v5.i4.604

67. Inamura K, Ishikawa Y. MicroRNA in lung cancer: novel biomarkers and potential tools for treatment. *J Clin Med*. (2016) 5:36. doi: 10.3390/jcm5030036

68. Shen J, Todd NW, Zhang H, Yu L, Lingxiao X, Mei Y, et al. Plasma microRNAs as potential biomarkers for non-small-cell lung cancer. *Lab Investig*. (2011) 91:579–87. doi: 10.1038/labinvest.2010.194

69. Carrier M, Apparicio P, Séguin AM, Crouse D. The application of three methods to measure the statistical association between different social groups and the concentration of air pollutants in Montreal: a case of environmental equity. *Transp Res Part D: Transp Environ*. (2014) 30:38–52. doi: 10.1016/j.trd.2014.05.001

70. Dai Z, Lakshmanan RR, Zhu WG, Smiraglia DJ, Rush LJ, Frühwald MC, et al. Global methylation profiling of lung cancer identifies novel methylated genes. *Neoplasia*. (2001) 3:314–23. doi: 10.1038/sj.neo.7900162

71. Rauch TA, Wang Z, Wu X, Kernstine KH, Riggs AD, Pfeifer GP. DNA methylation biomarkers for lung cancer. *Tumour Biol*. (2012) 33:287–96. doi: 10.1007/s13277-011-0282-2

72. Tsou JA, Galler JS, Siegmund KD, Laird PW, Turla S, Cozen W, et al. Identification of a panel of sensitive and specific DNA methylation markers for lung adenocarcinoma. *Mol Cancer*. (2007) 6:1–13. doi: 10.1186/1476-4598-6-70

73. Vaissière T, Hung RJ, Zaridze D, Moukeria A, Cuenin C, Fasolo V, et al. Quantitative analysis of DNA methylation profiles in lung cancer identifies aberrant DNA methylation of specific genes and its association with gender and cancer risk factors. *Cancer Res*. (2009) 69:243–52. doi: 10.1158/0008-5472.CAN-08-2489

74. Tam KW, Zhang W, Soh J, Stastny V, Chen M, Sun H, et al. CDKN2A/p16 inactivation mechanisms and their relationship to smoke exposure and molecular features in non–small-cell lung cancer. *J Thorac Oncol*. (2013) 8:1378–88. doi: 10.1097/JTO.0b013e3182a46c0c

75. Belinsky SA, Klinge DM, Stidley CA, Issa JP, Herman JG, March TH, et al. Inhibition of DNA methylation and histone deacetylation prevents murine lung cancer. *Cancer Res*. (2003) 63:7089–93.

76. Vendetti FP, Rudin CM. Epigenetic therapy in non-small-cell lung cancer: targeting DNA methyltransferases and histone deacetylases. *Expert Opin Biol Ther*. (2013) 13:1273–85. doi: 10.1517/14712598.2013.819337

77. Zöchbauer-Müller S, Minna JD, Gazdar AF. Aberrant DNA methylation in lung cancer: biological and clinical implications. *Oncologist*. (2002) 7:451–7. doi: 10.1634/theoncologist.7-5-451

78. Huffman K, Martinez ED. Pre-clinical studies of epigenetic therapies targeting histone modifiers in lung cancer. *Front Oncol*. (2013) 3:235. doi: 10.3389/fonc.2013.00235

79. Schiffmann I, Greve G, Jung M, Lübbert M. Epigenetic therapy approaches in non-small cell lung cancer: update and perspectives. *Epigenetics*. (2016) 11:858–70. doi: 10.1080/15592294.2016.1237345

80. Barger JF, Nana-Sinkam SP. MicroRNA as tools and therapeutics in lung cancer. *Respir Med*. (2015) 109:803–12. doi: 10.1016/j.rmed.2015.02.006

81. Wu M, Wang G, Tian W, Deng Y, Xu Y. MiRNA-based therapeutics for lung cancer. *Curr Pharm Des*. (2017) 23:5989–96. doi: 10.2174/1381612823666170714151715

82. Cheng H, Zou Y, Shah CD, Fan N, Bhagat TD, Gucalp R, et al. First-in-human study of inhaled Azacitidine in patients with advanced non-small cell lung cancer. *Lung Cancer*. (2021) 154:99–104. doi: 10.1016/j.lungcan.2021.02.015

83. Vendetti FP, Topper M, Huang P, Dobromilskaya I, Easwaran H, Wrangle J, et al. Evaluation of azacitidine and entinostat as sensitization agents to cytotoxic chemotherapy in preclinical models of non-small cell lung cancer. *Oncotarget*. (2015) 6:56–70. doi: 10.18632/oncotarget.2695

84. Komatsu N, Kawamata N, Takeuchi S, Yin D, Chien W, Miller CW, et al. SAHA, a HDAC inhibitor, has profound anti-growth activity against non-small cell lung cancer cells. *Oncol Rep*. (2006) 15:187–91. doi: 10.3892/or.15.1.187

85. Platta CS, Greenblatt DY, Kunnimalaiyaan M, Chen H. The HDAC inhibitor trichostatin a inhibits growth of small cell lung cancer cells. *J Surg Res*. (2007) 142:219–26. doi: 10.1016/j.jss.2006.12.555

86. Wang P, Yang D, Zhang H, Wei X, Ma T, Cheng Z, et al. Early detection of lung cancer in serum by a panel of microRNA biomarkers. *Clin Lung Cancer*. (2015) 16:313–319.e1. doi: 10.1016/j.cllc.2014.12.006

frontiers | Frontiers in Public Health

TYPE Original Research
PUBLISHED 13 November 2024
DOI 10.3389/fpubh.2024.1402421

OPEN ACCESS

EDITED BY
Goutam Kumar Kundu,
University of Dhaka, Bangladesh

REVIEWED BY
Guilherme Sgobbi Zagui,
University of Ribeirão Preto, Brazil
Lili Li,
Northwest A&F University, China

*CORRESPONDENCE
Sathiavelu Arunachalam
✉ asathiavelu@vit.ac.in

RECEIVED 03 June 2024
ACCEPTED 30 September 2024
PUBLISHED 13 November 2024

CITATION
Gupta N and Arunachalam S (2024) Assessment of human health risks posed by toxic heavy metals in Tilapia fish (*Oreochromis mossambicus*) from the Cauvery River, India.
Front. Public Health 12:1402421.
doi: 10.3389/fpubh.2024.1402421

Assessment of human health risks posed by toxic heavy metals in Tilapia fish (*Oreochromis mossambicus*) from the Cauvery River, India

Nikita Gupta[1,2] and Sathiavelu Arunachalam[2]*

[1]School of BioSciences and Technology, Vellore Institute of Technology, Vellore, India, [2]VIT School of Agricultural Innovation and Advanced Learning, Vellore Institute of Technology, Vellore, India

Heavy metal toxicity is a serious threat to human health due to its bioaccumulation, biomagnification, and persistent nature in the environment including aquatic systems. In the recent past, heavy metal contamination in the environment has occurred due to various anthropogenic sources. The concentration of potentially toxic heavy metals was determined by Atomic Absorption Spectroscopy in Tilapia (*Oreochromis mossambicus*), a highly farmed and consumed fish species in southern parts of India. The mean levels of Fe were found to be higher in major organs of the fish with the highest levels in liver (Mean 1554.4 ± 1708.7 mg/kg) and lowest in the muscles (Mean 130.757 ± 33.3 mg/kg). Correlation Matrix analysis revealed relationships between the occurrence of various heavy metals in different organs of fish and indicated similar origins and chemical properties. Target hazard quotient for Cd, Co, Pb, and Cr in the Liver, Co and Cr in the Gills, and Co in Muscle were > 1 for adults, which showed a significant health risk from the combined effects of these metals. The potential health risk to humans, according to the cancer risk (CR) assessment is attributed mainly to Cd and Cr levels. Overall, moderate fish consumption is advised to limit the bioaccumulation of heavy metals over prolonged exposure and associated health risks.

KEYWORDS

aquatic pollution, Cauvery River, environmental pollution, heavy metal, health risk assessment, Tilapia fish, toxicity

1 Introduction

The anthropogenic pollution of freshwater bodies is of major concern globally and so is in India (1). In this study, the authors emphasized the impact of anthropogenic activities on the fish fauna in the Ujjani Reservoir in Maharashtra, India. They also reported higher levels of heavy metals in the fish from the reservoir than normal. India is a country with rich biodiversity along with a number of freshwater reserves in the form of rivers, lakes, ponds, etc. However, in the past decade, there has been an indiscriminate discharge of industrial and agricultural pollutants into the water bodies through various anthropogenic activities creating severe deterioration of water quality, thereby affecting aquatic life (2–5). Over the years, efforts have been made by different environmental protection agencies to control the amount of pollutants dumped into the rivers. The government also supported some studies on anthropogenic activities and their influence on heavy metals in Indian rivers (6). Nevertheless, much needs

to be done to restore the water bodies to their native state and mitigate the impact of pollution on aquatic and human health.

Trace heavy metals present in the aquatic ecosystem are released through agriculture and industries which accumulate at various trophic levels of the food chain. However, this accumulation can slowly reach hazardous levels and turn into an environmental problem. There have been several studies about the prominent presence of heavy metals on sediments and their impact on seawater, and aquatic organisms (7–9). A few studies on rivers in India have also discussed the potential impacts of heavy metals on humans (2, 4). Several studies have explored the bioaccumulation of heavy metals in fishes (10–12). The consensus seems to be that fishes in heavy metal-contaminated areas tend to absorb certain heavy metals in ionic forms from their immediate environment. Environmental factors such as pH and temperature modulate this uptake. The gills and skin, directly exposed to the contaminated water act as hotspots for its absorption. Following the uptake, heavy metals are transported to various organs via blood flow where the coupling of heavy metals with various proteins takes place. Although, fishes do regulate their body metal concentration to some degree via excretion through gills, skin, kidneys, and bile. Studies all around the world have reported various risks and health hazards associated with fishes' bodies which results from disturbances in normal cellular activities, oxidative damage to biological macromolecules such as DNA and RNA caused by heavy metals (12, 13). Accumulation of heavy metal also depends on the habitat of the fishes, sedimentary fishes that stay in stagnant water in muddy streams that are contaminated have been reported to have higher heavy metal content (14). Heavy metal accumulation has a multidirectional toxic effect on fish. In some cases, it manifests changes in the physiochemical processes of the body. Structural lesions and functional disturbances could also result from the bioaccumulation of metals (15).

Eating fish contaminated with heavy metals can have significant adverse effects on human health. Heavy metals such as cadmium, mercury, lead, and arsenic, when accumulated in fish tissues, can pose severe health risks when these fish are consumed by humans. These metals are known to be potent carcinogens and mutagens. Cadmium is known to be primarily toxic to the kidneys, cadmium can accumulate in the human body over time, potentially leading to kidney damage. Mercury is shown to affect the central nervous system, and high exposure can lead to neurological and behavioral disorders. Mercury is particularly dangerous to pregnant women as it can affect fetal development. Lead exposure can cause damage to the nervous system, kidney function, and the cardiovascular system. In children, lead exposure can result in developmental issues and reduced cognitive function. Arsenic exposure can lead to skin lesions, cancer, cardiovascular diseases, and diabetes. Long-term exposure to heavy metals through contaminated fish consumption can result in chronic conditions such as Alzheimer's disease, Parkinson's disease, muscular dystrophy, multiple sclerosis, and other neurological and muscular diseases. Allergies and increased cancer risk are also associated with prolonged heavy metal exposure (16, 17).

In India, fishes are considered a staple food source and the *per capita* consumption in some states reaches as high as 29.29 kg/year (18). Most of the fishing needs are met with inland fish production which is more susceptible to various sources of water pollution. Inland fishes thus are more hazardous to human health. Consumption of a heavy metal-contaminated diet can lead to the depletion of vital nutrients which can cause severe damage to immunological defenses, malnutrition-related disabilities, and impaired psychosocial behavior. Hence, the regular risk assessment of these heavy metals intake via diet is of utmost concern (19–21).

Mozambique Tilapia (*Oreochromis mossambicus*) is a variety of edible freshwater fish that has an omnivorous nature with high local demand in several developing countries like Malaysia. Commercial production of Tilapia fish takes place in almost 10 countries around the world (22, 23). It is one of the most important farmed fishes in the world next to carp and salmon. The low cost and high production coupled with its suitability for aquaculture and marketability make it a lucrative option for people in developing countries. Tilapias can adapt to various environmental conditions and demonstrate higher resistance to diseases but are susceptible to leachate toxicity (24). The wide acceptability of the Tilapias is evident from the production boost over the last decade resulting in a four-fold increase in its production (25, 26).

The present study is focused on monitoring the levels of various heavy metals in Tilapia, an exotic fish of the Cauvery River. Tilapia fish (*Oreochromis mossambicus*) is widely popular and highly consumed in southern parts of India (27, 28–33). It has high nutritional value and is a rich source of proteins, amino acids, vitamins, minerals, PUFA (polyunsaturated fatty acids), and some essential heavy metals. Heavy metals such as Manganese, Zinc, and Iron in optimal concentrations are supportive for the normal growth of humans and animals (34). However, some heavy metals such as arsenic, cadmium, mercury, lead, etc. do not play any beneficial role in the biological systems and can lead to a variety of diseases (1). Despite fish aiding in fulfilling our food, particularly protein demand, which in turn reduces the burden on agriculture, the presence of high amounts of essential as well as harmful heavy metals poses a serious risk to human health.

In the current scenario, Genetically Improved Farmed Tilapia (GIFT), is considered a candidate species for aquaculture in India. Its affordability and animal protein content make it a fish of choice among consumers (35). Various business organizations positively argue for the expansion of tilapia production in India to meet fish and marine export goals. This species has a relatively high survival rate and faster growth makes it lucrative for small-scale and large-scale GIFT farmers (36, 37). On the other hand, environmentalists argue over responsible aquaculture and strict regulations. Overall, Tilapia is currently seen as the next billion-dollar enterprise in India. Our study aims to understand and estimate the heavy metal content in this widely consumed, and important fish species in India, whose consumption is further likely to be increased in the coming years (34). Therefore, a study on this species not only provides us with the overall scenario of heavy metal load in the Cauvery River but also acts as a reference for further studies in the upcoming years with the aim to determine the levels of heavy metal concentrations in various organs of Tilapia fish.

2 Materials and methods

2.1 Ethics statement

Our study did not require ethical board approval because it did not contain human or animal trials. The fish used in this study were

Abbreviations: HM, Heavy Metal; PI, Pollution Index; EDI, Estimation of Daily Intake; THQ, Target hazard quotient; CR, Cancer Risk; CMA, Correlation matrix analysis; RfD, Reference dose; CSF, Cancer Slope Factor.

procured dead from local fishermen. All surgical operations were performed on dead fish. Care was taken to ensure that the least number of fish was utilized to reach satisfactory statistical conclusions.

2.2 Sample collection

The Cauvery River in southern India is vital for agriculture, industry, and urban populations in Karnataka and Tamil Nadu, but it faces significant metal contamination due to anthropogenic activities. Agricultural runoff, industrial discharges, and urban waste contribute to the presence of heavy metals like lead, chromium, and cadmium in the river (38). These metals bio-accumulate in fish, posing health risks to humans and disrupting aquatic ecosystems (39). Effective mitigation requires stringent regulatory measures, sustainable agricultural practices, and robust waste management systems, alongside regular monitoring and community engagement (40). Figure 1 represents the four sampling sites near the Erode region across the Cauvery River in Tamil Nadu state in India. The sampling sites were carefully chosen to cover the maximum stretch of the river possible, there is also quite a few textile industries and other industries in the area near Erode. The sampling stations were as follows: R1 (11°74′75.34" N; 77°78′69.66″ E); R2 (11°43′36.68" N;77°68′27.9″ E); R3 (11°31′02.94" N;77°77′87.36″ E); R4 (11°15′72.31" N;77°88′11.61″ E). A total of sixteen (16) fresh and adult, Tilapia fish involved in the study were purchased from the local fishermen in each area depending on the sites from where the fish were planned to be sampled (41, 42). Samples collected were the maximum feasible given only one species of fish was targeted with similar size and body weight. All the fish were dead and stored in ice after purchase and carried forward for further analysis. On arrival, all the samples were labeled and stored at -20°C for further analysis. All 16 samples collected were analyzed as per the standard protocols published and raw data is provided as Supplementary file S1.

2.3 Sample analysis

The fishes collected had average lengths and weights of 17.7 cm (measured with a ruler) and 112.5 g (measured with a weighing balance (Mettler Toledo ME204)), respectively Supplementary file S1. Fish sample collection was done in the pre-monsoon period. A stainless-steel scalpel was used to dissect various portions of the raw sampled fish, which were Muscle, Liver and Gills and taken for further analysis. A digestion tube containing 0.1–1 g of the sample (dry weight) was weighed, and 5 mL of HNO_3 and 5 mL of H2SO4 were then added. The reaction was allowed to complete, and when it did, the tubes were put in a hot-block digestion device from BioBee® with 12 slots and temperature control and heated for 30 min at 60°C before being heated again to 150°C. When the samples' color turned black,

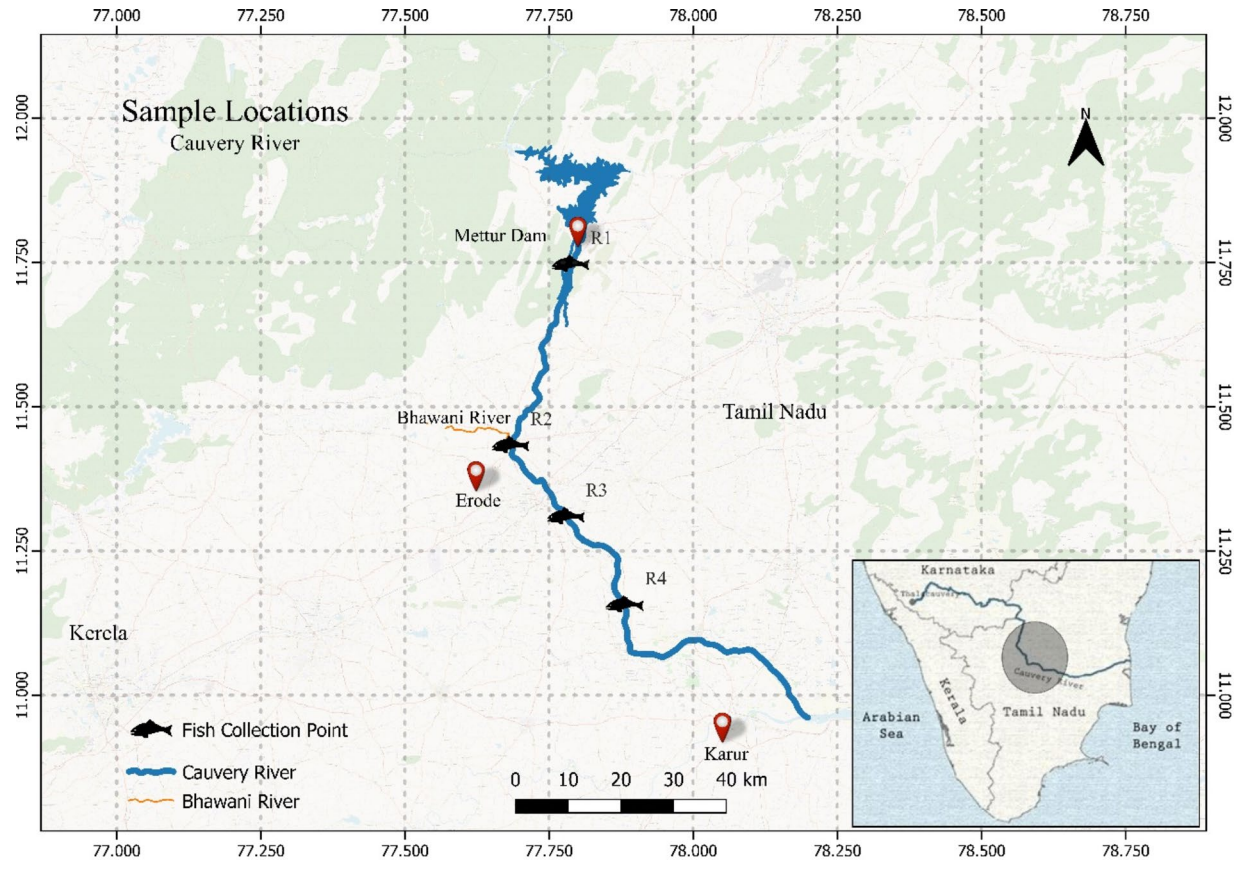

FIGURE 1
Location map of the study area showing sampling locations and important places.

the tubes were taken out of the experiment. After allowing the tubes to cool, 1 mL of H_2O_2 was added. The tubes were repositioned on the block after a strong reaction. Slowly adding H2O2 made the sample's solution appear clear. The tubes were taken out, and the sample solution was diluted with deionized water to a volume of 50 mL (12, 43).

The heavy metals (Cr, Cd, Fe, Ni, Zn, Co, Pb, and Cu) concentration was determined using a Varian - Atomic Absorption Spectrophotometer (AA240 Atomic Absorption Spectrometer). To test the instrument's accuracy, standard solutions, and samples were run simultaneously. Analytical conditions for the measurement of the heavy metals in the sample using AAS were tabulated in Table 1. All the fish samples were measured in triplicates and the mean was taken forward for further calculation and reported as it is, as no randomization was performed given the samples were collected directly from rivers. All chemicals and reagents were of analytical reagent-grade quality. Before use, all glass and plastic ware were soaked in 14% HNO_3 for 24 h. The washing was done with distilled water. Measurements were done simultaneously for each group to avoid batch effects if any. Data analysis was performed on a Spreadsheet and GraphPad Prism (Version 8.0).

2.4 Relevant parameter estimations

2.4.1 Calculation of heavy metal (HM) in tissues

The concentration of minerals is calculated according to the equation given below (44),

$$Mineral\left(\frac{mg}{L}\right) = Reading\ of\ mineral\ in\ AAS \times \frac{50(made-up\ volume)}{weight\ of\ sample(g)}$$

2.4.2 Pollution index (PI)

To determine the PI of the elements, statistical analysis was performed on the elemental concentrations in fish samples. The PI is the ratio of element x concentration in the sample to the element's maximum allowable level (41).

TABLE 1 Analytical conditions for the measurement of the heavy metals in the sample using AAS.

Heavy Metal	Wavelength	Slit (nm)	Lamp current (mA)
Cd	228.8	0.5	4
Cu	222.6	0.2	4
Cr	428.9	0.5	7
Fe	372.0	0.2	5
Pb	283.3	0.5	5
Zn	213.9	1	5
Co	304.4	0.5	7
Ni	341.5	0.2	4

$$PI(x) = \frac{Metal\ concentration\ in\ the\ sample}{Permissible\ limit\ or\ background\ value}$$

It is generally accepted that if an element's PI value is more than 1.0, the element is highly likely to have contaminated the sample and may even be dangerous at the amount it is present.

2.4.3 Estimated daily intake (EDI)

The estimated daily intake (EDI) was calculated using the following formula (45).

$$EDI = \frac{E_F \times E_D \times FIR \times C_F \times C}{W_{AB} \times T_A} \times 10^{-3}$$

where ED, EF, *CF*, WAB, FIR, C, and TA stand for the exposure duration (60 years), exposure frequency (365 days annually), conversion factor (0.208) to convert fish's dry weight to wet weight, average adult weight of the body (70 kg), consumption rate (25.2 g per day), heavy metal concentrations in fish's muscle tissues, and average exposure time, respectively (45–49). The daily intake values were compared with reference values established by the United States Environmental Protection Agency (50), making the USEPA the legislation that will serve as the bibliographic tool in the comparative analysis. All the calculations in this study were made for adult human with standard fish intake over lifetime.

2.4.4 Target hazard quotient (THQ) or non-carcinogenic health hazard

THQ measures the risk of side events other than cancer by comparing the exposure dosage to the reference dose (RfD). The exposure level is lower than the RfD if it is less than 1. This suggests that lifetime unfavorable effects are unlikely to result from daily exposure at this level and vice versa. Standard assumptions from the integrated USEPA risk study were used to construct the dosage estimations (41, 50).

The target hazard quotient (THQ) was estimated using the following formula.

$$THQ = \frac{EDI}{RfD}$$

In this study, the total THQ was calculated as the arithmetic sum of the individual THQ values of the metal of concern (51).

$$Total\ THQ(TTHQ) = THQ(toxicant\ 1) + THQ(toxicant\ 2) + ...THQ(toxicant\ n)$$

2.4.5 Carcinogenic risk or cancer risks (CR)

The Cancer Risk over a lifetime of Cd, Pb, and Cr exposure was calculated by applying the following formula (45, 46).

$$CR = EDI \times CSF$$

2.5 Data analysis

2.5.1 Principal component analysis (PCA)

Principal Component Analysis was used to reduce the dimensionality of the dataset. It was used to identify patterns in the distribution of heavy metals across different fish organs. The analysis was performed in GraphPad Prism version V.10. Principal Component Analysis transformed the original variables into a new set of uncorrelated variables which are also known as principal components these components are ordered by the amount of variance they explain in the data. This method allows for the visualization of the data structure and the identification of the most significant variables contributing to the observed variance. PCA can identify linear relationships between different inter-associated variables. PCA extracts eigenvalues and eigenvectors from the covariance matrix of the original associated variables. The principal component (PC) is an orthogonal variable, which is attained by multiplying the eigenvector with the original associated variables. The first few principal components, which capture the majority of the variance, were used to interpret the relationships between the heavy metal concentrations and the fish organs. Since there were various factors influencing the accumulation of heavy metals in fish muscles, Principal Component Analysis was used to explore the effects of size and body weight of fish on the accumulation of heavy metals in different organs using the analyzed heavy metal concentrations matrix.

2.5.2 Correlation matrix analysis

A correlation matrix was computed to analyze the associations between the various concentrations of heavy metals within various organs of fish. The correlation matrix was also analyzed with GraphPad Prism v.10. The correlation matrix is a summary of all the pair-wise correlations between the variables, measured by means of Pearson correlation coefficients. Correlations are meaningful, and a heatmap is used to see significant correlations in the matrix. A correlation coefficient-the value ranging from −1, for a perfect inverse relation, through 0, for no relation, to 1, for a perfect direct relation-evaluates any two variables on a scale from −1 to 0 to 1. High values and positive significant correlation may indicate chemical affinity between the metals, common genetic origin and /or a background level present in the samples; negative correlation might point toward different origins for the metals or a non-chemical relationship. Considering the various trends in the level of correlation, we explained the strength of the correlation of heavy metals within each organ separately. Beyond the statistical tools used in this study, additional hidden features and strength of the data set could be unearthed by the linkage of variables using non-linear tools.

3 Results

3.1 Heavy metal concentrations

The metal concentrations in various body organs of Tilapia fish species are presented in Figure 2. Since most of the heavy metal concentrations did not significantly differ between the sample sites (R1 – R4), all four sites were combined for further analyses and correlation studies. In fish samples, iron concentration was found to be relatively higher than the other metals. The heavy metal concentration varied across different organs in the following sequence: Muscle Fe > Ni > Cr > Co > Pb > Cd > Zn > Cu, Gills Fe > Ni > Co > Cr > Pb > Cd > Zn > Cu, Liver Fe > Ni > Cr > Co > Cu > Pb > Cd > Zn. The maximum Fe levels were detected in the Liver (Mean: 1554.4 ± 1708.7 mg/kg) of Tilapia, while the minimum Fe levels were observed in the muscles (Mean: 130.757 ± 33.3 mg/kg). Muscles contained a low Fe level compared to the other organs. Apart from Iron other heavy metals like Cr, Co, Pb, and Cd were also found to be well above the standard permissible limits (Table 2) for the respective heavy metals in respective tissue samples.

3.2 Pollution index (PI) of the heavy metals

To assess the degree of contamination or pollution linked to the obtained fish samples, the PI of heavy metals in the Tilapia fish samples was determined. Table 3 displays the PI values for the analyzed metals. We found that Zn and Cu pollution index were lower than 1 across the various organs. Fe, Cd, Pb, Cr, Ni, and Co had high pollution index across all the organs. Overall, the pollution index values for heavy metals in Gills and Liver far surpassed those in Muscle.

3.3 Human health risk assessment

3.3.1 Estimation of estimated daily intake (EDI) and target hazard quotient (THQ)

According to the United States Environmental Protection Agency's (50), recommended oral reference dose is shown in Table 4. Our results showed that the EDI for the investigated metals was lower than the RfD (oral reference dose) with some exceptions which are Liver (Cd, Co, Pb, and Cr), Gills (Co and Cr), Muscle (Co). The THQ of each metal from ingestion of Tilapia was generally less than 1 except in the Liver (Cd, Co, Pb, and Cr), Gills (Co and Cr), and Muscle (Co) (see Table 5). THQ values for Cd, Co, Pb, and Cr in the Liver, Co and Cr in Gills, and, Co in Muscle were > 1 for adults (see Table 6).

3.3.2 Calculation of the cancer risk (CR) for cd, Pb, and Cr

Figure 3 showcases the estimated cancer risk factors for Cd, Pb, and Cr. The USEPA has assigned a 10–5 acceptable limit for the lifetime carcinogenic risk. Based on the findings, the muscle, liver, and gills Pb cancer risk factor determined in this study is within the established tolerable level. However, Cd and Cr are higher than the set tolerable limit.

3.4 Results of principal component analysis (PCA)

Two principal components were estimated using the JMP for our dataset comprising of body weight, Length and heavy metal concentration of different organs of fish (Figure 4). Both components together were able to explain ~88% of total variance in the data, with PC1 and PC2 accounting for 56.1 and 31.4%, respectively. The general trend shows negative loading of heavy metals in various fish organs in Tilapia Fish when compared with fish size and body weight. From PC1

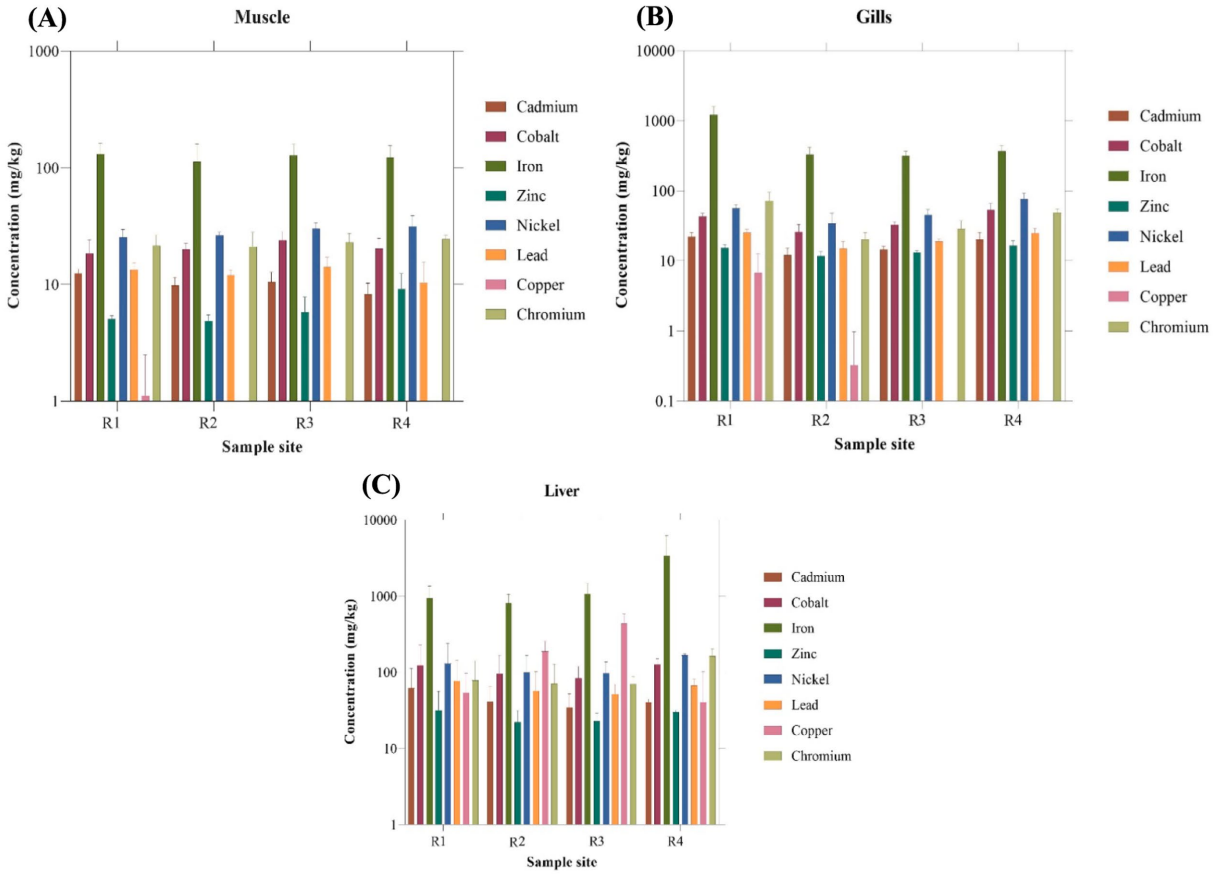

FIGURE 2
Concentration (mg/kg) of heavy metals in **(A)** Muscle, **(B)** Gills, and **(C)** Liver of *Oreochromis mossambicus*.

TABLE 2 The permissible limit of heavy metals in fisheries.

Institute/Organization	Zn	Cu	Pb	Ni	Cd	Mn	Fe	Cr	Reference
MFA (Malaysian Food Act)	100	30	2	-	1	–	–		MFA (65)
FAO (Food and Agriculture Organization) (1983)	30/40	30	0.5	-	0.5	–	–		FAO (66),
EC (Commission of the European Communities)	–	–	0.2–0.4	-	0.05	–	–	–	EC (67)
USFDA (Food and Drug Administration)	–	–	0.5	-	0.01–0.21	–	–		USFDA (68)
WHO (1989)/(2013)	100/5	30/2.25	2	–	1	1/0.5	100/0.30	–	Mokhtar et al. (69)
England	50	20	2	–	0.2	–	–		Contaminants (70)
FAO/WHO limits	40	30	2	–	0.5	–			Joint and Additives (71)
Median International Standard (Tolerable levels) (ug/g)	45	20	2	–	0.3	–	–	1	Phillips (72), Senarathne (73), and Senarathne and Pathiratne (74)
USEPA (United State Environmental Protection Agency) (ug/g)	5	2.25	0.11	–	0.01	0.02	0.5	–	Anim-Gyampo et al. (75)
WPCL (Water Pollution Control Legislation)	4.25	2	0.05	–	0.03	0.02	0.45	–	Anim-Gyampo et al. (75)

we can observe that heavy metal content more specifically in the Gills and Liver is loaded heavily on PC1 and seems to decrease with an increase in the length and weight of the fish. However, the loading of heavy metals in muscles seems to be dependent on both PC1 and PC2, which suggests some other factors influencing the loading apart from the length and weight of the Tilapia fish. This observation corroborates

TABLE 3 Pollution index (PI) of the studied heavy metals in the Tilapia Fish samples.

	Pollution index muscle				Pollution index liver				Pollution index gills			
HM	R1	R2	R3	R4	R1	R2	R3	R4	R1	R2	R3	R4
Cd	12.42	9.83	10.47	8.22	62.05	41.02	34.35	40.63	22.05	12.00	14.42	20.20
Co	65.82	71.52	85.77	72.27	440.29	342.92	296.75	450.00	154.15	92.05	117.59	190.85
Fe	261.51	225.93	255.35	243.59	1878.87	1615.56	2151.31	6789.50	2430.51	658.47	631.99	737.07
Zn	0.05	0.05	0.06	0.09	0.32	0.22	0.23	0.30	0.15	0.12	0.13	0.17
Ni	50.64	52.75	60.05	62.74	260.12	197.54	192.62	334.25	113.16	68.92	91.55	153.61
Pb	6.72	6.00	7.05	5.19	38.64	28.63	25.82	33.44	12.69	7.44	9.49	12.38
Cu	0.04	0.00	0.00	0.00	1.79	6.30	14.70	1.35	0.23	0.01	0.00	0.00
Cr	21.40	21.01	22.92	24.44	77.82	70.62	69.79	162.69	72.00	20.27	28.69	48.57

TABLE 4 Reference dose (RfD) and cancer slope factor (CSF) for different metals reported in the literature.

Metal	RfD	CSF (mg/kg/day)	Reference
Cd	0.001	6.3	Mohammadi et al. (64) and Adebiyi et al. (41)
Co	0.0003		Saha et al. (49)
Fe	0.3		Adebiyi et al. (41)
Zn	0.3		Adebiyi et al. (41)
Ni	0.02		Miri et al. (45)
Pb	0.004	0.0085	Mohammadi et al. (64) and Adebiyi et al. (41)
Cu	0.04		Adebiyi et al. (41)
Cr	0.003	0.5	Mohammadi et al. (64) and Adebiyi et al. (41)

TABLE 5 Calculation of adult's estimated daily intake (EDI) for identified elements from eating tilapia fish.

	EDI muscle				EDI gills				EDI liver			
HM	R1	R2	R3	R4	R1	R2	R3	R4	R1	R2	R3	R4
Cd	0.0009	0.0007	0.0008	0.0006	0.0017	0.0009	0.0011	0.0015	0.0046	0.0031	0.0026	0.0030
Co	0.0014	0.0015	0.0018	0.0015	0.0032	0.0019	0.0025	0.0040	0.0092	0.0072	0.0062	0.0094
Fe	0.0098	0.0085	0.0096	0.0091	0.0910	0.0247	0.0237	0.0276	0.0703	0.0605	0.0805	0.2542
Zn	0.0004	0.0004	0.0004	0.0007	0.0011	0.0009	0.0010	0.0012	0.0024	0.0017	0.0017	0.0022
Ni	0.0019	0.0020	0.0022	0.0023	0.0042	0.0026	0.0034	0.0058	0.0097	0.0074	0.0072	0.0125
Pb	0.0010	0.0009	0.0011	0.0008	0.0019	0.0011	0.0014	0.0019	0.0058	0.0043	0.0039	0.0050
Cu	0.0001	0.0000	0.0000	0.0000	0.0005	0.0000	0.0000	0.0000	0.0040	0.0141	0.0330	0.0030
Cr	0.0016	0.0016	0.0017	0.0018	0.0054	0.0015	0.0021	0.0036	0.0058	0.0053	0.0052	0.0122

various similar studies performed by researchers over the past decades (52).

3.5 Results of correlation matrix analysis (CMA)

Figure 5 shows the Correlation matrix analysis results of the studied metals in the Tilapia muscle samples: positive and strong significant correlations exist between Cr/Zn and Cr/Ni, also Ni/Zn shows some positive correlation. Considering other organs: in the Liver, positive and strong significant correlations exist between Cd/Pb, Co/Pb, Zn/Pb, Co/Zn, Cr/Fe, and Cr/Ni, also some positive correlation is displayed between Ni/Co. while strong and negative correlation exists between Cu/Co, some negative correlation exists between Pb/Cu, Cu/Zn, and Cu/Ni; in Gills, positive and strong significant correlations were shown by Zn/Cd, Zn/Co, Ni/Co, Ni/Zn, Pb/Cd, Pb/Co, Pb/Zn, Cu/Fe, Cr/Cd, and Cr/Pb, also some positive correlation was shown between Ni/Pb.

4 Discussion

Although excessive amounts of iron are linked to heart disease, cancer, and reduced insulin sensitivity, iron is a necessary element for biological activity (53). High iron content in the fish organs could be attributed to the prolonged exposure given that the Cauvery River water iron content is high (54, 55). As per prior studies, Iron content

TABLE 6 Calculation of target hazard quotient (THQ) for analyzed metals from Tilapia fish consumption by adults.

	THQ Muscle				THQ Gills				THQ Liver			
HM	R1	R2	R3	R4	R1	R2	R3	R4	R1	R2	R3	R4
Cd	0.930	0.736	0.784	0.616	1.651	0.898	1.080	1.513	4.646	3.072	2.572	3.042
Co	4.600	4.998	5.994	5.050	10.773	6.433	8.218	13.338	30.771	23.966	20.740	31.450
Fe	0.033	0.028	0.032	0.030	0.303	0.082	0.079	0.092	0.234	0.202	0.268	0.847
Zn	0.001	0.001	0.001	0.002	0.004	0.003	0.003	0.004	0.008	0.006	0.006	0.007
Ni	0.095	0.099	0.112	0.117	0.212	0.129	0.171	0.288	0.487	0.370	0.361	0.626
Pb	0.252	0.225	0.264	0.194	0.475	0.279	0.355	0.463	1.447	1.072	0.967	1.252
Cu	0.002	0.000	0.000	0.000	0.013	0.001	0.000	0.000	0.101	0.354	0.825	0.076
Cr	0.534	0.524	0.572	0.610	1.797	0.506	0.716	1.212	1.942	1.763	1.742	4.061
TTHQ	**6.446**	**6.611**	**7.760**	**6.621**	**15.228**	**8.331**	**10.623**	**16.910**	**39.636**	**30.803**	**27.481**	**41.361**

Total Target Hazard Quotient (TTHQ).

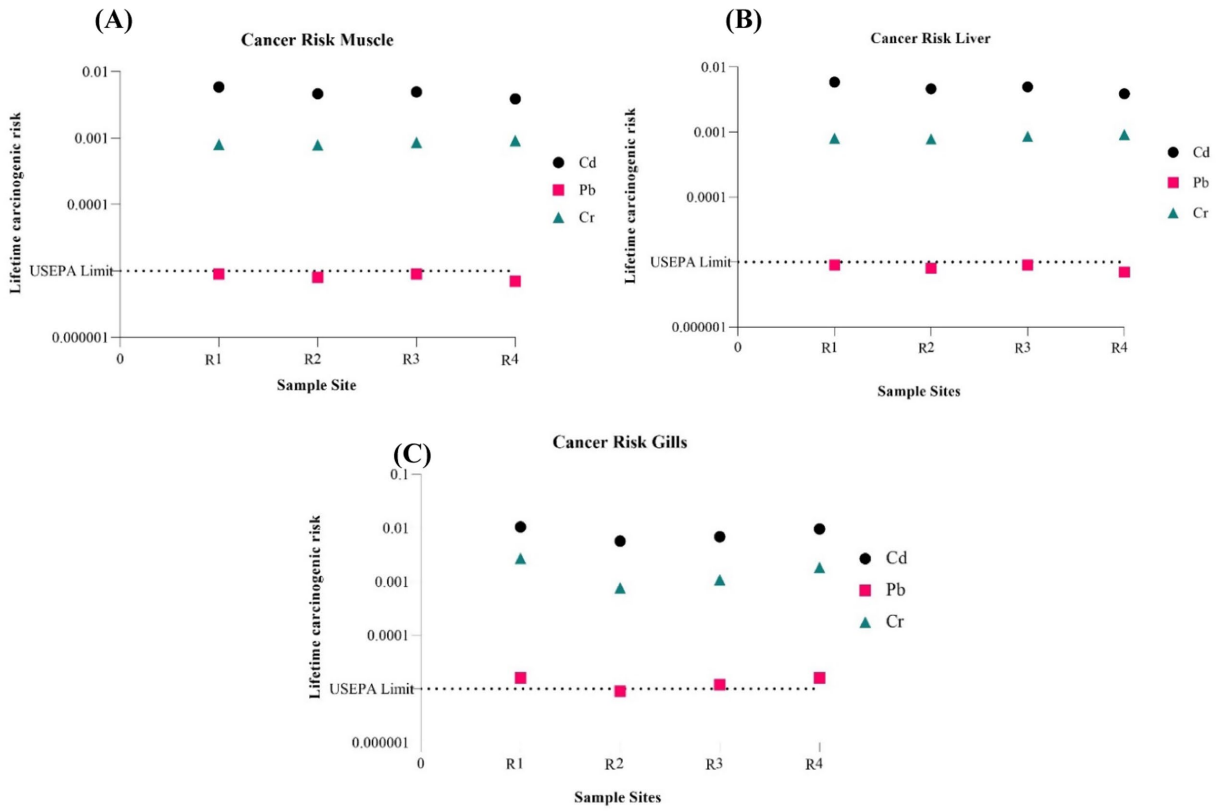

FIGURE 3
Estimated cancer risk for analyzed metals associated with consumption of **(A)** Muscle, **(B)** Liver, and **(C)** Gills from *Oreochromis mossambicus*.

in river water is mostly due to the tributaries from mineralized zones (56). PCA points out that Cu concentration in the Liver of Tilapia loads positively with the length and size of the fish (57). High concentration of Cu in the liver has been demonstrated to have significant poisonous effect on fish (58). The loading of rest of the metals in Liver and Gills shows negative loading when compared to size and weight of the fish. This seems to indicate younger fishes tend to have a higher accumulation of heavy metals than older fishes. This phenomenon has been observed in some earlier studies on other fish species as well. Our study also highlights the higher heavy metal concentration is there in the Gills and Liver of fishes when compared to muscles this is in line with the previous researches in similar area, according to which gills are exposed to the immediate environment and hence more exposed to the heavy metal pollution, on the other hand the Liver is metabolically active and despite the route of exposure be it food or via gills the accumulation of heavy metals take place here (59). Mozambique Tilapia are omnivorous and feed on a variety of food sources, including algae, detritus, and small invertebrates. This diverse diet can lead to the ingestion of metals present in the sediment and water, which can then accumulate in their tissues (60). Muscle however is not metabolically active and thus high heavy metal concentration in Tilapia's muscles raises concerns. In an earlier study

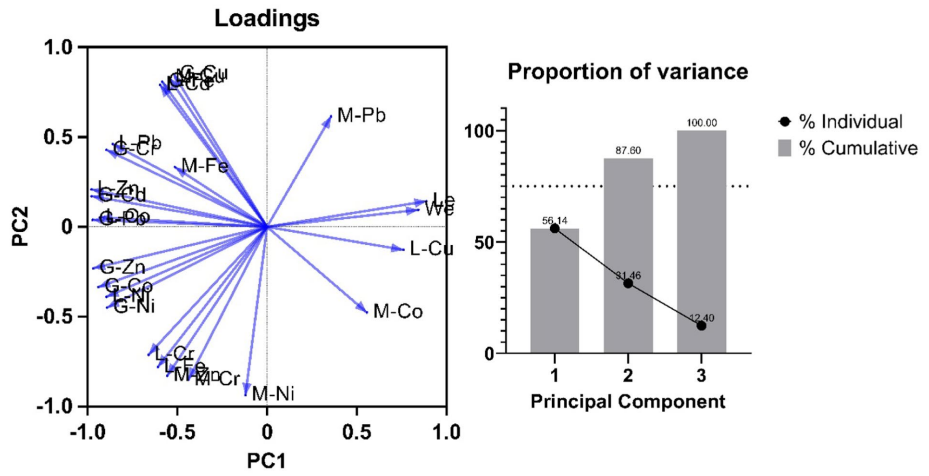

FIGURE 4
A plot of PCA of heavy metals in various tissue systems (M-Muscle, L-Liver, G-Gills) of *Oreochromis mossambicus,* **(A)** Loadings **(B)** variance covered by individual Principal component.

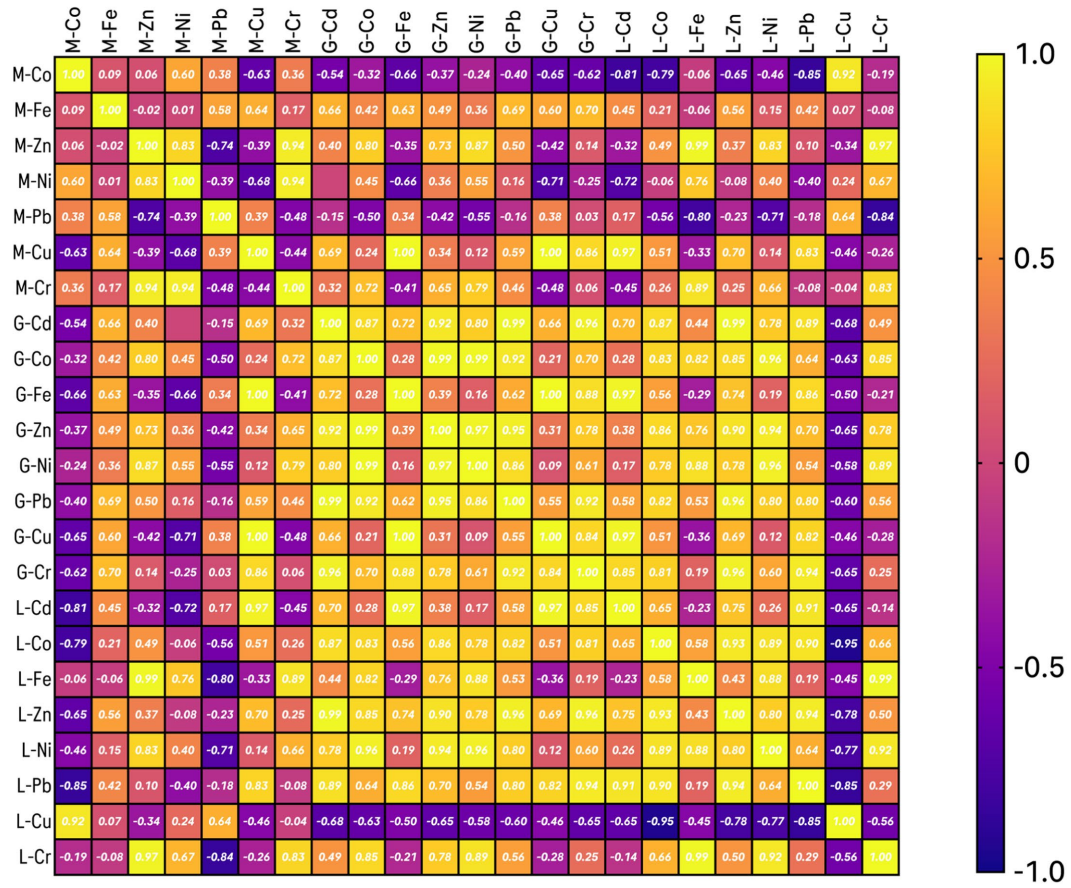

FIGURE 5
Correlation matrix of the studied metals in various tissue systems of *Oreochromis mossambicus.*

(61), which was performed on three economically important fish species (*Anguilla anguilla, Mugil cephalus, and Oreochromis niloticus*) in Turkey, it was also found that the concentrations of cadmium (Cd) and lead (Pb) were generally lower in the muscles compared to other tissues like the liver and gills, but still present in measurable amounts. The study also highlighted that omnivorous fish like Nile tilapia tend to accumulate metals in their muscles, albeit at different levels depending on the specific metal and environmental conditions.

The strong positive correlation of Chromium (Cr) with Zinc (Zn) and Nickel (Ni) may suggest that these are metals from a common source or with similar pathways of accumulation in the muscle tissue. This can be seen as an indicator of industrial discharge or runoff with these metals. The correlation between Nickel (Ni) and Zinc (Zn) further supports the above hypothesis to have an equal source or has similar environmental behavior, probably from industrial activities or urban runoff.

High correlations between Cadmium (Cd), Lead (Pb), Cobalt (Co), Zinc (Zn), Chromium (Cr), and Iron (Fe) within the liver organ indicate that these metals might be co-contaminants from industrial processes, mining activities, or agricultural runoff (62). It is also likely that the liver organ contains heavy metals because it is a primary detoxifying organ, in which it may accumulate metals reflecting environmental presence. The positive covariance of Nickel (Ni) and Cobalt (Co) could mean that they share a common source, perhaps from either of the metal plating industries or even natural geological sources. The negative correlation of Copper (Cu) and Cobalt (Co) might be interpreted as competition in uptake or different sources. For example, Cu may be more related to agricultural runoff in instances of pesticides (63), whereas Co may be more related to industrial discharge. These negative correlations could be related to other sources or antagonist interactions in the environment itself or within the fish's biological system.

Strong positive correlations among these metals in gills suggest they should co-exist within the water body, possibly through industrial effluent or urban runoff. As gills are directly exposed to the water, they could indicate water-borne metal contamination. The positive correlation between Nickel and Lead gives further support to a shared source from industrial activity.

The amount of heavy metals like Cr, Co, Pb, and Cd needs to be strictly regulated given these metals have been established as toxic to human health. Studying the Pollution Index shows that the Tilapia fish Muscle and Gills samples are contaminated with Cd, Cr, Fe, Co, Ni, and Pb given the PI > 1. Other examined metals with PI values below 1 include Zn and Cu. This may indicate that the fish samples are free of these metals' contamination. The correlation matrix indicated a significant relationship between the analyzed metals, suggesting similar sources and/or genetic origin. EDI and THQ for certain metals suggest that prolonged consumption of Tilapia in higher quantities could lead to serious health impacts. Only certain metals such as Cd, Cr, and Pb have been established to have cancer-causing roles in humans. The CR factor for Cd and Cr were found to be higher than the USEPA set tolerable limit. This suggests cancer risk due to Cd and Cr can be there over prolonged exposure. Pb in fish organs was found to have no such risk due to its presence within the tolerable limit. Overall, the data indicates that a higher intake of Tilapia fish might harm the health of the populace consuming it.

5 Conclusion and recommendation

Our study looked into a few particular potentially hazardous metals and the risks they pose to human health. According to the metal pollution index values, the amount of contamination in the samples of tilapia fish for Cd, Cr, Fe, Co, Ni, and Pb is greater than 1. The Target hazard quotient for Cd, Co, Pb, and Cr in the Liver, Co, and Cr in Gills, and Co in Muscle were > 1 for adults, which showed a significant health risk other than cancer from the combined effects of these metals. In the muscle, liver, and gills, the cancer risk (Cd and Cr) was higher than the established tolerable level, suggesting that consuming tilapia fish may carry a risk of these heavy metals causing cancer. There is a growing need for more active monitoring regarding the food safety of the Indian population that consumes fish, it would also help generate more data on the state of edible fish species in other Indian rivers. It would be prudent to limit the daily consumption of tilapia to prevent long-term detrimental effects on human health based on the results obtained for the cancer risk. Among the metals taken into consideration, the greatest risk for human health can be associated with the level of Cd and Cr. Further studies and data generation is recommended to study the impact of contaminated fish consumption on the local population over the extended time period.

6 Limitations

Although our study offers insightful information about the levels of heavy metals and related hazards in different fish organs, there are a few things to keep in mind. First off, our findings might not be as broadly applicable as they could be because of the sample size and geographic reach, which might not accurately reflect the larger fish population. Furthermore, the results may be impacted by variations in heavy metal buildup brought on by fish species, age, and size that were not fully controlled. Even with its robustness, the risk assessment based on USEPA recommendations might not take into consideration all potential exposure situations and individual susceptibilities, like dietary habits or pre-existing medical disorders. Moreover, possible interactions between various heavy metals that could increase or decrease the total risk were not assessed in the study. Future research should aim to address these limitations by incorporating a larger, more diverse sample set, and by considering additional variables and potential synergistic effects of multiple contaminants.

Data availability statement

The original contributions presented in the study are included in the article/Supplementary material, further inquiries can be directed to the corresponding author/s.

Ethics statement

Ethical approval was not required for the study involving animals in accordance with the local legislation and institutional requirements because our study did not require ethical board approval because it did not contain human or animal trials. The fish used in this study was procured dead from local fishermen. All surgical operations were performed on dead fish. Care was taken to ensure that the least number of fish was utilized to reach satisfactory statistical conclusions.

Author contributions

NG: Conceptualization, Data curation, Formal analysis, Investigation, Methodology, Visualization, Writing – original draft, Writing – review & editing. SA: Data curation, Funding acquisition, Supervision, Writing – review & editing.

Funding

The author(s) declare that no financial support was received for the research, authorship, and/or publication of this article.

Acknowledgments

The authors express their gratitude toward the Vellore Institute of Technology for providing the lab facilities for conducting our research and financial support. The authors are thankful to the VIT-TBI for providing AAS facilities to carry out this work. ChatGPT 3.5 was used in some paragraphs to refine language and enhance clarity and readability.

Conflict of interest

The authors declare that the research was conducted in the absence of any commercial or financial relationships that could be construed as a potential conflict of interest.

Publisher's note

All claims expressed in this article are solely those of the authors and do not necessarily represent those of their affiliated organizations, or those of the publisher, the editors and the reviewers. Any product that may be evaluated in this article, or claim that may be made by its manufacturer, is not guaranteed or endorsed by the publisher.

Supplementary material

The Supplementary material for this article can be found online at: https://www.frontiersin.org/articles/10.3389/fpubh.2024.1402421/full#supplementary-material

References

1. Shinde D, Kamble P, Mahajan DM, Devkar V, Chakane S. Analysis of accumulated heavy metal concentrations in various body parts of Chillapi (*Oreochromis Mossambicus*) fish from Ujjani reservoir of Maharashtra, India. *Adv Zool Bot*. (2020) 8:37–44. doi: 10.13189/azb.2020.080201

2. Goyal VC, Singh O, Singh R, Chhoden K, Malyan SK. Appraisal of heavy metal pollution in the water resources of Western Uttar Pradesh. *India Assoc Risks Environ Adv*. (2022) 8:100230. doi: 10.1016/j.envadv.2022.100230

3. Majumdar A, Avishek K. Assessing heavy metal and physiochemical pollution load of Danro River and its management using floating bed remediation. *Sci Rep*. (2024) 14:9885. doi: 10.1038/s41598-024-60511-x

4. Paul D. Research on heavy metal pollution of river ganga: a review. *Ann Agrar Sci*. (2017) 15:278–86. doi: 10.1016/j.aasci.2017.04.001

5. Singh V, Ahmed G, Vedika S, Kumar P, Chaturvedi SK, Rai SN, et al. Toxic heavy metal ions contamination in water and their sustainable reduction by eco-friendly methods: isotherms, thermodynamics and kinetics study. *Sci Rep*. (2024) 14. doi: 10.1038/s41598-024-58061-3

6. Khan R, Saxena A, Shukla S, Sekar S, Senapathi V, Wu J. Environmental contamination by heavy metals and associated human health risk assessment: a case study of surface water in Gomti River Basin, India. *Environ Sci Pollut Res*. (2021) 28:56105–16. doi: 10.1007/s11356-021-14592-0

7. Kumar P, Sivaperumal P, Manigandan V, Rajaram R, Hussain M. Assessment of potential human health risk due to heavy metal contamination in edible finfish and shellfish collected around Ennore coast, India. *Environ Sci Pollut Res*. (2021) 28:8151–67. doi: 10.1007/s11356-020-10764-6

8. Kumar SB, Padhi RK, Mohanty AK, Satpathy KK. Elemental distribution and trace metal contamination in the surface sediment of south east coast of India. *Mar Pollut Bull*. (2017) 114:1164–70. doi: 10.1016/j.marpolbul.2016.10.038

9. Rushinadha Rao K., Sreedhar U., Sreeramulu K. (2016). Spatial variation of heavy metal accumulation in coastal sea water, east coastof Andhra Pradesh, India. 2, 394–399. Available at: www.allresearchjournal.com (Accessed October 07, 2024).

10. Ali H, Khan E, Ilahi I. Environmental chemistry and ecotoxicology of hazardous heavy metals: environmental persistence, toxicity, and bioaccumulation. *J Chem*. (2019) 2019:1–14. doi: 10.1155/2019/6730305

11. Gashkina NA, Moiseenko TI, Kudryavtseva LP. Fish response of metal bioaccumulation to reduced toxic load on long-term contaminated lake Imandra. *Ecotoxicol Environ Saf*. (2020) 191:110205. doi: 10.1016/j.ecoenv.2020.110205

12. Rubalingeswari N, Thulasimala D, Giridharan L, Gopal V, Magesh NS, Jayaprakash M. Bioaccumulation of heavy metals in water, sediment, and tissues of major fisheries from Adyar estuary, southeast coast of India: an ecotoxicological impact of a metropolitan city. *Mar Pollut Bull*. (2021) 163:111964. doi: 10.1016/j.marpolbul.2020.111964

13. Tolulope A., Fawole O., Adewoye S., Akinloye O. M. (2009). Bioconcentration of metals in the body muscle and gut of *Clarias gariepinus* exposed to sublethal concentrations of soap and detergent effluent. Available at: http://www.academicjournals.org/JCAB (Accessed October 07, 2024).

14. Gupta A, Rai DK, Pandey RS, Sharma B. Analysis of some heavy metals in the riverine water, sediments and fish from river Ganges at Allahabad. *Environ Monit Assess*. (2009) 157:449–58. doi: 10.1007/s10661-008-0547-4

15. Javed M, Usmani N. An overview of the adverse effects of heavy metal contamination on fish health. *Proceed Nat Acad Sci India Sec B*. (2019) 89:389–403. doi: 10.1007/s40011-017-0875-7

16. Asuquo Isangedighi I, Samuel David G. Heavy metals contamination in fish: effects on human health. *J Aquatic Sci Marine Biol*. (2019) 2:7–12. doi: 10.22259/2638-5481.0204002

17. Azaman F, Juahir H, Yunus K, Azid A, Kamarudin MKA, Toriman ME, et al. Heavy metal in fish: analysis and human health-a review. *J Teknol*. (2015) 77:61–9. doi: 10.11113/jt.v77.4182

18. DOF (2020). Handbook on fisheries statistics.

19. Ahmed MK, Bhowmik AC, Rahman S, Haque MR. Heavy metal concentration in water, sediments, freshwater mussels and fishes of the river Shitalakhya, Bangladesh. *Asian Journal of Water, Environment and Pollution*. (2010) 7:77–90. doi: 10.3233/AJW-2010-7_1_11

20. González N, Calderón J, Rúbies A, Timoner I, Castell V, Domingo JL, et al. Dietary intake of arsenic, cadmium, mercury and lead by the population of Catalonia, Spain: analysis of the temporal trend. *Food Chem Toxicol*. (2019) 132:110721. doi: 10.1016/j.fct.2019.110721

21. Rabiul Islam GM, Habib MR, Waid JL, Rahman MS, Kabir J, Akter S, et al. Heavy metal contamination of freshwater prawn (*Macrobrachium rosenbergii*) and prawn feed in Bangladesh: a market-based study to highlight probable health risks. *Chemosphere*. (2017) 170:282–9. doi: 10.1016/j.chemosphere.2016.11.163

22. Raihana U., Rahman A. (2014). Landfill leachate toxicity analysis with Orechromis mossambicus (Mozambique Tilapia): a Review Available at: http://gssrr.org/index.php?journal=JournalOfBasicAndApplied (Accessed October 07, 2024).

23. Raihana U., Rahman A., Norkhadijah S., Ismail S., Abidin E. Z., Praveena S. M. (2019). Heavy metals accumulation in gills and muscles of Mozambique Tilapia (*Oreochromis mossambicus*) exposed to crude leachate.

24. Mangitung S. F., Hasan V., Isroni W., Serdiati N., Valen F. S. (2021). Mozambique Tilapia *Oreochromis mossambicus* (Peters, 1852) (Perciformes: Cichlidae): New Record from Masalembo Island, Indonesia: Ecology Environment and Conservation. 27:1091–109.

25. Debnath SC, McMurtrie J, Temperton B, Delamare-Deboutteville J, Mohan CV, Tyler CR. Tilapia aquaculture, emerging diseases, and the roles of the skin microbiomes in health and disease. *Aquac Int*. (2023) 31:2945–76. doi: 10.1007/s10499-023-01117-4

26. Siddique MAB, Mahalder B, Haque MM, Shohan MH, Biswas JC, Akhtar S, et al. Forecasting of tilapia (*Oreochromis niloticus*) production in Bangladesh using ARIMA model. *Heliyon*. (2024) 10:e27111. doi: 10.1016/j.heliyon.2024.e27111

27. Laxmappa B., Sreedhar Sharma M., Nagaraju C. (2015). International journal of fisheries and aquatic studies 2015; 3(1): 93–96 impact study of the feral population of Tilapia (*Oreochromis mossambicus*) on growth of Indian major carp in Veeranna tank of Tatikonda Village in Mahabubnagar District, Telangana, India. Available at: www.fisheriesjournal.com (Accessed October 07, 2024).

28. Roshni K. (2016). Fishery of Mozambique Tilapia *Oreochromis mossambicus* (Peters) in Poringalkuthu Reservoir of Chalakudy River, Kerala, India. Available at: https://www.researchgate.net/publication/316124730 (Accessed October 07, 2024).

29. Balamanikandan V, Shalini R, Arisekar U, Shakila RJ, Padmavathy P, Sivaraman B, et al. Bioaccumulation and health risk assessment of trace elements in Tilapia (*Oreochromis mossambicus*) from selected inland water bodies. *Environ Geochem Health*. (2024) 46:187. doi: 10.1007/s10653-024-01909-4

30. Khan MF, Panikkar P., Salim SM, Leela RV, Sarkar UK, Das BK, et al. (2021). Modeling impacts of invasive sharp tooth African catfish *Clarias gariepinus* (Burchell 1822) and Mozambique tilapia *Oreochromis mossambicus* (Peters, 1852) on the ecosystem of a tropical reservoir ecosystem in India. Environmental Science and Pollution Research, 28:58310–21.

31. RK LKKPG, Roshith M, Kumar CSMSV, Suresh MEVR, Das SSB. Composition and distribution of non-native fishes in relation to water quality parameters in river Cauvery. *J Inland Fish Soc India*. (2021) 53:185–193. doi: 10.47780/jifsi.53.3-4.2021.122367

32. Canciyal J, Kosygin L, Mogalekar HS, Das BK. Fish fauna of Kodayar River. Tamil Nadu, India: Kanyakumari district (2018).

33. Raj S, Prakash P, Reghunath R, Tharian JC, Raghavan R, Kumar AB. Distribution of alien invasive species in aquatic ecosystems of the southern Western Ghats, India. *Aquat Ecosyst Health Manag*. (2021) 24:64–75. doi: 10.14321/aehm.024.02.10

34. Arumugam M, Jayaraman S, Sridhar A, Venkatasamy V, Brown PB, Abdul Kari Z, et al. Recent advances in tilapia production for sustainable developments in Indian aquaculture and its economic benefits. *Fishes* (2023) 8:176. doi: 10.3390/fishes8040176

35. Tilapia (GIFT) – MPEDA (2020). Available at: https://mpeda.gov.in/?page_id=764 (Accessed November 29, 2022).

36. Manyise T, Lam RD, Lozano Lazo DP, Padiyar A, Shenoy N, Chadag MV, et al. Exploring preferences for improved fish species among farmers: a discrete choice experiment applied in rural Odisha. *India Aquaculture*. (2024) 583:740627. doi: 10.1016/j.aquaculture.2024.740627

37. Tran N, Shikuku KM, Rossignoli CM, Barman BK, Cheong KC, Ali MS, et al. Growth, yield and profitability of genetically improved farmed tilapia (GIFT) and non-GIFT strains in Bangladesh. *Aquaculture*. (2021) 536:736486. doi: 10.1016/j.aquaculture.2021.736486

38. Rajaram T, Das A. Water pollution by industrial effluents in India: discharge scenarios and case for participatory ecosystem specific local regulation. *Futures*. (2008) 40:56–69. doi: 10.1016/j.futures.2007.06.002

39. Sarkar SK, Bhattacharya BD, Bhattacharya A, Chatterjee M, Alam A, Satpathy KK, et al. Occurrence, distribution and possible sources of organochlorine pesticide residues in tropical coastal environment of India: an overview. *Environ Int*. (2008) 34:1062–71. doi: 10.1016/j.envint.2008.02.010

40. CPCB (2021). Status of trace and toxic metals in Indian Rivers.

41. Adebiyi FM, Ore OT, Ogunjimi IO. Evaluation of human health risk assessment of potential toxic metals in commonly consumed crayfish (*Palaemon hastatus*) in Nigeria. *Heliyon*. (2020) 6:e03092. doi: 10.1016/j.heliyon.2019.e03092

42. Taweel A, Shuhaimi-Othman M, Ahmad AK. Assessment of heavy metals in tilapia fish (*Oreochromis niloticus*) from the Langat River and engineering Lake in Bangi, Malaysia, and evaluation of the health risk from tilapia consumption. *Ecotoxicol Environ Saf*. (2013) 93:45–51. doi: 10.1016/j.ecoenv.2013.03.031

43. Agemian H, Sturtevant DP, Austen KD. Simultaneous acid extraction of six trace metals from fish tissue by hot-block digestion and determination by atomic-absorption spectrometry. *Analyst*. (1980) 105:125. doi: 10.1039/an9800500125

44. Ajeeshkumar KK, Vishnu KV, Bineesh KK, Mathew S, Sankar TV, Asha KK. Macromineral and heavy metal profiles of selected deep-sea fish from the Kochi coast of the Arabian Sea. *India Mar Pollut Bull*. (2021) 167. doi: 10.1016/j.marpolbul.2021.112275

45. Miri M, Akbari E, Amrane A, Jafari SJ, Eslami H, Hoseinzadeh E, et al. Health risk assessment of heavy metal intake due to fish consumption in the Sistan region. *Iran Springer*. (2017) 189:583. doi: 10.1007/s10661-017-6286-7

46. Kwaansa-Ansah EE, Nti SO, Opoku F. Heavy metals concentration and human health risk assessment in seven commercial fish species from Asafo market, Ghana. *Food Sci Biotechnol*. (2019) 28:569–79. doi: 10.1007/s10068-018-0485-z

47. NCAER (2023). Fish consumption in India in 2022–23 and future prospects - NCAER | quality. Relevance. Impact. NCAER. Available at: https://www.ncaer.org/news/fish-consumption-in-india-in-2022-23-and-future-prospects (Accessed August 29, 2024).

48. Ramesh R, Purvaja R, Lakshmi A. Coastal pollution loading and water quality criteria-Bay of Bengal Coast of India In: Surface and sub-surface water in Asia. (2015) 47–71. doi: 10.3233/978-1-61499-540-1-47

49. Saha N, Mollah MZI, Alam MF, Safiur Rahman M. Seasonal investigation of heavy metals in marine fishes captured from the bay of Bengal and the implications for human health risk assessment. *Food Control*. (2016) 70:110–8. doi: 10.1016/j.foodcont.2016.05.040

50. USEPA. Supplementary guidance for conducting health risk assessment of chemical mixtures risk assessment forum technical panel. Washington: (2000).

51. Chien LC, Hung TC, Choang KY, Yeh CY, Meng PJ, Shieh MJ, et al. Daily intake of TBT, cu, Zn, cd and as for fishermen in Taiwan. *Sci Total Environ*. (2002) 285:177–85. doi: 10.1016/S0048-9697(01)00916-0

52. Dobicki W., Polechoński R. (2003). Relationship between age and heavy metal bioaccumulation by tissues of four fish species inhabiting Wojnowskie lakes. Available at: https://www.researchgate.net/publication/283902142 (Accessed October 07, 2024).

53. Peto MV. Aluminium and iron in humans: bioaccumulation, pathology, and removal. *Rejuvenation Res*. (2010) 13:589–98. doi: 10.1089/rej.2009.0995

54. Tamilmani A, Venkatesan G. Assessment of trace metals and its pollution load indicators in water and sediments between upper and grand Anicuts in the Cauvery. *Int J Environ Sci Technol*. (2021) 18:3807–18. doi: 10.1007/s13762-020-03034-y

55. Venkatesha Raju K, Somashekar RK, Prakash KL. Heavy metal status of sediment in river Cauvery, Karnataka. *Environ Monit Assess*. (2012) 184:361–73. doi: 10.1007/s10661-011-1973-2

56. Vaithiyanathan P, Ramanathan AL, Subramanian V. Transport and distribution of heavy metals in Cauvery river. *Water Air Soil Pollut*. (1993) 71:13–28. doi: 10.1007/BF00475509

57. Masresha AE, Skipperud L, Rosseland BO, Z GM, Meland S, Salbu B. Bioaccumulation of trace elements in liver and kidney of fish species from three freshwater lakes in the Ethiopian Rift Valley. *Environ Monit Assess*. (2021) 193:329. doi: 10.1007/s10661-021-09083-1

58. Karayakar F, Cicik B, Ciftci N, Karaytug S, Erdem C, Ozcan AY. Accumulation of copper in liver, gill and muscle tissues of *Anguilla anguilla* (Linnaeus, 1758). *J Anim Vet Adv*. (2010) 9:2271–4. doi: 10.3923/javaa.2010.2271.2274

59. Authman MM. Use of fish as bio-indicator of the effects of heavy metals pollution. *J Aquac Res Dev*. (2015) 6:1–13. doi: 10.4172/2155-9546.1000328

60. Canli M, Atli G. The relationships between heavy metal (cd, Cr, cu, Fe, Pb, Zn) levels and the size of six Mediterranean fish species. *Environ Pollut*. (2003) 121:129–36. doi: 10.1016/S0269-7491(02)00194-X

61. Yilmaz F. (2009). The comparison of heavy metal concentrations (cd, cu, Mn, Pb, and Zn) in tissues of three economically important fish (Anguilla anguilla, Mugil cephalus and Oreochromis niloticus) Inhabiting Koycegiz Lake-Mugla (Turkey). Turkish Journal of Science & Technology, 4.

62. Zhu F, Qu L, Fan W, Wang A, Hao H, Li X, et al. Study on heavy metal levels and its health risk assessment in some edible fishes from Nansi Lake. *China Environ Monit Assess*. (2015) 187:161. doi: 10.1007/s10661-015-4355-3

63. Sapozhnikova Y, Zubcov N, Hungerford S, Roy LA, Boicenco N, Zubcov E, et al. Evaluation of pesticides and metals in fish of the Dniester River, Moldova. *Chemosphere*. (2005) 60:196–205. doi: 10.1016/j.chemosphere.2004.12.061

64. Mohammadi AA, Zarei A, Majidi S, Ghaderpoury A, Hashempour Y, Saghi MH, et al. Carcinogenic and non-carcinogenic health risk assessment of heavy metals in drinking water of Khorramabad. *Iran MethodsX*. (2019) 6:1642–51. doi: 10.1016/j.mex.2019.07.017

65. MFA (1983). vdocument.in_malasia-food-act-1983. Available at: https://r.search.yahoo.com/_ylt=Awrx_zh14QJnBAIAp7e7HAx.;_ylu=Y29sbwNzZzMEcG9zAzEEdnRpZAMEc2VjA3Ny/RV=2/RE=1729451637/RO=10/RU=https%3a%2f%2fhq.moh.gov.my%2ffsq%2fxs%2fdl.php%3ffilename%3dFood%2bAct%2b1983-doc.pdf/RK=2/RS=vZPM4WogmXrjUjkwEK07HpcEsko-

66. FAO (1983). Compilation of legal limits for hazardous substances in fish and fishery products. Fisheries circular. No. 764. | inland fisheries | food and agriculture Organization of the United Nations. Available at: https://www.fao.org/inland-fisheries/tools/detail/en/c/1150083/ (Accessed November 29, 2022).

67. EC (2001). Commission regulation (EC) no 466/2001 of 8 march 2001 setting maximum levels for certain contaminants in foodstuffs (text with EEA relevance) (repealed). Available at: https://webarchive.nationalarchives.gov.uk/eu-exit/https://eur-lex.europa.eu/legal-content/EN/TXT/?uri=CELEX:02001R0466-20070301 (Accessed October 07, 2024).

68. USFDA (1993). US FDA: Guidance document for arsenic in shellfish | EVISA's links database. Available at: https://speciation.net/Database/Links/US-FDA-Guidance-Document-for-Arsenic-in-Shellfish-;i762 (Accessed November 29, 2022).

69. Mokhtar M., Aris A., Munusamy V., Res S. P.-E. J. S., and 2009, undefined (2009). Assessment level of heavy metals in Penaeus monodon and Oreochromis spp. in selected aquaculture ponds of high densities development area. researchgate.net 30, 348–360. Available at: https://www.researchgate.net/profile/Ahmad-Zaharin-Aris/publication/233951795_European_Journal_of_Scientific_Research_2009_Mokhtar/data/09e4150d43ab5659e5000000/European-Journal-of-Scientific-Research-2009-Mokhtar.pdf (Accessed November 29, 2022).

70. Contaminants N. (1994). Monitoring and surveillance of non-radioactive Contaminants in the aquatic environment and activities regulating the disposal of wastes

at sea, 1993 Cefascouk. Centre for Environment Fisheries and Aquaculture Science. Available at: https://www.cefas.co.uk/Publications/aquatic/aemr40.pdf (Accessed November 29, 2022).

71. Joint F., and Additives, W. E. C. on F. (1972). Evaluation of certain food additives and the contaminants mercury, lead, and cadmium: Sixteenth report of the Joint FAO. Available at: https://apps.who.int/iris/bitstream/handle/10665/40985/WHO_TRS_505.pdf?sequenc (Accessed November 29, 2022).

72. Phillips D. (1993). Developing-country aquaculture, trace chemical contaminants, and public health concerns. Available at: https://agris.fao.org/agris-search/search.do?recordID=PH9410452 (Accessed November 29, 2022).

73. Senarathne P., Pathiratne K., Pathiratne A. (2006). Heavy metal levels in food fish, *Etroplus suratensis* inhabiting Bolgoda Lake, Sri Lanka. Available at: http://www.dr.lib.sjp.ac.lk/handle/123456789/1053 (Accessed November 29, 2022).

74. Senarathne P, Pathiratne KAS. Accumulation of heavy metals in a food fish, *Mystus gulio* inhabiting Bolgoda Lake, Sri Lanka. *Pathiratne/ Sri Lanka J Aquat Sci.* (2007) 12:61–75.

75. Anim-Gyampo M., Kumi M., and, M. Z.-J. of E., and 2013, undefined (2013). Heavy metals concentrations in some selected fish species in Tono irrigation reservoir in Navrongo, Ghana. Academiaedu. Available at: https://www.academia.edu/download/30633116/Heavy_Metals_Concentrations_in_some_selected_Fish_Species_in_Tono_Irrigation_Reservoir_in_Navrongo__Ghana.pdf (Accessed November 29, 2022).

frontiers | Frontiers in Public Health

TYPE Review
PUBLISHED 22 November 2024
DOI 10.3389/fpubh.2024.1458727

OPEN ACCESS

EDITED BY
Renata Sisto,
National Institute for Insurance against Accidents at Work (INAIL), Italy

REVIEWED BY
Sadaf Shabbir,
Université du Québec à Rimouski, Canada
Worradorn Phairuang,
Chiang Mai University, Thailand

*CORRESPONDENCE
Jin Su Kim
kjs@kirams.re.kr

RECEIVED 03 July 2024
ACCEPTED 29 October 2024
PUBLISHED 22 November 2024

CITATION
Hong AR and Kim JS (2024) Biological hazards of micro- and nanoplastic with adsorbents and additives.
Front. Public Health 12:1458727.
doi: 10.3389/fpubh.2024.1458727

Biological hazards of micro- and nanoplastic with adsorbents and additives

Ah Reum Hong[1,2] and Jin Su Kim[1,2]*

[1]Division of Applied RI, Korea Institute of Radiological and Medical Sciences (KIRAMS), Seoul, Republic of Korea, [2]Radiological and Medico-Oncological Sciences, University of Science and Technology (UST), Seoul, Republic of Korea

With the increased worldwide production of plastics, interest in the biological hazards of microplastics (MP) and nanoplastics (NP), which are widely distributed as environmental pollutants, has also increased. This review aims to provide a comprehensive overview of the toxicological effects of MP and NP on *in vitro* and *in vivo* systems based on studies conducted over the past decade. We summarize key findings on how the type, size, and adsorbed substances of plastics, including chemical additives, impact organisms. Also, we address various exposure routes, such as ingestion, inhalation, and skin contact, and their biological effects on both aquatic and terrestrial organisms, as well as human health. Additionally, the review highlights the increased toxicity of MP and NP due to their smaller size and higher bioavailability, as well as the interactions between these particles and chemical additives. This review emphasizes the need for further research into the complex biological interactions and risks posed by the accumulation of MP and NP in the environment, while also proposing potential directions for future studies.

KEYWORDS

microplastics, nanoplastics, heavy metals, chemical additives, biological effects

Introduction

With accelerated industrialization globally, plastics, widely used in packaging, construction, and other industrial sectors have been mass-produced since the 1950s (1, 2). The production and consumption of lightweight, convenient, and useful plastics are increasing exponentially worldwide owing to their low manufacturing cost, safety, and hygiene (1, 3, 4). Following the COVID-19 pandemic in 2020, global plastic production reached 390.7 million tons in 2021 and is projected to be 34 billion metric tons by 2050 (5, 6).

MP are generated from various environmental factors and human activities. They are transported, dispersed, and deposited by wind flow, direction, and precipitation in the atmosphere. Through the atmosphere, which serves as a major pathway for MP transportation, all environmental compartments, including freshwater and terrestrial environments, can be impacted by MP pollution (7, 8). MP can be released into the air from plastic recycling processes in industries and waste disposal, synthetic fibers in carpets and clothing, as well as from friction activities like tire wear, which is also known to be a source of MP emissions (9, 10).

Plastic waste introduced into the environment is broken down into MP over time due to physical, chemical, and biological factors such as microbial degradation, ultraviolet (UV) exposure, and physical abrasion (11). Plastic fragments can be classified into categories based on their size, including megaplastics (>100 mm), macroplastics (>20 mm), mesoplastics (5–20 mm) microplastics (<5 mm), and nanoplastics (1–1,000 nm) (12–16). Both MP and NP are considered serious environmental problem due to their persistence and potential to be ingested by various organisms (15).

The most produced plastic polymers include polypropylene (PP, 19.3%), low density polyethylene (PE-LD, 14.4%), polyvinyl chloride (PVC, 12.9%), and high density polyethylene (PE-HD, 12.5%), polyethylene terephthalate (PET, 6.2%), polyurethane (PUR, 5.5%), and polystyrene (PS, 5.3%), in that order (5, 11). Additionally, environmentally friendly plastics are estimated to account for approximately 9.8% of global production (5). Consequently, plastic waste has become widespread in the environment and has accumulated in aquatic ecosystems worldwide, from Antarctica to the deep oceans (4, 17–19). By 2016, an estimated maximum of 23 million metric tons (Mt), approximately 11% of global plastic waste, had reached the aquatic ecosystems. If plastic waste continues to increase, the amount of plastic waste entering the world's aquatic ecosystems is predicted to reach 90 Mt/year by 2030 (19).

The number of studies on the toxicity of MP/NP has been increasing (20, 21). The MP/NP generated after plastic waste decomposition are continuously dispersed accumulated in the environment, exerting toxic effects on aquatic and terrestrial wildlife and on humans (1, 21, 22).

MP originate from both primary plastics, which are manufactured in small sizes, and secondary plastics, which are created through the fragmentation of larger plastic waste (23). Several studies have indicated that MP negatively impacts the reproductive and feeding functions of crustaceans such as oysters (24) and mussels (25, 26). Furthermore, MP have been found in the feces of gentoo penguins in Antarctica (27), and research has reported the first occurrence of MP in demersal sharks in the UK (28). These findings suggest that MP can traverse the food chain, posing serious health risks to organisms (29).

MP degrade in the environment through physical, chemical, and biological processes, resulting in the formation of NP. Due to their smaller size, NP are more easily ingested by aquatic organisms, which can lead to bioaccumulation and serious health impacts on these organisms (30). These NP can also bind with heavy metals (31, 32) and chemicals (33, 34), exhibiting harmful effects such as reproductive toxicity (35, 36), intestinal toxicity (37, 38), and neurotoxicity (39, 40). Additionally, there are research studies that have confirmed that Antarctic krill, when consuming MP labeled with fluorescent substances, break them down into NP during the digestive process through the action of digestive enzymes (41). This study indicates that when most organisms ingest MP, they effectively consume NP simultaneously. This suggests that MP can serve as a resource for the formation of NP.

Also, researchers worldwide are increasingly focusing on the toxicity of mixtures formed by the adsorption of MP/NP with the additives used in their production and pollutants in the environment. However, current knowledge in this area is limited. Therefore, we emphasize the need for more research to reveal the interactions and biological hazards of chemicals associated with MP/NP accumulating in the environment. Our review of literature published over the past 10 years revealed that research on the toxicity of MP as well as NP, which are smaller and potentially more harmful than the MP, has rapidly increased (42, 43). In this review, we emphasized the need for more; the findings from this review can contribute to conducting systematic research on the biological hazards of not only MP/NP but also composite compounds.

Abbreviations: PP, Polypropylene; PE-LD, Low density polyethylene; PVC, Polyvinyl chloride; PE-HD, High density polyethylene; PET, Polyethylene terephthalate; PUR, Polyurethane; PS, Polystyrene; DEHP, Di-(2-ethylhexyl) phthalate; BPA, Bisphenol A; PBDE, Polybrominated diphenyl ether; BHA, Butylated hydroxyanisole; PMC, PubMed Central; PMMA, Polymethyl methacrylate; PLA, Polylactic acid; PA, Polyamide; HDF, Human-derived dermal fibroblasts; PBMC, Peripheral blood mononuclear cells; ROS, Reactive oxygen species.

Classification of biohazards of microplastics

We conducted a search for articles published from 2012 to 2022 in PubMed Central (PMC). To search for papers related to all types of MP, we conducted searches using both the abbreviations and full names. Examples of keywords used in the search included PS, polymethyl methacrylate (PMMA), PA, PE, PVC, PP, PET, and polylactic acid (PLA). Research articles related to the biological effects of MP, excluding those from an environmental perspective, reviews, and other types of articles such as editorial materials, were selected from the retrieved hits. To find papers related to the biological effects of MP from 2012 to 2022, data queried using keywords such as the abbreviations and full names of MP were classified using Microsoft Excel 2019 (Microsoft Corporation, Santa Rosa, California, United States). Briefly, the list of papers was filtered using the filter function to analyze the data and derive related figures based on the type and size of the plastic and the presence or absence of additives. Supplementary Figure S1 presents a schematic of the literature search and process for extracting numerical data related to the biological impact of plastics. Supplementary Figure S2 shows the number of papers published by year. The number of papers related to the microplastics has dramatically increased over the last 12 years (2012–2024). Between 2012 and 2022, a total of 7,899 papers were published. In 2023 alone, 4,085 papers were published. In the first half of 2024, 2,490 papers were published, and a similar number is expected for the second half, indicating that even more papers will likely be released by the end of the year.

Current status of research on the biological effects of microplastics

Out of 7,899 papers searched for MP-related keywords in PubMed, 457 papers were related to biological impacts (Figure 1A). Among the studies focusing on the biological effects of MP, the most commonly studied plastic types were PS, PE, PVC, PP, and PET. Interestingly, research on PMMA, which is less frequently detected in natural ecosystems, has recently been conducted. On classifying 457 papers that evaluated biological hazards according to the type of MP, PS was the most common (326), followed by PE at 86, PVC at 25, and PS at 326. Fourteen articles on PP, 13 on PET, 8 on PA, 8 on PMMA, and 5 on PLA were published (Figure 1B). After classifying papers for NP of each type of plastic, there were 155 papers for PS, 6 for PE, 3 for PVC, 1 for PP, 3 for PET, 5 for PMMA, and 1 for PLA (Figure 2A). Regarding the MP, there were 210 cases for PS, 84 for PE, 23 for PVC, 13 for PP and 10 for PET. Also, there were published in 8 cases for PA, 5 for PMMA and 5 for PLA (Figure 2B). For papers evaluating the biological hazards of adding mixtures, such as heavy metals, according to the type and size of MP, 32 papers on PS were investigated for NP (Figure 2C). Among the NP, only PS has been used to evaluate biological hazards using mixtures, and the addition of mixtures to other types of NP has not yet been published. However,

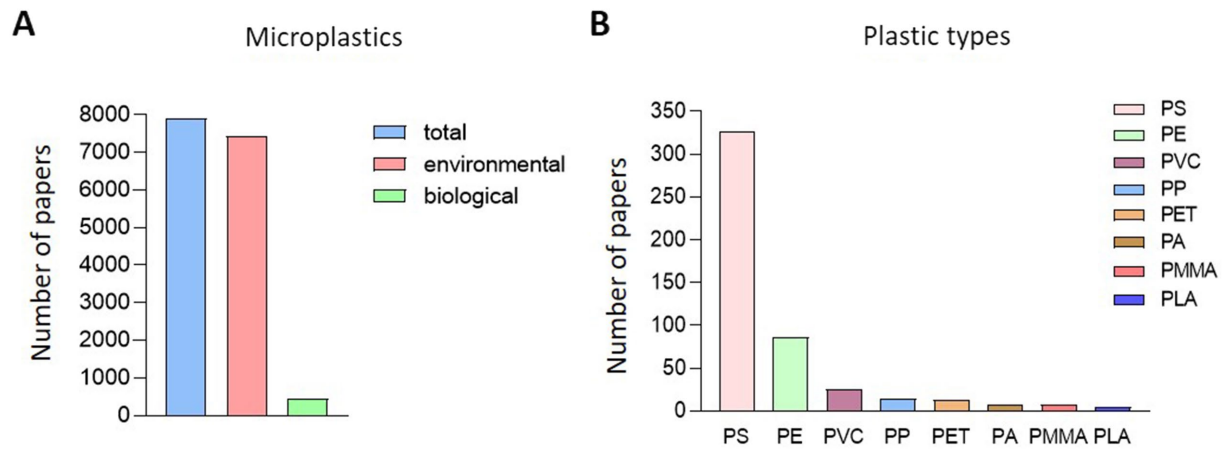

FIGURE 1
Research status of papers related to microplastics. **(A)** Overview of research on the biological effects of microplastics. **(B)** Classification of research by type of plastic.

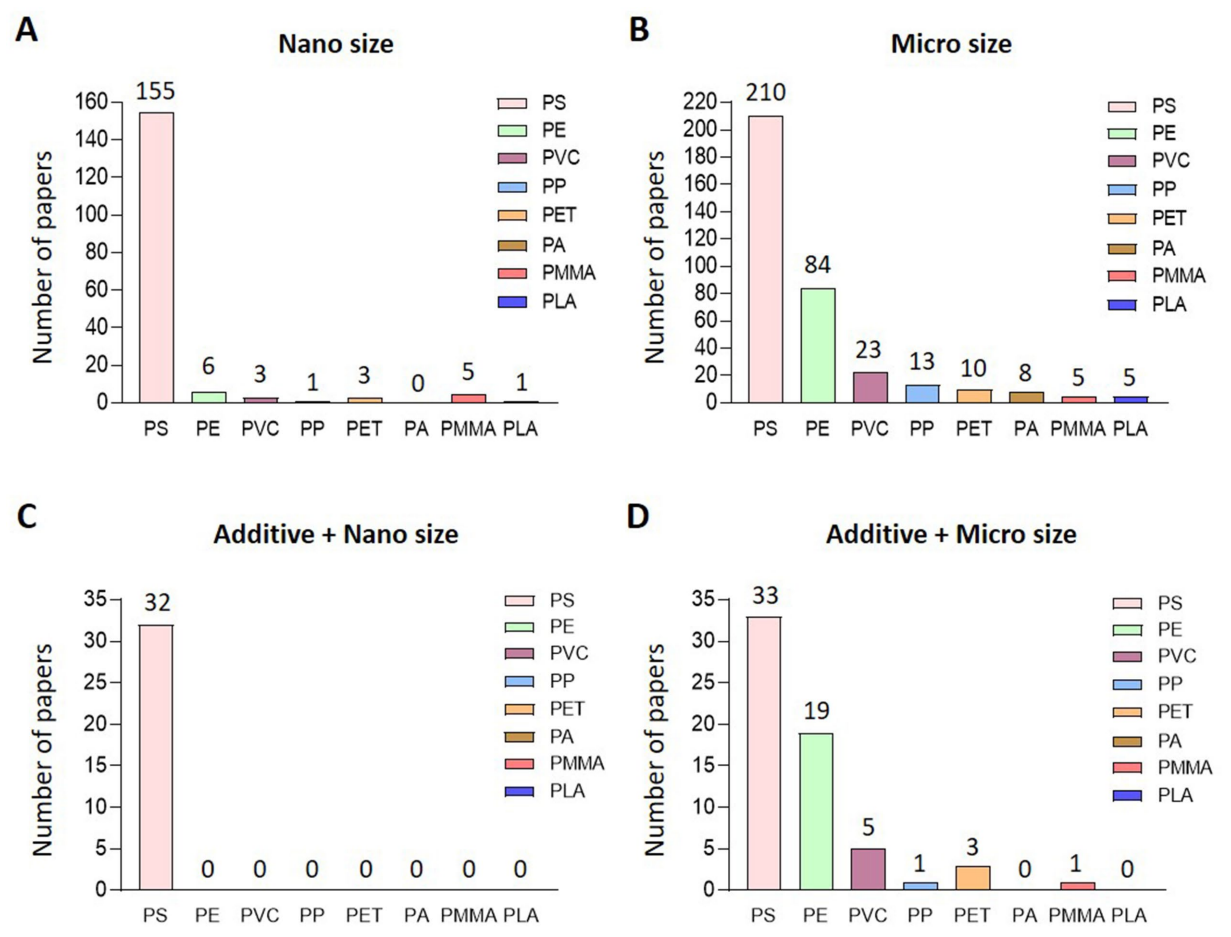

FIGURE 2
Current status of research on classification and additives according to size and type. Research classification of each type of plastic classified into **(A)** nano size and **(B)**. Micro size, **(C)** additive and nano sized, **(D)** additive and micro sized plastic.

in studies evaluating the biological hazards of adding mixtures to MP, PS was the most common with 33, followed by PE with 19, PVC with 5, and PP was investigated in 1 article, PET in three articles, and PMMA in one article. No study has yet been conducted to evaluate the biological hazards of mixtures of microsized PA (MP-PA) and microsized PLA (MP-PLA) (Figure 2D). Based on an investigation of

papers published on MP over the last decade, extensive research has been conducted to evaluate their biological hazards. Therefore, we summarized the type- and size-based characterization of MP *in vitro* and *in vivo* and the toxic effects of combined exposure to MP and additives, providing new evidence and insights into the potential biohazards of MP.

Evaluation of the biological effects of micro/nanosized plastics on specific organs in biological samples

MP present in the environment can have harmful biological effects by penetrating not only fish and land mammals but also the human body by inhalation of air or consumption of food contaminated with MP. However, the unique characteristics and complexity of biological samples make the detection of MP in them more difficult than that in environmental samples. Therefore, we compiled an overview and analysis of methods used for detecting MP in recently published papers (Tables 1–4) with the aim of providing a reference for research exploring the distribution and characteristics of MP in biological samples from fish, terrestrial mammals, and humans. We conducted a recent literature search to compile information on the types, exposure durations, methods, and concentrations of MP detected in biological samples from fish, terrestrial mammals, and humans. We categorized the data based on the organs, including the skin, intestines, lungs, and brain, and summarized the associated biological effects.

Skin

Table 1 summarizes the effects of microsized polypropylene (MP-PP) on skin cells. Human-derived dermal fibroblasts (HDF) were exposed to various concentrations of MP-PP for 48 h. MP-PP showed cytotoxicity in HDF, rodent macrophages (Raw 264.7), and human peripheral blood mononuclear cells (PBMC), linked to increased reactive oxygen species (ROS). Cytokine production (IL-6, TNF-α, histamine), associated with immune responses, also varied with particle size and concentration (44).

In another experiment, HDFs treated with various concentrations of microsized polystyrene (MP-PS) for 24 h showed particle penetration and accumulation within the cells. This induced the inflammatory cytokine IL-6, indicating potential local inflammation. Moreover, MP-PS infiltration into the cytoplasm triggered acute inflammatory responses in immune cells, increased ROS production, and released cytokines, leading to higher cell death in fibroblasts (45, 46). However, in an experiment using rodents and terrestrial mammals in which MP-PP was orally administered for 4 weeks, there was no toxicity or mutagenic potential. Additionally, 3D reconstructed human skin cell culture models showed no signs of skin irritation. This suggested that PP exposure does not have a negative effect on humans (47).

In a 96-h experiment with zebrafish embryos, exposure to nanosized polystyrene (NP-PS) reduced survival rates and damaged skin keratinocyte villi. Also, this exposure inhibited antioxidant responses, induced oxidative stress, caused mitochondrial damage, and led to ionocyte death, impairing ion uptake, pH regulation, and ammonia excretion (48). In conclusion, MP can induce cytotoxicity in skin cells, increase inflammatory cytokines, and trigger acute inflammatory responses in immune cells. Additionally, experiments using zebrafish embryos demonstrate that MP can reduce survival rates and damage skin keratinocytes.

Intestine

Table 2 summarizes the effects of plastics on the intestine. Human-derived colon cell lines (HT-29, Caco-2, and CCD 841CoN) were treated with nanosized polystyrene (NP-PS) at various times and concentrations. The results showed that PS was absorbed by colon cancer cells in a time- and concentration-dependent manner, leading to cytotoxicity. Specifically, HT-29 cells internalized PS, resulting in ultrastructural changes and cell death. Co-exposure to PS and F-further increased HT-29 cell death (38). The biological effects of exposing zebrafish to microsized PE (MP-PE) in water tanks were investigated. MP-PE reduced the range of intestinal goblet cells and altered the abundance of dominant microorganisms in the intestines. This exposure also activated intestinal immune network pathways responsible for mucosal immunoglobulin production (49). In experiments using terrestrial mammals, such as rodents and chickens, MP-PS was provided as drinking water and food, and its biological effects on the intestines were evaluated (50–52). In a mouse colitis model, PS disrupted colonic epithelium, induced liver inflammation, and exacerbated colitis, suggesting long-term exposure to PS poses significant health risks despite no significant accumulation in intestinal tissues (50). In chickens exposed to MP-PS in drinking water, PS damaged the intestinal vascular barrier, disrupted intestinal flora, caused intestinal necrosis, and induced inflammatory cell death (pyroptosis) due to microbial infections. Additionally, PS triggered hepatic immune responses, leading to lipid metabolism disorders and cell death in the liver (51). In mice, PS exposure primarily caused gut microbiota dysbiosis, tissue inflammation, and plasma lipid metabolism disorders, without significant PS accumulation in the intestines or liver. Gut microbiota changes were closely related to PS concentration and size, while intestinal damage and abnormal lipid metabolism were not significantly linked to PS exposure (52). In conclusion, plastics induce cytotoxicity in a size-dependent manner, with smaller sizes leading to internalization and subsequent cell death. Furthermore, MP has been shown to reduce the range of goblet cells and alter gut microbiota composition in zebrafish. In mammals, they cause damage to the colonic epithelium, liver inflammation, and disruption of gut microbial communities, which may result in gut microbiota dysbiosis and tissue inflammation.

Lung

Table 3 shows results for the biological effects of plastics on lungs. Research using human lung carcinoma cells (A549) investigated the biological effects of different-sized PS, PE, and PET particles (53–55). PS could be internalized by cells through phagocytosis, and could the findings facilitate the understanding of health risks caused by such accumulation (53). At 1,000 μg/mL, PE slightly reduced A549 cell viability and induced high levels of nitric oxide (NO) and nitrite. This suggests PE exposure may increase susceptibility to NO-mediated toxicity and immune modulation (54). PET was internalized by A549 cells, reducing cell viability at high concentrations and inducing oxidative stress. Increased PET concentrations correlated with decreased mitochondrial membrane potential and higher levels of reactive oxygen species (ROS), leading to an increase in late-stage apoptotic cells (55). In experiments with terrestrial mammals,

TABLE 1 Summary of the biological effects of microplastics and nanoplastics on the skin.

Reference	Model	Polymer	Size	Route	Duration	Dose	Additive	Limitation	Actual result
(44)	Human-derived dermal fibroblasts (HDF cells)	PP	~20 μm, 25–200 μm	*In vitro*	48 h	10, 50, 100, 500, 1,000 μg/mL	x		Elevated ROS levels induced toxicity and larger particles demonstrated lower cellular toxicity
(45)	Human-derived dermal fibroblasts (HDF cells)	PS	PS (10, 40, 100 μm), PS-FITC (460 nm, 1 μm, 3 μm)	*In vitro*	24 h	0, 1, 10, 100, 500 or 1,000 μg/mL	x	Hemolytic impact of nano-sized PS was unknown	Small-sized PS particles induced hemolysis in red blood cells
(46)	Human-derived dermal fibroblasts (HDF cells)	PS	5–25 μm, 25–75 μm, 75–200 μm	*In vitro*	1 and 4 d	10, 100, 1,000 μg/mL	x		PS generated reactive oxygen species (ROS)
(47)	Human skin reconstructed 3D model	PP	86 μm	*In vitro* (3D-reconstructed epidermal tissue)	22 h	40 mg	x	The 3D reconstructed human skin model lacks pores	No cell toxicity
(48)	Skin keratinocytes in zebrafish embryos	PS	25 nm	*In vitro* (zebrafish embryos)	96 h	10, 25, 50 mg/L	x		PS induced mitochondrial damage and ionocyte apoptosis

TABLE 2 Summary of the biological effects of microplastics and nanoplastics on the intestine.

Reference	Model	Polymer	Size	Route	Duration	Dose	Additive	Limitation	Actual result
(49)	Adult zebrafish (*Danio rerio*)	PE	30 μm	Oral (in water)	7 d	1, 10, 100, 1,000 μg/mL	x		Altered intestinal microbiota activated the intestinal immune network
(50)	Mouse	PS	5 μm	Oral	42 d	100 μg/L	x		PS disrupts the homeostasis of colonic epithelium
(52)	Mouse	PS	40–60 μm, 60–100 μm	Oral	21 weeks	50, 500 mg/kg food	x	Significant PS accumulation was not observed in the intestine or liver	Imbalance in gut microbiota, tissue inflammation
(51)	Chickens (*Gallus gallus*)	PS	5 μm	Oral	6 weeks	1, 10, 100 mg/L	x	Lack of data that PS disrupt the intestinal barrier and penetrate into the gut	PS disrupts the intestinal vascular barrier, disturbs gut microbiota, and promotes the accumulation of lipids and carbohydrates
(38)	Human colonocytes (HT-29, Caco-2, CCD 841 CoN)	PS	100 nm	*In vitro*	24, 48, 72 h	PS-NP: 50, 100, 250, 500 μg/mL, F^-: 1 mM	Fluoride	Intracellular internalization of PS in cells was conducted solely through TEM	Alterations in cellular microstructure

10.3389/fpubh.2024.1458727

10.3389/fpubh.2024.1458727

TABLE 3 Summary of the biological effects of microplastics and nanoplastics on the lung.

Reference	Model	Polymer	Size	Route	Duration	Dose	Additive	Limitation	Actual result
(39)	Mouse	PS	99 nm, 5 μm	Intranasal	5 weeks	10 μg/μL	x		Imbalance of microbiota
(53)	Human lung carcinoma, (A549)	PS	70, 200, 500 nm	*In vitro*	4, 10, 24 h	5, 15, 50, 150, 500, 1,500 mg/L	x		Internalized to cells
(54)	Human lung carcinoma, (A549l)	PE	7 μm (±2.0), 31 μm (±10.5)	*In vitro*	48 h	1, 10, 100, 500, 1,000 μg/mL	x		NO-mediated toxicity
(55)	Human alveolar type II epithelial cell line (A549)	PET	<20 nm	*In vitro*	24 h	1, 5, 10, 25, 50, 99, 197 μg/mL	x		Internalized to cells reactive oxygen species (ROS) detected
(56)	Mouse	PS	5 μm	Oral/ intratracheal	7 d and 3 weeks	Oral administration: 100 mg/kg, intratracheal administration: 2, 7, 12 mg/kg	x	Assessment of the Wnt/β-catenin signaling pathway in mouse lung	Pulmonary epithelial damage

intranasal administration of NP-PS and MP-PS to mice induced nasal microbiota imbalance, with MP-PS showing a stronger effect on lung microorganisms. Suggesting microbial changes could serve as biomarkers for PS-induced airway imbalance (39). Inhalation exposure to intratracheal PS via spray induced dose-dependent pulmonary fibrosis in mice, increasing α-SMA, vimentin, and Col1a expression. This exposure also caused intensive lung oxidative stress, suggesting PS inhalation may lead to pulmonary fibrosis through oxidative stress and Wnt/β-catenin signaling activation (56). In conclusion, plastic particles can be internalized by cells, increasing health risks, reducing the viability of lung cells, and inducing oxidative stress while affecting immune modulation. Additionally, in mammals, nanosized plastics have been shown to disrupt lung microbiota balance, and inhalation exposure may lead to pulmonary fibrosis, potentially linked to oxidative stress.

Brain

Table 4 summarizes the search results for the biological effects of plastics detected in the brain. Zebrafish embryos exposed to MP-PS exhibited seizures, increased seizure-like brainwave signals, and altered seizure-related gene expression. PS disrupts cholinergic, dopaminergic, and GABAergic neurotransmitter systems, impacting brain development in zebrafish embryos (57). In experiments with adult zebrafish, exposure to NP-PE and NP-PP in aquariums increased brain catalase activity but inhibited lactate dehydrogenase at high doses. Brain respiratory chain complexes II and IV significantly decreased, indicating impaired mitochondrial function. In the liver, mitochondrial respiration was also impaired, correlating with decreased mitochondrial membrane potential due to respiratory chain complex inhibition (58). In an experiment with common carp (*Cyprinus carpio*), exposure to NP-PE and MP-PE in aquariums significantly reduced acetylcholinesterase (AChE), monoamine oxidase (MAO), and nitric oxide (NO) levels in the brain. Smaller PE particle sizes correlated with more pronounced reductions in these markers. Additionally, damage such as necrosis, fibrosis, capillary changes, tissue disintegration, edema, and degenerative connective tissue was observed in cerebellar neurons, ganglion cells, and the retina, indicating potential neurotoxic effects of PE exposure (59). Furthermore, an experiment in terrestrial mammals investigated the effects of consuming MP-PS in drinking water. It found that PS disrupted the blood-brain barrier, increased brain dendritic spine density, and induced hippocampal inflammation. Mice exposed to PS exhibited impaired cognition and memory, with concentration-dependent effects on learning abilities, irrespective of PS particle size (60). In experiments with chickens exposed to MP-PS in drinking water, significant effects on the brain were observed, including hemorrhage, microthrombi formation, and loss of Purkinje cells. Plastic-induced brain hemorrhage triggered inflammation, disrupted mitochondrial function, and activated signaling pathways like ASC-NLRP3-GSDMD and AMPK (61). In conclusion, plastics impact neurotransmitter systems in zebrafish embryos, while they increase brain catalase activity and inhibit lactate dehydrogenase in adult zebrafish. In common carp, exposure to plastics leads to decreased levels of acetylcholinesterase (AChE), monoamine oxidase (MAO), and nitric oxide (NO). Furthermore, in mammals, the blood-brain barrier is disrupted, resulting in impaired cognition and memory, with significant observations in chickens, including brain hemorrhage and loss of Purkinje cells.

TABLE 4 Summary of the biological effects of microplastics and nanoplastics on the brain.

Reference	Model	Polymer	Size	Route	Duration	Dose	Additive	Limitation	Actual result
(57)	Zebrafish embryo	PS	1, 6, 10, 25 μm	*In vitro* (zebrafish embryos)	6 hpf (hours post-fertilization) ~ 120 hpf	500, 5,000, 50,000 particles/mL	x		Neurotoxicity (seizure effects)
(58)	Adult zebrafish (*Danio rerio*)	PE, PP	179 ± 77 nm	Oral (in water)	21 d	1 mg/L	x		Mitochondrial respiration deficiency
(59)	Common carp, (*Cyprinus carpio*)	PE	MaPs > 5 mm, 5 mm > MPs > 100 nm, NPs <100 nm	Oral (in water)	15 d	100 mg/L	x	Behavioral experiment data are needed to assess the neurotoxicity of PE	Neurotoxicity (decreased acetylcholinesterase (AChE), monoamine oxidase (MAO), and nitric oxide (NO))
(60)	Mouse	PS	1, 4, 10 μm	Oral	180 d	100, 1,000 μg/L	x	The underlying mechanisms of neurotoxicity and cognitive dysfunction induced by PS was unclear	The destruction of the blood-brain barrier, increased dendritic spine density, inflammation responses in the hippocampus, and impaired cognition and memory
(61)	Chicken	PS	5 μm	Oral	6 weeks	1, 10, 100 mg/L	x	Immunohistochemical staining methods to show clearly the presence of hemorrhage	Brain hemorrhage, loss of Purkinje cells

MaPs, macroplastics.

Assessments of biological effects of combined exposure to micro/nanoplastics and additives

Recently, the number of studies evaluating the biological hazards of mixtures containing MP and heavy metals or additives, rather than focusing solely on the biological toxicity of individual MP substances, is increasing. In this section, findings from studies that have assessed the biological effects of mixtures involving MP/NP of varying sizes and types combined with heavy metals or additives are summarized.

A summary of the combined exposure of nanoplastics with heavy metals or additives

Nanoplastics with heavy metals

Chen et al. (62) demonstrated that co-exposure of cadmium (Cd) and NP-PS in grass carp (*Ctenopharyngodon idellus*) decreases antioxidant enzyme activity and causes organ damage. Feng et al. (31) showed that co-exposure to MP-PS and lead (Pb) in female mice aggravated ovarian toxicity and increased Pb bioaccumulation. Estrela et al. (63) demonstrated that zinc oxide nanoparticles (ZnO) in combination with NP-PS influenced the behavior of *Ctenopharyngodon idella* (*C. idella*) in mirror tests, inducing inactivity and showing signs of DNA damage and increased oxidative stress. In mice, Estrela et al. (40) evaluated the toxicity of ZnO and NP-PS through intraperitoneal administration, revealing increased levels of nitric oxide (NO), reactive oxygen species, decreased acetylcholinesterase (AChE) activity, and brain accumulation of nanomaterials, indicating their potential neurotoxicity. Yu et al. (32) used single-cell sequencing to reveal heterogeneous effects of NP and Pb on zebrafish intestinal cells. Simultaneous exposure to NP-PS and Pb altered immune recognition, induced cell death, and caused oxidative stress, lipid metabolism disturbance, and similar intestinal toxicity.

Nanoplastics with chemicals

Steckiewicz et al. (38) demonstrated that fluoride alone was not cytotoxic but enhanced the cytotoxicity of NP-PS in colonocytes, causing ultrastructural changes through cellular internalization. Yu et al. (37) demonstrated that co-exposure to MP/NP and oxytetracycline in zebrafish led to altered intestinal histopathology, microbiome changes, and increased antibiotic-resistance genes. Li et al. (35) found that NP-PS enhanced the adverse effects of di-(2-ethylhexyl) phthalate (DEHP) on the male reproductive system in mice, causing gene and pathway alterations. Also, Liao et al. (64) showed that DEHP exacerbates the toxicity of NP-PS through histological damage and intestinal microbiota dysbiosis in freshwater fish. Wang et al. (65) demonstrated the Simultaneous exposure to NP-PS and BDE-47 in zebrafish exacerbated developmental deformities, decreased survival rates, and caused tissue damage. Santos et al. (66) demonstrated combined exposure to NP and phenmedipham (PHE) in zebrafish embryos exhibited greater toxicity than single exposures. Martínez-Álvarez et al. (67) showed that combined exposure to NP-PS and benzo(a)pyrene (B(a)P) in brine shrimp larvae and zebrafish embryos increased toxicity. Qin et al. (68) showed that chlorine disinfection increased NP-PS toxicity in human cells by inducing mitochondria-dependent apoptosis. Liu et al. (69) showed that NP and avobenzone (AVO) exposure affected neural and

retinal development in zebrafish. Liu et al. (70) demonstrated NP-PS and butyl methoxydibenzoylmethane (BMDBM) affected zebrafish brain development and inhibited motor activity. Wu et al. (34) showed that parental co-exposure to NP-PS and microcystin-LR (MCLR) aggravated hatching inhibition in zebrafish offspring, affecting enzyme activity, disrupting the cholinergic system, and impairing muscle development. Similarly, Zuo et al. (71) demonstrated that combined exposure to NP-PS and MCLR altered the expression of HPT axis-related genes and GH/IGF axis genes in F1 zebrafish larvae, exacerbating growth inhibition and increasing MCLR transfer to offspring. Wang et al. (33) demonstrated the NP-PS and bisphenol A (BPA) in human cells showed increased adsorption and cytotoxicity. Singh et al. (72) demonstrated that NP-PS and polycyclic aromatic hydrocarbons (PAHs) altered nanoparticle stability and toxicity, leading to DNA damage in zebrafish. He et al. (36) demonstrated co-exposure to NP and triphenyl phosphate (TPhP) in zebrafish led to significant reproductive impairment. Yan et al. (73) demonstrated NP and tetracycline (TC) in gastric cancer cells reduced cell viability and induced oxidative stress. Zhang et al. (74) showed NP-PS combined with roxithromycin (ROX) in freshwater fish red tilapia (*Oreochromis niloticus*) increased bioaccumulation and disrupted metabolism. Chen et al. (75) showed that NP and 17α-ethynylestradiol (EE2) exposure in zebrafish suppressed locomotor activity and altered swimming behavior. Bhagat et al. (76) demonstrated that co-exposure to NP and metal oxide nanoparticles (nMOx) like aluminum oxide and cerium oxide induced oxidative stress in zebrafish embryos. Zhao et al. (77) showed that NP-PS and synthetic phenolic antioxidants like butylated hydroxyanisole (BHA) in zebrafish disrupted thyroid function and metabolism.

Nanoplastics with others

Alaraby et al. (78) demonstrated antagonistic interactions between silver compounds and NP-PS in *Drosophila*, where nanosilver, known for inducing oxidative stress, significantly decreased oxidative stress and DNA damage when combined with NP-PS, thereby reducing genotoxicity. In contrast, Ilić et al. (79) showed a synergistic interaction between silver nanoparticles (AgNP) and NP-PS in human intestinal cells, with combined exposure leading to increased cell death, expression of inflammatory cytokines (IL-6, IL-8, and TNF-α), oxidative stress, and mitochondrial dysfunction. Guo et al. (80) showed that NP-PS significantly altered the gut microbial community in zebrafish, with commercial PS having stronger toxic effects, which were mitigated by co-treatment with enrofloxacin (ENR). Brandts et al. (81) demonstrated the immunomodulatory effects of NP and humic acids on European seabass. The study assessed whether NP-PS act as stressors in juvenile European seabass, affecting immune response, and whether humic acid mitigates these effects. Shi et al. (82) found that NP-PS and phthalate esters together reduced cell viability in human lung epithelial A549 cells, emphasizing their combined toxic effects and risks of co-exposure to NP and organic pollutants in humans. Hou et al. (83) showed significant NP accumulation in human intestinal organoids, investigating their absorption, toxicity in human intestinal cells, and proposing inhibiting intracellular uptake as a potential therapy to reduce NP toxicity in humans.

In conclusion, combined exposure to NP and heavy metals or additives has been shown to increase cytotoxicity, resulting in reproductive and intestinal toxicity, as well as organ damage. This exposure leads to heightened DNA damage and oxidative stress, which in turn contributes to increased inflammation. Additionally, alterations in gut microbial communities have been observed.

A summary of the combined exposure of microsized plastics with heavy metals or additives

Microsized polystyrene

Microsized polystyrene with heavy metals

Wang et al. (84) reported distinct adverse outcomes on erythrocytes' lipid profiles following single and combined exposure to Cd and MP. Co-treatment of MP-PS and CdCl2 showed a clear antagonistic relationship, indicating impaired membrane function of red blood cells (RBCs). Chen et al. (85) demonstrated that co-exposure to MP-PS and Cd in early-stage zebrafish reduced body weight and intensified growth abnormalities, oxidative stress, and cell death-related gene expression compared to individual exposures. These findings suggest that MP may worsen Cd's adverse effects during early zebrafish development. Zhang et al. (86) studied the combined toxicity of MP and Cd in zebrafish embryos. They exposed the embryos to varying concentrations of MP along with environmentally relevant levels of Cd, which adversely affected their survival and heart rate (HR). Yan et al. (87) showed that the individual and combined toxicogenetic effects of MP and heavy metals (Cd, Pb, and Zn) disrupted gut microbiota and gonadal development in marine medaka. This affected gut function and specific bacterial species in male fish. Lu et al. (88) found that MP increase Cd levels in zebrafish organs, including the liver, viscera, and gills. This combined exposure to MP and Cd resulted in increased toxicity, leading to oxidative damage and inflammation. The study emphasizes the chronic risks of MP and Cd exposure in zebrafish. Zuo et al. (89) demonstrated the individual and combined effects of MP and Cd on juvenile grass carp (*Ctenopharyngodon idellus*). They found that intestinal Cd levels were elevated in grass carp exposed to both Cd and MP-PS. Histological analysis showed significant intestinal damage following acute exposure, accompanied by changes in proinflammatory cytokine expression. Yang et al. (90) compared the combined toxicity of MP-PS and different Cd concentrations in zebrafish. They found that MP-PS increased Cd toxicity at low concentrations (LCd) but reduced toxicity at high concentrations (HCd), indicating a concentration-dependent interaction between MP-PS and Cd in zebrafish. Zhang et al. (91) found that combined exposure of goldfish to MP and Cu induced oxidative stress, inflammation, apoptosis, and impaired autophagy in the pancreas and intestines. MP enhanced Cu accumulation in the liver, pancreas, and intestines, worsening oxidative stress. This combined exposure also leads to inflammation, excessive cell death, and impaired autophagy in the liver and pancreas, further emphasizing the risks associated with MP-mediated heavy metal adsorption. Zheng et al. (92) found that particles, rather than Zn^{2+} released from ZnO nanoparticles, exacerbated MP toxicity in early-stage exposure in zebrafish and their offspring. ZnO particles attached to MP surfaces facilitated ZnO transport into larvae, intensifying effects on growth inhibition, oxidative stress, apoptosis, and GH/IGF axes.

Microsized polystyrene with chemicals

Yu et al. (37) showed that combined exposure to MP/NP and oxytetracycline in zebrafish affected intestinal histopathology and microbiome. Co-exposure increased antibiotic resistance gene abundance in the intestine. Cheng et al. (93) studied the combined effects of MP-PS and BPA on human embryonic stem cell-derived liver organoids, highlighting metabolism-related health risks even at low doses equivalent to human internal exposure levels. Wang et al. (33) studied the combined effects of BPA and NP-PS, MP-PS on particle uptake and toxicity in human Caco-2 cells. They examined how BPA adsorbs onto different sizes of PS particles using colon cancer Caco-2 cells and assessed resulting cell toxicity, confirming increased toxicity with BPA adsorption during MP exposure. Sun et al. (94) discovered that simultaneous ingestion of MP-PS and epoxiconazole increases health risks in mice due to synergistic bioaccumulation. Intestinal damage caused by EPO allows significant PS penetration, impacting gut microbiota and exacerbating oxidative stress and metabolic disorders. Lu et al. (95) investigated the combined toxicity of MP-PS and sulfamethoxazole (SMZ) on zebrafish embryos. Despite observing an antagonistic effect between PS and SMZ toxicity, which slightly reduced their combined impact, co-exposure still exhibited significant toxicity. Jiang et al. (96) investigated the effects of MP and tributyltin (TBT), alone and combined, on bile acid and gut microbiota interactions in mice. They observed that MP, either alone or with TBT, induced liver inflammation, altered gut microbiota composition, and disrupted fecal bile acid profiles. However, combined exposure to MP and TBT mitigated the toxic effects observed with individual exposures. Domenech et al. (97) showed the interaction of silver nanoparticles and silver nitrate with PS as metal carriers and their effects on human intestinal Caco-2 cells. In this study, we confirmed that a composite of silver compounds and PS was internalized by Caco-2 cells, exhibiting harmful cellular effects, such as genetic toxicity and oxidative DNA damage. Xu et al. (98) investigated the toxic effects of MP and phenanthrene in zebrafish. Combined exposure led to higher accumulation in zebrafish and increased expression of immune and oxidative stress genes due to oxidative stress. MP also demonstrated a synergistic effect by altering gut microbiota, thereby enhancing the toxicity of phenanthrene. He et al. (36) demonstrated enhanced toxicity of triphenyl phosphate (TPhP) in zebrafish when combined with MP and NP. MP-PS was used to study TPhP toxicity, revealing that MP further inhibited sperm and oocyte formation and significantly impaired zebrafish reproductive performance compared to TPhP alone. Li et al. (99) showed that hydrogen sulfide (NaHS) mitigates MP-PS-induced hepatotoxic effects by upregulating the Keap1-Nrf2 pathway. NaHS significantly reduced inflammation, cell death, and oxidative stress in the liver caused by MP-PS, promoting Nrf2 accumulation and alleviating its hepatotoxic effects. Yang et al. (100) discovered that MP-PS reduced 6:2 chlorinated polyfluorinated ether sulfonate (F-53B) bioaccumulation in larval zebrafish while promoting its adsorption, thereby lowering its bioavailability. This combined exposure also induced inflammatory stress in the zebrafish larvae. Wang et al. (101) showed that MP and DEHP together induced pancreatic cell apoptosis in mice through oxidative stress and activation of the GRP78/CHOP/Bcl-2 pathway. This study showed increased ROS levels, inhibited antioxidant enzyme activity, and altered expression of key pathway proteins, ultimately leading to cell death. Hanslik et al. (102) studied biomarker responses in zebrafish (*Danio rerio*) exposed long-term to MP-bound chlorpyrifos (CPF) and benzo(k)fluoranthene (BkF). They found that CPF, an organophosphate insecticide, adsorbed onto MP-PS during exposure to adult zebrafish, while BkF, a polycyclic aromatic hydrocarbon (PAH), adsorbed onto microsized polymethyl methacrylate (MP-PMMA). Importantly, these MP-bound substances did not induce adverse effects in aquatic ecosystems. Luo et al. (103) showed that exposure to both MP-PS and imidacloprid (IMI) in adult zebrafish led to enhanced liver toxicity by affecting genes involved in glycolipid metabolism and inflammation. This highlights the synergistic hepatotoxic effects of MP and IMI in zebrafish.

Microsized polystyrene with others

Qiao et al. (104) explored the combined effects of MP-PS and natural organic matter (NOM) on Cu accumulation and toxicity in zebrafish. They found that smaller MPs absorbed more Cu, and NOM facilitated Cu adsorption onto MPs. This combination increased Cu accumulation in the liver and gut in a size-dependent manner, suggesting heightened Cu toxicity in these organs. Deng et al. (105) demonstrated that MP worsen the toxicity of organophosphorus flame retardants (OPFRs) in mice. Co-exposure increased lactate dehydrogenase levels and decreased AChE activity, alongside significant metabolic changes in amino acid pathways and energy metabolism compared to controls. Zhang et al. (74) demonstrated that MP-PS interact with ROX to enhance its bioaccumulation and distribution in freshwater red tilapia. Co-exposure to PS and ROX potentially affects ROX metabolism in the liver of red tilapia. Zhao et al. (77) showed that microplastics worsened the developmental toxicity of synthetic phenolic antioxidants in zebrafish by disrupting thyroid function and metabolism, leading to increased BHA accumulation, lower hatching rates, more deformities, and reduced bone calcification. Yan et al. (73) investigated the toxicity of TC in combination with PS spheres in gastric cancer cells. They confirmed that PS had a concentration-dependent adsorption capacity for TC using two different sizes of PS. Moreover, the PS-TC mixture reduced the viability of gastric cancer cells (AGS) by inducing oxidative stress, ultimately leading to cell death.

In conclusion, the combined exposure of MP with heavy metals or additives has been shown to increase cytotoxicity, negatively impact erythrocytes, and induce developmental abnormalities. Furthermore, this combined exposure may enhance toxicity through accumulation in organs, leading to intestinal damage and alterations in gut microbial communities.

Microsized polyethylene

Microsized polyethylene with heavy metals

Tarasco et al. (106) studied the effects of pristine and contaminated MP-PE on zebrafish development, finding impaired reproductive capacity with BaP and MP-PE co-exposure. They noted increased skeletal deformities and bone disorders during development, alongside intestinal inflammation indicated by histological analysis. Banaee et al. (107) investigated the effects of Cd and MP particles on common carp (*Cyprinus carpio*), focusing on biochemical and immunological parameters. They found that combined exposure to Cd and MP reduced lysozyme and alternative complement (ACH50) activity, as well as total immunoglobulin and

complements C3 and C4 levels compared to controls. These changes indicated heightened toxicity on immunological parameters. Miranda et al. (108) investigated the neurotoxic, behavioral, and lethal effects of Cd, MP, and their mixtures on juvenile *pomatoschistus microps* under lab conditions. They found that while mortality rates did not significantly differ between groups exposed to Cd alone versus the MP-Cd mixture, MP did influence the sublethal neurotoxic effects of Cd. Luís et al. (109) demonstrated that MP influence the acute toxicity of chromium (Cr) (VI) in early juvenile common gobies (*Pomatoschistus microps*). They found a significant decrease in predatory performance and inhibition of AChE activity when juveniles were co-exposed to Cr (VI) and MP-PE. Additionally, confriming that co-exposure led to increased lipid peroxidation (LPO).

Microsized polyethylene with chemicals

Menéndez-Pedriza et al. (110) investigated the lipidomic impacts of MP-PE and PCBs on human hepatoma cells. They found that while MP-PE alone was non-toxic, its combination with PCBs led to concentration-dependent changes in lipid composition and membrane permeability, indicating potential adverse effects from this interaction. Huang et al. (111) investigated the combined impact of MP and tetrabromobisphenol A (TBBPA) on the human gut using *in vitro* simulations with human colon cancer cells and microbial communities. They found that this combined exposure disrupted gut homeostasis and metabolic pathways in gut microbiota, leading to significant adverse effects. Yu et al. (112) found that cosmetic-derived plastic microbeads enhance TBBPA adsorption and increase oxidative stress in zebrafish. The integrated biomarker response (IBR) index revealed significant detrimental effects from combined PE and TBBPA exposure. Zhang et al. (113) studied the combined effects of PE and 9-nitroanthracene (9-NAnt) on zebrafish, finding that this co-exposure induced neurotoxicity, disrupted energy metabolism, and altered gut microbiota composition. Deng et al. (114) demonstrated that phthalate-contaminated MP increased PAE accumulation in the liver and intestine of male mice, leading to enhanced reproductive toxicity. Combined exposure to PAEs and MP adversely affected sperm physiology and formation. Deng et al. (52) found that MP adsorb and transport PAEs to the mouse intestine, where they accumulate. Combined exposure to MP and PAEs increased intestinal permeability, altered gut microbiota, and exacerbated inflammation and metabolic disorders more than individual exposures. Sheng et al. (115) demonstrated that different types of MP affect triclosan (TCS) adsorption, accumulation, and toxicity in zebrafish. PE increased TCS accumulation in the liver and intestines by adsorbing TCS. Combined exposure to TCS and PE led to increased lipid toxicity due to TCS accumulation. Deng et al. (105) showed that MP worsen the toxicity of organophosphorus flame retardants (OPFRs) in mice. Mice exposed to MP-PE along with OPFRs like TCEP and TDCPP experienced more pronounced changes in biochemical markers and metabolites compared to exposure to these substances individually, indicating increased toxicity from the combined exposure. Tong et al. (116) demonstrated that MP-PE cooperate with *Helicobacter pylori* to promote gastric injury and inflammation in mice. In this study, exposure to a combination of *Helicobacter pylori* and MP-PE resulted in increased infiltration of inflammatory cells into gastric or intestinal tissues, along with an elevation in inflammatory factors.

Microsized polyethylene with others

Khan et al. (117) found that MP-PE beads did not significantly change silver (Ag) absorption and localization in zebrafish. However, MP-PE increased Ag accumulation in the intestines, suggesting alterations in the bioavailability and absorption of metal contaminants. Boyle et al. (118) demonstrated that PVC plastic fragments release bioavailable Pb additives in zebrafish. They compared the impact of PVC exposure with PE-HD and PET exposure, noting that PE did not significantly alter biomarker expression. Schirinzi et al. (119) studied the cytotoxic effects of nanomaterials and MP on human cerebral and epithelial cells. They assessed individual cell toxicity for PE, metal nanoparticles (nMOx), and carbon nanomaterials, observing heightened oxidative stress in both cell lines. This suggests that combined exposure to PE and these additives induces cellular toxicity. Batel et al. (120) found that PE transferred BaP to *Artemia nauplii* and zebrafish in a food web experiment. PE moved through zebrafish intestines without causing significant damage but was absorbed by epithelial cells. It also facilitated the release of persistent organic pollutants (POPs) in the intestines, transferring them to the intestinal epithelium and liver. Araújo et al. (121) examined the combined effects of emerging pollutants and MP-PE on zebrafish, focusing on genotoxicity and redox balance. They found that both MP-PE alone and in combination with new pollutants caused DNA damage and nuclear abnormalities in erythrocytes. This indicates that the combined exposure did not increase toxicity beyond that of MP-PE alone, highlighting complex interactions among substances in aquatic environments. Batel et al. (122) investigated the long-term ingestion effects of differently sized MP on zebrafish. Their study focused on BaP combined with PE, demonstrating that BaP-PE particles accumulated in the zebrafish intestine but particles were transported along the intestine and excreted without inducing adverse effects.

In conclusion, the combined exposure of MP with heavy metals and additives has been shown to enhance cellular toxicity and induce developmental disorders, neurotoxicity, and dysbiosis in gut microbiota. Additionally, as bioaccumulation within the body increases, it may lead to organ damage and alterations in the bioavailability of these substances.

Microsized polyvinyl chloride

Microsized polyvinyl chloride with heavy metals

Chen et al. (123) used the SBRC (Soluble Bioavailability Research Consortium) digestion model to study the bioaccessibility of heavy metals (As, Cr, Cd, Pb) associated with MP and PVC. They found that Pb (II) exhibited higher bioaccessibility compared to As (V), Cr (VI), and Cd (II), highlighting potential health risks related to the interactions between heavy metals and MP. Boyle et al. (118) demonstrated that PVC plastic fragments release bioavailable Pb additives in zebrafish. Their study assessed the effects of PVC and Pb additives on zebrafish biomarker expression, confirming that MP-PVC serves as an environmental reservoir for Pb, impacting biomarkers. Hoseini et al. (124) demonstrated severe hepatic stress and inflammation in common carp (*Cyprinus carpio*) exposed to copper (Cu) and MP-PVC. The combined exposure induced significant liver damage and inflammation, as evidenced by hepatic transcriptomic and histopathological responses.

Microsized polyvinyl chloride with chemicals

Wang et al. (125) demonstrated that single exposure to MP-PVC and DEHP delayed hatching and caused mortality in juvenile zebrafish. Single exposure affected cardiac development, while combined exposure showed an antagonistic effect. Sheng et al. (115) studied the impact of different MP types on triclosan (TCS) adsorption, accumulation, and toxicity in zebrafish. They observed PVC's ability to adsorb both forms of TCS, altering its tissue distribution and increasing TCS accumulation in the liver and intestines. This highlights potential harmful effects of PVC-TCS mixtures on zebrafish.

In conclusion, combined exposure to MP with heavy metals and additives has been shown to induce significant hepatic stress and inflammation, leading to liver damage. Furthermore, this exposure may also result in developmental disorders and has the potential to adsorb and accumulate specific substances in the liver and intestines, which could pose harmful effects.

Microsized polypropylene

Sheng et al. (115) studied the impact of different MP types, including PP, on triclosan (TCS) adsorption, accumulation, and toxicity in zebrafish. They found that MP-PP had the highest TCS adsorption capacity, leading to increased accumulation in the liver and intestines. Co-exposure to MP-PP and TCS also heightened oxidative stress, lipid peroxidation in the liver, and neurotoxic effects in the brain.

Microsized polyethylene terephthalate

Boyle et al. (118) found that PVC plastic fragments release bioavailable Pb additives in zebrafish. They studied both PVC and microsized polyethylene terephthalate (MP-PET) regarding Pb release in zebrafish. The study concluded that PET did not alter biomarker expression in zebrafish larvae, indicating it had no effect on Pb release. Liu et al. (126) found that MP-PET reduced the bioaccumulation of SMZ in various tissues of mice but worsened its effects on gut microbiota and antibiotic resistance genes. While SMZ levels in the liver, lungs, spleen, heart, and kidneys were lower with MP-PET, the interaction exacerbated impact of SMZ on gut microbiota and antibiotic resistance gene profiles. Cheng et al. (127) studied the effects of MP fibers and granules on zebrafish embryos, both alone and in combination with Cd. They found that PET granules (p-PET) increased blood flow velocity and heart rate and inhibited embryo hatching, while PET fibers (f-PET) reduced Cd accumulation in the chorion by dissolving in the culture medium. Overall, both p-PET and f-PET decreased Cd toxicity, with fibers showing a stronger detoxification effect.

Microsized polymethyl methacrylate

Hanslik et al. (102) studied biomarker responses in zebrafish exposed long-term to MP-associated chlorpyrifos (CPF) and benzo(k) fluoranthene (BkF). They found that BkF adsorbed onto MP-PMMA in zebrafish, and combined exposure reduced BkF bioavailability compared to exposure to BkF alone, suggesting no adverse effects from PMMA-bound BkF in zebrafish.

Discussion

In this review, we set a 10-year period from 2012 to 2022 and conducted a comprehensive search for relevant studies in PubMed. We identified any biological hazards depending on the size and type of plastic and classified and organized the results of mixed exposure with chemicals and heavy metals included during plastic preparation as well as numerous chemicals pre-exposed in the environment.

Hazard tests conducted on various organs, including the skin, intestine, lungs, and brain, to assess the biological effects of exposure to MP/NP revealed that in the skin they inhibit antioxidant responses, induce oxidative stress, and lead to cell death, potentially damaging skin function (45–48). In the intestines, they alter the microflora, cause tissue inflammation, destruct the vascular barrier, and cause metabolic disorders (38, 50–52). In the lungs, they cause an increase in oxidative stress and an imbalance in nasal microorganisms, potentially causing lung fibrosis (39, 53, 54, 56). Finally, in the brain they impact the regulatory disorders associated with seizures. They could cross the blood-brain barrier, induce inflammatory responses in the hippocampus, and trigger inflammatory cell infiltration into the brain as a result of brain hemorrhage, potentially leading to intracerebral inflammation (57, 60, 61). These findings suggest that the toxic effects induced by MP/NP could be significant, potentially reaching humans at the top of the food chain (128).

Majority of the global plastic is produced for use as packaging material in food, cosmetics, and pharmaceuticals (2, 129). Plastics are composed of numerous compounds including various chemicals. When manufacturing plastics for specific purposes, various chemical additives such as lubricants, plasticizers, antioxidants, heat stabilizers, and pigments are used during production and formulation (20, 130, 131). Plastics manufactured by incorporating numerous chemicals, when exposed to various environments, decompose into MP and cause biological hazards because of their ability to adsorb contaminants from the surrounding environment (93, 94, 110, 114, 122, 132).

DEHP, a commonly used plasticizer enhances the toxic effects on the male reproductive system when simultaneously exposed with plastics (35), causing histological damage microbial imbalance in the intestine (52, 64). Similarly, BPA, an endocrine-disrupting substance, has been used as an additive to render plastics transparent. Concurrent exposure to BPA and plastics increases metabolism-related hazards in human embryonic stem cell-derived liver organoids and can cause diseases (93). Simultaneous exposure to plastics and PBDE, which are used as flame retardants in plastics and fabrics, induces morphological developmental disorders, damages muscle and cartilage tissues, and exacerbates toxic effects on the thyroid (65). Additionally, BHA, an antioxidant widely used in plastics, food, and cosmetics, accumulates in plastics, disrupts thyroid function and metabolism, and worsens developmental toxicity (77).

Heavy metals such as Pb, Cd, Al, and ZnO are also used during plastic manufacturing and exist in a relatively stable form within plastics (133). However, studies have also demonstrated that MP/NP break down into small particles (134), and adsorb heavy metals present in the surrounding environment. These composite compounds have been shown to induce various side effects and diseases (76, 92,

108, 124). Co-exposure to Pb and plastics increases Pb accumulation in the ovaries of female mice, exacerbating ovarian toxicity (31). In aquatic organisms such as zebrafish (*Danio rerio*), they induced toxicity and immune recognition disorders in intestinal epithelial cells (32), and disrupted intestinal microbial homeostasis and reproductive development (87). Cd co-exposure with plastics causes damage to the gills, kidneys, liver, and muscles of aquatic organisms (62) and has negative effects on growth, survival, and heart rate (85). Moreover, when Al is co-exposed with plastics, they inhibit efflux pumps and induce oxidative stress in zebrafish embryos (76). When co-exposed with plastics, another heavy metal, ZnO, can cause DNA damage in zebrafish (72), leading to growth inhibition and cell death (92). In mice, the accumulation of nanomaterials in the brain because of co-exposure results in cognitive impairments (40). A variety of models, including aquatic organisms, higher terrestrial organisms, and human-derived cells, have been utilized in such research, and the experimental results varied depending on the size and type of plastics and additives (44, 52, 93, 118).

In this review, we searched PMC for papers related to MP over the past 10 years. Through this, we were able to visualize comprehensive information on the current status of MP research. According to our data, many publications over the past 10 years have confirmed the growing interest of researchers in MP/NP. MP/NP, which exist after plastic waste enters the environment and decomposes into fragments of various sizes, are already exposed to living organisms through oral ingestion, inhalation, or skin contact. Many studies have been conducted to date on the hazards caused by these various exposure routes. In addition, research has shown that decomposed plastic fragments can combine with various adsorbents, such as various surrounding chemicals or heavy metals, and that these composite compounds can cause more toxic reactions than the previously known harmful effects of MP/NP. However, research on the toxicity mechanisms of MP/NP is limited, and studies on the toxicity of composite compounds formed by various adsorbents are either biased towards specific sizes or types or lack sufficient evidence for established results.

Adsorbents and additives play a crucial role in shaping the fate and toxicity of MP and NP. This review critically assesses how different types of adsorbents and additives influence the bioavailability, persistence, and transport of plastics in various environments. Additionally, we explore the potential synergistic or antagonistic effects that may arise from the combination of plastics with different adsorbents and additives.

Building on the existing body of knowledge, this review proposes a new understanding that synthesizes the complex interactions between MP and NP, adsorbents, additives, and biological systems. By acknowledging the multifaceted nature of these interactions, we aim to move beyond a simplistic view of plastic pollution and biological hazards. This nuanced perspective allows for a more accurate assessment of risks and the formulation of targeted mitigation strategies. The added value of this review lies in its synthesis of disparate research findings, offering a comprehensive and up-to-date overview of the biological hazards associated with micro- and nano-plastics in the presence of adsorbents and additives.

By establishing a new position that considers the interplay of multiple factors, this review provides a roadmap for future research, guiding scientists, policymakers, and stakeholders toward more effective and sustainable solutions for mitigating the impacts of plastic pollution. This review contributes to the evolving discourse on the biological hazards of MP and NP by providing a nuanced understanding of the role of adsorbents and additives. By recognizing the complexities inherent in these interactions, we pave the way for targeted research efforts and informed decision-making to address the challenges posed by plastic pollution.

This review emphasized the need for further research to understand and establish the biological hazards of MP/NP and their interactions with plastic additives and different chemical substances in the environment. This review will provide researchers around the world with an understanding of the interactions of MP/NP with additives and suggests new research directions.

Conclusion

Accordingly, it is expected that this paper will contribute to active research on the toxicity mechanisms of MP/NP, or the toxic effects of composite compounds that have not been revealed to date.

Author contributions

ARH: Investigation, Visualization, Writing – original draft. JSK: Conceptualization, Supervision, Writing – review & editing.

Funding

The author(s) declare that financial support was received for the research, authorship, and/or publication of this article. This work was supported partly by Program Ministry of Science and ICT (Nos. NRF-2021M2E8A1039980, RS-2024-00353966, 50461-2024, 50462-2024), partly by Korea Environment Industry & Technology Institute (KEITI) through Measurement and Risk assessment Program for Management of Microplastics Program, funded by Korea Ministry of Environment (MOE) (RS-2022-KE002132).

Conflict of interest

The authors declare that the research was conducted in the absence of any commercial or financial relationships that could be construed as a potential conflict of interest.

Publisher's note

Supplementary material

The Supplementary material for this article can be found online at: https://www.frontiersin.org/articles/10.3389/fpubh.2024.1458727/full#supplementary-material

References

1. Liu M, Liu J, Xiong F, Xu K, Pu Y, Huang J, et al (2023). Research advances of microplastics and potential health risks of microplastics on terrestrial higher mammals: a bibliometric analysis and literature review. *Environ Geochem Health* 45:2803–38. doi: 10.1007/s10653-022-01458-8

2. Geyer R, Jambeck JR, Law KL (2017). Production, use, and fate of all plastics ever made. *Sci Adv* 3:e1700782. doi: 10.1126/sciadv.1700782

3. PlasticsEurope. Plastics–the facts 2019. An analysis of European plastics production, demand and waste data. Brussels, Belgium: Plastics Europe (2019).

4. Rangel-Buitrago N, Neal W, Williams A (2022). The Plasticene: time and rocks. *Mar Pollut Bull* 185:114358. doi: 10.1016/j.marpolbul.2022.114358

5. PlasticsEurope. Plastics–the facts 2022. Brussels, Belgium: PlasticsEurope (2022).

6. Petersen F, Hubbart JA (2021). The occurrence and transport of microplastics: the state of the science. *Sci Total Environ* 758:143936. doi: 10.1016/j.scitotenv.2020.143936

7. Zhang Y, Gao T, Kang S, Sillanpää M (2019). Importance of atmospheric transport for microplastics deposited in remote areas. *Environ Pollut* 254:112953. doi: 10.1016/j.envpol.2019.07.121

8. Dris R, Gasperi J, Rocher V, Saad M, Renault N, Tassin B (2015). Microplastic contamination in an urban area: a case study in greater Paris. *Environ Chem* 12:592–9. doi: 10.1071/EN14167

9. Zhu X, Huang W, Fang M, Liao Z, Wang Y, Xu L, et al (2021). Airborne microplastic concentrations in five megacities of northern and Southeast China. *Environ Sci Technol* 55:12871–81. doi: 10.1021/acs.est.1c03618

10. Gaston E, Woo M, Steele C, Sukumaran S, Anderson S (2020). Microplastics differ between indoor and outdoor air masses: insights from multiple microscopy methodologies. *Appl Spectrosc* 74:1079–98. doi: 10.1177/0003702820920652

11. Rede D, Delerue-Matos C, Fernandes VC (2023). The microplastics iceberg: filling gaps in our understanding. *Polymers* 15:3356. doi: 10.3390/polym15163356

12. Blasing M, Amelung W (2018). Plastics in soil: analytical methods and possible sources. *Sci Total Environ* 612:422–35. doi: 10.1016/j.scitotenv.2017.08.086

13. Banerjee A, Shelver WL (2021). Micro- and nanoplastic induced cellular toxicity in mammals: a review. *Sci Total Environ* 755:142518. doi: 10.1016/j.scitotenv.2020.142518

14. Dhaka V, Singh S, Anil AG, Sunil Kumar Naik TS, Garg S, Samuel J, et al (2022). Occurrence, toxicity and remediation of polyethylene terephthalate plastics. A review. *Environ Chem Lett* 20:1777–800. doi: 10.1007/s10311-021-01384-8

15. Zuri G, Karanasiou A, Lacorte S (2023). Human biomonitoring of microplastics and health implications: a review. *Environ Res* 237:116966. doi: 10.1016/j.envres.2023.116966

16. Zhou X, Luo Z, Wang H, Luo Y, Yu R, Zhou S, et al (2023). Machine learning application in forecasting tire wear particles emission in China under different potential socioeconomic and climate scenarios with tire microplastics context. *J Hazard Mater* 441:129878. doi: 10.1016/j.jhazmat.2022.129878

17. Obbard RW, Sadri S, Wong YQ, Khitun AA, Baker I, Thompson RC (2014). Global warming releases microplastic legacy frozen in Arctic Sea ice. *Earth's Future* 2:315–20. doi: 10.1002/2014EF000240

18. Woodall LC, Robinson LF, Rogers AD, Narayanaswamy BE, Paterson GLJ (2015). Deep-sea litter: a comparison of seamounts, banks and a ridge in the Atlantic and Indian Oceans reveals both environmental and anthropogenic factors impact accumulation and composition. *Front Mar Sci* 2:3. doi: 10.3389/fmars.2015.00003

19. Borrelle SB (2020). Predicted growth in plastic waste exceeds efforts to mitigate plastic pollution. *Science* 369:1515–8. doi: 10.1126/science.aba3656

20. Ullah S, Ahmad S, Guo X, Ullah S, Ullah S, Nabi G, et al (2023). A review of the endocrine disrupting effects of micro and nano plastic and their associated chemicals in mammals. *Front Endocrinol* 13:1084236. doi: 10.3389/fendo.2022.1084236

21. Sangkham S, Faikhaw O, Munkong N, Sakunkoo P, Arunlertaree C, Chavali M, et al (2022). A review on microplastics and nanoplastics in the environment: their occurrence, exposure routes, toxic studies, and potential effects on human health. *Mar Pollut Bull* 181:113832. doi: 10.1016/j.marpolbul.2022.113832

22. Barcelo D, Pico Y, Alfarhan AH (2023). Microplastics: detection in human samples, cell line studies, and health impacts. *Environ Toxicol Pharmacol* 101:104204. doi: 10.1016/j.etap.2023.104204

23. Thompson RC. Microplastics in the marine environment: sources, consequences and solutions In: Marine Anthropogenic Litter. Cham: Springer (2015). 185–200.

24. Sussarellu R, Suquet M, Thomas Y, Lambert C, Fabioux C, Pernet MEJ, et al (2016). Oyster reproduction is affected by exposure to polystyrene microplastics. *Proc Natl Acad Sci USA* 113:2430–5. doi: 10.1073/pnas.1519019113

25. Green DS, Colgan TJ, Thompson RC, Carolan JC (2019). Exposure to microplastics reduces attachment strength and alters the haemolymph proteome of blue mussels (*Mytilus edulis*). *Environ Pollut* 246:423–34. doi: 10.1016/j.envpol.2018.12.017

26. Berglund E, Fogelberg V, Nilsson PA, Hollander J (2019). Microplastics in a freshwater mussel (*Anodonta anatina*) in northern Europe. *Sci Total Environ* 697:134192. doi: 10.1016/j.scitotenv.2019.134192

27. Bessa F, Ratcliffe N, Otero V, Sobral P, Marques JC, Waluda CM, et al (2019). Microplastics in gentoo penguins from the Antarctic region. *Sci Rep* 9:14191. doi: 10.1038/s41598-019-50621-2

28. Parton KJ, Godley BJ, Santillo D, Tausif M, Omeyer LC, Galloway TS (2020). Investigating the presence of microplastics in demersal sharks of the North-East Atlantic. *Sci Rep* 10:12204. doi: 10.1038/s41598-020-68680-1

29. Issac MN, Kandasubramanian B (2021). Effect of microplastics in water and aquatic systems. *Environ Sci Pollut Res Int* 28:19544–62. doi: 10.1007/s11356-021-13184-2

30. Pashaei R, Dzingelevičienė R, Abbasi S, Szultka-Młyńska M, Buszewski B (2022). Determination of the pharmaceuticals-nano/microplastics in aquatic systems by analytical and instrumental methods. *Environ Monit Assess* 194:93. doi: 10.1007/s10661-022-09751-w

31. Feng Y, Yuan H, Wang W, Xu Y, Zhang J, Xu H, et al (2022). Co-exposure to polystyrene microplastics and lead aggravated ovarian toxicity in female mice via the PERK/eIF2alpha signaling pathway. *Ecotoxicol Environ Saf* 243:113966. doi: 10.1016/j.ecoenv.2022.113966

32. Yu J, Chen L, Gu W, Liu S, Wu B (2022). Heterogeneity effects of nanoplastics and lead on zebrafish intestinal cells identified by single-cell sequencing. *Chemosphere* 289:133133. doi: 10.1016/j.chemosphere.2021.133133

33. Wang Q, Bai J, Ning B, Fan L, Sun T, Fang Y, et al (2020). Effects of bisphenol A and nanoscale and microscale polystyrene plastic exposure on particle uptake and toxicity in human Caco-2 cells. *Chemosphere* 254:126788. doi: 10.1016/j.chemosphere.2020.126788

34. Wu Q, Li G, Huo T, Du X, Yang Q, Hung TC, et al (2021). Mechanisms of parental co-exposure to polystyrene nanoplastics and microcystin-LR aggravated hatching inhibition of zebrafish offspring. *Sci Total Environ* 774:145766. doi: 10.1016/j.scitotenv.2021.145766

35. Li D, Sun W, Jiang X, Yu Z, Xia Y, Cheng S, et al (2022). Polystyrene nanoparticles enhance the adverse effects of di-(2-ethylhexyl) phthalate on male reproductive system in mice. *Ecotoxicol Environ Saf* 245:114104. doi: 10.1016/j.ecoenv.2022.114104

36. He J, Yang X, Liu H (2021). Enhanced toxicity of triphenyl phosphate to zebrafish in the presence of micro- and nano-plastics. *Sci Total Environ* 756:143986. doi: 10.1016/j.scitotenv.2020.143986

37. Yu Z, Zhang L, Huang Q, Dong S, Wang X, Yan C (2022). Combined effects of micro-/nano-plastics and oxytetracycline on the intestinal histopathology and microbiome in zebrafish (*Danio rerio*). *Sci Total Environ* 843:156917. doi: 10.1016/j.scitotenv.2022.156917

38. Steckiewicz KP, Adamska A, Narajczyk M, Megiel E, Inkielewicz-Stepniak I (2022). Fluoride enhances polystyrene nanoparticles cytotoxicity in colonocytes *in vitro* model. *Chem Biol Interact* 367:110169. doi: 10.1016/j.cbi.2022.110169

39. Zha H, Xia J, Li S, Lv J, Zhuge A, Tang R, et al (2023). Airborne polystyrene microplastics and nanoplastics induce nasal and lung microbial dysbiosis in mice. *Chemosphere* 310:136764. doi: 10.1016/j.chemosphere.2022.136764

40. Estrela FN, Guimaraes ATB, Araujo A, Silva FG, Luz TMD, Silva AM, et al (2021). Toxicity of polystyrene nanoplastics and zinc oxide to mice. *Chemosphere* 271:129476. doi: 10.1016/j.chemosphere.2020.129476

41. Dawson AL, Kawaguchi S, King CK, Townsend KA, King R, Huston WM, et al (2018). Turning microplastics into nanoplastics through digestive fragmentation by Antarctic krill. *Nat Commun* 9:1001. doi: 10.1038/s41467-018-03465-9

42. Marsden P, Koelmans B, Bourdon-Lacombe J. Microplastics in drinking water. Geneva: World Health Organization (2019).

43. Moller P, Roursgaard M (2023). Exposure to nanoplastic particles and DNA damage in mammalian cells. *Mutat Res Rev Mutat Res* 792:108468. doi: 10.1016/j.mrrev.2023.108468

44. Hwang J, Choi D, Han S, Choi J, Hong J (2019). An assessment of the toxicity of polypropylene microplastics in human derived cells. *Sci Total Environ* 684:657–69. doi: 10.1016/j.scitotenv.2019.05.071

45. Hwang J, Choi D, Han S, Jung SY, Choi J, Hong J (2020). Potential toxicity of polystyrene microplastic particles. *Sci Rep* 10:7391. doi: 10.1038/s41598-020-64464-9

46. Choi D, Bang J, Kim T, Oh Y, Hwang Y, Hong J (2020). *In vitro* chemical and physical toxicities of polystyrene microfragments in human-derived cells. *J Hazard Mater* 400:123308. doi: 10.1016/j.jhazmat.2020.123308

47. Kim J, Maruthupandy M, An KS, Lee KH, Jeon S, Kim JS, et al (2021). Acute and subacute repeated oral toxicity study of fragmented microplastics in Sprague-Dawley rats. *Ecotoxicol Environ Saf* 228:112964. doi: 10.1016/j.ecoenv.2021.112964

48. Kantha P, Liu ST, Horng JL, Lin LY (2022). Acute exposure to polystyrene nanoplastics impairs skin cells and ion regulation in zebrafish embryos. *Aquat Toxicol* 248:106203. doi: 10.1016/j.aquatox.2022.106203

49. Yuan Y, Sepulveda MS, Bi B, Huang Y, Kong L, Yan H, et al (2023). Acute polyethylene microplastic (PE-MPs) exposure activates the intestinal mucosal immune network pathway in adult zebrafish (*Danio rerio*). *Chemosphere* 311:137048. doi: 10.1016/j.chemosphere.2022.137048

50. Xie S, Zhang R, Li Z, Liu C, Chen Y, Yu Q (2023). Microplastics perturb colonic epithelial homeostasis associated with intestinal overproliferation, exacerbating the severity of colitis. *Environ Res* 217:114861. doi: 10.1016/j.envres.2022.114861

51. Yin K, Wang D, Zhang Y, Lu H, Wang Y, Xing M (2022). Dose-effect of polystyrene microplastics on digestive toxicity in chickens (*Gallus gallus*): multi-omics reveals critical role of gut-liver axis. *J Adv Res* 52:3–18. doi: 10.1016/j.jare.2022.10.015

52. Deng Y, Yan Z, Shen R, Wang M, Huang Y, Ren H, et al (2020). Microplastics release phthalate esters and cause aggravated adverse effects in the mouse gut. *Environ Int* 143:105916. doi: 10.1016/j.envint.2020.105916

53. Zhang YX, Wang M, Yang L, Pan K, Miao AJ (2022). Bioaccumulation of differently-sized polystyrene nanoplastics by human lung and intestine cells. *J Hazard Mater* 439:129585. doi: 10.1016/j.jhazmat.2022.129585

54. Gautam R, Jo J, Acharya M, Maharjan A, Lee D, Pramod Bahadur KC, et al (2022). Evaluation of potential toxicity of polyethylene microplastics on human derived cell lines. *Sci Total Environ* 838:156089. doi: 10.1016/j.scitotenv.2022.156089

55. Zhang H, Zhang S, Duan Z, Wang L (2022). Pulmonary toxicology assessment of polyethylene terephthalate nanoplastic particles *in vitro*. *Environ Int* 162:107177. doi: 10.1016/j.envint.2022.107177

56. Li X, Zhang T, Lv W, Wang H, Chen H, Xu Q, et al (2022). Intratracheal administration of polystyrene microplastics induces pulmonary fibrosis by activating oxidative stress and Wnt/beta-catenin signaling pathway in mice. *Ecotoxicol Environ Saf* 232:113238. doi: 10.1016/j.ecoenv.2022.113238

57. Jeong S, Jang S, Kim SS, Bae MA, Shin J, Lee KB, et al (2022). Size-dependent seizurogenic effect of polystyrene microplastics in zebrafish embryos. *J Hazard Mater* 439:129616. doi: 10.1016/j.jhazmat.2022.129616

58. Felix L, Carreira P, Peixoto F (2023). Effects of chronic exposure of naturally weathered microplastics on oxidative stress level, behaviour, and mitochondrial function of adult zebrafish (*Danio rerio*). *Chemosphere* 310:136895. doi: 10.1016/j.chemosphere.2022.136895

59. Hamed M, Martyniuk CJ, Naguib M, Lee JS, Sayed AEH (2022). Neurotoxic effects of different sizes of plastics (nano, micro, and macro) on juvenile common carp (*Cyprinus carpio*). *Front Mol Neurosci* 15:1028364. doi: 10.3389/fnmol.2022.1028364

60. Jin H, Yang C, Jiang C, Li L, Pan M, Li D, et al (2022). Evaluation of neurotoxicity in BALB/c mice following chronic exposure to polystyrene microplastics. *Environ Health Perspect* 130:107002. doi: 10.1289/EHP10255

61. Yin K, Lu H, Zhang Y, Hou L, Meng X, Li J, et al (2022). Secondary brain injury after polystyrene microplastic-induced intracerebral hemorrhage is associated with inflammation and pyroptosis. *Chem Biol Interact* 367:110180. doi: 10.1016/j.cbi.2022.110180

62. Chen X, Wang J, Xie Y, Ma Y, Zhang J, Wei H, et al (2022). Physiological response and oxidative stress of grass carp (*Ctenopharyngodon idellus*) under single and combined toxicity of polystyrene microplastics and cadmium. *Ecotoxicol Environ Saf* 245:114080. doi: 10.1016/j.ecoenv.2022.114080

63. Estrela FN, Batista Guimaraes AT, Silva FG, Marinho da Luz T, Silva AM, Pereira PS, et al (2021). Effects of polystyrene nanoplastics on *Ctenopharyngodon idella* (grass carp) after individual and combined exposure with zinc oxide nanoparticles. *J Hazard Mater* 403:123879. doi: 10.1016/j.jhazmat.2020.123879

64. Liao H, Liu S, Junaid M, Gao D, Ai W, Chen G, et al (2022). Di-(2-ethylhexyl) phthalate exacerbated the toxicity of polystyrene nanoplastics through histological damage and intestinal microbiota dysbiosis in freshwater *Micropterus salmoides*. *Water Res* 219:118608. doi: 10.1016/j.watres.2022.118608

65. Wang Q, Li Y, Chen Y, Tian L, Gao D, Liao H, et al (2022). Toxic effects of polystyrene nanoplastics and polybrominated diphenyl ethers to zebrafish (*Danio rerio*). *Fish Shellfish Immunol* 126:21–33. doi: 10.1016/j.fsi.2022.05.025

66. Santos J, Barreto A, Sousa EML, Calisto V, Amorim MJB, Maria VL (2022). The role of nanoplastics on the toxicity of the herbicide phenmedipham, using *Danio rerio* embryos as model organisms. *Environ Pollut* 303:119166. doi: 10.1016/j.envpol.2022.119166

67. Martinez-Alvarez I, Le Menach K, Devier MH, Cajaraville MP, Budzinski H, Orbea A (2022). Screening of the toxicity of polystyrene nano- and microplastics alone and in combination with benzo(a)pyrene in brine shrimp larvae and zebrafish embryos. *Nanomaterials* 12:941. doi: 10.3390/nano12060941

68. Qin J, Xia PF, Yuan XZ, Wang SG (2022). Chlorine disinfection elevates the toxicity of polystyrene microplastics to human cells by inducing mitochondria-dependent apoptosis. *J Hazard Mater* 425:127842. doi: 10.1016/j.jhazmat.2021.127842

69. Liu Y, Wang Y, Li N, Jiang S (2022). Avobenzone and nanoplastics affect the development of zebrafish nervous system and retinal system and inhibit their locomotor behavior. *Sci Total Environ* 806:150681. doi: 10.1016/j.scitotenv.2021.150681

70. Liu Y, Wang Y, Ling X, Yan Z, Wu D, Liu J, et al (2021). Effects of nanoplastics and butyl methoxydibenzoylmethane on early zebrafish embryos identified by single-cell RNA sequencing. *Environ Sci Technol* 55:1885–96. doi: 10.1021/acs.est.0c06479

71. Zuo J, Huo T, Du X, Yang Q, Wu Q, Shen J, et al (2021). The joint effect of parental exposure to microcystin-LR and polystyrene nanoplastics on the growth of zebrafish offspring. *J Hazard Mater* 410:124677. doi: 10.1016/j.jhazmat.2020.124677

72. Singh N, Bhagat J, Tiwari E, Khandelwal N, Darbha GK, Shyama SK (2021). Metal oxide nanoparticles and polycyclic aromatic hydrocarbons alter nanoplastic's stability and toxicity to zebrafish. *J Hazard Mater* 407:124382. doi: 10.1016/j.jhazmat.2020.124382

73. Yan X, Zhang Y, Lu Y, He L, Qu J, Zhou C, et al (2020). The complex toxicity of tetracycline with polystyrene spheres on gastric cancer cells. *Int J Environ Res Public Health* 17:2808. doi: 10.3390/ijerph17082808

74. Zhang S, Ding J, Razanajatovo RM, Jiang H, Zou H, Zhu W (2019). Interactive effects of polystyrene microplastics and roxithromycin on bioaccumulation and biochemical status in the freshwater fish red tilapia (*Oreochromis niloticus*). *Sci Total Environ* 648:1431–9. doi: 10.1016/j.scitotenv.2018.08.266

75. Chen Q, Gundlach M, Yang S, Jiang J, Velki M, Yin D, et al (2017). Quantitative investigation of the mechanisms of microplastics and nanoplastics toward zebrafish larvae locomotor activity. *Sci Total Environ* 584-585:1022–31. doi: 10.1016/j.scitotenv.2017.01.156

76. Bhagat J, Zang L, Kaneco S, Nishimura N, Shimada Y (2022). Combined exposure to nanoplastics and metal oxide nanoparticles inhibits efflux pumps and causes oxidative stress in zebrafish embryos. *Sci Total Environ* 835:155436. doi: 10.1016/j.scitotenv.2022.155436

77. Zhao HJ, Xu JK, Yan ZH, Ren HQ, Zhang Y (2020). Microplastics enhance the developmental toxicity of synthetic phenolic antioxidants by disturbing the thyroid function and metabolism in developing zebrafish. *Environ Int* 140:105750. doi: 10.1016/j.envint.2020.105750

78. Alaraby M, Abass D, Villacorta A, Hernandez A, Marcos R (2022). Antagonistic *in vivo* interaction of polystyrene nanoplastics and silver compounds. A study using *Drosophila*. *Sci Total Environ* 842:156923. doi: 10.1016/j.scitotenv.2022.156923

79. Ilić K, Kalcec N, Krce L, Aviani I, Turcic P, Pavicic I, et al (2022). Toxicity of nanomixtures to human macrophages: joint action of silver and polystyrene nanoparticles. *Chem Biol Interact* 368:110225. doi: 10.1016/j.cbi.2022.110225

80. Guo X, Lv M, Li J, Ding J, Wang Y, Fu L, et al (2022). The distinct toxicity effects between commercial and realistic polystyrene microplastics on microbiome and histopathology of gut in zebrafish. *J Hazard Mater* 434:128874. doi: 10.1016/j.jhazmat.2022.128874

81. Brandts I, Balasch JC, Goncalves AP, Martins MA, Pereira ML, Tvarijonaviciute A, et al (2021). Immuno-modulatory effects of nanoplastics and humic acids in the European seabass (*Dicentrarchus labrax*). *J Hazard Mater* 414:125562. doi: 10.1016/j.jhazmat.2021.125562

82. Shi Q, Tang J, Wang L, Liu R, Giesy JP (2021). Combined cytotoxicity of polystyrene nanoplastics and phthalate esters on human lung epithelial A549 cells and its mechanism. *Ecotoxicol Environ Saf* 213:112041. doi: 10.1016/j.ecoenv.2021.112041

83. Hou Z, Meng R, Chen G, Lai T, Qing R, Hao S, et al (2022). Distinct accumulation of nanoplastics in human intestinal organoids. *Sci Total Environ* 838:155811. doi: 10.1016/j.scitotenv.2022.155811

84. Wang L, Xu M, Chen J, Zhang X, Wang Q, Wang Y, et al (2022). Distinct adverse outcomes and lipid profiles of erythrocytes upon single and combined exposure to cadmium and microplastics. *Chemosphere* 307:135942. doi: 10.1016/j.chemosphere.2022.135942

85. Chen X, Peng LB, Wang D, Zhu QL, Zheng JL (2022). Combined effects of polystyrene microplastics and cadmium on oxidative stress, apoptosis, and GH/IGF axis in zebrafish early life stages. *Sci Total Environ* 813:152514. doi: 10.1016/j.scitotenv.2021.152514

86. Zhang R, Wang M, Chen X, Yang C, Wu L (2020). Combined toxicity of microplastics and cadmium on the zebrafish embryos (*Danio rerio*). *Sci Total Environ* 743:140638. doi: 10.1016/j.scitotenv.2020.140638

87. Yan W, Hamid N, Deng S, Jia PP, Pei DS (2020). Individual and combined toxicogenetic effects of microplastics and heavy metals (Cd, Pb, and Zn) perturb gut microbiota homeostasis and gonadal development in marine medaka (*Oryzias melastigma*). *J Hazard Mater* 397:122795. doi: 10.1016/j.jhazmat.2020.122795

88. Lu K, Qiao R, An H, Zhang Y (2018). Influence of microplastics on the accumulation and chronic toxic effects of cadmium in zebrafish (*Danio rerio*). *Chemosphere* 202:514–20. doi: 10.1016/j.chemosphere.2018.03.145

89. Zuo Z, Wang Q, Zhang C, Zou J (2022). Single and combined effects of microplastics and cadmium on juvenile grass carp (*Ctenopharyngodon idellus*). *Comp Biochem Physiol C* 261:109424. doi: 10.1016/j.cbpc.2022.109424

90. Yang H, Zhu Z, Xie Y, Zheng C, Zhou Z, Zhu T, et al (2022). Comparison of the combined toxicity of polystyrene microplastics and different concentrations of cadmium in zebrafish. *Aquat Toxicol* 250:106259. doi: 10.1016/j.aquatox.2022.106259

91. Zhang C, Ye L, Wang C, Xiong X, Li Y, Li P, et al (2022). Toxic effect of combined exposure of microplastics and copper on goldfish (*Carassius auratus*): insight from oxidative stress, inflammation, apoptosis and autophagy in hepatopancreas and intestine. *Bull Environ Contam Toxicol* 109:1029–36. doi: 10.1007/s00128-022-03585-5

92. Zheng JL, Chen X, Peng LB, Wang D, Zhu QL, Li J, et al (2022). Particles rather than released Zn^{2+} from ZnO nanoparticles aggravate microplastics toxicity in early stages of exposed zebrafish and their unexposed offspring. *J Hazard Mater* 424:127589. doi: 10.1016/j.jhazmat.2021.127589

93. Cheng W, Zhou Y, Xie Y, Li Y, Zhou R, Wang H, et al (2022). Combined effect of polystyrene microplastics and bisphenol A on the human embryonic stem cells-derived liver organoids: the hepatotoxicity and lipid accumulation. *Sci Total Environ* 854:158585. doi: 10.1016/j.scitotenv.2022.158585

94. Sun W, Yan S, Meng Z, Tian S, Jia M, Huang S, et al (2022). Combined ingestion of polystyrene microplastics and epoxiconazole increases health risk to mice: based on

their synergistic bioaccumulation *in vivo*. *Environ Int* 166:107391. doi: 10.1016/j.envint.2022.107391

95. Lu J, Wu J, Gong L, Cheng Y, Yuan Q, He Y (2022). Combined toxicity of polystyrene microplastics and sulfamethoxazole on zebrafish embryos. *Environ Sci Pollut Res* 29:19273–82. doi: 10.1007/s11356-021-17198-8

96. Jiang P, Yuan GH, Jiang BR, Zhang JY, Wang YQ, Lv HJ, et al (2021). Effects of microplastics (MPs) and tributyltin (TBT) alone and in combination on bile acids and gut microbiota crosstalk in mice. *Ecotoxicol Environ Saf* 220:112345. doi: 10.1016/j.ecoenv.2021.112345

97. Domenech J, Cortés C (2021). Polystyrene nanoplastics as carriers of metals. interactions of polystyrene nanoparticles with silver nanoparticles and silver nitrate, and their effects on human intestinal Caco-2 cells. *Biomol Ther* 11:859. doi: 10.3390/biom11060859

98. Xu K, Zhang Y, Huang Y, Wang J (2021). Toxicological effects of microplastics and phenanthrene to zebrafish (*Danio rerio*). *Sci Total Environ* 757:143730. doi: 10.1016/j.scitotenv.2020.143730

99. Li S, Shi M, Wang Y, Xiao Y, Cai D, Xiao F (2021). Keap1-Nrf2 pathway up-regulation via hydrogen sulfide mitigates polystyrene microplastics induced-hepatotoxic effects. *J Hazard Mater* 402:123933. doi: 10.1016/j.jhazmat.2020.123933

100. Yang H, Lai H, Huang J, Sun L, Mennigen JA, Wang Q, et al (2020). Polystyrene microplastics decrease F-53B bioaccumulation but induce inflammatory stress in larval zebrafish. *Chemosphere* 255:127040. doi: 10.1016/j.chemosphere.2020.127040

101. Wang Y, Zhang Y, Sun X, Shi X, Xu S (2022). Microplastics and di (2-ethylhexyl) phthalate synergistically induce apoptosis in mouse pancreas through the GRP78/CHOP/Bcl-2 pathway activated by oxidative stress. *Food Chem Toxicol* 167:113315. doi: 10.1016/j.fct.2022.113315

102. Hanslik L, Seiwert B, Huppertsberg S, Knepper TP, Reemtsma T, Braunbeck T (2022). Biomarker responses in zebrafish (*Danio rerio*) following long-term exposure to microplastic-associated chlorpyrifos and benzo(k)fluoranthene. *Aquat Toxicol* 245:106120. doi: 10.1016/j.aquatox.2022.106120

103. Luo T, Weng Y, Huang Z, Zhao Y, Jin Y (2021). Combined hepatotoxicity of imidacloprid and microplastics in adult zebrafish: endpoints at gene transcription. *Comp Biochem Physiol C* 246:109043. doi: 10.1016/j.cbpc.2021.109043

104. Qiao R, Lu K, Deng Y, Ren H, Zhang Y (2019). Combined effects of polystyrene microplastics and natural organic matter on the accumulation and toxicity of copper in zebrafish. *Sci Total Environ* 682:128–37. doi: 10.1016/j.scitotenv.2019.05.163

105. Deng Y, Zhang Y, Qiao R, Bonilla MM, Yang X, Ren H, et al (2018). Evidence that microplastics aggravate the toxicity of organophosphorus flame retardants in mice (*Mus musculus*). *J Hazard Mater* 357:348–54. doi: 10.1016/j.jhazmat.2018.06.017

106. Tarasco M, Gavaia PJ, Bensimon-Brito A, Cordelieres FP, Santos T, Martins G, et al (2022). Effects of pristine or contaminated polyethylene microplastics on zebrafish development. *Chemosphere* 303:135198. doi: 10.1016/j.chemosphere.2022.135198

107. Banaee M, Soltanian S, Sureda A, Gholamhosseini A, Haghi BN, Akhlaghi M, et al (2019). Evaluation of single and combined effects of cadmium and micro-plastic particles on biochemical and immunological parameters of common carp (*Cyprinus carpio*). *Chemosphere* 236:124335. doi: 10.1016/j.chemosphere.2019.07.066

108. Miranda T, Vieira LR, Guilhermino L (2019). Neurotoxicity, behavior, and lethal effects of cadmium, microplastics, and their mixtures on *Pomatoschistus microps* juveniles from two wild populations exposed under laboratory conditions-implications to environmental and human risk assessment. *Int J Environ Res Public Health* 16:2857. doi: 10.3390/ijerph16162857

109. Luís LG, Ferreira P, Fonte E, Oliveira M, Guilhermino L (2015). Does the presence of microplastics influence the acute toxicity of chromium(VI) to early juveniles of the common goby (*Pomatoschistus microps*)? A study with juveniles from two wild estuarine populations. *Aquat Toxicol* 164:163–74. doi: 10.1016/j.aquatox.2015.04.018

110. Menendez-Pedriza A, Jaumot J, Bedia C (2022). Lipidomic analysis of single and combined effects of polyethylene microplastics and polychlorinated biphenyls on human hepatoma cells. *J Hazard Mater* 421:126777. doi: 10.1016/j.jhazmat.2021.126777

111. Huang W, Yin H, Yang Y, Jin L, Lu G, Dang Z (2021). Influence of the co-exposure of microplastics and tetrabromobisphenol A on human gut: simulation *in vitro* with human cell Caco-2 and gut microbiota. *Sci Total Environ* 778:146264. doi: 10.1016/j.scitotenv.2021.146264

112. Yu Y, Ma R, Qu H, Zuo Y, Yu Z, Hu G, et al (2020). Enhanced adsorption of tetrabromobisphenol A (TBBPA) on cosmetic-derived plastic microbeads and combined effects on zebrafish. *Chemosphere* 248:126067. doi: 10.1016/j.chemosphere.2020.126067

113. Zhang J, Meng H, Kong X, Cheng X, Ma T, He H, et al (2021). Combined effects of polyethylene and organic contaminant on zebrafish (*Danio rerio*): accumulation of 9-nitroanthracene, biomarkers and intestinal microbiota. *Environ Pollut* 277:116767. doi: 10.1016/j.envpol.2021.116767

114. Deng Y, Yan Z, Shen R, Huang Y, Ren H, Zhang Y (2021). Enhanced reproductive toxicities induced by phthalates contaminated microplastics in male mice (*Mus musculus*). *J Hazard Mater* 406:124644. doi: 10.1016/j.jhazmat.2020.124644

115. Sheng C, Zhang S, Zhang Y (2021). The influence of different polymer types of microplastics on adsorption, accumulation, and toxicity of triclosan in zebrafish. *J Hazard Mater* 402:123733. doi: 10.1016/j.jhazmat.2020.123733

116. Tong X, Li B, Li J, Li L, Zhang R, Du Y, et al (2022). Polyethylene microplastics cooperate with *Helicobacter pylori* to promote gastric injury and inflammation in mice. *Chemosphere* 288:132579. doi: 10.1016/j.chemosphere.2021.132579

117. Khan FR, Syberg K, Shashoua Y, Bury NR (2015). Influence of polyethylene microplastic beads on the uptake and localization of silver in zebrafish (*Danio rerio*). *Environ Pollut* 206:73–9. doi: 10.1016/j.envpol.2015.06.009

118. Boyle D, Catarino AI, Clark NJ, Henry TB (2020). Polyvinyl chloride (PVC) plastic fragments release Pb additives that are bioavailable in zebrafish. *Environ Pollut* 263:114422. doi: 10.1016/j.envpol.2020.114422

119. Schirinzi GF, Perez-Pomeda I, Sanchis J, Rossini C, Farre M, Barcelo D (2017). Cytotoxic effects of commonly used nanomaterials and microplastics on cerebral and epithelial human cells. *Environ Res* 159:579–87. doi: 10.1016/j.envres.2017.08.043

120. Batel A, Linti F, Scherer M, Erdinger L, Braunbeck T (2016). Transfer of benzo[a]pyrene from microplastics to *Artemia nauplii* and further to zebrafish via a trophic food web experiment: CYP1A induction and visual tracking of persistent organic pollutants. *Environ Toxicol Chem* 35:1656–66. doi: 10.1002/etc.3361

121. Araújo APDC, Luz TMD, Rocha TL, Ahmed MAI, Silva DME, Rahman MM, et al (2022). Toxicity evaluation of the combination of emerging pollutants with polyethylene microplastics in zebrafish: perspective study of genotoxicity, mutagenicity, and redox unbalance. *J Hazard Mater* 432:128691. doi: 10.1016/j.jhazmat.2022.128691

122. Batel A, Baumann L, Carteny CC, Cormier B, Keiter SH, Braunbeck T (2020). Histological, enzymatic and chemical analyses of the potential effects of differently sized microplastic particles upon long-term ingestion in zebrafish (*Danio rerio*). *Mar Pollut Bull* 153:111022. doi: 10.1016/j.marpolbul.2020.111022

123. Chen XJ, Ma JJ, Yu RL, Hu GR, Yan Y (2022). Bioaccessibility of microplastic-associated heavy metals using an *in vitro* digestion model and its implications for human health risk assessment. *Environ Sci Pollut Res Int* 29:76983–91. doi: 10.1007/s11356-022-20983-8

124. Hoseini SM, Khosraviani K, Hosseinpour Delavar F, Arghideh M, Zavvar F, Hoseinifar SH, et al (2022). Hepatic transcriptomic and histopathological responses of common carp, *Cyprinus carpio*, to copper and microplastic exposure. *Mar Pollut Bull* 175:113401. doi: 10.1016/j.marpolbul.2022.113401

125. Wang H, Wang Y, Wang Q, Lv M, Zhao X, Ji Y, et al (2022). The combined toxic effects of polyvinyl chloride microplastics and di(2-ethylhexyl) phthalate on the juvenile zebrafish (*Danio rerio*). *J Hazard Mater* 440:129711. doi: 10.1016/j.jhazmat.2022.129711

126. Liu J, Lv M, Sun A, Ding J, Wang Y, Chang X, et al (2022). Exposure to microplastics reduces the bioaccumulation of sulfamethoxazole but enhances its effects on gut microbiota and the antibiotic resistome of mice. *Chemosphere* 294:133810. doi: 10.1016/j.chemosphere.2022.133810

127. Cheng H, Feng Y, Duan Z, Duan X, Zhao S, Wang Y, et al (2021). Toxicities of microplastic fibers and granules on the development of zebrafish embryos and their combined effects with cadmium. *Chemosphere* 269:128677. doi: 10.1016/j.chemosphere.2020.128677

128. Jeong J, Choi J (2019). Adverse outcome pathways potentially related to hazard identification of microplastics based on toxicity mechanisms. *Chemosphere* 231:249–55. doi: 10.1016/j.chemosphere.2019.05.003

129. Groh KJ, Backhaus T, Carney-Almroth B, Geueke B, Inostroza PA, Lennquist A, et al (2019). Overview of known plastic packaging-associated chemicals and their hazards. *Sci Total Environ* 651:3253–68. doi: 10.1016/j.scitotenv.2018.10.015

130. Zimmermann L, Bartosova Z, Braun K, Oehlmann J, Volker C, Wagner M (2021). Plastic products leach chemicals that induce *in vitro* toxicity under realistic use conditions. *Environ Sci Technol* 55:11814–23. doi: 10.1021/acs.est.1c01103

131. Cai Z, Li M, Zhu Z, Wang X, Huang Y, Li T, et al (2023). Biological degradation of plastics and microplastics: a recent perspective on associated mechanisms and influencing factors. *Microorganisms* 11:1661. doi: 10.3390/microorganisms11071661

132. Kannan K, Vimalkumar K (2021). A review of human exposure to microplastics and insights into microplastics as obesogens. *Front Endocrinol* 12:724989. doi: 10.3389/fendo.2021.724989

133. Cao Y, Zhao M, Ma X, Song Y, Zuo S, Li H, et al (2021). A critical review on the interactions of microplastics with heavy metals: mechanism and their combined effect on organisms and humans. *Sci Total Environ* 788:147620. doi: 10.1016/j.scitotenv.2021.147620

134. Hurley R, Woodward J, Rothwell J (2018). Microplastic contamination of river beds significantly reduced by catchment-wide flooding. *Nat Geosci* 11:251–7. doi: 10.1038/s41561-018-0080-1

frontiers | Frontiers in Public Health

TYPE Original Research
PUBLISHED 17 January 2025
DOI 10.3389/fpubh.2024.1437519

OPEN ACCESS

EDITED BY
Pu Xia,
University of Birmingham, United Kingdom

REVIEWED BY
Giovanni Tarantino,
University of Naples Federico II, Italy
Brigitte Le Magueresse-Battistoni,
INSERM U1060 Laboratoire de Recherche en Cardiovasculaire, Métabolisme, diabétologie et Nutrition, France

*CORRESPONDENCE
Chengyu Liu
✉ chengyu@seu.edu.cn
Anhua Huang
✉ iamseric@163.com

†These authors have contributed equally to this work and share first authorship

RECEIVED 23 May 2024
ACCEPTED 27 December 2024
PUBLISHED 17 January 2025

CITATION
Shao W, Gong P, Wang Q, Ding F, Shen W, Zhang H, Huang A and Liu C (2025) Association of exposure to multiple volatile organic compounds with ultrasound-defined hepatic steatosis and fibrosis in the adult US population: NHANES 2017–2020. *Front. Public Health* 12:1437519. doi: 10.3389/fpubh.2024.1437519

Association of exposure to multiple volatile organic compounds with ultrasound-defined hepatic steatosis and fibrosis in the adult US population: NHANES 2017–2020

Wentao Shao[1,2†], Pan Gong[3†], Qihan Wang[2†], Fan Ding[2], Weiyi Shen[2], Hongchao Zhang[2], Anhua Huang[2*] and Chengyu Liu[1*]

[1]School of Instrument Science and Engineering, Southeast University, Nanjing, China, [2]Center of Gallstone Disease, Shanghai East Hospital, Tongji University School of Medicine, Shanghai, China, [3]Hongkou District Center for Disease Control and Prevention (Hongkou District Institute of Health Supervision), Shanghai, China

Objective: Volatile organic compounds (VOCs) are pervasive environmental pollutants known to impact human health, but their role in liver steatosis or fibrosis is not fully understood. This study investigates the association of urinary VOC mixtures with the risk of liver steatosis and fibrosis in U.S. adult population.

Methods: Data of 1854 adults from the National Health and Nutrition Examination Survey (NHANES) from 2017.01 to 2020.03 were collected. Vibration Controlled Transient Elastography (VCTE) assessed hepatic steatosis and liver fibrosis via the controlled attenuation parameter (CAP) and liver stiffness measurement (LSM), respectively. The study examined the relationship between urinary exposure biomarkers for 20 VOCs and liver health outcomes using multivariate logistic regression and Bayesian Kernel Machine Regression (BKMR) to evaluate the effects of both individual and mixed VOC exposures.

Results: Multivariate logistic regression analysis revealed that exposure biomarkers for acrolein and crotonaldehyde were positively associated with hepatic steatosis. Conversely, biomarkers for styrene, ethylbenzene, and propylene oxide were negatively associated with hepatic steatosis. Furthermore, biomarkers for 1,3-butadiene and xylene were positively associated with liver fibrosis, while ethylbenzene was negatively associated with this condition. BKMR analysis identified a significant positive joint effect of VOC biomarkers on CAP. Notably, when other VOC-EBs were held at median levels, biomarkers for acrolein and 1,3-butadiene exhibited linear correlations with Ln CAP and hepatic Ln LSM, respectively.

Conclusion: The study highlights the potential hepatotoxic effects of VOC mixtures, particularly noting the roles of acrolein and 1,3-butadiene in exacerbating liver steatosis and fibrosis. These findings advocate for further research to explore the mechanistic pathways and conduct longitudinal studies to establish causality and enhance understanding of VOCs' impact on liver health.

KEYWORDS

volatile organic compound, urinary metabolites, hepatic steatosis, liver fibrosis, NHANES

1 Introduction

Non-alcoholic fatty liver disease (NAFLD) affects approximately 25% of the adult population and has become the most prevalent chronic liver disorder (1). By 2030, it is projected that NAFLD will affect 33.5% of the adult population (2). NAFLD encompasses a disease continuum related to metabolic dysfunction, ranging from steatosis to steatohepatitis, fibrosis, cirrhosis, and eventually hepatocellular carcinoma (1, 3). Although the specific pathogenic factors have not been fully elucidated, it is clear that genetic, epigenetic, and environmental factors influence liver steatosis and fibrosis progression (4). Recent evidence suggests that persistent exposure to certain environmental contaminants can initiate and promote the pathogenesis of NAFLD (5). Elucidating how these environmental contaminants, particularly volatile organic compounds (VOCs), either independently or in combination, affect hepatic steatosis and fibrosis is critical for disease prevention.

VOCs are among the most common environmental pollutants, originating from a variety of anthropogenic and natural sources, including cigarette smoke (6), vehicular exhaust (7), biomass burning, and industrial emissions (8). The United States Environmental Protection Agency (US EPA) has classified VOCs such as toluene, xylene, styrene, propylene oxide, 1,3-butadiene, vinyl chloride, trichloroethylene, tetrachloroethylene, acrylamide, acrylonitrile, acrolein, and carbon disulfide as hazardous air pollutants (9). Human exposure to VOCs through inhalation (the main exposure route), ingestion, and dermal contact is ubiquitous in daily life (10). Exposure to VOCs is associated with increased risks of leukemia, cancer, respiratory illnesses, birth defects, and neurocognitive impairment in humans (8). Tobacco smoking, a major source of VOC exposure, has been linked to sarcopenia, a condition characterized by reduced skeletal muscle mass and strength. Recent studies have demonstrated the association between smoking and muscle health, including reduced handgrip strength (11) and impaired respiratory muscle function (12). Sarcopenia, which is prevalent in advanced liver disease, has also been identified as a significant comorbidity in aging populations, with smoking serving as a key contributing factor (13). Additionally, sarcopenia is emerging as a therapeutic target, given its shared pathophysiology across multiple chronic diseases (14). These findings underscore the importance of considering smoking and VOC exposure as contributors to both sarcopenia and liver-related outcomes.

As the central hub of xenobiotic metabolism, including VOCs, the liver is a general target for the toxicity of environmental chemicals (15, 16). After exposure, VOCs quickly reach the liver via systemic circulation and are metabolized by hepatic cytochrome P450 (CYP450) enzymes (17, 18). In the liver, VOCs are transformed into water-soluble metabolites that are subsequently excreted in urine. Due to their specificity and longer half-lives in the human body compared to their parent compounds, urinary VOC metabolites may serve as reliable biomarkers of exposure (VOC-EBs) (19). Previous studies have demonstrated that workers occupationally exposed to VOCs can develop liver injury (20, 21). The scientific plausibility of VOCs influencing liver health and function is also supported by animal studies (22). However, most studies have primarily consisted of vulnerable or occupational populations and were usually based on recognized hazardous materials. Recent epidemiological studies conducted among 663 United States adults reported that metabolites of residential VOCs were positively associated with alkaline phosphatase (ALP), a biomarker for cholestatic injury (23). Another study involving 3,950 Canadian adults found that certain compounds in the benzene series were associated with poor liver function parameters (24).

Moreover, the association between VOCs and both NAFLD and liver fibrosis in humans remains unclear. A recent epidemiological study illustrated the relationship between VOC exposure and NAFLD, where NAFLD was defined using the US fatty liver index (USFLI) and the hepatic steatosis index (HSI), based on 12 serum markers (25). However, serum scores (HSI and FLI) performed poorly in detecting NAFLD and grading steatosis (26). These serum biomarkers can appear normal in patients with NAFLD and are influenced by comorbid conditions, potentially lacking sensitivity in defining NAFLD (26, 27). Liver vibration-controlled transient elastography (VCTE) using FibroScan, known for its high sensitivity and specificity, can directly assess hepatic steatosis and liver fibrosis via the controlled attenuation parameter (CAP) and liver stiffness measurement (LSM), respectively (1, 26–28). In the 2017–2018 survey cycle, for the first time, NHANES employed VCTE to measure CAP, indicating liver steatosis, and LSM, indicating liver fibrosis.

Thus, this study aims to examine the cross-sectional association between urinary VOC-EB levels and the prevalence of liver steatosis (measured by median CAP) and liver fibrosis (quantified as liver stiffness) detected by VCTE in NHANES participants from 2017 to 2020.

2 Materials and methods

2.1 Data source and study population

The NHANES is a national, multi-year, population-based, cross-sectional study conducted by the US National Center for Health Statistics (Centers for Disease Control and Prevention, Atlanta, GA, United States). Approval for the NHANES was granted by the National Center for Health Statistics Research Ethics Review Board, ensuring a representative sample of the non-institutionalized civilian US population. Liver steatosis and hepatic fibrosis were assessed using VCTE exclusively during the 2017.01–2020.03 cycle of NHANES; thus, this study is based on the dataset from this specific cycle.

A total of 15,560 eligible participants aged 6 years and older were included. Initially, participants with unavailable or incomplete VCTE exams were excluded ($n = 6,537$). Subsequently, we excluded participants younger than 20 years ($n = 1,627$); those with positive HBV surface antigens ($n = 40$), confirmed HCV antibodies ($n = 165$), or incomplete body indices and questionnaire data ($n = 1,333$). Further exclusions were made for participants lacking data on urine

VOC metabolites (n = 4,004). Ultimately, 1,854 participants with complete data were enrolled (Figure 1).

2.2 Quantification of urine VOCs metabolites

Urine specimens were processed, stored, and shipped to the Division of Laboratory Sciences at the National Center for Environmental Health, Centers for Disease Control and Prevention, for analysis. Measurement of VOC metabolites was performed using ultra-performance liquid chromatography coupled with electrospray tandem mass spectrometry (UPLC-ESI/MSMS), as previously described (19). Twenty-one VOC metabolites were quantified in urine, including N-ace-S-(3,4-dihidxybutl)-L-cys (DHBMA), N-A-S-(4-hydrxy-2-butenyl)-L-cys (MHBMA3), 2-methylhippuric acid (2MHA), 3-methipurc acd + 4-methipurc acd (3MHA +4MHA), N-ace-S-(2-carbxyethyl)-L-cys (CEMA), N-ace-S-(3-hydroxypropyl)-L-cys (3HPMA), N-ace-S-(2-carbamoylethyl)-L-cys (AAMA), N-ac-S-(2-carbmo-2-hydxel)-L-cys (GAMA), mandelic acid (MA), phenylglyoxylic acid (PGA), N-ace-S-(1-cyano-2-hydroxyethyl)-L-cys (CHEMA), N-ace-S-(2-cyanoethyl)-L-cys (CEMA), N-ace-S-(2-hydroxyethyl)-L-cys (2HEMA), N-ace-S-(4-hydroxy-2-methyl-2-buten-1-yl)-L-cys (IPMA3), N-ace-S-(N-methlcarbamoyl)-L-cys (AMCC), 2-aminothiazoline-4-carboxylic acid (ATCA), N-ace-S-(benzyl)-L-cys (BMA), N-ace-S-(n-propyl)-L-cys (BPMA), N-ace-S-(2-hydroxypropyl)-L-cys (2HPMA), N-ace-S-(3-hydrxprpl-1-metl)-L-cys (HPMMA), and 2-Thioxothiazolidine-4-carboxylic acid (TTCA). As indicated by previous studies (17, 23, 25), when VOCs possess two or more metabolites, the levels of these metabolites are summed to represent the total exposure to the parent VOCs in this study, including ΣUBUM for 1,3-butadiene (DHBMA+MHBMA3), ΣUXM for xylene (2MHA + 3MHA + 4MHA), ΣUACLM for acrolein (CEMA+3HPMA), ΣUAAM for acrylamide (AAMA+ GAMA), ΣUSEBM for styrene and ethylbenzene (MA+PGA), and ΣUACLNM for acrylonitrile (CHEMA+ CEMA+2HEMA). TTCA was excluded from this study to maintain adequate statistical power, as it is the only metabolite of carbon disulfide with a detectable rate below 60%. Values below the lower limit of detection (LOD) for each metabolite were replaced by LOD/$\sqrt{2}$ (19). Finally, 13 urinary VOC-EBs were included in this analysis. Supplementary Table S1 lists 20 VOC metabolites, their parent compounds, and detectable rates.

2.3 Assessment of liver steatosis and fibrosis outcomes

CAP and LSM, indicators of liver steatosis and fibrosis respectively, were measured using VCTE. Trained technicians conducted VCTE assessments using a FibroScan model 502 V2 Touch (Echosens, Paris,

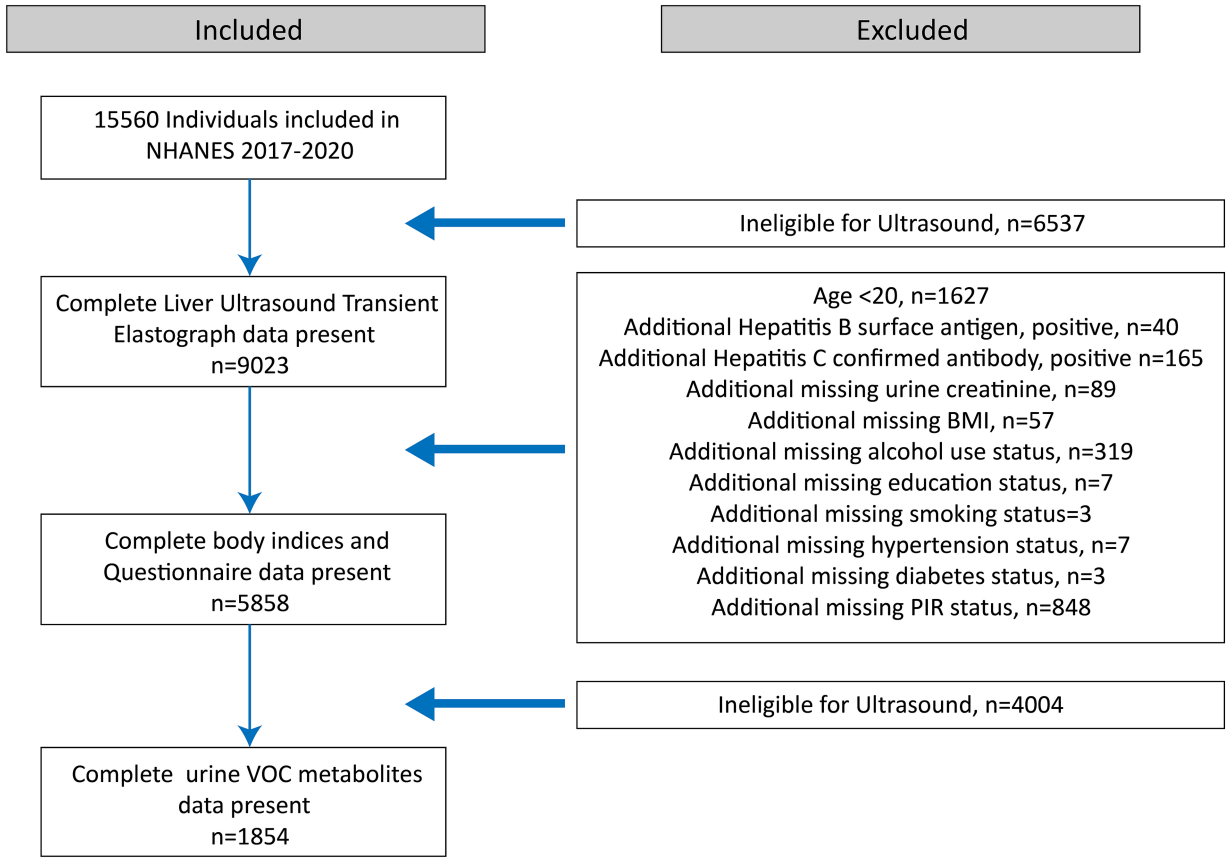

FIGURE 1
Flowchart illustrating the selection of the study population (N = 1854) for the final analysis, after applying exclusion criteria. Data were derived from the National Health and Nutrition Examination Survey (NHANES) conducted in the United States from 2017 to 2020.

France) equipped with either a medium (M) or extra-large (XL) probe. The medium probe was initially used. An XL probe was utilized if recommended by the manufacturer's instructions. Examinations were deemed reliable if participants had fasted for at least 3 h before the exam, at least 10 complete stiffness measures were obtained, and the liver stiffness interquartile range to median LSM ratio was less than 30%. Detailed procedures are available in the Liver Ultrasound Transient Elastography Procedures Manual. Liver steatosis was defined as a CAP of ≥274 dB/m, a threshold demonstrating 90% sensitivity in identifying NAFLD (29). A threshold of LSM ≥8 kPa was established for liver fibrosis.

2.4 Assessment of covariates

Potential confounders associated with levels of VOC-EBs and liver steatosis/fibrosis, derived from NHANES questionnaires, examinations, and laboratory data, included gender, age, race-ethnicity, education level, smoking status, alcohol use, diabetes, hypertension, physical activity, and PIR (poverty income ratio). Given that the liver regulates energy homeostasis in a sex-dependent manner, we have included sex as one of the covariates. Covariate categories included: gender (male or female), race-ethnicity (Mexican American, Hispanic, non-Hispanic white, non-Hispanic black, or other), education level (high school or less, college, graduate or higher), smoking status (never: <100 cigarettes in lifetime; former: >100 cigarettes in lifetime and currently not smoking; current: >100 cigarettes in lifetime and smokes every day or occasionally), alcohol use (30) (never drinkers; low-moderate drinkers: ≤2 drinks per day on average for men and ≤1 drink per day on average for women, on days alcohol was consumed during the past year; heavy drinkers: >2 drinks per day on average for men and >1 drink per day on average for women, on days alcohol was consumed during the past year), diabetes (defined by an FPG level ≥ 7.0 mmol/L, an HbA1c ≥ 6.5%, or a self-reported history of diagnosis by a physician), overweight/obesity (BMI ≥ 25 kg/m^2), hypertension (defined as systolic blood pressure ≥ 140 mmHg, diastolic blood pressure ≥ 90 mmHg, or a self-reported history of hypertension diagnosed by a physician), and physical activity (identified as having regular physical activity if they engaged in vigorous or moderate recreational activities). Additionally, to control for the urinary dilution effect of spot urine samples, urinary creatinine levels were adjusted for in all models as a covariate.

2.5 Statistical analysis

Descriptive statistics for continuous predictors, such as age, were obtained by calculating the mean value and standard deviation. Descriptive statistics for categorical variables were determined by calculating the number and frequency distributions for factors including gender, race, education, smoking status, alcohol use, diabetes, overweight/obesity, hypertension, physical activity, and PIR. We adjusted urinary VOC-EB concentrations for creatinine to minimize the effects of urine dilution. Although samples in the NHANES survey were weighted to reduce selection bias across subgroups based on age, sex, and ethnicity, we utilized unweighted estimations in our regression models, as the variables used for sample weighting were already incorporated in our study (31).

Initially, Pearson correlation coefficients were calculated between pairs of creatinine-adjusted VOC-EBs. These coefficients were categorized as weak ($r \leq 0.3$), medium ($0.3 < r \leq 0.8$), and strong ($r > 0.8$).

Secondly, we utilized multiple logistic regression models to evaluate the odds ratios (OR) with 95% confidence intervals (CIs) for the relationship between creatinine-adjusted VOC-EBs and liver steatosis and fibrosis. Creatinine-adjusted VOC-EB concentrations were categorized into quartiles, with the lowest quartile (Q1) serving as the reference group. The logistic regression analysis was adjusted for age, gender, race, obesity, diabetes, hypertension, smoking status, alcohol use, physical activity, education level, and poverty income ratio (PIR). Given that energy homeostasis exhibits sexual dimorphic traits and fatty liver diseases exhibit a strong sexual bias (32, 33), we constructed separate regression models for males and females.

Subsequently, the Bayesian kernel machine regression (BKMR) model, a non-parametric Bayesian variable selection framework, was employed to assess the joint effects of creatinine-adjusted VOC-EBs on liver steatosis and fibrosis (31). Data for CAP and LSM were transformed to natural logarithms to achieve a normal distribution. The BKMR model estimates the posterior inclusion probability (PIP) for each creatinine-adjusted VOC-EB, as well as the overall effect of VOC-EB mixtures on Ln CAP and Ln LSM, with adjustments for potential confounders. The final model utilized 10,000 iterations in a Markov Chain Monte Carlo (MCMC) sampler (31). A PIP threshold of 0.5 is commonly applied to determine the significance of the VOC-EBs. Estimates at any percentile, where the 95% confidence intervals excluded zero relative to the 50th percentile, were considered statistically significant (25, 34).

Data analysis was performed using R version 4.2.3, and BKMR analyses were conducted using the "bkmr" package. A two-tailed *p*-value of less than 0.05 was considered to indicate statistical significance.

3 Results

3.1 Baseline characteristics of study population

A total of 1,854 participants were included in the study. Descriptive characteristics of the study population are detailed in Table 1. Among the participants, 44.0% (816/1,854) had liver steatosis and 10.0% (186/1,854) had liver fibrosis. Participants with liver steatosis and fibrosis were predominantly male, tended to be older, of Mexican American ethnicity, past smokers, and had conditions such as diabetes, overweight/obesity, hypertension, and lower levels of physical activity. The distribution, parent compounds, and detectable rates of 20 VOC metabolites among the 1,854 participants are detailed in Supplementary Table S1. Strong correlations were observed between HPMMA and ΣUACLM ($r = 0.92$), HPMMA and IPMA3 ($r = 0.92$), HPMMA and ΣUACLNM ($r = 0.86$), ΣUACLM and ΣUACLNM ($r = 0.84$), IPMA3 and ΣUACLNM ($r = 0.81$), and IPMA3 and ΣUACLM ($r = 0.85$), as shown in Supplementary Figure S1. The concentrations of creatinine-adjusted urinary VOC-EBs from four consecutive NHANES cycles are shown in Supplementary Figure S2. A

TABLE 1 Descriptive characteristics of participants stratified by the presence of liver steatosis (CAP score ≥ 274 dB/m) and fibrosis (LSM score ≥ 8 kPa).

Characteristics	Total (*n* = 1,854)	Stestosis (CAP score ≥ 274 dB/m)			Fibrosis (LSM ≥ 8 k.Pa)		
		No (*n* = 1,038)	Yes (*n* = 816)	*p*-value	No (*n* = 1,668)	Yes (*n* = 186)	*p*-value
Gender (%)				<0.001			0.002
Male	922 (49.73)	474 (45.66)	448 (54.90)		809 (48.50)	113 (60.75)	
Female	932 (50.27)	564 (54.34)	368 (45.10)		859 (51.50)	73 (39.25)	
Age (years)	50.28 (16.76)	48.28 (17.34)	52.83 (15.63)	<0.001	49.76 (16.84)	54.99 (15.31)	<0.001
Race-ethnicity (%)				<0.001			0.137
Mexican American	217 (11.70)	85 (8.19)	132 (16.18)		192 (11.51)	25 (13.44)	
Hispanic	174 (9.39)	98 (9.44)	76 (9.31)		152 (9.23)	20 (10.75)	
Non-Hispanic White	657 (35.44)	353 (34.01)	304 (37.26)		587 (35.19)	70 (37.63)	
Non-Hispanic Black	491 (26.46)	313 (30.15)	178 (21.81)		439 (26.32)	52 (27.96)	
Others	315 (16.99)	189 (18.21)	126 (15.44)		296 (17.75)	19 (10.22)	
Education (%)				0.083			0.074
High school or less	763 (41.15)	407 (39.21)	356 (43.63)		677 (40.59)	86 (46.24)	
College	616 (33.23)	347 (33.43)	269 (32.97)		551 (33.03)	65 (34.95)	
Graduate or higher	475 (25.62)	284 (27.36)	191 (23.41)		440 (26.38)	35 (18.82)	
Smokers (%)				0.042			0.584
Never	1,058 (57.07)	594 (57.23)	464 (56.86)		954 (57.19)	104 (55.91)	
Former	465 (25.08)	242 (23.31)	223 (27.33)		413 (24.76)	52 (27.96)	
Current	331 (17.85)	202 (19.46)	129 (15.81)		301 (18.05)	30 (16.13)	
Alcohol use (%)				0.292			0.197
Never drinkers	492 (26.54)	276 (26.59)	216 (26.47)		434 (26.02)	58 (31.18)	
Low-moderate drinkers	687 (37.06)	370 (35.65)	317 (38.65)		617 (36.99)	70 (37.63)	
Heavy drinkers	675 (36.41)	392 (37.76)	283 (34.68)		617 (36.99)	58 (31.18)	
Diabetes (%)				<0.001			<0.001
No	1,611 (86.89)	963 (92.77)	648 (79.41)		1,487 (89.15)	124 (66.67)	
Yes	243 (13.11)	75 (7.23)	168 (20.59)		181 (10.85)	62 (33.33)	
Overweight/obesity (%)				<0.001			<0.001
No	481 (25.94)	416 (40.08)	65 (7.97)		463 (27.76)	18 (9.68)	
Yes	1,373 (74.06)	622 (59.92)	751 (92.03)		1,205 (72.24)	168 (90.32)	
Hypertension (%)				<0.001			<0.001

(Continued)

10.3389/fpubh.2024.1437519

10.3389/fpubh.2024.1437519

TABLE 1 (Continued)

Characteristics	Total (n = 1,854)	Stestosis (CAP score ≥ 274 dB/m)			Fibrosis (LSM ≥ 8 k.Pa)		
		No (n = 1,038)	Yes (n = 816)	p-value	No (n = 1,668)	Yes (n = 186)	p-value
No	1,171 (63.16)	721 (69.46)	450 (55.15)		1,086 (65.11)	85 (45.7)	
Yes	683 (36.84)	317 (30.54)	366 (44.85)		582 (34.89)	101 (54.3)	
Physical activity (%)				<0.001			0.030
No	947 (51.08)	486 (46.82)	461 (56.50)		838 (50.24)	109 (58.60)	
Yes	907 (48.92)	552 (53.18)	355 (43.51)		830 (49.76)	77 (41.40)	
PIR (%)				0.382			0.822
<1	318 (17.15)	171 (16.47)	147 (18.01)		285 (17.09)	33 (17.74)	
≥1	1,536 (82.85)	867 (83.53)	669 (81.99)		1,383 (82.91)	153 (82.26)	

Data are based on the National Health and Nutrition Examination Survey (NHANES) from 2017 to 2020, with a total sample size of 1,854 participants.

continuous increasing trend in the concentrations of creatinine-adjusted urinary ΣUBUM, ΣUACLM, ΣUAAM, ΣUSEBM, and BPMA was observed.

3.2 Association of single urinary VOC-EBs with liver steatosis and fibrosis

Binary logistic regression models were employed to assess the individual effects of each urinary VOC-EB on hepatic steatosis and fibrosis. As depicted in Figure 2, after adjusting for covariates, a significant positive association was observed between ΣUACLM and liver steatosis in a dose–response pattern (p-trend < 0.05). Additionally, HPMMA was positively associated with liver steatosis in the third quartile compared to the first quartile [OR 1.51 (95% CI 1.02–2.23)]. Meanwhile, negative associations with liver steatosis were observed for ΣUSEBM and 2HPMA. The adjusted OR for liver steatosis was 0.62 (95% CI 0.40–0.96) among participants in the highest urinary ΣUSEBM quartile. The adjusted OR for urinary 2HPMA with liver steatosis was 0.66 (95% CI 0.47–0.93) in the Q3 compared to Q1. Notable differences were observed in the sex-stratified analysis. For example, ΣUACLM and ΣUSEBM exhibited similar correlations in both men and women. However, high concentrations of ACTA and HPMMA were positively associated with liver steatosis, while high concentrations of IPMA3 were negatively associated with liver steatosis in men. For women, high concentrations of AMCC and 2HPMA were negatively associated with liver steatosis (Figure 2).

Regarding liver fibrosis, as illustrated in Figure 3, binary logistic regression analysis indicated that participants in the highest quartile of ΣUBUM (Q4 vs. Q1: OR = 1.91, 95% CI: 1.02–3.57) and ΣUXM (Q3 vs. Q1: OR = 1.64, 95% CI: 1.00–2.68) exhibited a higher prevalence of liver fibrosis compared to those in the first quartile. Additionally, a negative association was observed between ΣUSEBM and liver fibrosis in the third quartile compared to the first quartile [OR 0.42 (95% CI 0.21–0.84)]. However, the analysis stratified by sex revealed several inconsistencies. High concentrations of ΣUXM were positively associated with liver fibrosis in men, a finding consistent with the overall population. Meanwhile, high concentrations of ΣUSEBM and AMCC were negatively associated with liver fibrosis, and high concentrations of ΣUACLM were positively associated with liver fibrosis in women. Associations of urinary VOC-EBs mixture exposure with Ln CAP and Ln LSM.

Ln-transformed CAP, LSM, and concentrations of each VOC-EB were treated as continuous variables, and the BKMR model was fitted to assess their joint effects on CAP and LSM. Although the confidence intervals were broad, a significant decrease in Ln CAP was observed at the 35th percentile or below compared to the 50th percentile, indicating a significant positive association (Figure 4A). A decreasing trend was observed in the Ln LSM values, although these did not reach statistical significance (Figure 4B). The PIPs of ΣUACLM and ΣUACLNM for Ln CAP exceeded 0.5 (Supplementary Table S2), suggesting these VOC-EBs largely contributed to the observed increase in Ln CAP. Significant associations for ΣUACLM and ΣUACLNM with Ln CAP were observed regardless of other VOC-EBs being fixed at their 25th, 50th, or 75th percentiles (Supplementary Figure S3A), similar to BPMA and ΣUBUM with Ln LSM (Supplementary Figure S3B).

The dose–response relationships of the 13 VOC-EBs were illustrated after adjusting for covariates with other VOC-EBs set at

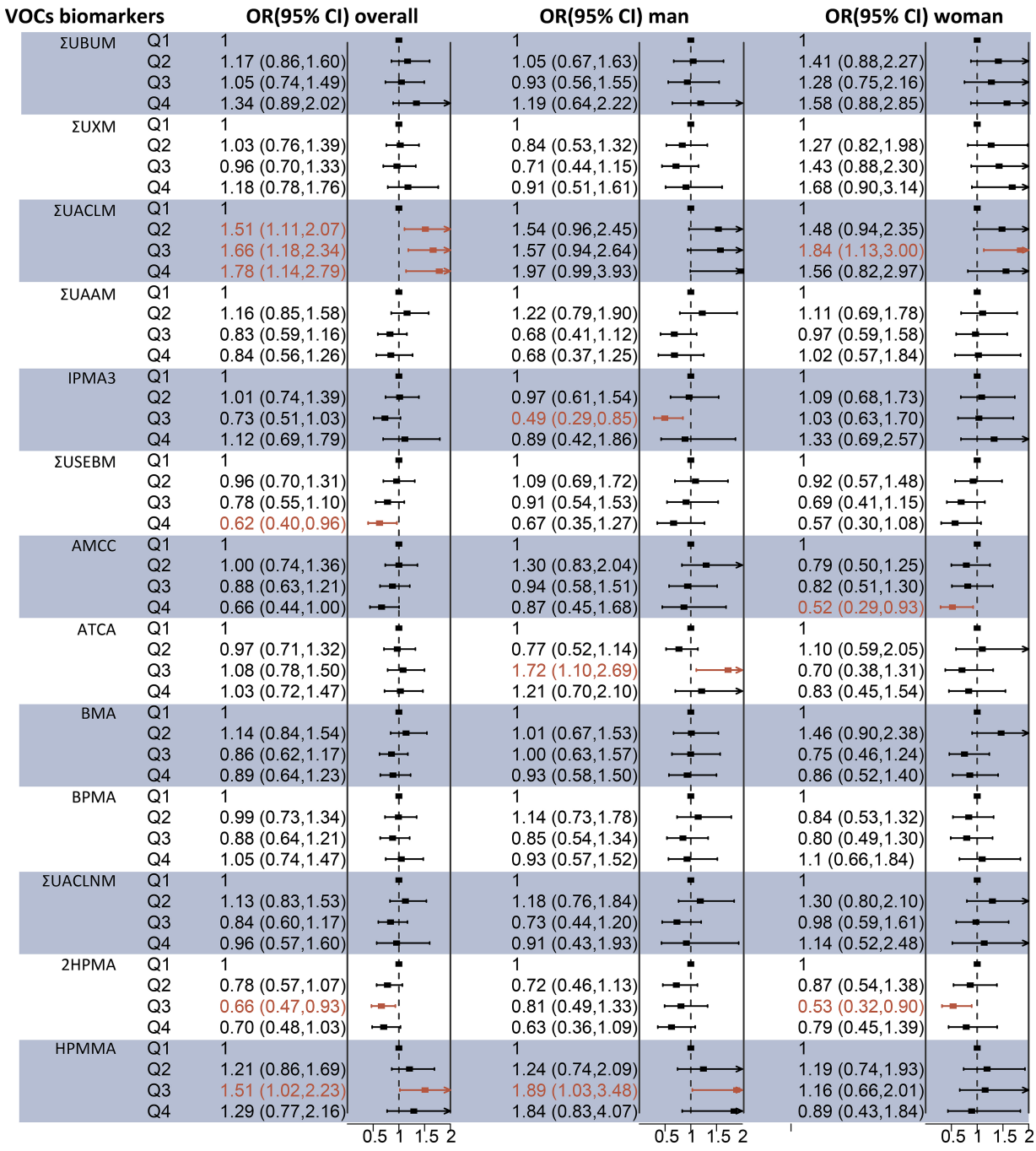

FIGURE 2
Association between individual urinary VOC-EB concentrations and the risk of liver steatosis, analyzed overall and stratified by sex, using multivariable logistic regression models. All VOC-EB concentrations were normalized to urinary creatinine levels (units: μg/g creatinine). Results are presented as odds ratios (OR) with 95% confidence intervals (CI). The regression model was adjusted for age, gender, race, obesity status, diabetes status, hypertension status, smoking status, alcohol use, physical activity, education level, and poverty income ratio (PIR). A bold segment indicates a p-value < 0.05.

their median levels (Figure 5). Positive exposure-response relationships were observed between ΣUACLM and Ln CAP, whereas negative associations were noted for ΣUSEBM and ΣUACLNM (Figure 5A). Variable patterns were noted in Ln LSM: ΣUBUM demonstrated a positive relationship, while ΣUSEBM, AMCC, BPMA, and 2HPMA showed inverse relationships (Figure 5B).

4 Discussion

To our knowledge, this study is the first to characterize the distributions of 20 urinary VOC metabolites in the general population from 2011 to 2020 and to assess their associations with hepatic steatosis and liver fibrosis using VCTE and diverse statistical methods. The results demonstrated a continuous increasing trend

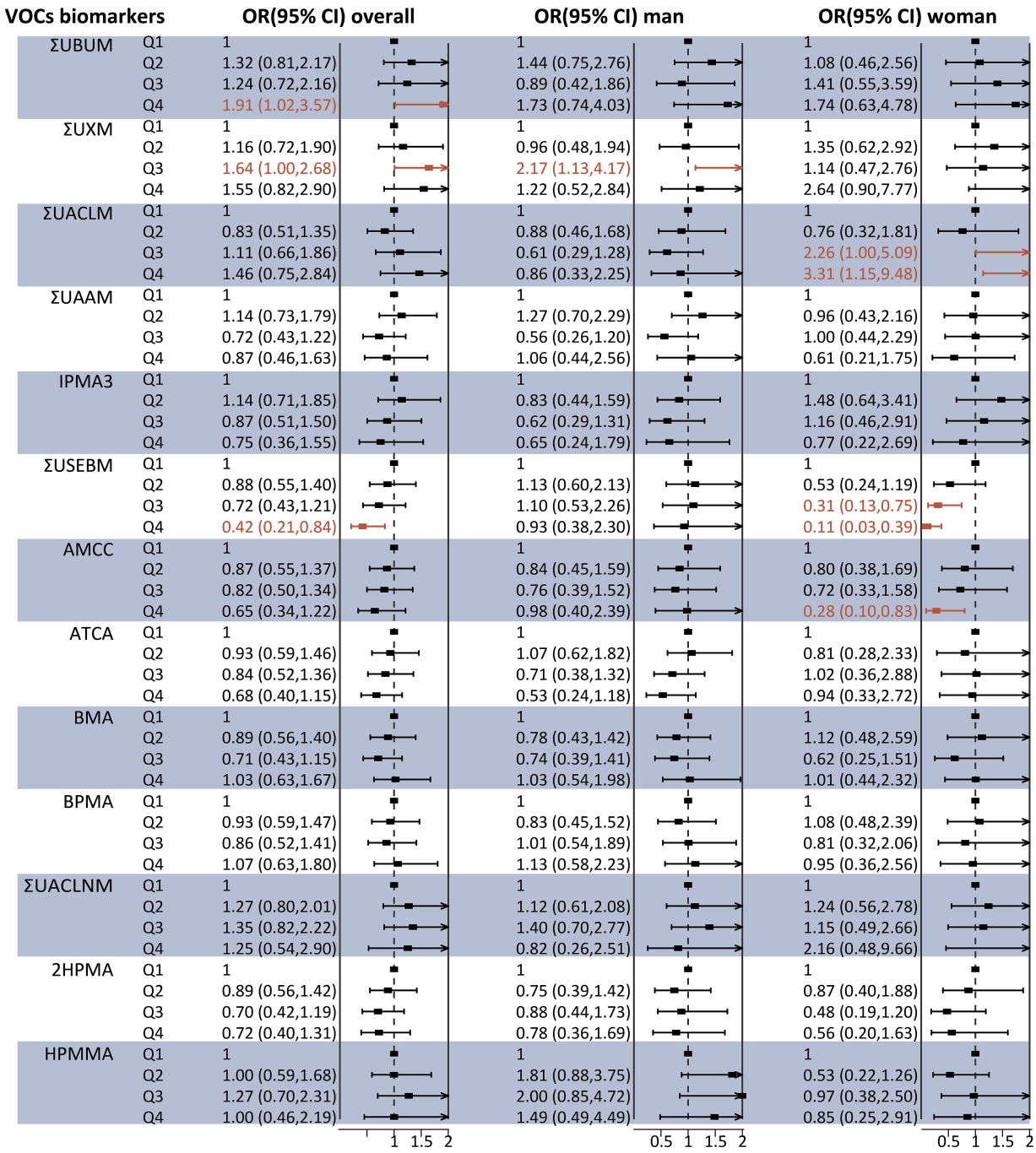

FIGURE 3
Association between individual urinary VOC-EB concentrations and the risk of liver fibrosis, analyzed overall and stratified by sex, using multivariable logistic regression models. All VOC-EB concentrations were normalized to urinary creatinine levels (units: μg/g creatinine). Results are presented as odds ratios (OR) with 95% confidence intervals (CI). The model was adjusted for age, gender, race, obesity status, diabetes status, hypertension status, smoking status, alcohol use, physical activity, education level, and poverty income ratio (PIR). Segments highlighted in bold indicate a p-value < 0.05.

in several urinary VOC-EBs from 2011 to 2020. On one hand, from 2017 to 2020, multivariate logistic regression indicated that several urinary VOC-EBs were significantly associated with an increased risk of hepatic steatosis and liver fibrosis, while several urinary VOC-EBs significant negative associations. Furthermore, the relationships of VOC-EBs with liver steatosis and fibrosis in men and women were found to be sporadic and inconsistent. On the other hand, BKMR analysis revealed that overall mixed exposure was significantly positively associated with Ln CAP. The univariate exposure-response function identified associations between several urinary VOC-EBs and the risk of hepatic steatosis and liver fibrosis. Both multivariate logistic regression and BKMR analysis found that ΣUACLM (acrolein metabolites) was positively associated with hepatic steatosis, ΣUBUM (1,3-butadiene metabolites) with liver

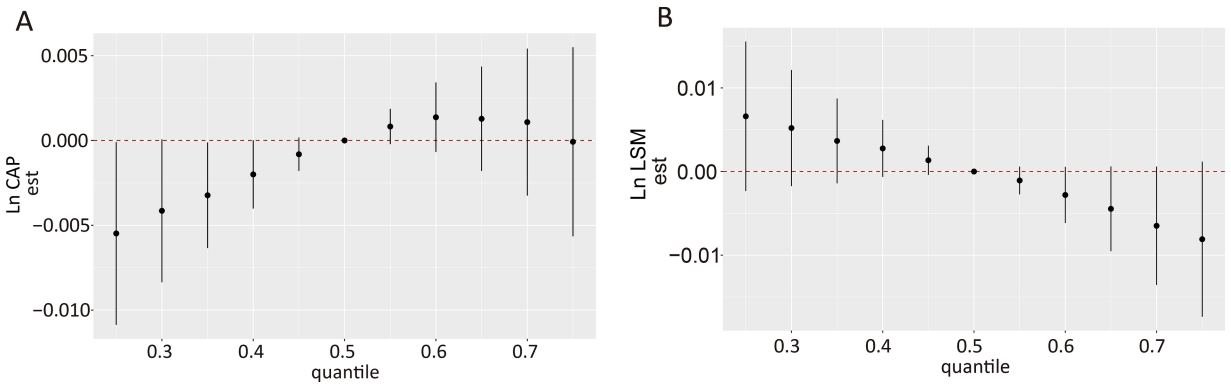

FIGURE 4
Overall association of VOC-EB mixtures with Ln CAP and Ln LSM using the Bayesian Kernel Machine Regression (BKMR) model. **(A)** Association of the urinary VOC-EB mixture with Ln CAP. **(B)** Association of the urinary VOC-EB mixture with Ln LSM. Both panels depict results adjusted for age, gender, race, obesity status, diabetes status, hypertension status, smoking status, alcohol use, physical activity, education level, and poverty income ratio (PIR).

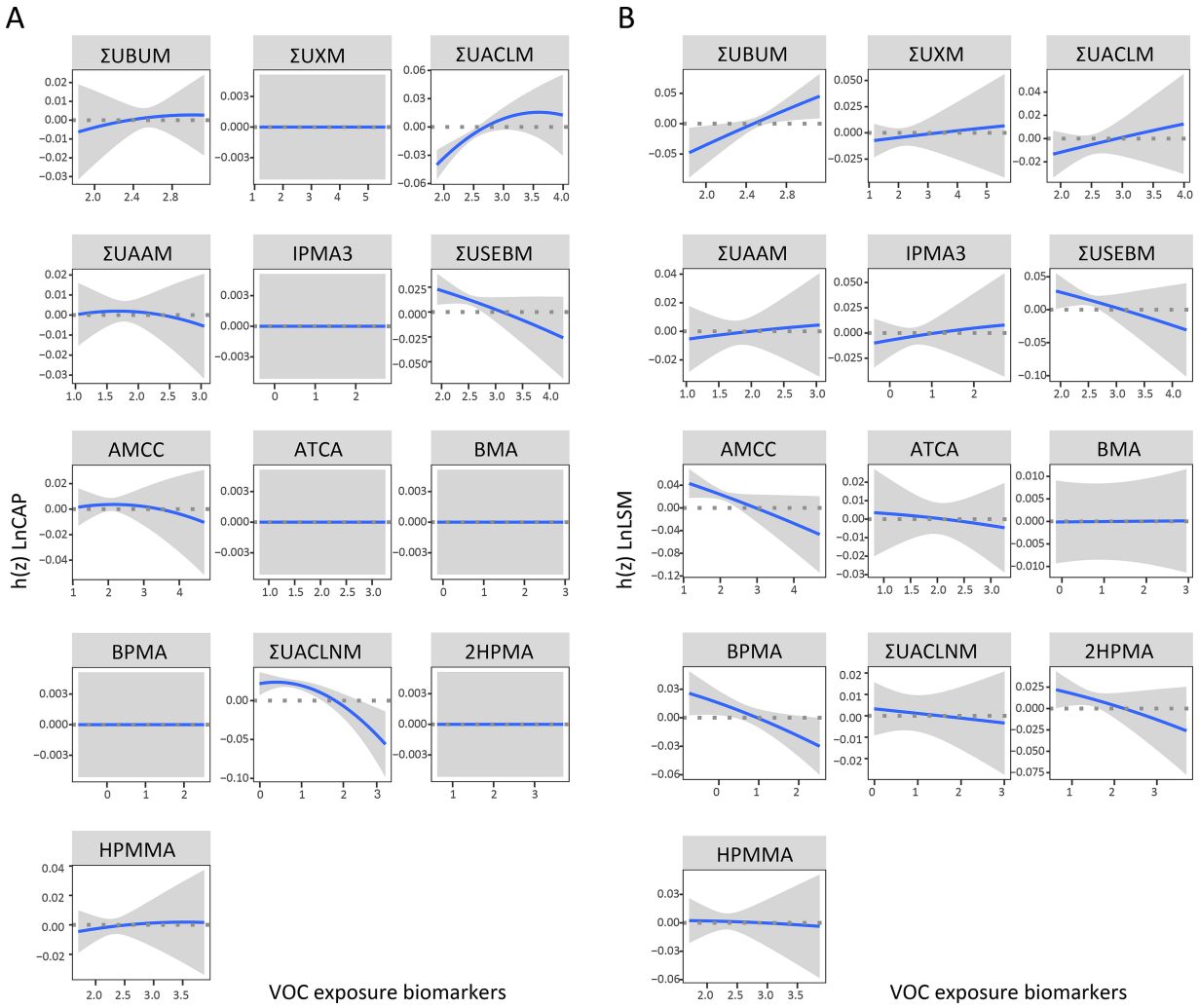

FIGURE 5
Univariate exposure-response functions displaying the associations of selected VOC-EBs with Ln CAP **(A)** and Ln LSM **(B)**. Each function is plotted with 95% confidence intervals (CIs) and analyzes the relationship while fixing the concentrations of other chemicals at their median values. The BKMR models used for these analyses were adjusted for age, gender, race, obesity status, diabetes status, hypertension status, smoking status, alcohol use, physical activity, education level, and poverty income ratio (PIR).

fibrosis, and ΣUSEBM (ethylbenzene metabolites) negatively with both conditions. These findings underscore the role of environmental VOC exposure in the development of hepatic steatosis and fibrosis.

VOCs originate from various sources, with road traffic emissions constituting the largest share before 2010. The replacement of older vehicles and the gradual reduction in gasoline consumption contributed to a rapid decline in VOC emissions until 2010 (35). From 2010 onwards, the use of solvents is believed to have surpassed road traffic as the primary source of VOCs, stabilizing pollution levels (36). In this study, we observed a trend of continuous increase in the urinary concentrations of ΣUBUM, ΣUACLM, ΣUAAM, ΣUSEBM, and BPMA, derived from parent compounds such as 1,3-butadiene, acrolein, acrylamide, styrene, ethylbenzene, and 1-bromopropane. Most governments have not yet to implement regulations on the use of solvents (35), which may partially explain these findings. In fact, the US EPA has found that the levels of about a dozen VOCs are 2 to 5 times higher inside homes than outside, whether in rural or highly industrial areas (37). Additionally, VOCs detected in indoor air and tap water are often as numerous and varied as those found outdoors (10). Clearly, exposure to these ambient VOCs is inevitable in everyday life. Further research is required to confirm these findings, and increased attention should be directed toward the rising exposure to VOCs among the general population.

While epidemiological studies on the association between combined VOC exposures and hepatic steatosis or fibrosis are sporadic, individual VOC exposures have been implicated in liver injury within the general population. A cross-sectional study within the Canadian population demonstrated that blood concentrations of xylene, styrene, and toluene were associated with elevated levels of ALP and AST (24). An earlier study involving 663 US adults showed a positive association between ALP levels and urinary exposure biomarkers for acrolein, xylene, and 1,3-butadiene (23). Furthermore, a recent study of the US general adult population reported significant correlations between urinary metabolites of acrolein, 1,3-butadiene, and xylene, and NAFLD as defined by the USFLI (25). However, levels of these serum liver enzymes may be comparable in patients with or without liver steatosis (38), and these biomarkers are influenced by comorbid conditions, potentially reducing their sensitivity in defining steatosis (26, 27). According to guidelines from the American Gastroenterological Association, VCTE is preferred for the precise quantification of liver fat (CAP) and fibrosis (LSM) (39, 40). We initially discovered significant associations between urinary ΣUACLM (an exposure biomarker for acrolein) and hepatic steatosis, and between urinary ΣUBUM and ΣUXM (exposure biomarkers for 1,3-butadiene and xylene, respectively) and liver fibrosis, as diagnosed by VCTE, aligning with findings from previous studies. Interestingly, urinary ATCA and HPMMA was positively associated with liver steatosis in men, but not in women, while ΣUACLM was positively associated with liver steatosis and fibrosis in women, but not in men. The sex differences in the health hazards of urinary VOCs have also been reported. A previous study showed that sex significantly interacted with ΣUAAM in influencing the liver steatosis biomarker (25). Another study indicated that increasing levels of VOCs were associated with increases in C-reactive protein for women, but not for men (24). The hypothesis explains the sex-based differential susceptibility, including sex hormones, anatomical differences, gut microbiota, and epigenetic effects (33). Furthermore, obesity, with its increasing prevalence worldwide, has been recognized as a significant contributor to VOC toxicity and a key driver of NAFLD onset and progression, including fibrosis. Recent studies have demonstrated the association between VOC exposure and obesity in the general U.S. population (41), underscoring the complex interaction between environmental pollutants and metabolic disorders. Furthermore, high body mass index (BMI), a major risk factor for NAFLD, frequently coexists with sarcopenia, a condition characterized by loss of muscle mass and strength (42). Sarcopenia is prevalent in advanced liver disease and is closely associated with obesity, forming a "sarcopenic obesity" phenotype that exacerbates liver injury and fibrosis progression. Given the role of obesity in liver steatosis and fibrosis, and its association with sarcopenia, it is plausible that VOC exposure contributes to both conditions. Sarcopenia and obesity not only exacerbate NAFLD progression but also amplify susceptibility to environmental toxins such as VOCs, leading to a compounded health burden. Future studies are warranted to explore the mechanistic pathways underlying the interaction between VOC exposure, obesity, and sarcopenia.

Traditional generalized linear regression models, including multivariable linear and logistic regression, typically offer straightforward relationships between individual VOCs and health outcomes (43, 44). However, these models often overlook mixed environmental exposures, joint effects, and their nonlinear interactions, potentially leading to false negative or positive results (34, 43, 45). Moreover, a strong correlation among several urinary VOC-EBs was detected in our study, which can distort the outcomes of generalized linear regression models (46). Thus, we utilized the BKMR model, a recently developed nonparametric statistical method, to analyze the joint effects of VOC-EBs on liver health. This novel mixture modeling approach accommodates a range of VOC-EBs, even those with high correlations (31). Furthermore, BKMR analysis tests the overall mixture effect and captures nonlinear exposure-response relationships, with other chemicals fixed at specified levels. In our analysis, a significant positive joint effect of the VOC-EBs mixture on Ln CAP was observed, particularly when urinary VOC-EB concentrations were below the 35th percentile. This finding suggests that VOC-EBs may be linked to the severity of liver steatosis. The PIPs of ΣUACL and ΣUACLNM for CAP exceeded 0.5, indicating that these VOC-EBs significantly contributed to the association with Ln CAP. A previous study demonstrated that a mixture of VOC-EBs was positively associated with liver steatosis as defined by USFLI, although the results differed when defined by HSI (25). This discrepancy may stem from the unreliability of serum biomarkers in predicting liver injury, whereas liver VCTE is likely more sensitive (38–40). Additionally, no associations were found between the mixture of VOC-EBs and LSM. A recent study found that a mixture of VOC-EBs was associated with liver fibrosis as defined by the Hepamet Fibrosis Score (HFS), but not when using the Non-Alcoholic Fatty Liver Disease Fibrosis Score (NFS) (25). Indeed, some studies suggest that VOC exposure may be linked to liver fibrosis, as smoking—a known contributor to advanced liver fibrosis—typically results in higher urinary VOC metabolite levels in smokers than in nonsmokers (23, 47, 48). The association between cigarette smoking and the risk of

sarcopenia also warrants attention (11–13). Sarcopenia, common across various diseases, is one of the most frequent complications in advanced liver disease. This inconsistency could be attributed to low levels of VOC exposure in the general population and the adjustment for smoking as a confounder, considering that smoking significantly contributes to urinary VOC levels and is independently associated with sarcopenia. Furthermore, traditional risk assessment procedures, based on single chemical evaluations, do not align with the characteristics of low-level, multiple chemical exposures typical of modern life, thus overlooking the cocktail effect of mixtures, which can underestimate the health risks of pollutants. Mixtures at concentrations that individually do not cause observable adverse effects can produce harmful effects, as reviewed elsewhere (49). A possible explanation is that multiple molecular pathways can be affected by the same chemical, often exhibiting nonlinear dose–response relationships, or different pathways are affected by chemicals at various doses (50). Further research with larger sample sizes is necessary to clarify this association.

The BKMR analysis also allows for the identification of exposure-response relationships with other chemicals held at fixed levels. In our analysis, ΣUACLM (exposure biomarker for acrolein) demonstrated a positive association with CAP, consistent with the findings from individual VOC analyses, thus reinforcing this result. Furthermore, our study is the first to report that ΣUBUM (exposure biomarker for 1,3-butadiene) displayed a linear correlation with liver fibrosis, a finding more pronounced than in individual VOC analyses. Although associations between 1,3-butadiene and liver fibrosis have not been extensively studied, the liver is considered the primary site of 1,3-butadiene-induced carcinogenesis (51). DNA damage, the primary toxic effect of 1,3-butadiene in hepatocytes (52), also plays a crucial role in the pathogenesis of liver fibrosis (53). Additionally, ΣUSEBM and ΣUACLNM showed negative associations with CAP. Meanwhile, ΣUSEBM and AMCC were negatively associated with LSM, especially in the lowest concentration. These results contradict previous findings that utilized liver injury markers (20, 54, 55). Several explanations are possible for these results. First, given the lack of significant associations in individual analyses, this negative association could be due to complex antagonistic interactions among VOCs. The interactions are common among VOCs because VOCs are mostly metabolized by CYP450 enzymes in liver (17, 18, 56). Another explanation might be that, unlike high-dose occupational VOC exposure, which is positively correlated with liver injury (20, 54), generally VOCs exposure may not necessarily exert a same effect. Nevertheless, caution should be exercised in interpreting the results, and the above hypothetical explanations need to be further validated in future studies.

Although the biological mechanisms underlying the hepatotoxicity of VOCs have not been fully elucidated, evidence from numerous animal studies supports our findings with plausible molecular mechanisms. Oxidative stress is a common hepatotoxic effect induced by VOCs. Most VOCs are metabolized by CYP450 enzymes primarily during biotransformation, forming active electrophilic intermediates (17). These intermediates then conjugate with glutathione (57), the most abundant *in vivo* antioxidant, thereby indirectly aggravating oxidative stress (58). Oxidative stress is considered a potential mechanism for the development of liver steatosis and fibrosis (53). The inflammatory response plays an integral role in the progression of liver fibrosis from liver steatosis. Accumulation of VOCs such as acrolein in the liver can induce neutrophil recruitment and activation, leading to the formation of neutrophil extracellular traps (59). Exposure to 1,3-butadiene was found to upregulate genes involved in oxidative and inflammatory responses in the lungs of mice (60). Furthermore, acrolein can significantly increase the expression of endoplasmic reticulum (ER) stress markers in hepatocytes (61), Furthermore, acrolein can significantly increase the expression of endoplasmic reticulum (ER) stress markers in hepatocytes (62). However, the causal role of VOCs in the initiation and progression of liver diseases, as discussed in this study, warrants further investigation.

There are several limitations of our study. First, the cross-sectional design of this study precludes definitive conclusions about the causal relationships between urinary VOC mixtures and liver steatosis or hepatic fibrosis. Case–control or cohort studies are needed to address this methodological limitation. Second, although VCTE offers many benefits, it is not the gold standard for diagnosing liver conditions. Liver biopsy remains the gold standard for diagnosing liver steatosis and fibrosis, but recruiting sufficient participants from the general population is challenging. In this study, VCTE was performed by trained NHANES health technicians to maximize the accuracy of the results. Third, while our models adjusted for many confounders, the potential for unmeasured confounding remains. Specifically, data on genetic susceptibility, drug usage and dosages, and treatment adherence were lacking. Finally, as this study was conducted among U.S. adults, the generalizability of our findings to other populations is uncertain.

5 Conclusion

In conclusion, our study suggests that exposure to VOC mixtures increases the prevalence of liver steatosis among U.S. adults. Acrolein may play a significant role in the association between VOC mixture exposure and liver steatosis, while 1,3-butadiene may be linked to an increased risk of liver fibrosis. These findings underscore the significant role of environmental VOC mixture exposure in the development of liver steatosis and hepatic fibrosis. Further prospective cohort studies and mechanistic research are required to validate these conclusions.

Data availability statement

Publicly available datasets were analyzed in this study. This data can be found here: https://wwwn.cdc.gov/nchs/nhanes/Default.aspx.

Ethics statement

The studies involving humans were approved by National Center for Health Statistics Research Ethics Review Board. The studies were conducted in accordance with the local legislation and institutional requirements. The participants provided their written informed consent to participate in this study.

Author contributions

WenS: Conceptualization, Methodology, Writing – original draft. PG: Data curation, Software, Writing – original draft. QW: Software, Visualization, Writing – original draft. FD: Supervision, Writing – review & editing. WeiS: Validation, Writing – review & editing. HZ: Methodology, Writing – review & editing. AH: Writing – review & editing. CL: Writing – review & editing.

Funding

The author(s) declare that financial support was received for the research, authorship, and/or publication of this article. This study was funded by the Key Specialty Construction Project of Shanghai Pudong New Area Health Commission (PWZzk2022-17) and the Youth Research Fund of Tongji University Affiliated East Hospital (DFPY2023007).

Acknowledgments

The authors thank all participants in the NHANES.

Conflict of interest

The authors declare that the research was conducted in the absence of any commercial or financial relationships that could be construed as a potential conflict of interest.

Publisher's note

Supplementary material

The Supplementary material for this article can be found online at: https://www.frontiersin.org/articles/10.3389/fpubh.2024.1437519/full#supplementary-material

References

1. Powell EE, Wong VW, Rinella M. Non-alcoholic fatty liver disease. *Lancet*. (2021) 397:2212–24. doi: 10.1016/S0140-6736(20)32511-3

2. Estes C, Razavi H, Loomba R, Younossi Z, Sanyal AJ. Modeling the epidemic of nonalcoholic fatty liver disease demonstrates an exponential increase in burden of disease. *Hepatology*. (2018) 67:123–33. doi: 10.1002/hep.29466

3. Ekstedt M, Hagstrom H, Nasr P, Fredrikson M, Stal P, Kechagias S, et al. Fibrosis stage is the strongest predictor for disease-specific mortality in Nafld after up to 33 years of follow-up. *Hepatology*. (2015) 61:1547–54. doi: 10.1002/hep.27368

4. Loomba R, Friedman SL, Shulman GI. Mechanisms and disease consequences of nonalcoholic fatty liver disease. *Cell*. (2021) 184:2537–64. doi: 10.1016/j.cell.2021.04.015

5. Sen P, Qadri S, Luukkonen PK, Ragnarsdottir O, McGlinchey A, Jantti S, et al. Exposure to environmental contaminants is associated with altered hepatic lipid metabolism in non-alcoholic fatty liver disease. *J Hepatol*. (2022) 76:283–93. doi: 10.1016/j.jhep.2021.09.039

6. Pazo DY, Moliere F, Sampson MM, Reese CM, Agnew-Heard KA, Walters MJ, et al. Mainstream smoke levels of volatile organic compounds in 50 U.S. domestic cigarette brands smoked with the Iso and Canadian intense protocols. *Nicotine Tob Res*. (2016) 18:1886–94. doi: 10.1093/ntr/ntw118

7. Hong-Li W, Sheng-Ao J, Sheng-Rong L, Qing-Yao H, Li L, Shi-Kang T, et al. Volatile organic compounds (Vocs) source profiles of on-road vehicle emissions in China. *Sci Total Environ*. (2017) 607-608:253–61. doi: 10.1016/j.scitotenv.2017.07.001

8. Pal VK, Kannan K. Assessment of exposure to volatile organic compounds through urinary concentrations of their metabolites in pet dogs and cats from the United States. *Environ Pollut*. (2023) 316:120576. doi: 10.1016/j.envpol.2022.120576

9. USEPA. Initial list of hazardous air pollutants with modifications: United States Environmental Protection Agency (2023). Available at: https://www.epa.gov/haps/initial-list-hazardous-air-pollutants-modifications.

10. Caron-Beaudoin E, Whyte KP, Bouchard MF, Chevrier J, Haddad S, Copes R, et al. Volatile organic compounds (Vocs) in indoor air and tap water samples in residences of pregnant women living in an area of unconventional natural gas operations: findings from the Experiva study. *Sci Total Environ*. (2022) 805:150242. doi: 10.1016/j.scitotenv.2021.150242

11. Cho E, Soh HS, Lee JR, Yun J, Bae WK, Lee H. Association between smoking status and handgrip strength in Korean male adults: based on Korea National Health and nutrition examination survey 2016-2019. *Front Med (Lausanne)*. (2023) 10:1212946. doi: 10.3389/fmed.2023.1212946

12. Nogami E, Miyai N, Zhang Y, Onishi S, Sakaguchi M, Yokoi K, et al. Effects of cigarette smoking on the association between respiratory muscle strength and skeletal muscle mass in middle-aged and older adults: the Wakayama study. *Eur Geriatr Med*. (2022) 13:805–15. doi: 10.1007/s41999-022-00662-0

13. Lin J, Hu M, Gu X, Zhang T, Ma H, Li F. Effects of cigarette smoking associated with sarcopenia in persons 60 years and older: a cross-sectional study in Zhejiang Province. *BMC Geriatr*. (2024) 24:523. doi: 10.1186/s12877-024-04993-4

14. Tarantino G, Sinatti G, Citro V, Santini SJ, Balsano C. Sarcopenia, a condition shared by various diseases: can we alleviate or delay the progression? *Intern Emerg Med*. (2023) 18:1887–95. doi: 10.1007/s11739-023-03339-z

15. Ehrlich A, Duche D, Ouedraogo G, Nahmias Y. Challenges and opportunities in the Design of Liver-on-Chip Microdevices. *Annu Rev Biomed Eng*. (2019) 21:219–39. doi: 10.1146/annurev-bioeng-060418-052305

16. Kim JK, Eun JW, Bae HJ, Shen Q, Park SJ, Kim HS, et al. Characteristic molecular signatures of early exposure to volatile organic compounds in rat liver. *Biomarkers*. (2013) 18:706–15. doi: 10.3109/1354750X.2013.847121

17. Frigerio G, Mercadante R, Polledri E, Missineo P, Campo L, Fustinoni S. An Lc-Ms/Ms method to profile urinary mercapturic acids, metabolites of electrophilic intermediates of occupational and environmental toxicants. *J Chromatogr B Analyt Technol Biomed Life Sci*. (2019) 1117:66–76. doi: 10.1016/j.jchromb.2019.04.015

18. Pal VK, Li AJ, Zhu H, Kannan K. Diurnal variability in urinary volatile organic compound metabolites and its association with oxidative stress biomarkers. *Sci Total Environ*. (2022) 818:151704. doi: 10.1016/j.scitotenv.2021.151704

19. Alwis KU, Blount BC, Britt AS, Patel D, Ashley DL. Simultaneous analysis of 28 urinary Voc metabolites using ultra high performance liquid chromatography coupled with electrospray ionization tandem mass spectrometry (Uplc-Esi/Msms). *Anal Chim Acta*. (2012) 750:152–60. doi: 10.1016/j.aca.2012.04.009

20. Qi C, Gu Y, Sun Q, Gu H, Xu B, Gu Q, et al. Low-dose N,N-Dimethylformamide exposure and liver injuries in a cohort of Chinese leather industry workers. *J Occup Environ Med*. (2017) 59:434–9. doi: 10.1097/JOM.0000000000000983

21. Wang SY, Han D, Pan YL, Yu CP, Zhou XR, Xin R, et al. A urinary Metabolomic study from subjects after long-term occupational exposure to low concentration acrylamide using Uplc-Qtof/Ms. *Arch Biochem Biophys*. (2020) 681:108279. doi: 10.1016/j.abb.2020.108279

22. Niaz K, Mabqool F, Khan F, Ismail Hassan F, Baeeri M, Navaei-Nigjeh M, et al. Molecular mechanisms of action of styrene toxicity in blood plasma and liver. *Environ Toxicol*. (2017) 32:2256–66. doi: 10.1002/tox.22441

23. Wahlang B, Gao H, Rai SN, Keith RJ, McClain CJ, Srivastava S, et al. Associations between residential volatile organic compound exposures and liver injury markers: the role of biological sex and race. *Environ Res*. (2023) 221:115228. doi: 10.1016/j.envres.2023.115228

24. Cakmak S, Cole C, Hebbern C, Andrade J, Dales R. Associations between blood volatile organic compounds, and changes in hematologic and biochemical profiles, in a population-based study. *Environ Int*. (2020) 145:106121. doi: 10.1016/j.envint.2020.106121

25. Liu W, Cao S, Shi D, Yu L, Qiu W, Chen W, et al. Single-chemical and mixture effects of multiple volatile organic compounds exposure on liver injury and risk of non-alcoholic fatty liver disease in a representative general adult population. *Chemosphere*. (2023) 339:139753. doi: 10.1016/j.chemosphere.2023.139753

26. Garteiser P, Castera L, Coupaye M, Doblas S, Calabrese D, Dioguardi Burgio M, et al. Prospective comparison of transient Elastography, Mri and serum scores for grading steatosis and detecting non-alcoholic steatohepatitis in bariatric surgery candidates. *JHEP Rep*. (2021) 3:100381. doi: 10.1016/j.jhepr.2021.100381

27. Torres DM, Harrison SA. Diagnosis and therapy of nonalcoholic steatohepatitis. *Gastroenterology*. (2008) 134:1682–98. doi: 10.1053/j.gastro.2008.02.077

28. Chalasani N, Younossi Z, Lavine JE, Diehl AM, Brunt EM, Cusi K, et al. The diagnosis and Management of non-Alcoholic Fatty Liver Disease: practice guideline by the American Gastroenterological Association, American Association for the Study of Liver Diseases, and American College of Gastroenterology. *Gastroenterology*. (2012) 142:1592–609. doi: 10.1053/j.gastro.2012.04.001

29. Hsu C, Caussy C, Imajo K, Chen J, Singh S, Kaulback K, et al. Magnetic resonance vs transient Elastography analysis of patients with nonalcoholic fatty liver disease: a systematic review and pooled analysis of individual participants. *Clin Gastroenterol Hepatol*. (2019) 17:630–637.e8. doi: 10.1016/j.cgh.2018.05.059

30. US Department of Agriculture UDoHaHS. Dietary Guidelines for Americans, 2020–2025 (2020). Available at: http://dietaryguidelines.gov/.

31. Zhang Y, Dong T, Hu W, Wang X, Xu B, Lin Z, et al. Association between exposure to a mixture of phenols, pesticides, and phthalates and obesity: comparison of three statistical models. *Environ Int*. (2019) 123:325–36. doi: 10.1016/j.envint.2018.11.076

32. Grossmann M, Wierman ME, Angus P, Handelsman DJ. Reproductive endocrinology of nonalcoholic fatty liver disease. *Endocr Rev*. (2019) 40:417–46. doi: 10.1210/er.2018-00158

33. Le Magueresse-Battistoni B. Endocrine disrupting chemicals and metabolic disorders in the liver: what if we also looked at the female side? *Chemosphere*. (2021) 268:129212. doi: 10.1016/j.chemosphere.2020.129212

34. Valeri L, Mazumdar MM, Bobb JF, Claus Henn B, Rodrigues E, Sharif OIA, et al. The joint effect of prenatal exposure to metal mixtures on neurodevelopmental outcomes at 20-40 months of age: evidence from rural Bangladesh. *Environ Health Perspect*. (2017) 125:067015. doi: 10.1289/EHP614

35. Zhang C, Stevenson D. Characteristic changes of ozone and its precursors in London during Covid-19 lockdown and the ozone surge reason analysis. *Atmos Environ (1994)*. (2022) 273:118980. doi: 10.1016/j.atmosenv.2022.118980

36. Lewis AC, Hopkins JR, Carslaw DC, Hamilton JF, Nelson BS, Stewart G, et al. An increasing role for solvent emissions and implications for future measurements of volatile organic compounds. *Philos Trans A Math Phys Eng Sci*. (2020) 378:20190328. doi: 10.1098/rsta.2019.0328

37. USEPA. Volatile organic Compounds' impact on indoor air quality: United States Environmental Protection Agency (2024). Available at: https://www.epa.gov/indoor-air-quality-iaq/volatile-organic-compounds-impact-indoor-air-quality.

38. Hatziagelaki E, Paschou SA, Schon M, Psaltopoulou T, Roden M. Nafld and thyroid function: pathophysiological and therapeutic considerations. *Trends Endocrinol Metab*. (2022) 33:755–68. doi: 10.1016/j.tem.2022.08.001

39. Cusi K, Isaacs S, Barb D, Basu R, Caprio S, Garvey WT, et al. American Association of Clinical Endocrinology Clinical Practice Guideline for the diagnosis and Management of Nonalcoholic Fatty Liver Disease in primary care and endocrinology clinical settings: co-sponsored by the American Association for the Study of Liver Diseases (Aasld). *Endocr Pract*. (2022) 28:528–62. doi: 10.1016/j.eprac.2022.03.010

40. Kanwal F, Shubrook JH, Adams LA, Pfotenhauer K, Wai-Sun Wong V, Wright E, et al. Clinical care pathway for the risk stratification and Management of Patients with nonalcoholic fatty liver disease. *Gastroenterology*. (2021) 161:1657–69. doi: 10.1053/j.gastro.2021.07.049

41. Lei T, Qian H, Yang J, Hu Y. The association analysis between exposure to volatile organic chemicals and obesity in the General USA population: a cross-sectional study from Nhanes program. *Chemosphere*. (2023) 315:137738. doi: 10.1016/j.chemosphere.2023.137738

42. Liu C, Cheng KY, Tong X, Cheung WH, Chow SK, Law SW, et al. The role of obesity in sarcopenia and the optimal body composition to prevent against sarcopenia and obesity. *Front Endocrinol (Lausanne)*. (2023) 14:1077255. doi: 10.3389/fendo.2023.1077255

43. Kim S, Kim S, Won S, Choi K. Considering common sources of exposure in association studies - urinary Benzophenone-3 and Dehp metabolites are associated with altered thyroid hormone balance in the Nhanes 2007-2008. *Environ Int*. (2017) 107:25–32. doi: 10.1016/j.envint.2017.06.013

44. Scinicariello F, Buser MC. Serum testosterone concentrations and urinary bisphenol a, Benzophenone-3, Triclosan, and paraben levels in male and female children and adolescents: Nhanes 2011-2012. *Environ Health Perspect*. (2016) 124:1898–904. doi: 10.1289/EHP150

45. Czarnota J, Gennings C, Colt JS, De Roos AJ, Cerhan JR, Severson RK, et al. Analysis of environmental chemical mixtures and non-Hodgkin lymphoma risk in the Nci-seer Nhl study. *Environ Health Perspect*. (2015) 123:965–70. doi: 10.1289/ehp.1408630

46. Marill KA. Advanced statistics: linear regression, part ii: multiple linear regression. *Acad Emerg Med*. (2004) 11:94–102. doi: 10.1197/j.aem.2003.09.006

47. Mantaka A, Koulentaki M, Samonakis D, Sifaki-Pistolla D, Voumvouraki A, Tzardi M, et al. Association of Smoking with liver fibrosis and mortality in primary biliary cholangitis. *Eur J Gastroenterol Hepatol*. (2018) 30:1461–9. doi: 10.1097/MEG.0000000000001234

48. Chambers DM, Ocariz JM, McGuirk MF, Blount BC. Impact of cigarette smoking on volatile organic compound (Voc) blood levels in the U.S. population: Nhanes 2003-2004. *Environ Int*. (2011) 37:1321–8. doi: 10.1016/j.envint.2011.05.016

49. Le Magueresse-Battistoni B, Vidal H, Naville D. Environmental pollutants and metabolic disorders: the multi-exposure scenario of life. *Front Endocrinol (Lausanne)*. (2018) 9:582. doi: 10.3389/fendo.2018.00582

50. Suvorov A. The dose disrupts the pathway: application of Paracelsus principle to mechanistic toxicology. *Toxicol Sci*. (2024) 200:228–34. doi: 10.1093/toxsci/kfae059

51. Melnick RL, Huff J, Matanoski GM. Carcinogenicity of 1,3-butadiene. *Lancet*. (1992) 340:724–5. doi: 10.1016/0140-6736(92)92259-i

52. Lewis L, Chappell GA, Kobets T, O'Brian BE, Sangaraju D, Kosyk O, et al. Sex-specific differences in genotoxic and epigenetic effects of 1,3-butadiene among mouse tissues. *Arch Toxicol*. (2019) 93:791–800. doi: 10.1007/s00204-018-2374-x

53. Gui R, Li W, Li Z, Wang H, Wu Y, Jiao W, et al. Effects and potential mechanisms of Igf1/Igf1r in the liver fibrosis: a review. *Int J Biol Macromol*. (2023) 251:126263. doi: 10.1016/j.ijbiomac.2023.126263

54. Brodkin CA, Moon JD, Camp J, Echeverria D, Redlich CA, Willson RA, et al. Serum hepatic biochemical activity in two populations of workers exposed to styrene. *Occup Environ Med*. (2001) 58:95–102. doi: 10.1136/oem.58.2.95

55. Wahlang B, Gripshover TC, Gao H, Krivokhizhina T, Keith RJ, Sithu ID, et al. Associations between residential exposure to volatile organic compounds and liver injury markers. *Toxicol Sci*. (2021) 185:50–63. doi: 10.1093/toxsci/kfab119

56. Toftgard R, Nilsen OG. Effects of xylene and xylene isomers on cytochrome P-450 and *in vitro* enzymatic activities in rat liver, kidney and lung. *Toxicology*. (1982) 23:197–212. doi: 10.1016/0300-483x(82)90098-1

57. Commandeur JNM. Mercapturic acids as biomarkers of exposure to electrophilic chemicals: applications to environmental and industrial chemicals. *Biomarkers*. (1998) 3:239–303. doi: 10.1080/135475098231101

58. Townsend DM, Tew KD, Tapiero H. The importance of glutathione in human disease. *Biomed Pharmacother*. (2003) 57:145–55. doi: 10.1016/s0753-3322(03)00043-x

59. Arumugam S, Girish Subbiah K, Kemparaju K, Thirunavukkarasu C. Neutrophil extracellular traps in Acrolein promoted hepatic ischemia reperfusion injury: therapeutic potential of Nox2 and P38mapk inhibitors. *J Cell Physiol*. (2018) 233:3244–61. doi: 10.1002/jcp.26167

60. Noel A, Xiao R, Perveen Z, Zaman HM, Rouse RL, Paulsen DB, et al. Incomplete lung recovery following sub-acute inhalation of combustion-derived ultrafine particles in mice. *Part Fibre Toxicol*. (2016) 13:10. doi: 10.1186/s12989-016-0122-z

61. Mohammad MK, Avila D, Zhang J, Barve S, Arteel G, McClain C, et al. Acrolein cytotoxicity in hepatocytes involves endoplasmic reticulum stress, mitochondrial dysfunction and oxidative stress. *Toxicol Appl Pharmacol*. (2012) 265:73–82. doi: 10.1016/j.taap.2012.09.021

62. Sozen E, Ozer NK. Impact of high cholesterol and endoplasmic reticulum stress on metabolic diseases: an updated Mini-review. *Redox Biol*. (2017) 12:456–61. doi: 10.1016/j.redox.2017.02.025

frontiers | Frontiers in Public Health

TYPE Original Research
PUBLISHED 29 January 2025
DOI 10.3389/fpubh.2024.1410056

OPEN ACCESS

EDITED BY
Nishant Raj Kapoor,
Academy of Scientific and Innovative Research (AcSIR), India

REVIEWED BY
Tommaso Filippini,
University of Modena and Reggio Emilia, Italy
Ali Mentes,
Marmara University, Türkiye

*CORRESPONDENCE
Yanhui Gao
✉ gaoyanhui@hrbmu.edu.cn
Yanmei Yang
✉ yangyanmei@hrbmu.edu.cn

RECEIVED 31 March 2024
ACCEPTED 27 December 2024
PUBLISHED 29 January 2025

CITATION
Wu J, Qin M, Gao Y, Liu Y, Liu X, Jiang Y, Yang Y and Gao Y (2025) Association between fluoride exposure and the risk of serum CK and CK-MB elevation in adults: a cross-sectional study in China.
Front. Public Health 12:1410056.
doi: 10.3389/fpubh.2024.1410056

Association between fluoride exposure and the risk of serum CK and CK-MB elevation in adults: a cross-sectional study in China

Junhua Wu, Ming Qin, Yue Gao, Yang Liu, Xiaona Liu, Yuting Jiang, Yanmei Yang* and Yanhui Gao*

Center for Endemic Disease Control, Chinese Center for Disease Control and Prevention, Harbin Medical University, Harbin, China

Background: This study aimed to investigate the relationship between urinary fluoride concentration and myocardial disease.

Methods: This is a cross-sectional study that was conducted in three villages in Wenshui County, Shanxi Province. A total of 737 villagers were included in this analysis. Urinary fluoride was detected using a fluoride-ion selective electrode. Myocardial enzymes were detected using an automatic biochemical analyzer. Myocardial ischemia and arrhythmia were diagnosed using 12-lead electrocardiogram.

Results: The median level of urinary fluoride concentration was 1.32 mg/L. Urinary fluoride was associated with serum creatine kinase (CK) elevation (odds ratio [OR] = 1.39 [95% confidence interval (CI)]: 1.09–1.78) and CK isoenzyme (CK-MB) elevation (OR = 1.49 [95% CI: 1.12–1.97]). Stratified analysis revealed that urinary fluoride concentration was associated with CK elevation in villagers under the age of 60 years (OR = 1.80 [95% CI: 1.26–2.59]). This study found that there was a positive association between urinary fluoride concentration and the risk of CK-MB elevation in participants under the age of 60 years(OR = 2.18 [95% CI: 1.39–3.42]), those who were of female gender (OR = 1.53 [95% CI: 1.07–2.19]), those who were overweight/obese (OR = 1.96 [95% CI: 1.28–2.99]), those who had central obesity (OR = 1.59 [95% CI: 1.12–2.25]), consumed alcohol (OR = 1.49 [95% CI: 1.09–2.05]), and smoked (OR = 1.50 [95% CI: 1.10–2.04]).

Conclusion: Our study suggests that fluoride exposure is associated with the risk of serum CK and CK-MB elevation; however, it is not associated with myocardial ischemia, arrhythmia, serum lactate dehydrogenase (LDH), serum alpha-hydroxybutyrate dehydrogenase (α-HBD), or serum aspartate aminotransferase (AST). Further investigations are needed to substantiate our findings and explore the potential underlying mechanisms.

KEYWORDS

creatine kinase, creatine kinase isoenzyme, fluoride, myocardial ischemia, arrhythmia

1 Introduction

Excessive fluoride exposure is identified by the World Health Organization as one of the top ten chemicals that pose significant public health problems (1). Long-term exposure to excessive fluoride can result in fluorosis, and it may cause systemic health problems, including skeletal damage, such as dental fluorosis and skeletal fluorosis (2), and non-skeletal damage affecting the cardiovascular system, renal function, and the nervous system, among others (3). Of particular concern is cardiovascular damage that can cause a heavy disease burden in populations with high fluoride exposure, potentially becoming a public health concern in areas endemic to fluorosis (4).

An increasing number of human epidemiological studies have linked fluoride exposure to several cardiovascular diseases. Some studies have reported a positive relationship between fluoride levels in drinking water and the prevalence of hypertension, specifically high systolic blood pressure (5–7). A systematic review reports that high fluoride exposure can increase thyroid stimulating hormone (TSH) release, which may rise the risk of cardiovascular diseases (8). A cross-sectional study reveals a significant positive relationship between excessive fluoride exposure and the prevalence of carotid artery atherosclerosis (9). Previous studies have confirmed that elastic properties of the aorta are impaired in fluorosis patients and that fluorosis patients have left ventricular diastolic and global dysfunctions despite normal left ventricular systolic function (10, 11).

A study involving 61 patients establishes a positive relationship between fluoride uptake by the coronary arteries and cardiovascular risk (12). Moreover, some studies have revealed the association between fluoride exposure and myocardial disease. A case of fluoride poisoning in children is presented as ventricular arrhythmias (13). A hospital-based study has also confirmed that fluoride could develop arrhythmias in children with fluorosis (14). However, a cohort study in Sweden investigates that long-term drinking-water fluoride exposure is not associated with myocardial infarction (15). To the best of our knowledge, no study focuses on the relationship between excessive fluoride exposure and myocardial ischemia or arrhythmias in adults.

Meanwhile, some human epidemiological studies have focused on the relationship between fluoride intake from drinking water and myocardial function biomarkers. The National Health and Nutrition Examination Survey (2013–2016) among United States adolescents finds that fluoride intake from drinking water does not associate with the serum aspartate aminotransferase (AST) level (16). An epidemiological study on children reports that serum lactate dehydrogenase (LDH) activity is associated with fluoride intake from drinking water (17). However, no human epidemiological studies have investigated the relationship between fluoride intake from drinking water and the other effective indicators of cardiac function in adults, such as creatine kinase (CK), CK isoenzyme (CK-MB), and alpha-hydroxybutyrate dehydrogenase (α-HBD).

Therefore, this cross-sectional study, conducted in areas of Shanxi Province, China, where fluoride levels in drinking water are elevated, aims to investigate the relationship between fluoride exposure and myocardial disease, specifically in relation to myocardial enzymes in adults.

2 Materials and methods

2.1 Study population

Three villages—Gaoche, Xishe, and Xihan—located in Wenshui County, Shanxi Province, China, were selected as the investigation sites based on long-term monitoring conducted by the Shanxi Institute of Endemic Disease Prevention and Control. The fluoride concentration of drinking water in Xishe village was 1.45 mg/L. In comparison, it was 1.5 mg/L in both Gaoche and Xihan villages, exceeding the Chinese government's stipulated limit for drinking water standards (1.2 mg/L). The inclusion criteria for our study were as follows: Villagers aged 18 years or above, who were born and have lived in these three villages. A total of 1,096 villagers were included. The exclusion criteria were as follows: (i) Villagers with diseases related to the heart, liver, muscle, or bone and had taken related medications in recent weeks ($n = 1$); (ii) villagers who did not provide a fasting blood sample ($n = 311$); (iii) villagers who did not provide their urinary sample ($n = 47$). In total, 737 villagers were enrolled for subsequent analysis.

2.2 General and physical information collection

General and physical information, including demographic data (age, sex, education, family income, alcohol consumption, and smoking), and disease history, were collected by trained doctoral and postgraduate students using face-to-face interviews. The height, weight, and waist circumference (WC) were also measured by trained doctoral and postgraduate students based on the Chinese government's weight control healthcare service standards (GB/T 34821–2017). Blood pressure was measured thrice in the morning using an electronic sphygmomanometer. The body mass index (BMI) was calculated based on the height and weight.

2.3 Sample collection, determination, and quality control

Nurses collected 5 mL of fasting peripheral blood samples from each participant. The blood sample was centrifuged at 3,000 rpm for 10 min in 2 h, and the serum was transferred into 1.5-ml Eppendorf (EP, Corning Incorporated, New York, USA) tubes to detect myocardial function biomarkers and blood glucose levels. A 5-ml morning urine sample was also collected from each participant. All serum and urine samples were stored at −80°C in a refrigerator until analysis.

Urinary fluoride, an accepted internal measurement index of fluoride exposure (18), was detected using fluoride-ion selective electrodes according to the industry-standard method in China (WS/T 89–2015, Beijing, China). Each sample was analyzed twice, and the average result was used as the final urinary fluoride concentration.

Serum CK, serum CK-MB, serum LDH, serum α-HBD, serum AST, and blood glucose were measured using an automatic biochemical analyzer 3,100 (Hitachi Hi-TECH international TRADE Co., LTD, Shanghai, China). The reagent used for the measurement

was provided by MedicalSystem Biotechnology Co. Ltd. (Ningbo, China), and the tests were performed according to standard operating procedures (details are shown at https://www.nbmksw.com/). Cut-off points of elevation for each myocardial enzyme are shown in Supplementary Table S1. These points are based on the industry standard of reference intervals for common clinical biochemistry tests in China (WS/T 404.1-2012, Beijing, China) and a previous study (19).

2.4 Diagnosis of diabetes mellitus, hypertension, skeletal fluorosis, and cardiac abnormality

Diabetes mellitus and hypertension were diagnosed through fasting blood glucose measurements and blood pressure readings. The cut-off points of fasting blood glucose for diabetes mellitus was 6.1 mmol/L, which was recommended by the Guideline for the Prevention and Treatment of Type 2 Diabetes Mellitus in China (2020 edition). The cut-off points of hypertension was 140/90 mm Hg, which was recommended by the Chinese Hypertension League Guidelines on Ambulatory Blood Pressure Monitoring (2020). Standard simultaneous 12-lead electrocardiogram (ECG) examinations were recorded at a sampling rate of 10,000 Hz (MedEx-1694, Beijing Madix Technology Co. Ltd, Beijing, China) and stored for subsequent analysis. The same technician conducted all ECG examinations and the diagnoses were made by a cardiologist and a specially trained ECG healthcare professional. Myocardial ischemia and arrhythmia were diagnosed based on the previous studies (20, 21). Skeletal fluorosis was diagnosed following the Chinese Diagnostic Criteria of Endemic Skeletal Fluorosis (WS 192–2008, Beijing, China).

2.5 Statistical analysis

Mean ± standard deviation (SD) or median (P25–P75) was employed to describe the continuous variables, and the categorical variables were expressed as numbers (percentages). The normal distribution test for the levels of each myocardial function biomarker was conducted by P–P chart. The urinary fluoride concentration was divided into four categorical values based on quartile and was used for further statistical analyses. Based on our prior knowledge and the directed acyclic graph, age, sex, educational level, family income, alcohol consumption, smoking, BMI, WC, diabetes mellitus, and hypertension were selected as potential confounders (Supplementary Figure S1). Binary logistic regression models were used to investigate the relationship between urinary fluoride concentration and myocardial damage.

Stratified analyses by age (<60 years and ≥ 60 years), sex (male and female), BMI (normal and overweight/obesity), WC (normal and central obesity), alcohol consumption (yes and no), and smoking (yes and no) were conducted. Furthermore, sensitivity analyses were used to test the robustness of the main results, while participants who had diabetes mellitus or hypertension were excluded.

Data analyses were performed using R statistical software (version 4.2.1; R Core Team, New Jersey, USA) and Statistical Package for the Social Sciences (SPSS) version 23.0 for Windows (SPSS, Inc., Chicago, IL, United States), and two-sided p-values less than 0.05 were considered statistically significant.

3 Results

3.1 Participant characteristics

The demographic statistics of 737 participants are presented in Table 1. The mean (±SD) age of the participants was 57.78 (±11.54) years and the age of 47.20% of them were above 60 years. There were more female individuals (67.17%) in this study than male counterparts (32.83%). The proportion of individuals with higher educational levels was low, those with primary or lower accounted for 36.50%, the junior high school graduates were 53.03%, and the senior high school or higher were only 10.47%. Approximately 19.75% of participants were alcohol consumers and smokers. In addition, the family income of 61.90% of participants was above 10,000 ¥/year.

Physical statistics found that 38.79% of participants had hypertension, 8.29% of participants had diabetes mellitus, and 32.47% of participants had skeletal fluorosis. The mean (±SD) BMI of participants was 25.70 (±3.60) kg/m^2 and 67.03% of participants were found to be overweight and obese. In addition, the mean (±SD) WC was 87.35 (±9.55) cm, and 72.95% of participants had central obesity. ECG examinations found that 88 (12.21%) participants had myocardial ischemia and 38 (5.27%) participants had arrhythmia.

Urinary fluoride, serum levels of myocardial enzymes, and the proportion of myocardial enzyme elevation were also shown in Table 1. The median (P25–P75) level of serum CK, CK-MB, LDH, α-HBD, and AST were 98.00 (71.00–131.00) U/L, 14.90 (12.90–17.90) U/L, 191.80 (174.05–214.73) U/L, 156.50 (140.50–174.03) U/L, and 21.50 (18.30–26.20) U/L. The level of urinary fluoride concentration was 1.32 (0.90–1.81) mg/L.

3.2 Association between urinary fluoride concentrations and the risk of myocardial damage

The relationship between urinary fluoride concentration and the risk of myocardial damage is shown in Table 2. Binary logistic regression analysis found that the urinary fluoride concentration was positively associated with the risk of serum CK elevation (OR = 1.39 [95% CI: 1.09–1.78]) and CK-MB elevation (OR = 1.49 [95% CI: 1.12–1.97]).

Sensitivity analysis showed that the urinary fluoride concentration was also positively associated with the risk of serum CK elevation (OR = 1.73 [95%CI, 1.25–2.39]) and CK-MB elevation (OR = 1.80 [95% CI: 1.23–2.63]) when excluding participants with hypertension (Supplementary Table S2). In addition, when excluding participants with diabetes mellitus, we still found a positive association between urinary fluoride concentration and the risk of serum CK elevation (OR = 1.56 [95% CI: 1.20–2.02]) and CK-MB elevation (OR = 1.55 [95% CI: 1.15–2.10]) (Supplementary Table S3).

3.3 Relationship between urinary fluoride concentration and the risk of CK and CK-MB elevation in different subgroups

Stratified analysis was conducted in subgroups according to age, sex, BMI, WC, alcohol consumption, and smoking, with the goal of

10.3389/fpubh.2024.1410056

TABLE 1 Basic characteristics of general population (n = 737).

Characteristics	All observations
Age (y, means ± SD)	57.78 ± 11.54
< 60	387 (52.80)
≥ 60	346 (47.20)
Sex (*n*, %)	
Male	241 (32.83)
Female	493 (67.17)
Educational level (*n*, %)	
Primary and below	265 (36.50)
Junior high school	385 (53.03)
Senior high school and above	76 (10.47)
Family income (*n*, %)	
< 10 000 ¥/year	277 (38.10)
≥ 10 000 ¥/year	450 (61.90)
Alcohol drinking	
No	589 (80.24)
Yes	145 (19.75)
Smoking	
No	589 (80.24)
Yes	145 (19.75)
Hypertension (*n*, %)	
Yes	282 (38.79)
No	445 (61.21)
Diabetes mellitus (*n*, %)	
Yes	61 (8.29)
No	675 (91.71)
Skeletal fluorosis (*n*, %)	
Yes	238 (32.47)
No	495 (67.53)
BMI (kg/m^2, means ± SD)	25.70 ± 3.60
Normal	242 (32.97)
Overweight/obesity	492 (67.03)
Waistline (cm, means ± SD)	87.35 ± 9.55
Normal	198 (27.05)
Central obesity	534 (72.95)
Urinary fluoride (mg/L, median, P25-P75)	1.32 (0.90, 1.81)
Myocardial disease (*n*, %)	
Myocardial ischemia	88 (12.21)
Arrhythmia	38 (5.27)
AST (U/L, median, P25-P75)	21.50 (18.30, 26.20)
AST elevation	46 (6.35)
CK (U/L, median, P25-P75)	98.00 (71.00, 131.00)
CK elevation	66 (9.11)
CK-MB (U/L, median, P25-P75)	14.90 (12.90, 17.90)
CK-MB elevation	51 (7.02)
α-HBD (U/L, median, P25-P75)	156.50 (140.50, 174.03)
α-HBD elevation	122 (16.80)
LDH (U/L, median, P25-P75)	191.80 (174.05, 214.73)
LDH elevation	60 (8.26)

The number of AST, CK, CK-MB is 727, and α-HBD, LDH is 726.

revealing the association between urinary fluoride concentration and the risk of CK elevation, as presented in Table 3. There was a positive association between urinary fluoride concentration and the risk of serum CK elevation in participants under the age of 60 years (OR = 1.80 [95% CI: 1.26–2.59]). In addition, no interaction effect was found between urinary fluoride concentration and the remaining subgroups regarding the risk of serum CK elevation.

The same stratified analysis was conducted to assess the risk of CK-MB elevation in Table 4. There was a positive association between urinary fluoride concentration and the risk of CK-MB elevation in participants under the age of 60 years (OR = 2.18 [95% CI: 1.39–3.42]), female (OR = 1.53 [95% CI: 1.07–2.19]), overweight/obesity (OR = 1.96 [95% CI: 1.28–2.99]), central obesity (OR = 1.59 [95% CI: 1.12–2.25]), alcohol consumption (OR = 1.49 [95% CI: 1.09–2.05]), and smoking (OR = 1.50 [95% CI: 1.10–2.04]). No interaction effects were observed on the risk of serum CK-MB elevation.

4 Discussion

Cell experiments revealed that fluoride could induce damage in H9c2 cardiomyocytes (22), and myocardial damage would lead to a change in the level of myocardial enzymes. Some studies have reported that an association between fluoride exposure and myocardial infarction, serum CK, and LDH, although their conclusions remain inconsistent. In addition to CK and LDH, the most common myocardial enzyme spectrum in clinical practice include CK-MB, α-HBD, and AST (23, 24). Therefore, our study focused not only on the relationship between urinary fluoride concentration and the risk of myocardial enzymes (serum CK, serum CK-MB, serum LDH, serum α-HBD, and serum AST) but also on myocardial ischemia and arrhythmia in a population-based cross-sectional study. We found that urinary fluoride concentration was only positively associated with the risk of serum CK and CK-MB elevation; however, it was not associated with myocardial ischemia, arrhythmia, or the remaining myocardial enzymes.

Our research found the urinary fluoride concentration was not associated with myocardial ischemia, which was consistent with the study conducted in a large cohort study of 455,619 people in Sweden (15). However, our findings regarding the relationship between urinary fluoride concentration and arrhythmia were inconsistent with previous studies conducted on children with acute fluoride poisoning or chronic fluorosis (13, 14). These inconsistent findings of arrhythmia might be caused by the different doses of fluoride intake, duration of exposure, and specific age group.

There were three tissue- and compartment-specific CK isoenzymes, including CK-BB (brain), CK-MM (skeletal muscle), and CK-MB (cardiac muscle), which mainly catalyzed the reversible conversion of creatine and ATP to phosphocreatine and adenosine diphosphate (25). Previous studies have reported considerable controversy regarding the relationship between fluoride and CK. Animal experiments revealed that fluoride did not affect CK's activity *in vitro* (26). However, it also found that the activity of serum CK was significantly increased with sodium fluoride in another animal experiment (27). Our study's binary logistic regression analysis indicated that the urinary fluoride concentration was positively associated with serum CK elevation. Moreover, at the same time, this kind of positive relationship was confirmed by the sensitivity analyses in participants without diabetes or hypertension. According to these

TABLE 2 Associations between urinary fluoride concentrations and the risk of myocardial damage.

Outcomes	Urinary fluoride			*P* for trend
	Q_2	Q_3	Q_4	
Myocardial ischemia	1.07 (0.52, 2.21)	0.95 (0.46, 1.97)	1.53 (0.77, 3.03)	0.242
Arrhythmia	0.90 (0.35, 2.33)	0.63 (0.23, 1.72)	0.72 (0.27, 1.94)	0.404
CK	1.81 (0.79, 4.17).	1.68 (0.72, 3.90)	**3.09 (1.39, 6.87)**	**0.008**
CK-MB	1.72 (0.65, 4.55)	1.33 (0.48, 3.70)	**3.66 (1.47, 9.09)**	**0.006**
LDH	0.36 (0.13, 0.99)	1.06 (0.49, 2.30)	1.16 (0.55, 2.47)	0.245
α-HBD	1.01 (0.54, 1.90)	1.30 (0.71, 2.38)	1.22 (0.67, 2.24)	0.384
AST	0.61 (0.23, 1.65)	1.17 (0.50, 2.75)	1.11 (0.46, 2.68)	0.523

Models were adjusted for age, sex, educational level, family income, BMI, waistline, alcohol drinking, smoking, hypertension and diabetes mellitus. Q_1 as reference group. The bold values means the difference among groups have statistical significant.

TABLE 3 Associations between urinary fluoride concentrations and the risk of CK elevation in subgroups.

Subgroup	No of events (%)	Urinary fluoride			*P*-interaction
		Q_2	Q_3	Q_4	
Age (years)					0.29
< 60	35 (9.19)	**7.21 (1.51, 34.40)**	**5.57 (1.15, 26.96)**	**12.79 (2.69, 60.93)**	
≥ 60	31 (9.06)	0.64 (0.19, 2.10)	0.74 (0.23, 2.31)	1.22 (0.45, 3.23)	
Sex					0.75
Male	26 (11.02)	2.37 (0.64, 8.75)	2.05 (0.52, 8.09)	2.88 (0.75, 11.13)	
Female	40 (8.20)	1.55 (0.52, 4.69)	1.52 (0.52, 4.48)	**2.95 (1.09, 8.00)**	
BMI (kg/m^2)					0.25
Normal	21 (8.90)	4.39 (0.83, 23.17)	3.36 (0.56, 20.14)	**7.94 (1.42, 44.45)**	
Overweight/obesity	45 (9.28)	1.36 (0.49, 3.78)	1.42 (0.53, 3.80)	2.39 (0.94, 6.10)	
Waistline (cm)					0.11
Normal	14 (7.14)	**10.90 (1.13, 104.95)**	3.32 (0.26, 42.07)	**17.69 (1.59, 197.27)**	
Central obesity	52 (9.89)	1.31 (0.50, 3.41)	1.64 (0.66, 4.08)	**2.53 (1.06, 6.04)**	
Alcohol drinking					0.75
No	52 (8.93)	1.39 (0.53, 3.62)	1.61 (0.64, 4.06)	**2.97 (1.22, 7.19)**	
Yes	14 (9.86)	4.44 (0.69, 28.57)	2.09 (0.24, 18.19)	4.21 (0.59, 30.07)	
Smoking					0.98
No	54 (9.26)	1.54 (0.61, 3.91)	1.83 (0.75, 4.44)	**2.75 (1.17, 6.48)**	
Yes	12 (8.51)	6.14 (0.59, 63.95)	1.01 (0.05, 19.72)	**15.79 (1.23, 203.35)**	

Models were adjusted for age, sex, educational level, family income, BMI, waistline, alcohol drinking, smoking, hypertension and diabetes mellitus, with stratified variables not adjusted in the stratified analysis. *P*-interaction values was adjusted by FDR - corrected. Q_1 as reference group. The bold values means the difference among groups have statistical significant.

analyses, it prompted that the fluoride could be associated with estimated myocardial damage. In addition, our study found that the urinary fluoride concentration was positively associated with serum CK elevation in people under the age of 60 years. It might be caused by more physical labor and muscle in people under the age of 60 years. Hence, further research should be conducted to determine the potential underlying mechanisms of this effect.

As a type of CK isoenzyme, CK-MB had higher sensitivity in detecting acute myocardial infarction, which was close to 100% (28). Animal experiments revealed that sodium fluoride intervention (set at 300 mg/mL for 10 days) could increase serum CK-MB in male rats (29). Coincidentally, this relationship was also confirmed in a study involving a group of male rats exposed to high doses of sodium fluoride (administered at 45 and 90 mg F-/kg body weight/24 hours treated rats) (30). To the best of our knowledge, there were no studies focused on the relationship between urinary fluoride concentration and serum CK-MB elevation in a natural population. In addition, in contrast to previous studies that focused on male animals, our study found that fluoride exposure was a risk factor for CK-MB elevation in females rather than males. It might be caused by the different concentrations of calcium between males and females, and further studies on female rats should be conducted. Moreover, we also found that fluoride exposure was a risk factor for CK-MB elevation in participants without alcohol consumption or smoking, which the sex distribution might cause. Previous studies revealed that obesity was a risk factor for cardiomyopathy caused by the calcium homeostasis disequilibrium in mitochondria and oxidative stress (31). Our research also found that fluoride exposure was a risk factor for serum

TABLE 4 Associations between urinary fluoride concentrations and the risk of CK-MB elevation in subgroups.

Subgroup	No of events (%)	Urinary fluoride			*P*-interaction
		Q_2	Q_3	Q_4	
Age (years)					0.26
< 60	26 (6.82)	1.37 (0.29, 6.59)	2.89 (0.71, 11.85)	**8.70 (2.19, 34.54)**	
≥ 60	25 (7.31)	1.71 (0.48, 6.17)	0.39 (0.07, 2.27)	1.92 (0.56, 6.56)	
Sex					0.99
Male	18 (7.63)	2.83 (0.53, 15.25)	2.16 (0.36, 12.90)	4.12 (0.74, 22.84)	
Female	33 (6.76)	1.30 (0.38, 4.48)	0.98 (0.27, 3.60)	**3.46 (1.17, 10.22)**	
BMI (kg/m^2)					0.99
Normal	24 (10.08)	1.69 (0.47, 6.10)	1.68 (0.42, 6.77)	1.68 (0.42, 6.73)	
Overweight/obesity	27 (5.56)	1.55 (0.33, 7.24)	1.29 (0.28, 6.06)	**6.22 (1.69, 22.97)**	
Waistline (cm)					0.99
Normal	17 (8.67)	3.15 (0.51, 19.37)	4.38 (0.70, 27.45)	3.39 (0.51, 22.45)	
Central obesity	34 (6.46)	1.41 (0.42, 4.68)	0.83 (0.21, 3.22)	**3.84 (1.32, 11.20)**	
Alcohol drinking					0.99
No	42 (6.34)	1.41 (0.48, 4.16)	1.29 (0.43, 3.88)	**3.39 (1.25, 9.17)**	
Yes	9 (7.22)	3.84 (0.31, 48.14)	1.21 (0.06, 25.06)	8.84 (0.70, 110.96)	
Smoking					0.93
No	42 (6.38)	1.29 (0.45, 3.73)	0.95 (0.31, 2.92)	**3.35 (1.32, 8.50)**	
Yes	9 (7.20)	-	-	-	

Models were adjusted for age, sex, educational level, family income, BMI, waistline, alcohol drinking, smoking, hypertension and diabetes mellitus, with stratified variables not adjusted in the stratified analysis. *P*-interaction values was adjusted by FDR - corrected. Q_1 as reference group. The bold values means the difference among groups have statistical significant.

CK-MB elevation in obese participants, which the additive effect of fluoride exposure and obesity might cause.

Epidemiological studies in children found that serum LDH activity was associated with drinking water fluoride in children (17), and this relationship was also found in cell and animal experiments (9, 26, 32, 33). However, our study found no significant association between urinary fluoride concentration and the risk of serum LDH elevation. This inconsistent result in the population study might be due to the potential confounders we had controlled in our research, but not in those previous studies. α-HBD comprised the total activity of some LDH isoenzymes, namely LDH1 and LDH2, which were mainly found in myocardial damage (34, 35). As a serological biomarker for myocardial alteration, no studies that investigated the relationship between fluoride and α-HBD before. Hence, our study first reported that fluoride exposure in the population could not increase the risk of serum α-HBD elevation.

AST was still the most important biomarker for myocardial injury (36). Our study found there was no association between urinary fluoride concentration and the risk of AST elevation, which was consistent with a study based on 1,742 adolescents (16).

Our research had some limitations. First, our study was a natural population cross-sectional investigation, which could not determine the exact causality between urinary fluoride concentration and the risk of serum CK, CK-MB elevation. Second, some known cardiovascular-related confounders were not included in our research. Meanwhile, the participants in our research might consume fluoride in different ways than drinking water, such as food, which needs further evaluation. Third, our assessment of fluoride exposure was limited to urinary fluoride measurements, thereby excluding other potential sources of exposure, such as drinking water and dietary intake. Finally, this was a single-center study and did not include the different types of fluorosis, such as brick-tea-type fluorosis or chronic coal-burning fluorosis.

5 Conclusion

In conclusion, our study provides population-based evidence for the relationship between urinary fluoride concentration and myocardial disease related to myocardial enzymes, including CK, CK-MB, LDH, α-HBD, and AST. Notably, fluoride exposure may be associated with the risk of serum CK and CK-MB elevation in adults but not with myocardial ischemia, arrhythmia, serum LDH, serum α-HBD, and serum AST. Further investigations are needed to substantiate our findings, elucidate the potential mechanism underlying fluoride-induced elevation of CK and CK-MB, and explore how fluoride-induced changes in myocardial enzymes may affect myocardial injury.

Data availability statement

The original contributions presented in the study are included in the article/Supplementary material, further inquiries can be directed to the corresponding authors.

Ethics statement

The studies involving humans were approved by Ethical Review Board of Center for Endemic Disease Control, Chinese Center for

Disease Control and Prevention. The studies were conducted in accordance with the local legislation and institutional requirements. Written informed consent for participation in this study was provided by the participants' legal guardians/next of kin. The manuscript presents research on animals that do not require ethical approval for their study.

Author contributions

JW: Formal analysis, Writing – original draft, Writing – review & editing. MQ: Data curation, Methodology, Writing – review & editing. YuG: Data curation, Methodology, Writing – review & editing. YL: Data curation, Formal analysis, Writing – review & editing. XL: Data curation, Formal analysis, Investigation, Methodology, Writing – review & editing. YJ: Investigation, Writing – review & editing. YY: Formal analysis, Investigation, Methodology, Project administration, Writing – review & editing. YaG: Data curation, Formal analysis, Funding acquisition, Investigation, Methodology, Project administration, Resources, Writing – review & editing.

Funding

The author(s) declare that financial support was received for the research, authorship, and/or publication of this article. This study was supported by the National Key R&D Program of China (2022YFC2503000).

Acknowledgments

We sincerely thank for the participants and the Institute of Endemic Disease Prevention and Control of Shanxi Province for their selfless contribution.

Conflict of interest

The authors declare that the research was conducted in the absence of any commercial or financial relationships that could be construed as a potential conflict of interest.

Publisher's note

All claims expressed in this article are solely those of the authors and do not necessarily represent those of their affiliated organizations, or those of the publisher, the editors and the reviewers. Any product that may be evaluated in this article, or claim that may be made by its manufacturer, is not guaranteed or endorsed by the publisher.

Supplementary material

The Supplementary material for this article can be found online at: https://www.frontiersin.org/articles/10.3389/fpubh.2024.1410056/full#supplementary-material

References

1. World Health Organization. Lead poisoning and health. (2018) Available at: http://www.who.int/news-room/fact-sheets/detail/lead-poisoning-and-health (Accessed March 05, 2020).

2. Veneri F, Iamandii I, Vinceti M, Birnbaum LS, Generali L, Consolo U, et al. Fluoride exposure and skeletal fluorosis: a systematic review and dose-response Meta-analysis. *Curr Environ Health Rep*. (2023) 10:417–41. doi: 10.1007/s40572-023-00412-9

3. Zhou J, Sun D, Wei W. Necessity to pay attention to the effects of low fluoride on human health: an overview of skeletal and non-skeletal damages in epidemiologic investigations and laboratory studies. *Biol Trace Elem Res*. (2023) 201:1627–38. doi: 10.1007/s12011-022-03302-7

4. Kurdi MS. Chronic fluorosis: the disease and its anaesthetic implications. *Indian J Anaesth*. (2016) 60:157–62. doi: 10.4103/0019-5049.177867

5. Koh S, Park S. The association between fluoride in water and blood pressure in children and adolescents. *Pediatr Res*. (2022) 92:1767–72. doi: 10.1038/s41390-022-01982-4

6. Sun L, Gao Y, Liu H, Zhang W, Ding Y, Li B, et al. An assessment of the relationship between excess fluoride intake from drinking water and essential hypertension in adults residing in fluoride endemic areas. *Sci Total Environ*. (2013) 443:864–9. doi: 10.1016/j.scitotenv.2012.11.021

7. Liu Y, Téllez-Rojo M, Sánchez BN, Ettinger AS, Osorio-Yáñez C, Solano M, et al. Association between fluoride exposure and cardiometabolic risk in peripubertal Mexican children. *Environ Int*. (2020) 134:105302. doi: 10.1016/j.envint.2019.105302

8. Iamandii I, De Pasquale L, Giannone ME, Veneri F, Generali L, Consolo U, et al. Does fluoride exposure affect thyroid function? A systematic review and dose-response meta-analysis. *Environ Res*. (2024) 242:117759. doi: 10.1016/j.envres.2023.117759

9. Liu H, Zeng Q, Cui Y, Yu L, Zhao L, Hou C, et al. The effects and underlying mechanism of excessive iodide on excessive fluoride-induced thyroid cytotoxicity. *Environ Toxicol Pharmacol*. (2014) 38:332–40. doi: 10.1016/j.etap.2014.06.008

10. Varol E, Akcay S, Ersoy IH, Koroglu BK, Varol S. Impact of chronic fluorosis on left ventricular diastolic and global functions. *Sci Total Environ*. (2010) 408:2295–8. doi: 10.1016/j.scitotenv.2010.02.011

11. Varol E, Akcay S, Ersoy IH, Ozaydin M, Koroglu BK, Varol S. Aortic elasticity is impaired in patients with endemic fluorosis. *Biol Trace Elem Res*. (2010) 133:121–7. doi: 10.1007/s12011-009-8578-4

12. Li Y, Berenji GR, Shaba WF, Tafti B, Yevdayev E, Dadparvar S. Association of vascular fluoride uptake with vascular calcification and coronary artery disease. *Nucl Med Commun*. (2012) 33:14–20. doi: 10.1097/MNM.0b013e32834c187e

13. Yolken R, Konecny P, McCarthy P. Acute fluoride poisoning. *Pediatrics*. (1976) 58:90–3. doi: 10.1542/peds.58.1.90

14. Karademir S, Akçam M, Kuybulu AE, Olgar S, Oktem F. Effects of fluorosis on QT dispersion, heart rate variability and echocardiographic parameters in children. *Anadolu Kardiyol Derg*. (2011) 11:150–5. doi: 10.5152/akd.2011.038

15. Näsman P, Granath F, Ekstrand J, Ekbom A, Sandborgh-Englund G, Fored CM. Natural fluoride in drinking water and myocardial infarction: a cohort study in Sweden. *Sci Total Environ*. (2016) 562:305–11. doi: 10.1016/j.scitotenv.2016.03.161

16. Malin AJ, Lesseur C, Busgang SA, Curtin P, Wright RO, Sanders AP. Fluoride exposure and kidney and liver function among adolescents in the United States: NHANES, 2013-2016. *Environ Int*. (2019) 132:105012. doi: 10.1016/j.envint.2019.105012

17. Xiong X, Liu J, He W, Xia T, He P, Chen XM, et al. Dose-effect relationship between drinking water fluoride levels and damage to liver and kidney functions in children. *Environ Res*. (2007) 103:112–6. doi: 10.1016/j.envres.2006.05.008

18. Zhao L, Yu C, Lv J, Cui Y, Wang Y, Hou C, et al. Fluoride exposure, dopamine relative gene polymorphism and intelligence: a cross-sectional study in China. *Ecotoxicol Environ Saf*. (2021) 209:111826. doi: 10.1016/j.ecoenv.2020.111826

19. Huang S, Liu Z, Ge X, Luo X, Zhou Y, Li D, et al. Occupational exposure to manganese and risk of creatine kinase and creatine kinase-MB elevation among ferromanganese refinery workers. *Am J Ind Med*. (2020) 63:394–401. doi: 10.1002/ajim.23097

20. Elhaj FA, Salim N, Harris AR, Swee TT, Ahmed T. Arrhythmia recognition and classification using combined linear and nonlinear features of ECG signals. *Comput Methods Prog Biomed*. (2016) 127:52–63. doi: 10.1016/j.cmpb.2015.12.024

21. Ibanez B, James S, Agewall S, Antunes MJ, Bucciarelli-Ducci C, Bueno H, et al. 2017 ESC guidelines for the management of acute myocardial infarction in patients presenting with ST-segment elevation: the task force for the management of acute myocardial infarction in patients presenting with ST-segment elevation of the European Society of Cardiology (ESC). *Eur Heart J*. (2018) 39:119–77. doi: 10.1093/eurheartj/ehx393

22. Yan X, Wang L, Yang X, Qiu Y, Tian X, Lv Y, et al. Fluoride induces apoptosis in H9c2 cardiomyocytes via the mitochondrial pathway. *Chemosphere*. (2017) 182:159–65. doi: 10.1016/j.chemosphere.2017.05.002

23. Li SW, Sun X, He Y, Guo Y, Zhao HJ, Hou ZJ, et al. Assessment of arsenic trioxide in the heart of *Gallus gallus*: alterations of oxidative damage parameters, inflammatory cytokines, and cardiac enzymes. *Environ Sci Pollut Res Int*. (2017) 24:5781–90. doi: 10.1007/s11356-016-8223-7

24. Wang L, Zheng M, Tang Y, Yin Y, Liu Y, Liu G. Impact of various periods of perfusion-pause and reperfusion on the severity of myocardial injury in the langenodorff model. *Perfusion*. (2023) 38:1609–16. doi: 10.1177/02676591221122349

25. Del Franco A, Ambrosio G, Baroncelli L, Pizzorusso T, Barison A, Olivotto I, et al. Creatine deficiency and heart failure. *Heart Fail Rev*. (2022) 27:1605–16. doi: 10.1007/s10741-021-10173-y

26. Nedeljković M, Matović V, Soldatović D. Levels of lactate dehydrogenase and creatine kinase in plasma of fluoride-treated rabbits. *J Appl Toxicol*. (1985) 5:11–3. doi: 10.1002/jat.2550050103

27. Hassan HA, Yousef MI. Mitigating effects of antioxidant properties of black berry juice on sodium fluoride induced hepatotoxicity and oxidative stress in rats. *Food Chem Toxicol*. (2009) 47:2332–7. doi: 10.1016/j.fct.2009.06.023

28. Mair J, Morandell D, Genser N, Lechleitner P, Dienstl F, Puschendorf B. Equivalent early sensitivities of myoglobin, creatine kinase MB mass, creatine kinase isoform ratios, and cardiac troponins I and T for acute myocardial infarction. *Clin Chem*. (1995) 41:1266–72. doi: 10.1093/clinchem/41.9.1266

29. Oyagbemi AA, Omobowale TOAsenuga ER, Adejumobi AO, Ajibade TOIge TM, et al. Sodium fluoride induces hypertension and cardiac complications through generation of reactive oxygen species and activation of nuclear factor kappa beta. *Environ Toxicol*. (2017) 32:1089–101. doi: 10.1002/tox.22306

30. Panneerselvam L, Govindarajan V, Ameeramja J, Nair HR, Perumal E. Single oral acute fluoride exposure causes changes in cardiac expression of oxidant and antioxidant enzymes, apoptotic and necrotic markers in male rats. *Biochimie*. (2015) 119:27–35. doi: 10.1016/j.biochi.2015.10.002

31. Ren J, Wu NN, Wang S, Sowers JR, Zhang Y. Obesity cardiomyopathy: evidence, mechanisms, and therapeutic implications. *Physiol Rev*. (2021) 101:1745–807. doi: 10.1152/physrev.00030.2020

32. Chen L, Ning H, Yin Z, Song X, Feng Y, Qin H, et al. The effects of fluoride on neuronal function occurs via cytoskeleton damage and decreased signal transmission. *Chemosphere*. (2017) 185:589–94. doi: 10.1016/j.chemosphere.2017.06.128

33. Pal P, Mukhopadhyay PK. Fluoride induced testicular toxicities in adult Wistar rats. *Toxicol Mech Methods*. (2021) 31:383–92. doi: 10.1080/15376516.2021.1891489

34. Lee S, Koppensteiner R, Kopp CW, Gremmel T. α-Hydroxybutyrate dehydrogenase is associated with atherothrombotic events following infrainguinal angioplasty and stenting. *Sci Rep*. (2019) 9:18200. doi: 10.1038/s41598-019-54899-0

35. Ruzich RS. Cardiac enzymes. How to use serial determinations to confirm acute myocardial infarction. *Postgrad Med*. (1992) 92:85–92. doi: 10.1080/00325481.1992.11701533

36. Lofthus DM, Stevens SR, Armstrong PW, Granger CB, Mahaffey KW. Pattern of liver enzyme elevations in acute ST-elevation myocardial infarction. *Coron Artery Dis*. (2012) 23:22–30. doi: 10.1097/MCA.0b013e32834e4ef1

frontiers | Frontiers in Public Health

TYPE Original Research
PUBLISHED 14 March 2025
DOI 10.3389/fpubh.2025.1416264

OPEN ACCESS

EDITED BY
Pu Xia,
University of Birmingham, United Kingdom

REVIEWED BY
Slawomir Gonkowski,
University of Warmia and Mazury in Olsztyn, Poland
Brigitte Reimann,
University of Hasselt, Belgium
Gülcan Gencer,
Afyonkarahisar Health Sciences University, Türkiye

*CORRESPONDENCE
Jung-Wei Chang
✉ jungwei723@nycu.edu.tw

RECEIVED 12 April 2024
ACCEPTED 25 February 2025
PUBLISHED 14 March 2025

CITATION
Huang P-C, Chen H-C, Huang H-B, Lin Y-L, Chang W-T, Leung S-H, Chen H and Chang J-W (2025) Mediating effects of insulin resistance on lipid metabolism with elevated paraben exposure in the general Taiwan population.
Front. Public Health 13:1416264.
doi: 10.3389/fpubh.2025.1416264

Mediating effects of insulin resistance on lipid metabolism with elevated paraben exposure in the general Taiwan population

Po-Chin Huang[1,2,3], Hsin-Chang Chen[4], Han-Bin Huang[5], Yu-Lung Lin[1], Wan-Ting Chang[1], Shih-Hao Leung[6], Hsi Chen[6] and Jung-Wei Chang[6]*

[1]National Institute of Environmental Health Sciences, National Health Research Institutes, Miaoli, Taiwan, [2]Department of Medical Research, China Medical University Hospital, China Medical University, Taichung, Taiwan, [3]Research Center for Precision Environmental Medicine, Kaohsiung Medical University, Kaohsiung, Taiwan, [4]Department of Chemistry, Tunghai University, Taichung, Taiwan, [5]School of Public Health, National Defense Medical Center, Taipei, Taiwan, [6]Institute of Environmental and Occupational Health Sciences, School of Medicine, National Yang Ming Chiao Tung University, Taipei, Taiwan

Introduction: Parabens are commonly used to prevent bacteria from growing in cosmetics and foodstuffs. Parabens have been reported to influence hormone regulation, potentially leading to metabolic anomalies, including insulin resistance and obesity. However, there is a paucity of knowledge regarding the relationship between urinary paraben levels and lipid metabolism in the general Taiwanese population. Therefore, the objective of this study was to determine whether the mediating role of insulin resistance exists between paraben exposure and lipid metabolism.

Methods: We selected the data of 264 adult participants from a representative survey in five major Taiwan area in 2013. UPLC tandem mass spectrometry was used to examine four urine parabens: methyl- (MeP), ethyl- (EtP), propyl- (PrP) and butyl- (BuP). Blood samples were analyzed for concentrations of glucose and lipid metabolic indices using the DxI 800 immunoassay analyzer and immunoradiometric assay kit. The relationship between urinary paraben levels and metabolism indices were evaluated through a multiple linear regression analysis. Finally, a mediation analysis was employed to understand the underlying mechanism by which paraben exposure influences lipid metabolism through insulin resistance.

Results: The significant positive association between MeP exposure and Castelli risk index I (CRI-I; $\beta = 0.05$, $p = 0.049$) was found, and also exhibited the similar associations between EtP exposure and low-density lipoprotein cholesterol ($\beta = 0.10$, $p = 0.001$), total cholesterol ($\beta = 0.06$, $p = 0.003$), and non-HDL cholesterol (NHC; $\beta = 0.08$, $p = 0.005$). EtP exhibited a significant positive association with triglyceride BMI (TyG-BMI; $\beta = 0.02$, $p = 0.040$). Additionally, TyG-BMI was positively associated with CRI-I ($\beta = 0.98$, $p < 0.001$), CRI-II ($\beta = 1.03$, $p < 0.001$) and NHC ($\beta = 0.63$, $p < 0.001$). Moreover, insulin resistance served as mediators for the effects of EtP exposure on lipid metabolism indices.

Discussion: The results indicate that changes in insulin resistance mediated the relationship between urinary paraben and lipid metabolism. Large-scale epidemiological and animal studies are warranted to identify biological mechanisms underlying validate these relationships.

KEYWORDS

parabens, endocrine disruptors, lipid metabolism, insulin resistance, mediation analysis

1 Introduction

Obesity has reached epidemic proportions globally, imposing a considerable public health burden in both developed and developing countries (1). According to the Nutrition and Health Survey in Taiwan (NAHSIT), the prevalence of general and abdominal obesity has been increasing from 16–20% and 27–47% from 1993–2016, respectively (55), and it increases the risk of chronic diseases such as cardiovascular disease, and type 2 diabetes (2). In Taiwan, the average body mass index (BMI) of adults is 24.5 kg/m^2, which exceeds the standard for overweight set by Taiwan's Health Promotion Administration (BMI $\geq$ 24 kg/m^2). The prevalence of overweight and obesity in adults was reported to be 50.7%, indicating that approximately half of the adult population has obesity (56). Factors such as genetic predisposition and lifestyle choices, including diet and physical activity, contribute to the complex etiology of obesity (3, 4). There is more evidence that certain endocrine disruptors, such as parabens, could play a role in the development of obesity and diabetes (5–7).

Parabens are extensively used as artificial preservatives in cosmetics and foodstuffs (8, 9) due to their chemical stability, low cost, and broad-spectrum antimicrobial properties (10). The chemical structure of parabens comprises a benzene ring, with a hydroxyl group and an ester group on the para position (11). Parabens differ in the alkyl chain length on the ester group and can be categorized into two types, including short alkyl-chain parabens (e.g., methylparaben, MeP) and long alkyl-chain parabens (e.g., butylparaben, BuP) (9). In addition, methyl paraben (MeP), ethyl paraben (EtP), propyl paraben (PrP), and butyl paraben (BuP) are the most commonly used parabens in commercial products (12), with the maximum usage level of 0.4% for a single compound and 0.8% for mixtures (13). Moreover, benzylparaben (BzP) and heptyl paraben (HeP) were not always incorporated into exposure assessments and statistical analyses due to their low frequency of detection in previous studies, unless stated otherwise (14).

Typical exposure routes for parabens include inhalation, ingestion, and dermal absorption; the latter is the primary exposure route for the general population, primarily owing to the widespread use of parabens in Personal care products (PCPs) (10). In recent years, the potential of parabens to cause endocrine disruption has elevated concerns about exposure to these chemicals.

In vitro studies have found that parabens have abilities in activating the glucocorticoid receptor and peroxisome proliferator-activated receptor γ (PPARγ) in 3 T3-L1 preadipocytes. Parabens could promote the differentiation of 3 T3-L1 adipocytes and increase their adipogenic potency, such as by increasing the synthesis and accumulation of triglycerides (15). Furthermore, animal studies have indicated that parabens can stimulate adipocyte differentiation and lipogenesis in white adipose tissue and liver fat cells in female rats, which includes the processes of fatty acid synthesis and subsequent triglyceride synthesis (16).

In epidemiology, studies have also evaluated associations between paraben exposure and human lipid-related traits. Parabens can cause a range of adverse health effects, particularly in the endocrine system. A growing body of evidence from epidemiological and toxicological studies indicates that paraben exposure may be associated with metabolic disorders, including obesity and diabetes mellitus (DM). A longitudinal study conducted on a sub-sample of the Granada EPIC-Spain cohort (n = 670) revealed that individuals with elevated levels of PrP exhibited an elevated risk of developing type 2 diabetes after a 23-year follow-up period (57). Furthermore, exposure to MeP and EtP has been linked to an increased risk of DM, with EtP exhibiting a positive association with a higher risk of obesity (17). Blood plasma samples were collected from 27 healthy women at various points throughout their menstrual cycles in order to examine the potential correlation between paraben exposure and obesity (58). The plasma levels of methylparaben, as well as the sum of parabens, were found to be positively associated with plasma adipsin levels. Conversely, a negative correlation was observed between methylparaben levels and glucagon, leptin, and PAI-1.

Some critical indices for assessing lipid metabolism include Triglyceride (TG), Total cholesterol (TC), high-density lipoprotein cholesterol (HDLC), and low-density lipoprotein cholesterol (LDLC). Additionally, other indices such as Castelli risk index (CRI-I and CRI-II), non-HDLC (NHC), and the atherogenic coefficient (AC) have been used to assess cardiovascular disease status and coronary artery disease risk (18–20). Disruptions in glucose homeostasis could also affect lipid metabolism. Moreover, insulin resistance can alter systemic lipid metabolism, leading to dyslipidemia. It can lead to elevated TG and LDLC levels and reduced HDLC levels (21, 22).

The above studies suggest that endocrine disrupters may affect human lipid metabolism. Moreover, the literature also reveals that the Taiwanese is commonly exposed to parabens (23, 24). However, the knowledge gap that exists between paraben exposure and lipid metabolism in the general Taiwanese population. Furthermore, fewer studies have investigated the mechanism through which insulin resistance mediates the relationship between urinary paraben levels and lipid metabolism.

To address the aforementioned research gaps, we aimed to investigate the relationship between urinary paraben levels, insulin resistance, and lipid metabolism in Taiwanese adults. Additionally, we explored whether insulin resistance served as mediators for the effects of paraben exposure on lipid metabolism indices. It is hypothesized that parabens may contribute to the development of obesity and cardiovascular disease through the promotion of insulin resistance and dyslipidaemia.

2 Methods

2.1 Characteristics of participants

Participants for this study were selected from the Taiwan Environmental Survey for Toxicants (TEST) 2013. A number of studies have previously detailed the participant recruitment, selection methods and approval from the Institutional Review Board of National Yang Ming Chiao Tung University in Taiwan (23–25).

Abbreviations: AC, atherogenic coefficient; BuP, butylparaben; CRI-I, Castelli risk index I; CRI-II, Castelli risk index II; EDCs, endocrine-disrupting chemicals; EtP, ethylparaben; HDLC, high-density lipoprotein cholesterol; HOMA-IR, homeostasis model assessment of insulin resistance; LDLC, low-density lipoprotein cholesterol; LOD, limit of detection; LLOQ, lower limit of quantification; NHC, non-HDL cholesterol; PrP, propylparaben; PPARγ, peroxisome proliferator-activated receptor gamma; TC, total cholesterol; TG, triglyceride; TyG-BMI, triglyceride body mass index.

For the present study, participants aged ≥18 years were included and selected from 11 counties and cities from 5 regions in Taiwan: Northern, Central, Southern, Eastern, and one remote island. The sampling period spanned from May to December 2013. A total of 394 individuals were included through events held at elementary schools and community centers, yielding a response rate of approximately 78%. Before enrollment, all individuals provided informed consent and volunteered to participate in the NAHSIT. After the participants provided informed consent, their first-morning urine samples and fasting blood samples were collected; The concentration of parabens in the urine of an individual may fluctuate considerably over time due to a number of factors, including age, sex, lifestyle, diet, medical history, and environmental exposures. The precise impact of these variables on urinary paraben exposure among study participants remains unclear. Each participant was requested to complete a retrospective questionnaire encompassing demographic information (age and sex), BMI (body mass index) categories (i.e., <24 kg/m^2, 24 < = & <27 kg/m^2, and ≥ 27 kg/m^2), geographical location (northern, central, southern, eastern, and remote islands), and educational attainment (≤elementary school, junior high school, senior high school, and ≥ college/graduates), annual family income (<15,625, 15,625–31,250, >31,250 USD), lifestyle factors (cigarette smoking and alcohol consumption) and PCP uses. Participants were categorized into different groups for the purpose of comparison, including different age groups (18–40, 40–65, and 65 and older). In addition, the term "cigarette smoking" is defined as the act of consuming at least one cigarette per day, as reported by the subjects. The subjects were self-reported lifelong non-smokers (never-smokers) who had involuntarily inhaled smoke from cigarettes or other tobacco products. The term "alcohol consumption" is defined as the ingestion of at least one bottle of alcohol per week. Subject who self-reported using at least one kind of PCPs (personal care products), including body wash, lotion, perfume, and nail polishes. The BMI standard for adults was divided into three groups: weight standard (BMI < 24 kg/m^2), overweight (24≦BMI < 27 kg/m^2) and obesity (BMI≧27 kg/m^2) (59).

Anthropometric variables, including height, body weight, percentage body fat, and body mass index (BMI), were measured in accordance with standardized procedures outlined by Lohman et al. (60). Body height was measured with a portable stadiometer (model AD-6227R, manufactured by A&D Co., Ltd., Tokyo, Japan) to the nearest 0.1 cm. Body mass (0.1 kg) was evaluated by a bioelectrical impedance analyzer (model BC-418, manufactured by Tanita, Japan). BMI was calculated by dividing body weight (kg) by body height squared (m).

Of the original 394 subjects, a total of 28 were excluded from the study due to an insufficient number of urine samples and 27 were excluded due to an insufficient number of biochemical indicators. Additionally, 75 minors were excluded from the study. Our study included 264 TEST participants aged >18 years. Of these participants, 55 were excluded owing to inadequate urine or blood samples. Accordingly, a total of 264 participants were recruited in this study, comprising 125 men and 139 women. Participants aged between 40 and 65 years constituted the largest proportion of our study population (47.7%) (Table 1; Supplementary Figure S1). Moreover, 50.0% of the participants were of standard body weight, and 24.1 and 26.3% were overweight and obese, respectively. Regarding education level, 29.2% of the participants held a college degree or above. Furthermore, 58.1% of the participants reported having an annual household income of <NT$500,000. Approximately 75% of the participants were nonsmokers; however, nearly half of the participants were exposed to secondhand smoke. In addition, 74.6% of the participants reported using PCPs.

2.2 Paraben analysis

Parabens and their metabolites do not accumulate in the body, and are eliminated within a few hours of exposure (26, 27). Serum paraben concentrations, even after intravenous injection, decline quickly and remain low in the blood (28). Given the short half-life of parabens in blood, the parent compounds and their metabolites are conjugated and excreted in urine. Therefore, urinary measurements in humans can be used to estimate paraben uptake (29). Urinary levels of parent parabens can be used as biomarkers of recent human monitoring (30–33). Significant positive correlations between urinary and blood levels were also observed in a Chinese study, suggesting that urinary concentrations are good predictors of human exposure to parabens and metabolites (34). In the present study, the reagents and chemical standards as well as the measurement procedures for the four parabens used in our study are comprehensively described elsewhere (35). Briefly, spot urine samples were kept and stored at −80°C until analysis. For analysis, the collected urine samples were thawed at 4°C for 24 h. Each sample was extracted through a supported liquid extraction (SLE) column, and the extract was then eluted twice with 0.9 mL of dichloromethane. Finally, the extract was dried under vacuum conditions, followed by the addition of MeOH and Milli-Q water (both 100 μL) were added to reconstitute the extract for injection. Paraben concentrations were measured using a Waters Acquity UPLC system equipped with a Thermo Scientific™ Hypersil Gold™ column (50 × 2.1 mm, 1.9 μm) (35). The coefficient of determination for parabens (r^2) was higher than 0.9952. We observed that the average recovery rates of the parabens at low, medium, and high concentrations were 91.6–100.9% (5.4–10.5%), 84.4–99.5% (1.9–7.1%), and 86.8–98.4% (1.7–13.7%), respectively. Furthermore, the within-run and between-run accuracy (>85%) and precision (<14.2%) of our measurements were noted to meet the standards set by the European Medicines Agency (36). In instances where the paraben concentrations fell below the LOD, the measured concentrations were substituted with half the LOD. The LOD and LLOQ of each paraben were evaluated by SLE using paraben-spiked artificial urine and were 0.1 and 0.3 ng/mL, respectively (23, 24, 35). The present study has revealed that parabens Urinary creatinine levels were measured by spectrophotometry using a picric acid reagent with a wavelength of 520 nm (DXC 800 Synchron; Coulter, Brea, CA, United States).

2.3 Measurement of concentrations of metabolism indices

The UniCel DxI 800 Access Immunoassay System analyzer and an immunoradiometric assay kit (DIAsource, Louvain-la-Neuve, Belgium) were used to measure the concentrations of insulin resistance indices (e.g., glucose and insulin) and lipid

TABLE 1 Demographic characteristics of the study participants (N = 264).

Variables	Item	N	%	Mean ± SD
Gender	Male	125	47.3	
	Female	139	52.7	
Age (years, mean ± SD)	All	264		53.5 ± 17.1
	18–40	62	23.5	
	40–65	126	47.7	
	65 and older	76	28.8	
BMI[a] (kg/m^2) (mean ± SD)	All	264		24.7 ± 4.38
	Normal	132	50.0	
	Overweight	64	24.2	
	Obese	68	25.8	
Region	Northern Taiwan	83	31.4	
	Central Taiwan	36	13.6	
	Southern Taiwan	73	27.7	
	Eastern Taiwan	45	17.0	
	Remote island	27	10.2	
Marriage status	Single	44	16.7	
	Married	193	73.1	
	Divorce/widowed	27	10.2	
Education	≤Elementary school	73	27.7	
	Junior high school	38	14.4	
	Senior high school	76	28.8	
	≥College/graduates	77	29.2	
Annual family income[b] (NTD)	<15,625	147	58.1	
	15,625–31,250	69	27.3	
	>31,250	37	14.6	
Cigarette smoking[c]	Yes/No	64/200	24.2/75.8	
Passive smoker[d]	Yes/No	132/132	50.0/50.0	
Alcohol consumption[e]	Yes/No	34/226	13.1/86.9	
PCPs usage[f]	Yes/No	197/67	74.6/25.4	

[a]BMI standard for adults: weight standard (BMI < 24 kg/m^2), overweight (24≦BMI < 27 kg/m^2) and obesity (BMI≧27 kg/m^2) (59).
[b]The currency exchange rate of converting USD to new Taiwan dollar (NTD) is 1:32.
[c]Subjects who self-reported consuming at least one cigarette per day.
[d]Subject who self-reported as lifelong nonsmokers (never-smokers) but involuntary inhalation of smoke from cigarettes or other tobacco.
[e]Subject consuming at least one bottle of alcohol drink per week.
[f]Subject who self-reported using at least one kind of PCPs (personal care products), including body wash, lotion, perfume, and nail polishes.

metabolism indices (e.g., TG, HDLC, LDLC, and TC). The measurements were conducted randomly by technicians who were not aware of the metabolic status in Taiwan accredited laboratories (37, 38). Among our participants, 17.4 and 26.4% exhibited fasting blood glucose and insulin concentrations outside the reference range, respectively, and 13.6, 9.5, 29.9, and 37.9% exhibited TG, HDLC, LDLC, and TC levels outside the reference range, respectively. Furthermore, metabolic status was calculated using metabolism indices used in previous studies, including TG glucose-body mass index (TyG-BMI), CRI-I, CRI-II, NHC, and atherogenic coefficient (AC). TyG-BMI is an effective indicator for assessing insulin resistance Equation 1. TG metabolites affect the insulin sensitivity of adipose and muscle tissues and have been extensively studied for predicting diabetes. CRI-I, also known as the cardiac hazard ratio, reflects coronary plaque formation Equation 2. Moreover, CRI-II and AC are effective predictors of coronary artery disease risk Equations 3, 5. NHC is an indicator for predicting cardiovascular disease Equation 4. These indices can be calculated as follows (18–20, 39):

$$\mathrm{TyG-BMI} = \mathrm{Ln}\left(\frac{\mathrm{TG}\times\mathrm{glucose}}{2}\right)\times\mathrm{BMI} \quad (1)$$

where glucose represents fasting glucose (mg/dL), and TG (mg/dL) and BMI (kg/m^2) are already defined earlier (39).

$$\mathrm{CRI-I} = \frac{\mathrm{TC}}{\mathrm{HDLC}} \quad (2)$$

$$CRI - II = \frac{LDLC}{HDLC} \quad (3)$$

where TC (mg/dL), LDLC (mg/dL) and HDLC (mg/dL) are already defined earlier (20).

$$NHC = TC - HDLC \quad (4)$$

where TC (mg/dL) and HDLC (mg/dL) are already defined earlier (19).

$$AC = \frac{(TC - HDLC)}{HDLC} \quad (5)$$

where TC (mg/dL) and HDLC (mg/dL) are already defined earlier (18).

2.4 Statistical methods

The medians and geometric means (GMs) of the concentrations of urinary parabens and lipid metabolism indices are first calculated. Subsequently, we used the Mann–Whitney U test to assess differences in the concentrations of parabens and lipid metabolism indices between the genders. The correlation between parabens and lipid metabolism indices was evaluated through a Spearman correlation analysis.

In this study, a multiple linear regression analysis was conducted; for this analysis, the measured concentrations of parabens and metabolism indices were subjected to a natural logarithm transformation to satisfy the normality assumptions via the Kolmogorov–Smirnov test. Moreover, age (continuous), sex (categorical), BMI (categorical), education (categorical), income (categorical) and use of PCPs (categorical) were selected as covariates; this selection was based on the findings of relevant studies (17, 40) and on whether the inclusion of any of these covariates would engender a > 10% change in the estimated coefficient. Additionally, we adjusted for endocrine disease status to minimize potential interference effects of endocrine diseases on our analysis results. We also adjusted for the metabolite di(2-ethylhexyl) phthalate, considering its association with lipid metabolism, as indicated in previous research (23–25). Directed Acyclic Graphs (DAGs) were utilised to investigate the potential role of confounding variables in the association between urinary paraben levels and lipid metabolism indicator (see Supplementary Figure S2). The minimum sufficient adjustment sets for estimating the total effect of urinary paraben levels on lipid metabolism indicator were determined to be age, sex, BMI, education, income and use of personal care products (PCPs). The directed acyclic graph (DAG) was constructed using a web-based tool (DAGitty® version 3.1; 61). A mediation analysis was conducted using PROCESS v4.2 to explore the effect of insulin resistance on the relationship between parabens and lipid metabolism. In the mediation analysis, both indirect and direct effects were assessed, and the proportion of insulin resistance mediated the relationship between parabens and lipid metabolism was estimated (62). All data analyses were performed using SPSS software (version 24.0), and a p-value below 0.05 was considered statistically significant.

3 Results

3.1 Urinary concentrations of parabens and blood lipid metabolism indices

Table 2 presents the detection rate for the parabens as well as the medians and GMs of the concentrations of the parabens. The detection rate for the parabens was 100%. The parabens could be ordered as follows (in descending order) in terms of the GMs of their concentrations: MeP (383 μg/L), PrP (109 μg/L), EtP (39.5 μg/L), and BuP (6.35 μg/L). After stratifying our participants by gender, we observed that the GM of the concentrations of the parabens was higher in men than in women (MeP: 411 vs. 360 μg/L; EtP: 40.8 vs. 38.4 μg/L; PrP: 115 vs. 104 μg/L; BuP: 6.65 vs. 6.10 μg/L). However, the Mann–Whitney U test revealed no significant difference in urinary paraben concentrations between the genders.

We also observed that the detection rate for all lipid metabolism indices was 100% (Table 3). The GMs of the concentrations of TG, LDLC, HDLC, and TC were 109, 110, 56.4, and 190 mg/dL, respectively. After stratifying our participants by gender, we observed that the GM of the concentration of TG was significantly higher in men than in women (125 vs. 96.0 mg/dL, $p < 0.001$). The GM of the concentration of LDLC was also higher in men than in women (112 vs. 107 mg/dL, $p = 0.299$). By contrast, the concentration of HDLC was significantly higher in women than in men (62.5 vs. 50.1 mg/dL, $p < 0.001$), and the concentration of TC was higher in women than in men (192 vs. 188 mg/dL, $p = 0.334$).

3.2 Associations of urinary parabens with lipid metabolism and insulin resistance indices

As indicated in Table 4 and Figure 1, our Spearman correlation analysis revealed a significant positive association between urinary parabens and lipid metabolism indices ($p < 0.01$). EtP was significantly positively correlated with LDLC ($r = 0.139$, $p = 0.024$) and TC ($r = 0.123$, $p = 0.047$).

The multiple linear regression model was also used to explore the association of urinary parabens with lipid metabolism indices and insulin resistance indices (Table 5). After controlling for confounders, we observed that MeP exhibited a significant positive association with CRI-I ($\beta = 0.05$, $p = 0.049$). EtP also exhibited significant positive associations with LDLC ($\beta = 0.10$, $p = 0.001$), TC ($\beta = 0.06$, $p = 0.003$), and NHC ($\beta = 0.08$, $p = 0.005$). Furthermore, regarding the associations between urinary parabens and insulin resistance indices, EtP was positively associated with TyG-BMI ($\beta = 0.02$, $p = 0.040$).

3.3 Associations between lipid metabolism and insulin resistance indices

Concerning the association between lipid metabolism and insulin resistance indices, TyG-BMI exhibited positive associations with TG ($\beta = 3.02$, $p < 0.001$), CRI-I ($\beta = 0.98$, $p < 0.001$), CRI-II ($\beta = 1.03$, $p < 0.001$), NHC ($\beta = 0.63$, $p < 0.001$), and AC ($\beta = 1.07$, $p < 0.001$). However, a negative association was observed between TyG-BMI and HDLC (Supplementary Table S1).

TABLE 2 Distribution of parabens concentration (μg/L) in the general Taiwanese adult population by sex (*N* = 264).

Parabens	Group	DR (%)[a]	N	GM (95%CI)	Min	25th (95%CI)	50th (95%CI)	75th (95%CI)	95th (95%CI)	Max	*p*-value[b]
MeP	Adults	100	264	383 (356–412)	64.2	257 (225–277)	399 (360–456)	622 (542–690)	1,025 (936–1,103)	1,188	
	Men	100	125	411 (369–457)	90.4	266 (239–310)	419 (368–471)	654 (548–767)	1,059 (972–1,116)	1,134	0.152
	Women	100	139	360 (323–404)	64.2	234 (209–273)	376 (321–456)	615 (499–697)	1,015 (909–1,094)	1,188	
EtP	Adults	100	264	39.5 (36.7–42.6)	6.86	25.9 (23.8–28.0)	38.8 (35.1–43.5)	64.3 (56.9–76.7)	107 (99.3–112)	130	
	Men	100	125	40.8 (36.1–45.3)	6.86	25.9 (22.6–31.1)	40.5 (34.5–44.2)	74.6 (54.5–85.5)	110 (100–120)	130	0.484
	Women	100	139	38.4 (34.6–42.5)	7.16	25.5 (21.7–28.1)	37.9 (32.7–45.3)	60.7 (54.3–71.7)	107 (90.2–111)	112	
PrP	Adults	100	264	109 (102–116)	26.5	77.7 (67.4–82.1)	117 (105–124)	165 (149–180)	226 (217–239)	258	
	Men	100	125	115 (104–124)	26.5	80.5 (72.1–92.2)	115 (97.1–139)	179 (153–195)	228 (216–238)	253	0.134
	Women	100	139	104 (96–114)	31.2	65.6 (57.0–79.7)	117 (101–125)	156 (139–170)	225 (205–243)	258	
BuP	Adults	100	264	6.35 (5.98–6.77)	1.39	4.46 (4.18–4.92)	6.60 (6.00–7.36)	9.47 (8.93–10.0)	14.2 (13.4–15.0)	16.7	
	Men	100	125	6.65 (6.08–7.20)	1.40	4.84 (4.21–5.42)	6.84 (5.81–8.02)	9.60 (8.65–10.9)	14.8 (13.9–15.7)	15.8	0.305
	Women	100	139	6.10 (5.61–6.74)	1.39	4.34 (3.91–4.84)	6.54 (5.55–7.45)	9.47 (8.36–9.99)	13.4 (12.3–14.7)	16.7	

GM = Geometric mean.

[a]DR = Detection rate: number of urine sample with level of each paraben above detection limit/all analyzed urine samples.

[b]Comparison of urinary paraben levels between men and women using Mann–Whitney U test; *** $p < 0.001$.

TABLE 3 Distribution of lipid metabolism indicators in the general Taiwanese adult population by sex (*N* = 264).

	Group	DR (%)[b]	N	GM (95%CI)	Min	25th (95%CI)	50th (95%CI)	75th (95%CI)	95th (95%CI)	Max	*p*-value[c]
TG (mg/dL)[a]	Adults	100	264	109 (101–117)	35.0	72.0 (66.0–76.5)	102 (94.0–111)	147 (132–164)	284 (258–361)	3,821	
	Men	100	125	125 (112–139)	35.0	79.5 (74,0–92.5)	119 (103–133)	184 (157–224)	383 (280–582)	1,512	<0.001***
	Women	100	139	96.0 (88.5–107)	35.0	66.8 (60.0–72.5)	93.5 (85.0–104)	126 (116–137)	221 (175–274)	3,821	
HDLC (mg/dL)[a]	Adults	100	264	56.4 (54.6–58.5)	23.2	46.5 (45.6–48.9)	56.3 (54.4–58.3)	68.7 (64.3–70.8)	85.1 (81.0–96.0)	118	
	Men	100	125	50.1 (47.7–52.6)	23.2	42.7 (40.8–45.2)	48.9 (46.3–53.3)	58.2 (55.8–62.2)	73.5 (69.9–105)	117	<0.001***
	Women	100	139	62.5 (60.2–65.2)	30.7	52.8 (50.7–55.9)	62.2 (59.8–64.4)	73.0 (70.7–77.1)	89.5 (83.1–110)	118	
LDLC (mg/dL)[a]	Adults	100	264	110 (105–113)	30.0	90.0 (85.5–95.0)	112 (109–116)	139 (128–145)	174 (166–189)	271	
	Men	100	125	112 (106–118)	40.0	94.0 (83.0–101)	112 (109–121)	144 (129–149)	175 (161–199)	271	0.299
	Women	100	139	107 (101–113)	30.0	88.8 (83.0–94.0)	112 (98.0–118)	134 (124–144)	173 (166–190)	199	
TC (mg/dL)[a]	Adults	100	264	190 (186–195)	92.0	168 (163–173)	190 (184–195)	220 (211–229)	263 (252–276)	493	
	Men	100	125	188 (181–195)	120	166 (155–174)	185 (180–195)	220 (205–230)	263 (246–284)	365	0.334
	Women	100	139	192 (185–200)	92.0	168 (162–178)	192 (185–198)	222 (209–234)	267 (248–286)	493	

GM = Geometric mean TG = Triglycerides, HDLC = High Density Lipoprotein Cholesterol, LDLC = Low Density Lipoprotein Cholesterol, and TC = Total cholesterol.

[a]The laboratory reference ranges of adults for TG, HDL-C, LDL-C, and TC were < 150 mg/dL, > 40 mg/dL, < 130 mg/dL, and < 200 mg/dL, respectively.

[b]DR = Detection rate: number of urine sample with each lipid metabolism indicators concentration above detection limit/all analyzed urine samples.

[c]Comparison of lipid metabolism indicators concentration between men and women using Mann–Whitney U test; *$p < 0.05$; **$p < 0.01$; *** $p < 0.001$.

10.3389/fpubh.2025.1416264

10.3389/fpubh.2025.1416264

TABLE 4 Spearman's correlation coefficients between urinary paraben concentrations in adults and lipid metabolism indicators (N = 264).

	MeP	EtP	PrP	BuP	TG (mg/dL)	HDLC (mg/dL)	LDLC (mg/dL)	TC (mg/dL)	BMI (kg/m²)
MeP (μg/L)	1.000	**0.414****	**0.613****	**0.577****	0.068	−0.044	0.074	0.087	−0.062
EtP (μg/L)		1.000	**0.649****	**0.548****	0.090	0.027	**0.139***	**0.123***	−0.025
PrP (μg/L)			1.000	**0.719****	0.062	0.027	0.074	0.075	−0.037
BuP (μg/L)				1.000	0.028	0.025	0.056	0.070	−0.052
TG (mg/dL)					1.000	**−0.482****	**0.260****	**0.225****	**0.443****
HDLC (mg/dL)						1.000	0.066	**0.344****	**−0.314****
LDLC (mg/dL)							1.000	**0.849****	0.097
TC (mg/dL)								1.000	−0.023
BMI (kg/m²)									1.000

TG = Triglycerides, HDLC = High Density Lipoprotein Cholesterol, LDLC = Low Density Lipoprotein Cholesterol, and TC = Total cholesterol. *$p < 0.05$; **$p < 0.01$; *** $p < 0.001$ Bold: $p < 0.05$.

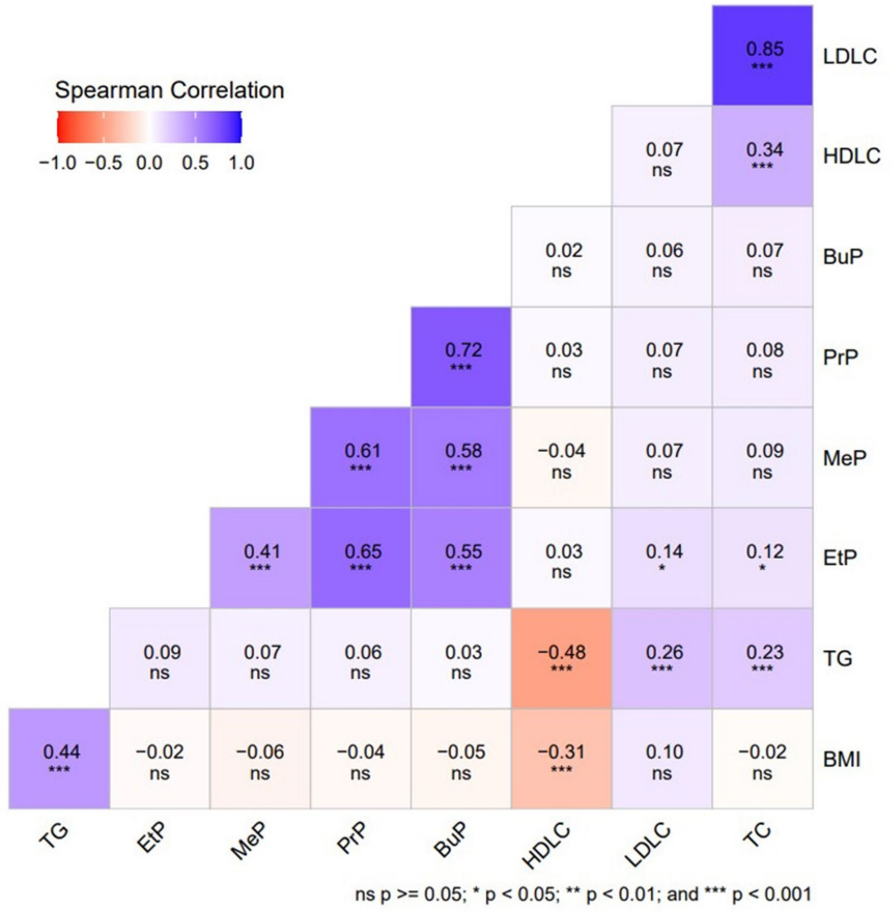

FIGURE 1
Spearman's correlation coefficients between urinary paraben concentrations in adults and lipid metabolism indices (N = 264).

3.4 Mediating role of insulin resistance in the association between urinary paraben levels and lipid metabolism

We selected parabens that, upon exposure, were significantly associated with lipid metabolism and insulin resistance indices to conduct a mediation analysis; in this analysis, we identified that insulin resistance could serve as mediators for the effects of paraben exposure on lipid metabolism indices. In mediation analysis, TyG-BMI mediated 17.2% of the association between EtP and NHC (indirect effect = 0.014, 95% confidence interval [CI] = 0.003–0.029); the mediation effect was significant (shown in Supplementary Table S2 and Figure 2).

4 Discussion

Our study revealed that MeP was positively associated with CRI-I and that EtP was positively associated with LDLC, TC, and NHC. The

TABLE 5 Adjusted regression coefficients (β), 95% confidence intervals (CI), and *p*-values (*p*) for change in lipid and glucose metabolism indicators in relation to unit-increased in Ln-parabens (μg/L) in Taiwanese adults (*N* = 264).

Variable	MeP (μg/L)			EtP (μg/L)			PrP (μg/L)			BuP (μg/L)		
	β	95% CI	*p* value	β	95% CI	*P* value	β	95% CI	*P* value	β	95% CI	*P* value
Model 1[a]												
TG (mg/dL)	0.08	(−0.03, 0.18)	0.147	0.06	(−0.05, 0.17)	0.300	0.03	(−0.11, 0.16)	0.711	0.06	(−0.06, 0.19)	0.318
HDLC (mg/dL)	−0.03	(−0.07, 0.02)	0.250	0.03	(−0.02, 0.08)	0.192	0.03	(−0.03, 0.09)	0.306	0.01	(−0.04, 0.07)	0.684
LDLC (mg/dL)	0.03	(−0.03, 0.09)	0.340	**0.10**	**(0.04, 0.16)**	**0.001**	0.07	(−0.01, 0.15)	0.083	0.07	(<0.01, 0.14)	0.050
TC (mg/dL)	0.02	(−0.02, 0.06)	0.261	**0.06**	**(0.02, 0.10)**	**0.003**	0.04	(−0.01, 0.09)	0.134	0.04	(−0.01, 0.09)	0.086
CRI-I	**0.05**	**(<0.01, 0.10)**	**0.049**	0.03	(−0.02, 0.08)	0.229	0.01	(−0.06, 0.07)	0.788	0.03	(−0.03, 0.09)	0.312
CRI-II	0.06	(−0.01, 0.13)	0.115	0.07	(> − 0.01, 0.14)	0.059	0.04	(−0.05, 0.13)	0.410	0.06	(−0.02, 0.14)	0.155
NHC	0.04	(−0.01, 0.10)	0.123	**0.08**	**(0.02, 0.13)**	**0.005**	0.04	(−0.03, 0.11)	0.230	0.06	(−0.01, 0.12)	0.096
AC	0.07	(> − 0.01, 0.14)	0.057	0.05	(−0.03, 0.12)	0.205	0.01	(−0.08, 0.11)	0.793	0.04	(−0.04, 0.13)	0.316
TyG-BMI	0.01	(−0.01, 0.03)	0.271	**0.02**	**(<0.01, 0.05)**	**0.040**	0.01	(−0.02, 0.04)	0.648	0.01	(−0.02, 0.03)	0.705
Model 2[b]												
TG (mg/dL)	0.07	(−0.05, 0.18)	0.250	0.06	(−0.05, 0.17)	0.282	0.02	(−0.12, 0.16)	0.798	0.07	(−0.06, 0.20)	0.269
HDLC (mg/dL)	−0.02	(−0.06, 0.03)	0.479	0.03	(−0.02, 0.08)	0.189	0.03	(−0.03, 0.10)	0.258	0.02	(−0.04, 0.07)	0.546
LDLC (mg/dL)	0.03	(−0.03, 0.09)	0.347	**0.11**	**(0.05, 0.17)**	**0.001**	0.07	(−0.01, 0.15)	0.075	**0.08**	**(<0.01, 0.15)**	**0.048**
TC (mg/dL)	0.02	(−0.02, 0.07)	0.259	**0.07**	**(0.02, 0.11)**	**0.002**	0.04	(−0.02, 0.09)	0.157	0.04	(> − 0.01, 0.09)	0.075
CRI-I	0.04	(−0.01, 0.09)	0.119	0.03	(−0.02, 0.09)	0.209	<0.01	(−0.06, 0.07)	0.906	0.03	(−0.03, 0.09)	0.374
CRI-II	0.05	(−0.03, 0.12)	0.202	**0.08**	**(0.01, 0.15)**	**0.034**	0.04	(−0.05, 0.13)	0.417	0.06	(−0.03, 0.14)	0.187
NHC	0.04	(−0.02, 0.10)	0.175	**0.08**	**(0.03, 0.14)**	**0.004**	0.04	(−0.03, 0.11)	0.273	0.06	(−0.01, 0.13)	0.094
AC	0.06	(−0.02, 0.13)	0.139	0.05	(−0.02, 0.13)	0.178	0.01	(−0.09, 0.10)	0.899	0.04	(−0.05, 0.13)	0.369
TyG-BMI	0.01	(−0.01, 0.03)	0.361	**0.03**	**(<0.01, 0.05)**	**0.018**	0.01	(−0.02, 0.04)	0.438	0.01	(−0.02, 0.04)	0.546

[a]Model 1: adjustment for age, sex, BMI, urinary creatinine levels, endocrine disease status, and Ln ΣDEHPm. Bold: $p < 0.05$.

[b]Model 2: adjustment for age, sex, education, income, PCPs use, BMI, urinary creatinine, endocrine disease status, and Ln ΣDEHPm. Bold: $p < 0.05$.

10.3389/fpubh.2025.1416264

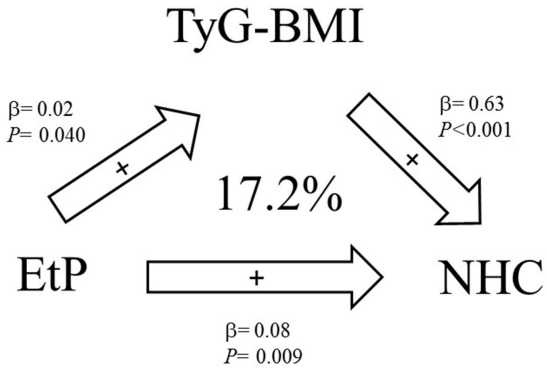

FIGURE 2
Mediation effects of exposure to parabens on the homeostatic model assessment of estimated lipid metabolism indices through insulin resistance indices (N = 264).

findings of this study indicate that exposure to parabens may be associated with obesity and indicators of lipid metabolism, as well as adverse health outcomes, in adults. These findings are consistent with those reported in previous epidemiological studies. In an ongoing three-year cycle cross-sectional biomonitoring programme [KoNEHS Cycle 3 (2015–2017)], an adult population (aged 19 years or older) was investigated to ascertain the current level of exposure to major environmental chemicals among the general Korean population. The KoNEHS study also revealed a positive association between urinary EtP levels in adults and obesity [β = 0.03, p = 0.038; (17)]. A total of 1,454 children, 891 adolescents, and 3,758 adults (for BMI) and 3,424 adults (for TG/HDL) from the Korean National Environmental Health Survey (2015 to 2017) were included in this cross-sectional study. The findings of Kim's study suggest that exposure to EDC mixtures is associated with elevated BMI and TG/HDL levels in both adolescents and adults. The association is more pronounced in adults than in adolescents. Moreover, adolescence may signify a critical period for EDC mixtures in terms of outcomes (41).

In a related study, blood plasma samples were collected from 27 healthy women at various points throughout their menstrual cycles in order to examine the potential correlation between paraben exposure and obesity (58). The plasma levels of methylparaben, as well as the sum of parabens, were found to be positively associated with plasma adipsin levels. Conversely, a negative correlation was observed between methylparaben levels and glucagon, leptin, and PAI-1. These inconsistencies in the impact of urinary paraben concentrations on lipid metabolism indices could be attributed to differences in study design or participant characteristics, including sex, age, or ethnicity.

It is hypothesised that paraben exposure may impact insulin sensitivity in human organs, thus providing an underlying mechanism that could explain the observed association. Hu et al. (15) found that parabens promote adipogenesis in 3 T3-L1 cells, contributing to obesity by disrupting lipid synthesis and decomposition via the PPARγ receptor. Their findings showed a significant positive association between EtP and TyG-BMI. Animal studies suggest that paraben exposure can damage pancreatic islet cells. For example, zebrafish embryos exhibited enlarged islet areas, abnormal shapes, and increased aberrant β-cells (42). Pereira-Fernandes et al. (43) demonstrated that parabens strongly bind to and activate PPARγ, a key regulator of insulin sensitivity. Our results showed a significant positive association between EtP and TyG-BMI, suggesting that paraben exposure may disrupt blood glucose regulation and increase insulin resistance risk. These findings align with the KoNEHS Cycle 3 study (2015–2017) in South Korea, which reported positive associations between MeP (OR = 1.68, 95% CI = 1.08–2.60) and EtP (OR = 2.74, 95% CI = 1.77–4.24) with diabetes (17). Similarly, Bai et al. (44) found a significant positive association between PrP and insulin resistance (OR = 1.72, 95% CI = 1.15–2.57) in NHANES (2009–2016). A case–control study from the Henan Rural Cohort Study, including 1,713 participants (880 with type 2 diabetes and 833 controls), used generalized linear regression models to assess the effects of parabens on T2DM and insulin resistance indicators (63). The study found a linear positive association between MeP or paraben mixtures and T2DM risk, while EtP and BuP showed a non-linear association, with moderate-to-high exposure levels contributing to T2DM development (63). The findings of this study demonstrated that exposure to MeP or paraben mixtures was found to have a linear positive association with the risk of T2DM. EtP and BuP demonstrated a non-linear association with insulin resistance, with moderate-high exposure levels contributing to the development of T2DM (63).

A prospective study of 1,087 pregnant women from a single tertiary medical center also shows that urinary EtP was associated with gestational DM, with risk ratios of 1.12, 1.11 and 1.70 for the second, third and highest quartiles, respectively (64). Furthermore, a case–control study of adults (n = 101) in Jeddah, Saudi Arabia during 2015–2016 also found that increased parabens (including MeP, EtP, and PrP) exposure could lead to an over six-fold increase in the risk of diabetes (65).

We found that insulin resistance indices were positively linked to LDLC and lipid metabolism markers but negatively associated with HDLC, suggesting a role in dyslipidemia and obesity. Previous studies indicate that insulin resistance and type 2 diabetes can elevate TG or reduce HDLC levels (45, 46). Insulin resistance may impair VLDL degradation, leading to increased VLDL synthesis (47). VLDL transports fat from the liver to tissues and converts to LDLC after unloading most of its fat (48, 49).

Consequently, insulin resistance may lead to elevated TG levels, resulting in hypertriglyceridemia. Insulin resistance also reduces the activity of lipoprotein lipase, a key mediator of VLDL clearance (50). This reduction in VLDL and LDLC uptake by the liver prolongs the duration of these lipoproteins in the plasma (22, 47). Gencer et al. (51) confirmed that insulin resistance in polycystic ovary syndrome (PCOS) is linked to fasting insulin, HOMA index, BMI, and right ovarian volume. In PCOS with Hashimoto's thyroiditis (PCOS+HT), insulin resistance also correlates with fasting insulin, HOMA index, BMI, SHBG, and left ovarian volume. Among PCOS patients with insulin resistance, 37.5% had increased right ovarian volume, while left ovarian volume was elevated in 35.7% of those without insulin resistance and 68.8% of those with it. PCOS shares clinical similarities with certain thyroid diseases, particularly hypothyroidism and autoimmune thyroid diseases (AITDs) (52). Its coexistence with hyperthyroidism is rare, suggesting thyroid influence on PCOS through metabolism and immunity. Thyroid function affects insulin resistance, a key factor in PCOS, with hypothyroidism exacerbating it more than hyperthyroidism. The rising prevalence of obesity further impacts health, as hypothyroid patients are prone to obesity, and those with both PCOS and hypothyroidism often have a higher BMI and greater metabolic disease risk. Further research is required to confirm these findings and to elucidate the underlying mechanisms. Nevertheless, it is evident that strategies to reduce EDC exposure from early life stages may be necessary to lower the risk of metabolic disease.

Our mediation analysis revealed that TyG-BMI could mediate the association between EtP and NHC. Therefore, TyG-BMI may be a mediator in the association between EtP exposure and NHC. Parabens increase the risk of obesity and cardiovascular disease by fostering the development of insulin resistance and dyslipidemia. Extensive epidemiological and mechanistic studies (both *in vivo* and *in vitro*) are warranted to validate these associations and elucidate the potential corresponding biological mechanisms.

There are four key strengths in this study. First, our current data were obtained from a representative survey including participants aged 7 to 97 years. Therefore, our study can accurately reflect the exposure profile of the general population in Taiwan. Second, few studies have explored the association between paraben exposure and metabolism indices in the general Taiwanese adult. Third, we employed various metabolic indices that are currently used in clinical practice but are rarely used in research, thus enriching the understanding of overall metabolic conditions. Finally, we conducted a mediation analysis to explore the potential mediating role of insulin resistance in the association between paraben exposure and lipid metabolism in the general Taiwanese adult population.

Despite its strengths, our study has some limitations that warrant consideration. First, we applied a cross-sectional design; hence, we could not establish a causal relationship between exposure and health effects. Second, our sample size was relatively small, which could potentially affect the reliability and interpretability of our statistical findings. Future research should consider a larger sample size for improved representativeness and robustness. Third, the measurement of urinary paraben concentrations using morning urine samples may not fully capture long-term exposure; however, this limitation is mitigated by evidence suggesting that daily exposure patterns for parabens could be consistent over time (53, 54).

5 Conclusion

The present study has revealed that parabens have the capacity to affect metabolic homeostasis. The potential mediation of the association between paraben exposure and lipid metabolism by insulin resistance is also indicated. The risk of obesity and cardiovascular disease is increased by parabens via the fostering of the development of insulin resistance and dyslipidemia. Whilst the participants in the present study were selected from the general population, the findings are limited to Taiwanese individuals. Therefore, future studies must include a greater number of samples in order to elucidate these underlying mechanisms and increase the generalizability of the results.

Data availability statement

The raw data supporting the conclusions of this article will be made available by the authors, without undue reservation.

Ethics statement

The studies involving humans were approved by Institutional Review Board of National Yang Ming Chiao Tung University in Taiwan. The studies were conducted in accordance with the local legislation and institutional requirements. The participants provided their written informed consent to participate in this study.

Author contributions

P-CH: Conceptualization, Methodology, Resources, Software, Supervision, Writing – original draft. H-CC: Investigation, Methodology, Resources, Writing – review & editing. H-BH: Investigation, Methodology, Writing – review & editing. Y-LL: Investigation, Methodology, Resources, Writing – review & editing. W-TC: Investigation, Writing – review & editing. S-HL: Investigation, Writing – review & editing. HC: Investigation, Writing – review & editing. J-WC: Data curation, Formal analysis, Methodology, Resources, Software, Supervision, Validation, Writing – review & editing, Writing – original draft.

Funding

The author(s) declare financial support was received for the research and/or publication of this article. We sincerely appreciate the assistance from our research team in data and sample collection. We would also like to express our thanks and gratitude to the Ministry of Science and Technology (grant nos. MOST 106-3114-B-400-001, 111-2314-B-400-039, and 111-2314-B-A49A-522) and National Health Research Institutes for research financial support (grant nos. EM-110-PP-11, EM-111-PP-11). This work was supported partially by the Research Center for Precision Environmental Medicine, Kaohsiung Medical University, Kaohsiung, Taiwan from The Featured Areas Research Center Program within the framework of the Higher Education Sprout Project by the Ministry of Education (MOE) in Taiwan and by Kaohsiung Medical University Research Center Grant (KMU-TC114A01).

Conflict of interest

The authors declare that the research was conducted in the absence of any commercial or financial relationships that could be construed as a potential conflict of interest.

Publisher's note

Supplementary material

The Supplementary material for this article can be found online at: https://www.frontiersin.org/articles/10.3389/fpubh.2025.1416264/full#supplementary-material

SUPPLEMENTARY FIGURE S1
Flow chart of the recruitment for the study.

SUPPLEMENTARY FIGURE S2
Visualized directed acyclic graph (DAG) to apply the minimal sufficient adaptation set as covariates.

References

1. Lind PM, Lind L. Endocrine-disrupting chemicals and risk of diabetes: an evidence-based review. *Diabetologia*. (2018) 61:1495–502. doi: 10.1007/s00125-018-4621-3

2. Mottillo S, Filion KB, Genest J, Joseph L, Pilote L, Poirier P, et al. The metabolic syndrome and cardiovascular risk a systematic review and meta-analysis. *J Am Coll Cardiol*. (2010) 56:1113–32. doi: 10.1016/j.jacc.2010.05.034

3. Alberti KG, Eckel RH, Grundy SM, Zimmet PZ, Cleeman JI, Donato KA, et al. Harmonizing the metabolic syndrome: a joint interim statement of the international diabetes federation task force on epidemiology and prevention; National Heart, Lung, and Blood Institute; American Heart Association; world heart federation; international atherosclerosis society; and International Association for the Study of obesity. *Circulation*. (2009) 120:1640–5. doi: 10.1161/circulationaha.109.192644

4. Moller DE, Kaufman KD. Metabolic syndrome: a clinical and molecular perspective. *Annu Rev Med*. (2005) 56:45–62. doi: 10.1146/annurev.med.56.082103.104751

5. Darbre PD. Endocrine disruptors and obesity. *Curr Obes Rep*. (2017) 6:18–27. doi: 10.1007/s13679-017-0240-4

6. Mimoto MS, Nadal A, Sargis RM. Polluted pathways: mechanisms of metabolic disruption by endocrine disrupting chemicals. *Curr Environ Health Rep*. (2017) 4:208–22. doi: 10.1007/s40572-017-0137-0

7. Song Y, Chou EL, Baecker A, You NC, Song Y, Sun Q, et al. Endocrine-disrupting chemicals, risk of type 2 diabetes, and diabetes-related metabolic traits: a systematic review and meta-analysis. *J Diabetes*. (2016) 8:516–32. doi: 10.1111/1753-0407.12325

8. Myridakis A, Fthenou E, Balaska E, Vakinti M, Kogevinas M, Stephanou EG. Phthalate esters, parabens and bisphenol-a exposure among mothers and their children in Greece (Rhea cohort). *Environ Int*. (2015) 83:1–10. doi: 10.1016/j.envint.2015.05.014

9. Soni MG, Carabin IG, Burdock GA. Safety assessment of esters of p-hydroxybenzoic acid (parabens). *Food Chem Toxicol*. (2005) 43:985–1015. doi: 10.1016/j.fct.2005.01.020

10. Wei F, Mortimer M, Cheng H, Sang N, Guo LH. Parabens as chemicals of emerging concern in the environment and humans: a review. *Sci Total Environ*. (2021) 778:146150. doi: 10.1016/j.scitotenv.2021.146150

11. Haman C, Dauchy X, Rosin C, Munoz JF. Occurrence, fate and behavior of parabens in aquatic environments: a review. *Water Res*. (2015) 68:1–11. doi: 10.1016/j.watres.2014.09.030

12. Junaid M, Wang Y, Hamid N, Deng S, Li W-G, Pei D-S. Prioritizing selected PPCPs on the basis of environmental and toxicogenetic concerns: a toxicity estimation to confirmation approach. *J Hazard Mater*. (2019) 380:120828. doi: 10.1016/j.jhazmat.2019.120828

13. Nowak K, Jablonska E, Ratajezak-Wrona W. Controversy around parabens: alternative strategies for preservative use in cosmetics and personal care products. *Environ Res*. (2021) 198:110488. doi: 10.1016/j.envres.2020.110488

14. Honda M, Robinson M, Kannan K. Parabens in human urine from several Asian countries, Greece, and the United States. *Chemosphere*. (2018) 201:13–9. doi: 10.1016/j.chemosphere.2018.02.165

15. Hu P, Chen X, Whitener RJ, Boder ET, Jones JO, Porollo A, et al. Effects of parabens on adipocyte differentiation. *Toxicol Sci*. (2013) 131:56–70. doi: 10.1093/toxsci/kfs262

16. Hu P, Overby H, Heal E, Wang S, Chen J, Shen CL, et al. Methylparaben and butylparaben alter multipotent mesenchymal stem cell fates towards adipocyte lineage. *Toxicol Appl Pharmacol*. (2017) 329:48–57. doi: 10.1016/j.taap.2017.05.019

17. Lee I, Park YJ, Kim MJ, Kim S, Choi S, Park J, et al. Associations of urinary concentrations of phthalate metabolites, bisphenol a, and parabens with obesity and diabetes mellitus in a Korean adult population: Korean National Environmental Health Survey (KoNEHS) 2015–2017. *Environ Int*. (2021) 146:106227. doi: 10.1016/j.envint.2020.106227

18. Bhardwaj S, Bhattacharjee J, Bhatnagar M, Tyagi S, Delhi N. Atherogenic index of plasma, Castelli risk index and atherogenic coefficient-new parameters in assessing cardiovascular risk. *Int J Pharm Biol Sci*. (2013) 3:359–64. Available at: https://ijpbs.com/ijpbsadmin/upload/ijpbs_526938e855804.pdf

19. Packard CJ, Saito Y. Non-HDL cholesterol as a measure of atherosclerotic risk. *J Atheroscler Thromb*. (2004) 11:6–14. doi: 10.5551/jat.11.6

20. Salcedo-Cifuentes M, Belalcazar S, Acosta EY, Medina-Murillo JJ. Conventional biomarkers for cardiovascular risks and their correlation with the Castelli risk index-indices and TG/HDL-c. *Archivos de Medicina (Manizales)*. (2020) 20:11–22. doi: 10.30554/archmed.20.1.3534.2020

21. Monnier L, Colette C, Percheron C, Descomps B. Insulin, diabetes and cholesterol metabolism. *C R Seances Soc Biol Fil*. (1995) 189:919–31.

22. Ormazabal V, Nair S, Elfeky O, Aguayo C, Salomon C, Zuñiga FA. Association between insulin resistance and the development of cardiovascular disease. *Cardiovasc Diabetol*. (2018) 17:122. doi: 10.1186/s12933-018-0762-4

23. Huang HB, Cheng PK, Siao CY, Lo YC, Chou WC, Huang PC. Mediation effects of thyroid function in the associations between phthalate exposure and lipid metabolism in adults. *Environ Health*. (2022) 21:61. doi: 10.1186/s12940-022-00873-9

24. Huang PC, Chen HC, Chou WC, Lin HW, Chang WT, Chang JW. Cumulative risk assessment and exposure characteristics of parabens in the general Taiwanese using multiple hazard indices approaches. *Sci Total Environ*. (2022) 843:156821. doi: 10.1016/j.scitotenv.2022.156821

25. Huang H-B, Siao C-Y, Lo Y-TC, Shih S-F, Lu C-H, Huang P-C. Mediation effects of thyroid function in the associations between phthalate exposure and insulin resistance in adults. *Environ Pollut*. (2021) 278:116799. doi: 10.1016/j.envpol.2021.116799

26. Aubert N, Ameller T, Legrand JJ. Systemic exposure to parabens: pharmacokinetics, tissue distribution, excretion balance and plasma metabolites of [14C]-methyl-, propyl- and butylparaben in rats after oral, topical or subcutaneous administration. *Food Chem Toxicol*. (2012) 50:445–54. doi: 10.1016/j.fct.2011.12.045

27. Wang L, Kannan K. Alkyl protocatechuates as novel urinary biomarkers of exposure to p-hydroxybenzoic acid esters (parabens). *Environ Int*. (2013) 59:27–32. doi: 10.1016/j.envint.2013.05.001

28. Abbas S, Greige-Gerges H, Karam N, Piet MH, Netter P, Magdalou J. Metabolism of parabens (4-hydroxybenzoic acid esters) by hepatic esterases and UDP-glucuronosyltransferases in man. *Drug Metab Pharmacokinet*. (2010) 25:568–77. doi: 10.2133/dmpk.dmpk-10-rg-013

29. Boberg J, Taxvig C, Christiansen S, Hass U. Possible endocrine disrupting effects of parabens and their metabolites. *Reprod Toxicol*. (2010) 30:301–12. doi: 10.1016/j.reprotox.2010.03.011

30. Calafat AM, Ye X, Wong LY, Bishop AM, Needham LL. Urinary concentrations of four parabens in the U.S. population: NHANES 2005-2006. *Environ Health Perspect*. (2010) 118:679–85. doi: 10.1289/ehp.0901560

31. Ma WL, Wang L, Guo Y, Liu LY, Qi H, Zhu NZ, et al. Urinary concentrations of parabens in Chinese young adults: implications for human exposure. *Arch Environ Contam Toxicol*. (2013) 65:611–8. doi: 10.1007/s00244-013-9924-2

32. Wang L, Wu Y, Zhang W, Kannan K. Characteristic profiles of urinary p-hydroxybenzoic acid and its esters (parabens) in children and adults from the United States and China. *Environ Sci Technol*. (2013) 47:2069–76. doi: 10.1021/es304659r

33. Ye X, Bishop AM, Reidy JA, Needham LL, Calafat AM. Parabens as urinary biomarkers of exposure in humans. *Environ Health Perspect*. (2006) 114:1843–6. doi: 10.1289/ehp.9413

34. Zhang H, Quan Q, Li X, Sun W, Zhu K, Wang X, et al. Occurrence of parabens and their metabolites in the paired urine and blood samples from Chinese university students: implications on human exposure. *Environ Res*. (2020) 183:109288. doi: 10.1016/j.envres.2020.109288

35. Chen HC, Chang JW, Sun YC, Chang WT, Huang PC. Determination of parabens, bisphenol a and its analogs, Triclosan, and Benzophenone-3 levels in human urine by isotope-dilution-UPLC-MS/MS method followed by supported liquid extraction. *Toxics*. (2022) 10:21. doi: 10.3390/toxics10010021

36. European Medicines Agency, Committee for Medicinal Products for Human Use. Guideline on Bioanalytical Method Validation. London, UK: European Medicines Agency. (2011).

37. Huang HB, Pan WH, Chang JW, Chiang HC, Guo YL, Jaakkola JJ, et al. Does exposure to phthalates influence thyroid function and growth hormone homeostasis? The Taiwan environmental survey for toxicants (TEST) 2013. *Environ Res*. (2017) 153:63–72. doi: 10.1016/j.envres.2016.11.014

38. Waits A, Chen HC, Kuo PL, Wang CW, Huang HB, Chang WH, et al. Urinary phthalate metabolites are associated with biomarkers of DNA damage and lipid peroxidation in pregnant women—Tainan birth cohort study (TBCS). *Environ Res*. (2020) 188:109863. doi: 10.1016/j.envres.2020.109863

39. Er LK, Wu S, Chou HH, Hsu LA, Teng MS, Sun YC, et al. Triglyceride glucose-body mass index is a simple and clinically useful surrogate marker for insulin resistance in nondiabetic individuals. *PLoS One*. (2016) 11:e0149731. doi: 10.1371/journal.pone.0149731

40. Lee I, Kim S, Park S, Mok S, Jeong Y, Moon H-B, et al. Association of urinary phthalate metabolites and phenolics with adipokines and insulin resistance related markers among women of reproductive age. *Sci Total Environ*. (2019) 688:1319–26. doi: 10.1016/j.scitotenv.2019.06.125

41. Kim J, Chevrier J. Exposure to parabens and prevalence of obesity and metabolic syndrome: an analysis of the Canadian health measures survey. *Sci Total Environ*. (2020) 713:135116. doi: 10.1016/j.scitotenv.2019.135116

42. Brown SE, Sant KE, Fleischman SM, Venezia O, Roy MA, Zhao L, et al. Pancreatic beta cells are a sensitive target of embryonic exposure to butylparaben in zebrafish (*Danio rerio*). *Birth Defects Res*. (2018) 110:933–48. doi: 10.1002/bdr2.1215

43. Pereira-Fernandes A, Demaegdt H, Vandermeiren K, Hectors TL, Jorens PG, Blust R, et al. Evaluation of a screening system for obesogenic compounds: screening of endocrine disrupting compounds and evaluation of the PPAR dependency of the effect. *PLoS One*. (2013) 8:e77481. doi: 10.1371/journal.pone.0077481

44. Bai J, Ma Y, Zhao Y, Yang D, Mubarik S, Yu C. Mixed exposure to phenol, parabens, pesticides, and phthalates and insulin resistance in NHANES: a mixture approach. *Sci Total Environ*. (2022) 851:158218. doi: 10.1016/j.scitotenv.2022.158218

45. Liu H, Liu J, Liu J, Xin S, Lyu Z, Fu X. Triglyceride to high-density lipoprotein cholesterol (TG/HDL-C) ratio, a simple but effective Indicator in predicting type 2

diabetes mellitus in older adults. *Front Endocrinol (Lausanne)*. (2022) 13:828581. doi: 10.3389/fendo.2022.828581

46. Liu H, Yan S, Chen G, Li B, Zhao L, Wang Y, et al. Association of the Ratio of triglycerides to high-density lipoprotein cholesterol levels with the risk of type 2 diabetes: a retrospective cohort study in Beijing. *J Diabetes Res*. (2021) 2021:5524728–8. doi: 10.1155/2021/5524728

47. Vergès B. Pathophysiology of diabetic dyslipidaemia: where are we? *Diabetologia*. (2015) 58:886–99. doi: 10.1007/s00125-015-3525-8

48. Gershkovich P, Hoffman A. Effect of a high-fat meal on absorption and disposition of lipophilic compounds: the importance of degree of association with triglyceride-rich lipoproteins. *Eur J Pharm Sci*. (2007) 32:24–32. doi: 10.1016/j.ejps.2007.05.109

49. Lambert D, Mourot J. Vitamin E and lipoproteins in hyperlipoproteinemia. *Atherosclerosis*. (1984) 53:327–30. doi: 10.1016/0021-9150(84)90133-3

50. Semenkovich CF. Insulin resistance and atherosclerosis. *J Clin Invest*. (2006) 116:1813–22. doi: 10.1172/JCI29024

51. Gencer G, Serin AN, Gencer K. Analysis of the effect of hashimoto's thyroiditis and insulin resistance on ovarian volume in patients with polycystic ovary syndrome. *BMC Womens Health*. (2023) 23:86. doi: 10.1186/s12905-023-02200-x

52. Fan H, Ren Q, Sheng Z, Deng G, Li L. The role of the thyroid in polycystic ovary syndrome. *Front Endocrinol*. (2023) 14:1242050. doi: 10.3389/fendo.2023.1242050

53. Pollack AZ, Perkins NJ, Sjaarda L, Mumford SL, Kannan K, Philippat C, et al. Variability and exposure classification of urinary phenol and paraben metabolite concentrations in reproductive-aged women. *Environ Res*. (2016) 151:513–20. doi: 10.1016/j.envres.2016.08.016

54. Smith KW, Braun JM, Williams PL, Ehrlich S, Correia KF, Calafat AM, et al. Predictors and variability of urinary paraben concentrations in men and women, including before and during pregnancy. *Environ Health Perspect*. (2012) 120:1538–43. doi: 10.1289/ehp.1104614

55. Wong TJ, Yu T. Trends in the distribution of body mass index, waist circumference and prevalence of obesity among Taiwanese adults, 1993-2016. *PLoS One*. (2022) 17:e0274134. doi: 10.1371/journal.pone.0274134

56. Pan W-H. In: Nutrition and Health Survey in Taiwan 2017–2020: Preliminary Results. *Health Promotion Administration, Ministry of Health and Welfare, editor*. Health Promotion Administration, Ministry of Health and Welfare; Taipei, Taiwan. (2020).

57. Salamanca-Fernández E, Iribarne-Durán LM, Rodríguez-Barranco M, Vela-Soria F, Olea N, Sánchez-Pérez MJ, et al. Historical exposure to non-persistent environmental pollutants and risk of type 2 diabetes in a Spanish sub-cohort from the European Prospective Investigation into Cancer and Nutrition study. *Environ Res*. (2020) 185:109383. doi: 10.1016/j.envres.2020.109383

58. Kolatorova L, Sramkova M, Vitku J, Vcelak J, Lischkova O, Starka L, et al. Parabens and their relation to obesity. *Physiol Res*. (2018) 67:S465–S472. doi: 10.33549/physiolres.934004

59. Health Promotion Administration, Ministry of Health and Welfare. Taiwan's Obesity Prevention and Management Strategy. 1st edn, 1:55. (Health Promotion Administration, Ministry of Health and Welfare), (2018).

60. Lohman TG, Roche AF, Martorell R. *Anthropometric Standardization Reference Manual*. Human Kinetics; Champaign, IL, USA. (1988).

61. Textor J, van der Zander B, Gilthorpe MS, Li´skiewicz M, Ellison GT. Robust causal inference using directed acyclic graphs: The R package 'dagitty'. *Int J Epidemiol*. (2016) 45:1887–94.

62. VanderWeele TJ. *Explanation in Causal Inference: Methods for Mediation and Interaction*. (2015) New York: Oxford University Press.

63. Song Y, Wang M, Nie L, Liao W, Wei D, Wang L, et al. Exposure to parabens and dysglycemia: Insights from a Chinese population. *Chemosphere*. (2023) 340:139868. doi: 10.1016/j.chemosphere.2023.139868

64. Liu W, Zhou Y, Li J, Sun X, Liu H, Jiang Y, et al. Parabens exposure in early pregnancy and gestational diabetes mellitus. *Environ Int*. (2019) 126:468–75. doi: 10.1016/j.envint.2019.02.040

65. Li AJ, Xue J, Lin S, Al-Malki AL, Al-Ghamdi MA, Kumosani TA, et al. Urinary concentrations of environmental phenols and their association with type 2 diabetes in a population in Jeddah, *Saudi Arabia. Environ Res*. (2018) 166:544–52. doi: 10.1016/j.envres.2018.06.040

frontiers | Frontiers in Public Health

TYPE Original Research
PUBLISHED 19 March 2025
DOI 10.3389/fpubh.2025.1457630

OPEN ACCESS

EDITED BY
Pu Xia,
University of Birmingham, United Kingdom

REVIEWED BY
Janneke Hogervorst,
University of Hasselt, Belgium
Peymaneh Habibi,
Tabriz University of Medical Sciences, Iran

*CORRESPONDENCE
Ming Dong
✉ dongge@jlu.edu.cn

RECEIVED 01 July 2024
ACCEPTED 10 March 2025
PUBLISHED 19 March 2025

CITATION
Gan L, Wang J, Qu K, Jiang W, Lei Y and Dong M (2025) Association of acrylamide exposure with markers of systemic inflammation and serum alpha-klotho concentrations in middle-late adulthood. *Front. Public Health* 13:1457630. doi: 10.3389/fpubh.2025.1457630

Association of acrylamide exposure with markers of systemic inflammation and serum alpha-klotho concentrations in middle-late adulthood

Lin Gan[1], Jiaoyang Wang[1], Kang Qu[1], Wei Jiang[1], Yuhong Lei[2] and Ming Dong[1]*

[1]Department of Neurology and Neuroscience Center, The First Hospital of Jilin University, Changchun, China, [2]Cancer Institute, The First Hospital of Jilin University, Changchun, China

Background: Acrylamide (AA) is a ubiquitous environmental contaminant linked to systemic inflammation and oxidative stress in animal studies; however, the epidemiological evidence is still lacking. This study aimed to evaluate the association of AA exposure with markers of systemic inflammation and serum concentrations of an anti-aging protein, α-klotho.

Methods: The study used data of 1,545 adults aged 40–79 years from the National Health and Nutrition Examination Survey (NHANES) 2013–2016. Internal AA exposure was assessed using hemoglobin adducts of acrylamide and glycidamide (HbAA and HbGA, respectively), the sum of HbAA and HbGA (HbAA + HbGA), and the ratio of HbGA and HbAA (HbGA/HbAA). Two novel indicators, systemic immune-inflammation index (SII) and system inflammation response index (SIRI), were calculated using the lymphocyte, platelet, neutrophil, and monocyte counts. The serum concentration of soluble α-klotho was measured using enzyme-linked immunosorbent assay. Multivariable linear regression models were used to estimate the associations of AA hemoglobin biomarkers with systemic inflammation indicators and serum concentration of α-klotho.

Results: Each one-unit increase in ln-transformed HbAA, HbGA, and HbAA+HbGA was associated with an increase in SII in models adjusted for age, sex, and race/ethnicity [regression coefficient (β) = 32.16, 95% confidence interval (CI): 3.59, 60.73; β =36.37, 95% CI: 5.59, 67.15; and β = 37.17, 95% CI: 6.79, 67.55, respectively]. However, the associations were no longer significant after additional adjustment for lifestyle factors. Higher HbAA and HbAA+HbGA predicted lower serum α-klotho concentrations (β = −35.76 pg./mL, 95% CI: −63.27, −8.25; β = −33.82 pg./mL, 95% CI: −62.68, −4.96, respectively).

Conclusion: The hemoglobin adducts of AA parameters, as biomarkers of internal AA exposure, were associated with reduced serum concentrations of α-klotho among the United States population in their middle-late adulthood. The findings indicated that exposure to AA may have impacts on the molecular pathways of aging and related diseases by influencing α-klotho concentrations.

KEYWORDS

acrylamide, glycidamide, systemic immune-inflammation index, system inflammation response index, α-klotho

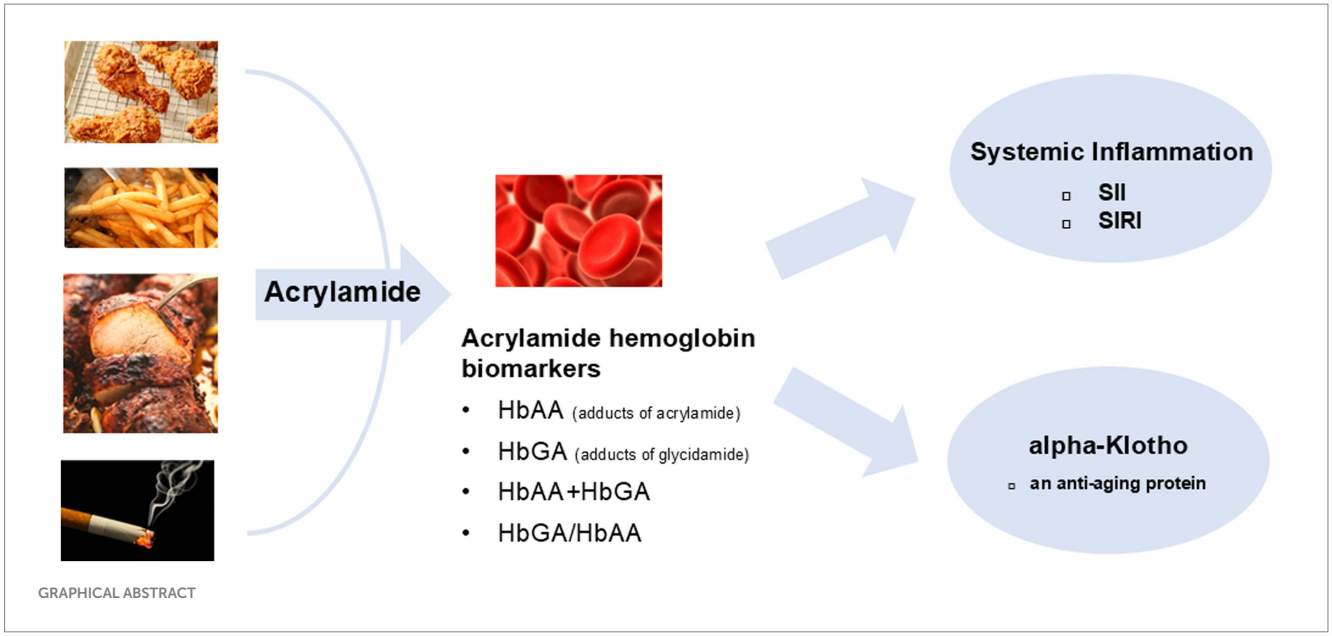

GRAPHICAL ABSTRACT

1 Introduction

Acrylamide (AA) is a reactant extensively used to synthesize polyacrylamide polymers, gels, and binding agents (1). AA has attracted public attention in the last decades because it can be developed via Maillard reaction during food processing at high temperatures, such as frying and baking (2). Meanwhile, it is also found in the smoke generated when tobacco burns in a lit cigarette (3). Thus, AA can be absorbed into the body through ingestion, inhalation, and dermal contact with AA-containing products (3, 4). Diet contributes to an average daily intake of 0.02–1.53 μg/(kg body weight · day) AA for the general population (5). Once absorbed, AA is widely distributed to various organs and metabolized to a major metabolite, glycidamide (GA), in the liver (6). Hemoglobin adducts of AA (HbAA) and GA (HbGA) are validated biomarkers in human biomonitoring and commonly found in the United States (US) population (7). The ubiquitous presence of AA has raised health concerns worldwide owing to its toxicological effects (1, 2).

AA exposure has been related to various adverse health outcomes, such as cancer (8, 9), cardiovascular diseases (10), respiratory diseases (11), diabetes (12), and depression (13, 14). It impacts human health through multiple mechanisms. Particularly, AA exposure increases systemic inflammation (2). *In vitro* and *in vivo* studies indicated that AA treatment activated the nuclear factor-κB (NF-κB) pathway and enhanced the release of pro-inflammatory cytokines (15, 16). However, evidence of AA exposure associated with systemic inflammation in humans is still scarce. Recently, two novel indicators derived from lymphocyte, neutrophil, monocyte, and platelet counts were introduced: the systemic immune-inflammation index (SII) and the system inflammation response index (SIRI) (17). Initially, SII was used to assess the prognosis of patients with liver cancer, whereas SIRI predicted survival after chemotherapy in patients with cancer (18, 19). These indicators were widely used for evaluating systemic inflammation response in the general population because of their easy access and biological significance (20, 21).

Another toxicological mechanism of AA-associated health outcomes is oxidative stress damage. AA or GA contributes to the depletion of glutathione, overproduction of reactive oxygen species (ROS), and alteration of the nuclear factor erythroid 2-related factor 2 pathway (22). Oxidative stress may be inhibited by soluble α-klotho, which is a transmembrane protein related to the aging process (23). α-klotho downregulates ROS-associated stress and prolongs cellular lifespan (24, 25). It also maintains the anti-aging process and prevents aging-related diseases. Therefore, exploring a potential link between AA exposure and soluble α-klotho may have significant public health implications.

AA exposure induces systemic inflammation and oxidative stress in animals (1); however, the epidemiological evidence related to this is quite limited. Previous epidemiological studies suggested that hemoglobin or urinary biomarkers of AA and GA were associated with increased levels of pro-inflammatory cytokines and inflammatory markers, including low-grade inflammation score (INFLA-score), C-reactive protein (CRP), circulating mean platelet volume (MPV), and high-sensitivity interleukin-6 (IL-6) (10, 26–28). However, few studies have addressed the associations of HbAA and HbGA with novel markers of systemic inflammation and serum concentrations of α-klotho. Therefore, this study aimed to explore the associations of AA exposure with markers of systemic inflammation and serum concentrations of α-klotho in general adults aged 40–79 years using the National Health and Nutrition Examination Survey (NHANES) 2013–2016 cycles.

2 Materials and methods

2.1 Study design and population

The study data were extracted from the NHANES database (29). NHANES is a population-based survey aiming to evaluate the health and nutrition of participants in the US. This nationally representative survey included physical examinations, laboratory tests, dietary information, and health-related questionnaires. The NHANES team captured informed consent from each participant *prior to* enrollment. The study protocol (Protocol #2011–17) was reviewed and approved by the NCHS Research Ethics Review Board.

The NHANES 2013–2014 and 2015–2016 cycles were selected owing to data availability. A total of 20,146 participants were enrolled in NHANES 2013–2016 cycles (Figure 1). Adults aged 40–79 years were included ($N = 6,853$). Pregnant women were excluded at the examination ($N = 7$). Furthermore, participants with missing blood cell counts ($N = 478$), missing HbAA and HbGA measurements ($N = 4,495$), and missing α-klotho concentrations in serum ($N = 328$) were excluded from the analysis.

2.2 Measurements of AA and GA concentrations

The concentrations of HbAA and HbGA in human whole blood or erythrocytes were measured (7) as described in a previous study (30). Briefly, the adducts of AA and GA were cleaved using a modified Edman reaction. The Edman products were prepared by liquid–liquid extraction and quantified using high-performance liquid chromatography–tandem mass spectrometry. The limit of detection of AA and GA was 3.90 pmol/g Hb and 4.90 pmol/g Hb, respectively. Laboratory quality assurance and quality control protocols are available on the NHANES website (29).

2.3 Systemic immune-inflammation index

The whole blood specimens were analyzed at NHANES mobile examination centers using automated hematology analyzing devices (29). After analysis in duplicate, the observed results were averaged to improve the data quality. We calculated SII using the counts of peripheral blood cells (1,000 cells/μL):

$$\frac{Platelet\ count \times neutrophil\ count}{Lymphocyte\ count}$$

SIRI was also calculated as follows (19):

$$\frac{Monocyte\ count \times neutrophil\ count}{Lymphocytes\ count}$$

2.4 Serum concentrations of α-klotho

Serum concentrations of soluble α-klotho from the participants were quantified using an extensively validated IBL enzyme-linked immunosorbent assay method (31). The sensitivity of the assay was 6 pg./mL. The samples were analyzed in duplicate to ensure the precision. The final values were calculated using the average of the two observed values.

2.5 Covariables

As reported in previous studies (10, 28), several potential confounding factors in relation to AA exposure and systemic inflammation/α-klotho were considered, including socio-demographic characteristics, physical examination, dietary information, and lifestyles. The covariables were included if they changed the coefficient of AA hemoglobin biomarkers by greater than 10% in simple linear regression models. The following covariables were selected: sex, age, race/ethnicity, educational level, family poverty-income ratio (PIR), body mass index (BMI), cigarette smoking (smoker or non-smoker), alcohol consumption (days per year) and physical activity (minutes per week). Cigarette smoking was assessed by individual's self-report. Smoker was defined as participants who smoked at least 100 cigarettes in life. In the smoking subgroup analysis, an additional continuous variable of an average number of cigarettes smoked per day over the past 30 days was adjusted in the models for smokers. A continuous variable of alcohol consumption was generated from three components: consumption of at least 12 alcohol drinks/lifetime (yes or no), frequency of drinking alcohol over past 12 months (0 to 365) and days of alcohol consumption per week, month, or year. "0" was assigned to individuals who did not have at least 12 alcohol drinks/lifetime. The amount of alcohol consumption was calculated by day × frequency for those who had 12 or more alcohol drinks. Physical activity was calculated as the total weekly minutes of vigorous work activities, moderate work activities, walking or bicycling, vigorous recreational activities, and moderate recreational activities (32).

2.6 Statistical analysis

The general characteristics of participants were summarized using the median and interquartile range for continuous variables

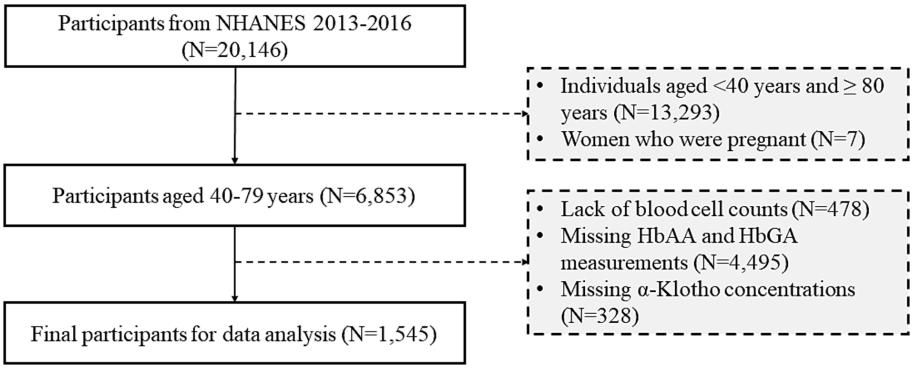

FIGURE 1
The number of participants included in the current analysis in NHANES survey 2013–2016.

TABLE 1 Descriptive statistics of general characteristics of 1,545 participants from NHANES 2013–2016.

Characteristics	N (%)	Variables	Median (25th-75th percentile)
Age (years)		BMI (kg/m^2)	28.7 (24.9, 33.1)
40–59	851 (55.1)	PIR	2.20 (1.15, 4.39)
60–79	694 (44.9)	Endpoints	
Sex		SII	455 (332, 623)
Male	763 (49.4)	SIRI	1.07 (0.75, 1.58)
Female	782 (50.6)	α-klotho (pg/mL)	779 (649, 961)
Race/Ethnicity		Target analytes	
Mexican American	265 (17.2)	HbAA (pmol/g Hb)	41.5 (32.2, 60.6)
Other Hispanic	185 (12.0)	HbGA (pmol/g Hb)	36.2 (26.7, 51.0)
Non-Hispanic White	614 (39.7)	HbAA+HbGA (pmol/g Hb)	78.2 (60.1, 111.0)
Non-Hispanic Black	269 (17.4)	HbGA/HbAA	0.822 (0.689, 0.982)
Other race - including multi-racial	212 (13.7)		
Education			
Less than 9th grade	197 (12.8)		
9th–11th grade	181 (11.7)		
High school grade	333 (21.5)		
Some college	417 (27.0)		
College graduate or above	417 (27.0)		
Cigarette smoking			
Smoker	738 (47.8)		
Non-smoker	807 (52.2)		

N, frequency; %, proportion; BMI, body mass index; PIR, poverty income ratio; SII, systemic immune-inflammation index; SIRI, system inflammation response index.

and frequency and proportion for categorical variables. HbAA, HbGA, HbAA + HbGA, and HbGA/HbAA were natural logarithm (ln) transformed owing to the skewed distribution of residuals. Spearman correlation coefficients were calculated to evaluate pairwise correlations of AA hemoglobin indicators. Multiple imputations with chained equations were applied for a few missing covariables, including family PIR, BMI, cigarette smoking, and alcohol consumption.

Multivariable linear regression models were used to explore the associations of AA hemoglobin biomarkers with SII, SIRI, and serum concentration of α-klotho. The collinearity of the linear regression models was assessed using a variance inflation factor, revealing no multi-collinearity. Regarding covariables, three models were used. Model 1 was a crude model without any adjustment. Model 2 was a basic model adjusted for sex, age, and race/ethnicity. Model 3 was adjusted for all the aforementioned covariables as the primary model. Generalized additive models with 3-degrees-of-freedom natural cubic splines were fitted to estimate the potential nonlinear associations of AA hemoglobin biomarkers with markers of systemic inflammation and serum concentrations of α-klotho. Tobacco smoke is a major source of AA exposure (33). Therefore, an interaction term between cigarette smoking and target biomarkers (data shown in Supplementary Table S1) was further introduced, and then stratified analysis based on cigarette smoking was performed.

Statistical analysis was performed using Stata version 17.0 (Stata Corp, TX, United States) and R version 4.2.1.[1] Statistical significance was considered as a two-sided $p < 0.05$ and $p < 0.10$ for interaction terms.

3 Results

A total of 1,545 participants were included in the present analysis. The general characteristics and outcomes are presented in Table 1. The frequency and proportion of adults aged 40–59 years were 851 and 55.1%, respectively. A majority of participants were non-Hispanic White (39.7%) and had higher educational levels (54.0%).

HbAA and HbGA were detected in all the samples. The median values (25th percentile, 75th percentile) of HbAA, HbGA, and HbAA + HbGA were 41.5 (32.2, 60.6) pmol/g Hb and 36.2 (26.7, 51.0) pmol/g Hb and 78.2 (60.1, 111) pmol/g Hb, respectively. The median value of HbGA/HbAA was 0.822 (0.689, 0.982) (Table 1). HbAA and HbGA were highly correlated with a Spearman correlation coefficient of 0.822 ($p < 0.001$). The median (25th percentile, 75th percentile) SII and SIRI values were 455 (332, 623) and 1.07 (0.75, 1.58), respectively.

1 https://www.r-project.org/

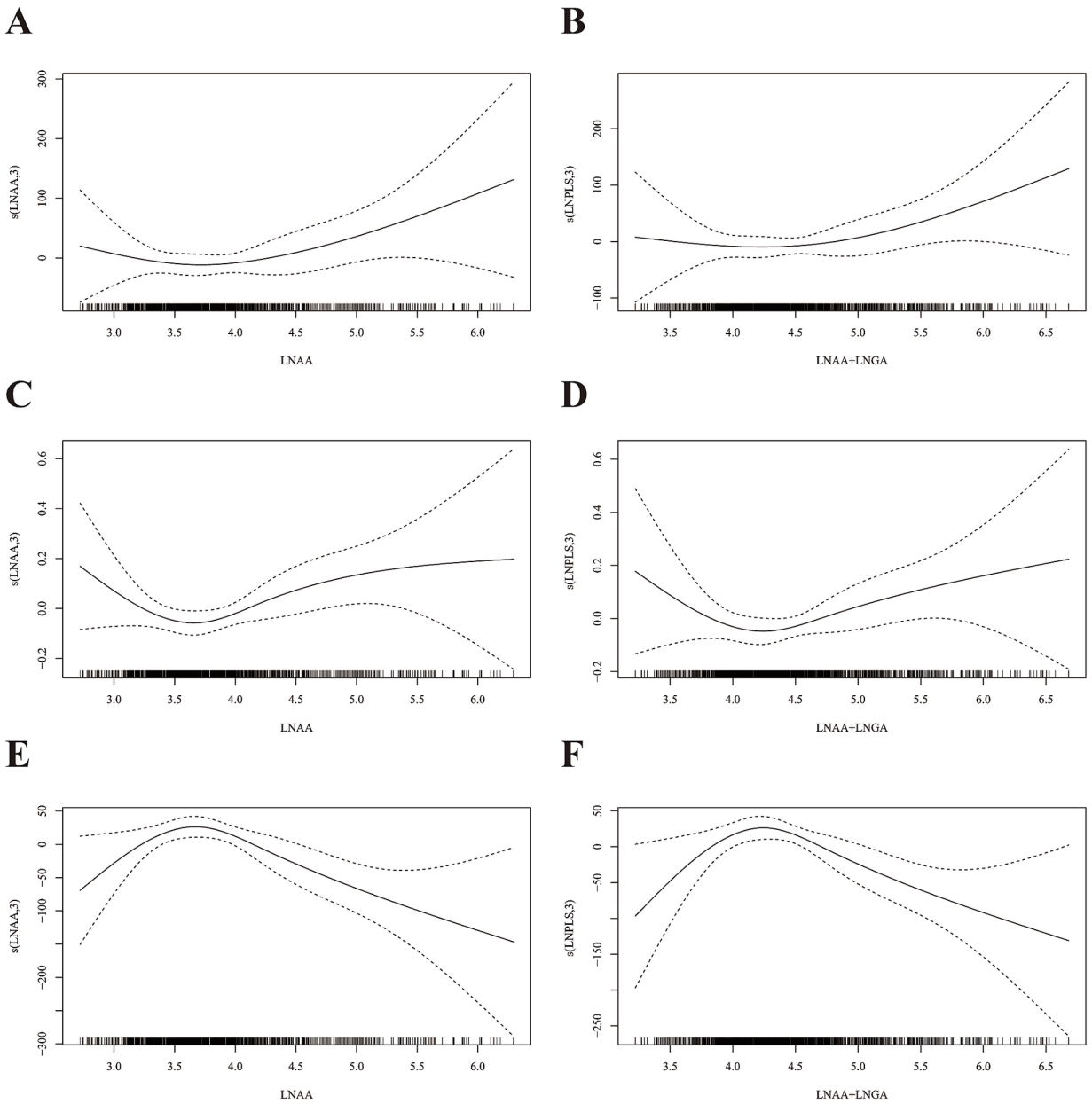

FIGURE 2
Dose–response relationships of AA hemoglobin biomarkers and markers of systemic inflammation and α-Klotho concentrations in serum. **(A)** HbAA and SII; **(B)** HbAA+HbGA and SII; **(C)** HbAA and SIRI; **(D)** HbAA+HbGA and SIRI; **(E)** HbAA and α-Klotho; **(F)** HbAA+HbGA and α-Klotho. LNAA, ln-transformed HbAA; LNAA+LNGA, ln-transformed HbAA+HbGA. The dose–response relationships were assessed by generalized additive models with adjustment for age, sex, race/ethnicity, educational level, body mass index, family poverty income ratio, cigarette smoking, alcohol consumption, and physical activity.

A high correlation was observed between SII and SIRI (Spearman correlation coefficient: 0.747, $p < 0.001$). The median α-klotho concentration in serum was 779 (649, 961) pg./mL (Table 1).

Nonlinear and linear associations between AA hemoglobin biomarkers and markers of systemic inflammation are displayed in Figure 2 and Table 2, respectively. No evidence of statistically significant nonlinear associations between AA hemoglobin biomarkers and systemic inflammation markers was found ($p_{\text{nonlinearity}} > 0.05$, Figure 2). HbAA, HbGA, and HbAA + HbGA were significantly positively correlated with SII and SIRI in the crude models (Model 1) and basic adjusted models (Model 2). No statistically significant association between AA hemoglobin biomarkers and SII or SIRI was observed after adjusting for potential confounders in Model 3.

Table 3 illustrates the associations of AA hemoglobin biomarkers with serum concentrations of α-klotho. Higher HbAA concentration in whole blood was statistically significantly related to decreased serum concentrations of α-klotho ($\beta = -35.76$ pg./mL, 95% CI: −63.27, −8.25; $p = 0.011$), after adjustment for potential confounders. A negative association between HbAA + HbGA and serum concentrations of α-klotho was also observed ($\beta = -33.82$ pg./mL, 95% CI: −62.68, −4.96; $p = 0.022$).

TABLE 2 Estimated regression coefficients and 95% CI for markers of systemic inflammation and AA hemoglobin biomarkers.

	Model 1		Model 1		Model 1	
	β (95% CI)	*P*	β (95% CI)	*P*	β (95% CI)	*P*
SII						
HbAA	32.94 (5.05, 60.84)	0.021	32.16 (3.59, 60.73)	0.028	23.48 (−8.12, 55.08)	0.145
HbGA	47.43 (17.53, 77.34)	0.002	36.37 (5.59, 67.15)	0.021	24.88 (−7.85, 57.61)	0.136
HbAA+HbGA	42.17 (12.52, 71.82)	0.005	37.17 (6.79, 67.55)	0.017	26.84 (−6.29, 59.97)	0.112
HbGA/HbAA	27.42 (−23.63, 78.47)	0.293	−2.92 (−56.32, 50.48)	0.915	−0.97 (−58.63, 56.69)	0.974
SIRI						
HbAA	0.11 (0.03, 0.18)	0.008	0.08 (0.01, 0.16)	0.036	0.07 (−0.02, 0.15)	0.133
HbGA	0.10 (0.01, 0.18)	0.023	0.08 (−0.01, 0.16)	0.075	0.03 (−0.05, 0.12)	0.456
HbAA+HbGA	0.11 (0.03, 0.20)	0.008	0.09 (0.01, 0.17)	0.034	0.06 (−0.03, 0.15)	0.188
HbGA/HbAA	−0.07 (−0.21, 0.07)	0.342	−0.06 (−0.21, 0.08)	0.414	−0.11 (−0.27, 0.04)	0.154

β, regression coefficient; CI, confidence interval; SII, systemic immune-inflammation index; SIRI, system inflammation response index. AA biomarker data was ln-transformed. Model 1 was unadjusted. Model 2 was adjusted for age, sex, race/ethnicity. Model 3 was adjusted for age, sex, race/ethnicity, educational level, body mass index, family poverty income ratio, cigarette smoking, alcohol consumption, physical activity.

TABLE 3 Estimated regression coefficients and 95% CI for serum α-Klotho concentrations and AA hemoglobin biomarkers.

	Model 1		Model 2		Model 3	
	β (95% CI)	*P*	β (95% CI)	*P*	β (95% CI)	*P*
HbAA	−31.54 (−55.93, −7.14)	0.011	−30.73 (−55.60, −5.85)	0.016	−35.76 (−63.27, −8.25)	0.011
HbGA	−18.22 (−44.45, 8.00)	0.173	−21.92 (−48.75, 4.92)	0.110	−24.98 (−53.51, 3.55)	0.086
HbAA+HbGA	−28.63 (−54.59, −2.67)	0.031	−29.64 (−56.12, −3.17)	0.028	−33.82 (−62.68, −4.96)	0.022
HbGA/HbAA	52.52 (7.92, 97.11)	0.021	41.27 (−5.20, 87.73)	0.082	41.50 (−8.73, 91.73)	0.106

β, regression coefficient; CI, confidence interval. AA biomarker data was ln-transformed. Model 1 was unadjusted. Model 2 was adjusted for age, sex, race/ethnicity. Model 3 was adjusted for age, sex, race/ethnicity, educational level, body mass index, family poverty income ratio, cigarette smoking, alcohol consumption, physical activity.

The interaction term based on the multiplication of cigarette smoking and AA hemoglobin biomarkers was statistically significant in the associations between HbAA/HbGA and SII, as well as between HbAA+HbGA and α-klotho (Supplementary Table S1). After stratification by cigarette smoking, HbAA and HbAA + HbGA were borderline significantly associated with decreased serum concentrations of α-klotho only in smokers (β = −40.69 pg./mL, 95% CI: −87.15, 5.77; $p = 0.086$; β = −39.88 pg./mL, 95% CI: −88.23, 8.47; $p = 0.106$, respectively). No statistically significant association was observed with other AA hemoglobin biomarkers in the stratified analyses (Figure 3).

4 Discussion

This cross-sectional analysis revealed negative associations of HbAA and HbAA + HbGA with serum concentrations of α-klotho; the associations were more pronounced in smokers. HbAA and HbAA + HbGA showed no association with SII and SIRI, as calculated using blood cell counts.

Several epidemiological studies have addressed the association of AA exposure at environmentally relevant doses with systemic inflammation measured using various indicators. Our findings were consistent with those of previous studies (10, 26–28). In a pilot study, 14 healthy volunteers (6 smokers) were administered 160 g/day AA-containing potato chips (27). After 4 weeks, the concentrations of inflammation markers, plasma high-sensitivity CRP, high-sensitivity IL-6, gamma-glutamyltransferase significantly increased ($p < 0.10$) compared with baseline (before consumption) among smokers and nonsmokers (27). The urinary AA biomarkers in a Chinese population were significantly associated with increased concentrations of systemic inflammatory marker plasma CRP (28). This increase in plasma CRP concentration mediated 6.34–11.1% of the associations of urinary AA biomarkers with reduced pulmonary function. In a prospective study, Wang et al. (10) reported an association of the urinary AA biomarkers with 10-year cardiovascular disease risks in general adults, mediated by systemic inflammation (plasma CRP and circulating MPV), oxidative stress, and plasma transforming growth factor-β1. In NHANES 2003–2014 cycles, AA hemoglobin biomarkers were related to an increase in cancer mortality (mediated by low-grade INFLA-score), an inflammatory marker derived from CRP, white blood cell and platelet counts, and granulocyte/lymphocyte ratio (26). On the contrary, the present study indicated that AA exposure might not increase systemic inflammation in general adults. The reasons for inconsistent findings may be due to the heterogeneity between populations, outcome measurements, and time window of assessment. We cannot be ruled out that manifestations of inflammatory effects of AA may be temporarily masked by compensatory processes in this population and maybe become apparent in other study population. Moreover, CRP used in the previous studies may be a more sensitive biomarker in measuring inflammation, compared with SII and SIRI (21).

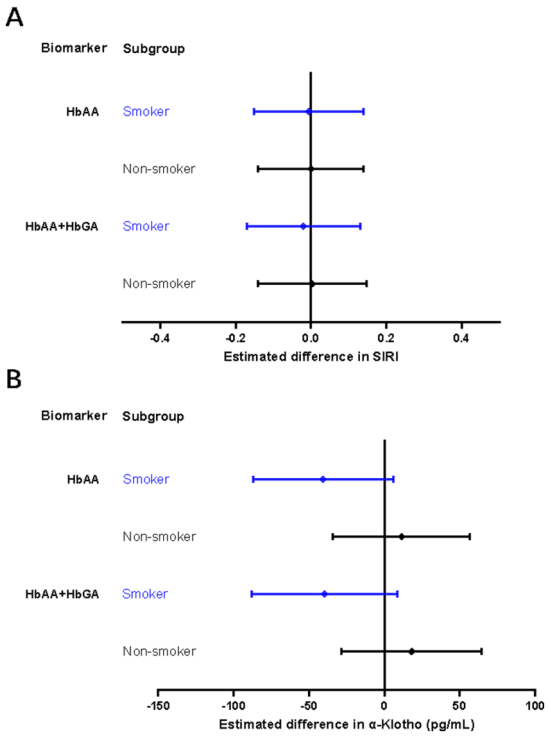

FIGURE 3
Stratified analysis by cigarette smoking for associations of AA hemoglobin biomarkers with SIRI **(A)** or serum α-Klotho concentrations **(B)**. SIRI, system inflammation response index. Models for smokers were adjusted for sex, age, race/ethnicity, educational level, family poverty-income ratio, body mass index, average cigarettes per day during past 30 days, alcohol consumption and physical activity. Models for non-smokers were adjusted for sex, age, race/ethnicity, educational level, family poverty-income ratio, body mass index, alcohol consumption, and physical activity.

Furthermore, given the short half-life of HbAA in humans, there may be exposure misclassification and the relevant time window for AA exposure and inflammation may not overlap.

Both *in vitro* and *in vivo* experimental studies have indicated that AA exposure increased inflammation in various tissues, including the neurons, brain, liver, and kidney (1). AA exposure induced an inflammatory response *in vitro* via the nuclear factor-κB (NF-κB) pathway in human PC12 cells (16). The transcription of inflammatory genes was enhanced after NF-κB activation, and pro-inflammatory cytokines, such as tumor necrosis factor-α (TNF-α), interleukin 6 (IL-6), pro-IL-1β, and pro-IL-18, were released. These findings were further observed in rodent models. AA treatment enhanced the serum concentrations of cytokines, including TNF-α, pro-IL-1β, and IL-6 (15, 34).

Several epidemiological studies have reported that reductions in serum α-Klotho levels were associated with several environmental contaminants, including heavy metals (35), perfluoroalkyl and polyfluoroalkyl substances (36), and polycyclic aromatic hydrocarbons (37). The exact biological mechanisms of action of AA exposure on the reduction in serum concentrations of α-klotho are still unclear. The most possible underlying mechanism was AA-induced oxidative stress. Several animal and epidemiological studies showed that AA exposure increases the levels of oxidative stress markers, such as urinary 8-hydroxydeoxyguanosine and 8-iso-prostaglandin-F2α (10, 15). The α-klotho stimulation upregulated the expression of phosphorylation forkhead box protein O3a, inhibiting ROS-related oxidative stress damage (24). ROS production and oxidative stress damage were negatively correlated with serum concentrations of α-klotho (25).

Stratified analyses revealed more prominent associations between AA exposure and serum concentrations of α-klotho in smokers than nonsmokers. This was also observed previously in associations of AA exposure with other health-related outcomes, including diabetes (12), cardiovascular diseases (38, 39), depressive symptoms (13). Cigarette smoking, a critical source of AA exposure, was associated with increases in local and systemic inflammation (40) and a reduction in serum concentrations of α-klotho (3, 41). Smokers had higher exposure levels of AA and other toxic chemicals, such as tar, formaldehyde, polycyclic aromatic hydrocarbons, and heavy metals (40), compared with nonsmokers. We cannot exclude the possibility that AA in combination with a series of toxic chemicals in tobacco smoke contributes to the decrease in serum concentrations of α-klotho in smokers. Residual confounding by smoking may also play a role in association between AA exposure and serum α-klotho concentrations. More epidemiological studies should be conducted to assess the exposure to a mixture of toxic chemicals associated with systemic inflammation and biological aging among active smokers.

This epidemiological study was novel in exploring the associations of internal AA exposure with novel systemic inflammation markers and serum concentrations of α-klotho in the general population. However, this study had several limitations. First, causality could not be inferred between AA exposure and systemic inflammation or serum concentrations of α-klotho owing to the observational study design, especially for the cross-sectional study design. Second, despite adjusting for a broad set of covariables, we could not exclude the possibility of residual confounders, such as occupational factors (42), and other environmental contaminants (35, 36). These may have confounding effects on the exposure-outcome associations. Third, HbAA biomarkers were assessed only once and thus reflect AA exposure over a short time window (42). This single measurement may lead to exposure misclassification, as the relevant time window for AA exposure and inflammation may not overlap. Repeated measurements would have provided a more accurate or long-term assessment of exposure levels.

5 Conclusion

AA exposure assessed using hemoglobin biomarkers was associated with decreased serum concentrations of α-klotho in general adults aged 40–79 years. The findings of this study provide suggestive evidence regarding the potential health effects of AA exposure at environmentally relevant doses. Future studies are warranted to identify potential biological mechanisms and develop intervention strategies.

Data availability statement

The raw data supporting the conclusions of this article will be made available by the authors, without undue reservation.

Ethics statement

The study protocol (Protocol #2011–17) was reviewed and approved by the NCHS Research Ethics Review Board (ERB). The studies were conducted in accordance with the local legislation and institutional requirements. The participants provided their written informed consent to participate in this study.

Author contributions

LG: Conceptualization, Data curation, Formal analysis, Methodology, Writing – original draft, Writing – review & editing. JW: Data curation, Formal analysis, Methodology, Software, Supervision, Writing – review & editing. KQ: Data curation, Formal analysis, Supervision, Writing – review & editing. WJ: Conceptualization, Formal analysis, Supervision, Writing – review & editing. YL: Conceptualization, Formal analysis, Writing – review & editing. MD: Conceptualization, Funding acquisition, Project administration, Supervision, Writing – review & editing.

Funding

The author(s) declare that financial support was received for the research and/or publication of this article. This work was supported by the Jilin Provincial Health Science and Technology Capacity Enhancement Program Project (2024A015)and the National Key Research and Development Program of China (2023YFC2508701).

Acknowledgments

We appreciated the adults for participation in the NHANES survey. We are also grateful for the U.S. Centers for Disease Control and Prevention (CDC) for providing the publicly available data.

Conflict of interest

The authors declare that the research was conducted in the absence of any commercial or financial relationships that could be construed as a potential conflict of interest.

Publisher's note

Supplementary material

The Supplementary material for this article can be found online at: https://www.frontiersin.org/articles/10.3389/fpubh.2025.1457630/full#supplementary-material

References

1. Yan F, Wang L, Zhao L, Wang C, Lu Q, Liu R. Acrylamide in food: occurrence, metabolism, molecular toxicity mechanism and detoxification by phytochemicals. *Food Chem Toxicol*. (2023) 175:113696. doi: 10.1016/j.fct.2023.113696

2. Koszucka A, Nowak A, Nowak I, Motyl I. Acrylamide in human diet, its metabolism, toxicity, inactivation and the associated European Union legal regulations in food industry. *Crit Rev Food Sci Nutr*. (2020) 60:1677–92. doi: 10.1080/10408398.2019.1588222

3. Esposito F, Squillante J, Nolasco A, Montuori P, Macri PG, Cirillo T. Acrylamide levels in smoke from conventional cigarettes and heated tobacco products and exposure assessment in habitual smokers. *Environ Res*. (2022) 208:112659. doi: 10.1016/j.envres.2021.112659

4. Liao KW, Chang FC, Chang CH, Huang YF, Pan WH, Chen ML. Associating acrylamide internal exposure with dietary pattern and health risk in the general population of Taiwan. *Food Chem*. (2022) 374:131653. doi: 10.1016/j.foodchem.2021.131653

5. Timmermann CAG, Molck SS, Kadawathagedara M, Bjerregaard AA, Tornqvist M, Brantsaeter AL, et al. A review of dietary intake of acrylamide in humans. *Toxics*. (2021) 9:155. doi: 10.3390/toxics9070155

6. Sumner SC, Williams CC, Snyder RW, Krol WL, Asgharian B, Fennell TR. Acrylamide: a comparison of metabolism and hemoglobin adducts in rodents following dermal, intraperitoneal, oral, or inhalation exposure. *Toxicol Sci*. (2003) 75:260–70. doi: 10.1093/toxsci/kfg191

7. Vesper HW, Caudill SP, Osterloh JD, Meyers T, Scott D, Myers GL. Exposure of the U.S. population to acrylamide in the National Health and nutrition examination survey 2003-2004. *Environ Health Perspect*. (2010) 118:278–83. doi: 10.1289/ehp.0901021

8. Filippini T, Halldorsson TI, Capitão C, Martins R, Giannakou K, Hogervorst J, et al. Dietary acrylamide exposure and risk of site-specific cancer: a systematic review and dose-response Meta-analysis of epidemiological studies. *Front Nutr*. (2022) 9:875607. doi: 10.3389/fnut.2022.875607

9. Pelucchi C, Bosetti C, Galeone C, La Vecchia C. Dietary acrylamide and cancer risk: an updated meta-analysis. *Int J Cancer*. (2015) 136:2912–22. doi: 10.1002/ijc.29339

10. Wang B, Wang X, Yu L, Liu W, Song J, Fan L, et al. Acrylamide exposure increases cardiovascular risk of general adult population probably by inducing oxidative stress, inflammation, and TGF-beta1: a prospective cohort study. *Environ Int*. (2022) 164:107261. doi: 10.1016/j.envint.2022.107261

11. Liu S, Ben X, Liang H, Fei Q, Guo X, Weng X, et al. Association of acrylamide hemoglobin biomarkers with chronic obstructive pulmonary disease in the general population in the US: NHANES 2013-2016. *Food Funct*. (2021) 12:12765–73. doi: 10.1039/D1FO02612G

12. Yin G, Liao S, Gong D, Qiu H. Association of acrylamide and glycidamide haemoglobin adduct levels with diabetes mellitus in the general population. *Environ Pollut*. (2021) 277:116816. doi: 10.1016/j.envpol.2021.116816

13. Li Z, Sun J, Zhang D. Association between acrylamide hemoglobin adduct levels and depressive symptoms in US adults: NHANES 2013-2016. *J Agric Food Chem*. (2021) 69:13762–71. doi: 10.1021/acs.jafc.1c04647

14. Wang A, Wan X, Zhuang P, Jia W, Ao Y, Liu X, et al. (2023) high fried food consumption impacts anxiety and depression due to lipid metabolism disturbance and neuroinflammation. *Proc Natl Acad Sci USA*. (2023) 120:e2221097120. doi: 10.1073/pnas.2221097120

15. Alturfan AA, Tozan-Beceren A, Sehirli AO, Demiralp E, Sener G, Omurtag GZ. Resveratrol ameliorates oxidative DNA damage and protects against acrylamide-induced oxidative stress in rats. *Mol Biol Rep*. (2012) 39:4589–96. doi: 10.1007/s11033-011-1249-5

16. Pan X, Wu X, Yan D, Peng C, Rao C, Yan H. Acrylamide-induced oxidative stress and inflammatory response are alleviated by N-acetylcysteine in PC12 cells: involvement of the crosstalk between Nrf2 and NF-κB pathways regulated by MAPKs. *Toxicol Lett*. (2018) 288:55–64. doi: 10.1016/j.toxlet.2018.02.002

17. Luo S, Liu Z, Jiao R, Li W, Sun J, Ma S, et al. The associations of two novel inflammation indexes, systemic immune-inflammation index (SII) and system inflammation response index (SIRI), with periodontitis: evidence from NHANES 2009-2014. *Clin Oral Investig*. (2024) 28:129. doi: 10.1007/s00784-024-05529-1

18. Hu B, Yang XR, Xu Y, Sun YF, Sun C, Guo W, et al. Systemic immune-inflammation index predicts prognosis of patients after curative resection for hepatocellular carcinoma. *Clin Cancer Res*. (2014) 20:6212–22. doi: 10.1158/1078-0432.CCR-14-0442

19. Qi Q, Zhuang L, Shen Y, Geng Y, Yu S, Chen H, et al. A novel systemic inflammation response index (SIRI) for predicting the survival of patients with

pancreatic cancer after chemotherapy. *Cancer*. (2016) 122:2158–67. doi: 10.1002/cncr.30057

20. Wang P, Guo X, Zhou Y, Li Z, Yu S, Sun Y, et al. Monocyte-to-high-density lipoprotein ratio and systemic inflammation response index are associated with the risk of metabolic disorders and cardiovascular diseases in general rural population. *Front Endocrinol*. (2022) 13:944991. doi: 10.3389/fendo.2022.944991

21. Xia Y, Xia C, Wu L, Li Z, Li H, Zhang J. Systemic immune inflammation index (SII), system inflammation response index (SIRI) and risk of all-cause mortality and cardiovascular mortality: a 20-year follow-up cohort study of 42,875 US adults. *J Clin Med*. (2023) 12:1128. doi: 10.3390/jcm12031128

22. Gao H, Xue Y, Wu L, Huo J, Pang Y, Chen J, et al. Protective effect of Lycium ruthenicum polyphenols on oxidative stress against acrylamide induced liver injury in rats. *Molecules*. (2022) 27:4100. doi: 10.3390/molecules27134100

23. Kuro OM. The klotho proteins in health and disease. *Nat Rev Nephrol*. (2019) 15:27–44. doi: 10.1038/s41581-018-0078-3

24. Brooke M, Emerling 1 FW, Liu J-L, Mak TW, Chandel NS. PTEN regulates p300-dependent hypoxia-inducible factor 1 transcriptional activity through Forkhead transcription factor 3a (FOXO3a). *Proc Natl Acad Sci USA*. (2008) 105:2622–7. doi: 10.1073/pnas.0706790105

25. Hsieh CC, Kuro-o M, Rosenblatt KP, Brobey R, Papaconstantinou J. The ASK1-signalosome regulates p38 MAPK activity in response to levels of endogenous oxidative stress in the klotho mouse models of aging. *Aging*. (2010) 2:597–611. doi: 10.18632/aging.100194

26. Gu W, Zhang J, Ren C, Gao Y, Zhang T, Long Y, et al. The association between biomarkers of acrylamide and cancer mortality in U.S. adult population: evidence from NHANES 2003-2014. *Front Oncol*. (2022) 12:970021. doi: 10.3389/fonc.2022.970021

27. Naruszewicz M, Zapolska-Downar D, Kosmider A, Nowicka G, Kozlowska-Wojciechowska M, Vikstrom AS, et al. Chronic intake of potato chips in humans increases the production of reactive oxygen radicals by leukocytes and increases plasma C-reactive protein: a pilot study. *Am J Clin Nutr*. (2009) 89:773–7. doi: 10.3945/ajcn.2008.26647

28. Wang B, Wang X, Yang S, Cheng M, Zhou Y, Zhou M, et al. Acrylamide exposure and pulmonary function reduction in general population: the mediating effect of systemic inflammation. *Sci Total Environ*. (2021) 778:146304. doi: 10.1016/j.scitotenv.2021.146304

29. Centers for Disease Control and Prevention (CDC). National Health and Nutrition Examination Survey (NHANES). Available online at: https://www.cdc.gov/nchs/nhanes/index.htm (Accessed January 2, 2024).

30. Vesper HWSN, Hallmans G, Tjonneland A, Agudo A, Benetou V. Cross-sectional study on acrylamide hemoglobin adducts in subpopulations from the European prospective investigation into Cancer and nutrition (EPIC) study. *J Agric Food Chem*. (2008) 56:6046–53. doi: 10.1021/jf703750t

31. Yamazaki Y, Urakawa AI, Shimada T, Murakami J, Aono Y, Hasegawa H, et al. Establishment of a sandwich ELISA for soluble alpha-klotho measurements: age-dependent change of soluble alpha-klotho levels in healthy subjects. *Biochem Biophys Res Comm*. (2017) 398:513–8. doi: 10.1016/j.bbrc.2010.06.110

32. Dong JX, Jiang LL, Liu YP, Zheng AX. Association between composite dietary antioxidant index and metabolic dysfunction-associated fatty liver disease: a cross-sectional study from NHANES. *BMC Gastroenterol*. (2024) 24:465. doi: 10.1186/s12876-024-03556-6

33. Kenwood BM, Zhu W, Zhang L, Bhandari D, Blount BC. Cigarette smoking is associated with acrylamide exposure among the U.S. population: NHANES 2011-2016. *Environ Res*. (2022) 209:112774. doi: 10.1016/j.envres.2022.112774

34. Zhang L, Wang E, Chen F, Yan H, Yuan Y. Potential protective effects of oral administration of allicin on acrylamide-induced toxicity in male mice. *Food Funct*. (2013) 4:1229–36. doi: 10.1039/c3fo60057b

35. Kim D, Lee S, Choi JY, Lee J, Lee HJ, Min JY, et al. Association of alpha-klotho and lead and cadmium: a cross-sectional study. *Sci Total Environ*. (2022) 843:156938. doi: 10.1016/j.scitotenv.2022.156938

36. Li M, Ma Y, Cheng W, Zhang L, Zhou C, Zhang W, et al. Association between perfluoroalkyl and polyfluoroalkyl internal exposure and serum alpha-klotho levels in middle-old aged participants. *Front Public Health*. (2023) 11:1136454. doi: 10.3389/fpubh.2023.1136454

37. Chen YY, Chen WL. The relationship between polycyclic aromatic hydrocarbons exposure and serum klotho among adult population. *BMC Geriatr*. (2022) 22:198. doi: 10.1186/s12877-022-02924-9

38. Wang B, Cheng M, Yang S, Qiu W, Li W, Zhou Y, et al. Exposure to acrylamide and reduced heart rate variability: the mediating role of transforming growth factor-β. *J Hazard Mater*. (2020) 395:122677. doi: 10.1016/j.jhazmat.2020.122677

39. Zhang Y, Huang M, Zhuang P, Jiao J, Chen X, Wang J, et al. Exposure to acrylamide and the risk of cardiovascular diseases in the National Health and nutrition examination survey 2003-2006. *Environ Int*. (2018) 117:154–63. doi: 10.1016/j.envint.2018.04.047

40. Johannsen A, Susin C, Gustafsson A. Smoking and inflammation: evidence for a synergistic role in chronic disease. *Periodontol*. (2014) 64:111–26. doi: 10.1111/j.1600-0757.2012.00456.x

41. Du R, Tang X, Jiang M, Qian S, Yang L, Tong X, et al. Association between cigarette smoking and serum alpha klotho levels among US adults over 40-years-old: a cross-sectional study. *Sci Rep*. (2023) 13:19519. doi: 10.1038/s41598-023-46698-5

42. Bergmark E, Calleman CJ, He F, Costa LG. Determination of hemoglobin adducts in humans occupationally exposed to acrylamide. *Toxicol Appl Pharmacol*. (1993) 120:45–54. doi: 10.1006/taap.1993.1085

frontiers | Frontiers in Public Health

TYPE Original Research
PUBLISHED 09 April 2025
DOI 10.3389/fpubh.2025.1459060

OPEN ACCESS

EDITED BY
Solomon Dan,
Beibu Gulf University, China

REVIEWED BY
Orazio Valerio Giannico,
Local Health Authority of Taranto, Italy
Mostafa Yuness Abdelfatah Mostafa,
Minia University, Egypt

*CORRESPONDENCE
Ching-Fu Lee
✉ leecf@mx.nthu.edu.tw

RECEIVED 03 July 2024
ACCEPTED 18 March 2025
PUBLISHED 09 April 2025

CITATION
Salah-Tantawy A, Chang C-SG, Young S-S and Lee C-F (2025) Multivariate analyses to evaluate the contamination, ecological risk, and source apportionment of heavy metals in the surface sediments of Xiang-Shan wetland, Taiwan.
Front. Public Health 13:1459060.
doi: 10.3389/fpubh.2025.1459060

Multivariate analyses to evaluate the contamination, ecological risk, and source apportionment of heavy metals in the surface sediments of Xiang-Shan wetland, Taiwan

Ahmed Salah-Tantawy[1,2,3], Ching-Sung Gavin Chang[4], Shuh-Sen Young[2] and Ching-Fu Lee[2]*

[1]International Ph.D. Program in Environmental Science and Technology, University System of Taiwan (UST), Hsinchu, Taiwan, [2]Institute of Analytical and Environmental Sciences, College of Nuclear Science, National Tsing Hua University, Hsinchu, Taiwan, [3]Marine Science Division, Department of Zoology, College of Science, Al-Azhar University, Assiut, Egypt, [4]Institute of Bioinformatics and Systems Biology, National Yang-Ming Chiao Tung University, Hsinchu, Taiwan

Nowadays, heavy metal (HM) contamination and their ecological risk in coastal sediments are global issues. This research provides insight into the heavy metals' contamination, source apportionment, and potential ecological risks in the surface sediments of the Xiang-Shan wetland in Taiwan, which is undergoing rapid economic development, mainly by the semiconductor industries. The levels of twelve metals and total organic matter (TOM) were measured in 44 samples of surface sediment during the spring and winter seasons of 2022. Subsequently, the single and comprehensive pollution indices were assessed. The findings showed that the average of HM contents exhibited a descending sequence of Al > Fe > Mn > Zn > Co > Ga > Cr > Cu > In > Ni > Pb = Cd during both seasons. The E_f, I_{geo}, and PI showed that the majority of sediment samples were uncontaminated to heavily contaminated by Fe, Al, Zn, Cu, Mn, Cr, Ni, Co and Ga, and extremely contaminated by In. Moreover, PLI and mC_{deg} unveiled that the surface sediments of DJ, OB, and KY stations were strongly or extremely polluted. PERI revealed that the sediment shows minimal to moderate ecological risk. The findings of multivariate analyses suggested that Fe, Al, Cu, Zn, and Ni derived from natural sources, while Ga, In, Co, Cr, and Mn originated from both anthropogenic and natural origins. Hence, it is critical that HM contamination, particularly Co, In, and Ga, be continuously monitored in the study area. Our data provide significant insights for more effective prevention and evaluation of HM contamination in the aquatic-sedimentary ecosystems of Taiwan.

KEYWORDS

sediments, ecological risk, Xiang-Shan, heavy metal, pollution index, sediment quality guidelines, wetlands, Taiwan

Introduction

Due to fast industrialization and urbanization, heavy metals (HMs) in marine ecosystems have been recognized as significant intermediary sources for the presence of contamination in marine environments and even population health (1). They are a grave hazard to people, living creatures, and natural settings owing to their unique physicochemical properties, such as high density, toxicity, persistence, bioaccumulation traits, and difficulty in removing them by self-purification (2–6). The accumulation of HM in living organisms and food webs is another manner in which HMs contribute to the deterioration of marine environments by diminishing species variety and richness (7, 8). Anthropogenically, HMs can enter marine and coastal ecosystems via multiple sources, e.g., agriculture, sewage, industries and household discharges (9). Additionally, they are triggered naturally by lithogenic events, including air deposition (10, 11).

Once heavy metals enter the aquatic system from different origins, some of them may dissolve, while others may bind to the suspended particles and eventually sink in the sedimentary substrate over time (12, 13). Due to fluctuations and discontinuities in water movement, sediment is an indispensable and dynamic factor in aquatic environments. It has biogeochemical and physical properties that assess the potential risks to the environment, and it has given us better tools for figuring out where heavy metals come from and how they are distributed than the water inspection over it (1). As a natural reservoir for the preponderance of metal contaminants dispersed into seawater, marine sediments can be utilized to evaluate the contamination level and environmental threat posed by HMs in various marine habitats (14–18). The evaluation of these characteristics offers crucial data about the effects of HM contamination and encourages environmentalists toward appropriate remediation solutions (19, 20). Likewise, such data will help authorities, legislators, and environmental activists understand the associations among coastal improvement and its efficient management to safeguard coastlines from global HM contamination (21).

Considering the vitality of the coastal ecosystem, several investigations on the contamination of sediments by HMs have been accomplished (22–26) and a number of geochemical and pollution indices, including the geoaccumulation index (I_{geo}), contamination factor (C_f), enrichment factor (E_f), pollution load index (PLI), modified contamination degree (mC_{deg}), potential ecological risk index (PERI), and sediment quality guidelines (SQGs), have been established in order to calculate the contamination level and environmental risk of HMs in marine sediments (25, 27–35). Furthermore, bivariate and multivariate statistical approaches, such as the Pearson's correlation coefficient (PCC), Principle component analysis (PCA), and Hierarchical cluster analysis (HCA), are being implemented progressively to discover the potential origins of HMs and measure their pollution degree in sediments (26, 36–39).

In Taiwan, the government and researchers devoted scant attention to environmental issues spurred by sediment pollution with heavy metals. Recently, human operations for economic growth, mainly by industry, have been consistently and swiftly intensified, especially in Hsinchu city. After the 1980s, Hsinchu City had a new era of industrial expansion, and Hsinchu Science Industrial Park (HSIP) rose to the top position of semiconductor production around the globe. Besides, this park contained numerous innovative manufacturers of light-emitting diodes, liquid crystal displays, and optoelectronic plates, etc. According to the fabrication procedures of high-tech devices, a wide variety of substances are utilized in huge quantities. Despite stringent surveillance, the ultimate effluent water from the treatment plant still contains a significant proportion of contaminants (25). In HSIP, the daily water intake exceeds 200 thousand CMD, and the final wastewater from the wastewater treatment plant of the HSIP (over 100 thousand CMD) is released into the KeYa river. The Xiang-Shan wetland receives a large amount of freshwater from the KeYa stream since the KeYa river is the primary terrestrial source of freshwater. Over 40 % of freshwater production is wastewater from the treatment plant; approximately 40 % is untreated household waste; and less than 20 % is natural water gathered in the catchment region of the river. The new era of technological advancement introduced different forms of contaminants that settled on the surface of sediment and were immobilized by the adsorption process (40, 41). Therefore, it is critical to explore the ecological concerns and determine the existing level of HM pollution in marine sediments as well as the probable sources in Xiang-Shan wetland.

Yet, there is little accessible knowledge regarding the Xiang-Shan wetland's heavy metal pollution and related health threats. Improving knowledge of sediment heavy metal pollution helps stakeholders, including the government and the public, safeguard the distinctive hydrological and biological ecosystem of the Xiang-Shan wetland. Therefore, 44 surface sediment samples were collected during two seasons to (1) investigate the sediment properties like, granulometric analysis (GSA) and total organic matter (TOM), (2) determine the total contents of twelve metals (e.g., Zn, Al, Ni, Fe, Cu, Mn, Co, Cr, In, Cd, Ga, and Pb), (3) assess the contamination level and possible risks associated with the studied elements, and (4) explore the potential origins of HMs by utilizing bivariate and multivariate statistical analysis. The findings on HM pollution and risks in the Xiang-Shan wetland's surface sediments described herein are likely to be useful to environmental researchers and lawmakers.

Materials and methods

Study area

The Xiang-Shan wetland is situated west of Hsinchu city in Taiwan, between the KeYa river and HaiShan Fishing Harbor (Figure 1). The study area is 17 km^2, with an 8-kilometer shoreline. It is characterized by fine sediments and a variety of species like crustaceans, prawns, benthic invertebrates, shellfish, and endangered avian species (42, 43). Since 1980, Hsinchu has been transformed into a significant center of high-tech industry, where the Hsinchu Science Industrial Park (HSIP) and its environs are home to the information technology (IT) industrial complex, commonly recognized as "Eastern Silicon Valley." The HSIP is one of the largest emitters of treated water discharges (104,842 m^3/d), according to Taiwan's EPA permit registration. In the late 1990s, there were a number of noteworthy ecological incidents, such as the foul river water odor, aberrant blood test results of local residents, and frequent dead fish episodes in the KeYa stream (44, 45). The KeYa River is the main river that runs across the industrialized urban area. In fact, the watershed contains over 500 manufacturing facilities, including factories for electroplating, glass, cement, paper, pulp mills, computer chip manufacturing, container assembly, dyeing, rubber production, chemical plants, fertilizer manufacturing, printing, and metallic analyzing. Nowadays, the KeYa

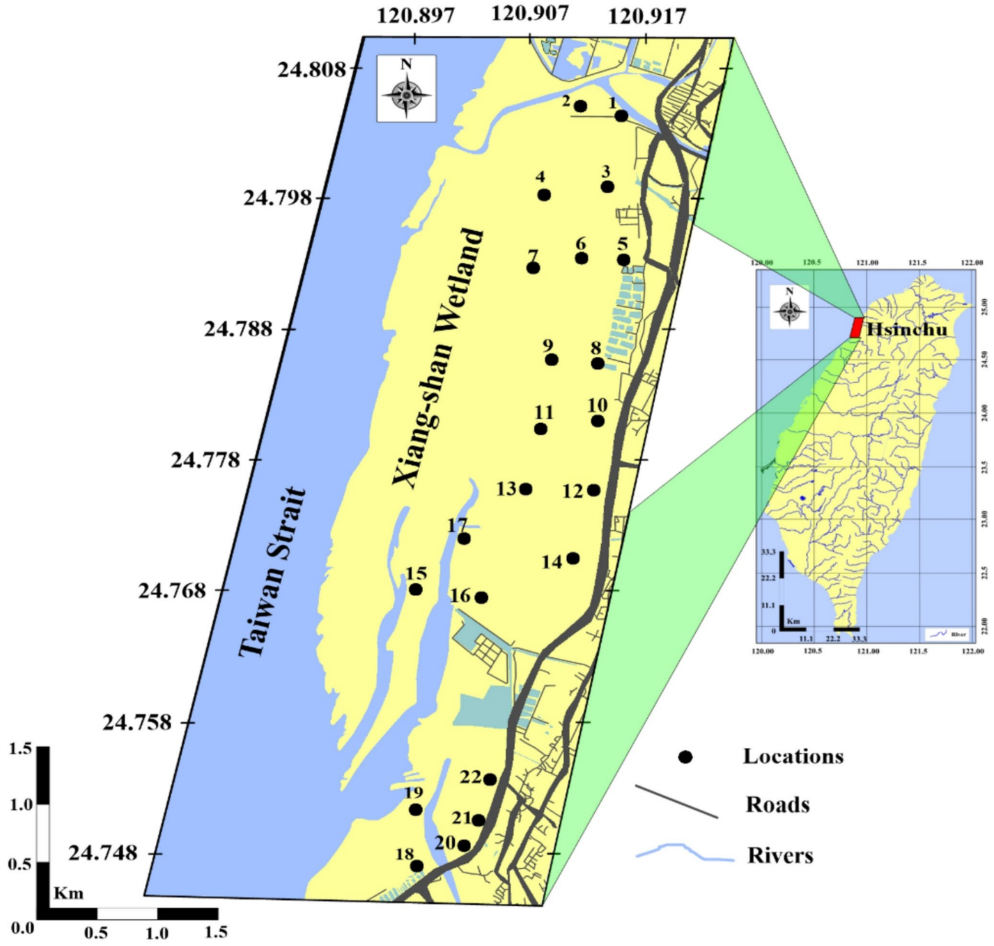

FIGURE 1
Map of the study stations illustrates the sampling locations (Surfer v. 10.7.972).

River continues to be the primary water body in Hsinchu City for collecting various pollutants dumped from domestic drainage from the surrounding population, agricultural and industrial effluent, and possibly occasionally illicit disposal of unprocessed wastewater from propagated industries (46). As a result, the Xiang-Shan wetland receives all of the freshwater from the KeYa river, and all contaminants from urban, agricultural, and industrial uses either sink in the sediments or are swept away by the shifting tides to the Taiwan Strait. Among the many contaminants, anthropogenic metals are extremely mobile and bioavailable and can harm aquatic creatures and human populations (47, 48).

Sediment sampling and preparation

The study area covers an area of about 1,600 hectares overall, with a shoreline of about 8 km and it was split up into nine primary stations (KeYa (KY), KeYa Water Supply Center (KW), DaJuang (DJ), HuiMin (HM), FongCin (FC), HaiShan (HS), Oyster Bed (OB), YenKan (YK), and Mangrove Area (MA)), each of which had a number of locations spaced approximately 400 meters apart that extended from the shore to the interior (perpendicular to the coast). The main sampling stations were divided into 2, 2, 3, 2, 2, 3, 3, 2, and 3 locations for KY, KW, DJ, HM, FC, HS, OB, YK, and MA, respectively (Figure 1). In this research, 44 samples of surface sediment (0–5 cm deep) were gathered from 22 locations in the spring and winter of 2022. The same approach was employed to gather sediment samples in the winter as in the spring ($n = 22$).

At each sampling location, surface sediments were collected in labeled plastic bags using a sanitized glass scraper in order to prevent possible cross-contamination, and each sample was obtained by combining four subsamples. Then, about 500 g of combined sediment subsamples were put in a sealed plastic bag to keep the sample clean, clearly marked, and immediately transferred to the laboratory in a cool container. In our lab, sediment samples were dried in a dust-free area. The semi-dried state, it was smashed using an unpolluted glass vessel and dried in the oven at 50°C for two hours to eliminate the moisture content. Once dry, we removed non-sediment impurities such as roots, shells, gravel, and other debris. Following this, each sediment sample was split into three groups as follows: 100 g for GSA, 20 g for TOM, and 50 g for HMs analysis, and preserved at room temperature in plastic bags until examination. For heavy metal and total organic carbon analyses, about 10 g of each dried sediment sample were disaggregated with agate mortar into very fine grains (< 0.063 mm).

Geochemical analyses

Grain size analysis

Mechanical sieve methods were used to perform grain size analysis (GSA) for Xiang-Shan sediments (49). The particle-size fractions were differentiated by passing 100 grams of dried sediment through a stainless-steel sieve. Particle sizes were expressed using the phi scale (Φ), since the logarithmic scale is more convenient than the equimultiple scale. Seven categories were acquired: gravel ($\Phi_{-1} > 2000$ µm), very coarse sand ($\Phi_0 > 1{,}000$ µm), coarse sand ($\Phi_1 > 500$ µm), medium sand ($\Phi_2 > 250$ µm), fine sand ($\Phi_3 > 125$ µm), very fine sand ($\Phi_4 > 63$ µm) and silt or clay ($\Phi_5 < 63$ µm). The resultant sediment categories were re-classified into three distinct classes: gravel (Φ_{-1}), sand ($\Phi_0 + \Phi_1 + \Phi_2 + \Phi_3$), and mud ($\Phi_4 + \Phi_5$) (25).

Total organic carbon

The Walkley-Black procedure was employed for quantifying total organic carbon (TOC) in surface sediments (50). 0.5 g of pulverized sediment was heated exothermically and oxidized with 1 N potassium dichromate ($Cr_2O_7^{-2}$) and sulfuric acid (1:2). To eradicate excess dichromate, the solution was then adjusted with 0.5 N ferrous sulfate heptahydrate ($FeSO_4$. $7H_2O$) solution after adding o-phenanthroline indicator (3 to 4 droplets). Accordingly, the results were multiplied by 1.8 to get the organic matter values. Likewise, the blank titration was carried out to standardize the $Cr_2O_7^{-2}$.

Bioavailable of heavy metals concentrations (mg/kg)

Twelve metals were measured in surface sediment samples using the acid digestion method (51). To evaluate the heavy metal contents, 0.5 gram of each homogenized sample was digested by a 12 mL combination of hydrochloric and nitric acids (1:3) and then heated inside a microwave oven (MarsXpress) for 12 min at 175°C. After the digestion process, each extract was dissolved into fifty milliliters of high-purity water (Millipore Direct-Q System), filtrated by filter paper with a pore size of 40 mm (ADVANTEC, Japan), and Zn, Al, Ni, Fe, Cu, Mn, Co, Cr, In, Cd, Ga, and Pb concentrations were measured using an inductively coupled plasma (ICP-OES) at National Tsing Hua University in Taiwan. The ICP multi-element standard solution (1,000 ppm) was employed to generate the calibration curves, and the samples were only examined when the r^2 was higher than 0.995. The instrument was recalibrated if there was a deviation of over 10% after the initial calibration and after the analysis of ten samples. Also, the recovery rates for the examined heavy metals fluctuated between 96.3 and 103%. For quality control, all apparatus was cleaned and sterilized for 24 h in a nitric acid solution (10%) before being rinsed in double-distilled water. In our research, Merck PA reagents were employed throughout the experiments. The results were displayed as mg/kg and three digestions of each sample were achieved.

Determination of pollution degree

Single pollution indices

Enrichment factor (E_f)

To assess the level of HM enrichment in sediment, the E_f was applied by comparing the measured element to a reference metal (52).

In our work, Iron (Fe) served as a conservative element to standardize the detected metal levels in sediment because it is the fourth most prevalent element in the shale, has a natural content that tends to be consistent, is a carrier of numerous metals, and has a fine uniform surface (53, 54). Ef values are given by the following formula (55):

$$Ef^{i} = \left(C_m^i \div Fe_m\right) Sample / \left(C_b^i \div Fe_b\right) crust$$

Where C_m^i and C_b^i are the ratios of the sample's heavy metal i value to its earth's crust value, respectively; whereas Fe_m and Fe_b are the detected iron level and its value in the crust, respectively. Here, we used the average shale values (ASVs) determined by Turwkian and Wedepohl as the reference, which are: Zn: 95, Al: 80,000, Ni: 68, Fe: 47,200, Cu: 45, Mn: 850, Pb: 20, Cr: 90, In: 0.1, Cd: 0.3, and Co = Ga: 19 $mg.kg^{-1}$ (56). Since the enrichment factor technique does not have a recognized classification scheme for contamination levels, seven professional classes have been offered in Table 1 (57).

Geo-accumulation index (I_{geo})

The geoaccumulation index is applied to calculate the HMs contamination without taking into consideration geogenic conditions (58). I_{geo} can be calculated as follows:

TABLE 1 Degrees of heavy metal contamination determined by single pollution indices.

Categories	E_f	Contamination degree	I_{geo}	Contamination degree	C_f / PI	Contamination degree
0	< 1	No enrichment	< 1	Nil to minor pollution	$C_f < 1$	Low pollution
1	$1 \leq E_f < 3$	Minor enrichment	$1 \leq I_{geo} < 2$	Moderate pollution	$1 \leq C_f < 3$	Moderate pollution
2	$3 \leq E_f < 5$	Moderate enrichment	$2 \leq I_{geo} < 3$	Severe pollution	$3 \leq C_f < 6$	Considerable pollution
3	$5 \leq E_f < 10$	Heavily enrichment	$3 \leq I_{geo} < 4$	Very severe pollution	$C_f > 6$	High pollution
4	$10 \leq E_f < 25$	Severe enrichment	$4 \leq I_{geo} < 5$	Significant pollution		
5	$25 \leq E_f < 50$	Very severe enrichment	$I_{geo} > 5$	Extreme pollution		
6	$E_f > 50$	Extremely enrichment				
Acevedo-Figueroa et al. (57)			Förstner et al. (124)		Chakraborty et al. (62) and Tian et al. (109)	

$$\text{Igeo}^i = \log_2\left(C_m^i \div 1.5\, C_b^i\right)$$

wherein 1.5 represents the baseline matrix adjustment factor that mitigates the influences of geological contributions (59, 60). Based on the I_{geo}, sediment samples can be allocated into different distinct categories (Table 1).

Comprehensive pollution indices

Pollution load index (PLI)

PLI is calculated as the *n*th root of the outcome of *n* C_f and can be used to ascertain the aggregate pollution at the studied stations. The subsequent equations were employed to compute C_f^i and PLI (61, 62):

$$C_f^i = \left(C_m^i \diagup C_b^i\right)$$

$$\text{PLI}^i = \sqrt[n]{\left(Cf_{Fe} \times Cf_{Al} \times Cf_{Mn} \times Cf_{Zn} \times Cf_{Cu} \times Cf_{Ni} \times Cf_{Co} \times Cf_{Cr} \times Cf_{Ga} \times Cf_{In}\right)}$$

whereas C_f^i refers to the single contamination factor for the metal *i*. As shown in Tables 1, 2, the C_f^i and PLI have been classified into several pollution levels.

Modified contamination factor (mC_{deg})

Likewise, the comprehensive pollution of multiple elements per sampling station was evaluated utilizing the modified degree of contamination (mC_{deg}) approach (30). mC_{deg} developed by Abrahim and Parker (63) and it calculated as follows:

$$C_f^i = \left(C_m^i \diagup C_b^i\right)$$

$$mC_{\text{deg}} = \Sigma C_f^i \diagup n$$

Since *n* indicates the number of measured elements. The mC_{deg} is classified into various classes; see Table 2.

Nemerow comprehensive pollution index (P_N)

The Nemerow comprehensive pollution index (P_N) is another method for determining the total pollution degree of heavy metals throughout all stations (64), and it was estimated using an individual pollution index (PI):

$$\text{PI} = \left(C_m^i \diagup C_b^i\right)$$

$$P_N = \sqrt{\frac{\left(\text{PI}_{ave}^i\right)^2 + \left(\text{PI}_{\max}^i\right)^2}{2}}$$

Where PI_{ave}^i represents the average singular pollution index level of a metal, and $\text{PI}_{\max}^i$ signifies its maximum level. Based on Yang et al. (65), P_N is categorized into five levels of pollution (Table 2).

Evaluate the potential ecological risk

Potential ecological risk index (PERI)

This study applied the PERI in order to evaluate the possible risks posed by heavy metals (66). This index extensively considers the synergy, hazardous threshold, heavy metal content, and environmental sensitivity of elements (67–69). The PERI is composed of three fundamental factors: potential ecological risk factor (E_R^i), toxic-response factor (T_r^i), and contamination level (C_m^i). Accordingly, both individual (E_R^i) and cumulative (PERI) ecological risks were computed via these equations:

$$C_f^i = \left(C_m^i \diagup C_b^i\right)$$

$$E_R^i = T_r^i \text{ x } C_f^i$$

$$\text{PERI} = \sum_{i=1}^{m} E_R^i$$

TABLE 2 Categories of heavy metal pollution by comprehensive pollution indices.

Classes	PLI	Pollution level	mC_{deg}	Pollution level	P_N	Pollution level
1	< 1	Unpolluted	< 2	Nil to very low contamination	< 0.7	Non-polluted
2	1 ≤ PLI < 2	Slightly polluted	2 ≤ mC_{deg} < 4	Slight contamination	0.7 ≤ P_N < 1	Minor pollution
3	2 ≤ PLI < 3	Strongly polluted	4 ≤ mC_{deg} < 8	Strong contamination	1 ≤ P_N < 2	Moderate pollution
4	PLI ≥ 3	Heavily polluted	8 ≤ mC_{deg} < 16	Heavy contamination	2 ≤ P_N < 3	Significant pollution
5			16 ≤ mC_{deg} < 32	Severe contamination	P_N > 3	Extremely pollution
6			mC_{deg} > 32	Extremely contamination		
Tian et al. (62)			Abrahim and Parker (63)		Yang et al. (65)	

Where C_f^i and E_R^i reflect to the single contamination factor and potential ecological risk index for the element *i*, respectively, while T_r^i is the biological toxic factor of a certain metal that is established for Mn = Zn = 1, Cd = 30, Cr = 2, and Cu = Ni = Co = Pb = 5 (66).

In this research, eight contaminants involving Zn, Ni, Cr, Pb, Mn, Co, Cu, and Cd are considered by the classical PERI method. The current work modified the classification guideline for the metal's ecological risk indices as a result of the variation in contaminant forms and quantities (70). The greatest value of T_r^i had been chosen to represent the minimal level limit of E_R^i, and the subsequent level limits were then doubled. Similarly, by setting the rounding digit of $\sum T_r^i$ as the smallest level limit of PERI, the subsequent level limits were then doubled (70). The modified classification guidelines of PERI in sediment are illustrated in Table 3.

Sediment quality guidelines (SQGs)

Our findings were compared with different worldwide guidelines to better express the quality and adverse effects of HMs in sediment. This method includes four international guidelines: (1) the Australian and New Zealand Environment and Conservation Council and the Agriculture and Resource Management Council of Australia and New Zealand (71); (2) the National Oceanic and Atmospheric Administration of the USA (NOAA) (72); (3) the Canadian Council of Ministers of the Environment (73); and (4) Taiwan's national standard guidelines (74). For different heavy metals, there are lower and upper limits for each of the four typical guidelines. Negative effects "infrequently or rarely emerge" if the metal level surpasses the lower limit, but they "frequently occur" if the level surpasses the upper limit (75).

Statistical analyses

The data were pre-processed utilizing the Excel Pro +2019 software, and they are demonstrated as averages for the studied locations. All descriptive data (e.g., maximum, minimum, average, and standard deviation) and the ANOVA were executed by SPSS version 25 ($p < 0.05$) (76, 77). In order to compute the HMs pollution and their probably risks in the sediment of the Xiang-Shan wetland, several ecological pollution indicators were computed and visualized by Origin 2021 (v. 9.8). Simultaneously, multivariate statistical analyses such as principal component analysis (PCA) and hierarchical cluster analysis (HCA) were conducted to identify probable heavy metal sources (78). Furthermore, the relationship among HMs and sediment properties was examined via Pearson's correlation coefficient (PCC) to validate the findings of multivariate analyses (26). PCC and PCA were displayed using the "*corrplot*" package in R programming v. 4.2.2 ($p < 0.001$, 0.01, and 0.05) (79, 80) and Origin 2021 (v. 9.8), respectively, while the HCA dendrogram was plotted by the PC-ORD 5 program (81) according to the Euclidean distance and the Ward methods.

TABLE 3 Classification of ecological risks posed by heavy metal pollution.

Classes	E_R	PERI	Single and comprehensive ecological risk level
1	< 30	< 40	Minimal risk
2	$30 \leq E_R < 60$	40 ≤ PERI <80	Moderate risk
3	$60 \leq E_R < 120$	80 ≤ PERI <160	Considerable risk
4	$120 \leq E_R < 240$	160 ≤ PERI <320	Strong risk
5	$E_R > 240$	PERI >320	Extremely risk
Hakanson (66) and Li et al. (70)			

Results

Sediment properties

Grain size analysis

The granulometry of surface sediment at Xiang-Shan wetland is depicted in Figure 2. Based on the GSA findings, sediment grains were divided into seven fractions with various sizes and further grouped into three major classes (gravel, sand, and mud). Seasonally, the mean particle size of surface sediment fluctuated between (0.00–0.38%) for gravel, (24.18–68.44%) for sand, and (31.35–75.44%) for mud in spring, while in winter it ranged from 0.03 to 0.51%, 29.10 to 68.64%, and 30.86 to 70.84% for gravel, sand, and mud, respectively. Geographically, the surface sediments of KY, KW, and HS stations were predominated by sand, while DJ, HM, FC, OB, and MA were characterized by mud sediments in both seasons. Overall, all studied stations were dominated by mud and sand sediments. In contrast, the gravel particles demonstrated minimal proportions at all stations.

Total organic matter (TOM)

The mean TOM contents in the surface sediment of the Xiang-Shan wetland are illustrated in Figure 3. The TOM levels at the surface sediments fluctuated between 0.72–5.45% and 0.65–3.09% in spring and winter, respectively. Moreover, the greatest content of TOM was recorded at KY station, followed by MA, OB, and DJ, while the lowest contents were recorded at HS station during different seasons. Specifically, the surface sediments of the KY and MA stations were highly enriched with TOM in both seasons.

Total concentrations of HM in surface sediments

Supplementary Table 1 illustrates the average levels of HMs in the surface sediment of the examined stations during the two seasons. The levels of Iron (Fe), Aluminum (Al), Magnesium (Mn), Copper (Cu), Zinc (Zn), Gallium (Ga), Indium (In), Nickel (Ni), Chromium (Cr), Cobalt (Co) varied in the ranges of 24115.00–42123.33, 19234.50–51850.00, 319.15–764.73, 12.17–117.80, 65.90–252.05, 64.05–121.63, 27.40–56.23, 15.55–45.25, 55.35–112.87, 69.25–134.60 mg/kg, respectively, for spring, and 23445.00–38624.67, 20785.00–48285.00, 266.05–667.37, 11.05–77.15, 60.20–233.80, 57.35–106.40, 17.90–48.57, 16.90–37.05,

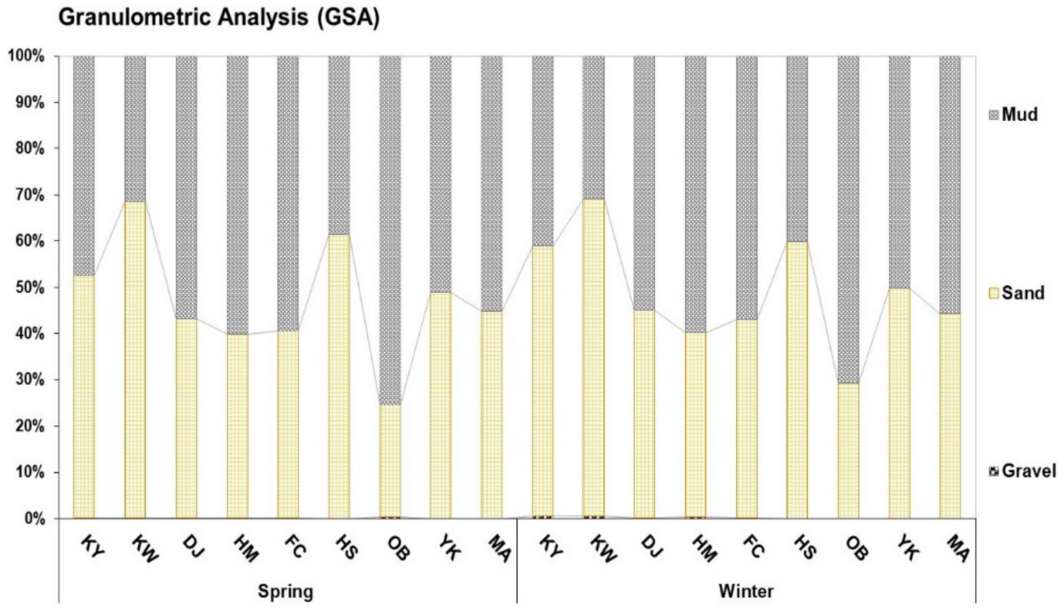

FIGURE 2
Grain size analysis of surface sediments at Xiang-Shan wetland during the spring and winter seasons (KY: KeYa, KW: KeYa Water Supply Center, DJ: DaJuang, HM: HuiMin, FC: FongCin, HS: HaiShan, OB: Oyster Bed, YK: YenKan, MA: Mangrove Area).

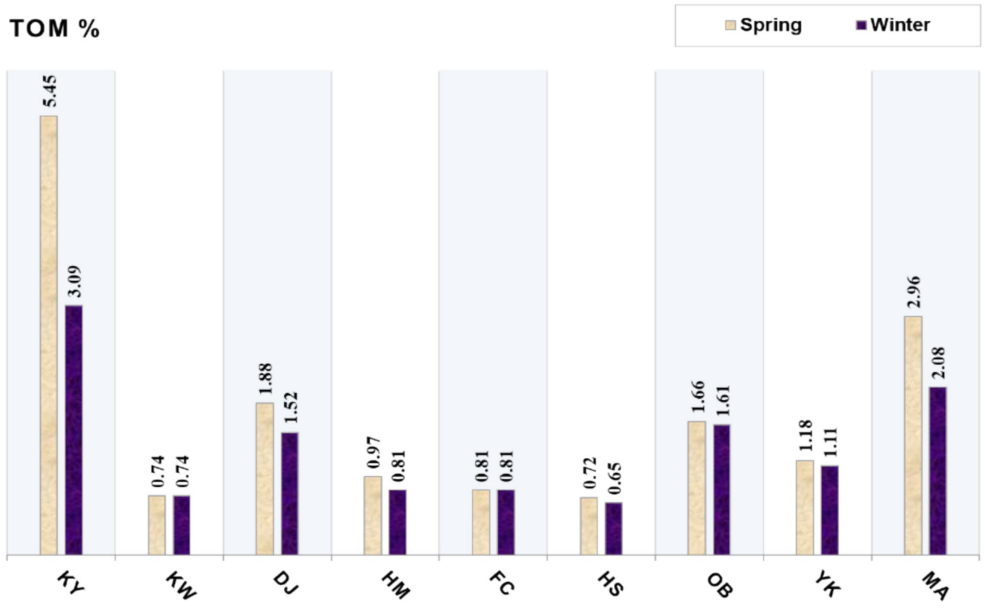

FIGURE 3
The mean contents of total organic matter in the Xiang-Shan wetlands' sediments during both seasons (KY: KeYa, KW: KeYa Water Supply Center, DJ: DaJuang, HM: HuiMin, FC: FongCin, HS: HaiShan, OB: Oyster Bed, YK: YenKan, MA: Mangrove Area).

46.90–109.23, 58.35–121.97 mg/kg, respectively, for winter. All stations had Pb and Cd concentrations below the detection limit for both seasons. Spatially, the maximum levels of HMs such as Al, Co, Cr, Ga, and In at DJ station (51850.00, 134.60, 112.87, 121.63, and 56.23 mg/kg, respectively) were observed in the spring season, while Zn, Cu, and Ni were detected at KY station (252.05, 117.80, and 45.25 mg/kg, respectively). OB and MA stations recorded high concentrations of Mn and Fe (764.73 and 42123.33, respectively). Inversely, surface sediments at KW station exhibited the minimum levels of Fe, Al, Co, Cr, and Ga (23445.00, 19234.50, 58.35, 46.90, and 57.35 mg/kg, respectively), and at YK station for Zn, Ni, and In (60.20, 15.55, and 17.90 mg/kg, respectively). Also, Mn and Cu concentrations (266.05 and 11.05 mg/kg) were low in KY and FC stations respectively, in the winter.

Assessment of heavy metal- polluted sediments

In our research, five reliable indicators were employed to estimate the extent of contamination by HMs in surface sediments, of which two indicators (E_f and I_{geo}) were employed to gauge the pollution by certain metals, and the other three (PLI, mC_{deg}, and P_N) were used for comprehensive pollution assessment.

Enrichment factor (E_f)

Figure 4 depicts the calculated E_f and contamination degree for each metal in Xiang-Shan wetland based on Iron (Fe) as the reference metal. The ranges (mean) of the E_f of Al, Mn, Cu, Zn, Co, Cr, Ni, Ga, and In at the study area during different seasons were 0.47–0.94 (0.70), 0.54–1.43 (1.02), 0.43–4.51 (1.35), 1.18–4.57 (1.99), 6.05–8.75 (7.40), 1.05–1.62 (1.31), 0.39–1.15 (0.58), 6.08–9.17 (7.52), and 334.00–666.93 (554.85), respectively. Based on the

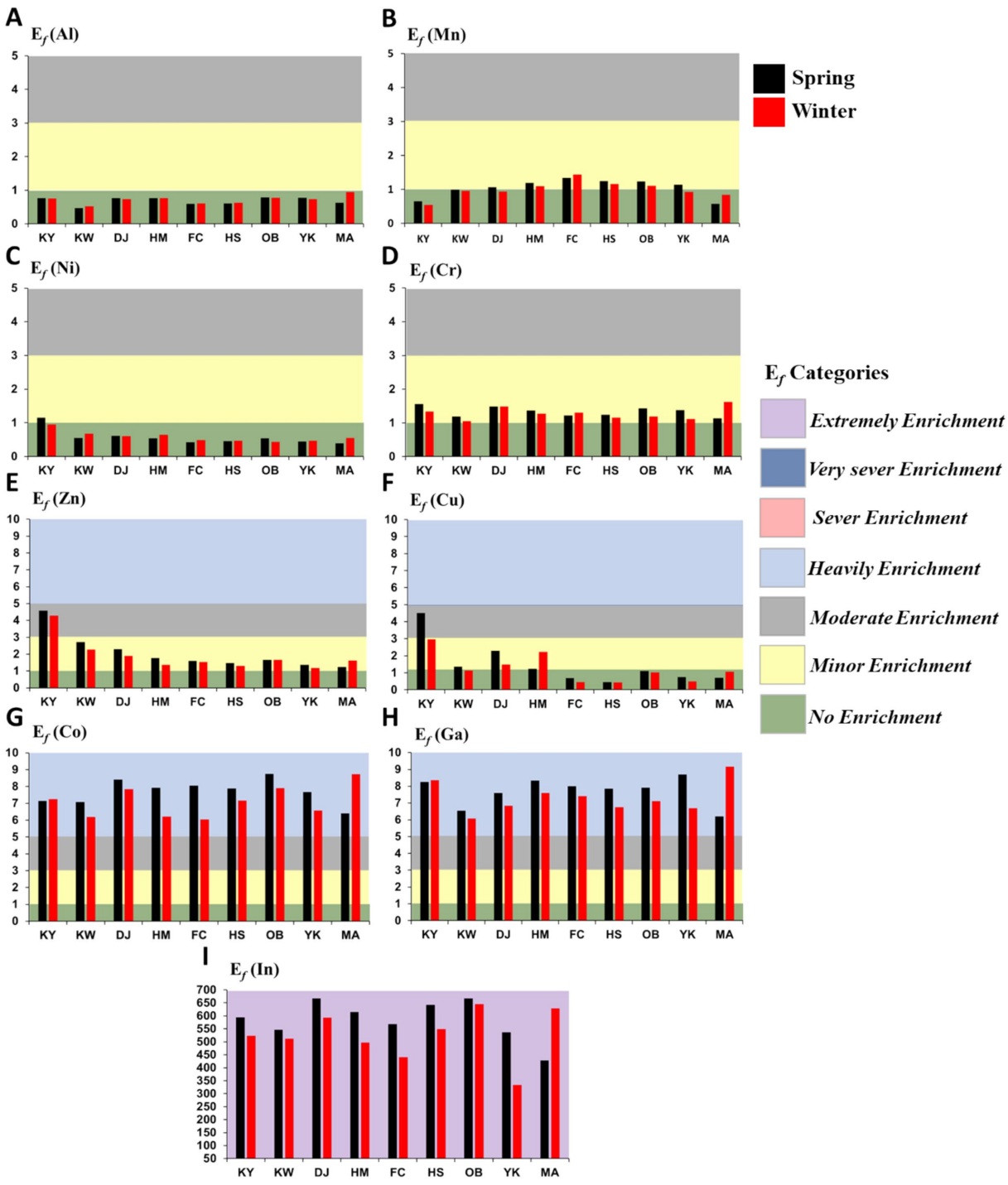

FIGURE 4
Enrichment factor (Ef) and contamination levels for studied HMs in the XiangShan wetland's sediments. (KY: KeYa, KW: KeYa Water Supply Center, DJ: DaJuang, HM: HuiMin, FC: FongCin, HS: HaiShan, OB: Oyster Bed, YK: YenKan, MA: Mangrove Area). **(A)** Al, **(B)** Mn, **(C)** Ni, **(D)** Cr, **(E)** Zn, **(F)** Cu, **(G)** Co, **(H)** Ga, **(I)** In.

categories of E_f (Table 1), Al, Cd, and Pb showed no enrichment (class 0) in all study stations, while Zn, Cu, Ni, and Cr fluctuated between class 0 (< 1) and class 2 (< 5). Moreover, E_f for Co and Ga were subjected to class 3 (< 10), and class 6 for In (> 50).

Geoaccumulation index (I_{geo})

The computed I_{geo} and contamination degree at all sampling stations in two seasons are demonstrated in Figure 5. The ranges (mean) of the I_{geo} of Fe, Al, Mn, Cu, Zn, Ni, Co, Cr, Ga, and In were 0.10–0.18 (0.13), 0.05–0.13 (0.09), 0.06–0.18 (0.13), 0.05–0.53 (0.17), 0.13–0.53 (0.25), 0.05–0.13 (0.07), 0.62–1.42 (0.94), 0.10–0.25 (0.17), 0.61–1.28 (0.94), and 35.92–112.84 (70.54), respectively. According to Table 1, the I_{geo} levels for all investigated metals at all studied stations in the spring and winter were unpolluted (< 1), except Co and Ga at DJ, OB, and MA stations showed moderate pollution (class 1), and In values subjected to class 5 (> 5) at all study stations.

Pollution load index (PLI)

The PLI, as a comprehensive index, served to measure the deposition levels of HMs in the Xiang-Shan wetland's surface sediments, as shown in Figure 6A. Seasonally, PLI varied from 1.37 to 2.80 and 1.03 to 1.11 with an average of 1.87 and 1.06 in the spring and winter samples, respectively, indicating the range of slightly polluted (< 1) to heavily polluted (> 2). The mean values of PLI at most studied stations fall under class 1 ($1 \leq PLI < 2$) in both spring and winter sediment samples, except at 3 stations (KY, DJ, and OB) where they were greater than 2 (class 2) in the spring season (Table 2).

Modified contamination degree (mC_{deg})

Modified degree of contamination (mC_{deg}) was implemented to compute the overall pollution level of all HMs in surface sediment samples (Figure 6B). mC_{deg} varied from 23.82 to 48.65 with an average of 32.88 and from 15.77 to 42.03 with an average of 28.10 in the sediments during spring and winter, respectively. According to the mC_{deg} classification (Table 2), the sampling stations fluctuated between severe and extremely polluted (classes 5 and 6, respectively) in the spring season, while, in the winter, the contamination degree ranged from heavy to extremely (classes 4 and 6, respectively) at the studied stations.

Nemerow integrated pollution index (P_N)

The P_N index was calculated to calculate the comprehensive contamination for each metal across all sediment samples; see Supplementary Table 2. In our study, the mean levels of P_N for each metal ranged from 0.00 to 479.66 with average (38.72), reflecting the range of unpolluted ($P_N < 0.7$) to extremely polluted ($P_N > 3$). The mean P_N values for In, Ga, and Co were subjected to class 4 ($P_N > 3$), while the other metals ranged from unpolluted ($P_N < 0.7$) to significant pollution ($2 \leq P_N < 3$).

Determine the potential ecological risks of heavy metals

Potential ecological risk index (PERI)

PERI is an integrative indicator that is calculated from the individual ecological risk (E_R) of each element. As shown in Figure 7A and Table 3, the mean E_R values for Cr, Mn, Cu, Zn, Pb, Cd, and Ni fall under class 1 ($E_R < 30$), while for Co ranged between minimal ($E_R < 30$) and moderate risk ($30 \leq E_R < 60$) throughout the Xiang-Shan wetland in both spring and winter. Additionally, PERI ranged between 25.32–52.97 (mean = 35.25) in summer and 21.77–45.37 (mean = 30.74) in winter (Figure 7B). Based on the PERI classes (Table 3), all studied stations displayed a minimal ecological risk to the environment, with PERI levels below 40 (class 1), except KY and OB stations in the spring and DJ in both seasons (class 2, > 40).

Discussion

Sediment characteristics

Granulometric analysis was performed mechanically to differentiate the surface sediment particles of the Xiang-Shan wetland and consequently establish the accumulation trend of organic matter and HMs in relation to the sediment size. The results of GSA revealed that mud sediments are the dominant grain size overall, followed by sand sediments ($p = 0.07$), and gravel ($p = 0.003$) across all sampling stations with averages (51.98, 47.82, and 0.19%, respectively). Specifically, DJ, HM, FC, OB, and MA stations were dominated by mud, while sand grains were dominant in KY, KW, and HS stations. Overall, the surface sediments of the Xiang-Shan wetland were characterized by fine-grained sediments (mud and sand). This may be attributed to flow rate, flow velocity, and calm conditions. Rea and Hovan (82) reported that fine-grained sediments are conveyed by suspension in the marine setting; therefore, they can readily be distributed throughout the water mass and transported for long distances before being re-deposited in the calm zone. The percentages of GSA among the studied stations decreased in the order of mud > sand > gravel.

Sediment organic matter is composed of light-weight materials, typically structural materials from marine creatures (83). In our study, KY station had the maximum TOM content with an average of 4.27%, followed by MA (2.52%) in both seasons. This could be attributed to the KeYa River, which supplies the KY station with an extensive amount of freshwater loaded with a high proportion of OM (25). Furthermore, the mangrove environment is regarded as a highly productive ecosystem with substantial rates of organic matter storage (84, 85). Also, DJ and OB stations had relatively significant values, with averages of 1.70 and 1.64%, respectively; this may be associated with the deposition of fine particles with excessive organic matter levels. The magnitude of TOM values among the surface sediments of Xiang-Shan wetland were in the order of KY > MA > DJ > OB > YK > HM < FC > KW > HS for both spring and winter seasons. The ANOVA revealed insignificant spatio-temporal variances in TOM ($p > 0.05$).

Heavy metal concentrations and comparison with worldwide studies

Heavy metals are pervasive and tenacious in marine settings, probably poisonous, and may be accumulated in food chains (86, 87). Multiple pathways, including air deposition, agriculture, and industrial activities, have been identified as the origins of HM contamination in sediments (88, 89). In our research, there was no discernible difference in the concentration of HMs between the spring and winter seasons ($p > 0.05$), despite an overall greater level observed during the spring season across all sampling stations. Higher heavy metal concentrations in the spring may be caused by seasonal changes

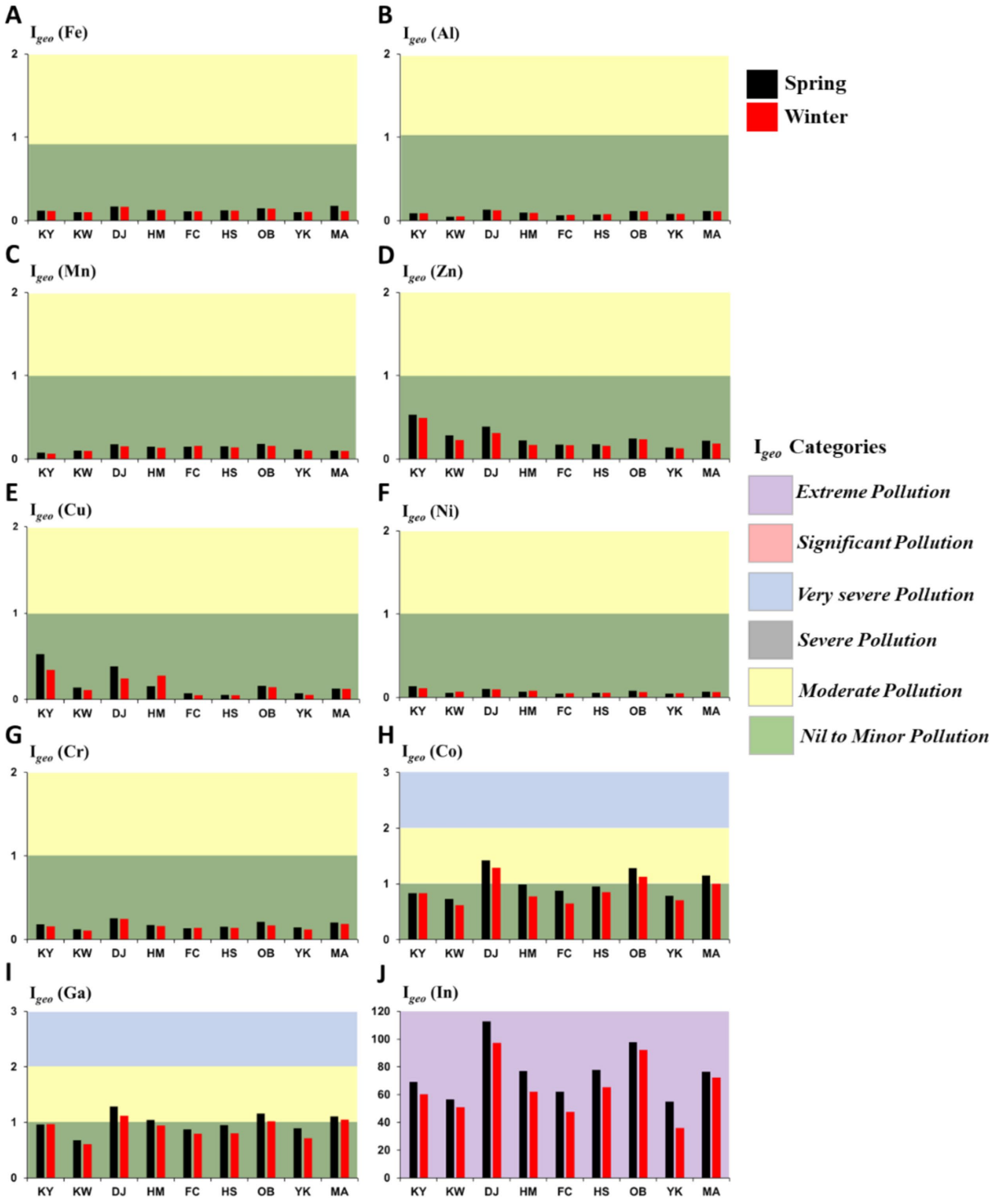

FIGURE 5
Geoaccumulation index (I_{geo}) and contamination categories for analyzed HMs in the Xiang-Shan wetlands' sediments (KY: KeYa, KW: KeYa Water Supply Center, DJ: DaJuang, HM: HuiMin, FC: FongCin, HS: HaiShan, OB: Oyster Bed, YK: YenKan, MA: Mangrove Area). **(A)** Fe, **(B)** Al, **(C)** Mn, **(D)** Zn, **(E)** Cu, **(F)** Ni, **(G)** Cr, **(H)** Co, **(I)** Ga, **(J)** In.

in the wetland's water flows; such as, water replenishment to the wetland is restricted in the spring, resulting in less mobility and greater deposition of HMs in surface sediments (90).

The average levels of Iron (Fe), Aluminum (Al), Manganese (Mn), Cobalt (Co), Zinc (Zn), copper (Cu), Gallium (Ga), Nickel (Ni), Chromium (Cr), and Indium (In) in the Xiang-Shan wetland's surface sediments ranged from 23445.00 to 42123.33, 19234.50 to 51850.00, 266.05 to 764.73, 58.35 to 134.60, 60.20 to 252.05, 11.05 to 117.80, 57.35 to 121.63, 15.55 to 45.25, 46.90 to 112.87, and 17.90 to 56.23 $mg.kg^{-1}$, respectively. While Lead (Pb) and Cadmium (Cd) were blow the detection limits at all studied stations in both seasons. The average contents of the 12 HMs in the Xiang-Shan

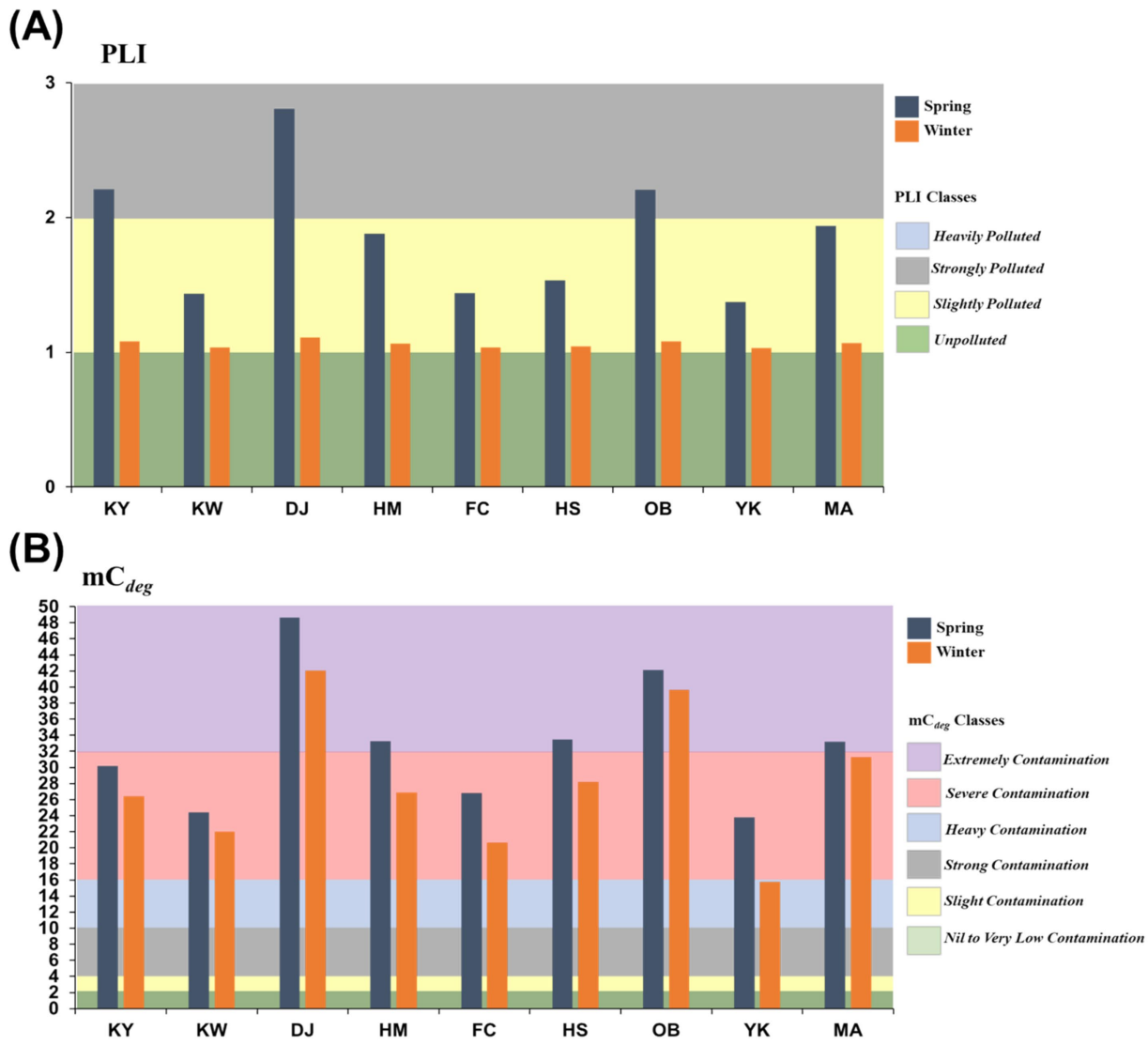

FIGURE 6
Comprehensive pollution indices with pollution classes at the studied stations. **(A)** Pollution load index and **(B)** Modified contamination degree (mC_{deg}) (KY: KeYa, KW: KeYa Water Supply Center, DJ: DaJuang, HM: HuiMin, FC: FongCin, HS: HaiShan, OB: Oyster Bed, YK: YenKan, MA: Mangrove Area).

wetland's surface sediments showed a decreasing sequence of Al > Fe > Mn > Zn > Co > Ga > Cr > Cu > In > Ni > Pb = Cd. The ANOVA revealed discernible variances for Mn, Cu, Co, Cr, and In values across stations ($p < 0.05$).

Spatially, the greatest mean annual Fe, Al, Co, Cr, In, and Ga concentrations were observed in the DJ station, Zn, Cu, and Ni in the KY station, and Mn in the OB station. This may be attributed to the prevalence of fine-grained sediments with considerable amounts of OM in these stations, that have a tendency to bind with HMs. In addition to the existence of terrigenous freshwater sources and unprocessed domestic sewage from the surrounding area (25, 91, 92). Previously, Barik et al. (93) and Dar and El-Saharty (94) observed that fine-grained sediments have a higher affinity for metals owing to their large surface area and abundance of organic matter. Also, this observation was consistent with an earlier study by Tian et al. (8), who reported that fine sediments serve a critical role in controlling the mobility of HMs and subsequently their distributions in sediments. Furthermore, the Pearson's correlation coefficient (Figure 8) revealed that most metals have high and significant positive associations with mud % and negative associations with sand % and gravel %, confirming the higher deposition and retention of metals by fine-grained sediments in the Xiang-Shan wetland. Conversely, in low-depth marine sediments, Giannico et al. (95, 96) investigated the concentrations and hazards of organic matters such as PCDD, PCDF, and PCBs. This study found high concentrations of dioxins and PCBs in marine sediments from Mar Piccolo 1st Inlet, Italian Taranto, due to industrial settlements nearby, which are known potential sources of PCDD/Fs and PCBs (e.g., groundwater and freshwater pollution in the northern area of the basin).

Besides, the obtained results were compared to those previously presented in other investigations, as well as the average shale values (ASVs), to better comprehend the contamination status of HMs in sediments (Supplementary Table 3). The seasonal mean of Fe, Co, Ga, and In (30,464.07, 92.27, 91.44, and 36.61 $mg.kg^{-1}$, respectively)

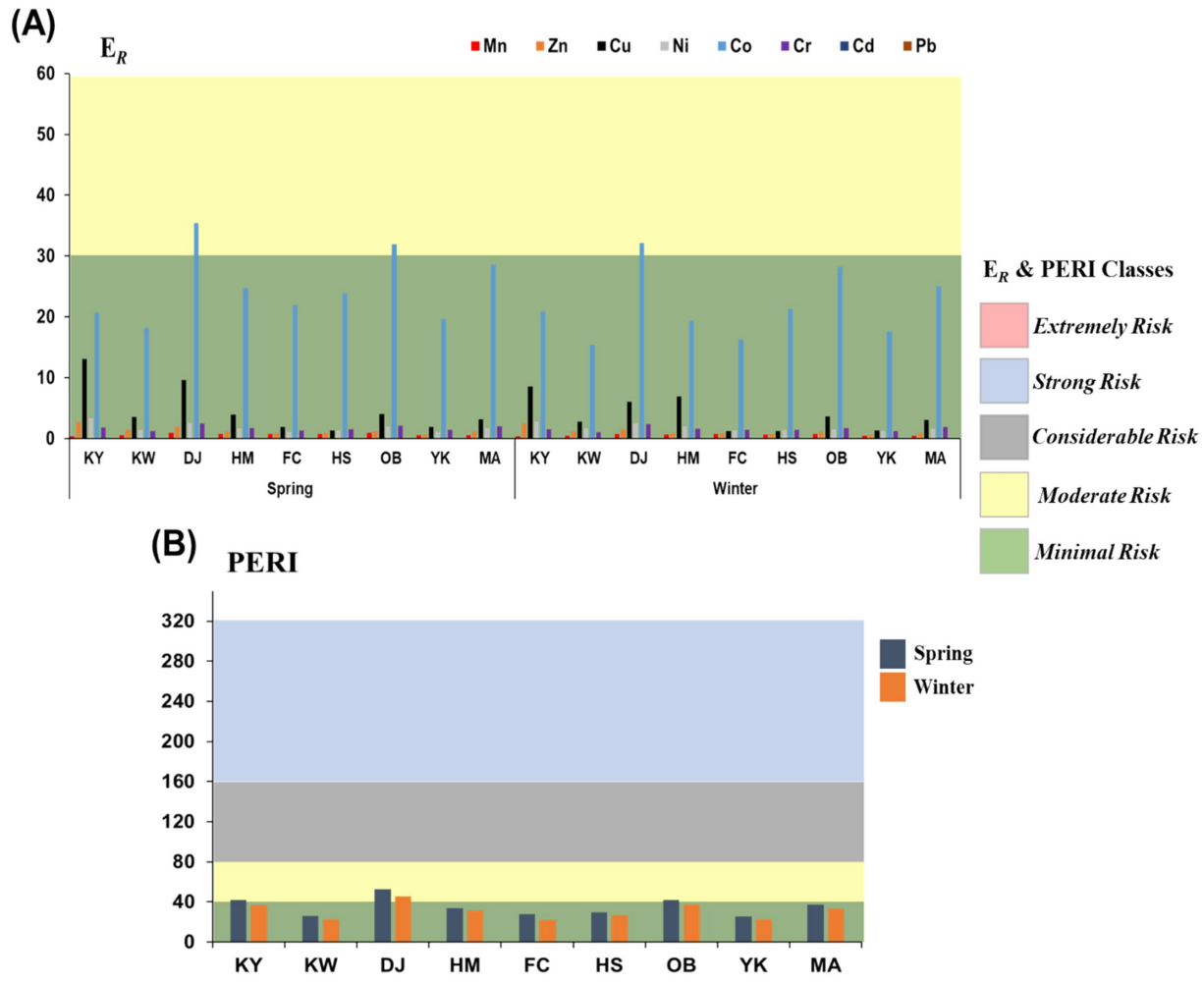

FIGURE 7
Potential ecological risk index with pollution classes for the studied HMs. **(A)** Single ecological risk (E_R) for each metal and **(B)** Integrated potential ecological risk index (PERI) (KY: KeYa, KW: KeYa Water Supply Center, DJ: DaJuang, HM: HuiMin, FC: FongCin, HS: HaiShan, OB: Oyster Bed, YK: YenKan, MA: Mangrove Area).

was greater than those of most other areas around the globe, such as the Western Saronikos Gulf, Greece (97), the Dhaleshwari River in Bangladesh (98), the Gulf of Aqaba along the Saudi Arabia coastline (99), Bafa Lake in Turkey (38), the Xiang-Shan wetland in Taiwan (100), and the wetlands and main rivers in Taiwan (101). While the total average of Al (36690.77 mg.kg^{-1}) was less than Changjiang River Estuary, China (102), and more than those of other earlier investigations. Likewise, the seasonal mean of Zn and Cu (116.52 and 38.21 mg.kg^{-1}, respectively) was greater than those observed in other studies (Table 3) but lower than the upper levels of baseline concentrations in Taiwan (103). The value of Mn (553.50 mg.kg^{-1}) was less than those of the Western Saronikos Gulf, Greece (97), but more than the levels in the Iranian Urmia Lake (90), and Bafa Lake in Turkey (38). Moreover, the mean annual Ni concentration (24.44 mg.kg^{-1}) across all sampling stations was lower than those of most previous studies and higher than the shorelines of the Bohai and Yellow Seas in China (8), the Aqaba Gulf along the Saudi Arabia coastline (99), and the Western Taiwan Strait, China (104), but it was similar to the results of wetlands and main rivers in Taiwan (101). When compared with the average shale values (ASVs) that were established by Turekian and Wedepohl (56), the mean annual levels of all analyzed metals were below the ASVs, with the exception of Zn, Co, Ga, and In were comparable (Supplementary Table 3).

As a result of the spatial variability observed in the sediments, the overall concentration of HMs may not accurately reflect the current contamination levels. Hence, the HM concentrations alone are insufficient to assess the pollution level of HM in the sediments. Further quantitative indicators (e.g., E_f, I_{geo}, PLI, mC_{deg}, P_N, E_R, and PERI) that consider the ASVs in the associated sediments are required.

Assessment of heavy metals contamination

Single-element contamination indices, such as the enrichment factor (Ef) and geoaccumulation index (Igeo), were applied to assess the contamination of HM in the sediments (105). These indices provide information about how a particular metal is concentrated at a location of interest in comparison to the background.

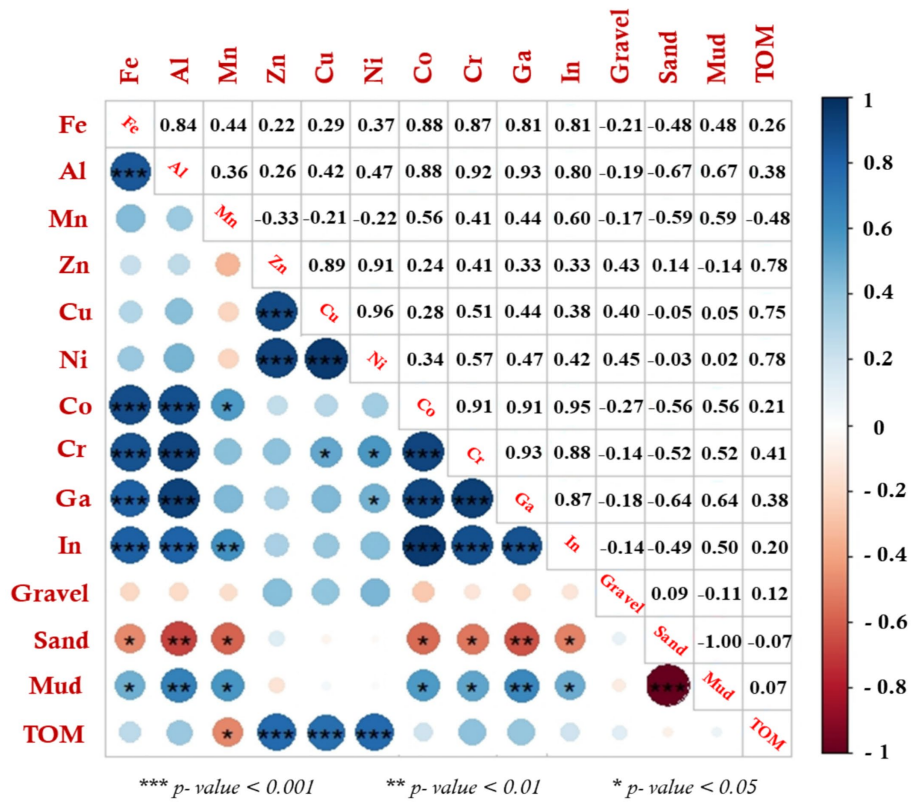

FIGURE 8
The association relationships among the analyzed parameters in Xiang-Shan wetlands' sediments using Pearson's correlation coefficient (KY: KeYa, KW: KeYa Water Supply Center, DJ: DaJuang, HM: HuiMin, FC: FongCin, HS: HaiShan, OB: Oyster Bed, YK: YenKan, MA: Mangrove Area).

Here, the mean E_f values of Al, Co, Zn, Pb, Cu, Cr, Ni, Ga, In, Mn, and Cd were 0.70, 7.40, 1.99, 0.00, 1.35, 1.31, 0.58, 7.52, 554.85, 1.02, 0.00, respectively. These results revealed that the surface sediments of Xiang-Shan wetland were extremely enriched with In ($E_f > 50$), heavily enriched with Co and Ga ($5 \leq E_f < 10$), and had nil to minor enrichment with the other heavy metals ($1 \leq E_f < 3$). The mean E_f values of Al, Pb, and Cd were below one at all studied stations in both seasons, suggesting no enrichment and proving that they are largely originating from shale components or natural weathering activities. Conversely, the E_f levels for Zn, Cr, Cu, Co, Ni, In, Mn, and Ga are almost more than one, implying a tendency from minor to extremely anthropogenic enrichment.

Regarding I_{geo} index, the surface sediments of Xiang-Shan wetland were marked as nil or minor polluted with Fe, Cu, Al, Cd, Mn, Ni, Zn, Cr, and Pb ($I_{geo} < 1$). Moreover, the average I_{geo} values of Co, and Ga are categorized as moderately polluted in DJ, OB, and MA stations. The seasonal mean I_{geo} values of Fe, Cu, Al, Cd, Mn, Ni, Zn, Cr, Ga, Pb, In, and Co were 0.13, 0.17, 0.09, 0.00, 0.13, 0.07, 0.25, 0.17, 0.94, 0.00, 70.54, and 0.94, respectively, indicating the range of uncontaminated ($I_{geo} < 1$) to extremely polluted ($I_{geo} > 5$).

The mean E_f levels for the examined HMs were in the decreasing sequence of In > Ga > Co > Zn > Cu > Cr > Mn > Al > Ni > Pb = Cd, and the mean I_{geo} declined in the following order: In > Ga ≥ Co > Zn > Cu ≥ Cr > Mn ≥ Fe > Al > Ni > Pb = Cd. As can be observed, the HMs have a similar order with regard to the estimated E_f and I_{geo}. Interestingly, E_f and I_{geo} values for Indium (In) metal at all sampling stations showed great values, suggesting extremely contamination; this is likely attributed to the industrial effluent from Hsinchu Science Industrial Park (HSIP). This park is the biggest industrial region in Taiwan, containing various high-tech companies producing photovoltaic plates, biomedical materials, liquid-crystal displayers (LCD), light-emitting diodes (LED), etc. (46). Gallium and Indium are crucial transition elements that are used in large quantities in the aforementioned industries, and they are discharged into the coastal zone of the study area via the KeYa river during the fabrication processes (i.e., cleaning operations, epitaxy, and chip fabrication in the production of high-speed semiconductors and LEDs), causing adverse impacts on humans (106–108).

To further determine the HM pollution in the surface sediments, the integrated pollution indices (PLI, mC_{deg}, and P_N) were used to estimate the overall HMs pollution in the Xiang-Shan wetland's surface sediments. These indices were quantified from the contamination factor (C_f) or pollution index (PI) of every single element. The pollution level identified by C_f or PI in the Xiang-Shan wetland was comparable to the findings by E_f and I_{geo} described earlier. The average levels of C_f or PI revealed a decreasing sequence of In (351.51) > Ga (4.70) > Co (4.68) > Zn (1.23) > Cu (0.86) > Cr (0.83) > Mn (0.64) > Fe (0.63) > Al (0.44) > Ni (0.36) > Pb = Cd (0.00). According to the classification of Chakraborty et al. (109) and Tian et al. (62) (Table 1), these data suggest that the surface sediments of Xiang-Shan wetland were highly contaminated with In ($C_f > 6$),

considerably polluted with Ga and Co ($3 < C_f \leq 6$), and unpolluted with the other metals ($C_f < 1$).

Due to the great contribution of Indium (In), Gallium (Ga), and Cobalt (Co) metals in our study, the obtained data of PLI, mC_{deg}, and P_N displayed a certain level of HM contamination. The seasonal mean values of PLI ranged between 1.96 and 1.20, indicating the surface sediment of the investigated area were slightly polluted ($1 \leq PLI < 2$). Specifically, the surface sediments of DJ, KY, and OB stations in the spring season are greater than 2, suggesting strong pollution with heavy metals, and the mean PLI showed the descending order of DJ (1.96) > KY (1.65) > OB (1.64) > MA (1.50) > HM (1.47) > HS (1.29) > FC (1.24) ≥ KW (1.24) > YK (1.20).

While the annual average mC_{deg} values at all sampling stations fluctuated from 45.34 to 19.80, reflecting the range of severe ($16 \leq mC_{deg} < 32$) to extreme pollution ($mC_{deg} > 32$). The mean value of mC_{deg} was higher than 32 for DJ and OB stations in both seasons, reflecting extremely contamination in the sediments of these two stations while other stations' sediments were heavily or severely polluted. The magnitude of mC_{deg} levels between investigated stations was in the sequence of DJ (45.34) > OB (40.89) > MA (32.23) > HS (30.82) > HM (30.10) > KY (28.29) > FC (23.74) > KW (23.19) > YK (19.80).

Additionally, The Nemerow integrated pollution index (P_N) is another widely employed proxy to quantify the pollution of HMs across all sampling stations. This index was calculated from the single pollution index (PI) of HMs mentioned previously. According to the mean P_N values, the surface sediments of Xiang-Shan wetland were extremely polluted with In, Ga, and Co (class 4, $P_N > 3$) in both two seasons and unpolluted (class 0, $P_N < 0.7$) to significantly polluted (class 3, $P_N < 3$) with the other metals (Table 2). The seasonal mean P_N levels for the twelve HMs decreased as follows: In > Ga > Co > Zn > Cu > Cr > Fe ≥ Mn > Al > Ni > Pb = Cd.

Evaluate the potential risks of metals to the environment

The possible hazards related to the examined elements in the Xiang-Shan wetland's surface sediments were evaluated utilizing the potential ecological risk index (PERI) and consensus-based sediment quality guidelines (SQGs).

PERI demonstrates the risks posed by pollutants and shows the susceptibility of ecological communities to given metals (110). The average E_R of HMs varied considerably. The E_R levels for the eight elements were ordered descendingly as follows: Co (23.39) > Cu (4.29) > Ni (1.79) > Cr (1.65) > Zn (1.23) > Mn (0.64) for both spring and winter sediments. Accordingly, all HMs across all sampling stations exhibited a minimal risk to the ecology with E_R levels below 30 ($E_R < 30$). Specifically, the E_R values for Co exceeded 30 at DJ (in both seasons) and OB (in the spring season) stations, indicating Co had moderate ecological risk in these two stations. Comprehensively, the seasonal mean PERI values of the surface sediments were 39.21, 24.38, 49.17, 32.59, 24.83, 28.22, 39.61, 23.91, and 35.02 in KY, KW, DJ, HM, FC, HS, OB, YK, and MA, respectively, with a total mean of 32.99. According to the PERI classifications, all sampling stations showed minimal ecological risk (PERI <40), with the exception of the OB station in the spring season and the DJ station in both seasons, which posed a moderate risk ($40 \leq$ PERI <80) to the environment, mostly due to Co contamination. Similar to mC_{deg} and PLI, the average PERI levels of the spring sediments were greater than those of the winter season, and they showed the descending order of DJ (49.17) > OB (39.61) > KY (39.21) > MA (35.02) > HM (32.59) > HS (28.22) > FC (24.83) > KW (24.38) > YK (23.91).

Similarly, sediment quality guidelines (SQGs) are the most prevalent conventional approach for determining the likely adverse impacts of HMs in sediments (75, 111, 112). Generally, these guidelines have low and high limits for various heavy metals. Supplementary Table 4 juxtaposes our results with numerous SQGs' reference values. The reference data imposed by the National Oceanic and Atmospheric Administration of the USA (NOAA) (72) are equivalent to those of the Australian and New Zealand Environment and Conservation Council and the Agriculture and Resource Management Council of Australia and New Zealand (71). Those developed by the Taiwan EPA (74) and the Canadian Council of Ministers of the Environment (73) are analogous to each other. Overall, the last two have somewhat lower values than the previous two, implying that the latter two reflect more rigorous values for the SQG technique. In comparison with the values of SQGs, the mean value of Cr greatly surpassed CCME's ISQG, but it was close to the lower limit of Taiwan's EPA. Similarly, the Cu value exceeded the lower limits of the CCME's ISQG and NOAA's effects range-low (ERL). Ni concentration in our work is between the lower and upper limits of NOAA's ERL and ANZECC & ARMCANZ, but it is comparable to the Taiwan EPA's lower limit. Meanwhile, the mean Zn value was considerably greater than the Taiwan EPA's lower limit. Finally, the contents of Pb and Cd in our research were below all of the referenced levels established in the other guidelines. Overall, the mean levels of Zn, Cr, Ni, and Cu in the current research exceeded the lower limits of various SQGs, indicating that HM risk rarely occurs in the sediment of the Xiang-Shan wetland (105).

Identify the potential sources of HMs in the Xiang-Shan wetland's sediments

The assessment of current contamination alone is inadequate to reduce the level of HMs pollution in the Xiang-Shan wetland's surface sediments. Various bivariate and multivariate statistical methods, including Pearson's correlation coefficient (PCC), Hierarchical cluster analysis (HCA), and principle component analysis (PCA), have been shown to be useful for examining the correlations and identifying the possible sources of HMs in sediments (26, 36).

Regarding PCC, a positive correlation among two variables implies that they originate from common origins and similar migration ways, while a negative correlation reflects distinct origins and is likely related to lithogenic or natural activities (39). Statistically, the correlation coefficient (r) can be categorized into four levels: $r < \pm 0.5$ negligible, $0.5 \pm \leq r < \pm 0.6$ significant, $0.6 \pm \leq r < \pm 0.7$ high, and $r \geq \pm 0.7$ strong. As shown in Figure 8, there were strong positive correlations ($r \geq 0.7$, $p < 0.001$) among some studied variables, and the strongest associations, in decreasing order of correlation coefficient, were between the content of Cu-Ni (0.96), Co-In (0.95), Al-Ga (0.93), Cr-Ga (0.93), Al-Cr (0.92), Zn-Ni (0.91), Co-Cr (0.91), Co-Ga (0.91), Zn-Cu (0.89), Fe-Co (0.88), Al-Co (0.88), Cr-In (0.88), Fe-Cr (0.87), Ga-In (0.87), Fe-Al (0.84), Fe-Ga (0.81), Fe-In (0.81), Al-In (0.80), Zn-TOM (0.78), Ni-TOM (0.78), and Cu-TOM (0.75). In addition, Al-Mud (0.67), Ga-Mud (0.64), and Mn-In (0.60) showed high positive

correlation ($0.6 \leq r < 0.7$, $p < 0.01$), while Mn-Mud (0.59), Ni-Cr (0.57), Mn-Co (0.56), Co-Mud (0.56), Cr-Mud (0.52), Cu-Cr (0.51), and In-Mud (0.50) showed significant correlation ($0.5 \leq r < 0.6$, $p < 0.05$). Contrarily, most metals had a negative and negligible relationship with sand and gravel, respectively. Similar findings were observed previously by Liang et al. (113) and Briki et al. (114), who confirmed that positive relationships between heavy metals imply similar anthropogenic pollution sources and migration processes, whereas negative correlations indicate that they originated from various sources, which are likely geogenic.

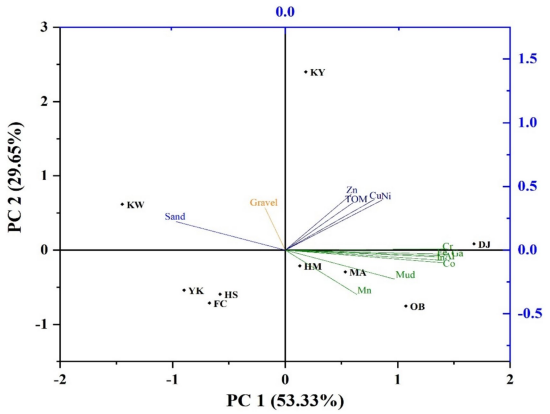

FIGURE 9
Biplot depicts the PCA analysis for HMs, TOM, and GSA in sediments of the Xiang-Shan wetland (KY: KeYa, KW: KeYa Water Supply Center, DJ: DaJuang, HM: HuiMin, FC: FongCin, HS: HaiShan, OB: Oyster Bed, YK: YenKan, MA: Mangrove Area).

PCA was performed to further investigate the association, HMs sources, and the linked interactions of HMs and sediment properties (i.e., TOM%, gravel%, sand%, and mud%). The PCA observations illustrated that the variance of HMs, TOM, and GSA can be described by two principal components that explained 82.98% of the cumulative variance. PC1 and PC2 explained 53.33 and 29.65%, respectively. As shown in Figure 9, Fe, Al, Co, Cr, Ga, In, Mn, and mud were positively associated with the first component (PC1), indicating that these variables predominantly came from similar sources, and PCC data confirm the possibility that these HMs had common origins. Inversely, sand and gravel variables were negatively loaded with PC1, indicating that the heavy metal distribution is highly affected by muddy sediments in DJ, OB, HM, and MA stations. Moreover, the PC2 had positively loaded Zn, Cu, Ni, and TOM, reflecting that these metals came from another source.

Similar to PCC and PCA, HCA (HCA-R mode) was conducted using the method of Euclidean distance to study similar heavy metal interrelationships and explore their potential origins (26). The HCA dendrogram provided data that split the PC1 and PC2 components into four distinct clusters with more precise similarities (Figure 10A). Cluster 1 contains Fe, Ga, Al, Cr, Co, In, Mn, and mud-grained size, proving that these metals emanated from a

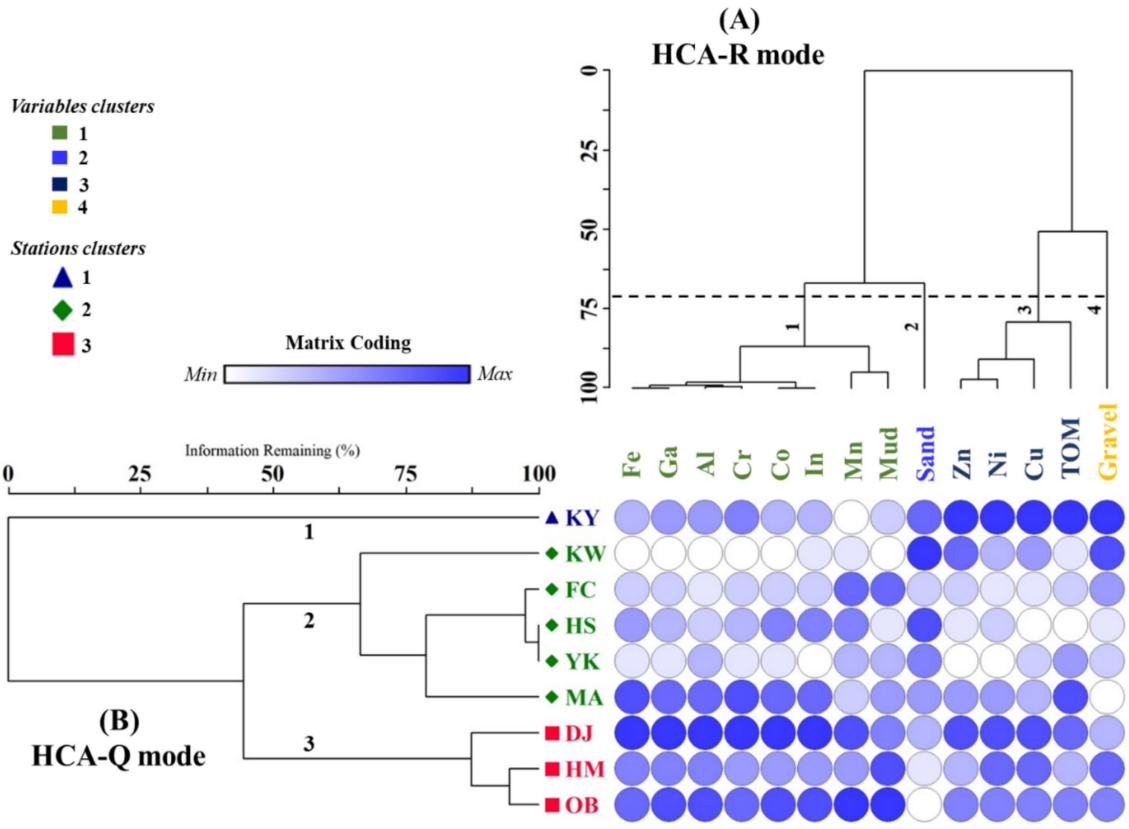

FIGURE 10
A dendrogram shows the hierarchical cluster analysis. **(A)** HCA for HMs, TOM, and GSA, and **(B)** HCA for studied stations (KY: KeYa, KW: KeYa Water Supply Center, DJ: DaJuang, HM: HuiMin, FC: FongCin, HS: HaiShan, OB: Oyster Bed, YK: YenKan, MA: Mangrove Area).

similar terrigenous source (115–117). Fe and Al elements are abundant in the crust of the earth and naturally enter aquatic environments, as well as serving a significant role in HMs scavenging and their incorporation into sediments (118). As a result, the presence of Fe and Al with Ga, Co, In, and Cr can suggest diversity in pollutant sources between natural and anthropogenic activities. Also, the strong positive correlation among Co, Ga, and In might be due to industrial effluent from the industrialized urban area. Furthermore, the significant positive relationship of mud with Mn, Al, Fe, Co, Cr, Ga, and In indicates that mud-grained particles can extensively influence the mobility of these seven metals (25, 119, 120). Cluster 3 consists of Zn, Ni, Cu, and TOM; this data implied that the TOM content may have an influence on the distribution of HMs in surface sediments owing to its strong affinity through adsorption or complexation (8, 121, 122). Our findings coincided with earlier observations by Liu et al. (123), who mentioned that the HM concentrations in the Luanhe Estuary sediments were influenced by the OM content. Additionally, cluster 2 and 4 comprise only sand and gravel, respectively; it seems that the gravel and sand sediments have a negligible influence on the HM distribution. Based on the heavy metal's distribution (HCA-Q mode), the main nine studied stations were categorized into three clusters (Figure 10B). The first cluster contains one station (KY). This cluster had the greatest contents of Zn, Cu, Ni, and TOM. The second cluster comprises four stations (KW, FC, HS, YK, and MA), which had the highest percentage of sand (KW) and relative high values of TOM, Fe, Ga, Al, Cr, Co, and In (MA). While the third one contains three stations (DJ, HM, and OB), which had the greatest values of Fe, Al, Co, Cr, In, and Ga (DJ), Mn, and mud (OB). The results of HCA were consistent with the PCC and PCA data.

In summary, Fe and Al in cluster 1 enter the sediment of the wetland from another natural origin unrelated to organic matter. In contrast, In, Ga, Co, Cr, and Mn are primarily derived in the wetland sediment from anthropogenic origins, in addition to natural sources related to Fe and Al. Unlike cluster 1, heavy metals in cluster 3 (Zn, Cu, and Ni) are linked to OM and carried into the wetland while affixed to OM that derives mostly from natural origins. These outcomes support other findings and are reinforced by the sediment contamination indices discussed in this work. Restoration of Xiang-Shan wetland requires the local government to implement measures to prevent HM pollution as a matter of urgency, particularly in relation to In, Ga, Co, Cr, and Mn. In order to reveal the full ecological risk posed by these HMs, extensive ecotoxicological studies are required on the responses of the biota of Xiang-Shan wetland to these toxic metals.

Conclusion

The Xiang-Shan wetland is a natural home for millions of crustaceans, prawns, benthic invertebrates, shellfish, and endangered avian species. Added to that, its economic value to the government of Hsinchu City. Thus, it is critical to evaluate the heavy metal contamination and identify its ecological threat. The average values of the 12 metals in the Xiang-Shan wetland's surface sediments showed a decreasing sequence of Al > Fe > Mn > Zn > Co > Ga > Cr > Cu > In > Ni > Pb = Cd. The single pollution indices proved that the majority of sampling stations were unpolluted to minor polluted by Fe, Al, Zn, Cu, Mn, Cr, and Ni, moderately to heavily polluted by Co and Ga, and extremely polluted by In at all studied stations. The findings of PLI demonstrated that about 67% of spring sediments and entirely of winter sediments were moderately polluted (PLI < 2). Based on PERI, about 67% of spring sediment and 89% of winter sediment posed "minimal ecological risk" (PERI <40). Multivariate analyses demonstrated that Fe, Al, Zn, Cu, and Ni came from natural origins, while the sources of Co, Ga, In, Cr, and Mn were both anthropogenic and natural. Our research sounds the alarm for stricter management of metal discharges, and it is critical for the integrity of the ecosystem that heavy metals in aquatic-sedimentary systems in the Xiang-Shan wetland are continuously monitored.

Data availability statement

The raw data supporting the conclusions of this article will be made available by the authors, without undue reservation.

Author contributions

AS-T: Conceptualization, Data curation, Formal analysis, Investigation, Methodology, Software, Visualization, Writing – original draft, Writing – review & editing. C-SGC: Data curation, Methodology, Software, Writing – review & editing. S-SY: Funding acquisition, Project administration, Resources, Supervision, Writing – review & editing. C-FL: Funding acquisition, Project administration, Resources, Supervision, Writing – review & editing.

Funding

The author(s) declare that no financial support was received for the research and/or publication of this article.

Conflict of interest

The authors declare that the research was conducted in the absence of any commercial or financial relationships that could be construed as a potential conflict of interest.

Publisher's note

Supplementary material

The Supplementary material for this article can be found online at: https://www.frontiersin.org/articles/10.3389/fpubh.2025.1459060/full#supplementary-material

References

1. Castillo MA, Trujillo IS, Alonso EV, de Torres AG, Pavón JC. Bioavailability of heavy metals in water and sediments from a typical Mediterranean Bay (Málaga Bay, region of Andalucía, southern Spain). *Mar Pollut Bull*. (2013) 76:427–34. doi: 10.1016/j.marpolbul.2013.08.031

2. Gopinath A, Nair S, Kumar N, Jayalakshmi K, Pamalal D. A baseline study of trace metals in a coral reef sedimentary environment, Lakshadweep archipelago. *Environ Earth Sci*. (2010) 59:1245–66. doi: 10.1007/s12665-009-0113-6

3. Nobi E, Dilipan E, Thangaradjou T, Sivakumar K, Kannan L. Geochemical and geo-statistical assessment of heavy metal concentration in the sediments of different coastal ecosystems of Andaman Islands, India. *Coastal Shelf Sci*. (2010) 87:253–64. doi: 10.1016/j.ecss.2009.12.019

4. Ramachandra T, Sudarshan P, Mahesh M, Vinay S. Spatial patterns of heavy metal accumulation in sediments and macrophytes of Bellandur wetland, Bangalore. *J Environ Manag*. (2018) 206:1204–10. doi: 10.1016/j.jenvman.2017.10.014

5. Rezapour S, Atashpaz B, Moghaddam SS, Damalas CA. Heavy metal bioavailability and accumulation in winter wheat (*Triticum aestivum* L.) irrigated with treated wastewater in calcareous soils. *Sci Total Environ*. (2019) 656:261–9. doi: 10.1016/j.scitotenv.2018.11.288

6. Shu Q, Ma Y, Liu Q, Zhang S, Hu Z, Yang P. Levels and ecological risk of heavy metals in the surface sediments of tidal flats along the North Jiangsu coast, China. *Mar Pollut Bull*. (2021) 170:112663. doi: 10.1016/j.marpolbul.2021.112663

7. Hosono T, Su C-C, Delinom R, Umezawa Y, Toyota T, Kaneko S, et al. Decline in heavy metal contamination in marine sediments in Jakarta Bay, Indonesia due to increasing environmental regulations. *Estuar Coast Shelf Sci*. (2011) 92:297–306. doi: 10.1016/j.ecss.2011.01.010

8. Tian K, Wu Q, Liu P, Hu W, Huang B, Shi B, et al. Ecological risk assessment of heavy metals in sediments and water from the coastal areas of the Bohai Sea and the Yellow Sea. *Environ Int*. (2020) 136:105512. doi: 10.1016/j.envint.2020.105512

9. Fu F, Wang QJ. Removal of heavy metal ions from wastewaters: a review. *J Environ Manag*. (2011) 92:407–18. doi: 10.1016/j.jenvman.2010.11.011

10. Barut IF, Ergin M, Meriç E, Avşar N, Nazik A, Suner F. Contribution of natural and anthropogenic effects in the Iznik Lake bottom sediment: geochemical and microfauna assemblages evidence. *Quat Int*. (2018) 486:129–42. doi: 10.1016/j.quaint.2017.10.026

11. Shajib MTI, Hansen HCB, Liang T, Holm PE. Metals in surface specific urban runoff in Beijing. *Environ Pollut*. (2019) 248:584–98. doi: 10.1016/j.envpol.2019.02.039

12. Zahra A, Hashmi MZ, Malik RN, Ahmed ZJ. Enrichment and geo-accumulation of heavy metals and risk assessment of sediments of the Kurang Nallah—feeding tributary of the Rawal Lake reservoir, Pakistan. *Sci Total Environ*. (2014) 470-471:925–33. doi: 10.1016/j.scitotenv.2013.10.017

13. Bastami KD, Neyestani MR, Molamohyedin N, Shafeian E, Haghparast S, Shirzadi IA, et al. Bioavailability, mobility, and origination of metals in sediments from Anzali wetland, Caspian Sea. *Caspian Sea Marine Pollution Bulletin*. (2018) 136:22–32. doi: 10.1016/j.marpolbul.2018.08.059

14. Xu X, Cao Z, Zhang Z, Li R, Hu B. Spatial distribution and pollution assessment of heavy metals in the surface sediments of the Bohai and yellow seas. *Mar Pollut Bull*. (2016) 110:596–602. doi: 10.1016/j.marpolbul.2016.05.079

15. Anbuselvan N, Sridharan M. Heavy metal assessment in surface sediments off Coromandel Coast of India: implication on marine pollution. *Mar Pollut Bull*. (2018) 131:712–26. doi: 10.1016/j.marpolbul.2018.04.074

16. Gholizadeh M, Patimar R. Ecological risk assessment of heavy metals in surface sediments from the Gorgan Bay, Caspian Sea. *Mar Pollut Bull*. (2018) 137:662–7. doi: 10.1016/j.marpolbul.2018.11.009

17. Nour HES. Distribution, ecological risk, and source analysis of heavy metals in recent beach sediments of Sharm El-sheikh, Egypt. *Environ Monit Assess*. (2019) 191:546. doi: 10.1007/s10661-019-7728-1

18. Ye Z, Chen J, Gao L, Liang Z, Li S, Li R, et al. 210Pb dating to investigate the historical variations and identification of different sources of heavy metal pollution in sediments of the Pearl River estuary, southern China. *Mar Pollut Bull*. (2020) 150:110670. doi: 10.1016/j.marpolbul.2019.110670

19. Xu F, Hu B, Yuan S, Zhao Y, Dou Y, Jiang Z, et al. Heavy metals in surface sediments of the continental shelf of the South Yellow Sea and East China Sea: sources, distribution and contamination. *Catena*. (2018) 160:194–200. doi: 10.1016/j.catena.2017.09.022

20. Şimşek A, Özkoç HB, Bakan G. Environmental, ecological and human health risk assessment of heavy metals in sediments at Samsun-Tekkeköy, north of Turkey. *Environ Sci Pollut Res*. (2022) 29:2009–23. doi: 10.1007/s11356-021-15746-w

21. Rezapour S, Siavash Moghaddam S, Nouri A, Khosravi AK. Urbanization influences the distribution, enrichment, and ecological health risk of heavy metals in croplands. *Sci Rep*. (2022) 12:3868. doi: 10.1038/s41598-022-07789-x

22. Adamo P, Arienzo M, Imperato M, Naimo D, Nardi G, Stanzione D. Distribution and partition of heavy metals in surface and sub-surface sediments of Naples city port. *Chemosphere*. (2005) 61:800–9. doi: 10.1016/j.chemosphere.2005.04.001

23. Bahloul M, Baati H, Amdouni R, Azri C. Assessment of heavy metals contamination and their potential toxicity in the surface sediments of Sfax solar Saltern, Tunisia. *Environ Earth Sci*. (2018) 77:1–22. doi: 10.1007/s12665-018-7227-7

24. Wang Q, Chen Q, Yan D, Xin S. Distribution, ecological risk, and source analysis of heavy metals in sediments of Taizihe River, China. *Environ Earth Sci*. (2018) 77:1–14. doi: 10.1007/s12665-018-7750-6

25. Salah-Tantawy A, Chang C-SG, Liu M-Y, Young S-S. Exploring the diversity and structural response of sediment-associated microbiota communities to environmental pollution at the siangshan wetland in Taiwan using environmental DNA metagenomic approach. *Front Mar Sci*. (2022) 9:990428. doi: 10.3389/fmars.2022.990428

26. Nour HE, Helal SA, Wahab MA. Contamination and health risk assessment of heavy metals in beach sediments of Red Sea and Gulf of Aqaba, Egypt. *Mar Pollut Bull*. (2022) 177:113517. doi: 10.1016/j.marpolbul.2022.113517

27. Ghrefat HA, Abu-Rukah Y, Rosen MA. Application of geoaccumulation index and enrichment factor for assessing metal contamination in the sediments of Kafrain dam, Jordan. *Environ Monit Assess*. (2011) 178:95–109. doi: 10.1007/s10661-010-1675-1

28. Bednarova Z, Kuta J, Kohut L, Machat J, Klanova J, Holoubek I, et al. Spatial patterns and temporal changes of heavy metal distributions in river sediments in a region with multiple pollution sources. *J Soils Sediments*. (2013) 13:1257–69. doi: 10.1007/s11368-013-0706-2

29. Nazeer S, Hashmi MZ, Malik RN. Heavy metals distribution, risk assessment and water quality characterization by water quality index of the river Soan, Pakistan. *Ecol Indic*. (2014) 43:262–70. doi: 10.1016/j.ecolind.2014.03.010

30. Cheng Q, Wang R, Huang W, Wang W, Li X. Assessment of heavy metal contamination in the sediments from the Yellow River wetland National Nature Reserve (the Sanmenxia section), China. *Environ Sci Pollut Res*. (2015) 22:8586–93. doi: 10.1007/s11356-014-4041-y

31. Mamat Z, Haximu S, Zhang ZY, Aji R. An ecological risk assessment of heavy metal contamination in the surface sediments of Bosten Lake, Northwest China. *Environ Sci Pollut Res*. (2016) 23:7255–65. doi: 10.1007/s11356-015-6020-3

32. Chai L, Li H, Yang Z, Min X, Liao Q, Liu Y, et al. Heavy metals and metalloids in the surface sediments of the Xiangjiang River, Hunan, China: distribution, contamination, and ecological risk assessment. *Environ Sci Pollut Res*. (2017) 24:874–85. doi: 10.1007/s11356-016-7872-x

33. Liu R, Jiang W, Li F, Pan Y, Wang C, Tian H. Occurrence, partition, and risk of seven heavy metals in sediments, seawater, and organisms from the eastern sea area of Shandong peninsula, Yellow Sea, China. *J Environ Manag*. (2021) 279:1117. doi: 10.1016/j.jenvman.2020.111771

34. Al-Kahtany K, Nour HE, El-Sorogy AS, Alharbi T. Ecological and health risk assessment of heavy metals contamination in mangrove sediments, Red Sea coast. *Mar Pollut Bull*. (2023) 192:115000. doi: 10.1016/j.marpolbul.2023.115000

35. Hossain MB, Sultana J, Pingki FH, Nur A-AU, Mia MS, Bakar MA, et al. Accumulation and contamination assessment of heavy metals in sediments of commercial aquaculture farms from a coastal area along the northern bay of Bengal. *Front Environ Sci*. (2023) 11:1148360. doi: 10.3389/fenvs.2023.1148360

36. Jamshidi-Zanjani A, Saeedi M. Metal pollution assessment and multivariate analysis in sediment of Anzali international wetland. *Environ Earth Sci*. (2013) 70:1791–808. doi: 10.1007/s12665-013-2267-5

37. Tang W, Shan B, Zhang H, Zhang W, Zhao Y, Ding Y, et al. Heavy metal contamination in the surface sediments of representative limnetic ecosystems in eastern China. *Sci Rep*. (2014) 4:7152. doi: 10.1038/srep07152

38. Algül F, Beyhan M. Concentrations and sources of heavy metals in shallow sediments in Lake Bafa, Turkey. *Sci Rep*. (2020) 10:11782. doi: 10.1038/s41598-020-68833-2

39. Zhang Q, Ren F, Xiong X, Gao H, Wang Y, Sun W, et al. Spatial distribution and contamination assessment of heavy metal pollution of sediments in coastal reclamation areas: a case study in Shenzhen Bay, China. *Environ Sci Eur*. (2021) 33:1–11. doi: 10.1186/s12302-021-00532-9

40. Du Laing G, Rinklebe J, Vandecasteele B, Meers E, Tack F. Trace metal behaviour in estuarine and riverine floodplain soils and sediments: a review. *Sci Total Environ*. (2009) 407:3972–85. doi: 10.1016/j.scitotenv.2008.07.025

41. Lin Y-C, Chang-Chien G-P, Chiang P-C, Chen W-H, Lin Y-C. Multivariate analysis of heavy metal contaminations in seawater and sediments from a heavily industrialized harbor in southern Taiwan. *Mar Pollut Bull*. (2013) 76:266–75. doi: 10.1016/j.marpolbul.2013.08.027

42. Young S, Jiang H, Syu R, Huang S. The biodiversity of siangshan wetland. government-authorized project final report (in Chinese), vol. *210*. Taiwan: Hsinchu City Government, National Hsinchu teacher's College (2005).

43. Young S. The study of polychaeta and sipuncula from hisinchu city costal wildlife sanctuary, habitats and species distribution on temporal and spatial scale. Government authorized project final report (in Chinese), vol. *169*. Taiwan: Taiwan governemnt (2009).

44. Chang S, Chiu H-M, Tu W. The silence of silicon lambs: speaking out health and environmental impacts within Taiwan's Hsinchu science-based industrial park. IEEE International Symposium on Electronics and the Environment, 2004. Conference Record. 2004; (2004). IEEE; 258–263. doi: 10.1109/ISEE.2004.1299726

45. Tu W-L. Challenges of environmental governance in the face of IT industrial dominance: a study of Hsinchu science-based Industrial Park in Taiwan. *Int J Environ Sustain Dev*. (2005) 4:290–309. doi: 10.1504/IJESD.2005.007742

46. Wei K-Y. Multivariate analyses of potentially toxic elements along an industrialized Urban River in northern Taiwan. *J Environ Prot*. (2021) 12:983–1000. doi: 10.4236/jep.2021.1211057

47. Modak D, Singh K, Chandra H, Ray P. Mobile and bound forms of trace metals in sediments of the lower Ganges. *Water Res*. (1992) 26:1541–8. doi: 10.1016/0043-1354(92)90075-F

48. Lin J-G, Chen S, Su C. Assessment of sediment toxicity by metal speciation in different particle-size fractions of river sediment. *Water Sci Technol*. (2003) 47:233–41. doi: 10.2166/wst.2003.0694

49. Folk RL. Petrology of sedimentary rocks. Austin: Hemphill Publishing Company (1974). 182 p.

50. Wakley A, Black C. Determination of organic matter in the soil by chromic acid digesion. *Soil Sci*. (1934) 63:251–64.

51. Element C. Method 3051A microwave assisted acid digestion of sediments, sludges, soils, and oils. *Für Anal Chem*. (2007) 111:362–6.

52. Sakan SM, Đorđević DS, Manojlović DD, Predrag PS. Assessment of heavy metal pollutants accumulation in the Tisza river sediments. *J Environ Manag*. (2009) 90:3382–90. doi: 10.1016/j.jenvman.2009.05.013

53. Daskalakis KD, O'Connor TP. Normalization and elemental sediment contamination in the coastal United States. *Environ Sci Technol*. (1995) 29:470–7. doi: 10.1021/es00002a024

54. Zhang L, Ye X, Feng H, Jing Y, Ouyang T, Yu X, et al. Heavy metal contamination in western Xiamen Bay sediments and its vicinity, China. *Marine Poll Bullet*. (2007) 54:974–82. doi: 10.1016/j.marpolbul.2007.02.010

55. Ergin M, Saydam C, Baştürk Ö, Erdem E, Yörük R. Heavy metal concentrations in surface sediments from the two coastal inlets (Golden Horn estuary and Izmit Bay) of the northeastern sea of Marmara. *Chem Geol*. (1991) 91:269–85. doi: 10.1016/0009-2541(91)90004-B

56. Turekian KK, Wedepohl KH. Distribution of the elements in some major units of the earth's crust. *Geological Society America Bullet*. (1961) 72:175–92. doi: 10.1130/0016-7606(1961)72[175:DOTEIS]2.0.CO;2

57. Acevedo-Figueroa D, Jiménez B, Rodríguez-Sierra C. Trace metals in sediments of two estuarine lagoons from Puerto Rico. *Environ Pollut*. (2006) 141:336–42. doi: 10.1016/j.envpol.2005.08.037

58. Muller G. Index of geoaccumulation in sediments of the Rhine River. *Geo J*. (1969) 2:108–18.

59. Chen C-W, Kao C-M, Chen C-F, Dong C-D. Distribution and accumulation of heavy metals in the sediments of Kaohsiung Harbor, Taiwan. *Chemosphere*. (2007) 66:1431–40. doi: 10.1016/j.chemosphere.2006.09.030

60. Zhang W, Feng H, Chang J, Qu J, Xie H, Yu L. Heavy metal contamination in surface sediments of Yangtze River intertidal zone: an assessment from different indexes. *Environ Pollut*. (2009) 157:1533–43. doi: 10.1016/j.envpol.2009.01.007

61. Tomlinson D, Wilson J, Harris C, Jeffrey D. Problems in the assessment of heavy-metal levels in estuaries and the formation of a pollution index. *Helgoländer meeresuntersuchungen*. (1980) 33:566–75. doi: 10.1007/BF02414780

62. Tian K, Huang B, Xing Z, Hu W. Geochemical baseline establishment and ecological risk evaluation of heavy metals in greenhouse soils from Dongtai, China. *Ecol Indic*. (2017) 72:510–20. doi: 10.1016/j.ecolind.2016.08.037

63. Abrahim G, Parker R. Assessment of heavy metal enrichment factors and the degree of contamination in marine sediments from Tamaki estuary, Auckland, New Zealand. *Environ Monit Assess*. (2008) 136:227–38. doi: 10.1007/s10661-007-9678-2

64. Nemerow NL. Stream, lake, estuary, and ocean pollution. (1991). Available at: https://www.osti.gov/biblio/7030475

65. Yang Z, Lu W, Long Y, Liu X. Prediction and precaution of heavy metal pollution trend in urban soils of Changchun City, urban environ. *Urban Ecol*. (2010) 23:1–4.

66. Hakanson L. An ecological risk index for aquatic pollution control. *Sedimentological Approach Water Research*. (1980) 14:975–1001. doi: 10.1016/0043-1354(80)90143-8

67. Nabholz J. Environmental hazard and risk assessment under the United States toxic substances control act. *Sci Total Environ*. (1991) 109-110:649–65.

68. Singh A, Sharma RK, Agrawal M, Marshall F. Health risk assessment of heavy metals via dietary intake of foodstuffs from the wastewater irrigated site of a dry tropical area of India. *Food Chem Toxicol*. (2010) 48:611–9. doi: 10.1016/j.fct.2009.11.041

69. Douay F, Pelfrêne A, Planque J, Fourrier H, Richard A, Roussel H, et al. Assessment of potential health risk for inhabitants living near a former lead smelter. Part 1: metal concentrations in soils, agricultural crops, and homegrown vegetables. *Environ Monit Assess*. (2013) 185:3665–80. doi: 10.1007/s10661-012-2818-3

70. Li R, Pan C, Xu J, Ding G, Zou Y. Application of potential ecological risk assessment model based on Monte Carlo simulation. *Res Environ Sci*. (2012) 25:1336–43. Available at: http://www.hjkxyj.org.cn

71. Anzecc A. Australian and New Zealand guidelines for fresh and marine water quality. Australian and New Zealand Environment and Conservation Council and Agriculture and Resource Management Council of Australia and New Zealand, Canberra. (2000) 1:1–314

72. Long ER, Macdonald DD, Smith SL, Calder FD. Incidence of adverse biological effects within ranges of chemical concentrations in marine and estuarine sediments. *Environ Manag*. (1995) 19:81–97. doi: 10.1007/BF02472006

73. CCME. Canadian environmental quality guidelines, vol. *2* Canadian Council of Ministers of the Environment (2002). Available at: https://ccme.ca/en

74. Taiwan EPA. Soil and groundwater pollution remediation act. Taipei, Taiwan: Taiwan Environmental Protection Administration (2010).

75. Lin Q, Liu E, Zhang E, Li K, Shen J. Spatial distribution, contamination and ecological risk assessment of heavy metals in surface sediments of Erhai Lake, a large eutrophic plateau lake in Southwest China. *Catena*. (2016) 145:193–203. doi: 10.1016/j.catena.2016.06.003

76. Patman P, Denny L, Churchill B. Using SPSS for descriptive statistical analysis. Oxford University Press: University of Tasmania (2013).

77. Arkkelin D. Using SPSS to understand research and data analysis. *Psychol Curricul Mat*. (2014) 1:1–194. Available at: https://scholar.valpo.edu/psych_oer/1

78. Varol M. Assessment of heavy metal contamination in sediments of the Tigris River (Turkey) using pollution indices and multivariate statistical techniques. *J Hazard Mater*. (2011) 195:355–64. doi: 10.1016/j.jhazmat.2011.08.051

79. Wei T, Simko V, Levy M, Xie Y, Jin Y, Zemla J. Package "corrplot": Visualization of a correlation matrix. R Foundation for Statistical Computing: Vienna, Austria (2017).

80. Team RD. R: A language and environment for statistical computing. Copenhagen Business School: R Foundation for Statistical Computing (2010).

81. Grandin U. PC-ORD version 5: a user-friendly toolbox for ecologists. *J Veg Sci*. (2006) 17:843–4. doi: 10.1111/j.1654-1103.2006.tb02508.x

82. Rea DK, Hovan SA. Grain size distribution and depositional processes of the mineral component of abyssal sediments: lessons from the North Pacific. *Paleoceanography*. (1995) 10:251–8. doi: 10.1029/94PA03355

83. Pontoni L, La Vecchia C, Boguta P, Sirakov M, D'Aniello E, Fabbricino M, et al. Natural organic matter controls metal speciation and toxicity for marine organisms: a review. *Environ Chem Lett*. (2022) 20:797–812. doi: 10.1007/s10311-021-01310-y

84. Odum WE, Heald EJ. The detritus-based food web of an. *Estuar Res Chem Biol Estuar Syst*. (1975) 1:265.

85. Huc A. Origin and formation of organic matter in recent sediments and its relation to kerogen. *Kerogen*. (1980)

86. Suresh G, Sutharsan P, Ramasamy V, Venkatachalapathy R. Assessment of spatial distribution and potential ecological risk of the heavy metals in relation to granulometric contents of Veeranam lake sediments. *India Ecotoxicol Environ Safety*. (2012) 84:117–24. doi: 10.1016/j.ecoenv.2012.06.027

87. Taweel A, Shuhaimi-Othman M, Ahmad A. Assessment of heavy metals in tilapia fish (*Oreochromis niloticus*) from the Langat River and engineering Lake in Bangi, Malaysia, and evaluation of the health risk from tilapia consumption. *Ecotoxicol Environ Saf*. (2013) 93:45–51. doi: 10.1016/j.ecoenv.2013.03.031

88. Li H, Davis A. Heavy metal capture and accumulation in bioretention media. *Environ Sci Technol*. (2008) 42:5247–53. doi: 10.1021/es702681j

89. Tang W, Ao L, Zhang H, Shan B. Accumulation and risk of heavy metals in relation to agricultural intensification in the river sediments of agricultural regions. *Environ Earth Sci*. (2014) 71:3945–51. doi: 10.1007/s12665-013-2779-z

90. Rezapour S, Asadzadeh F, Nouri A, Khodaverdiloo H, Heidari M. Distribution, source apportionment, and risk analysis of heavy metals in river sediments of the Urmia Lake basin. *Sci Rep*. (2022) 12:17455. doi: 10.1038/s41598-022-21752-w

91. Yu T, Zhang Y, Zhang Y. Distribution and bioavailability of heavy metals in different particle-size fractions of sediments in Taihu Lake, China. *Chem Spec Bioavailab*. (2012) 24:205–15. doi: 10.3184/095422912X13488240379124

92. El-Metwally ME, Madkour AG, Fouad RR, Mohamedein LI, Eldine HAN, Dar MA, et al. Assessment the leachable heavy metals and ecological risk in the surface sediments inside the Red Sea ports of Egypt. International. *J Mar Sci*. (2017):7. doi: 10.5376/ijms.2017.07.0023

93. Barik SS, Prusty P, Singh RK, Tripathy S, Farooq S, Sharma K. Seasonal and spatial variations in elemental distributions in surface sediments of Chilika Lake in response to change in salinity and grain size distribution. *Environ Earth Sci*. (2020) 79:1–18. doi: 10.1007/s12665-020-09009-z

94. Dar MA, El-Saharty AA. Recycling and retention of some trace metals in the mangrove sediments, Red Sea, Egypt. *Egypt J Aquat Res*. (2006) 32:34–47.

95. Giannico OV, Baldacci S, Desiante F, Basile FC, Franco E, Fragnelli GR, et al. PCDD/fs and PCBs in *Mytilus galloprovincialis* from a contaminated area in Italy: the role of mussel size, temperature and meteorological factors. *Food Additives Contaminants*. (2022) 39:1123–35. doi: 10.1080/19440049.2022.2059108

96. Giannico OV, Desiante F, Basile FC, Franco E, Baldacci S, Fragnelli GR, et al. Dioxins and PCBs contamination in mussels from Taranto (Ionian Sea, southern Italy): a seven years spatio-temporal monitoring study. *Ann Ist Super Sanita*. (2020) 56:452–61. doi: 10.4415/ANN_20_04_07

97. Filippi G, Dassenakis M, Paraskevopoulou V, Lazogiannis K. Sediment quality assessment in an industrialized Greek coastal marine area (western Saronikos gulf). *Biogeosciences*. (2023) 20:163–89. doi: 10.5194/bg-20-163-2023

98. Islam MAS, Hossain ME, Nahar K, Majed N. Assessment of environmental Hazard and heavy metal contamination in Dhaleshwari River sediment: a toxicity based study on pollution. *Pollution*. (2023) 9:67–83. doi: 10.22059/poll.2022.342243.1455

99. El-Sorogy AS, Youssef M, Al-Kahtany K, Saleh M. Distribution, source, contamination, and ecological risk status of heavy metals in the Red Sea-Gulf of Aqaba coastal sediments, Saudi Arabia. *Mar Pollut Bull*. (2020) 158:111411. doi: 10.1016/j.marpolbul.2020.111411

100. Young SS. The ecological and water quality monitoring on siangshan wetland (national scale) 2018–2019. Government-authorized project final report (in Chinese), vol. *204*. Taiwan: Hsinchu City Government, National Tsing Hua University (2019).

101. Ye YT, Young SS. An investigation of the heavy metals distribution of the main rivers and wetlands in Hsinchu [dissertation/master thesis in Chinese]. Taiwan: National Tsing Hua University. (2008).

102. Wang Q, Huang X, Zhang Y. Heavy metals and their ecological risk assessment in surface sediments of the Changjiang River estuary and contiguous East China Sea. *Sustain For*. (2023) 15:4323. doi: 10.3390/su15054323

103. Lai YJ, Chang PC, Lee YT, Hung YH, Huang YH, Chen SD, et al. Establishment and discussion of soil heavy metal background concentrations in Taiwan. *J Soil Groundwater Remediation*. (2018) 5:143–62. doi: 10.6499/JSGR.201807_5(3).0003

104. Zhai B, Liu Z, Wang X, Bai F, Wang L, Chen Z, et al. Assessment of heavy metal contamination in surface sediments in the western Taiwan Strait. *Mar Pollut Bull*. (2020) 159:111492. doi: 10.1016/j.marpolbul.2020.111492

105. Sarkar SK, Sarkar SK. Geochemical speciation and risk assessment of trace metals in sediments of sundarban wetland. *Ecotoxicol Relevance Remedial Measures*. (2018) 10:145–72. doi: 10.1007/978-981-10-2793-2_6

106. Bu-Olayan A, Thomas B. Bourgeoning impact of the technology critical elements in the marine environment. *Environ Pollut*. (2020) 265:115064. doi: 10.1016/j.envpol.2020.115064

107. Yang J-L, Chen L-H. Toxicity of antimony, gallium, and indium toward a teleost model and a native fish species of semiconductor manufacturing districts of Taiwan. *J Elem*. (2018) 23:191–199. doi: 10.5601/jelem.2017.22.3.1470

108. Nguyen CH, Field JA, Sierra-Alvarez RJ. Microbial toxicity of gallium-and indium-based oxide and arsenide nanoparticles. *J Environ Sci Health A*. (2020) 55:168–78. doi: 10.1080/10934529.2019.1676065

109. Chakraborty P, Ramteke D, Chakraborty S, Nath BN. Changes in metal contamination levels in estuarine sediments around India–an assessment. *Mar Pollut Bull*. (2014) 78:15–25. doi: 10.1016/j.marpolbul.2013.09.044

110. Fu J, Zhao C, Luo Y, Liu C, Kyzas GZ, Luo Y, et al. Heavy metals in surface sediments of the Jialu River, China: their relations to environmental factors. *J Hazard Mater*. (2014) 270:102–9. doi: 10.1016/j.jhazmat.2014.01.044

111. El Nemr A, El-Said GF, Ragab S, Khaled A, El-Sikaily A. The distribution, contamination and risk assessment of heavy metals in sediment and shellfish from the Red Sea coast, Egypt. *Chemosphere*. (2016) 165:369–80. doi: 10.1016/j.chemosphere.2016.09.048

112. Duodu GO, Ogogo KN, Mummullage S, Harden F, Goonetilleke A, Ayoko GA. Source apportionment and risk assessment of PAHs in Brisbane River sediment, Australia. *Ecol Indic*. (2017) 73:784–99. doi: 10.1016/j.ecolind.2016.10.038

113. Liang A, Wang Y, Guo H, Bo L, Zhang S, Bai Y. Assessment of pollution and identification of sources of heavy metals in the sediments of Changshou Lake in a branch of the three gorges reservoir. *PLoS One*. (2015) 22:16067–76. doi: 10.1007/s11356-015-4825-8

114. Briki M, Zhu Y, Gao Y, Shao M, Ding H, Ji H, et al. Distribution and health risk assessment to heavy metals near smelting and mining areas of Hezhang, China. *Environ Monit Assess*. (2017) 189:1–19. doi: 10.1007/s10661-017-6153-6

115. Li F, Huang J, Zeng G, Yuan X, Li X, Liang J, et al. Spatial risk assessment and sources identification of heavy metals in surface sediments from the Dongting Lake, middle China. *J Geochem Explor*. (2013) 132:75–83. doi: 10.1016/j.gexplo.2013.05.007

116. Zhang P, Qin C, Hong X, Kang G, Qin M, Yang D, et al. Risk assessment and source analysis of soil heavy metal pollution from lower reaches of Yellow River irrigation in China. *Sci Total Environ*. (2018) 633:1136–47. doi: 10.1016/j.scitotenv.2018.03.228

117. Nour HES, Ramadan F, Aita S, Zahran H. Assessment of sediment quality of the Qalubiya drain and adjoining soils, eastern Nile Delta, Egypt. *Arab J Geosci*. (2021) 14:1–13. doi: 10.1007/s12517-021-06891-0

118. Jagus A, Khak V, Rzetala MA, Rzetala M. Accumulation of heavy metals in the bottom sediments of the Irkutsk reservoir. *Int J Environ Health*. (2013) 6:350–62. doi: 10.1504/IJENVH.2013.056976

119. Gao X, Li P. Concentration and fractionation of trace metals in surface sediments of intertidal Bohai Bay, China. *Mar Pollut Bull*. (2012) 64:1529–36. doi: 10.1016/j.marpolbul.2012.04.026

120. Kim S, Yang DS, Kim YS. Distribution of metal contamination and grain size in the sediments of Nakdong River, Korea. *Environ Monit Assess*. (2020) 192:502. doi: 10.1007/s10661-020-08475-z

121. Jiang X, Teng A, Xu W, Liu X. Distribution and pollution assessment of heavy metals in surface sediments in the Yellow Sea. *Mar Pollut Bull*. (2014) 83:366–75. doi: 10.1016/j.marpolbul.2014.03.020

122. Li H, Kang X, Li X, Li Q, Song J, Jiao N, et al. Heavy metals in surface sediments along the Weihai coast, China: distribution, sources and contamination assessment. *Mar Pollut Bull*. (2017) 115:551–8. doi: 10.1016/j.marpolbul.2016.12.039

123. Liu J, Yin P, Chen B, Gao F, Song H, Li M. Distribution and contamination assessment of heavy metals in surface sediments of the Luanhe River estuary, northwest of the Bohai Sea. *Mar Pollut Bull*. (2016) 109:633–9. doi: 10.1016/j.marpolbul.2016.05.020

124. Förstner U, Ahlf W, Calmano W, Kersten M. Sediment criteria development: Contributions from environmental geochemistry to water quality management. Sediments and environmental geochemistry: Selected aspects and case histories. Springer, Berlin, Heidelberg. (1990) 311–338.

frontiers | Frontiers in Public Health

TYPE Original Research
PUBLISHED 17 April 2025
DOI 10.3389/fpubh.2025.1428772

OPEN ACCESS

EDITED BY
Dan Xu,
Dalian Maritime University, China

REVIEWED BY
Zhengrui Li,
Shanghai Jiao Tong University, China
Peng Tang,
Guangxi Medical University, China

*CORRESPONDENCE
Hao Zeng
✉ zenghao2019@126.com
Yongqiang Sun
✉ joint99@126.com

RECEIVED 07 May 2024
ACCEPTED 07 April 2025
PUBLISHED 17 April 2025

CITATION
Zhang P, Li S, Zeng H and Sun Y (2025) Exposure to polycyclic aromatic hydrocarbons and bone mineral density in children and adolescents: results from the 2011–2016 National Health and Nutrition Examination Survey.
Front. Public Health 13:1428772.
doi: 10.3389/fpubh.2025.1428772

Exposure to polycyclic aromatic hydrocarbons and bone mineral density in children and adolescents: results from the 2011–2016 National Health and Nutrition Examination Survey

Peng Zhang[1], Shuailei Li[2], Hao Zeng[3]* and Yongqiang Sun[2]*

[1]Department of Orthopedics, Huaihe Hospital Affiliated to Henan University, Kaifeng, Henan, China, [2]Henan Luoyang Orthopedic Hospital (Henan Provincial Orthopedic Hospital), Zhengzhou, Henan, China, [3]Department of Medical Insurance, Huaihe Hospital Affiliated to Henan University, Kaifeng, Henan, China

Introduction: Identifying factors that hinder bone development in children and adolescents is crucial for preventing osteoporosis. Exposure to polycyclic aromatic hydrocarbons (PAHs) has been linked to reduced bone mineral density (BMD), although available data, especially in children and adolescents, are limited. We examined the associations between urinary hydroxylated-PAHs (OH-PAHs) and lumbar spine BMD, pelvic BMD, and total BMD among 8–19 years participants (N = 1,332) of the 2011–2016 National Health and Nutrition Examination Survey.

Methods: Weighted linear regressions were employed to assess the associations between urinary OH-PAHs and BMD. Additionally, Bayesian kernel machine regression (BKMR) and quantile g-computation (Qgcomp) models were utilized to investigate the effect of co-exposure of PAHs on BMD.

Results: Several urinary OH-PAHs exhibited negative associations with lumbar spine BMD, pelvic BMD, and total BMD in children and adolescents. For instance, an increase of one unit in the natural log-transformed levels of urinary 1-hydroxypyrene and 2&3-Hydroxyphenanthrene was linked with a decrease of −0.014 g/cm^2 (95% CI: −0.026, −0.002) and −0.018 g/cm^2 (95% CI: −0.032, −0.004) in lumbar spine BMD, a decrease of −0.021 g/cm^2 (95% CI: −0.039, −0.003) and −0.017 g/cm^2 (95% CI: −0.033, −0.001) in pelvic BMD, and a decrease of −0.013 g/cm^2 (95% CI: −0.023, −0.002) and −0.016 g/cm^2 (95% CI: −0.026, −0.006) in total BMD. The body mass index modified the associations between urinary OH-PAHs and BMD, revealing negative effects on BMD primarily significant in overweight/obese individuals but not significant in underweight/normal individuals. Both the BKMR model and the Qgcomp model indicated a significant negative correlation between the overall effects of seven urinary OH-PAHs and lumbar spine BMD, pelvic BMD, and total BMD.

Conclusion: Our findings revealed that exposure to PAHs might hinder bone development in children and adolescents, potentially impacting peak bone mass—an essential factor influencing lifelong skeletal health.

KEYWORDS

polycyclic aromatic hydrocarbons, bone mineral density, children and adolescents, Bayesian kernel machine regression, quantile g-computation

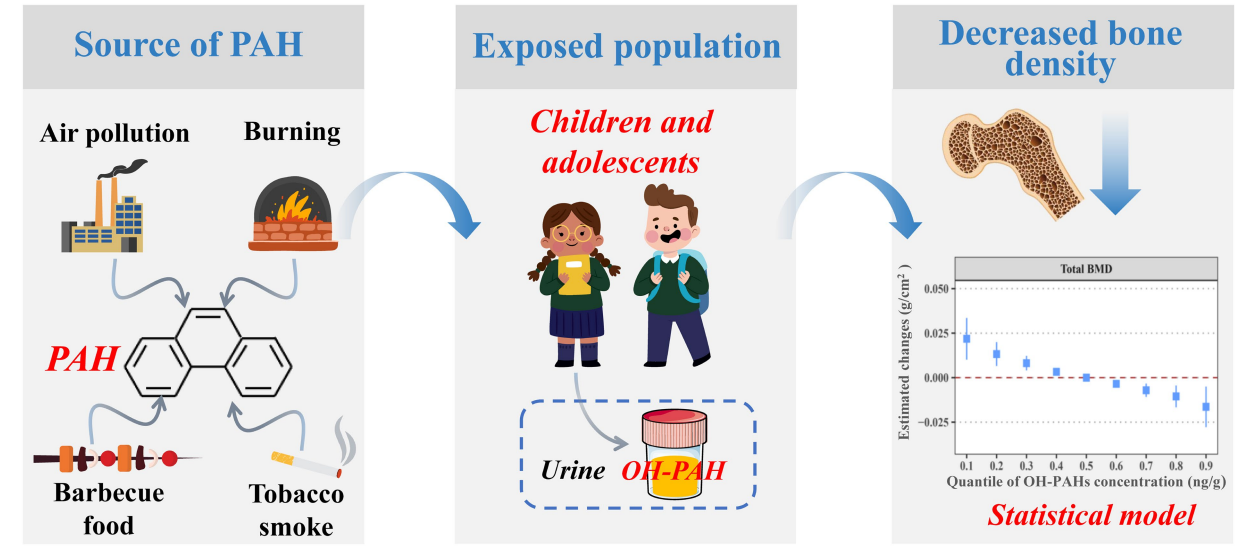

GRAPHICAL ABSTRACT

1 Introduction

Osteoporosis is a significant public health concern, with approximately 200 million adults worldwide affected by this condition (1). Osteoporosis leads to an increased incidence of bone fractures and mortality, imposing a substantial burden on families and society due to associated medical and caregiving costs. Skeletal accumulation occurs during childhood and adolescence, with peak bone mass in adolescence being a critical factor in the development of osteoporosis in later life (2). Approximately 90% of peak bone mass is attained by age 18–20, and failure to achieve optimal bone accrual during this window increases lifelong osteoporosis risk (3). Adolescents exhibit heightened susceptibility to environmental toxicants due to ongoing bone remodeling, rapid growth rates, and immature detoxification systems (4, 5). Identifying and addressing risk factors that lead to inadequate bone mass accumulation during childhood and adolescence is of paramount importance for osteoporosis prevention. Nevertheless, there has been limited research analyzing the impact of environmental factors on childhood and adolescence bone accrual.

Polycyclic aromatic hydrocarbons (PAHs) are a class of widely distributed environmental pollutants, and human exposure to PAHs can occur through various routes, including inhalation, skin contact, and ingestion (6). Children face unique exposure risks due to higher respiratory rates, and prolonged outdoor activities and proportionally higher intake of contaminated food (7). Emerging evidence suggests that urinary 1-hydroxypyrene (1-OHPyr), a key PAH metabolite, is 30% higher in children aged 6–11 compared to non-smoking adults under similar environmental conditions (8). A systematic review and meta-analysis of 40 studies involving 12,697 children and adolescents further corroborates this finding, demonstrating that urinary 1-OHPyr levels in pediatric populations are consistently elevated compared to non-occupational adults who do not smoke (9). The exposure to PAH is not only related to individual susceptibility and behavioral patterns, but also significantly influenced by geographic heterogeneity and pollution source distribution characteristics (10). Multiple studies have shown that the risk of PAH exposure is significantly increased in industrial intensive areas, transportation corridors, and during the winter heating season (11–13). For instance, monitoring in Rome detected 2.5-fold higher PAH levels in city centers compared to suburbs during heating seasons (13), while industrial cities like Slavonski Brod exhibited PAH concentrations 40% higher than background urban areas (11).

PAHs may affect bone mineral density (BMD) through multiple mechanisms. Experimental studies demonstrate that benzo [a] pyrene disrupts bone homeostasis through aryl hydrocarbon receptor (AhR) activation, suppressing osteoblast differentiation via ERK/MAPK pathway hyperphosphorylation (14). Additionally, PAHs can activate AhR pathways to accelerate osteoclast genesis or disrupt estrogen signaling, potentially altering bone homeostasis more profoundly in growing skeletons (15, 16). This is particularly concerning given that pediatric bone turnover rates are higher than adults (9), potentially amplifying toxicant impacts. Two previous studies have suggested an association between higher urinary hydroxylated-PAH (OH-PAH) concentrations in specific gender adult populations and lower BMD in different skeletal sites (17, 18).

However, few studies have examined PAH effects during the critical bone accrual window of 8–19 years. Current evidence gaps are threefold: (1) Limited data on dose–response relationships in pediatric populations; (2) Insufficient understanding of the unique susceptibility of developing skeletons to PAH exposure; and (3) Lack of analysis of combined exposure effects from multiple PAH congeners. Using a nationally representative sample from NHANES, this study investigates PAH-BMD associations in U.S. adolescents while addressing these knowledge gaps.

2 Materials and methods

2.1 Study design and population

National Health and Nutrition Examination Survey (NHANES) utilized a sophisticated multi-stage sampling weight design to

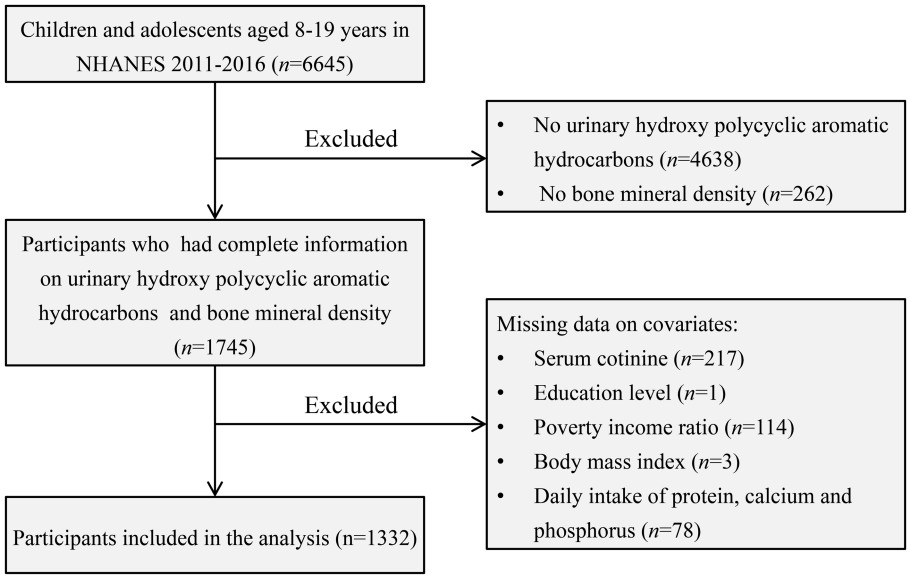

FIGURE 1
Flow chart of study participant selection process.

ensure the selection of a representative sample from the non-institutionalized civilian population of the United States. The survey was overseen by the National Center for Health Statistics (NCHS), and the data from questionnaires, laboratory tests, and physical examinations were made publicly available every 2 years.[1] Participants in the survey provided written informed consent, and the research protocol was approved by the NCHS Research Ethics Review Board.

Our study focused on children and adolescents aged 8–19, utilizing NHANES data spanning the years 2011–2016. Participants lacking data on BMD, urinary OH-PAHs, and relevant covariates were excluded from the analysis. Ultimately, a total of 1,332 subjects met the inclusion criteria for the final analysis. For a visual representation of the screening process, please refer to Figure 1.

2.2 Urinary OH-PAHs and BMD

Spot urine samples were collected from participants during their appointments at the NHANES Mobile Examination Center (MEC). These urine samples underwent processing, storage, and were subsequently shipped to the National Center for Environmental Health for analysis. The analysis included the measurement of seven urinary OH-PAHs, namely 1-Hydroxynaphthalene (1-OHNap), 2-Hydroxynaphthalene (2-OHNap), 3-Hydroxyfluorene (3-OHFlu), 2-Hydroxyfluorene (2-OHFlu), 1-Hydroxyphenanthrene (1-OHPhe), 1-Hydroxypyrene (1-OHPyr), and 2&3-Hydroxyphenanthrene (2&3-OHPhe). These measurements were carried out using isotope dilution high-performance liquid chromatography–tandem mass spectrometry. The detailed laboratory protocols can refer to the NHANES website.[2] When the concentrations of urinary metals fell below the limit of detection (LOD), they were replaced by LOD divided by the square root of 2. Additionally, the urinary concentrations of OH-PAHs in the study participants were adjusted for corresponding creatinine concentrations and expressed in units of ng/g.

In our study, we assessed three primary outcome variables: lumbar spine BMD, pelvic BMD, and total BMD (19). These measurements were conducted using Dual-Energy X-ray Absorptiometry (DXA) scans, administered by radiology technologists who were both trained and certified. Whole-body scans were performed using Hologic densitometers (Hologic, Inc., Bedford, Massachusetts). For a more comprehensive description of the DXA examination protocol, please consult the Body Composition Procedures Manual available on the NHANES website.[3]

2.3 Covariates

The covariates considered in our study, drawn from prior research (18, 20), encompassed demographic factors such as age, gender, race, and body mass index (BMI), poverty income ratio categories (<1, 1–3, >3) (21), education level (below junior school, junior school, high school or above), daily protein intake, daily calcium intake, daily phosphorus intake and serum cotinine. The information about the protein, calcium and phosphorus intake was derived from averaging the first and second 24 h dietary recall data.

1 https://www.cdc.gov/nchs/nhanes/index.htm

2 https://wwwn.cdc.gov/nchs/data/nhanes/2015-2016/labmethods/PAH-I-PAHS-I-MET-508.pdf

3 https://wwwn.cdc.gov/nchs/data/nhanes/2015-2016/manuals/2016_Body_Composition_Procedures_Manual.pdf

In instances where the second 24 h recall was unavailable, data from the first recall were utilized. Serum cotinine levels were categorized into high and low levels based on the median value (0.033 ng/mL) among study participants (22).

2.4 Statistical analysis

Following NHANES analytic guidelines, we incorporated 6-year sample weights to ensure that our results are representative of the national population aged 8–19 years and to correctly account for the complex, multistage sampling design of NHANES. To compare characteristics between genders, we used design-based methods appropriate for complex survey data: weighted chi-square tests for categorical variables (e.g., race, education) and weighted linear regression for continuous variables (e.g., age, BMI) (18, 23). For skewed urinary OH-PAH concentrations, natural log transformation was applied. Weighted multivariable linear regression models were then used to evaluate associations between log-transformed OH-PAH levels and BMD, adjusting for covariates. Results are reported as estimated BMD changes per unit increase in log-transformed OH-PAHs with 95% confidence intervals (CIs). Additionally, we employed restricted cubic splines regressions with three knots to explore potential non-linear relationships between urinary OH-PAH levels and BMD. We used three knots placed at the 10th, 50th, and 90th percentiles of each OH-PAH exposure distribution, following standard recommendations for restricted cubic splines that balance flexibility and stability. This approach allows for adequate flexibility to detect non-linear relationships while avoiding overfitting (24).

We evaluated potential modification effects of gender (male vs. female), age group (8–13 years vs. 14–19 years), and BMI (underweight/normal vs. overweight/obesity). This assessment involved estimating stratum-specific associations within each subgroup and introducing a multiplicative interaction term in the regression models. An interaction term with a *p*-value below 0.15 was considered statistically significant. The categorization of BMI was based on age-and sex-specific percentiles outlined in the Centers for Disease Control and Prevention growth charts (25).

Given the simultaneous exposure to multiple PAHs and their impact on BMD, we applied two statistical models—Bayesian kernel machine regression (BKMR) and quantile g-computation (Qgcomp) models—to explore the relationship between urinary OH-PAH mixtures and BMD.

(1) The BKMR model enables flexible assessment of the multivariable exposure-response function through kernel functions, allowing for non-linear and non-additive relationships between exposure and response (26). Considering the high correlation among urinary OH-PAHs, as illustrated in Supplementary Figure S1, all urinary OH-PAHs showed significant correlation ($p < 0.05$), with strong correlations observed among 3-OHFlu, 2-OHFlu, 1-OHPhe, 1-OHPyr, and 2&3-OHPhe (correlation coefficient ≥ 0.79). We employed a hierarchical variable selection method to construct the BKMR model for the urinary OH-PAHs mixture based on the magnitude of correlation among them. Urinary OH-PAHs were divided into three groups: Group 1 included 1-OHNap, Group 2 comprised 2-OHNap, and Group 3 encompassed 3-OHFlu, 2-OHFlu, 1-OHPhe, 1-OHPyr, and 2&3-OHPhe. The expression of the BKMR model is as follows:

$$\begin{aligned} Y_i = h[&Group_1 = 1 - OHNap_i, Group_2 = 2 - OHNap_i, Group_3 \\ &= (3 - OHFlu_i, 2 - OHFlu_i, 1 - OHPhe_i, 1 - OHPyr_i, \\ &2\,\&\,3 - OHPhe_i)] + \beta^T Z_i + e_i \end{aligned}$$

Where i corresponds to each participant. Y_i represents individual BMD. h () signifies the unknown exposure-response function. β denotes the estimated effects of all covariates Z_i. e_i indicates residuals. We used a Gaussian kernel function to model the exposure-response function, capable of handling high-dimensional parameter spaces, employing a Markov Chain Monte Carlo (MCMC) algorithm for 25,000 iterations. The BKMR analysis yielded the following results: (1) Overall OH-PAHs mixture effects on BMD, (2) Individual OH-PAH effects on BMD. For a detailed description, refer to previous researcher (26).

(2) The Qgcomp model is a parametric statistical method that merges weighted quantile sum regression and g-computation, allowing for the assessment of the effects of exposure mixtures (27). This method involves converting all exposure variables into quartiles and then fitting a linear model incorporating exposure, covariates, and outcomes. The aggregate effect of the exposure mixture is quantified as the estimated changes in outcomes corresponding to a quartile increase for all exposure variables. Additionally, each exposure variable is assigned a weight, indicating the significance of the association of each variable in either a positive or negative direction. Notably, the strength of Qgcomp model lies in its ability to avoid the assumption of directional homogeneity. This method allows for the computation of both positive and negative associations between individual exposure variables and outcomes. The detailed description referred to the previous study (27).

Sensitivity analysis comprised two key components: (1) Exclusion of individuals with abnormal creatinine values (<30 mg/dL or >300 mg/dL) was conducted to validate the association between urinary OH-PAHs and BMD (28). (2) An extended approach utilizing the Qgcompint model, which is an extension of the Qgcomp package, was employed to evaluate potential effect measure modifications of the overall mixture effect. This model incorporates interaction terms between the OH-PAH mixture and covariates such as gender, age group, and BMI to assess how these factors modify the effect of PAH exposure on BMD (29). (3) Given that 1-OHPyr had a detection rate of 85%, we conducted a secondary analysis excluding participants whose 1-OHPyr measurement fell below the detection limit.

All data analyses were performed with R (4.3.1). Except for the interaction *p*-value, all other significance levels were set at 0.05. Weighted linear regression, restricted cubic splines regression, bmkr, Qgcomp, and Qgcompint were implemented by R packages "survey," "rms," "bkmr," "qgcmop," and "Qgcompint," respectively.

3 Results

3.1 Characteristics of participants

As shown in Table 1, this study involved a total of 1,332 participants, including 690 males and 642 females. Their weighted average age and BMI were 13.6 years and 22.9 kg/m^2, respectively. The majority of the study subjects were non-Hispanic white, had high school or above education, and had a poverty income ratio of 1–3. Among males, the intake of serum cotinine, protein, calcium, and phosphorus was significantly higher compared to females ($p < 0.05$).

The weighted average BMD of the participants was 0.888 g/cm^2 for lumbar spine BMD, 1.09 g/cm^2 for pelvic BMD, and 0.965 g/cm^2 for total BMD. Female participants exhibited significantly higher lumbar spine BMD than males ($p < 0.05$), while there were no significant gender differences in pelvic BMD and total BMD. Supplementary Table S1 provides the descriptive statistics for the seven urinary OH-PAHs measured in our study. Detection frequencies ranged from 85.2% (1-OHPyr) to nearly 100%. The mean concentrations were highest for 2-OHNap and lowest for 3-OHFlu. Except for 2-OHNap and 2&3-OHPhe, the concentrations of other OH-PAHs did not show significant differences between different genders.

3.2 Association of urinary OH-PAHs with BMD: weighted linear regression model

As shown in Figure 2, the majority of OH-PAHs exhibit a significant negative correlation with BMD. Each unit increase of natural log-transformed urinary 1-OHNap, 1-OHPhe, 1-OHPyr, 2-OHFlu, 2&3-OHPhe, and 3-OHFlu was associated with a decrease of −0.010 g/cm^2 (95% CI: −0.018, −0.002), −0.013 g/cm^2 (95% CI: −0.024, −0.001), −0.014 g/cm^2 (95% CI: −0.026, −0.002), −0.021 g/cm^2 (95% CI: −0.035, −0.007), −0.018 g/cm^2 (95% CI: −0.032, −0.004), and −0.017 g/cm^2 (95% CI: −0.031, −0.003) in lumbar spine BMD. Pelvic BMD decreased by −0.013 g/cm^2 (95% CI: −0.022, −0.004), −0.017 g/cm^2 (95% CI: −0.033, −0.001), and −0.021 g/cm^2 (95% CI: −0.039, −0.003) with one unite increase of natural log-transformed urinary 1-OHNap, 2&3-OHPhe, and 1-OHPyr. Total BMD reduced by −0.010 g/cm^2 (95% CI: −0.018, −0.001), −0.016 g/cm^2 (95% CI: −0.026, −0.006), −0.015 g/cm^2 (95% CI: −0.026, −0.004), and −0.013 g/cm^2 (95% CI: −0.023, −0.002) with per unit increase of natural log-transformed urinary 3-OHFlu, 2&3-OHPhe, 1-OHPhe, and 1-OHPyr.

Supplementary Figures S2–S4 illustrate restricted cubic spline models depicting the nonlinear associations of urinary OH-PAH levels with lumbar spine BMD (Supplementary Figure S2), pelvic BMD (Supplementary Figure S3), and total BMD (Supplementary Figure S4). These plots suggest non-linear relationships between 1-OHPyr and pelvic BMD, as well as between 1-OHPhe and both pelvic BMD and total BMD (*P* for nonlinearity < 0.05).

Supplementary Figures S5, S6, respectively, illustrate subgroup analysis of the associations between urinary OH-PAHs and BMD among different gender (males and females) and age group (< 14 years and ≥ 14 years). Regarding gender, significant interactions between 1-OHPhe and gender for pelvic BMD and total BMD are observed, as well as between 3-OHFlu and gender for total BMD (all *P*-interaction < 0.15). Specifically, the effect of 1-OHPhe on pelvic BMD is not significant in both males and females, and the effect on total BMD is significant only in males, while the effect of 3-OHFlu on total BMD is significant only in females. Concerning age, only the interaction between 2-OHNap and age for the BMD is significant (*P*-interaction < 0.15); the effect of 2-OHNap on lumbar spine BMD and pelvic BMD is not significant in both age groups (<14 years and ≥14 years), while the negative effect on total BMD is significant only in the ≥14 years age group.

As shown in Figure 3, we also identified significant interactions between some OH-PAHs and BMI (underweight/normal and overweight/obesity) on BMD, such as 1-OHPhe, 2-OHFlu, 2-OHNap, 3-OHFlu, and BMI on lumbar spine BMD, 2-OHFlu and BMI on pelvic BMD, and 2-OHFlu and BMI on total BMD (all *P*-interaction < 0.15). These OH-PAHs exhibited a negative effect on BMD that was significant only in overweight/obesity individuals, while not significant in underweight/normal individuals.

3.3 Association of urinary OH-PAHs with BMD: BKMR model

As illustrated in Figure 4A, the significant negative linear associations exist between the overall effects of urinary OH-PAHs mixture with lumbar spine BMD, pelvic BMD, and total BMD. Figure 4B displays the associations between individual OH-PAH and BMD in the BMKR model. The results indicate that 1-OHPhe is the primary contributor to the decrease in lumbar spine BMD and total BMD, while 1-OHPyr is the main contributor to the decrease in pelvic BMD. When the concentrations of the other urinary OH-PAHs were held constant at the 50th percentile, each increase of one quartile range in the natural log-transformed of urinary 1-OHPhe was significantly associated with a decrease of −0.013 g/cm^2 (95% CI: −0.025, −0.001) in lumbar spine BMD and −0.015 g/cm^2 (95% CI: −0.022, −0.007) in total BMD. Additionally, each increase of one quartile range in the natural log-transformed of urinary 1-OHPyr was significantly associated with a decrease of −0.016 g/cm^2 (95% CI: −0.029, −0.003) in pelvic BMD.

Supplementary Figure S7 depicts exposure-response curves for the associations between individual OH-PAH and BMD in the BKMR model. These findings confirm significant negative associations between 1-OHPhe and lumbar spine BMD and total BMD, as well as between 1-OHPyr and pelvic BMD.

3.4 Association of urinary OH-PAHs with BMD: Qgcomp model

As shown in Supplementary Table S2, the Qgcomp model reveals a significant negative association between the overall effect of the urinary OH-PAHs mixture and BMD. For one quartile range increase in the natural log-transformed of urinary OH-PAHs mixture, lumbar spine BMD, pelvic BMD, and total BMD decreased by −0.012 g/cm^2 (95% CI: −0.021, −0.004), −0.014 g/cm^2 (95% CI: −0.025, −0.003), and −0.010 g/cm^2 (95% CI: −0.016, −0.003), respectively. As shown in Figure 5, 2&3-OHPhe is assigned the largest negative weight to the decrease in lumbar spine BMD (weight = 0.46), while 2&3-OHPhe

10.3389/fpubh.2025.1428772

TABLE 1 Weighted characteristics of participants (*N* = 1,332).

Characteristics	Total	Male	Female	*p*
N[a]	1,332	690	642	
Age, years	13.6 ± 3.30	13.5 ± 3.39	13.8 ± 3.21	0.283
BMI, kg/m^2	22.9 ± 6.31	22.4 ± 5.93	23.4 ± 6.68	0.114
Race, *n* (%)				0.259
Non-Hispanic White	726 (54.5%)	367 (53.2%)	359 (55.9%)	
Hispanic	304 (22.8%)	158 (23.0%)	146 (22.7%)	
Non-Hispanic Black	173 (13.0%)	100 (14.4%)	73 (11.4%)	
Other Race	129 (9.7%)	65 (9.4%)	64 (10.0%)	
Education level, *n* (%)				0.537
Below junior school	419 (31.5%)	224 (32.4%)	195 (30.3%)	
Junior school	397 (29.8%)	211 (30.6%)	187 (29.1%)	
High school or above	516 (38.7%)	255 (37.0%)	261 (40.6%)	
Poverty income ratio, *n* (%)				0.300
<1	310 (23.3%)	149 (21.6%)	161 (25.1%)	
1–3	555 (41.6%)	285 (41.3%)	269 (41.9%)	
>3	467 (35.1%)	256 (37.1%)	212 (33.0%)	
Cotinine, *n* (%)				0.017
Low	680 (51.0%)	327 (47.4%)	353 (55.0%)	
High	652 (49.0%)	363 (52.6%)	289 (45.0%)	
Protein, g	74.3 ± 32.7	84.1 ± 36.4	63.8 ± 24.2	<0.001
Calcium, g	1.05 ± 0.518	1.17 ± 0.540	0.922 ± 0.459	<0.001
Phosphorus, g	1.34 ± 0.552	1.49 ± 0.593	1.17 ± 0.448	<0.001
Lumbar spine BMD, g/cm^2	0.888 ± 0.186	0.855 ± 0.191	0.924 ± 0.174	<0.001
Pelvis BMD, g/cm^2	1.09 ± 0.230	1.07 ± 0.249	1.11 ± 0.205	0.069
Total BMD, g/cm^2	0.965 ± 0.150	0.969 ± 0.160	0.961 ± 0.138	0.501
1-OHNap, ng/g	886 (497, 1,631)	862 (481, 1,615)	893 (516, 1,693)	0.892
2-OHNap, ng/g	4,253 (2,580, 7,861)	3,813 (2,319, 6,589)	4,898 (2,830, 8,883)	<0.001
3-OHFlu, ng/g	70.5 (44.6, 109)	69.0 (44.2, 106)	71.1 (45.0, 111)	0.570
2-OHFlu, ng/g	156 (111, 245)	153 (107, 244)	163 (117, 246)	0.303
1-OHPhe, ng/g	95.5 (64.7, 142)	90.4 (61.0, 134)	100 (71.7, 153)	0.164
1-OHPyr, ng/g	132 (86.9, 202)	121 (79.8, 196)	142 (100, 211)	0.556
2&3-OHPhe, ng/g	108 (77.9, 155)	107 (74.0, 159)	110 (79.7, 152)	0.023

BMI, Body mass index; BMD, Bone mineral density; 1-OHNap, 1-Hydroxynaphthalene; 2-OHNap, 2-Hydroxynaphthalene; 3-OHFlu, 3-Hydroxyfluorene; 2-OHFlu, 2-Hydroxyfluorene; 1-OHPhe, 1-Hydroxyphenanthrene; 1-OHPyr, 1-Hydroxypyrene; 2&3-OHPhe, 2&3-Hydroxyphenanthrene.
[a]Unweighted sample number in the group.

(weight = 0.30) and 1-OHPyr (weight = 0.28) are the main contributors to the decrease in pelvic BMD. Additionally, 1-OHPyr has the highest negative weight to the decrease in BMD (weight = 0.42).

3.5 Sensitivity analysis

Supplementary Figure S8 displays the relationships between urinary OH-PAHs and BMD in subjects with normal creatinine levels (30–300 mg/dL). Except for the significant negative correlation between 1-OHPyr and lumbar and pelvic BMD, which shifted to marginal negative correlation ($p = 0.059$ and $p = 0.056$), the other results are consistent with the main analysis results. Supplementary Figure S9 demonstrates the differences in the overall effects of urinary OH-PAHs mixture on BMD among different genders, age groups, and BMI categories. Similar to the stratified analysis in the main study, we observe significant interactions between urinary OH-PAHs mixture and BMI for lumbar spine BMD (P-interaction = 0.05), with the overall negative effect of the mixture being significant only in overweight/obesity individuals, not in those with underweight/normal subjects. After excluding individuals with undetectable 1-OHPyr levels, we identified significant negative associations between urinary 1-OHPyr and BMD (Supplementary Table S3), consistent with our primary analysis results.

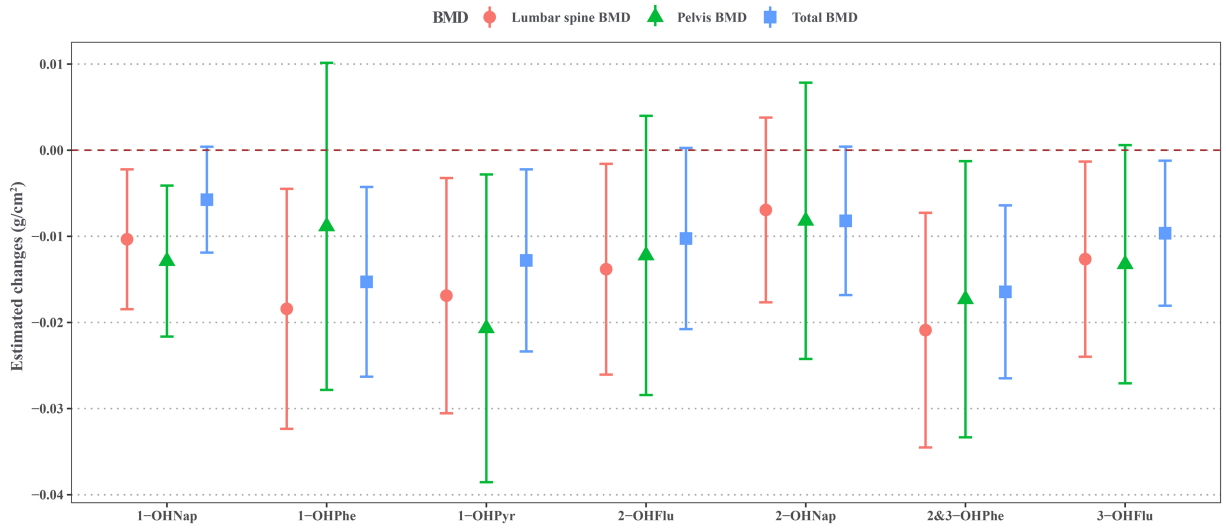

FIGURE 2
Estimated changes for associations of urinary OH-PAHs with lumbar spine BMD, pelvis BMD, and total BMD after adjusted for gender, age, race, poverty income ratio, education level, BMI, cotinine, and daily protein, calcium, and phosphorus intake. OH-PAHs, hydroxy polycyclic aromatic hydrocarbons; BMD, bone mineral density; BMI, body mass index.

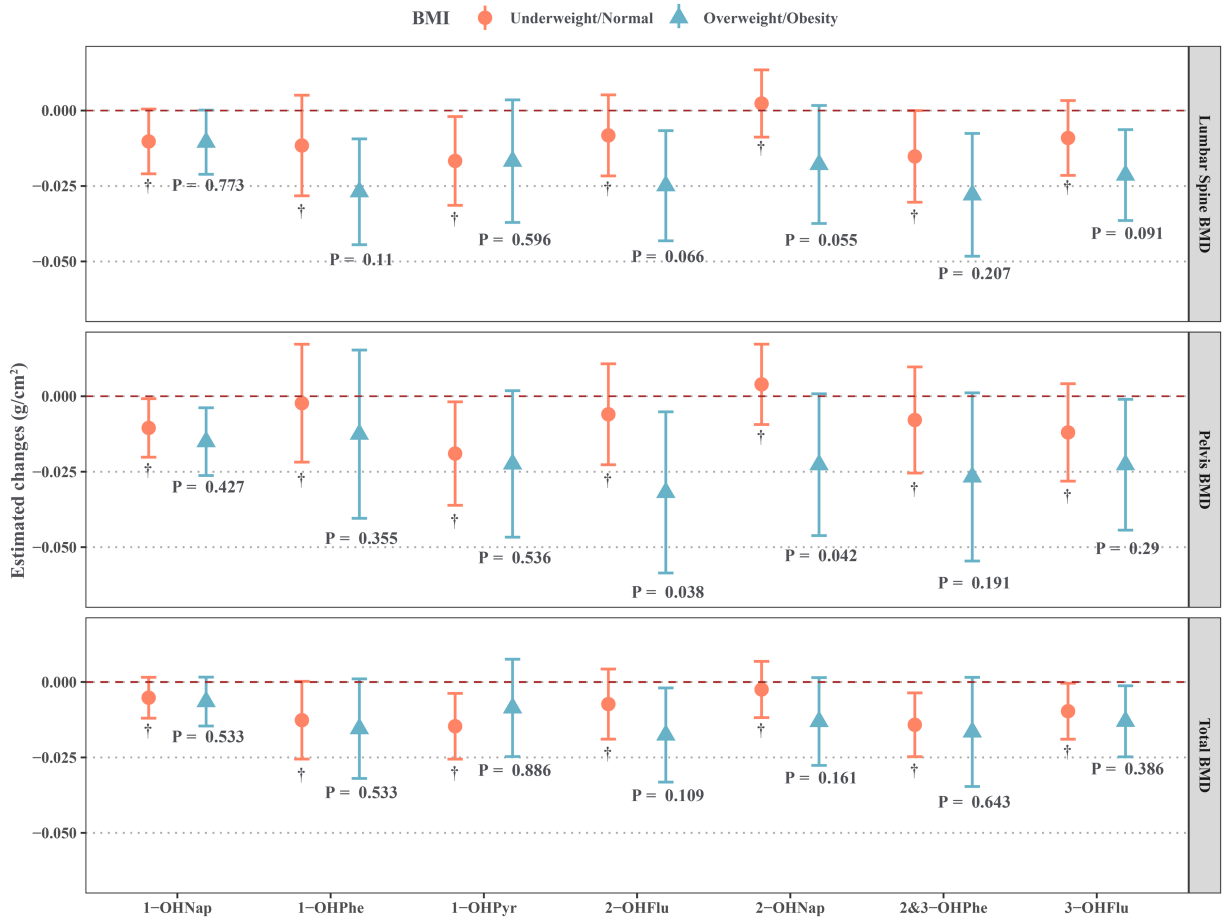

FIGURE 3
Estimated changes for associations of urinary OH-PAHs with lumbar spine BMD, pelvis BMD, and total BMD in different BMI groups after adjusted for gender, age, race, poverty income ratio, education level, cotinine, and daily protein, calcium, and phosphorus intake. OH-PAHs, hydroxy polycyclic aromatic hydrocarbons; BMD, bone mineral density; BMI, body mass index.

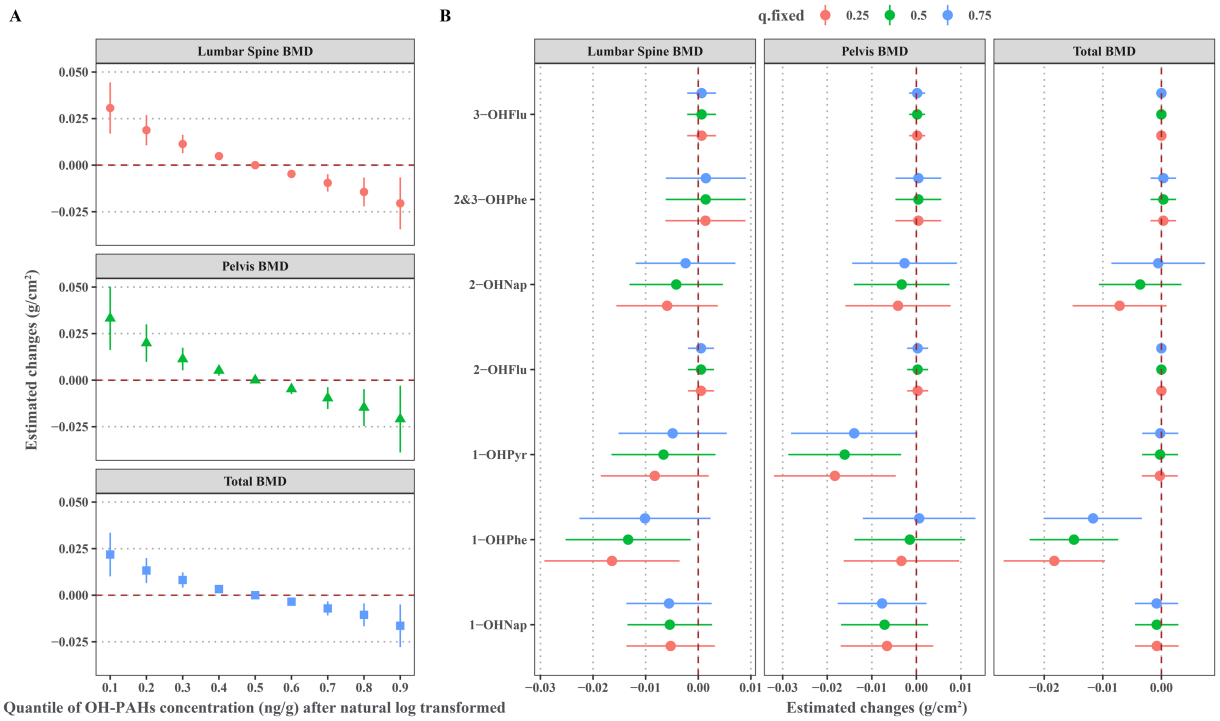

FIGURE 4
Associations of urinary OH-PAHs with BMD based BMKR model after adjusted for gender, age, race, poverty income ratio, education level, BMI, cotinine, and daily protein, calcium, and phosphorus intake. **(A)** Overall effect of urinary OH-PAHs mixture on BMD through comparing the estimated changes of BMD when urinary OH-PAHs fixing at the 10th-90th percentiles with these when urinary OH-PAHs fixing at the 50th percentiles; **(B)** Effects of individual urinary OH-PAH with BMD through comparing the estimated changes of BMD when each OH-PAH was in the 75th percentile with these in its 25th percentile and when all other urinary OH-PAHs were fixed at the 25th, 50th and 75th percentiles, respectively. OH-PAHs, hydroxy polycyclic aromatic hydrocarbons; BMD, bone mineral density; BMKR, Bayesian kernel machine regression; BMI, body mass index.

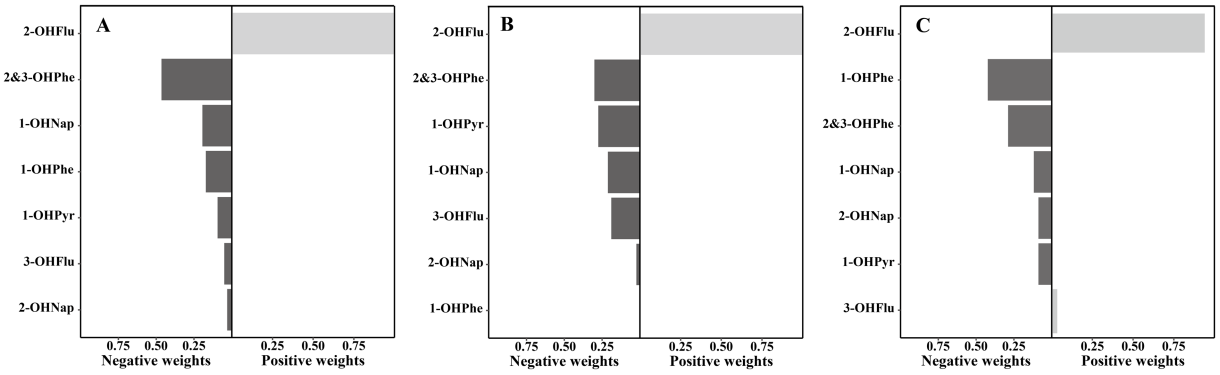

FIGURE 5
Weights of each urinary OH-PAH in associations with **(A)** lumbar spine BMD, **(B)** pelvis BMD, and **(C)** total BMD based on Qgcomp models after adjusted for gender, age, race, poverty income ratio, education level, BMI, cotinine, and daily protein, calcium, and phosphorus intake. OH-PAHs, hydroxy polycyclic aromatic hydrocarbons; BMD, bone mineral density; Qgcomp, quantile g-computation; BMI, body mass index.

4 Discussion

To our knowledge, this is the first study to examine the effects of urinary OH-PAHs on BMD among children and adolescents. We found that some urinary OH-PAHs were negatively associated with lumbar spine BMD, pelvic BMD, and total BMD. BMI modified the associations between urinary OH-PAHs and BMD, and some OH-PAHs exhibited negative effects on BMD, only significant in overweight/obesity individuals, while not significant in underweight/normal individuals. In mixture analysis, both the BKMR model and the Qgcomp model found a significant negative correlation between the overall effect of urinary OH-PAHS mixture and lumbar spine BMD, pelvic BMD, and total BMD; urinary 1-OHPyr and 1-OHPhe were identified as the primary contributors to the decrease in pelvic BMD and total BMD, respectively.

Currently, there is a lack of research on the impact of PAHs exposure on BMD in children and adolescents, making it difficult to directly compare our study's findings with existing literature. There are limited studies that have reported associations between PAHs exposure in adults and BMD, but the results are inconsistent. For instance, Di et al. found a significant negative association between adult urinary 3-OHFlu, 2-OHFlu, and 1-OHPhe levels and lumbar spine BMD in NHANES 2005–2010 and 2013–2014 ($N = 6,766$) (20). Conversely, another study in NHANES 2005–2010 ($N = 1768$) found that adult lumbar spine BMD was significantly negatively associated only with urinary 3-OHPhe at the second tertile, and this study also found a significant positive correlation between urinary 1-OHPyr and trochanteric BMD (18). Additionally, in NHANES 2001–2004 ($N = 2,987$), only female 2-OHPhe levels were significantly negatively correlated with total BMD (17). The disparities in these study results may be attributed to differences in sample size, levels of urinary OH-PAHs, and the skeletal sites. Our study extends the findings from these previous studies, and the discovery of the detrimental effects of PAHs exposure on BMD in children and adolescents holds significant implications for the field of research on the impact of PAHs exposure on bone health in the general population.

Exposure to PAHs, the potential biological mechanisms underlying the decrease in BMD remain unclear, but several pathways have been identified. First, PAH exposure can disrupt bone turnover equilibrium, leading to increased bone resorption (15). In an epidemiological study (30), a significant correlation was found between urinary OH-PAH levels in adults and elevated N-terminal peptide levels (a biomarker reflecting bone resorption). Second, PAHs exhibit estrogen-like effects, reducing the inhibitory action of estrogen on osteoclasts and increasing bone resorption (16). Third, PAHs can induce a pro-inflammatory state in the body, with increased levels of inflammatory mediators such as Tumor Necrosis Factor-α and Interleukin-6 (31), which can stimulate the expression of receptor activator of nuclear factor-κB ligand by osteoblasts. This, in turn, activates osteoclasts, leading to a reduction in bone mass (32). Fourth, PAHs can generate a substantial amount of reactive oxygen species by activating aryl hydrocarbon receptors, which can promote apoptosis of mesenchymal stem cells (precursors to osteoblasts), osteoblasts, and osteocytes, thereby reducing bone formation (33).

Our findings indicate a significant negative association between certain urinary OH-PAH levels and BMD, notably in overweight/obese children and adolescents. This suggests increased susceptibility within this demographic, aligning with previous research demonstrating that higher body fat percentage and total fat mass negatively impact lumbar spine BMD and total BMD (34). The mechanisms by which PAHs negatively influence bone density, particularly in the context of obesity, may involve several biological pathways: (1) Altered Metabolism and Lipid Homeostasis: PAHs have been shown to promote preadipocyte differentiation in adipose tissues while potentially disrupting lipid metabolism. Activation of peroxisome proliferator-activated receptors (PPARs) by PAHs may lead to altered adipocyte function, which can adversely affect bone health (35). This dual impact on both fat and bone tissues could exacerbate the negative effects of obesity on BMD. (2) Inflammation and Bone Remodeling: Obesity is associated with chronic low-grade inflammation, which is a known risk factor for bone loss. Adipose tissue secretes pro-inflammatory cytokines that can impair osteoblast function and promote osteoclastogenesis, leading to decreased bone formation and increased bone resorption (36). The presence of PAHs may further exacerbate this inflammatory state, intensifying the negative effects on BMD in overweight/obese individuals. (3) Hormonal Disruption: PAHs are recognized endocrine disruptors that may alter hormonal balance, particularly affecting sex hormones, which play critical roles in bone health. In adolescents, the relative abundance of estrogen and androgens is crucial for achieving peak bone mass (3, 16). Disruption of these hormonal signals by PAHs, combined with the altered hormonal milieu characteristic of obesity, may further contribute to compromised bone health. Previous studies have shown a significant positive correlation between urinary OH-PAH levels and BMI in children and adolescents, underscoring the importance of considering body composition when evaluating the health impacts of environmental exposures (37). This correlation reinforces our findings, suggesting that weight status amplifies the adverse effects of PAHs on bone density.

In real-life situations, the human body is typically exposed to various PAHs simultaneously. This study employed BKMR and Qgcomp to evaluate the joint effects of PAH mixtures on BMD. These models were selected based on their complementary strengths in addressing distinct aspects of environmental mixture analysis. The BKMR model was chosen to account for potential non-linear dose–response relationships and interactions among PAHs, which are biologically plausible given their diverse mechanisms of toxicity. For instance, certain PAHs may disrupt bone homeostasis through AhR activation or oxidative stress pathways, and their combined effects could be synergistic or non-additive (16, 38). BKMR's semi-parametric framework allows flexible modeling of such complexities without assuming linearity a priority (26). Conversely, the Qgcomp model was applied to quantify the overall linear effect of the PAH mixture while estimating component weights under an additive assumption (27). This parametric approach is advantageous for risk assessment, as it provides interpretable estimates of cumulative effects, which are critical for informing public health interventions. By integrating both approaches, this study balances methodological rigor with practical interpretability, addressing the dual need to explore mechanistic complexity (via BKMR) and quantify actionable risks (via Qgcomp). This strategy aligns with recent methodological frameworks advocating for multi-model analyses in environmental mixtures research (39). Furthermore, both the BKMR and Qgcomp models identified urinary 1-OHPyr and 1-OHPhe as the primary contributors to the decrease in pelvic BMD and total BMD, emphasizing the need for prioritizing the control of these specific PAHs in preventing BMD reduction in children and adolescents. However, for lumbar BMD, the primary contributors identified by the two models differed: BKMR highlighted 1-OHPhe, whereas Qgcomp emphasized 2&3-OHPhe. These metabolites, though derived from the same parent PAH (phenanthrene), may differentially influence bone health due to variations in hydroxylation patterns and bioavailability (40). The discrepancy between models could reflect distinct methodological approaches—BKMR's incorporation of nonlinearity and interactions versus Qgcomp's linear additive framework. This suggests both metabolites may contribute to lumbar BMD reduction through complementary pathways, necessitating further toxicological and epidemiological validation.

A critical aspect often overlooked is the potential synergistic or additive effects of PAHs in conjunction with other environmental contaminants. Studies investigating combined exposures have

indicated that phenolic compounds, chlorophenol pesticides, and phthalates may exacerbate the detrimental effects of PAHs on bone health. For instance, in a study examining the joint effects of these compounds, results indicated that co-exposure significantly impacted BMD, highlighting the importance of accounting for multiple environmental pollutants when assessing bone health (20). Research has shown that endocrine disruptors, including PAHs, can interact with pathways involved in bone metabolism, further complicating their effects (41). For example, a review highlighted that chronic exposure to endocrine disruptors like phthalates and per-and polyfluoroalkyl substances can lead to alterations in bone remodeling processes, which may compound the adverse effects of PAHs on BMD (42). The interplay between PAHs and these pollutants can create a cumulative burden on bone health, emphasizing the need for comprehensive studies that address multiple exposures to adequately assess risks to BMD. Despite the existing literature linking PAH exposure to impaired bone health, there is still limited research on the co-exposure of PAHs with other toxicants and their collective impact on bone density. Further investigations are warranted to better understand these interactions and their implications for public health.

This study has several notable strengths. First, our use of NHANES data—a nationally representative sample with rigorous protocols—enhances the generalizability of findings to U.S. children and adolescents. Second, we focused on a critical yet understudied developmental window (8–19 years), during which bone mass accrual peaks and environmental insults may exert lifelong consequences. Third, we employed advanced mixture modeling approaches (BKMR and Qgcomp) to evaluate co-exposure effects, addressing a key limitation of single-pollutant studies. Additionally, stratified analyses revealed heightened susceptibility in overweight/obese individuals, highlighting metabolic status as a modifier of PAH toxicity. Our findings underscore the need for targeted interventions to reduce PAH exposure in children and adolescents, contributing to the prevention of future osteoporosis and associated health outcomes.

However, this study also has the following drawbacks. Firstly, the cross-sectional study design cannot establish a causal temporal relationship between PAHs exposure and changes in BMD. Secondly, urinary OH-PAH levels may significantly change over time due to the stochastic nature of exposure and variations in PAH pharmacokinetics (43). Using single-point urine samples to measure individual PAH exposure concentrations may lead to exposure misclassification. Thirdly, this study did not include children under the age of 8 due to the lack of BMD data for this age group. As a result, it was not possible to explore the effect of PAHs exposure on early childhood BMD. Finally, the study focused only on the impact of PAHs exposure on BMD in children and adolescents. However, other toxic substances in the environment, such as per-and polyfluoroalkyl substances, phthalates, and lead, can also contribute to changes in BMD in children and adolescents (20, 44, 45). The study did not account for these potential confounding factors.

5 Conclusion

In conclusion, we found that higher levels of PAHs exposure in children and adolescents are associated with decreased BMD, with a potentially greater effect on overweight/obesity individuals. While further validation of our findings is necessary, reducing environmental PAHs exposure during childhood and adolescence may potentially mitigate bone mass loss, thus improving peak BMD and preventing osteoporosis.

Data availability statement

The raw data supporting the conclusions of this article will be made available by the authors, without undue reservation.

Ethics statement

The studies involving humans were approved by National Center for Health Statistics Research Ethics Review Board. The studies were conducted in accordance with the local legislation and institutional requirements. Written informed consent for participation in this study was provided by the participants' legal guardians/next of kin.

Author contributions

PZ: Writing – original draft, Writing – review & editing. SL: Supervision, Writing – review & editing. HZ: Conceptualization, Data curation, Formal analysis, Methodology, Software, Visualization, Writing – review & editing. YS: Formal analysis, Funding acquisition, Methodology, Writing – review & editing.

Funding

The author(s) declare that no financial support was received for the research and/or publication of this article.

Conflict of interest

The authors declare that the research was conducted in the absence of any commercial or financial relationships that could be construed as a potential conflict of interest.

Publisher's note

Supplementary material

The Supplementary material for this article can be found online at: https://www.frontiersin.org/articles/10.3389/fpubh.2025.1428772/full#supplementary-material

References

1. Vijayakumar R, Büsselberg D. Osteoporosis: an under-recognized public health problem. *J Local Glob Health Sci*. (2016) 2016:2. doi: 10.5339/jlghs.2016.2

2. Gordon CM, Zemel BS, Wren TAL, Leonard MB, Bachrach LK, Rauch F, et al. The determinants of peak bone mass. *J Pediatr*. (2017) 180:261–9. doi: 10.1016/j.jpeds.2016.09.056

3. Stagi S, Cavalli L, Iurato C, Seminara S, Brandi ML, de Martino M. Bone metabolism in children and adolescents: main characteristics of the determinants of peak bone mass. *Clin Cases Miner Bone Metab*. (2013) 10:172–9.

4. Carroquino MJ, Posada M, Landrigan PJ. Environmental toxicology: children at risk. In: Laws EA, editor. *Environmental toxicology: selected entries from the encyclopedia of sustainability science and technology*. New York, NY, USA: Springer (2013) p. 239–291.

5. Benjamin RM. Bone health: preventing osteoporosis. *Public Health Rep*. (2010) 125:368–70. doi: 10.1177/003335491012500302

6. Mallah MA, Changxing L, Mallah MA, Noreen S, Liu Y, Saeed M, et al. Polycyclic aromatic hydrocarbon and its effects on human health: an overeview. *Chemosphere*. (2022) 296:133948. doi: 10.1016/j.chemosphere.2022.133948

7. Au WW. Susceptibility of children to environmental toxic substances. *Int J Hyg Environ Health*. (2002) 205:501–3. doi: 10.1078/1438-4639-00179

8. Huang W, Caudill SP, Grainger J, Needham LL, Patterson DG Jr. Levels of 1-hydroxypyrene and other monohydroxy polycyclic aromatic hydrocarbons in children: a study based on U.S. reference range values. *Toxicol Lett*. (2006) 163:10–9. doi: 10.1016/J.TOXLET.2005.08.003

9. Huang X, Deng X, Li W, Liu S, Chen Y, Yang B, et al. Internal exposure levels of polycyclic aromatic hydrocarbons in children and adolescents: a systematic review and meta-analysis. *Environ Health Prev Med*. (2019) 24:1–15. doi: 10.1186/S12199-019-0805-9

10. Shen H, Tao S, Liu J, Huang Y, Chen H, Li W, et al. Global lung cancer risk from PAH exposure highly depends on emission sources and individual susceptibility. *Sci Rep*. (2014) 4:1–8. doi: 10.1038/srep06561

11. Jakovljević I, Štrukil ZS, Pehnec G, Horvat T, Sanković M, Šumanovac A, et al. Ambient air pollution and carcinogenic activity at three different urban locations. *Ecotoxicol Environ Saf*. (2025) 289:117704. doi: 10.1016/J.ECOENV.2025.117704

12. Zhang J, Li J, Wang P, Chen G, Mendola P, Sherman S, et al. Estimating population exposure to ambient polycyclic aromatic hydrocarbon in the United States – part I: model development and evaluation. *Environ Int*. (2017) 99:263–74. doi: 10.1016/J.ENVINT.2016.12.002

13. Gariazzo C, Lamberti M, Hänninen O, Silibello C, Pelliccioni A, Porta D, et al. Assessment of population exposure to polycyclic aromatic hydrocarbons (PAHs) using integrated models and evaluation of uncertainties. *Atmos Environ*. (2015) 101:235–45. doi: 10.1016/J.ATMOSENV.2014.11.035

14. Yu H, Du Y, Zhang X, Sun Y, Li S, Dou Y, et al. The aryl hydrocarbon receptor suppresses osteoblast proliferation and differentiation through the activation of the ERK signaling pathway. *Toxicol Appl Pharmacol*. (2014) 280:502–10. doi: 10.1016/J.TAAP.2014.08.025

15. Ye Q, Xi X, Fan D, Cao X, Wang Q, Wang X, et al. Polycyclic aromatic hydrocarbons in bonehomeostasis. *Biomed Pharmacother*. (2022) 146:112547. doi: 10.1016/j.biopha.2021.112547

16. Zhang Y, Dong S, Wang H, Tao S, Kiyama R. Biological impact of environmental polycyclic aromatic hydrocarbons (ePAHs) as endocrine disruptors. *Environ Pollut*. (2016) 213:809–24. doi: 10.1016/J.ENVPOL.2016.03.050

17. Yang R, Chen Z, Hu Y. Associations of urinary polycyclic aromatic hydrocarbons with bone mineral density at specific body sites in U.S. adults, National Health and nutrition examination survey 2001 to 2004. *Endocr Pract*. (2022) 28:867–74. doi: 10.1016/j.eprac.2022.06.008

18. Guo J, Huang Y, Bian S, Zhao C, Jin Y, Yu D, et al. Associations of urinary polycyclic aromatic hydrocarbons with bone mass density and osteoporosis in U.S. adults, NHANES 2005–2010. *Environ Pollut*. (2018) 240:209–18. doi: 10.1016/J.ENVPOL.2018.04.108

19. Fu Y, Wang G, Liu J, Li M, Dong M, Zhang C, et al. Stimulant use and bone health in US children and adolescents: analysis of the NHANES data. *Eur J Pediatr*. (2022) 181:1633–42. doi: 10.1007/S00431-021-04356-W

20. Di D, Zhang R, Zhou H, Wei M, Cui Y, Zhang J, et al. Joint effects of phenol, chlorophenol pesticide, phthalate, and polycyclic aromatic hydrocarbon on bone mineral density: comparison of four statistical models. *Environ Sci Pollut Res*. (2023) 30:80001–13. doi: 10.1007/s11356-023-28065-z

21. Gu L, Wang Z, Pan Y, Wang H, Sun L, Liu L, et al. Associations between mixed urinary phenols and parabens metabolites and bone mineral density: four statistical models. *Chemosphere*. (2023) 311:137065. doi: 10.1016/j.chemosphere.2022.137065

22. Fang L, Zhao H, Chen Y, Ma Y, Xu S, Xu S, et al. The combined effect of heavy metals and polycyclic aromatic hydrocarbons on arthritis, especially osteoarthritis, in the U.S. adult population. *Chemosphere*. (2023) 316:137870. doi: 10.1016/j.chemosphere.2023.137870

23. Xu H, Mao Y, Hu Y, Xu B. Association between exposure to polyfluoroalkyl chemicals and increased fractional exhaled nitric oxide in adults. *Environ Res*. (2021) 198:110450. doi: 10.1016/J.ENVRES.2020.110450

24. Gauthier J, Wu QV, Gooley TA. Cubic splines to model relationships between continuous variables and outcomes: a guide for clinicians. *Bone Marrow Transplant*. (2020) 55:675–80. doi: 10.1038/s41409-019-0679-x

25. Kuczmarski RJ, Ogden CL, Guo SS, Grummer-Strawn LM, Flegal KM, Mei Z, et al. 2000 CDC growth charts for the United States: methods and development. *Vital Health Stat*. *11*. (2002) 246:1–90.

26. Bobb JF, Claus Henn B, Valeri L, Coull BA. Statistical software for analyzing the health effects of multiple concurrent exposures via Bayesian kernel machine regression. *Environ Health*. (2018) 17:1–10. doi: 10.1186/S12940-018-0413-Y

27. Keil AP, Buckley JP, O'Brien KM, Ferguson KK, Zhao S, White AJ. A quantile-based g-computation approach to addressing the effects of exposure mixtures. *Environ Health Perspect*. (2020) 128:47004. doi: 10.1289/EHP5838

28. Desai G, Niu Z, Luo W, Frndak S, Shaver AL, Kordas K. Low-level exposure to lead, mercury, arsenic, and cadmium, and blood pressure among 8-17-year-old participants of the 2009–2016 National Health and nutrition examination survey. *Environ Res*. (2021) 197:111086. doi: 10.1016/J.ENVRES.2021.111086

29. Kuiper JR, Pan S, Lanphear BP, Calafat AM, Chen A, Cecil KM, et al. Associations of maternal gestational urinary environmental phenols concentrations with bone mineral density among 12-year-old children in the HOME study. *Int J Hyg Environ Health*. (2023) 248:114104. doi: 10.1016/J.IJHEH.2022.114104

30. Chen YY, Kao TW, Wang CC, Wu CJ, Zhou YC, Chen WL. Association between polycyclic aromatic hydrocarbons exposure and bone turnover in adults. *Eur J Endocrinol*. (2020) 182:333–41. doi: 10.1530/EJE-19-0750

31. Niu X, Ho SSH, Ho KF, Huang Y, Sun J, Wang Q, et al. Atmospheric levels and cytotoxicity of polycyclic aromatic hydrocarbons and oxygenated-PAHs in PM2.5 in the Beijing-Tianjin-Hebei region. *Environ Pollut*. (2017) 231:1075–84. doi: 10.1016/j.envpol.2017.08.099

32. Chinese Society of Osteoporosis and Bone Mineral. Guidelines for the diagnosis and treatment of primary osteoporosis (2022). *Chin Gen Pract*. (2023) 26:1671. doi: 10.12114/J.ISSN.1007-9572.2023.0121

33. Wu X, Cao X, Lintelmann J, Peters A, Koenig W, Zimmermann R, et al. Assessment of the association of exposure to polycyclic aromatic hydrocarbons, oxidative stress, and inflammation: a cross-sectional study in Augsburg, Germany. *Int J Hyg Environ Health*. (2022) 244:113993. doi: 10.1016/j.ijheh.2022.113993

34. Suárez CG, Singer BH, Gebremariam A, Lee JM, Singer K. The relationship between adiposity and bone density in U.S. children and adolescents. *PLoS One*. (2017) 12:e0181587. doi: 10.1371/JOURNAL.PONE.0181587

35. Grün F, Blumberg B. Environmental Obesogens: Organotins and endocrine disruption via nuclear receptor signaling. *Endocrinology*. (2006) 147:s50–5. doi: 10.1210/en.2005-1129

36. Coppack SW. Pro-inflammatory cytokines and adipose tissue. *Proc Nutr Soc*. (2001) 60:349–56. doi: 10.1079/PNS2001110

37. Bushnik T, Wong SL, Holloway AC, Thomson EM. Association of urinary polycyclic aromatic hydrocarbons and obesity in children aged 3–18: Canadian health measures survey 2009–2015. *J Dev Orig Health Dis*. (2020) 11:623–31. doi: 10.1017/S2040174419000825

38. Goedtke L, Sprenger H, Hofmann U, Schmidt FF, Hammer HS, Zanger UM, et al. Polycyclic aromatic hydrocarbons activate the aryl hydrocarbon receptor and the constitutive Androstane receptor to regulate xenobiotic metabolism in human liver cells. *Int J Mol Sci*. (2020, 2021) 22:372. doi: 10.3390/IJMS22010372

39. Joubert BR, Kioumourtzoglou M-A, Chamberlain T, Chen HY, Gennings C, Turyk ME, et al. Powering research through innovative methods for mixtures in epidemiology (PRIME) program: novel and expanded statistical methods. *Int J Environ Res Public Health*. (2022) 19:1378. doi: 10.3390/ijerph19031378

40. Ramesh A, Walker SA, Hood DB, Guillén MD, Schneider K, Weyand EH. Bioavailability and risk assessment of orally ingested polycyclic aromatic hydrocarbons. *Int J Toxicol*. (2004) 23:301–33. doi: 10.1080/10915810490517063

41. Park SY, Kong SH, Kim KJ, Ahn SH, Hong N, Ha J, et al. Effects of endocrine-disrupting chemicals on bone health. *Endocrinol Metab*. (2024) 39:539–51. doi: 10.3803/ENM.2024.1963

42. Baradaran Mahdavi S, Zamani S, Riahi R, Taheri E, Vahdatpour B, Sharifianjazi F, et al. Exposure to environmental chemicals and human bone health; a systematic review and Meta-analysis. *Expo Health*. (2024) 16:861–83. doi: 10.1007/S12403-023-00596-3

43. Zhu H, Martinez-Moral MP, Kannan K. Variability in urinary biomarkers of human exposure to polycyclic aromatic hydrocarbons and its association with oxidative stress. *Environ Int*. (2021) 156:106720. doi: 10.1016/J.ENVINT.2021.106720

44. Cluett R, Seshasayee SM, Rokoff LB, Rifas-Shiman SL, Ye X, Calafat AM, et al. Per-and Polyfluoroalkyl substance plasma concentrations and bone mineral density in Midchildhood: a cross-sectional study (project viva, United States). *Environ Health Perspect*. (2019) 127:87006. doi: 10.1289/EHP4918

45. Li T, Xie Y, Wang L, Huang G, Cheng Y, Hou D, et al. The association between Lead exposure and bone mineral density in childhood and adolescence: results from NHANES 1999–2006 and 2011–2018. *Nutrients*. (2022) 14:1523. doi: 10.3390/NU14071523/S1

Frontiers in Public Health

Explores and addresses today's fast-moving healthcare challenges

One of the most cited journals in its field, which promotes discussion around inter-sectoral public health challenges spanning health promotion to climate change, transportation, environmental change and even species diversity.

Discover the latest Research Topics

See more →

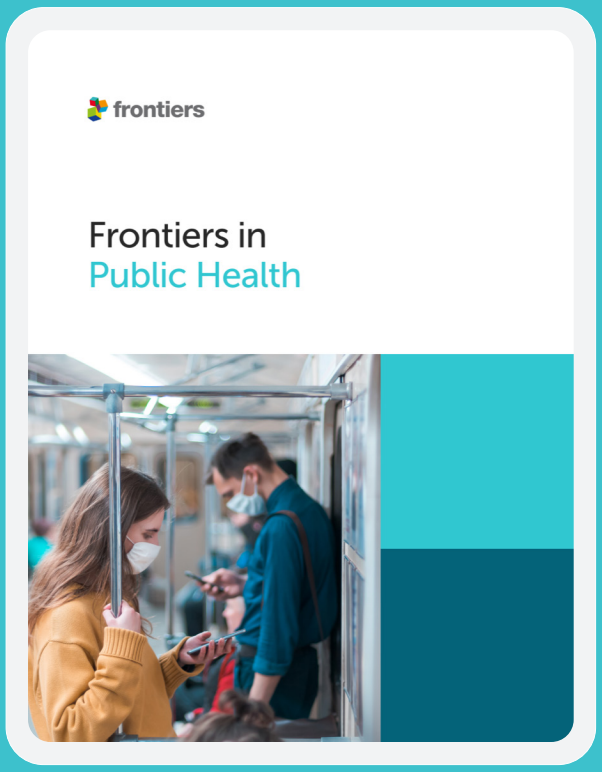

Frontiers

Avenue du Tribunal-Fédéral 34
1005 Lausanne, Switzerland
frontiersin.org

Contact us

+41 (0)21 510 17 00
frontiersin.org/about/contact